ZooKeys 1207: 1–149 (2024)
DOI: 10.3897/zookeys.1207.120068

Research Article

Systematic revision of the South American "*Nuncia*" (Opiliones, Laniatores, Triaenonychidae)

Willians Porto[1,2], Shahan Derkarabetian[3,4], Gonzalo Giribet[3], Abel Pérez-González[1]

1 *División Aracnología, Museo Argentino de Ciencias Naturales–CONICET, Av. Ángel Gallardo 470, C1405DJR Buenos Aires, Argentina*
2 *Sección Aracnología y Miriapodología, Universidad Nacional de La Plata, Facultad de Ciencias Naturales y Museo, Paseo del Bosque s/n, (1900) La Plata, Argentina*
3 *Museum of Comparative Zoology, Department of Organismic and Evolutionary Biology, Harvard University, Cambridge, MA 02138, USA*
4 *San Diego Natural History Museum, Department of Entomology, San Diego, CA 92101, USA*
Corresponding authors: Willians Porto (willians.porto@outlook.com); Abel Pérez-González (abelaracno@gmail.com)

Abstract

The genus *Nuncia* has long been the most speciose within the Opiliones family Triaenonychidae, comprising 63 species and subspecies distributed across New Zealand and South America. Recent molecular studies utilizing Sanger sequencing and ultraconserved elements (UCEs) have indicated that this genus is not monophyletic, and true *Nuncia* are actually confined to New Zealand. Here, the morphology of all South American triaenonychids is re-examined and DNA sequence data compiled from three markers (18S rRNA, 28S rRNA and cytochrome *c* oxidase subunit I) for a large number of triaenonychid species, including specimens from all areas with species currently and formerly classified in *Nuncia* to reassess their phylogenetic position. Based on our findings we 1) revalidate the genus *Chilenuncia* (Muñoz-Cuevas, 1971) **nom. rest.**; 2) describe five new genera: *Fresiax* **gen. nov.**, *Mistralia* **gen. nov.**, *Laftrachia* **gen. nov.**, *Lautaria* **gen. nov.**, *Nerudiella* **gen. nov.**; 3) redescribe five species: *Fresiax spinulosa* **comb. nov.**, *Mistralia verrucosa* **comb. nov.**, *Chilenuncia chilensis* **comb. nov.**, *Chilenuncia rostrata* **comb. nov.**, *Nerudiella americana* **comb. nov.**; and 4) describe 22 new species of South American triaenonychids: *Fresiax conica* **sp. nov.**, *Fresiax fray* **sp. nov.**, *Fresiax mauryi* **sp. nov.**, *Fresiax pichicuy* **sp. nov.**, *Mistralia ramirezi* **sp. nov.**, *Laftrachia robin* **sp. nov.**, *Lautaria ceachei* **sp. nov.**, *Nerudiella cachai* **sp. nov.**, *Nerudiella caramavida* **sp. nov.**, *Nerudiella cautin* **sp. nov.**, *Nerudiella choapa* **sp. nov.**, *Nerudiella curi* **sp. nov.**, *Nerudiella goroi* **sp. nov.**, *Nerudiella jaimei* **sp. nov.**, *Nerudiella malleco* **sp. nov.**, *Nerudiella penco* **sp. nov.**, *Nerudiella pichi* **sp. nov.**, *Nerudiella portai* **sp. nov.**, *Nerudiella quenes* **sp. nov.**, *Nerudiella vilches* **sp. nov.**, *Nerudiella wekufe* **sp. nov.**, and *Nerudiella zapallar* **sp. nov.** Furthermore, we provide detailed illustrations of all the South American species belonging to these lineages formerly classified in *Nuncia*.

Key words: Argentina, Chile, genital morphology, harvestmen, Insidiatores, phylogenetic analysis, systematics, taxonomy

Academic editor: Fedor Konstantinov
Received: 3 February 2024
Accepted: 28 April 2024
Published: 12 July 2024

ZooBank: https://zoobank.org/8B2E2B5D-CA1D-4B61-8736-ECF013EDC384

Citation: Porto W, Derkarabetian S, Giribet G, Pérez-González A (2024) Systematic revision of the South American "*Nuncia*" (Opiliones, Laniatores, Triaenonychidae). ZooKeys 1207: 1–149. https://doi.org/10.3897/zookeys.1207.120068

Introduction

Triaenonychidae Sørensen, 1886, stands as the fourth most diverse family of Opiliones, encompassing 404 known species (Kury et al. 2022). These Laniatores, which are characterized by their small to medium-sized bodies and ranging in color from yellowish to brown (Fig. 1), thrive in the southern temperate regions of the ancient supercontinent Gondwana (Giribet and Kury 2007). Their presence extends across Australia, Madagascar, New Caledonia, New Zealand, South Africa, and southern South America, with at least one species having dispersed to the Crozet Islands (Enderlein 1909; Roewer 1914; Hickman 1939; Kury 2007; Mendes and Kury 2008; Mendes and Kury 2012; Baker et al. 2020; Porto and Pérez-González 2020; Derkarabetian et al. 2021a). In their natural habitat, triaenonychids are primarily nocturnal, actively navigating the moist temperate forests they inhabit. During daytime, they often seek refuge beneath woody debris, rocks, and even in caves (Pérez-Schultheiss et al. 2021).

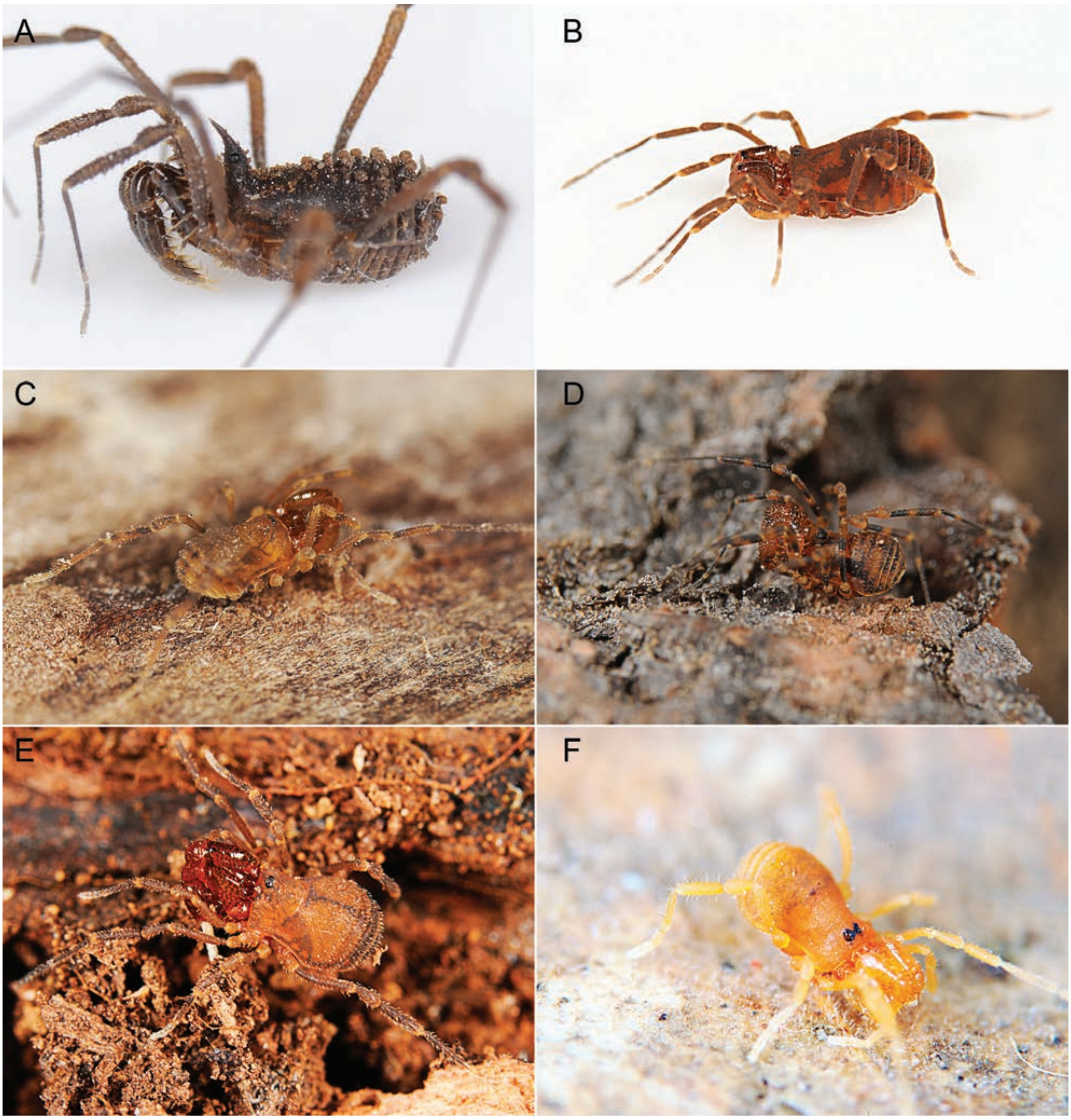

Figure 1. Photographs of live Triaenonychidae **A** *Mistralia verrucosa* comb. nov. **B** *Chilenuncia chilensis* comb. nov. **C** *Nerudiella* gen. nov. **D** *Fresiax spinulosa* comb. nov. **E** *Lautaria ceachei* sp. nov. **F** *Laftrachia robin* sp. nov. Photographs copyright of Abel Pérez-González.

Nuncia, described by Loman in 1902 from New Zealand, is recognized as the most speciose genus within Triaenonychidae, encompassing 63 species and subspecies (Kury et al. 2022). Initially, *Nuncia* was believed to have a distribution that included the Crozet Islands, New Zealand, and South America, a rare transoceanic distribution among triaenonychids (Mendes and Kury 2008). However, recent investigations incorporating molecular and morphological evidence have revealed that *Nuncia* does not form a monophyletic group, the nominal clade being exclusively confined to New Zealand (Porto and Pérez-González 2019; Baker et al. 2020; Derkarabetian et al. 2021a). Here we deal with the remaining *Nuncia*, as the *"Nuncia"* from the Crozet Islands is reinstated in its original genus, *Promecostethus* Enderlein 1909 (Kury et al. 2014; Porto and Pérez-González 2020).

The genus *Nuncia* was established by Loman (1902) for the species *Nuncia sperata* Loman, 1902. Forster (1954) considered it a junior synonym of *Triaenonyx obesus* Simon, 1899, and transferred *T. obesus* to *Nuncia* under the name *Nuncia obesa obesa* (Simon, 1899). Forster (1954) made a significant contribution to the taxonomy of *Nuncia* through his comprehensive revision of the New Zealand Laniatores. His work resulted in the revision and description of 53 new species and subspecies of *Nuncia*. Furthermore, Forster's revision encompassed the reorganization of the infra-generic status of *Nuncia*, resulting in the description of two subgenera (Forster 1954). In the subsequent years (Forster 1965) continued to contribute by documenting additional species of *Nuncia* from New Zealand.

The history of the South American *Nuncia* began when Roewer (1961) described *Nuncia americana*, which marked the first occurrence of a 'transcontinental' genus within Triaenonychidae. Subsequently, Soares (1968) added the Tasmanian *Parattahia* Roewer, 1915, to the list of transcontinental genera with the description of *Parattahia chilensis* Soares, 1968, from Chile. In his influential work, Maury (1990) strengthened and expanded the Roewerian concept of transcontinental *Nuncia* when he described three new species from Chile and Argentina, *N. rostrata*, *N. spinulosa*, and *N. verrucosa*, and also transferred *Parattahia chilensis* to this genus. Maury (1990) not only established the new combination *Nuncia chilensis* but also considered *Chilenuncia donosoi* Muñoz-Cuevas, 1971, its junior synonym; therefore, the hitherto monotypic Chilean genus *Chilenuncia* also fell into the synonymy of *Nuncia*. In the same work, Maury (1990) also reinstated the synonymy of Crozet Island's monotypic *Promecostethus* with *Nuncia*. Since this work, *Nuncia* has been considered the triaenonychid genus with the largest distributional range and a textbook example of transcontinental distribution in opilionid genera.

Recent studies that have examined the relationships within Triaenonychidae worldwide utilizing molecular Sanger markers and ultraconserved element (UCE) data (Baker et al. 2020; Derkarabetian et al. 2021a, 2021b), have confirmed that the South American and New Zealand *Nuncia* represent separate genetic lineages, thus constituting a polyphyletic group. Furthermore, while the New Zealand *Nuncia* are monophyletic, the South American *Nuncia* belong to multiple independent genetic lineages, necessitating taxonomic revision and the proposal of new names that more accurately reflect their systematic classification as was claimed in recent works (Baker et al. 2020; Derkarabetian et al. 2021b).

In this study, our primary focus is on the taxonomy and systematics of the South American triaenonychid species traditionally included in the genus *Nuncia* Loman, 1902, aiming to provide a comprehensive understanding of their phylogeny through molecular analysis and examination of external and genital morphology. Before this study, there were five known species of "*Nuncia*" in South America. Our study has resulted in the redefinition of the Neotropical lineage within this group, as well as the formalization of new taxa. As part of our research, we have revalidated one genus, described five new genera, redescribed the five previously known species, and described 22 additional species. Furthermore, we provide detailed illustrations of all the South American species belonging to these lineages.

Materials and methods

Sample preparation

The specimens used in this study are deposited in the following institutions: American Museum of Natural History (**AMNH**), California Academy of Sciences (**CAS**), Field Museum of Natural History (**FMNH**), Museo Argentino de Ciencias Naturales (**MACN**), Museum of Comparative Zoology (**MCZ**), and Museo Nacional de Historia Natural, Santiago de Chile (**MNHNCL**). Examination and photography of the specimens were conducted using a Leica M205A stereomicroscope equipped with a Leica DF295 digital camera. Specimens were carefully cleaned using a fine bristle paint brush. For scanning electron microscopy (SEM) preparations, body parts were dissected, cleaned, dehydrated using an ethanol series (80%–90%–96%–100%), mounted on aluminum stubs, and coated with gold-palladium using a VG Scientific SC 7620 mini sputter-coater. SEM micrographs were captured under high vacuum using a Philips FEI XL30 TMP at the MACN.

Male genitalia were dissected and temporarily mounted on microscope slides following the technique described in Acosta et al. (2007), with clove oil used as a clearing agent. Examination of male genitalia was conducted using an Olympus BH2 compound microscope, after which they were returned to 80% ethanol and stored in microvials alongside their respective specimens. The morphological nomenclature in this study adheres to the classifications provided by Mendes and Kury (2012), Murphree (1988) Pérez-González and Werneck (2018) and Porto and Pérez-González (2019). Scutum shape outline nomenclature follows the guidelines established by Kury and Medrano (2016). Other details about the external and genital morphology can be analyzed according to the models proposed herein (Fig. 2). All measurements in mm, unless otherwise stated.

Molecular data

We targeted three markers, including two conserved nuclear ribosomal genes (18S and 28S rRNAs) and the mitochondrial gene cytochrome *c* oxidase subunit I. Molecular data were obtained from Baker et al. (2020), with additional sequences obtained from sequence capture of ultraconserved element (UCE) data available from Derkarabetian et al. (2021a) as "bycatch" (Suppl. material 1). For these UCE-derived sequences, we used Geneious v. 11.0 (https://www.geneious.com) to conduct local nucleotide BLAST searches for the associated UCE assembly file for each sample against closely related COI sequences

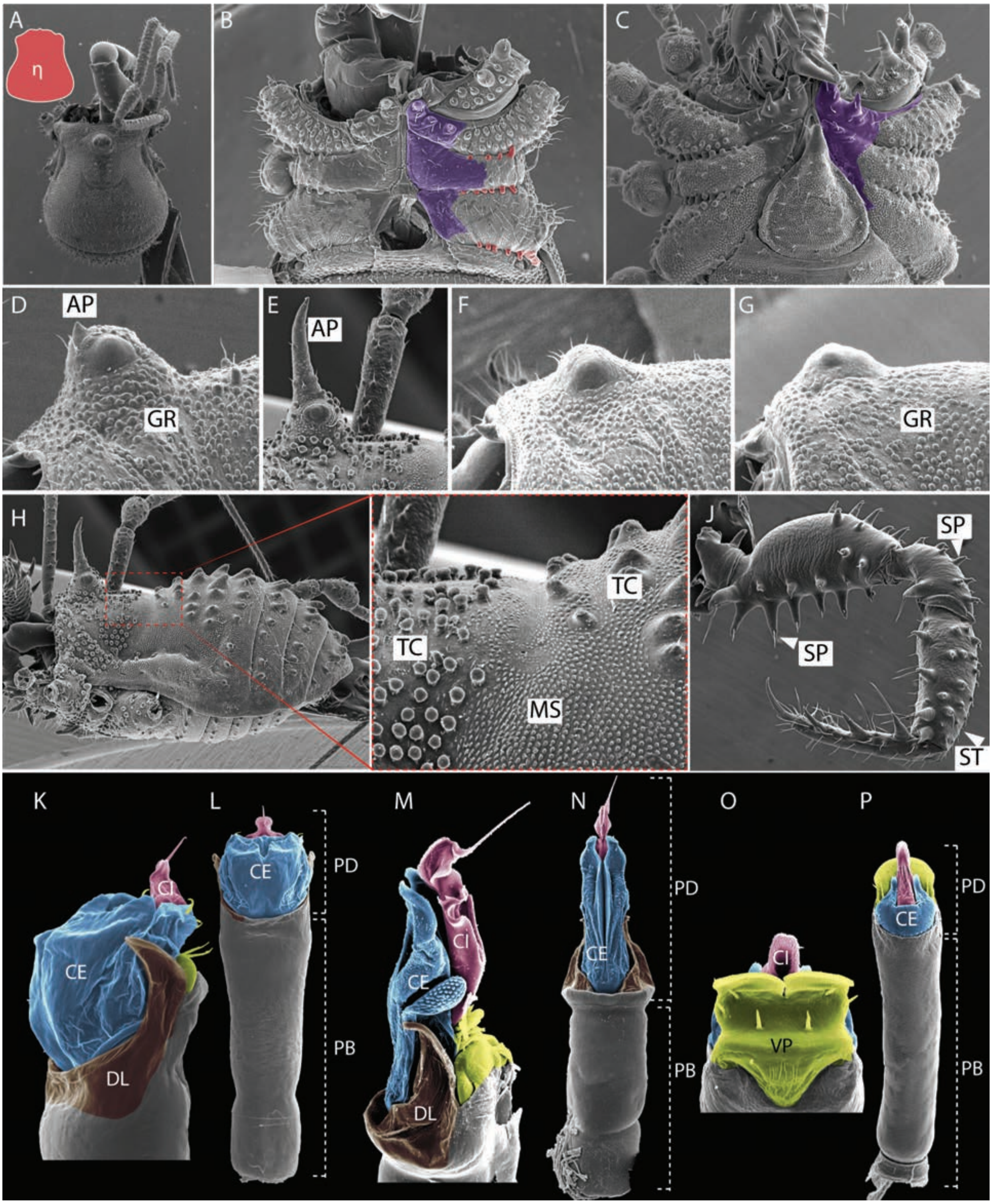

Figure 2. Guide to some taxonomic characters used in this study **A** shape dorsal scutum of Triaenonychidae **B, C** smooth areas of ventral coxae (purple) and ventral bridges(red) **D–G** shapes of ocularium **H, I** styles of integument **J** styles of pedipalps tubercles **K–P** styles of male genital morphology. Abbreviations: AP apophyses, CE capsula externa, CI capsula interna, DL dorsolateral plate,GR granules, MS microgranulation, PB pars basalis, PD pars distalis, SP (spines)large tubercles, ST setae, TC tubercles, VP ventral plate.

which were available from Baker et al. (2020). Sequences for 15 additional taxa were generated for this study from specimens deposited in the MACN collected in 96% ethanol and kept at -20 °C. All voucher specimens for this study are thus deposited in the MACN or in the MCZ, the latter being available through MCZbase (https://mczbase.mcz.harvard.edu/).

For the new sequences, DNA was extracted from leg muscle using Chelex 10%, with an overnight incubation. 18S rRNA was amplified in two non-overlapping fragments using primer pairs 1F–5R, and 18Sa2.0–9R (Giribet et al. 1996; Whiting et al. 1997). A portion of 28S rRNA was sequenced in two overlapping fragments using primer pairs 28Sa–28Srd5b and 28Srd4.8a–28Srd7bi (Schwendinger and Giribet 2005). COI was amplified with the primer pair LCO1490–HCO2198 (Folmer et al. 1994). PCR reactions were carried out with 0.5–1.5 μL of DNA template, using Taq DNA polymerase in a 25-mL reaction. A 1% agarose gel electrophoresis was used to visualize amplification reactions. Successful reactions were cleaned using ExoSAP. Sanger sequencing was conducted at Macrogen Inc., Korea. New sequences have been deposited in GenBank (Suppl. material 1).

Sequences for each marker were checked and trimmed with Geneious 7.1.3 and aligned with Muscle (Edgar 2004) in MEG. Azevedo-X (Kumar et al. 2018), with the gap opening set at -400.00, 100 maximum iterations, and using UPGMA as clustering method. Aligned fragments were concatenated in Sequence Matrix (Vaidya et al. 2011) and the concatenated dataset was then subjected to subsequent phylogenetic analysis.

Phylogenetic analysis

Model testing and phylogenetic analysis were performed in IQ-TREE (Nguyen et al. 2015), implementing the ModelFinder function (Kalyaanamoorthy et al. 2017) and partitioning by locus (Chernomor et al. 2016). Nodal support was assessed with a Shimodaira–Hasegawa approximate likelihood ratio test (SH-aLRT) and ultrafast bootstrap analysis (UFBoot) (Hoang et al. 2018), specifying 1000 replications for each. The runs were repeated 10 times and three topology tests were conducted: approximately unbiased AU (Shimodaira 2002), bootstrap proportion (Kishino et al. 1990), Kishino–Hasegawa (Kishino and Hasegawa 1989), and expected likelihood weight (Strimmer and Rambaut 2002), using 10,000 resampling-estimated log-likelihoods in IQ-TREE with the 10 trees. A consensus tree summarizing the 10 runs was constructed. This tree served as a reference for the discussion and was further refined and customized using FigTree v. 1.4.3 and Adobe Illustrator 2019. The maps in this study were constructed using shapefiles sourced from Natural Earth data. Additionally, the ecoregions shapefiles were obtained from WWF terrestrial ecoregions (Olson et al. 2001). The map visualization was performed using R Statistical Software (R Core Team 2022) and the following packages: sf (Pebesma 2018, Pebesma and Bivand 2023), ggplot2 (Wickham 2016), ggspatial (Dunnington et al. 2023), and ggpubr (Kassambara 2023).

Results and discussion

Phylogenetics of South American lineages

In our phylogenetic analysis (Fig. 3), we found support for the hypothesis that the previously known South American “*Nuncia*” species are polyphyletic assemblage of taxa, where “*Nuncia*” *spinulosa* and three related new species be-

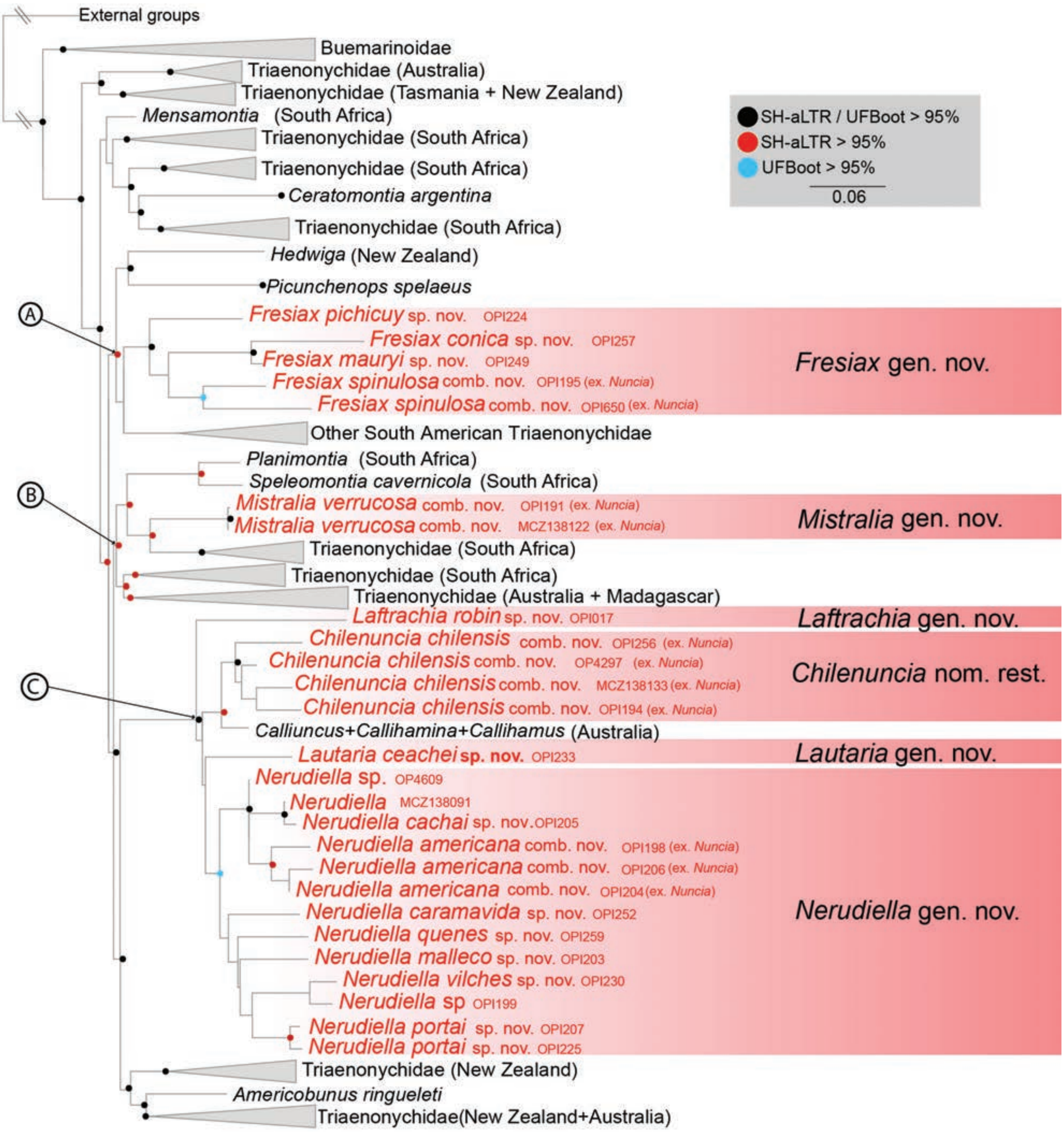

Figure 3. Phylogenetics relationships of Triaenonychidae, with clade names as discussed in the main text. Phylogeny is derived from the IQ-TREE analysis. Nodes without circles have < 95% bootstrap support to AH-aLR and UFBoot.

ing sister to other South American triaenonychids clade, "*Nuncia*" *verrucosa* being related to a core of South African species. Nevertheless, "*Nuncia*" *chilensis* being closely related to a series of Australian genera (*Calliuncus*, *Callihamina*, and *Callihamus*), and "*Nuncia*" *americana* form a clade with other six new South American species. This finding is in most part consistent with previous hypotheses based on both Sanger data and UCEs (Baker et al. 2020; Derkarabetian et al. 2021a; Porto et al. 2022).

Our analyses consistently recovered three independent lineages with SH-aLTR high support (clades A and B) or SH-aLTR and UFboot high support (clade

C) where the representatives of the South American *"Nuncia"* are nested. We discuss the phylogenetic relationships of the South American *"Nuncia"* based on the preferred tree obtained in the IQ-TREE results (Fig. 3).

We recovered the species originally described as *Nuncia spinulosa* Maury, 1990, deeply nested inside the big clade A (SH-aLTR > 95%). We herein combined under *Fresiax* gen. nov. the species: *Fresiax spinulosa* comb. nov. and related species (*F. conica* sp. nov., *F. mauryi* sp. nov., *F. pichicuy* sp. nov. – based on molecular and morphological evidence – and *F. fray* sp. nov. based on morphological evidence only). The monophyly of *Fresiax* gen. nov. received strong support from both SH-aLTR and UFBoot methods. This new genus exhibits a close relationship with other South American Triaenonychidae genera, including *Adrianonyx*, *Araucanobunus*, *Diasia*, *Nahuelonyx*, *Triaenonychoides*, *Triaenonyx* and *Valdivionyx* (see Suppl. material 2). Additionally, it shares connection with the New Zealand genus *Hedwiga* and the South American cave relictual species *Picunchenops spelaeus*. The early divergence within clade A suggests that *Picunchenops spelaeus* has more affinities with the New Zealand genus *Hedwiga* than with other South American representatives of this clade. Besides *Fresiax spinulosa* comb. nov., we described four other new species, three of which have accompanying molecular data.

In contrast "*Nuncia*" *verrucosa* Maury, 1990, does not show a relationship with South American triaenonychids. Instead, it is recovered as the sister group of South African species, including *Adaeulum*, *Larifuga*, *Larifugella*, and *Paradaeum* (SH-aLTR > 95%) (see Suppl. material 2). This group of species is deeply nested in the clade B (SH-aLTR > 95%), which is composed of South African, Malagasy, and Australian species (Fig. 3). To name this distinct genus, we described *Mistralia* gen. nov., and consequently, we introduce the new combination *Mistralia verrucosa*. Due to the external and genital morphological affinities (no molecular data available), we described a second species to this genus, *Mistralia ramirezi* sp. nov. The unique morphology of *Mistralia* was first noted by Maury (1990) when he established the "verrucosa group."

Clade C (SH-aLTR and UFBoot > 95%) represents the most diverse and intricate group, comprising triaenonychids that were previously classified or could be classified within the former concept of South American "*Nuncia*". Clade C includes the previously known species *"Nuncia" americana* and *"Nuncia" chilensis.* However, both species are recovered as part of different lineages. For *"Nuncia" chilensis*, we have reinstated the previously synonymized genus *Chilenuncia* Muñoz-Cuevas, 1971, and consequently established the new combination *Chilenuncia rostrata*. Unfortunately, we do not have molecular data of "*Nuncia*" *rostrata* Maury, 1990, but the morphological similarities with *Chilenuncia chilensis* support our decision of include this species in the genus *Chilenuncia* combining them as *Chilenuncia rostrata* comb. nov. Our four terminals identified as *Chilenuncia chilensis* comb. nov. were strongly (SH-aLTR > 95%) recovered as monophyletic and are sister of a monophyletic group that includes the Australian genera: *Calliuncus* Roewer, 1931, *Callihamina* Roewer, 1942, and *Callihamus* Roewer, 1931. This group exhibits an extraordinary stasis in their external morphology, but the genital morphology supports the South American representatives as a different genus as well as the molecular evidence. This morphological stasis could be responsible for the original description as *Parattahia chilensis* Soares, 1968, but the examination of the type species

Parattahia u-signata Roewer, 1914, and their male genital morphology (data not showed) not support the inclusion in the same genus and reinforce the restoration of *Chilenuncia*. The relationship and limits of the genera *Parattahia*, *Calliuncus*, *Callihamina*, and *Callihamus* deserve further attention. The phylogenetic relationship between *Chilenuncia* and the Australian genera was also recovered by Derkarabetian et al. (2021a) who estimated a divergence between the South American and Australian species of approximately 40 million years ago.

As part of the Clade C, we recovered a clade with strong UFBoot support that included the previous species *Nuncia americana* Roewer, 1961, plus several new species. We described the genus *Nerudiella* gen. nov. to accommodate all the species closely related with "*Nuncia*" *americana*. Besides *Nerudiella americana* comb. nov. we have described fifteen new species based on morphology and six of them also based on molecular evidence. This is a remarkably diverse group of South American triaenonychid that exhibits a very interesting radiation that deserves further studies. Finally, in the Clade C, we described two new monotypic genera, namely *Laftrachia* gen. nov. and *Lautaria* gen. nov.

The entire Clade C is recovered with high support (SH-aLTR and UFBoot > 95%) as sister of another clade, primarily composed of Australian and New Zealand species, were the South American monotypic relict taxon *Americobunus ringueleti* Muñoz-Cuevas, 1972, is nested.

Biogeographical remarks

A comprehensive biogeographic study of Triaenonychidae has been conducted by Derkarabetian et al. (2021a), where all South American lineages recovered in our study were represented. The lineages which are here called A, B, and C are equivalent to clades C, D, and E in Derkarabetian et al. (2021a). Our study contains a denser sampling of South American triaenonychids and thus, examining them in the context of the divergence dating in Derkarabetian et al. (2021a) reinforces interesting biogeographic relationships. We know that Triaenonychidae is an ancient group, they existed for ~ 237 million years, predating the fragmentation of Gondwana initiated around 180 million years ago. Our South American lineages A, B, and C exhibit a highly complex biogeographic history with their origin and early diversification predating Gondwanan fragmentation. Other groups like the new genus *Mistralia*, appear to have originated from a cladogenetic event coinciding with the split of West Gondwana into South America and Africa, occurring ~ 140 million years ago. The divergence between the Australian taxa *Calliuncus*–*Callihamus*–*Callihamina* and the South American restored genus *Chilenuncia* (clade C) is estimated to have occurred approximately 45 million years ago, suggesting the possibility of a land connection between South America and Australia via Antarctica (see Derkarabetian et al. 2021a). This is not only an interesting biogeographic pattern to be further studied—a pattern that nonetheless includes a remarkable long-distance oceanic dispersal to the Crozet Islands (Baker et al. 2020)—but also from a morphological point of view because it contains an astonishing stasis.

A time-calibrated phylogeny with denser sampling, including the new taxa described here and other representatives of South American triaenonychids, is currently underway where this and other biogeographic and evolutionary questions will be addressed on a more regional scale within South America.

Taxonomic section

Clade A

Genus *Fresiax* gen. nov.

https://zoobank.org/88A21A16-8380-4FDE-9EB5-DEC3BC2276DD
Figs 5–34

Nuncia [part] (only references to *Nuncia spinulosa*): Maury 1990: 108; Maury 1992: 5; Acosta and Maury 1998: 579; Kury 2003: 22.

Etymology. The genus name *Fresiax* is a combination of "Fresia," the name of the wife of Mapuche's military leader Caupolicán, and the Greek word ὄνυξ (onyx = nail, claw), which is part of the generic name *Triaenonyx*, the type genus of the family Triaenonychidae. The genus name *Fresiax* is feminine.

Diagnosis. The male genitalia of *Fresiax* exhibits a pars distalis considerably reduced (as in *F. mauryi* sp. nov.), a ventral plate longer than the capsula externa (as in *F. conica* sp. nov.), and a capsula externa divided into two lamellae, a character that distinguishes it from any other triaenonychid genus. Additionally, the pedipalp femora possesses at least three dorsal and four ventral spines.

Type species. *Nuncia spinulosa* Maury, 1990

Included species. *Fresiax conica* sp. nov., *Fresiax fray* sp. nov., *Fresiax mauryi* sp. nov., *Fresiax pichicuy* sp. nov., *Fresiax spinulosa* (Maury, 1990), comb. nov.

Distribution. Argentina: Río Negro Province. Chile: Coquimbo, Valparaíso, Araucanía, Los Ríos, Los Lagos (Fig. 4A).

Fresiax conica sp. nov.

https://zoobank.org/5E85033C-CB20-4C7D-B42D-EEE6FFFF443B
Figs 5–10

Material examined. ***Holotype***. ♂ **Chile.** Choapa: Cuesta Cavilolén, 31.76669°S, 71.32727°W, 300 m, M. Ramírez, A. Ojanguren, J. Pizarro coll. 11.II.2011 (MNHNCL). ***Paratypes*. Chile.** Choapa: Los Vilos, Cuesta Caviolén, 30 km NE de Los Vilos, E. Maury coll., 1 ♀ 12.XII.1987 (MACN). Choapa: Los Vilos, Cuesta Caviolén, 30 km NE de Los Vilos, E. Maury coll., 1 ♀ 12.XII.1987 (MACN).

Etymology. The term "conica" refers to the shape of the ocularium, which is conical and lacks an apophysis. The specific epithet was also a name "in schedula" by the late Dr. Emilio Maury that labeled the specimens. Maury early recognized this species as a new but never published. We keep the Maury's specific name to maintain the name preference of the researcher who first recognized this species as new.

Diagnosis. The conical ocularium, without acute apophysis, clearly distinguishes this species from others in the genus. There is only one row of tubercles on the anterior region of the dorsal scutum. The apical section of the tubular capsula interna is subtriangular.

Distribution. Chile: Coquimbo Region (Fig. 4A).

Description of male. Measurements: Total length 2.01, carapace length 0.78, dorsal scutum length 1.30, carapace max. width 1.05, mesotergum max. length 1.50. Appendage measurements: Pedipalps. Length of trochanter 0.13, length

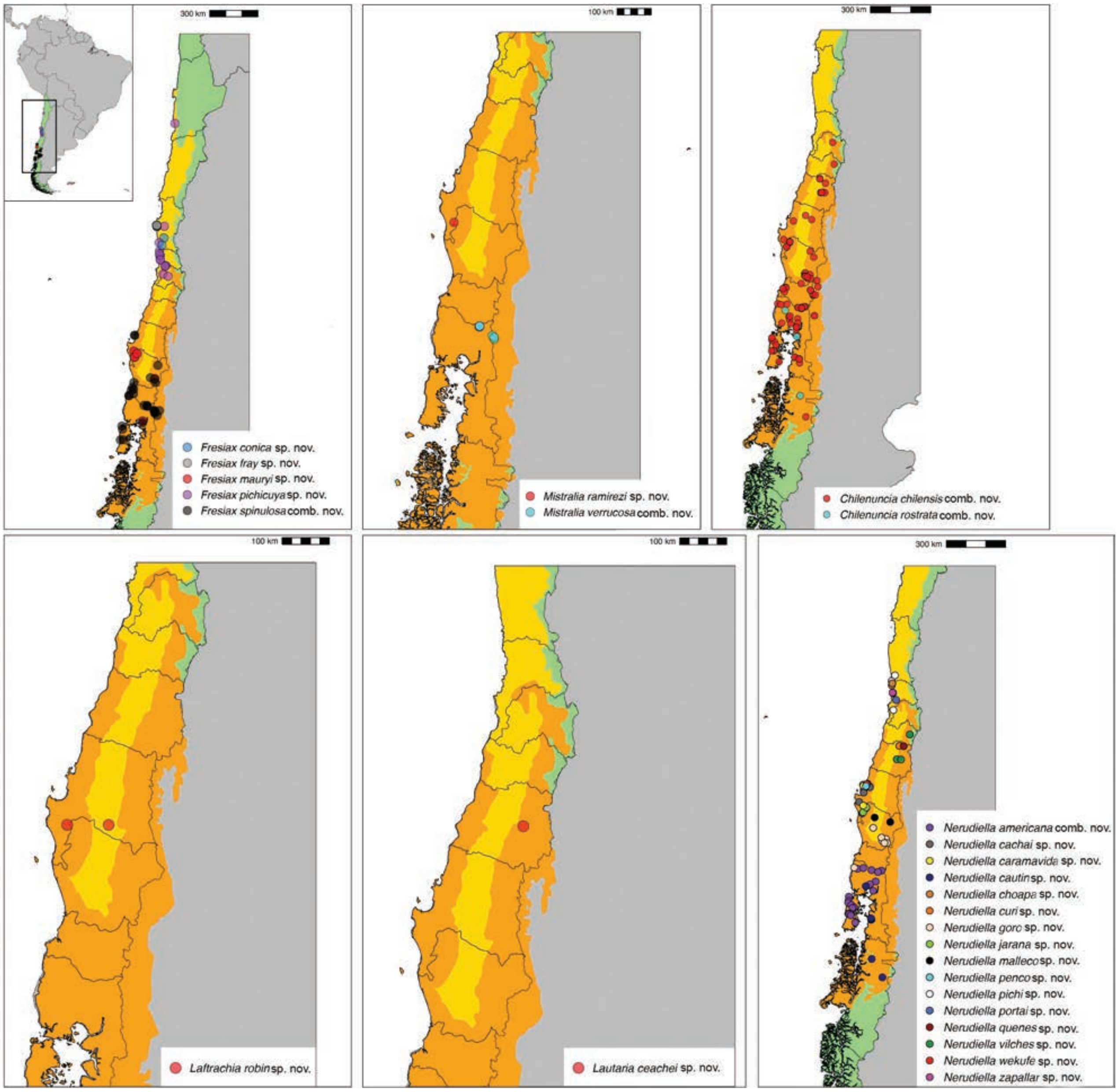

Figure 4. Maps showing the distribution of the species used in this work. South America (Chile and western Argentina inset). Chile in green, Argentina/ South America in grey. Terrestrial ecoregions (following Olson et al. 2001) highlighted in yellow (Chilean Matorral) and orange (Valdivian temperate forests).

of femora 0.80, length of patella 0.46, length of tibia 0.53, length of tarsus 0.62. Leg I: trochanter (tr) 0.16, femora (fe) 0.16, patella (pa) 0.74, tibia (ti) 0.38, metatarsus (mt) 0.51, tarsus (ta) 0.62. II: tr 0.46, fe 0.22, pa 1.03, ti 0.41, mt 0.80, ta 0.98. III: tr 0.93, fe 0.19, pa 0.68, ti 0.36, mt 0.60, ta 0.67. IV: tr 0.62, fe 0.26, pa 1.04, ti 0.46, mt 0.80, ta 1.11.

Dorsum (Fig. 5, 6). Eta (η) or hourglass-shaped dorsal scutum (Kury and Medrano 2016). Ocularium conical with a group of ~ 20 setiferous tubercles. Eyes located on the middle of the ocularium. Dorsal scutum microgranulate with a row of setiferous tubercles on each side of the ocularium, without clear delimitation of the mesotergal areas. Areas I–IV and posterior margin with seta, I with two, II and III with four, and IV and posterior margin with six. All free tergites bear a row of small, setiferous, rounded granules.

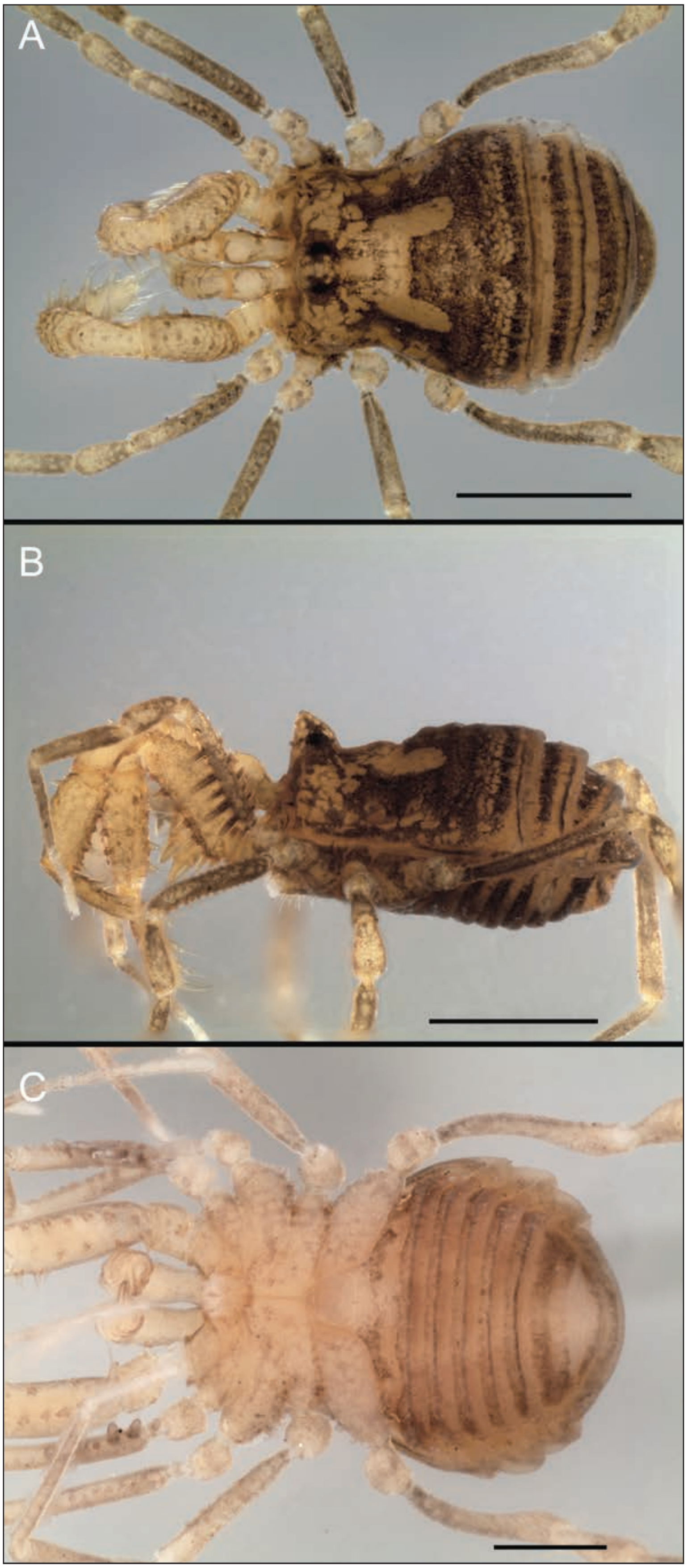

Figure 5. *Fresiax conica* sp. nov. male **A** dorsal view **B** lateral view **C** ventral view. Scale bars: 1 mm. Species of Clade A, see Fig. 3.

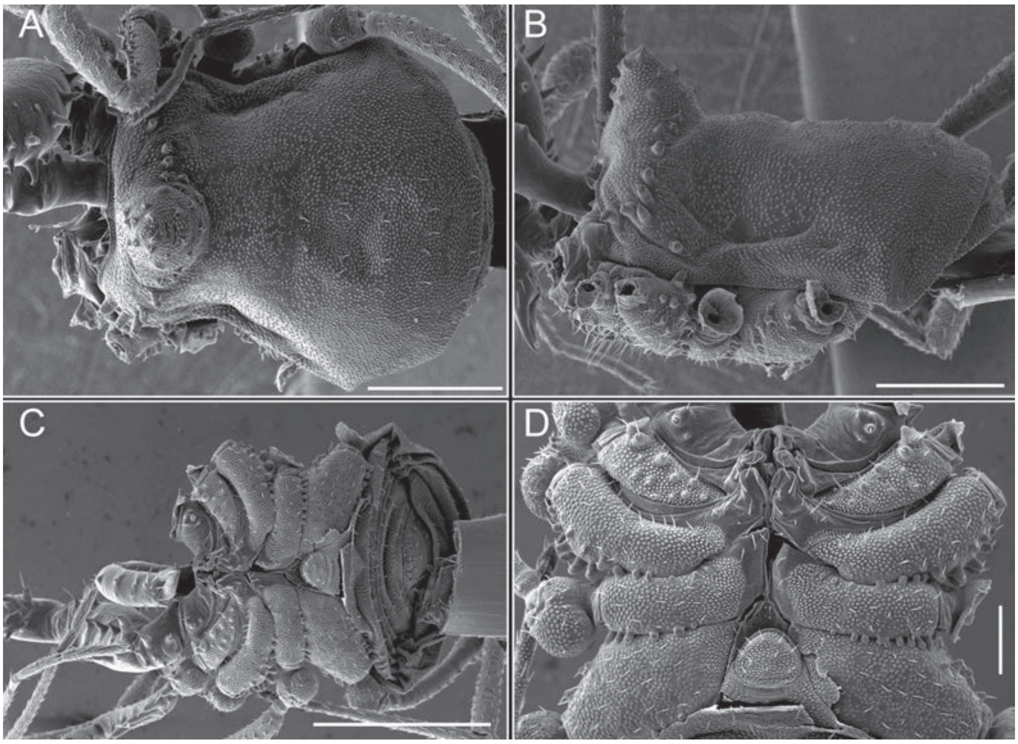

Figure 6. *Fresiax conica* sp. nov. male, SEM images of habitus **A** dorsal view **B** lateral view **C, D** ventral view. Scale bars: 500 μm (**A, B, C**); 200 μm (**D**).

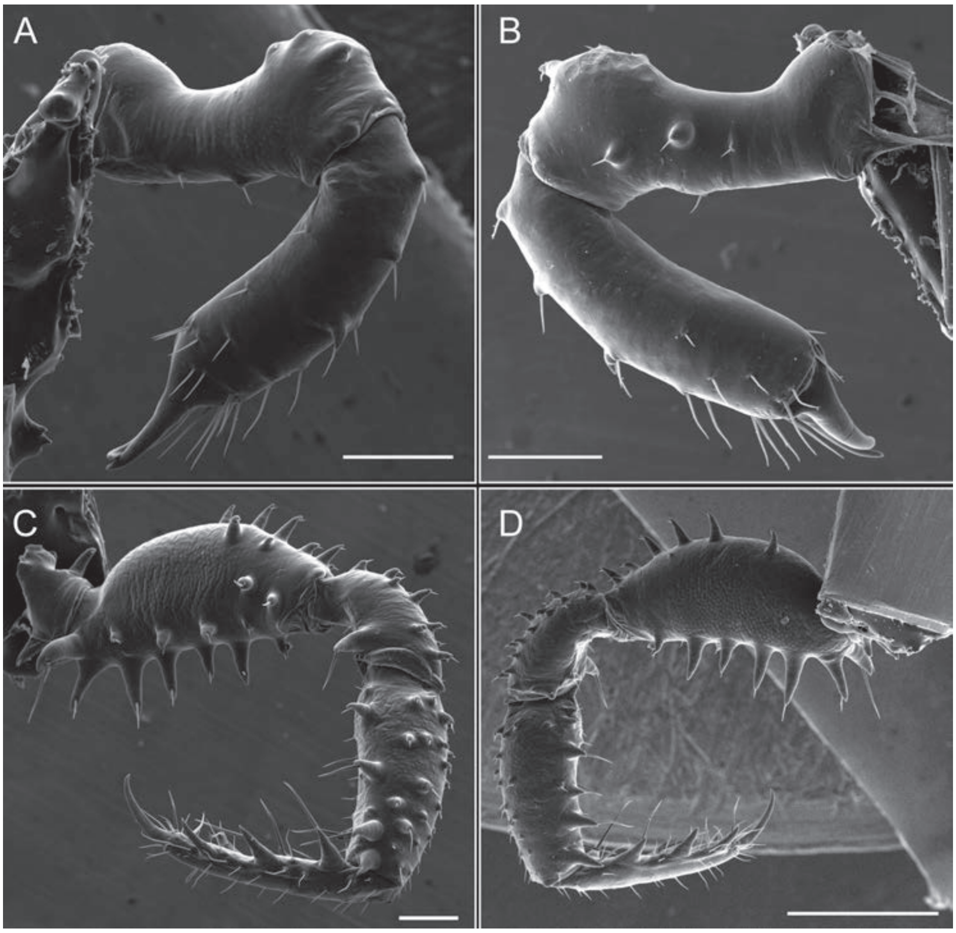

Figure 7. *Fresiax conica* sp. nov. chelicerae: mesal **A** ectal **B** pedipalps: mesal **C** ectal **D**. Scale bars: 200 μm.

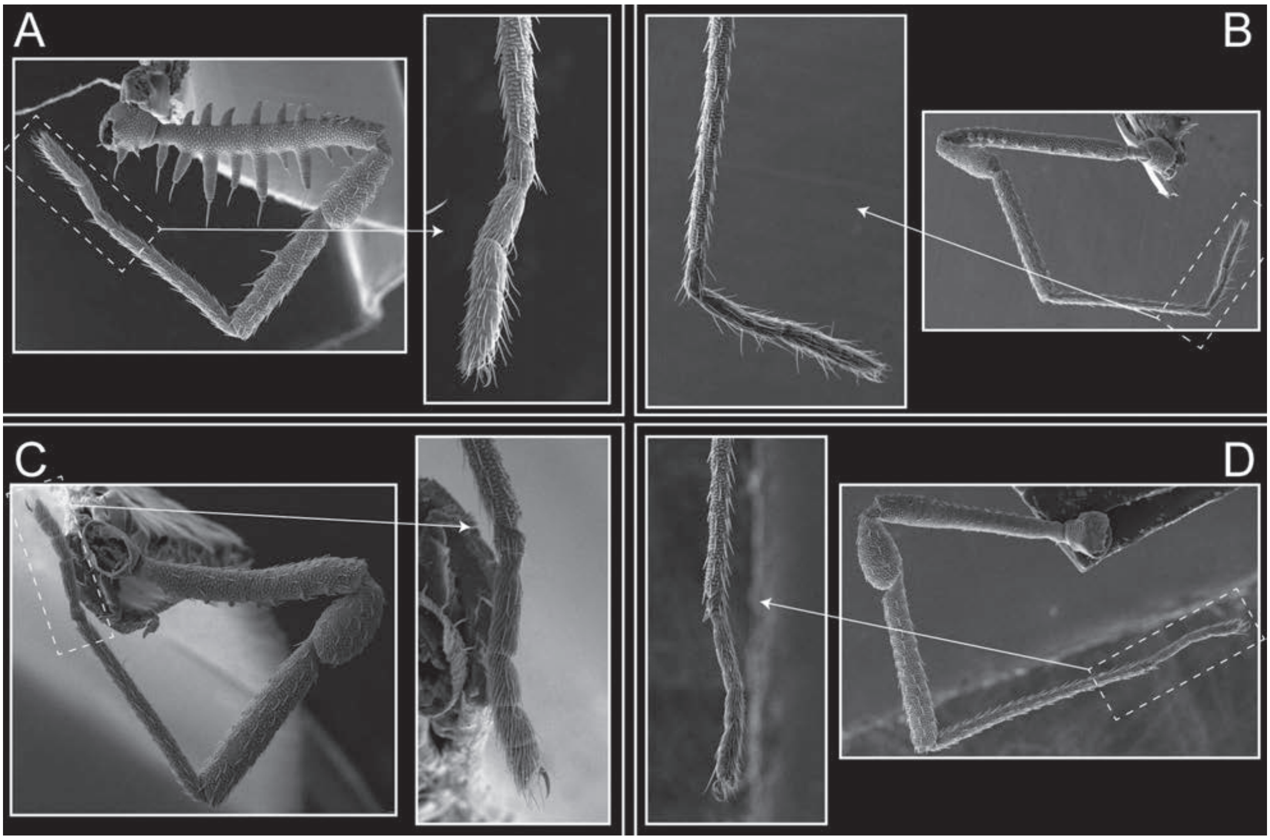

Figure 8. *Fresiax conica* sp. nov. legs I **A** II **B** III **C** IV **D**. Scale bars: 200 µm (**A, C**); 500 µm (**B, D**).

Chelicerae (Fig. 7A, B). Segment I with few sparse setae. Segment II with three small frontal tubercles and sparse setae.

Pedipalps (Fig. 7C, D). Trochanter with long ventral and dorsal spines. Femora bearing a remarkable ventral-proximal subtriangular spine with long subdistal setae; a row of four ventral spines, with subdistal setae and six dorsal small spines with setae. Patella bearing a notable mesal spine with long setae. There are two rows of small setiferous tubercles on the dorsal patella-tarsus. Tibia shows a ventral row of four long spines. Tarsus with three mesal and ectal setiferous spines.

Legs (Fig. 8). Coxa I with two rows of setiferous tubercles, the distal one with a subdistal setae. II–IV are microgranulate, with four bridges between the legs II and III, 6–8 bridges between the legs III and IV, seven between the leg IV and the opisthosoma. Spiracles not covered by bridges. The smooth surface represents < ¼ of coxa and leg III. Sternum arrow-shaped. Legs I–IV covered in setae, tarsal area and calcaneus are also setose. Trochanter I with small ventral granules. Femora I with a row of nine dorsal and ventral setiferous tubercles. Calcaneus is shorter than astragalus (7× shorter in leg I, 8× in II, 13× in III, 15× in IV). Tarsal count 3–6–4–4.

Penis (Figs 9, 10). Pars distalis has a large ventral plate with a cleft separating the plate into two lamellae. Each one bears three acute macrosetae on the ventral surface and one acute macroseta on the dorsal surface. Capsula externa is cleft and covers the dorsal and lateral surfaces. The Capsula interna is tubular with an apical subtriangular portion.

Female. Similar to male, with shorter pedipalpal femora.

Female measurements. Total length 1.91, length of carapace 0.76, length of dorsal scutum 1.29, max. width of carapace 1.04, max. width of mesoter-

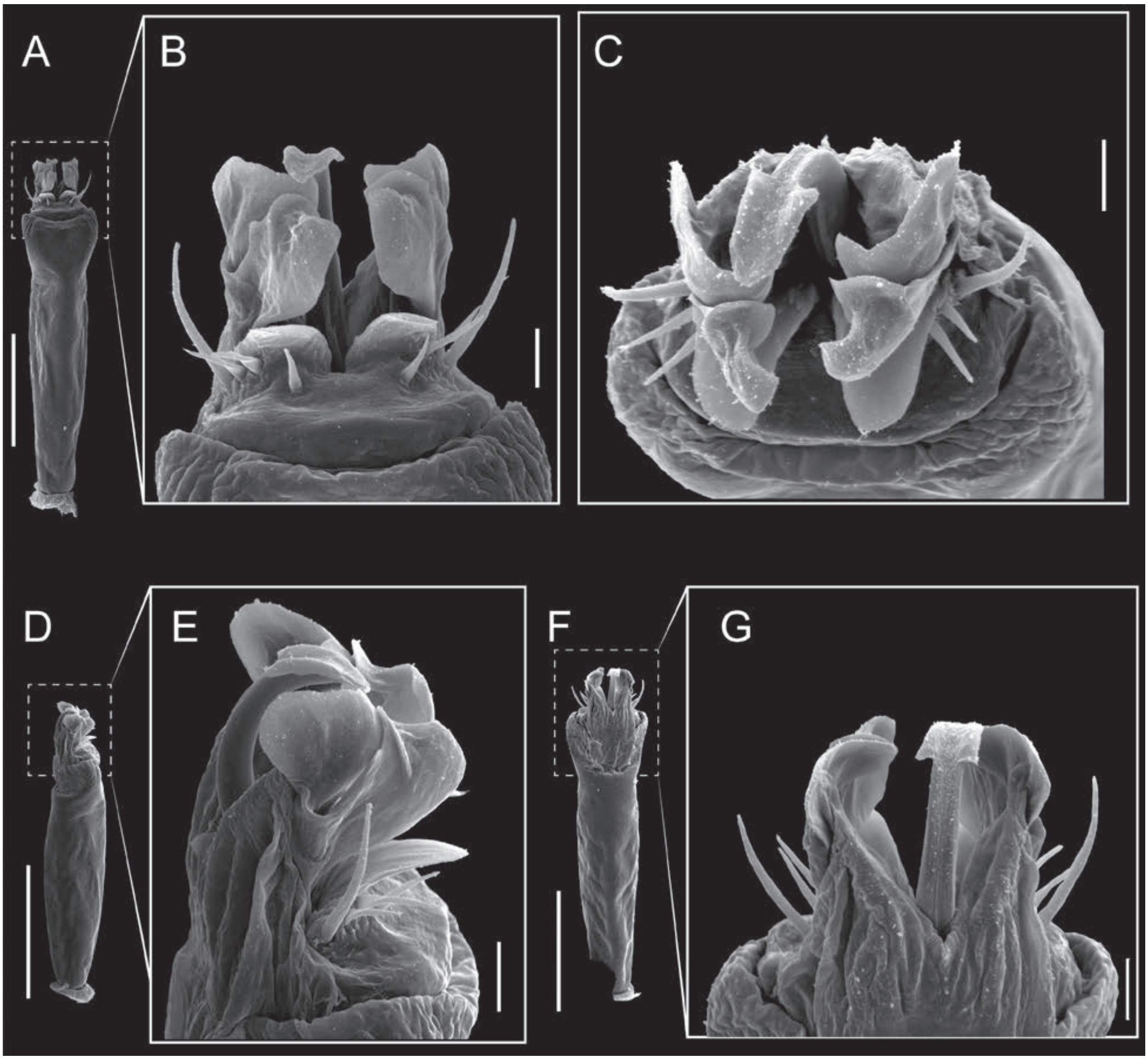

Figure 9. *Fresiax conica* sp. nov. penis: ventral **A, B** apical **C** lateral **D, E** dorsal **F, G**. Scale bars: 200 µm (**A, D, F**); 20 µm (**B, C**, **E, G**).

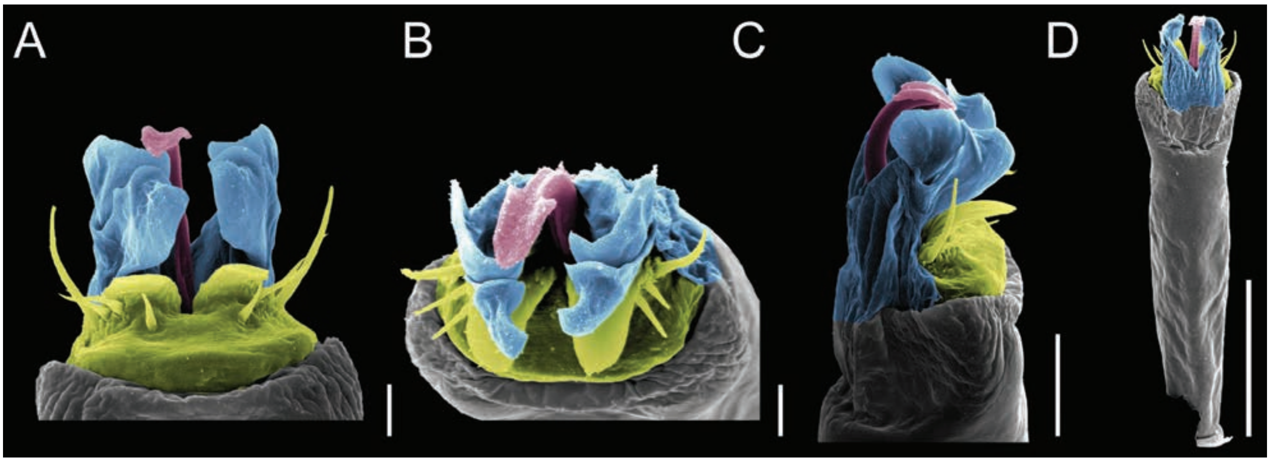

Figure 10. *Fresiax conica* sp. nov. penis: ventral **A** apical **B** lateral **C** dorsal **D**. Colors: ventral plate (yellow), capsula externa (blue), capsula interna (red). Scale bars: 20 µm (**A, B**); 50 µm (**C, D**).

gum 1.47. Appendage measurements: Pedipalps. Length of trochanter 0.20, length of femora 0.76, length of patella 0.43, length of tibia 0.63, length of tarsus 0.56. Leg I: trochanter (tr) 0.26, femora (fe) 0.88, patella (pa) 0.38, tibia (ti) 0.56, metatarsus (mt) 0.64, tarsus (ta) 0.384. II: tr 0.23, fe 1.14, pa 0.53, ti 0.84, mt 0.90, ta 0.73. III: tr 0.22, fe 0.88, pa 0.36, ti 0.69, mt 0.88, ta 0.43. iv: tr 0.23, fe 1.07, pa 0.49, ti 0.95, mt 1.26, ta 0.61.

Fresiax fray **sp. nov.**

https://zoobank.org/0F310737-611E-4AB6-B41D-FD12B585ECA5
Figs 11–16

Material examined. ***Holotype*****.** ♂ **CHILE.** Coquimbo: Bosque de Fray Jorge, E. Maury coll. 03.XI.1988 (MNHNCL). ***Paratypes*****. CHILE.** Coquimbo: Limarí, Bosque Fray Jorge, P.N. Fray Jorge, E. Maury coll. 03.XI.1988, 38 ♂ 24 ♀, amm. (MACN).

Additional material. CHILE: Coquimbo: Limarí, Bosque Talinay, P.N. Fray Jorge, relict Valdivian fog forest, R. Schuh, N. Platnick coll., 08.II.1986, 66 specimens (AMNH).

Etymology. The epithet *fray*, a noun in apposition, refers to the type locality of the species, Bosque Fray Jorge National Park.

Diagnosis. This species can be easily distinguished from the other species of the genus by its small size (< 2 mm long), conical ocularium, with an apophysis at an angle of 45 °.

Distribution. Chile, Coquimbo Region (Fig. 4A).

Description of male. Measurements: Total length 1.81, carapace length 0.69, dorsal scutum length 1.47, carapace max. width 1.14, mesotergum max. length 1.49. Appendage measurements: Pedipalps. Length of trochanter 0.13, length of femora 0.80, length of patella 0.46, length of tibia 0.53, length of tarsus 0.62. Leg I: trochanter (tr) 0.16, femora (fe) 0.74, patella (pa) 0.38, tibia (ti) 0.51, metatarsus (mt) 0.62, tarsus (ta) 0.46. II: tr 0.22, fe 1.03, pa 0.41, ti 0.80, mt 0.98, ta 0.93. III: tr 0.19, fe 0.68, pa 0.36, ti 0.60, mt 0.67, ta 0.62. IV: tr 0.26, fe 1.04, pa 0.46, ti 0.80, mt 1.11, ta 0.57.

Dorsum (Fig. 11, 12). Eta (η) hourglass-shaped dorsal scutum. Ocularium conical, with a small, forward-pointing apical spine and small setae. Eyes located on the distal region of the ocularium. Dorsal scutum microgranulate with no clear area delimitation. Areas I–III with two small setiferous granules, IV with three, posterior margin with a row of small setiferous granules. All free tergites with a row of small setiferous granules.

Chelicerae (Fig. 13A, B). Segment I characterized by a smooth surface without any prominent tubercles or setae. In contrast, segment II with a small frontal tubercle and covered in setae. Segment II with more pronounced texture and setal coverage compared to the smooth surface of segment I.

Pedipalps (Fig. 13C, D). Trochanter with a dorsal and a ventral spine, both with setae. Femora with a row of four dorsal spines with subdistal setae, a row of five ventral spines with setae, the proximal one with a subtriangular shape; two dorsal and distal tubercles with setae, a row of five small mesal tubercles with setae, and three small distal tubercles with setae. Patella with two rows of three tubercles with setae, two small mesal tubercles with setae, and few ventral granules. Tibia with four ectal and mesal spines with subdistal setae; three

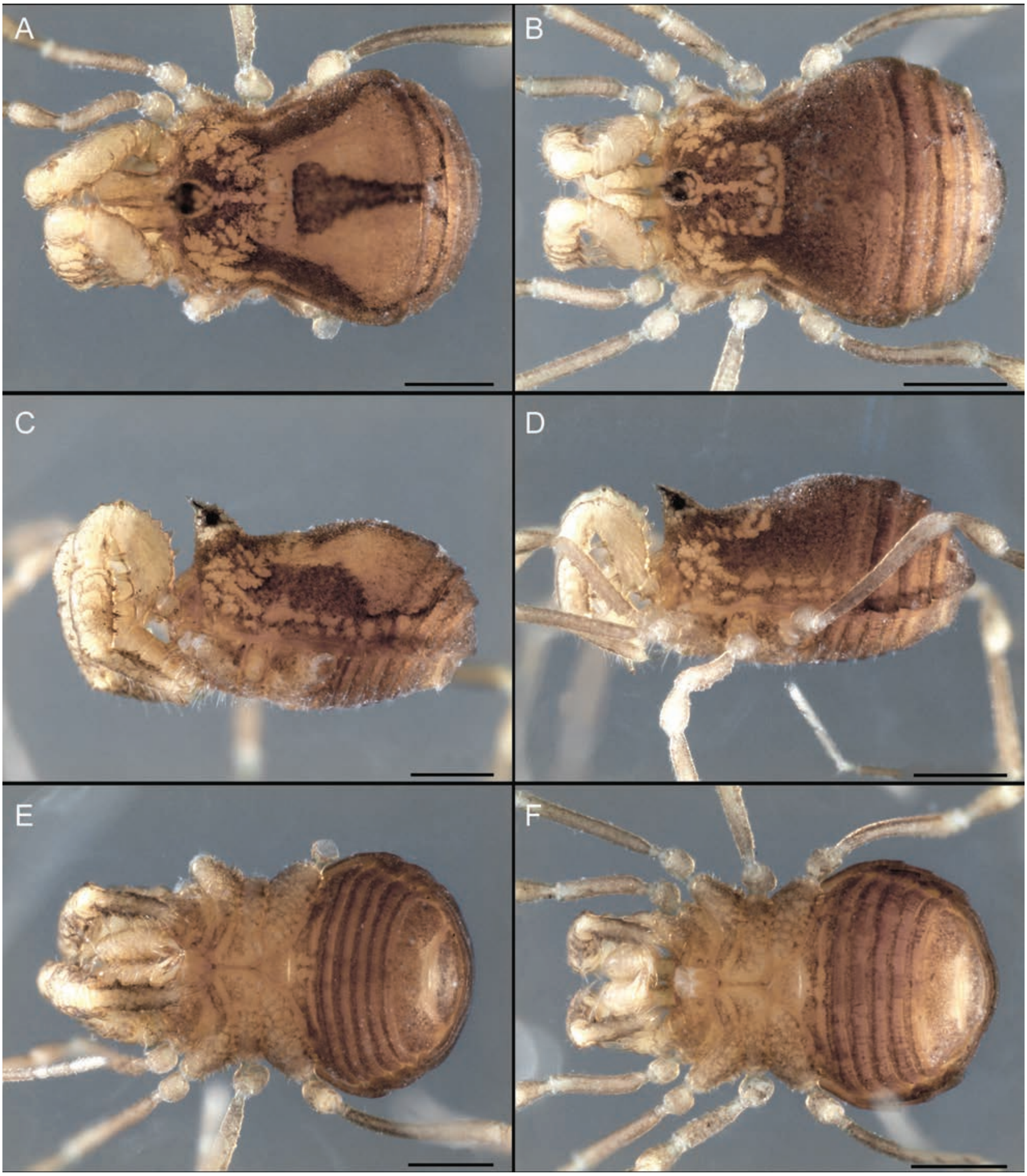

Figure 11. *Fresiax fray* sp. nov. habitus, male **A** dorsal view **C** lateral view **E** ventral view. Female **B** dorsal view **D** lateral view **F** ventral view. Scale bars: 500 µm. Species of Clade A, see Fig. 3.

ventral tubercles with setae and two rows of 4–5 granules with setae on the dorsal surface. Tarsus with three mesal and ectal spines with subdistal setae, as well as few setae and granules.

Legs (Fig. 14). Coxa I bearing small setiferous tubercles and a row of three long tubercles with subdistal setae; II–IV with microgranulation, bearing 4–6 bridges between legs II and III, five or six between III and IV, six or seven between

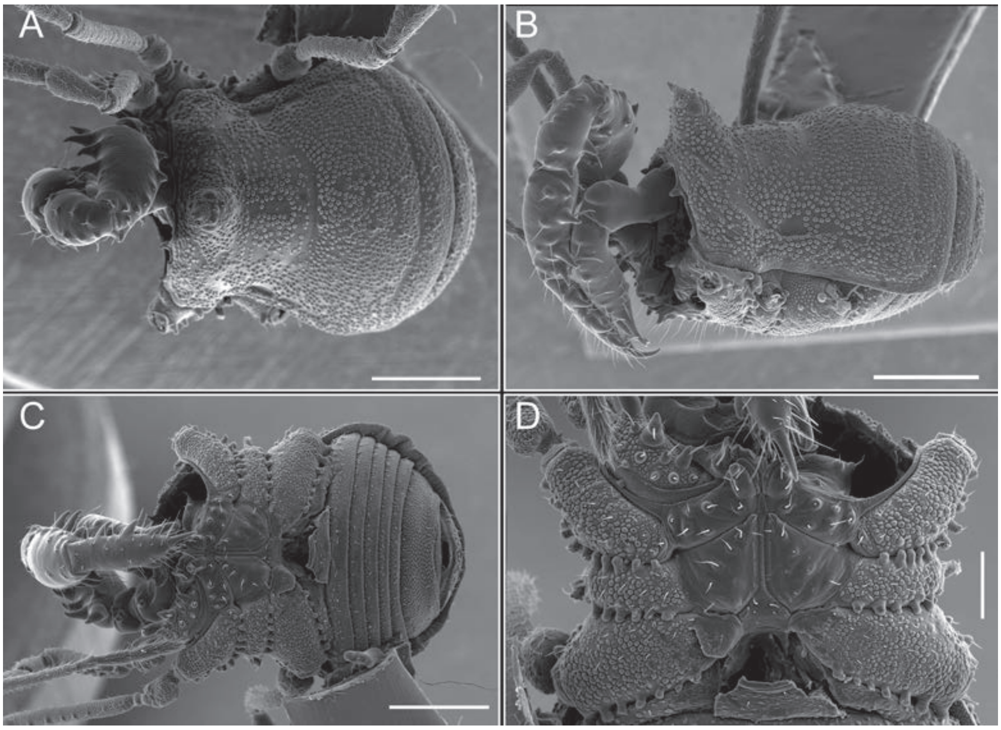

Figure 12. *Fresiax fray* sp. nov. male, SEM images of habitus **A** dorsal view **B** lateral view **C, D** ventral view. Scale bars: 500 µm (**A, B, C**); 200 µm (**D**).

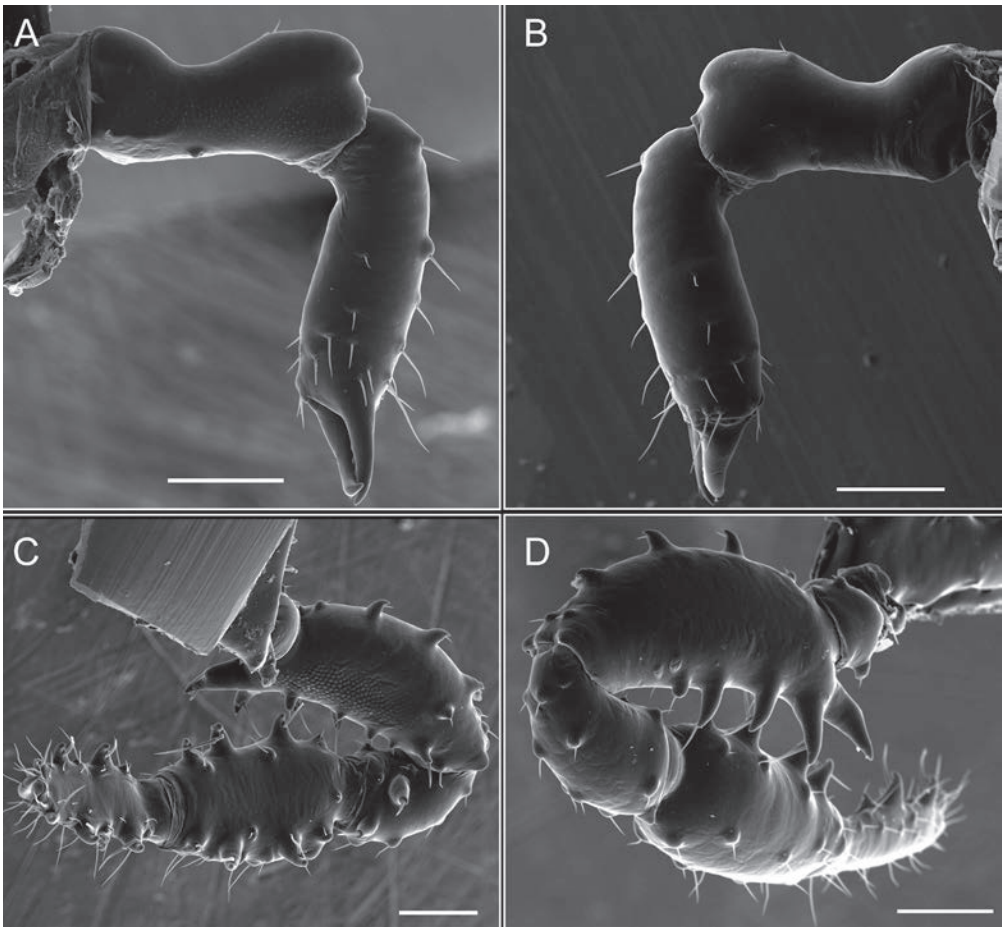

Figure 13. *Fresiax fray* sp. nov. chelicerae: mesal **A** ectal **B** pedipalps: mesal **C** ectal **D**. Scale bars: 200 µm.

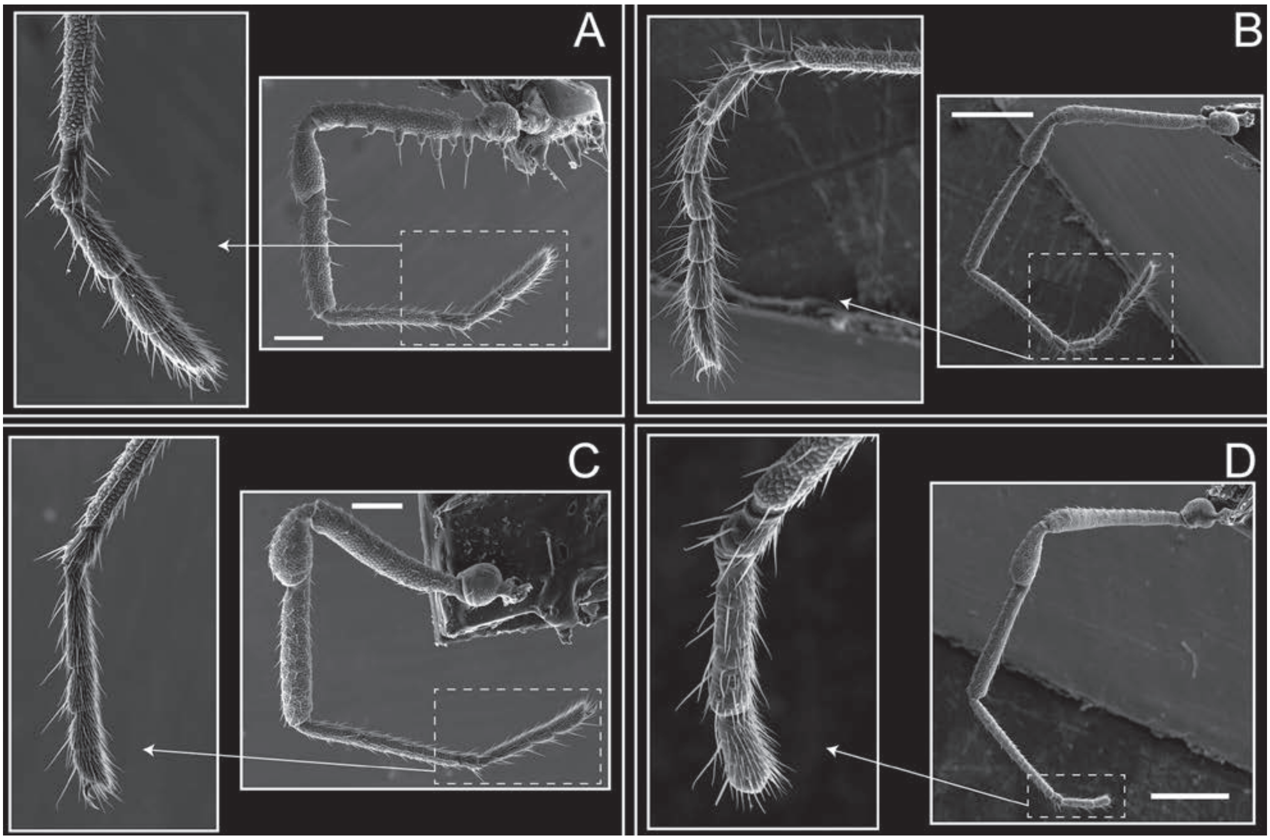

Figure 14. *Fresiax fray* sp. nov. legs I **A** II **B** III **C** IV **D**. Scale bars: 200 µm (**A, C**); 500 µm (**B, D**).

leg IV and the opisthosoma. Spiracles not visible. Smooth area occupies ⅓ of the leg II, almost ½ of III, and only a small proximal portion of the leg IV. Smooth area of leg II with five small setiferous tubercles, III with a row of four and an anterior process directed to the sternum. Sternum arrow-shaped, with a triangular posterior area. Leg I trochanter with three small ventral setiferous tubercles and one dorsal tubercle. Femora of leg I with a row of seven setiferous tubercles and a dorsal row of small setiferous tubercles. Tibia of leg I with 3–4 ventral tubercles with setae. Legs II–IV covered in setae, with the tarsus and calcaneus area densely covered in setae. Calcaneus smaller than astragalus, ≥ 4× smaller in leg I, 5× smaller in leg II, 8× smaller in leg III, and 7× smaller in leg IV. These differences in size ratios between the calcaneus and astragalus serve as distinguishing characteristics among the legs of this species. Tarsal count 3–6–4–4.

Penis (Figs 15, 16). Pars distalis with a ventral plate and a prominent cleft that divides the plate into two lamellae. Each lamella is equipped with three macrosetae on the ventral surface and one macroseta on the dorsal surface. Capsula externa nearly as long as the capsula interna, having a notch that divides the capsula externa into two halves.

Female. Similar to male, with shorter pedipalpal femora.

Female measurements. Total length 1.54, length of carapace 0.61, length of dorsal scutum 1.31, max. width of carapace 0.96, max. width of mesotergum 1.35. Appendage measurements: Pedipalps. Length of trochanter 0.11. Length of femora 0.58, length of patella 0.37, length of tibia 0.45, length of tarsus 0.46. Leg I: trochanter (tr) 0.18, femora (fe) 0.62, patella (pa) 0.33, tibia (ti)

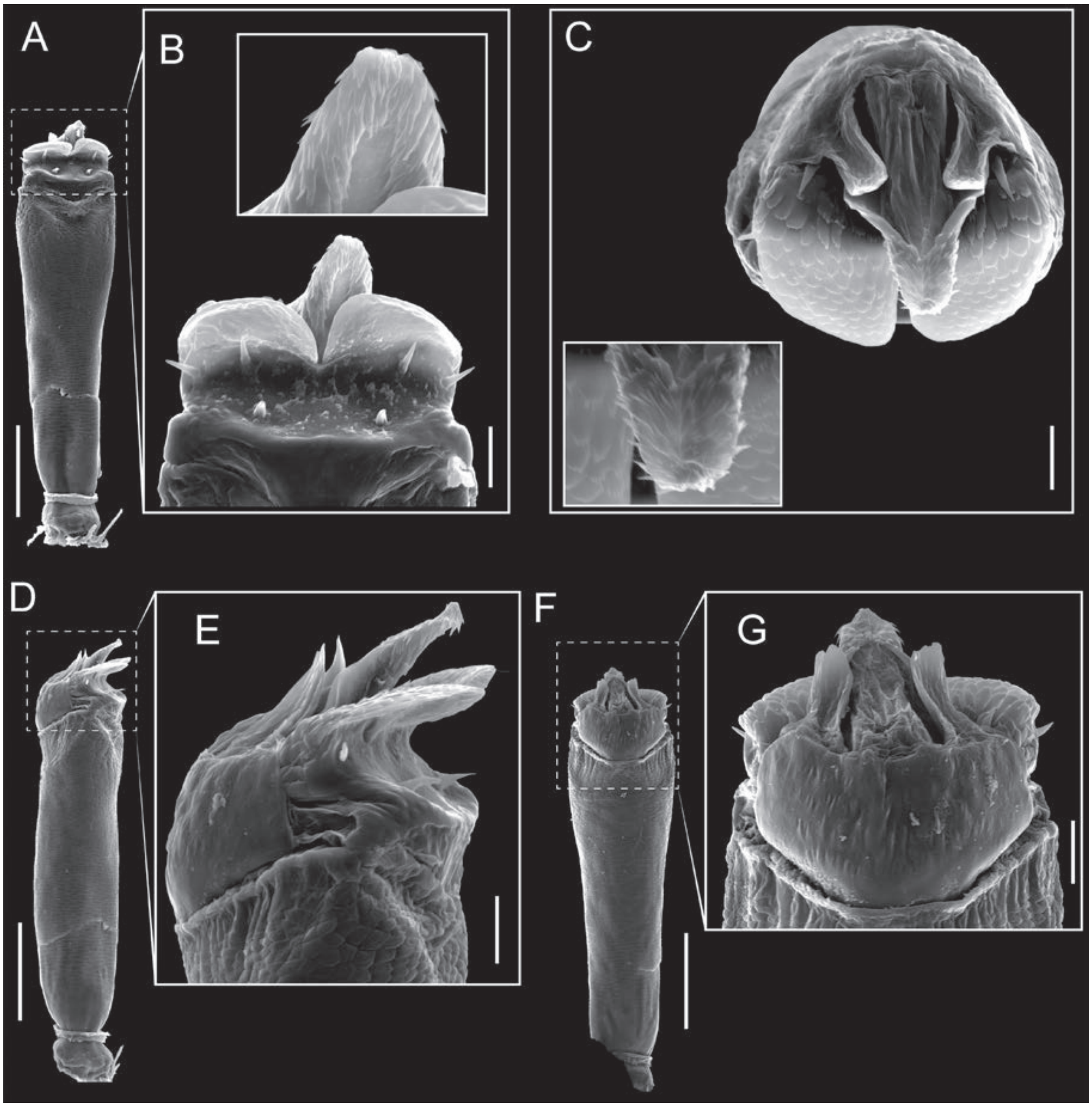

Figure 15. *Fresiax fray* sp. nov. penis: ventral **A, B** apical **C** lateral **D, E** dorsal **F, G**. Scale bars: 100 μm (**A, D, F**); 20 μm (**B, C, E, G**).

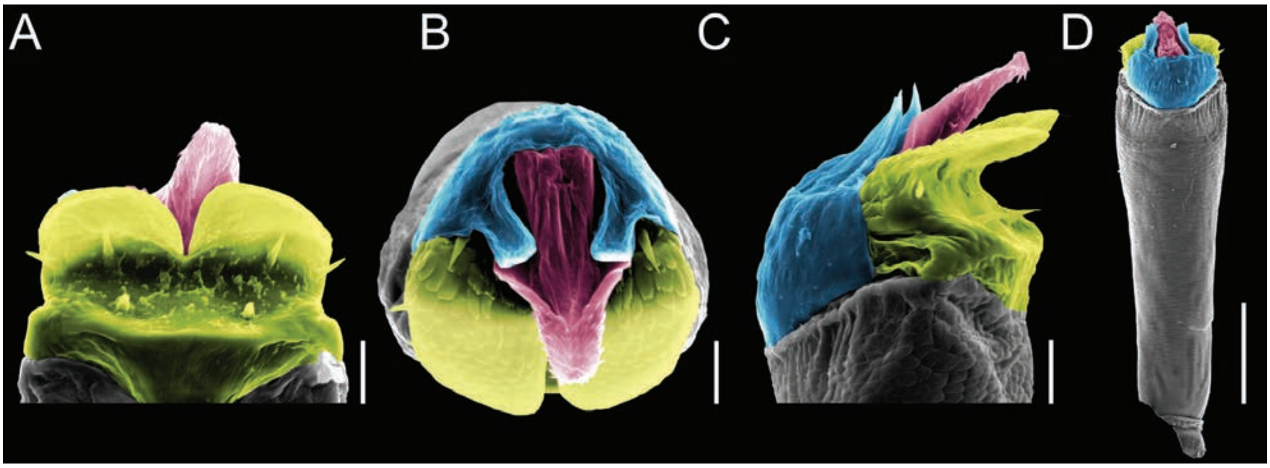

Figure 16. *Fresiax fray* sp. nov. penis: ventral **A** apical **B** lateral **C** dorsal **D**. Colors: ventral plate (yellow), capsula externa (blue), capsula interna (red). Scale bars: 20 μm.

0.46, metatarsus (mt) 0.53, tarsus (ta) 0.42. **II**: tr 0.18, fe 0.88, pa 0.34, ti 0.71, mt 0.84, ta 0.86. **III**: tr 0.18, fe 0.62, pa 0.26, ti 0.53, mt 0.68, ta 0.49. **IV**: tr 0.21, fe 0.80, pa 0.37, ti 0.73, mt 0.98, ta 0.57.

***Fresiax mauryi* sp. nov.**

https://zoobank.org/4DA933F8-1369-4BCE-B27B-E068D0A74188
Figs 17–22

Material examined. ***Holotype*.** ♂ **Chile.** Monumento Natural Contulmo, 38.01501°S, 73.17981°W, 360 m, M. Ramírez & F. Labarque coll., 10.II.2005 (MNHNCL). ***Paratypes*.** **Chile.** Cautín: Lago Caburgua, 39.20749°S, 71.80529°W, S. Peck J. Peck coll., 15.XII.1984, 1 ♂ (AMNH). Llanquihue: P.N. Alerce Andino, Correntoso, sendero Huillifoten, 41.58235°S, 72.61738°W, 135 m, M. Ramírez & F. Labarque coll., 03.II.2005, 1 ♀ (MACN). Malleco, Monumento Natural Contulmo, 38.01501°S, 73.17981°W, E. Maury coll., 13.I.1989, 1 ♂ 1 ♀ (MACN). Malleco: P.N. Nahuelbuta, 37.81477°S, 72.9967°W, M. Ramírez & F. Labarque coll., 12.II.2005, 1 ♂ (MACN). Malleco: Monumento Natural Contulmo, 38.01501°S, 73.17981°W, 360 m, M. Ramírez & F. Labarque coll., 10.II.2005, 1 ♀ (MACN), P.N. Nahuelbuta, 37.81477°S, 72.9967°W, M. Ramírez & F. Labarque coll., 12.II.2005, 5 ♂ 13 ♀ 6 imm. (MACN).

Additional material. Chile. Malleco, Monumento Natural Contulmo, 38.01624°S, 73.17942°W, 361 m, G. Giribet, G. Hormiga, A. Pérez-González coll. 13.XI.2014 (MACN). Same locality, 38.01625°S, 73.17902°W, M. Ramírez, M. Izquierdo, P. Michalik, C. Wirkner, K. Huckstorf coll., 09.II.2012, 1 imm. (MACN). Caramávida, San Alfonso, Quebrada Caramávida, San Alfonso, Reserva Arauco, 37.70942°S, 73.17107°W, 750 m, 15.I.2018, 1 ♀ (MACN), Quebrada Caramávida, "sector 9", Reserva Arauco, 37.66839°S, 73.22683°W, 800 m, 16.I.2018 (MACN).

Etymology. Patronym after the late Argentine arachnologist Emilio Maury, in honor of his contributions to the study of the Triaenonychidae (and Opiliones in general) of South America's Southern Cone.

Diagnosis. The prominent interocular apophysis, the carapace densely covered with rounded tubercles, the long tubercles of the mesotergum, the long drop-shaped genital operculum, the ectal-distal process of cheliceral segment II, and the hypertelic genitalia distinguish this species from all its congeners.

Distribution. Chile: Araucanía Region (Fig. 4A).

Description of male. Measurements: Total length 2.93, carapace length 0.97, dorsal scutum length 1.99, carapace max. width 1.40, mesotergum max. width 1.81. Appendage measurements: Pedipalps. Trochanter length 0.14, femora length 0.87, patella length 0.61, tibia length 0.66, tarsus length 0.56. Leg I: trochanter (tr) 0.25, femora (fe) 0.97, patella (pa) 0.42, tibia (ti) 0.73, metatarsus (mt) 0.90, tarsus (ta) 0.55. **II**: tr 0.29, fe 1.36, pa 0.43, ti 0.94, mt 1.55, ta 1.00. **III**: tr 0.28, fe 1.00, pa 0.41, ti 0.82, mt 1.24, ta 0.60. **IV**: tr 0.26, fe 1.33, pa 0.49, ti 1.11, mt 1.85, ta 0.72.

Dorsum (Fig. 17, 18). Eta (η) hourglass-shaped dorsal scutum. Ocularium raised, with a long backward-bending apophysis between the eyes, covered with rounded tubercles and with few setae on the apophysis. Carapace densely covered in rounded tubercles, mesotergum with areas delimited by strong tubercles. Areas **I** and **II** with straight rows of four and five setiferous tubercles,

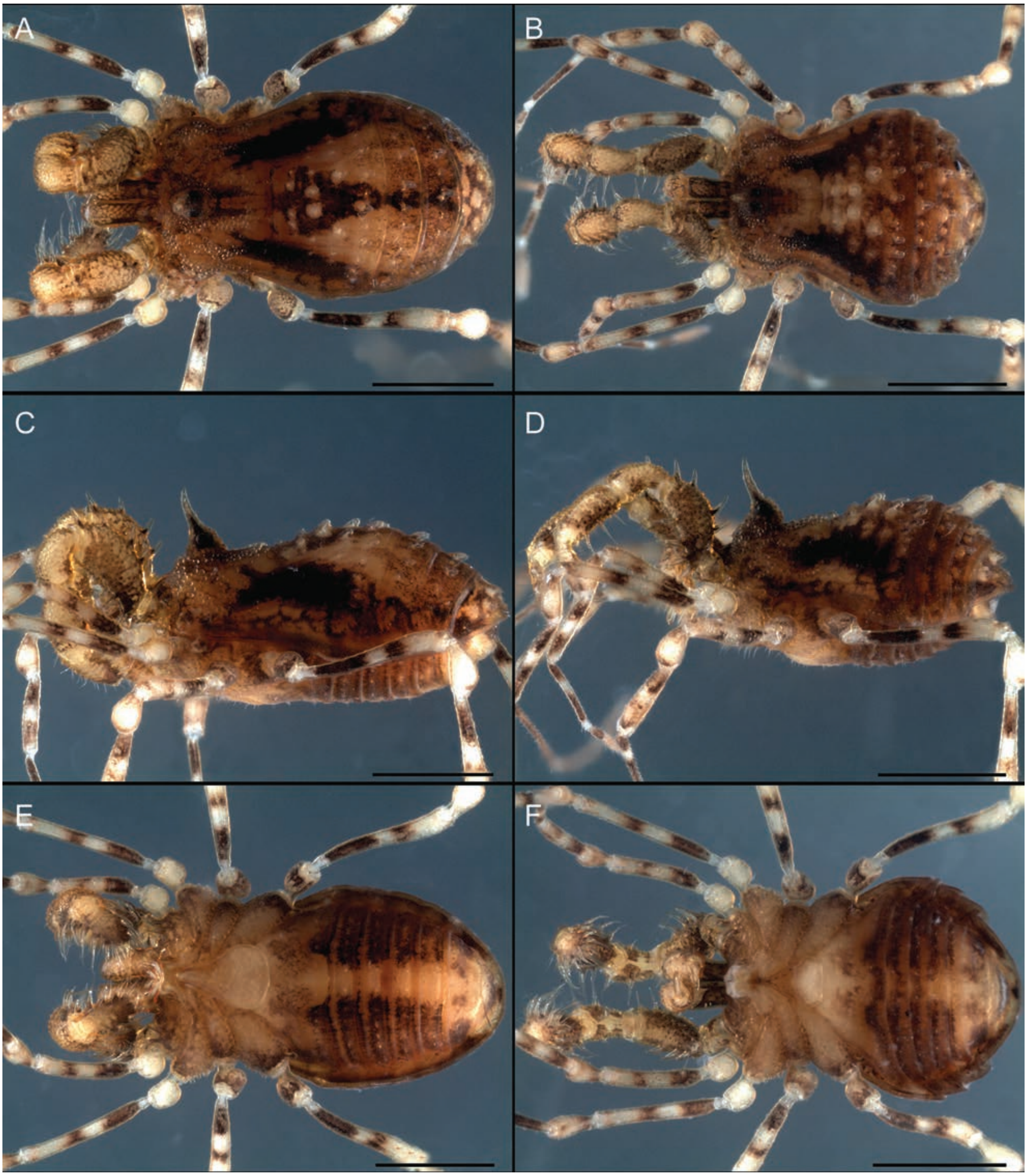

Figure 17. *Fresiax mauryi* sp. nov. habitus, male **A** dorsal view **C** lateral view **E** ventral view. Female **B** dorsal view **D** lateral view **F** ventral view. Scale bars: 1 mm. Species of Clade A, see Fig. 3.

respectively, and **III** and **IV** with a row of eight setiferous tubercles (the two central ones are stronger than others). Posterior margin with a row of 12–14 setiferous tubercles. Free tergites with a row of setiferous tubercles similar to the posterior margin of the dorsal scutum.

Chelicerae (Fig. 19A, B). Segment **I** with a small, granulated area on the dorso-distal surface and two ventral granules. Segment **II** with an ectal-distal process that bears a few setae.

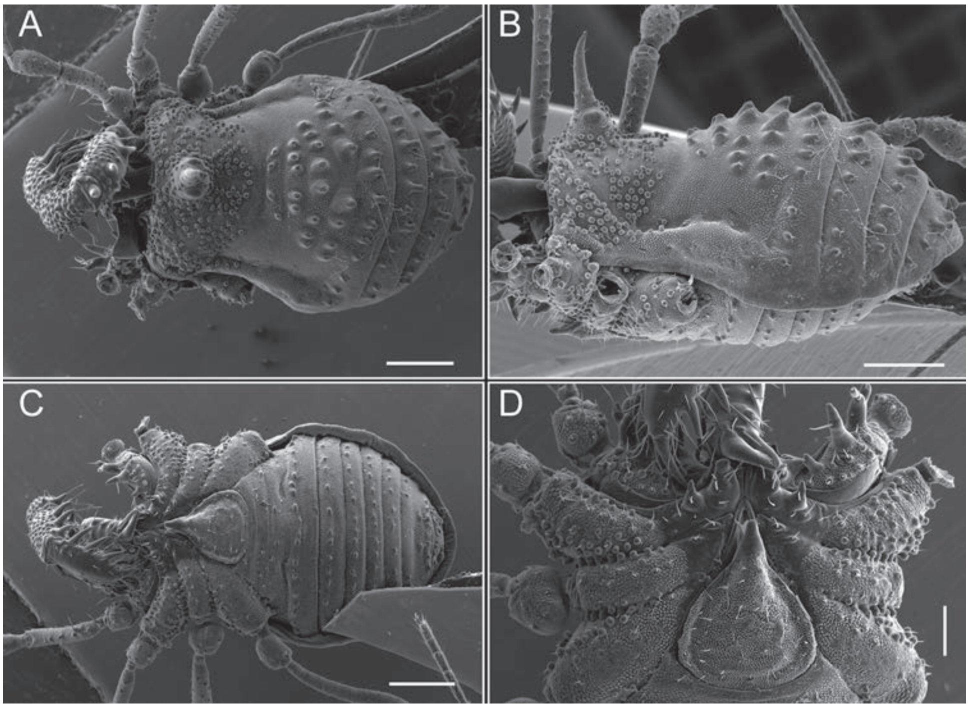

Figure 18. *Fresiax mauryi* sp. nov. male, SEM images of habitus **A** dorsal view **B** lateral view **C, D** ventral view. Scale bars: 500 µm (**A, B, C**); 200 µm (**D**).

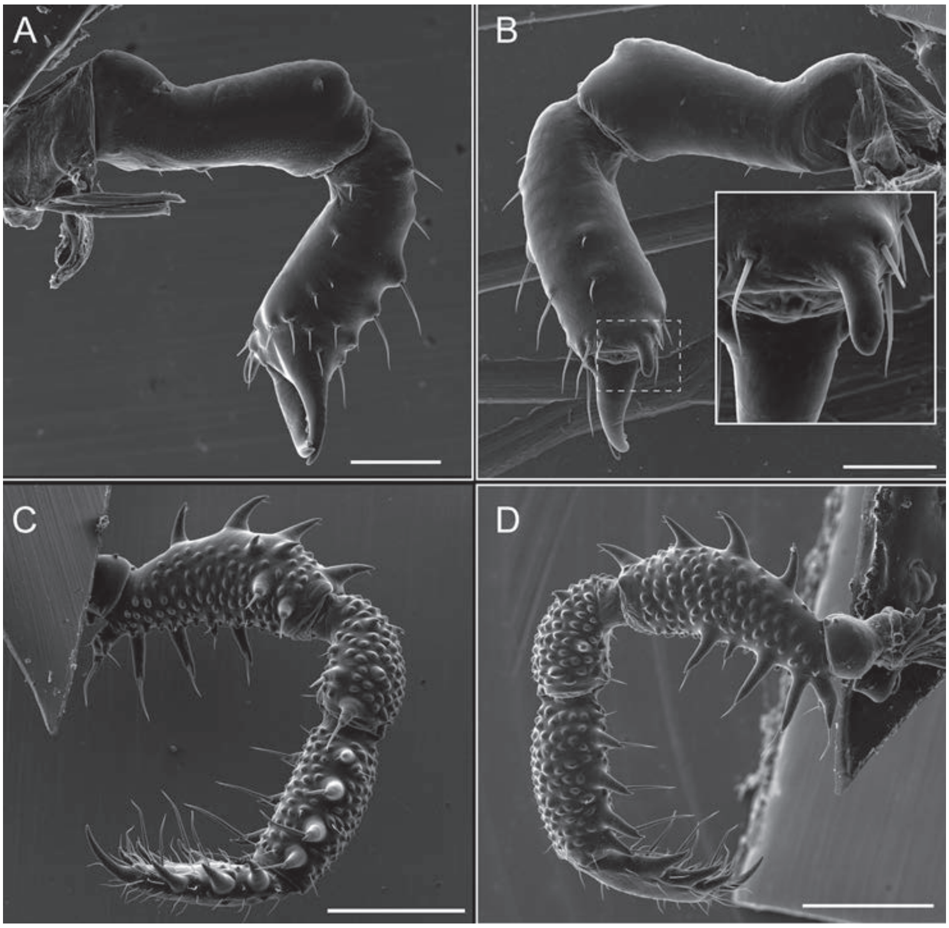

Figure 19. *Fresiax mauryi* sp. nov. chelicerae: mesal **A** ectal **B** pedipalps: mesal **C** ectal **D**. Scale bars: 200 µm (**A, B**); 500 µm (**C, D**).

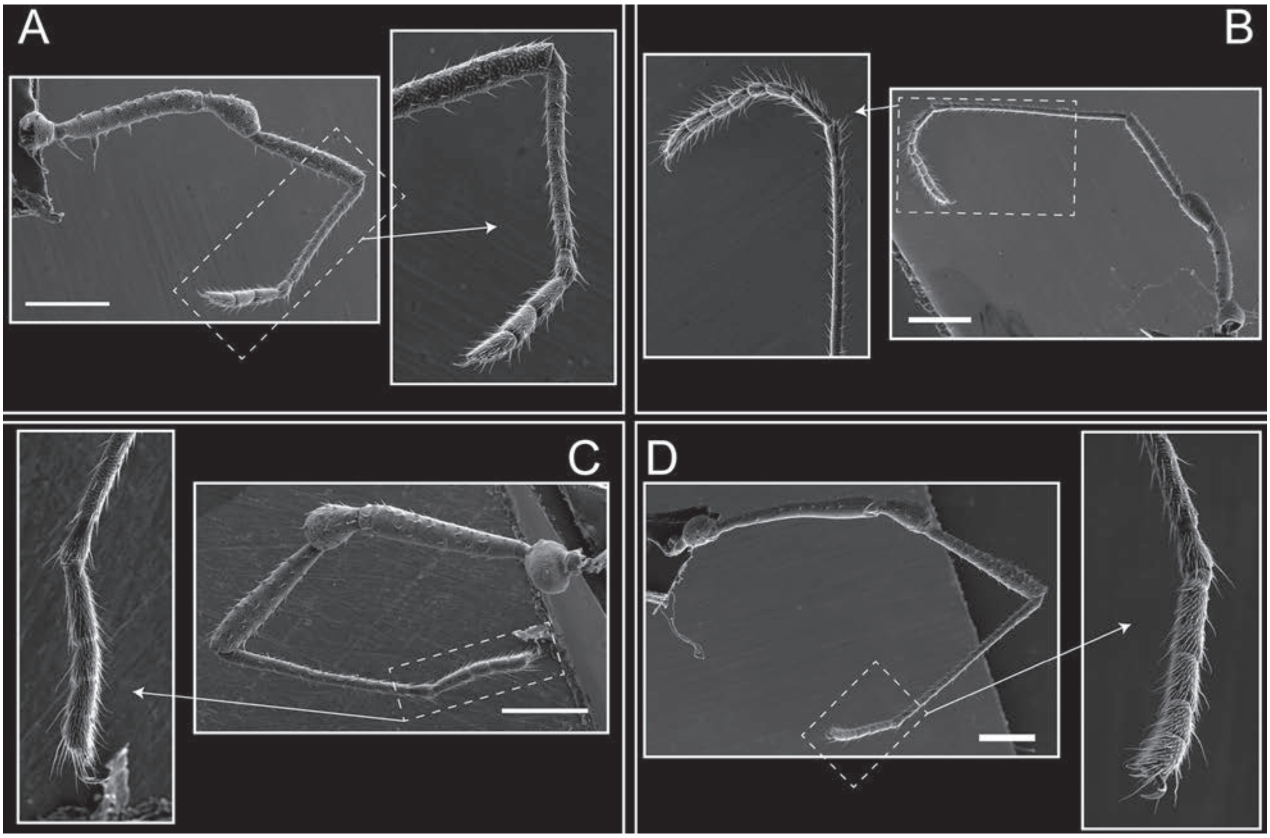

Figure 20. *Fresiax mauryi* sp. nov. legs I **A** II **B** III **C** IV **D**. Scale bars: 500 µm.

Pedipalps (Fig. 19C, D). Trochanter with three small dorsal granules, and two ventral and a small dorsal tubercle. Granules cover the femora, patella, tibia, and tarsus. Femora with a row of five spines with one subdistal seta, the proximal one bifurcated. Patella with three mesal spines and one ectal spine with subdistal setae. Tibia with four ectal and mesal spines with subdistal setae. Tarsus with three ectal and mesal spines with subdistal setae.

Legs (Fig. 20). Coxae I–IV bearing small setiferous tubercles, leg I with three long subdistal setiferous tubercles, the distal one forked at its terminal end. Spiracles visible. A smooth area occupies ¼ of legs II (which has a tubercle with subdistal seta) and III. The drop-shaped genital operculum is larger than all species of the genus. Opisthosomal sternites with a row of small setiferous tubercles. Sternum reduced due to the large size of the genital operculum.

Legs I–IV covered in setae; tarsal area and calcaneus densely covered in setae. Trochanter I with a small ventral tubercle. Tibia I with three proximal tubercles with setae, II–IV with sparse ventral granules. Calcaneus smaller than astragalus, ≥ 7× smaller in legs I, 9× (II), 8× (III), and 11× (IV). Tarsal count: 3–7–4–4.

Penis (Figs 21, 22). Pars distalis has a ventral plate with a notch that divides the plate into two halves, each with six long ventral macrosetae and one dorsal macroseta, a capsula externa shorter than the capsula interna, divided into two halves, and a finger-like apical region.

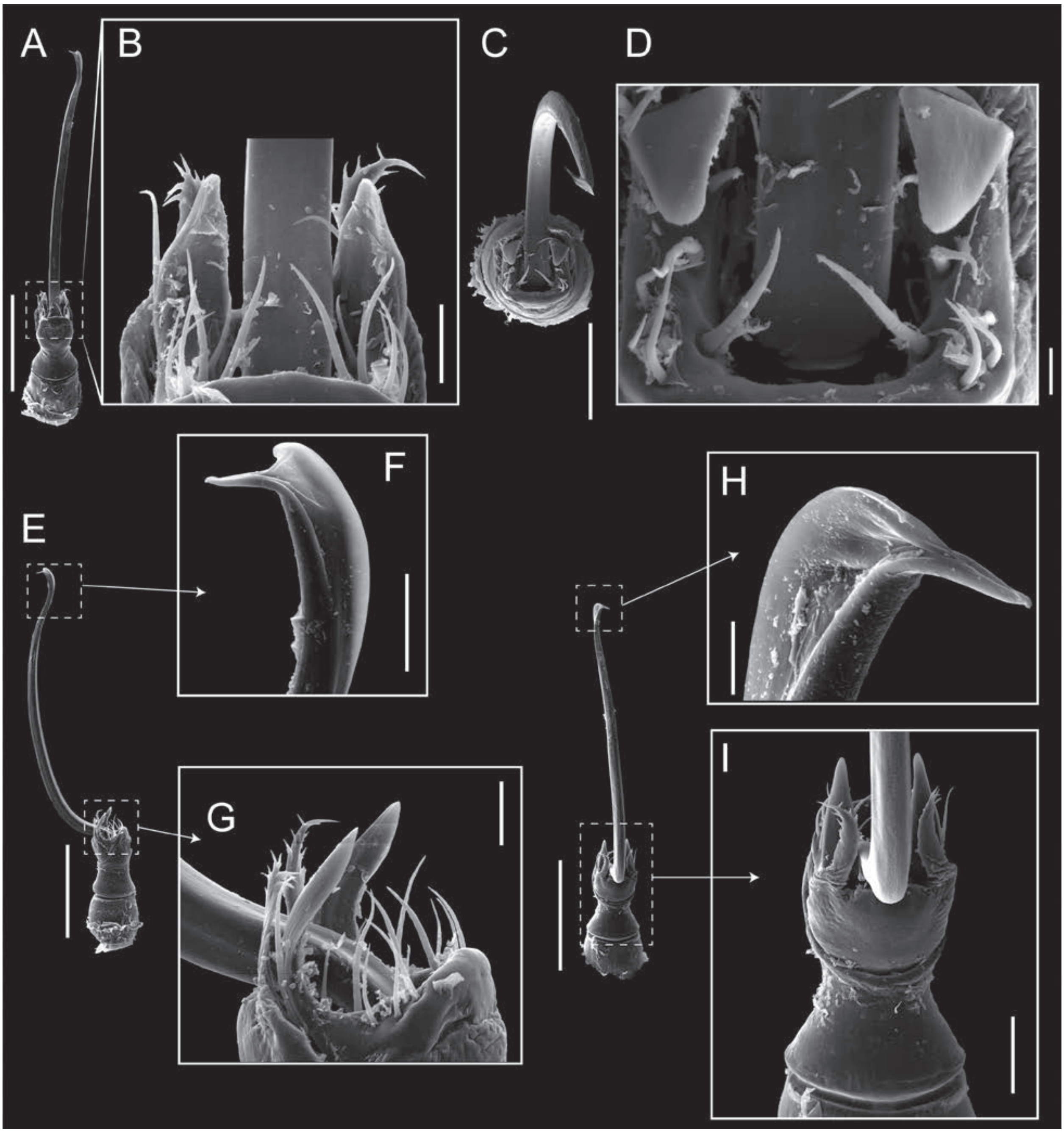

Figure 21. *Fresiax mauryi* sp. nov. penis: ventral **A, B** apical **C, D** lateral **E, G** dorsal **H, I**. Scale bars: 500 µm (**A, E**); 100 µm (**C**); 20 µm (**D, H**); 50 µm (**B, F, G**).

Female. Similar to male, with shorter pedipalpal femora and reduced genital operculum.

Female measurements. Total length 2.67, carapace length 0.80, dorsal scutum length 1.65, carapace max. width 1.25, mesotergum max. width 1.74. Appendage measurements: Pedipalps. Trochanter length 0.13, femora length 0.78, patella length 0.45, tibia length 0.56, tarsus length 0.53. Leg I: trochanter (tr) 0.19, femora (fe) 0.83, patella (pa) 0.35, tibia (ti) 0.66, metatarsus (mt) 0.80, tarsus (ta) 0.48. **II**: tr 0.27, fe 1.26, pa 0.43, ti 1.03, mt 1.45, ta 0.86. **III**: tr 0.23, fe 0.96, pa 0.38, ti 0.82, mt 1.15, ta 0.52. IV: tr 0.24, fe 1.29, pa 0.42, ti 1.04, mt 1.56, ta 0.64.

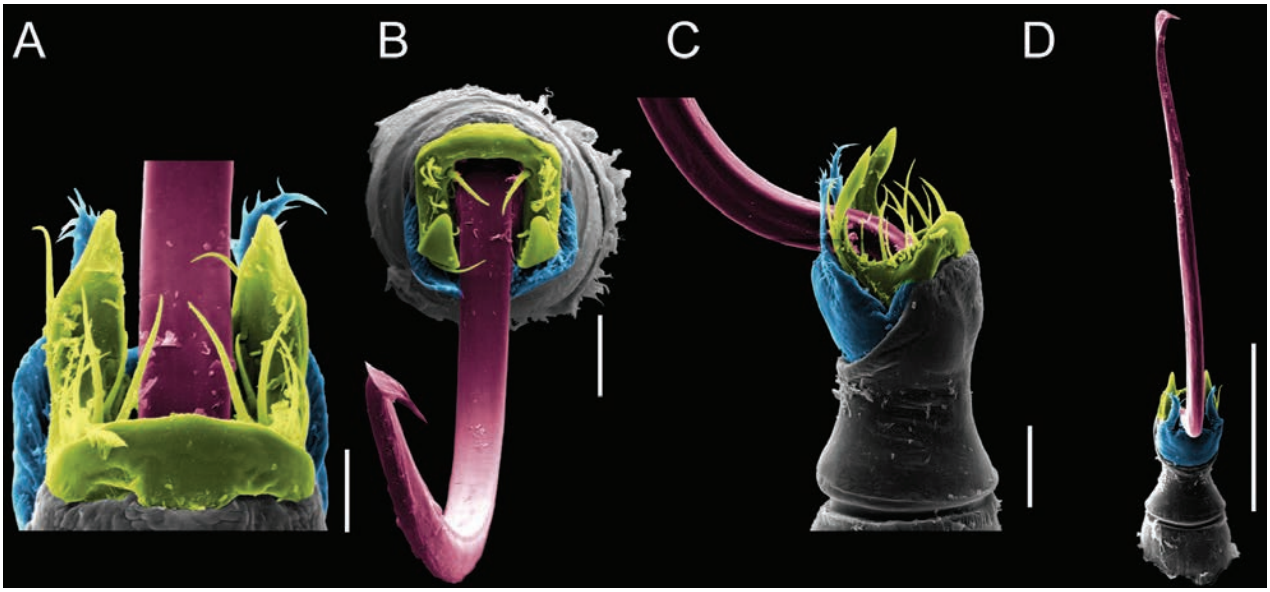

Figure 22. *Fresiax mauryi* sp. nov. penis: ventral **A** apical **B** lateral **C** dorsal **D**. Colors: ventral plate (yellow), capsula externa (blue), capsula interna (red). Scale bars: 50 µm (**A**); 100 µm (**B, C**); 500 µm (**D**).

Fresiax pichicuy **sp. nov.**

https://zoobank.org/58DB7CF4-A314-4B5F-9BB1-E7C4AF64C4CD
Figs 23–28

Material examined. ***Holotype.*** ♂ **Chile.** Choapa: Pichidangui, Coquimbo, Fundo Palo Colorado, 16 km N of Pichidangui, E. Maury coll. 21.X.1988 (MNHNCL). ***Paratypes.*** Chile. Choapa: Pichidangui, Coquimbo, Fundo Palo Colorado, 16 km N de Pichidangui, E. Maury coll. 21.X.1988, 1 ♀ (MACN). Cuesta de Zapata, A. Porta coll., 2018, 11 imm. (MACN). Petorca: Cachagua, Quebrada El Tigre, E. Maury coll., 08.XII.1988, 5 ♂ 2 ♀ (MACN). Quillota: Parque Nacional La Campana, Palmas de Ocoa, E. Maury coll., 08.XII.1987, 2 ♀ (MACN). Petorca: Pichicuy, V región Valparaíso, Quebrada Huaquén, E. Maury coll., 29.X.1988, 2 ♂ 3 ♀ (MACN). Choapa, Los Vilos, Quebrada a Playa, Agua Dulce 46 km N de Los Vilos, E. Maury coll., 05.XII.1988, 1 ♀ (MACN). Quillota: Parque Nacional La Campana, Palmas de Ocoa, E. Maury coll., 27.X.1988, 2 ♂ 2 ♀ (MACN). Coquimbo: Limarí, Bosque Talinay, P.N. Fray Jorge, relict Valdivian fog forest, R. Schuh, N. Platnick coll., 08.II.1986, 2 ♂ (AMNH). Petorca: Pichicuy, Quebrada con Peumusboldus, A. Roig coll., 07.I.1984, 1 ♂ (MACN). Valparaíso, Cerro de La Campana, G. Betancourt coll., 12.III.1979, 1 ♀. Coquimbo: Limarí, P.N. Fray Jorge, relict Valdivian fog forest, N. Platnick, K. Catley, M. Ramírez, T. Allen coll., 10.XI.1993, 1 ♂ (AMNH). Petorca: Cachagua, V región Valparaíso, Quebrada El Tigre, E. Maury coll., 14.XII.1987, 7 imm. (MACN).

Etymology. The species name derives from the species' distribution locality, Pichicuy, located in the commune of La Ligua, Petorca province, Chile. Noun in apposition.

Diagnosis. This species can be easily distinguished from the other species in the genus by its conical forward-facing ocularium, with a 45 ° angled process. Dorsal scutum only covered in small granules. Capsula interna with digitiform structures on the apical portion. Genitalia similar to that of *F. fray*, slightly longer and with variations in the surface of the ventral plate and apex of the capsula interna with longer projections.

Figure 23. *Fresiax pichicuy* sp. nov. habitus, male **A** dorsal view **C** lateral view **E** ventral view. Female **B** dorsal view **D** lateral view **F** ventral view. Scale bars: 1 mm. Species of Clade A, see Fig. 3.

Distribution. Chile: Valparaíso Region, Petorca Province (Fig. 4A).

Description of male. Measurements: Total length 2.01, carapace length 0.64, dorsal scutum length 1.37, carapace max. width 1.03, mesotergum max. width 1.42. Appendage measurements: Pedipalps. Trochanter length 0.17, femora length 0.76, patella length 0.44, tibia length 0.67, tarsus length 0.54. Leg **I**: trochanter (tr) 0.16, femora (fe) 0.75, patella (pa) 0.36, tibia (ti) 0.51, metatarsus (mt) 0.54, tarsus (ta) 0.55. **II**: tr 0.19, fe 0.94, pa 0.39, ti 0.79, mt 0.87, ta 1.11.

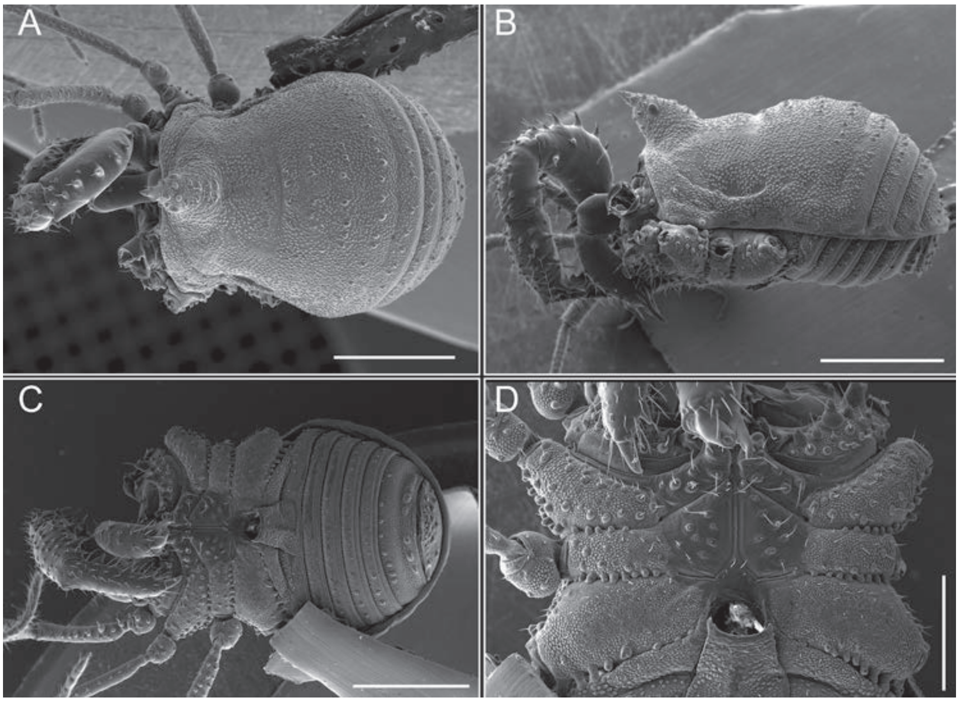

Figure 24. *Fresiax pichicuy* sp. nov. male, SEM images of habitus **A** dorsal view **B** lateral view **C, D** ventral view. Scale bars: 1 mm (**A, B, C**); 500 µm (**D**).

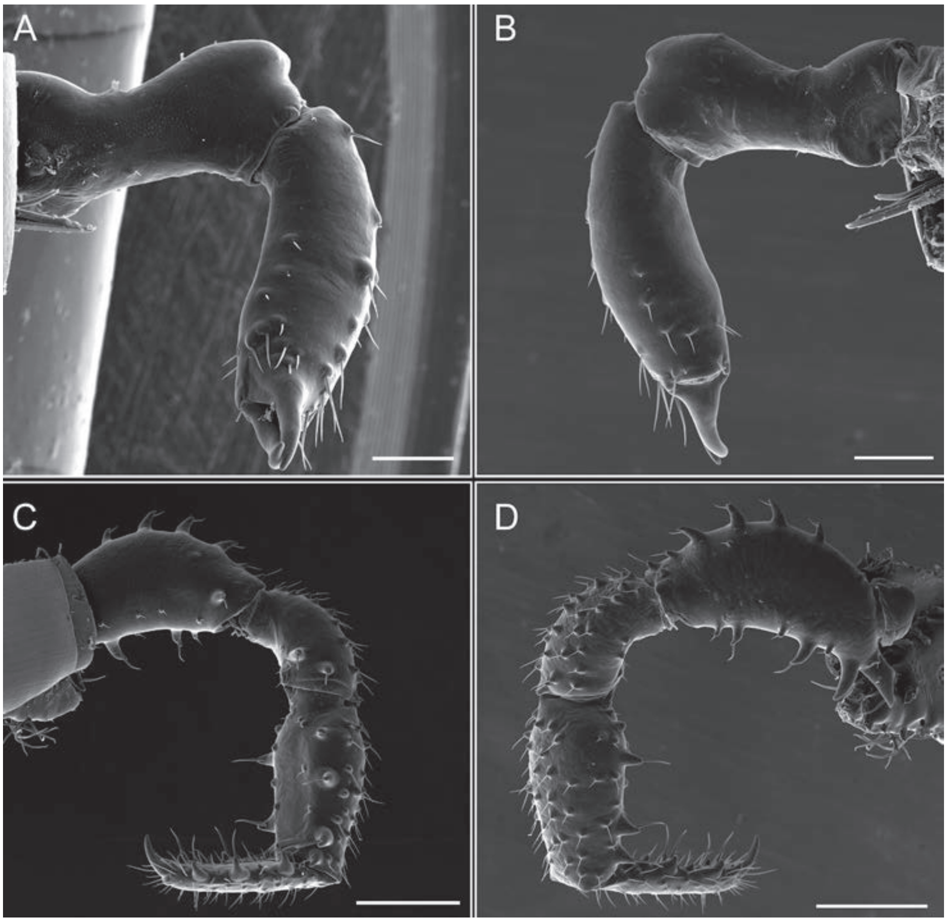

Figure 25. *Fresiax pichicuy* sp. nov. chelicerae: mesal **A** ectal **B** pedipalps: mesal **C** ectal **D**. Scale bars: 200 µm (**A, B**); 500 µm (**C, D**).

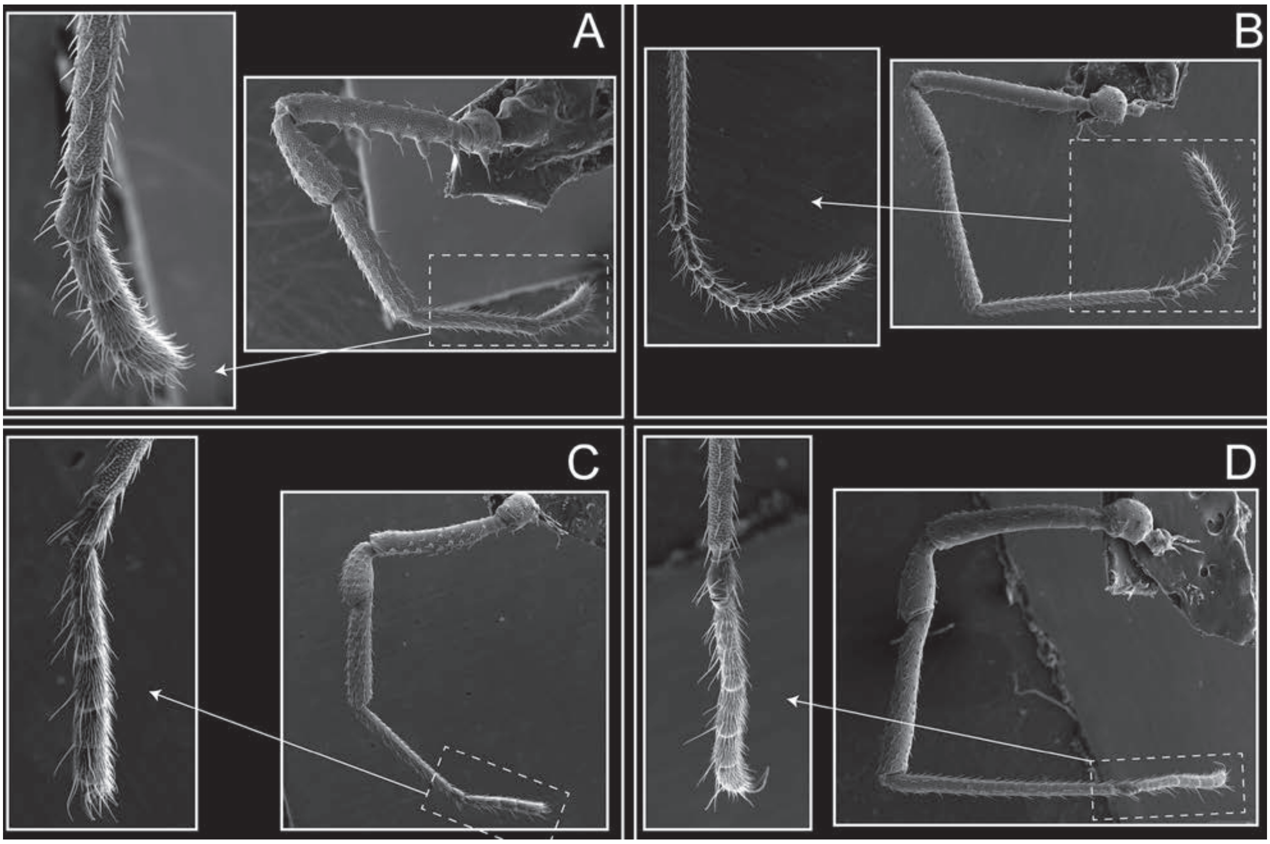

Figure 26. *Fresiax pichicuy* sp. nov. legs I **A** II **B** III **C** IV **D**. Scale bars: 200 µm (**A, C**); 500 µm (**B, D**).

III: tr 0.24, fe 0.72, pa 0.26, ti 0.34, mt 0.65, ta 0.62. IV: tr 0.18, fe 0.99, pa 0.43, ti 0.82, mt 1.03, ta 0.71.

Dorsum (Fig. 23, 24). Eta (η) hourglass-shaped dorsal scutum. Conical ocularium, forward-looking, with a small forward-pointing apical spine and two dorsal rows of small setiferous tubercles. Eyes located high. Dorsal scutum microgranulate, without clear delimitation of areas. Areas I–IV with four, six, eight, and ~ 17 small rounded setiferous tubercles with setae, respectively. Posterior border and free tergites with a row of small rounded setiferous tubercles. All free tergites with a row of small setiferous granules.

Chelicerae (Fig. 25A, B). Segment I smooth; segment II with setae and sparse granules.

Pedipalps (Fig. 25C, D). Trochanter smooth. Femora with a row of six dorsal spines with subdistal setae, a row of four ventral spines with setae interspersed by small tubercles with subdistal setae, the proximal one subtriangular in shape, a row of four small mesal granules with setae, and a small distal tubercle with mushroom-shaped tubercles. Patella covered in small tubercles with setae on the dorsal surface, with two small mesal setiferous tubercles. Tibia with four ectal and mesal spines with subdistal setae, nine ventral granules with setae, and dorsal surface covered in small tubercles with setae. Tarsus with three mesal and ectal spines, as well as a few setae and granules.

Legs (Fig. 26). Coxa I with small setiferous tubercles and a row of three long tubercles with subdistal setae, coxae II–IV microgranulate, bearing five or six bridges between legs II and III, eight between III and IV, 6–8 between leg IV

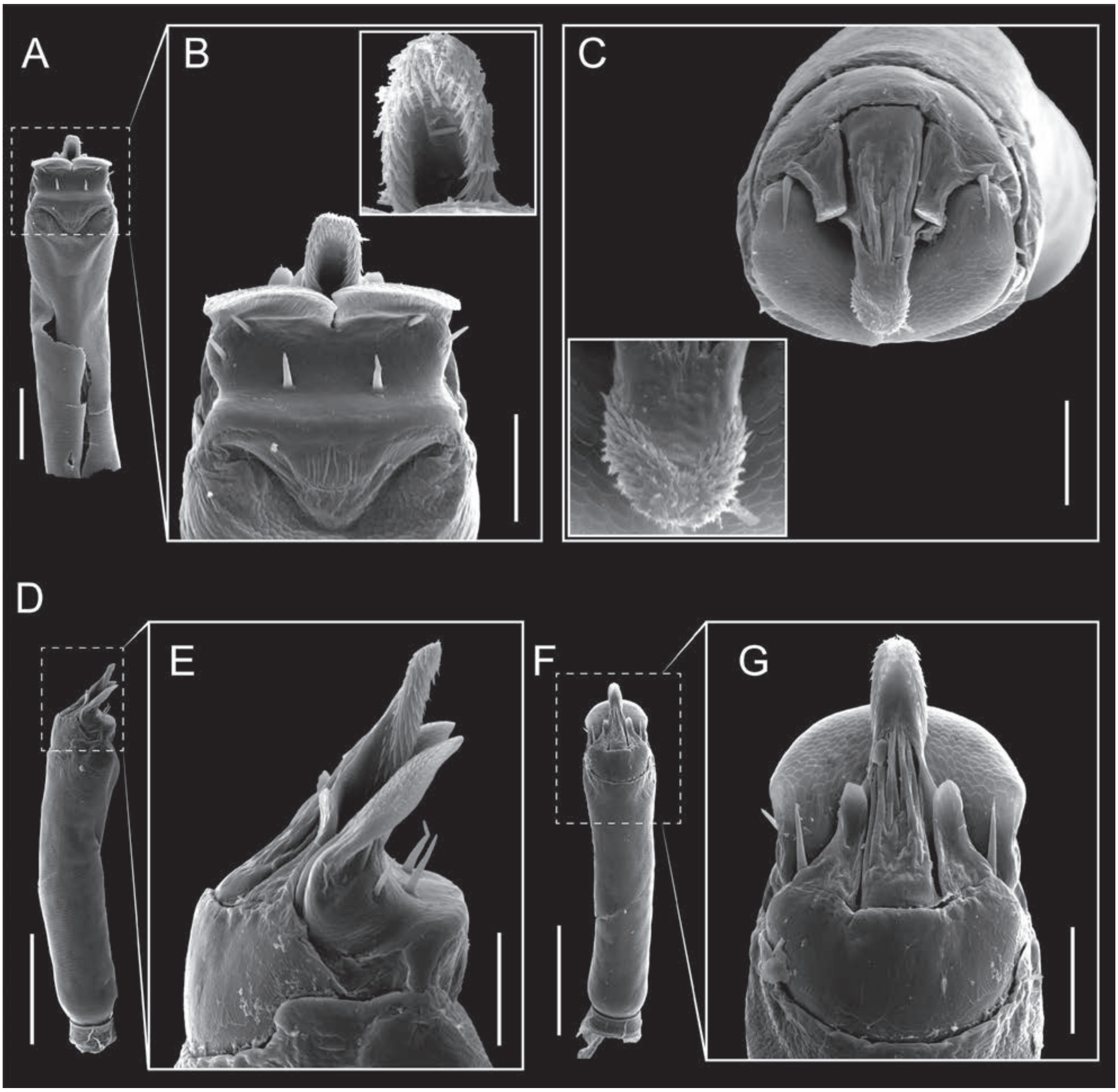

Figure 27. *Fresiax pichicuy* sp. nov. penis: ventral **A, B** apical **C** lateral **D, E** dorsal **F, G**. Scale bars: 200 µm (**A, D, F**); 50 µm (**B, C, E, G**).

and opisthosoma. Spiracles not visible. Smooth area occupies ⅓ of leg II, almost ½ of III, and only a small proximal portion of IV. Smooth area II with five small setiferous tubercles, III with eight small setiferous tubercles. Opisthosomal sternites III with four small setiferous tubercles on each side, IV with three small setiferous tubercles on each side, and V with an anterior row of small setiferous tubercles and a posterior row of rounded setiferous tubercles. Anal plate covered in small setiferous tubercles. Trochanter I with three small ventral and one dorsal setiferous tubercle; tibia I with a row of five tubercles with setae and a dorsal row of small setiferous tubercles; femora III with ~ 20 small setiferous tubercles. Legs II–IV covered in setae, tarsal area, and calcaneus densely setose. Calcaneus smaller than astragalus, ≥ 5× smaller in legs I, 6× (II), 7× (III) and 10× (IV). Tarsal count 3–9–4–4.

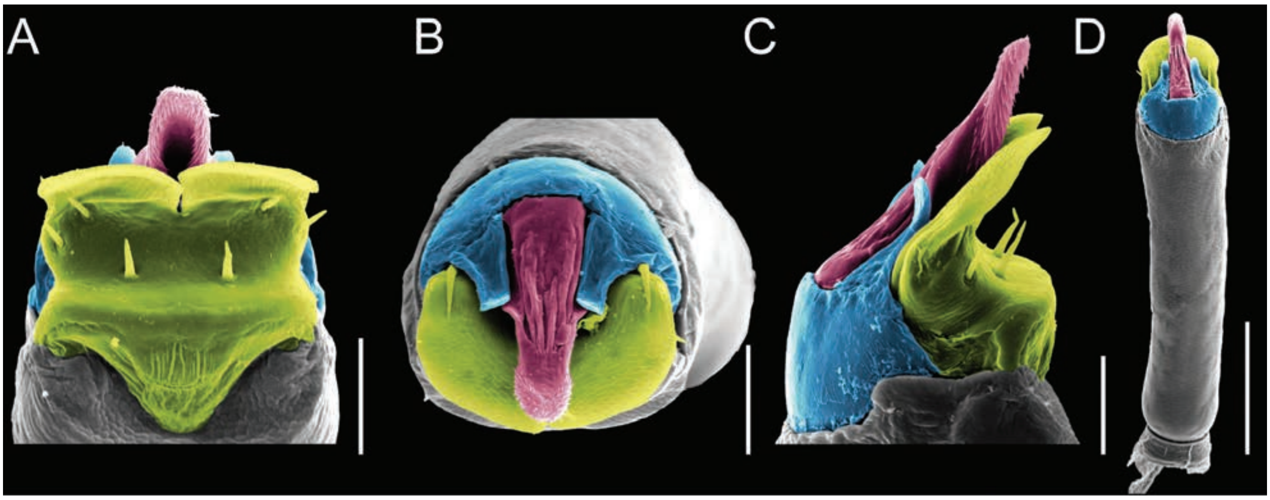

Figure 28. *Fresiax pichicuy* sp. nov. penis: ventral **A** apical **B** lateral **C** dorsal **D**. Colors: ventral plate (yellow), capsula externa (blue), capsula interna (red). Scale bars: 50 μm.

Penis (Figs 27, 28). Pars distalis with a ventral plate bearing a cleft dividing the plate into two halves. Ventral surface of each half with three macrosetae and dorsal surface with one macroseta; ventral plate covered in scale-like structures. Capsula externa shorter than capsula interna, having a notch that divides the capsula externa into two halves.

Female. Similar to male, with shorter pedipalpal femora.

Female measurements. Total length 1.93, carapace length 0.60, dorsal scutum length 1.34, carapace max. width 1.07, mesotergum max. width 1.45. Appendage measurements: Pedipalps. Trochanter length 0.15. Femora length 0.65, patella length 0.34, tibia length 0.53, tarsus length 0.49. Leg I: trochanter (tr) 0.15, femora (fe) 0.62, patella (pa) 0.34, tibia (ti) 0.51, metatarsus (mt) 0.53, tarsus (ta) 0.50. II: tr 0.18, fe 0.79, pa 0.37, ti 0.70, mt 0.81, ta 1.03. III: tr 0.18, fe 0.68, pa 0.31, ti 0.57, mt 0.67, ta 0.49. IV: tr 0.20, fe 0.94, pa 0.36, ti 0.72, mt 0.87, ta 0.62.

Fresiax spinulosa **(Maury, 1990), comb. nov.**

Figs 29–34

Nuncia spinulosa Maury, 1990: 108, figs 13–24; Maury 1992: 5; Acosta and Maury 1998: 579; Kury 2003: 22.

Material examined. ***Holotype***. ♂ **Argentina.** Neuquén Province, Hua Hum, E. Maury coll. (MACN 8689). ***Paratype*** **(allotype ♀). Argentina.** Neuquén Province, Hua Hum, E. Maury coll. (MACN 8690). ***Paratypes*. Argentina.** Tromen Lake, Neuquén Province, 3 ♂ and 4 ♀ (MACN 8691).

Additional material. Argentina. Neuquén: Parque Nacional Nahuel Huapi, Lago Ortiz Basualdo, M. Ramírez coll., I.1990, 2 ♀ 1 imm. (MACN). Río Negro: Parque Nacional Nahuel Huapi, Río Frías Superior, M. Ramírez coll., I.1990, 1 ♀ (MACN), D. Anghicante. coll., 26.01.1990, 1 ♀ 1 imm. Río Negro: P.N. Nahuel Huapi, Puerto Blest, M. Ramírez V. Werenkraut, S. Aysén coll., 28.XII.2010, 1 ♂ 2 ♀, Near Puerto Alegre, Lago Frías, M. Ramírez, V. Werenk-

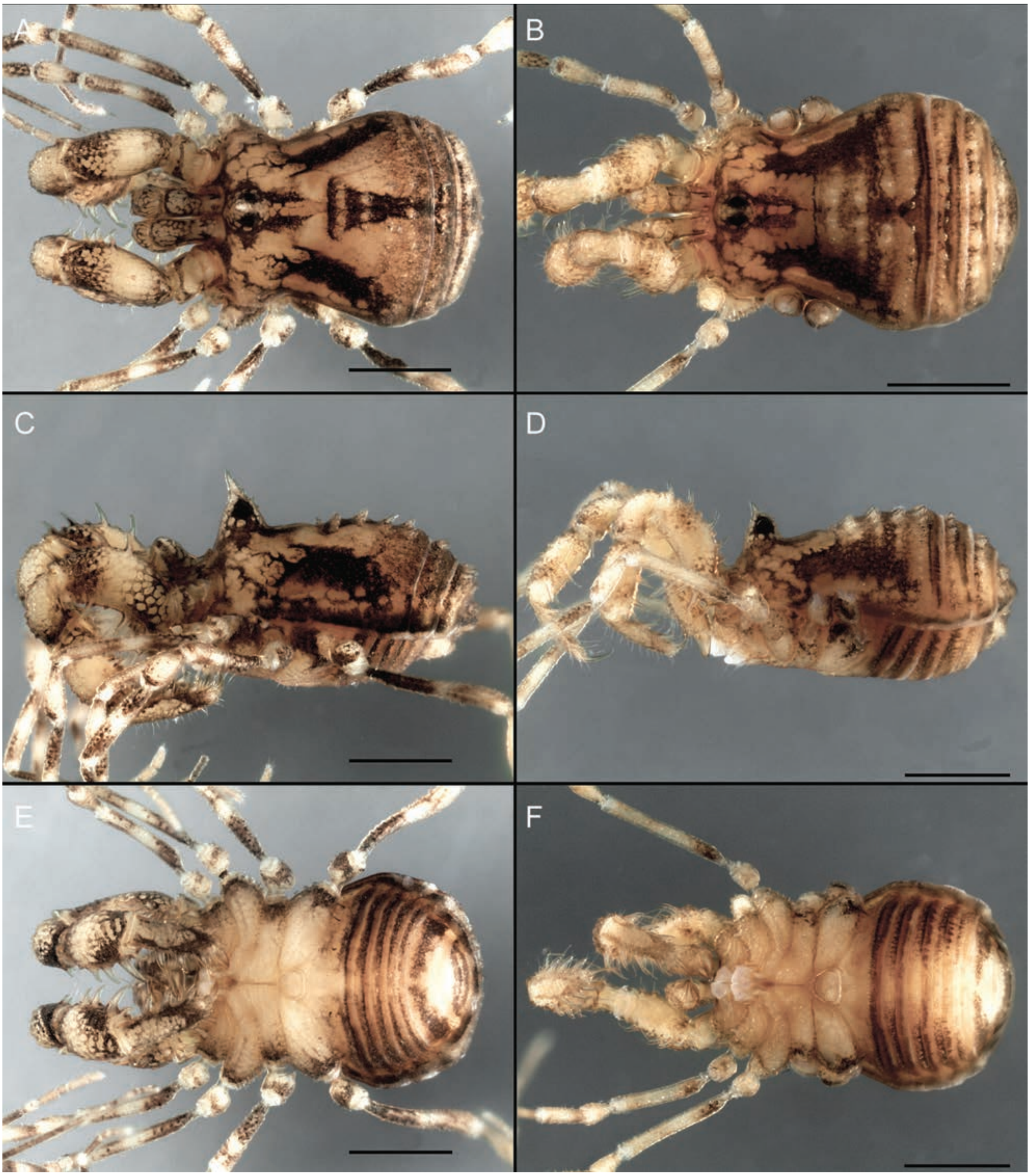

Figure 29. *Fresiax spinulosa* comb. nov. habitus, male **A** dorsal view **C** lateral view **E** ventral view. Female **B** dorsal view **D** lateral view **F** ventral view. Scale bars: 1 mm. Species of Clade A, see Fig. 3.

raut, S. Aysén coll., 29.XII.2010, 1 ♂, A. Quaglino, L. Lopardo coll., 07.I.2000, 1 ♀. Neuquén: P.N. Nahuel Huapi, Puerto Blest, M. Ramírez coll., 05.I.1998, 1 ♀ (MACN). Río Negro: Bariloche, Lago Mascardi, Near Tronador Hotel, E. Maury coll., 02.XI.1986, 1 ♂ 2 imm. (MACN). Neuquén: Parque Nacional Nahuel Huapi, Los Lagos, M. Ramírez coll., 30. I.1985, 1 ♀ (MACN), Base Glaciar Frias, D. Anghicante coll., 24.I.1988, 1 ♂ 1 ♀. Chile. Valdivia: Res. Valdivia, B. Borry coll., I.2007, 4 imm. Cautín: M. Ramírez, F. Labarque coll., 08.II.2005, 1

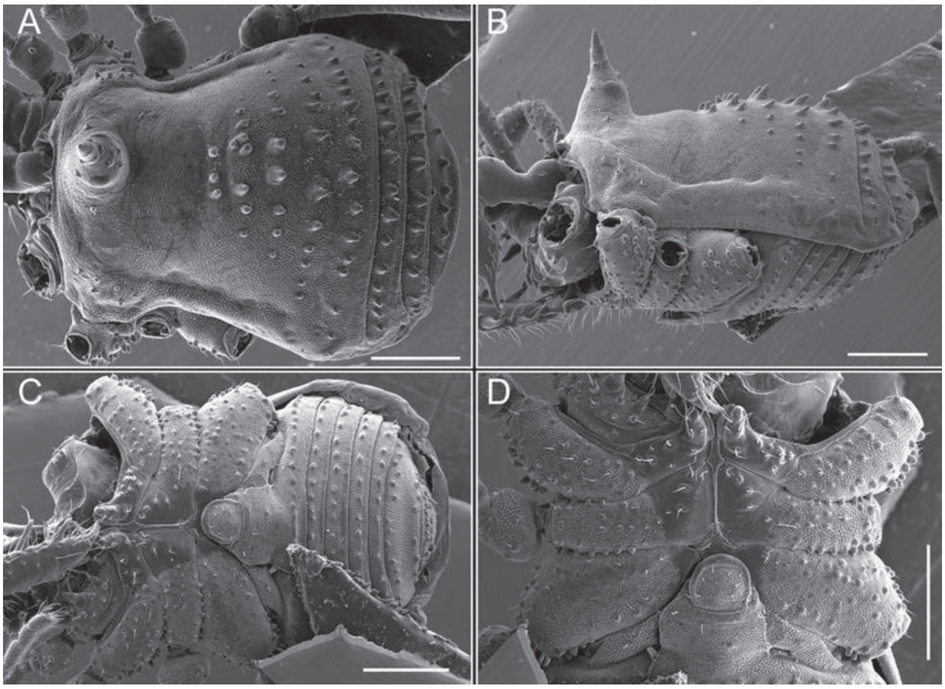

Figure 30. *Fresiax spinulosa* comb. nov. male, SEM images of habitus **A** dorsal view **B** lateral view **C, D** ventral view. Scale bars: 500 µm.

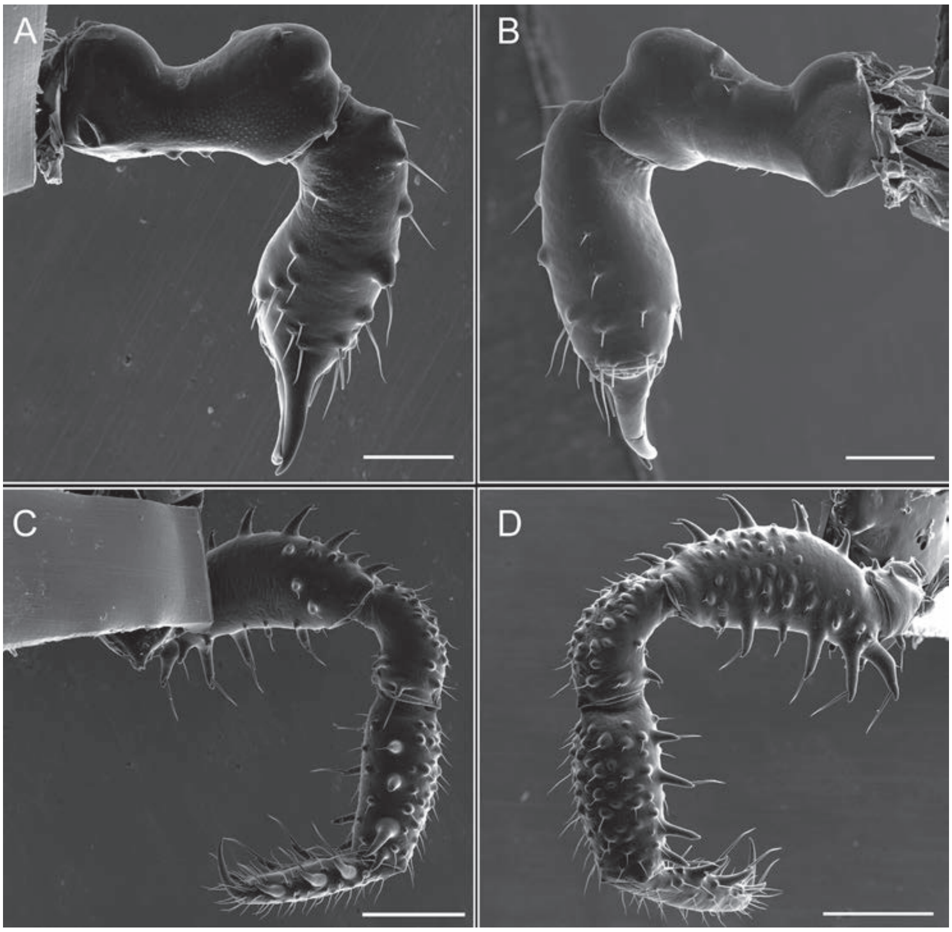

Figure 31. *Fresiax spinulosa* comb. nov. chelicerae: mesal **A** ectal **B** pedipalps: mesal **C** ectal **D**. Scale bars: 200 µm (**A, B**); 500 µm (**C, D**).

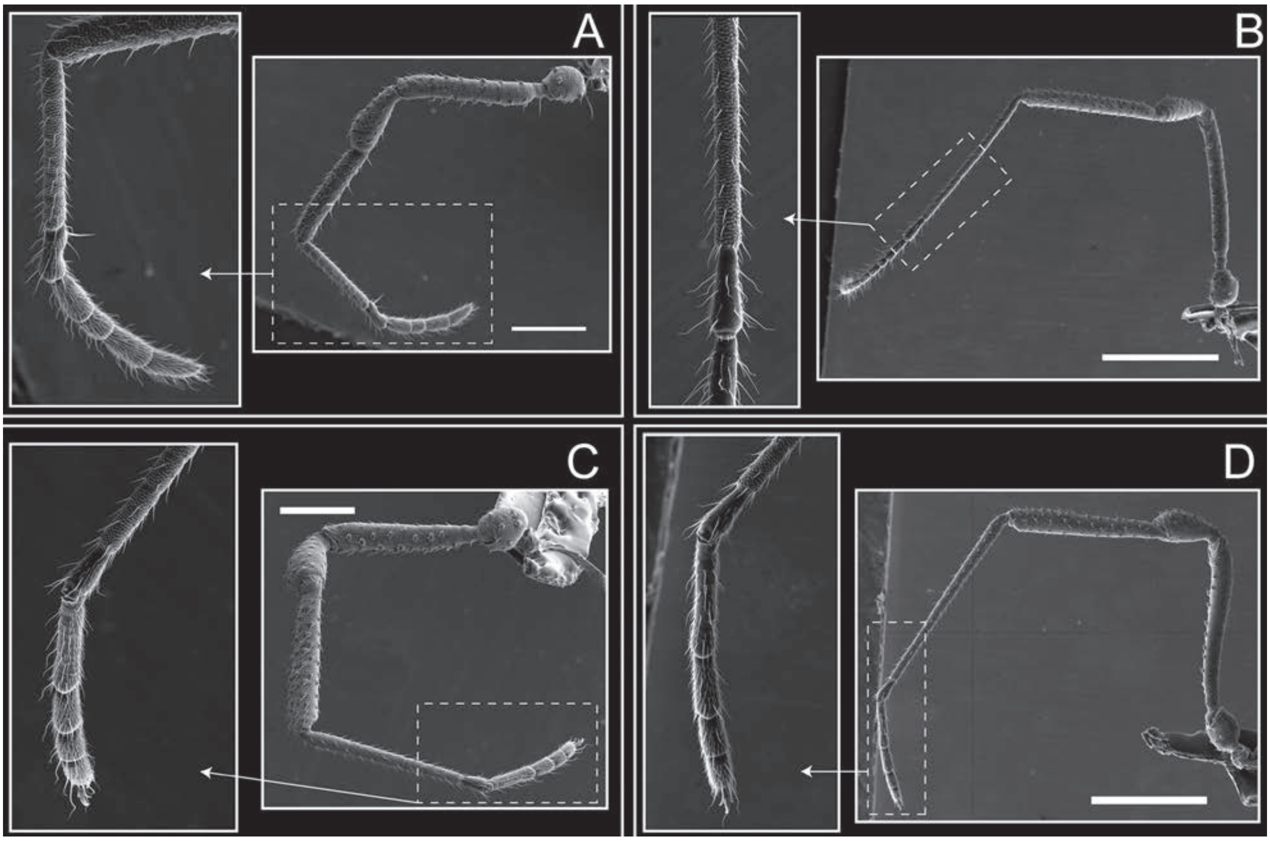

Figure 32. *Fresiax spinulosa* comb. nov. legs I **A** II **B** III **C** IV **D**. Scale bars: 500 µm (**A, C**); 100 µm (**B, D**).

♂ 1 imm. (MACN); Bellavista, Fundo Flor del Lago, M. Ramírez, F. Labarque coll., 09.II.2005, 1 ♀ (MACN). Osorno: Termas de Puyehue, R. Schuh, N. Platnick coll., 24–25.XI.1981, 4 ♂ 1 ♀ (AMNH), 36 km W. La Union, L. Peña coll., 25.III.1987, 2 ♂ (AMNH). Valdivia: Nehuin, X Reg. Los Lagos, E. Maury coll., 16.I.1989, 1 ♂ 1 ♀ 1 imm. (MACN). Chiloé: Chiloé island, 5 km N of Quellón, R. Schuh, N. Platnick coll., 01.XII.1981, 1 ♂ (AMNH). Osorno: 7 km E de Entrelagos, Camping "No me olvides", E. Maury coll., 30.I.1991, 1 ♂ 1 imm. (MACN). Llanquihue: P.N. Alerce Andino, M. Ramírez, F. Labarque coll., 02.IV.2005, 2 ♂ (MACN). Valdivia: Corral, X Reg. Los Lagos, Río Nahuelan 24 km E Corral, E. Maury coll., 16.I.1989, 1 ♂ 1 ♀ (MACN). Chiloé: 25 km N de Chepu, M. Ramírez coll., 08.II.1991, 1 ♀ (MACN). Valdivia: Niebla, Camping "La Herradura", 8 km east form Niebla, E. Maury coll., 23.I.1991, 1 ♂ 2 ♀ 1 imm. (MACN). Concepción: Hualpén, Estación de Biología terrestre Univ. de Concepción, A. Ojanguren, A. Pérez-González, M. Ramírez, G. Azevedo, W. Porto coll., 14.I.2018, 1 ♂ (MACN). Valdivia: Parque Oncol, Sendero Punucahua, M. Ramírez, E. Soto, J. Wilson, D. Poy coll., 13.I.2020, 1 ♀ (MACN). Concepción: Hualpén, Estación de Biología terrestre Univ. de Concepción, A. Ojanguren, A. Pérez-González, M. Ramírez, G. Azevedo, W. Porto coll., 14.I.2018, 1 ♂ 1 ♀ (MACN). Valdivia: Res. Valdivia, B. Borry coll., I.2007, 1 imm. Cautín: Pucón, Ojos del Caburgua, 15 km NE de Pucón, E. Maury coll., 16.I.1987, 1 ♂ 2 ♀ 3 imm. (MACN), Termas de Palguin, SE de Pucón, E. Maury coll., 17.I.1987, 1 ♀ (MACN). Chiloé: Chepu, E. Maury coll., 11.XII.1985, 1 ♂ (MACN). Malleco: Malalcahuello, E. Maury coll., 08.01.1987, 3 ♂ 1 ♀ (MACN). Chiloé: Cucao, E. Maury coll., 12.XII.1985, 2 ♂ 1 ♀ (MACN). Llanquihue: Puerto Montt, Carretera Austral, Caleta La Arena, E.

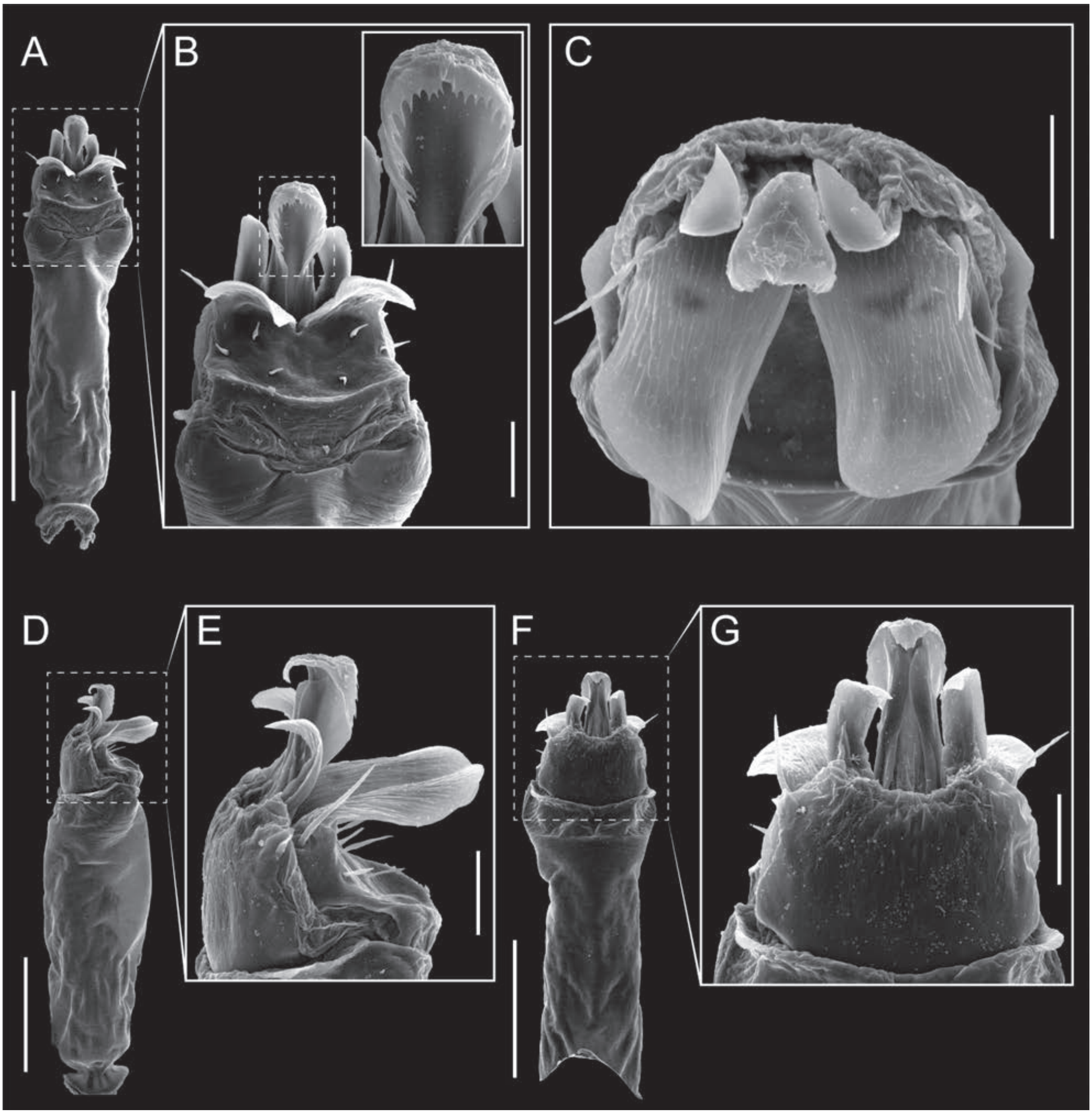

Figure 33. *Fresiax spinulosa* comb. nov. penis: ventral **A, B** apical **C** lateral **D, E** dorsal **F, G**. Scale bars: 200 μm (**A, D, F**); 50 μm (**B, C, E, G**).

Maury coll., 07.VIII.1985, 3 ♂ 3 ♀ (MACN). Osorno: Los Derrumbes, 5 km al S de Termas Puyehue, E. Maury coll., 03.I.1988, 1 ♀ (MACN). Same collector, 04.XII.1985, 5 ♂ 5 ♀ 8 imm. (MACN), 36 km W. La Union, 600 m, L. Peña coll., 25–28.III.1987, 1 ♂ (AMNH). Valdivia: Las Lajas (Las Trancas), W. La Unión, L. Peña coll., 19.XI.1990, 1 ♂ (AMNH).

Diagnosis. This species can be easily distinguished from the other species in the genus by its long interocular apophysis (not as long as in *F. mauryi*), the long mesotergal tubercles, and the penis with longer ventral plate than other species in the genus.

Distribution. Argentina: Provinces of Neuquén and Río Negro. Chile: Regions of Araucanía, Los Ríos, and Los Lagos (Fig. 4A).

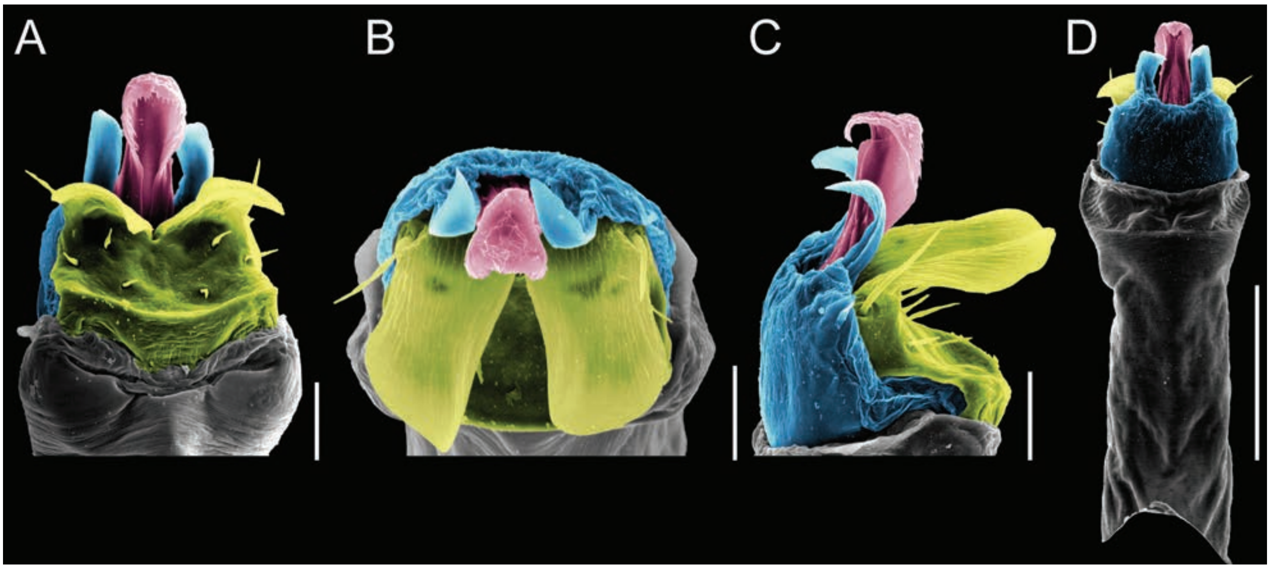

Figure 34. *Fresiax spinulosa* comb. nov. penis: ventral **A** apical **B** lateral **C** dorsal **D**. Colors: ventral plate (yellow), capsula externa (blue), capsula interna (red). Scale bars: 50 µm (**A–C**); 200 µm (**D**).

Description of male. Measurements: Total length 3.29, carapace length 0.77, dorsal scutum 2.22 length. max. width of the carapace 1.72. max. width of the mesotergum 2.01. Appendage measurements: Pedipalps. Trochanter length 0.28, femora length 1.27, patella length 0.64, tibia length 1.05, tarsus length 0.95. Leg I: trochanter (tr) 0.30, femora (fe) 1.13, patella (pa) 0.58, tibia (ti) 0.92, metatarsus (mt) 1.03, tarsus (ta) 0.76. II: tr 0.34, fe 1.71, pa 0.63, ti 1.47, mt 1.75, ta 1.55. III: tr 0.36, fe 1.17, pa 0.51, ti 1.13, mt 1.44, ta 0.97. IV: tr 0.41, fe 1.56, pa 0.71, ti 1.47, mt 1.98, ta 1.10.

Dorsum (Fig. 29, 30). Eta (η) hourglass-shaped dorsal scutum. Ocularium elevated, accompanied by a long apophysis located between the eyes. Additionally, there are two dorsal rows of setae present in the ocularium. Carapace with fine microgranulation, small tubercles located on each side of the ocular region. A group of five small tubercles can be observed near leg I. Mesotergum with fine microgranulation and features areas that are delineated by prominent tubercles. These tubercles create triangular patterns on the dorsal surface of the mesotergum. Areas I–IV with rows of three, nine, ten, and 12 setiferous tubercles, respectively. The two central tubercles of rows II and III more robust than the others. Posterior margin of the mesotergum with a row of 16 setiferous tubercles. Free tergites, similarly to the posterior margin of the dorsal scutum, display a row of setiferous tubercles.

Chelicerae (Fig. 31A, B). Segment I with two ventral granules and a tiny granule on the dorso-distal surface. Segment two with small granules.

Pedipalps (Fig. 31C, D). The pedipalps exhibit several distinctive features. Trochanter of the pedipalp possesses one ventral and three small dorsal setiferous tubercles. Femora and tibia covered with granules, visible in both dorsal and ectal views. Femora of the pedipalp particularly notable, with a series of six ventral spines with subdistal setae. Proximal process subtriangular in shape, while the fourth and sixth spines are smaller compared to the others. On the mesal surface of the femora, a row of small tubercles of varying sizes can be observed. Additionally, three small distal tubercles with setae and 6–8 granules are present. Dorsal surface of the femora with a row of six spines with subdistal setae. Patella with two mesal and one ectal small spines, each adorned with subdistal setae. In ventral view, tibia displays four ectal and mesal spines with subdistal setae, with a row of setiferous granules. Tarsus with three mesal and ectal tubercles, all covered in subdistal setae.

Legs (Fig. 32). Legs I to IV characterized by short setiferous tubercles. Leg I with three long tubercles with subdistal setae. Legs II and III are connected by four or five bridges, while leg IV is connected to the opisthosoma by 6–8 bridges. Spiracles not covered by these bridges. The smooth surface occupies < ¼ of leg IV, indicating the presence of microgranulation or other textural variations. Legs II and III each with ~ ⅓ of their surfaces covered in a row of four small tubercles. Leg II with seven small tubercles. On the opisthosomal sternites, a row of tiny setiferous tubercles can be observed. Sternum arrow-shaped, with a triangular-shaped posterior. Femora I–IV bearing small setiferous tubercles, metatarsus I with a distal notch.

Penis (Figs 33, 34). Pars distalis with a ventral plate that bears a groove dividing it into two long lamellae. Each lamella has three small macrosetae on the ventral surface and one macroseta on the dorsal surface, and the ventral plate is composed of scale-like structures. Capsula externa shorter than capsula interna, with a groove dividing the dorsal fold into two halves. Capsula interna with apical projections on the ventral view.

Female. Similar to male, with shorter pedipalpal femora.

Female measurements. Total length 3.10, carapace length 0.94, dorsal scutum length 2.00, carapace max. width 1.48, mesotergum max. width 1.95. Appendage measurements: Pedipalps. Trochanter length 0.21, femora length 1.00, patella length 0.61, tibia length 0.74, tarsus length 0.80. Leg I: trochanter (tr) 0.28, femora (fe) 1.02, patella (pa) 0.48, tibia (ti) 0.84, metatarsus (mt) 0.95, tarsus (ta) 0.68. II: tr 0.34, fe 1.55, pa 0.59, ti 1.37, mt 1.54, ta 1.34. III: tr 0.31, fe 1.16, pa 0.48, ti 0.93, mt 1.26, ta 0.78. IV: tr 0.38, fe 1.42, pa 0.61, ti 1.31, mt 1.79, ta 1.02.

Clade B

Genus *Mistralia* gen. nov.

https://zoobank.org/B295CFCF-0BC2-4562-B880-C549E61289C7
Figs 35–43

Nuncia [part] (only references to *Nuncia verrucosa*): Maury 1990: 106; Maury 1992: 5; Acosta and Maury 1998: 579; Kury 2003: 22.

Etymology. The generic epithet is a reference to the Chilean poet, diplomat, and educator Gabriela Mistral (1889–1957). Feminine grammatical gender.

Diagnosis. It differs from all other genera in Triaenonychidae by the morphology of the male genitalia, where the capsula interna features a lateral plate formed by a projection of the pars basalis onto the pars distalis. The dorsal scutum is covered in sharp tubercles (*M. ramirezi* sp. nov.) or wart-shaped (*M. verrucosa*). Ocularium with an apical apophysis.

Type species. *Nuncia verrucosa* Maury, 1990

Included species. *Mistralia ramirezi* sp. nov., *Mistralia verrucosa* comb. nov.

Distribution. Argentina: Neuquén, Río Negro. Chile, Regions: Bío-Bío, Los Lagos (Fig. 4B).

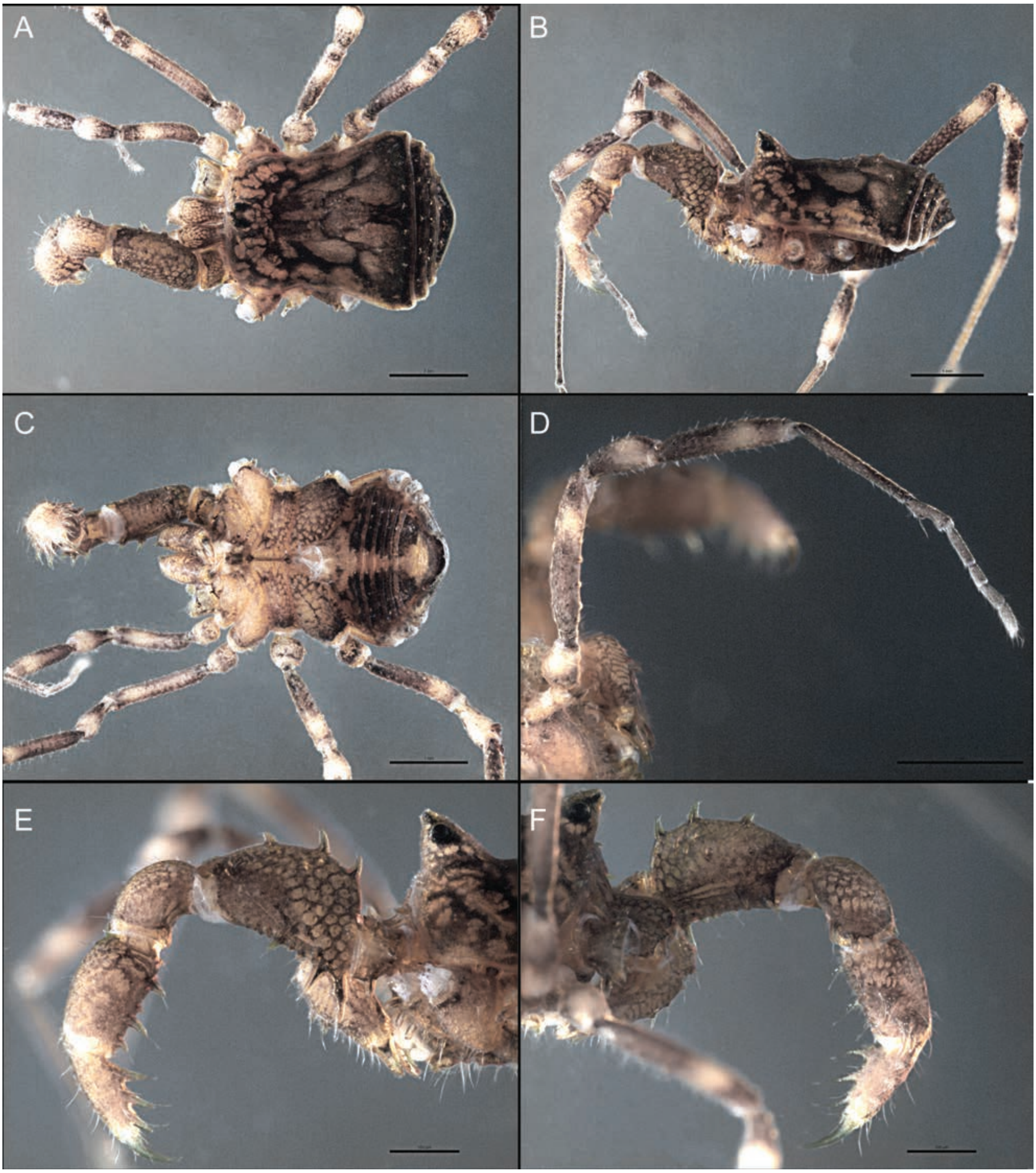

Figure 35. *Mistralia ramirezi*. sp. nov. habitus, male **A** dorsal view **B** lateral view **C** ventral view **D** leg I **E** pedipalp ectal **F** pedipalp mesal. Scale bars: 1 mm (**A–D**); 500 μm (**E, F**).

Mistralia ramirezi sp. nov.

https://zoobank.org/28A61E8F-6EC9-4908-A88C-791AB46769B5
Figs 35–37

Material examined. ***Holotype*.** ♂ **Chile.** Malleco: Monumento Natural Contulmo, 38.01314°S, 73.18648°W, M. Ramírez, F. Labarque coll. 10.II.2005 (MNHNCL).

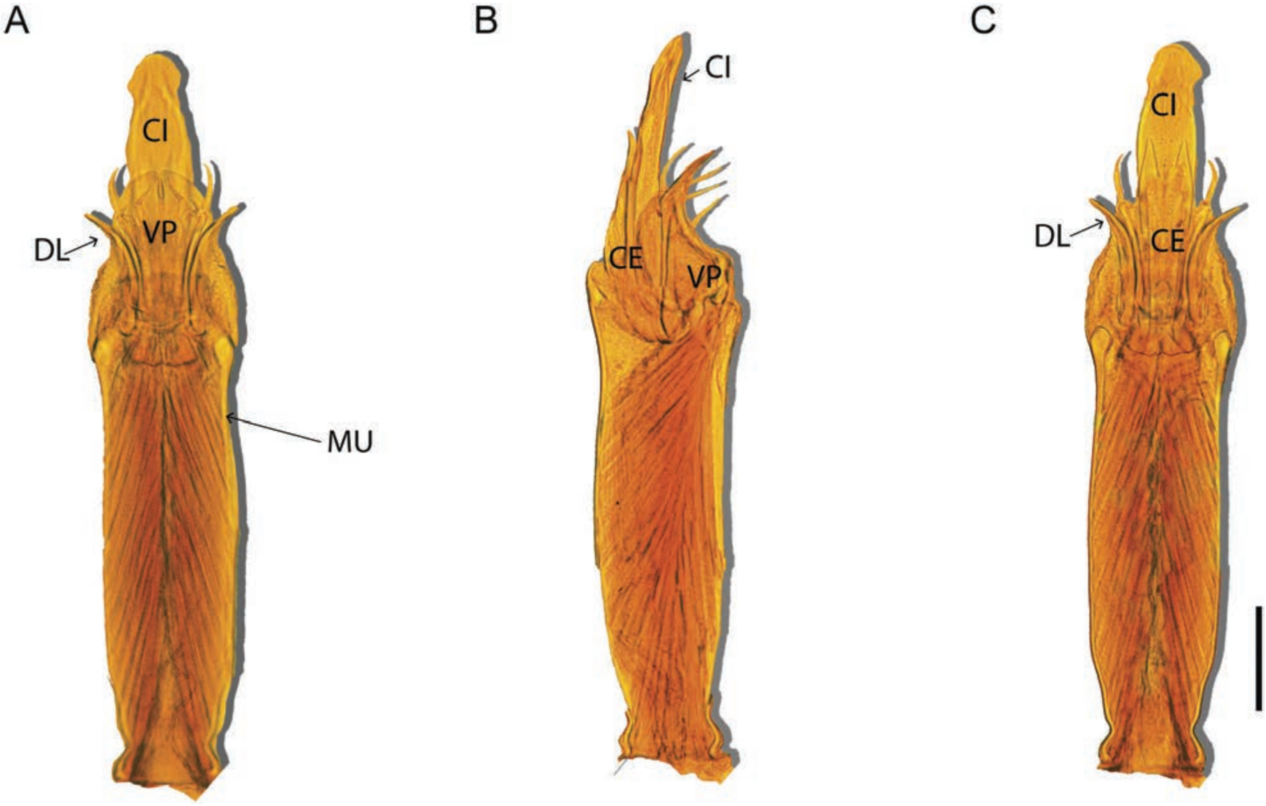

Figure 36. *Mistralia ramirezi* sp. nov. Penis ventral **A** lateral **B** dorsal **C**. Capsula interna (CI), Capsula externa (CE), dorsolateral plate (DL), ventral plate (VP), muscle (MU). Scale bar: 100 µm.

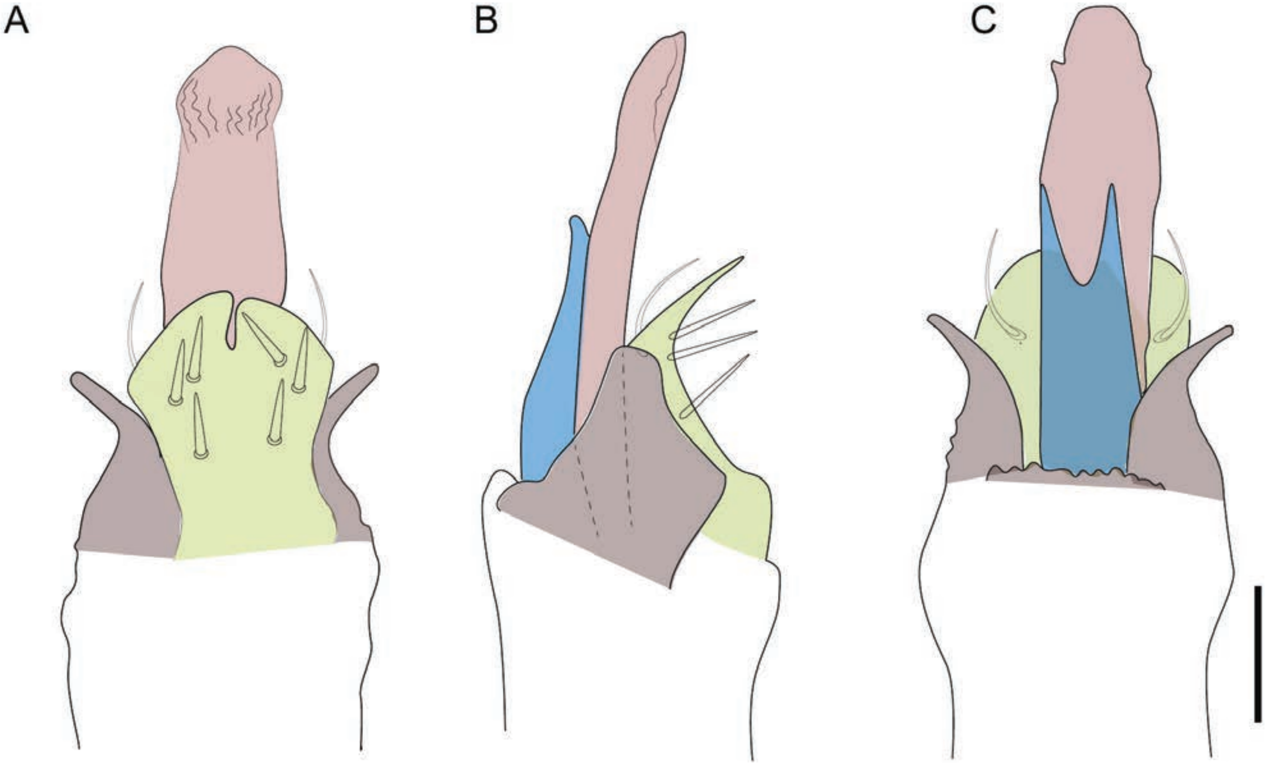

Figure 37. *Mistralia ramirezi* sp. nov. Penis ventral **A** lateral **B** dorsal **C** capsula interna (red), Capsula externa (blue), dorsolateral plate (brown), ventral plate (green). Scale bar: 100 µm.

Etymology. Patronym in honor to Argentine arachnologist, Martín Ramírez, esteemed colleague and friend, for his contributions to the field of spider taxonomy and systematics.

Diagnosis. This species can be easily distinguished from the other species in the genus by having sharp tubercles on the surface of the dorsal scute and by its unique genitalia, with a U-shaped capsula externa in dorsal view.

Distribution. Chile: Bío-Bío Region (Fig. 4B).

Description of male. Measurements: Total length 3.29, carapace length 0.77, dorsal scutum length 2.22, carapace max. width 1.72. Appendage measurements: Pedipalps. Trochanter length 0.28, femora length 1.27, patella length 0.64, tibia length 1.05, tarsus length 0.95. Leg I: trochanter (tr) 0.37, femora (fe) 0.30, patella (pa) 1.13, tibia (ti) 0.58, metatarsus (mt) 0.92, tarsus (ta) 1.03. II: tr 0.76, fe 0.34, pa 1.71, ti 0.63, mt 1.47, ta 1.75. III: tr 1.55, fe 0.36, pa 1.17, ti 0.51, mt 1.13, ta 1.44. IV: tr 0.97, fe 0.41, pa 1.56, ti 0.71, mt 1.47, ta 1.98.

Dorsum (Fig. 35). Eta (η) hourglass-shaped dorsal scutum. Ocularium elevated, with apophysis between eyes. Carapace smooth; mesotergum with areas delimited by tubercles. Areas I–IV characterized by two setiferous tubercles: posterior margin with a row of ca. 10 setiferous tubercles. Free tergites bear a row of setiferous tubercles, similar to those found on the posterior margin of the dorsal scutum.

Chelicerae. Segment II with two prominent tubercles and few granules.

Pedipalps. Femora and tibia covered with granules when viewed from dorsal and ectal perspectives. Femora with a row of three distinct ventral and dorsal spines. Patella with two mesal tubercles and one ectal tubercle, each accompanied by subdistal setae. In ventral view, tibia with four ectal and mesal spines with subdistal setae, as well as with a row of setiferous granules. Tarsus characterized by three mesal and ectal spines covered with subdistal setae.

Legs (Fig. 35D). Ventral surface: I–IV with small setiferous tubercles. Sternum arrow-shaped.

Penis (Figs 36, 37). Pars distalis with a ventral plate divided into two lamellae by a small cleft. Each lamella on the ventral surface bears three tiny macrosetae, while the dorsal surface has one macroseta. Capsula externa with a U-shaped slit, shorter in length compared to the capsula interna, which is tubular in shape.

Female. Unknown.

Mistralia verrucosa **(Maury, 1990), comb. nov.**

Figs 38–43

Nuncia verrucosa Maury, 1990: 106, figs 1–12; Maury 1992: 5; Acosta and Maury 1998: 579; Kury 2003: 22; Pérez-Schultheiss et al. 2021: 413, fig. 3c, f.

Material examined. ***Holotype*****.** ♂ **Chile.** Termas del Río Amarillo, Palena Province, E. Maury coll., 04.XII.1986 (MACN 8685). ***Paratype*** **(allotype ♀). Chile.** Los Derrumbes, Puyehue, Osorno Province, E. Maury coll., 04–05.XII.1985 (MACN 8686).

Paratypes**. Chile.** Río Palena, Aysén Province, 1 ♂ and 1 ♀, E. Maury coll., 06–07.XII.1986 (MACN 8687).

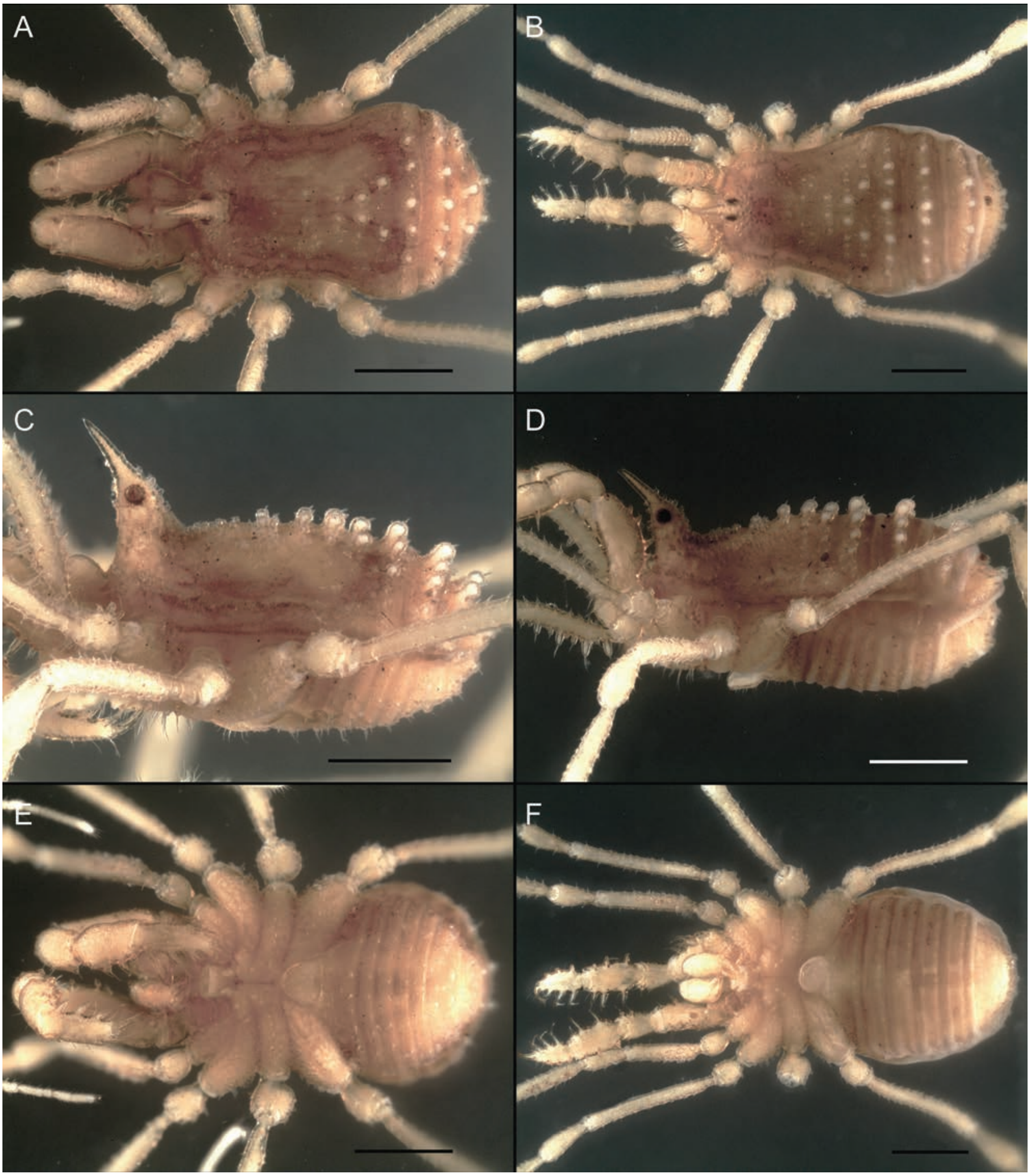

Figure 38. *Mistralia verrucosa* comb. nov. habitus, male **A** dorsal view **C** lateral view **E** ventral view. Female **B** dorsal view **D** lateral view **F** ventral view. Scale bars: 1 mm. Species of Clade B, see Fig. 3.

Additional material. Argentina. Río Negro: Parque Nacional Nahuel Huapi, Río Frías Superior, D. Anghicante coll., 26.I.1990, 2 imm. Neuquén: Lago Ortiz Basualdo, M. Ramírez coll., I.1990, 1 ♂ (MACN), P.N. Nahuel Huapi, Puerto Blest, M. Ramírez coll., 10.I.1998, 1 ♂ 1 ♀ 1 imm. (MACN). Osorno: Los Derrumbes, 5 km al S de Termas Puyehue, A. Roig coll., I.1988, 1 ♂ (MACN). Same locality, E. Maury coll., 18.I.1989, 1 ♂ (MACN). Los Derrumbes, 5 km al S de Termas Puyehue, 40.73807°S, 72.31114°W, 536 m, E. Maury coll., 04.12.1985, 1 ♀ (MACN).

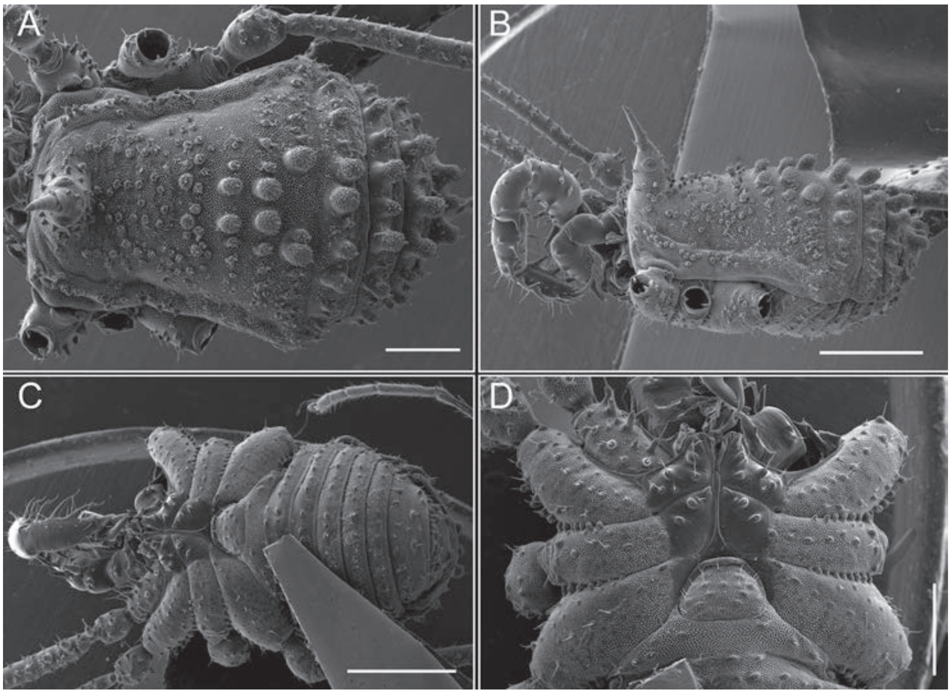

Figure 39. *Mistralia verrucosa* comb. nov. male, SEM images of habitus **A** dorsal view **B** lateral view **C, D** ventral view. Scale bars: 1 mm (**A, B, C**); 500 µm (**D**).

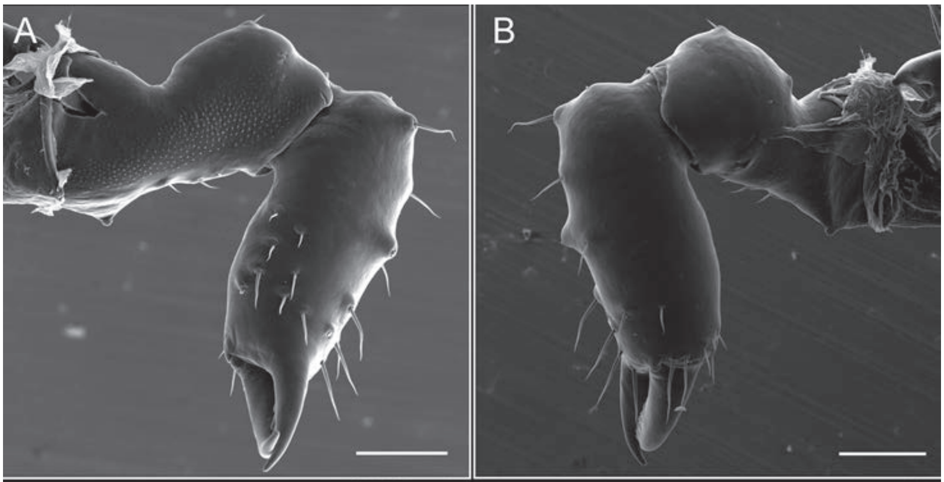

Figure 40. *Mistralia verrucosa* comb. nov. chelicerae: mesal **A** ectal **B** Pedipalps: mesal **C** ectal **D**. Scale bars: 200 µm (**A, B**); 500 µm (**C, D**).

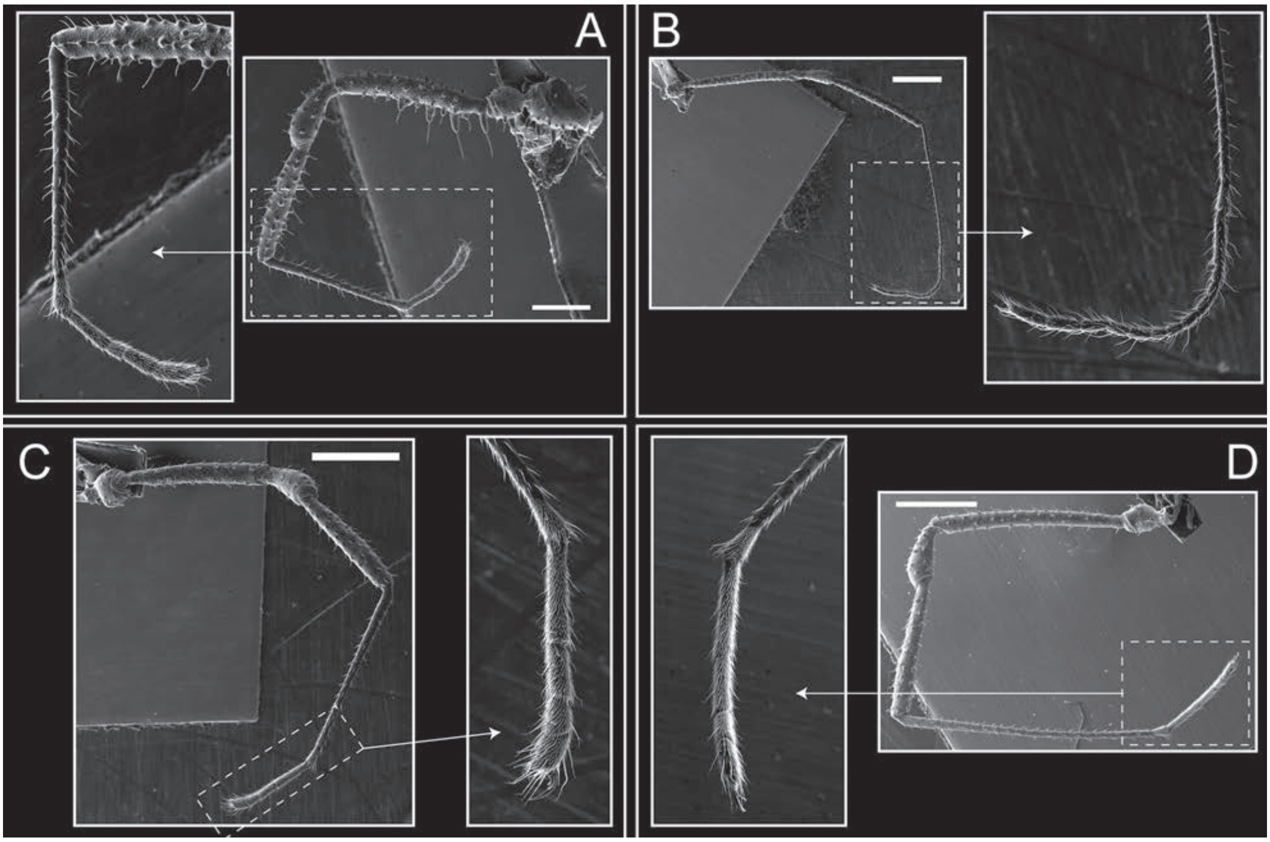

Figure 41. *Mistralia verrucosa* comb. nov. legs I **A** II **B** III **C** IV **D**. Scale bars: 1 mm.

Diagnosis. This species can be readily distinguished from other species within the genus by its distinctive ocularium with a prominent elongated process. The tubercles on the dorsal scutum are wart-like. The dorsal plate of the penis is divided into two elongated structures with small apical projections.

Distribution. Argentina: Provinces of Neuquén and Río Negro. Chile: Los Lagos Region (Fig. 4B).

Redescription of male. Measurements: Total length 3.60, length of carapace 1.16, length of dorsal scutum 2.70, max. width of carapace 1.74. max. width of mesotergum 2.00. Appendage measurements: Pedipalps. Length of trochanter 0.28, length of femora 1.15, length of patella 0.56, length of tibia 0.87, length of tarsus 0.91. Leg I: trochanter (tr) 0.36, femora (fe) 1.62, patella (pa) 0.66, tibia (ti) 1.27, metatarsus (mt) 1.44, tarsus (ta) 0.91. II: tr 0.39, fe 2.4, pa 0.73, ti 1.97, mt 2.57, ta 1.97. III: tr 0.37, fe 1.78, pa 0.63, ti 1.49, mt 2.17, ta 1.05. IV: tr 0.44, fe 2.52, pa 0.73, ti 1.77, mt 3.36, ta 1.12.

Dorsum (Fig. 38, 39). Eta (η) hourglass-shaped dorsal scutum. Anterior margin with 2–3 small setiferous tubercles on each side. Ocularium raised, with a long spine between eyes, covered in setiferous tubercles and with few setae on the spine. Carapace with fine microgranulation; adorned with warts-shaped tubercles, while the mesotergum microgranulate. Areas I–IV with setiferous tubercles, with area I having a pair of wart-shaped tubercles, and areas II–IV exhibiting 2–3 robust wart-shaped tubercles. Posterior margin adorned with a row of six wart-like tubercles. Free tergites also with a row of wart-shaped tubercles similar to those found on the posterior margin of the dorsal scutum.

Chelicerae (Fig. 40A, B). Segment I with few setae. Segment II with few granules.

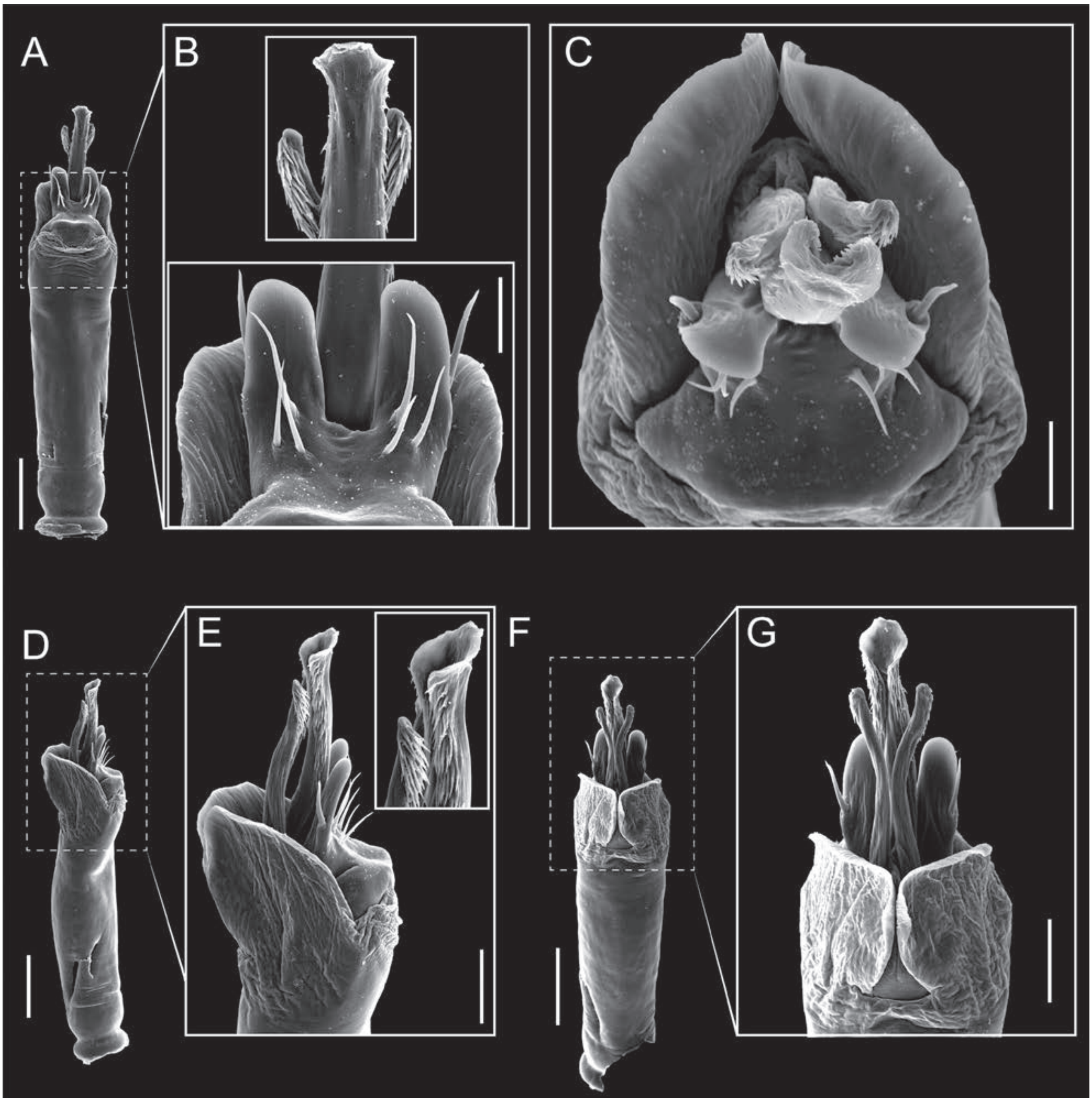

Figure 42. *Mistralia verrucosa* comb. nov. penis: ventral **A, B** apical **C** lateral **D, E** dorsal **F, G**. Scale bars: 200 µm (**A, D, F**); 100 µm (**B, E, G**); 50 µm (**C**).

Pedipalps (Fig. 40C, D). Trochanter with dorsal and ectal granules and a ventral spine with a seta. Ventral surface of femora with a row of four spines with subdistal setae and three small setiferous tubercles. In ectal view, there are 4–5 setiferous granules, while the dorsal surface features a row of three spines with subdistal setae. In mesal view, there are two distal tubercles with setae, with a row of setiferous granules on the top and bottom of the mesal surface. Dorsal surface of the patella with a few setiferous granules, while the mesal view exhibits two spines with setae, and the ectal view has setiferous granules. Tibia with setiferous granules on the dorsal and ventral surfaces, in addition to six ventral spines with subdistal setae. Tarsus with three mesal and ectal spines with subdistal setae.

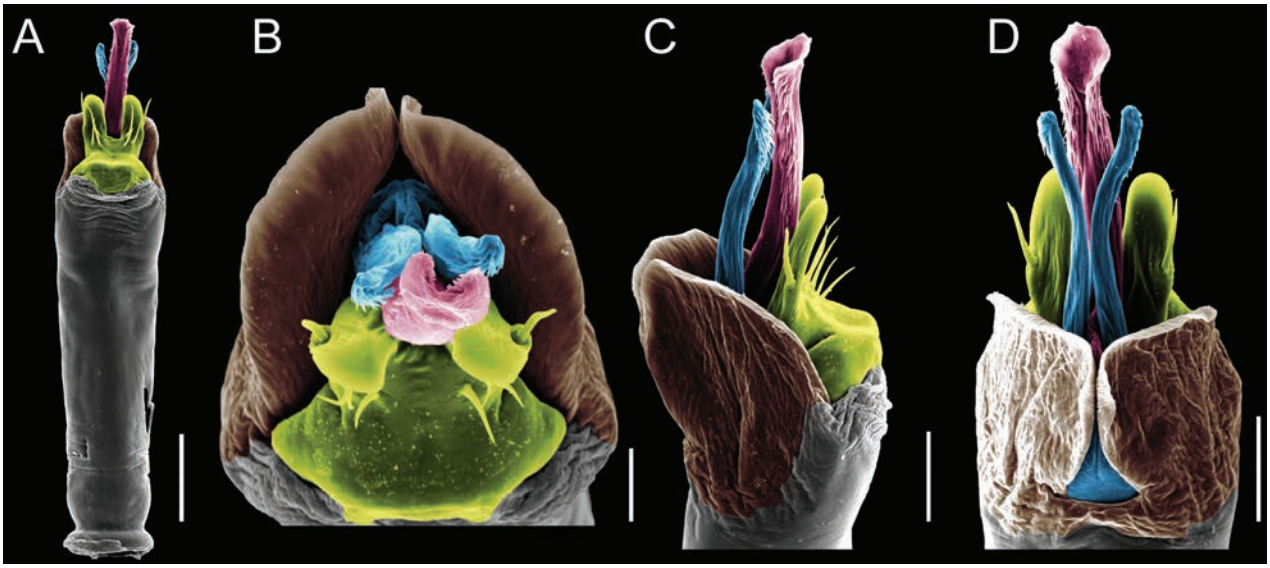

Figure 43. *Mistralia verrucosa* comb. nov. penis: ventral **A** apical **B** lateral **C** dorsal **D**. Colors: ventral plate (yellow), capsula externa (blue), capsula interna (red). Scale bars: 200 µm (**A**); 50 µm (**B**); 100 µm (**C, D**).

Legs (Fig. 41). I with three rows of small tubercles and one row of long tubercles with subdistal setae, II and III with one row of small tubercles each, and IV exhibiting microgranulation, with six bridges between coxa II–III, 8–9 eight or nine bridges between coxa III and IV, and three or four between coxa IV and opisthosoma. Spiracles visible. The smooth surface covers ~ ¼ of leg II (which features three tubercles with setae) and III and occupies < ¼ of the IV coxa (with a row of 2–3 small tubercles and a process directed towards the sternum). The opisthosomal sternites possess a row of small setiferous tubercles. Sternum arrow-shaped.

Trochanters I–IV bearing small dorsal setiferous tubercles, trochanter I with a ventral tubercle with setae. Femora I–IV bearing small setiferous tubercles. Femora I with a ventral row of remarkable spines with setae. Tarsal count: 5–10/12–4–4.

Penis (Figs 42, 43). Pars distalis equipped with a ventral plate featuring a long cleft, dividing it into two lamellae. Each lamella with three small macrosetae on its ventral surface and one macroseta on the dorsal surface. Capsula externa shorter in length compared to the capsula interna, divided into two cylindrical structures adorned with numerous small apical denticles. Capsula interna tubular in shape, with dorsal-apical denticles.

Female. Similar to the male, with shorter pedipalpal femora and without interocular apophysis.

Female measurements. Total length 3.15, length of carapace 1.52, length of dorsal scutum 2.62, max. width of carapace 1.73, max. width of mesotergum 2.28. Appendage measurements: Pedipalps. Length of trochanter 0.27, length of femora 1.21, length of patella 0.75, length of tibia 0.90, length of tarsus 1.26. Leg I: trochanter (tr) 0.34, femora (fe) 1.60, patella (pa) 0.73, tibia (ti), 1.24, metatarsus (mt) 1.51, tarsus (ta) 0.81. II: tr 0.45, fe 2.42, pa 0.83, ti 2.00, mt 2.65, ta 1.98. III: tr 0.45, fe 1.77, pa 0.75, ti 1.37, mt 2.12, ta 1.07. IV: tr 0.39, fe 2.59, pa 0.89, ti 1.88, mt 3.48, ta 1.36. Tarsal count: 4–9(10)–4–4.

Clade C

Genus *Chilenuncia* Muñoz-Cuevas, 1971, nom. rest.

Figs 44–55

Chilenuncia Muñoz-Cuevas, 1971: 873; Cekalovic 1985: 11 [considered syn. jr. of *Nuncia* Loman, 1902, by Maury 1990].
Parattahia [part]: Soares 1968: 266; Cekalovic 1985: 11; Maury and Roig Alsina 1985: 78.
Nuncia [part]: Maury 1990: 103, 105; Kury 2003: 21.

Diagnosis. It is distinguished from all other South American Triaenonychidae by the unique morphology of the male genitalia, characterized by a capsula externa that covers nearly the entire capsula interna, with a small apical cleft. The external morphology, particularly the presence of a small curved apophysis in the ocularium, allows for differentiation from other South American triaenonychid genera, although it bears resemblance to the Australian genus *Calliuncus*, which forms part of Clade C.

Type species. *Chilenuncia donosoi* Muñoz-Cuevas, 1971 (syn. jr. of *Parattahia chilensis* Soares, 1968)

Included species. *Chilenuncia chilensis* comb. nov., *Chilenuncia rostrata* comb. nov.

Distribution. Argentina: Neuquén, Río Negro. Chile, Metropolitan Region of Santiago, O'Higgins, Maule, Ñuble, Bío-Bío, Araucanía, Los Ríos, Los Lagos, and Aysén Regions (Fig. 4C).

Chilenuncia chilensis (Soares, 1968), comb. nov.

Figs 44–49

Parattahia chilensis Soares, 1968: 266, figs 13, 14; Muñoz-Cuevas 1971: 873, fig. 28; Cekalovic 1985: 11.
Nuncia chilensis: Maury 1990: 105; Acosta and Maury 1998: 579; Kury 2003: 21.
Chilenuncia donosoi Muñoz-Cuevas, 1971: 874, figs 1–28; Cekalovic 1985: 11. [Synonymy established by Maury, 1990].

Material examined. CHILE. Osorno: Puyehue, Anticura Sector, Parque Nacional Puyehue, Sendero Pionero, M. Ramírez, F. Labarque coll., 06.II.2005, 1 imm. (MACN). Llanquihue: Alerce Andino, Correntoso, M. Ramírez, F. Labarque coll., 03.II.2005, 1 imm. (MACN). Talca: RN Altos del Lircay, E Vilches Alto, A. Ojanguren, A. Pérez-González, M. Ramírez, G. Azevedo, W. Porto coll., 11.I.2018, 6 ♂ 9 ♀ 2 imm. (MACN). Cachapoal: Reserva Nacional Río de los Cipreses, near the El potrero, A. Ojanguren, A. Pérez-González, M. Ramírez, G. Azevedo, W. Porto coll., 09.I.2018, 1 ♀ 2 imm. (MACN). Curicó: El Potrero Grande, El Relvo, J. Barriga coll., 08.V.2004, 1 ♀ (MACN). Arauco: P.N. Nahuelbuta, Pichinahuel, J. Barriga coll., 22.XI.2004, 1 ♂ (MACN). Osorno: Camping "No me olvides", 7 km E de Entrelagos, E. Maury coll., 30.I.1991, 9 ♂ 7 ♀ 16 imm. (MACN). Puerto Cárdenas, T. Cekalovic coll., 31.I.1982, 1 imm. (MACN). Curicó: Los Queñes, E. Maury coll., 15.I.1984, 1 ♀ 1 imm. (MACN). Coyhaique: 10 km N de

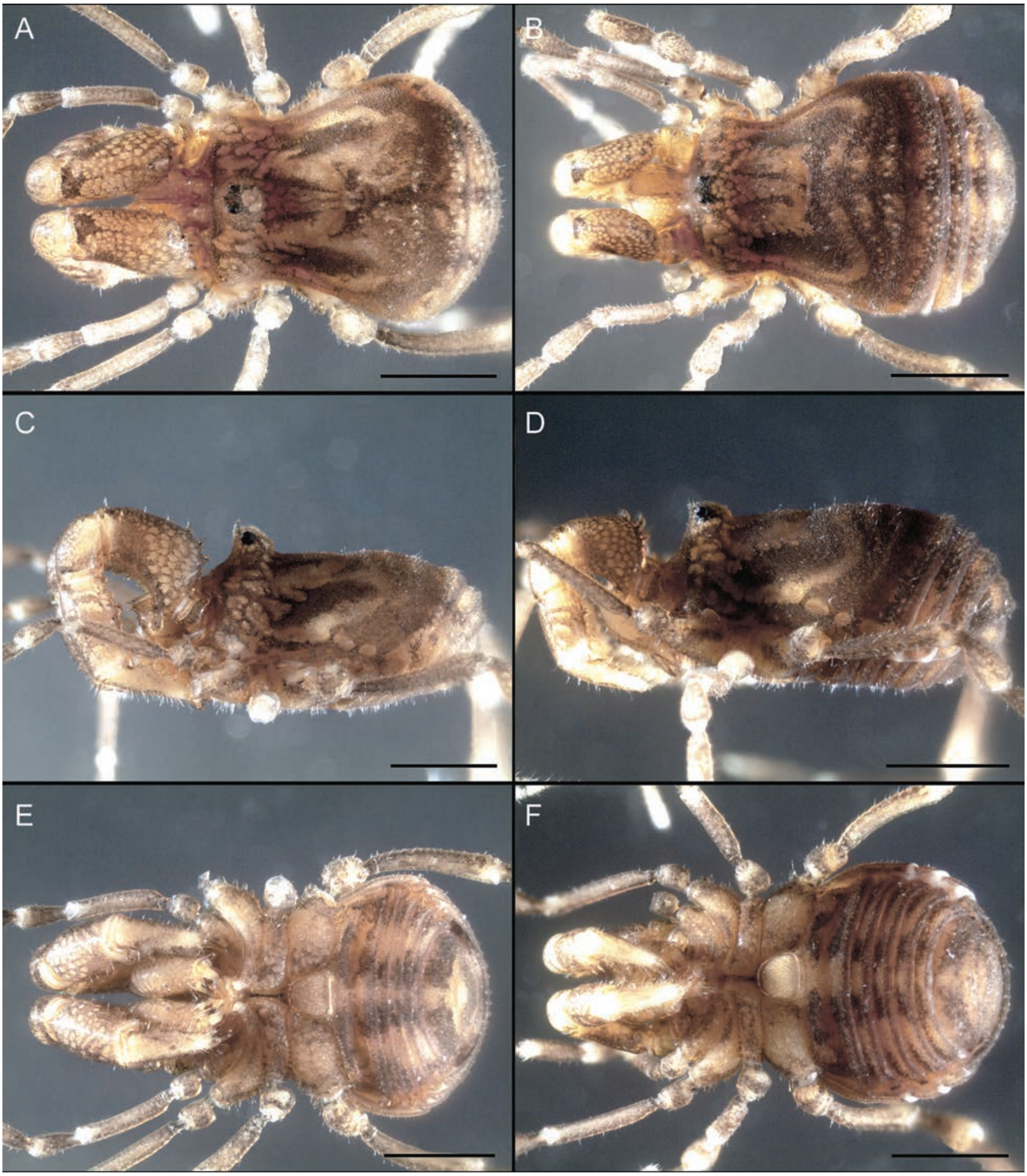

Figure 44. *Chilenuncia chilensis* comb. nov. habitus, male **A** dorsal view **C** lateral view **E** ventral view. Female **B** dorsal view **D** lateral view **F** ventral view. Scale bars: 1 mm. Species of Clade C, see Fig. 3.

Coyhaique, Reserva Nacional, S. Peck, J. Peck coll., 22.I.1985, 1 ♀ (AMNH). Frutillar Bajo, Univ. Chile Forest Res., S. Peck J. Peck coll., 22.XII.1984, 1 ♀ (AMNH). Palena: Near Chaitén, R.Schuh, N. Platnick coll., 05.XII.1981, 1 ♀ 3 imm. (AMNH); Chaitén, N. Platnick, R.Schuh coll., 07.XII.1981, 2 ♀ 1 imm. (AMNH); 25–27 km N Chaitén, N. Platnick, P. Goloboff, R.Schuh coll., 17.I.1986, 1 imm. (AMNH), Termas Río Amarillo, E. Maury coll., 04.XI.1986, 2 ♂ 1 ♀ (MACN), 11 km O de Río Negro, E. Maury coll., 08.XII.1985, 9 ♂ 1 ♀ (MACN).

La Cabaña, A. Hidalgo coll., 01.II.1982, 1 imm. Cautín: Bellavista, Fundo Flor del Lago, M. Ramírez, F. Labarque coll., 09.II.2005, 4 ♂ 1 ♀ 1 imm. (MACN), 3 ♂ 2 imm. (MACN). Llanquihue: Los Muermos, E.Ross, A.Michelbacher coll., 20. I.1951, 2 ♀; Frutillar, G. Kuschel coll., 29.IX.1954, 5 imm. Alerce Andino, Correntoso, M. Ramírez, F. Labarque coll., 03.II.2005, 6 imm. (MACN), 7 km N Enseada, N. Platnick, R.Schuh coll., 26.XI.1981, 1 imm. (AMNH), Lago Chapo, 11.7 km E Correntoso, A. Newton, M. Thayer coll., 16.XII.1982, 1 imm. (AMNH), 10–14 km E Correntoso, N. Platnick, O. Francke coll., 03.II.1985, 1 imm. (AMNH), Carretera Austral, Caleta La Arena, E. Maury coll., 07.XII.1985, 15 imm. (MACN); Playa Magui, 7 km NE Frutillar, E. Maury coll., 27.I.1991, 11 imm. (MACN); P.N. Alerce Andino, N. Platnick, K. Catley, M. Ramírez, T. Allen coll., 23.XI.1993, 1 imm. (AMNH). Argentina. Neuquén: 4 km W de Poracá, L. Herman coll., 21.I.1972, 2 imm., Road between Pucará y Laguna Venados, L. Herman coll., 25.I.1972, 4 imm., Hua Hum, E. Maury coll., 19.I.1983, 1 ♂ (MACN), Lago Huechulafquen, M. Ramírez coll., 07.I.1985, 1 imm. (MACN); Hua Hum, E. Maury coll., 17.I.1985, 2 imm. (MACN); Río Pucará S shore, Lago Lacar, 8 km E Hua Hum, N. Platnick, R.Schuh coll., 13.I.1986, 1 imm. (AMNH), Lago Tromen, E. Maury coll., 18.I.1987, 1 imm. (MACN), Nahuel Huapi, E. Maury coll., 23.XI.1987, 2 imm. (MACN). Chile. Chiloé: 5 km de Chepu, T.Cekalovic coll., 23.II.1968, 3 imm. (MACN), Cruce camino a San Pedro, T.Cekalovic coll., 26.II.1976, 8 imm. (MACN); Chepu, N. Platnick, R. Schuh coll., 29.XI.1981, 1 imm. (AMNH); 5 km N Quellón, N. Platnick, R.Schuh coll., 01.XII.1981, 2 imm. (AMNH), Piruquina, T. Cekalovic coll., 09.II.1983, 1 imm. (MACN), Isla Chiloé, 8 km S Ancud, S.Peck, J.Peck coll., 01.II.1985, 2 imm. (AMNH); Chepu, E. Maury coll., 11.XII.1985, 1 imm. (MACN); Cucas, E. Maury coll., 12.XII.1985, 5 imm. (MACN). Cautín: Parque Nacional Villarrica, M. Ramírez, F. Labarque coll., 08.II.2005, 6 imm. (MACN); Bellavista, Lago Villarrica, N. Platnick, K. Catley, M. Ramírez, T. Allen coll., 20.XI.1993, 1 imm. (AMNH); Huerquehue, Laguna Toro, M. Ramírez, F. Labarque coll., 02.VII.2005, 1 imm. (MACN), Volcán Villarrica, site 654, A. Newton, M. Thayer coll., 15.XII.1982, 7 imm. (AMNH), site 653, A. Newton, M. Thayer coll., 15.XII.1982, 1 imm. (AMNH), Molco, T. Cekalovic coll., 22.II.1983, 1 imm. (MACN), 15 km NE Villarrica, Flor del Lago, S. Peck, J. Peck coll., 01.XI.1985, 7 imm. (AMNH); Bellavista, Lago Villarrica, N. Platnick, O. Francke coll., 28.I.1985, 15 imm. (AMNH), R. Schuh, N. Platnick coll., 30.X.1986, 13 imm. (AMNH); Molco Alto, T.Cekalovic coll., 18.II.1986, 3 imm. (MACN); Ojos del Caburgua, 15 km NE de Pucón, E. Maury coll., 16.I.1987, 3 imm. (MACN), Termas de Palguin, SE de Pucón, E. Maury coll., 17.I.1987, 11 imm. (MACN). Maule: Talca, Parque Nacional Gil de Vilches, N. Platnick, P. Goloboff, M. Ramírez coll., 08.II.1992, 1 imm. (AMNH). Talca: Vilches, E. Maury coll., 16.1.1984, 3 imm. (MACN). Same collector, 07.I.1989, 10 imm. (MACN). Las Tacitas, Bordon coll., II.1972, 1 imm. Talca: A. Roig coll., 17.I.1984, 3 imm. (MACN). Maule: Curicó, Los Queñes, P. Goloboff, K. Catley coll., 17.X.1992, 2 imm. (AMNH). Malleco: Parque Nacional Nahuelbuta, M. Ramírez, F. Labarque coll., 12.II.2005, 2 ♂ 3 ♀ 4 imm. (MACN), E. Schlinger, E. Irwin coll., 09.IX.1966, 1 ♀ 1 imm., Monumento Nacional Contulmo, M. Ramírez, F. Labarque coll., 10.II.2005, 1 ♂ 1 ♀ (MACN), Puren Contulmo Nat. Mon, S.Peck, J.Peck coll., 13.II.1985, 1 ♂ (AMNH); Malalcahuello, E. Maury coll., 08.I.1987, 2 ♂ 1 ♀ (MACN); Parque Nacional Nahuelbuta, E. Maury coll., 23.XII.1985, 2 ♂ 1 ♀ (MACN). Arauco: Caramávida, E. Maury coll., 16.XII.1985, 2 ♂ 5 ♀ 7

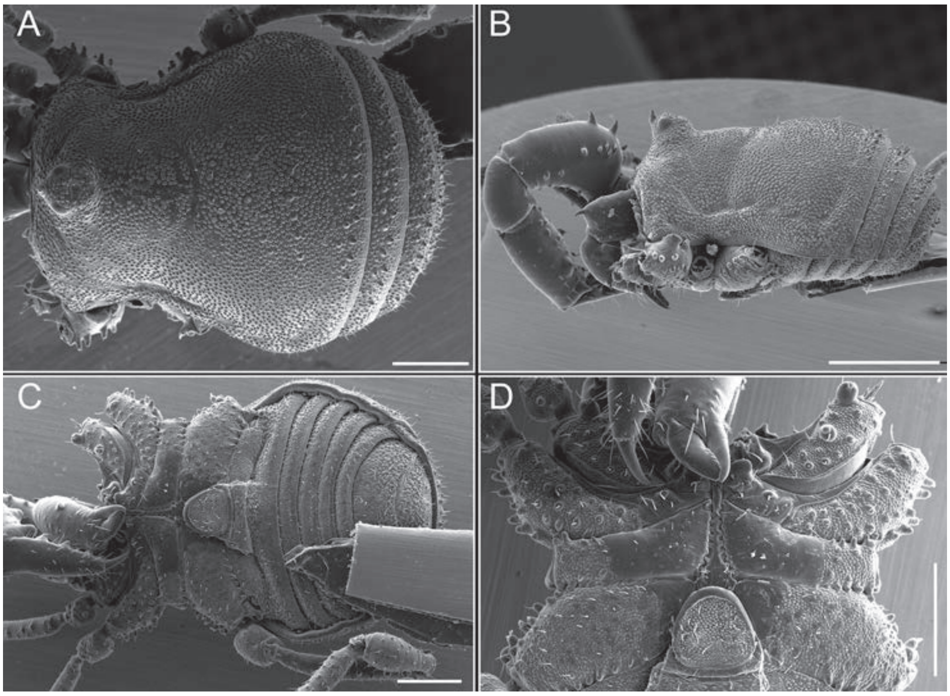

Figure 45. *Chilenuncia chilensis* comb. nov. male, SEM images of habitus **A** dorsal view **B** lateral view **C, D** ventral view. Scale bars: 500 µm.

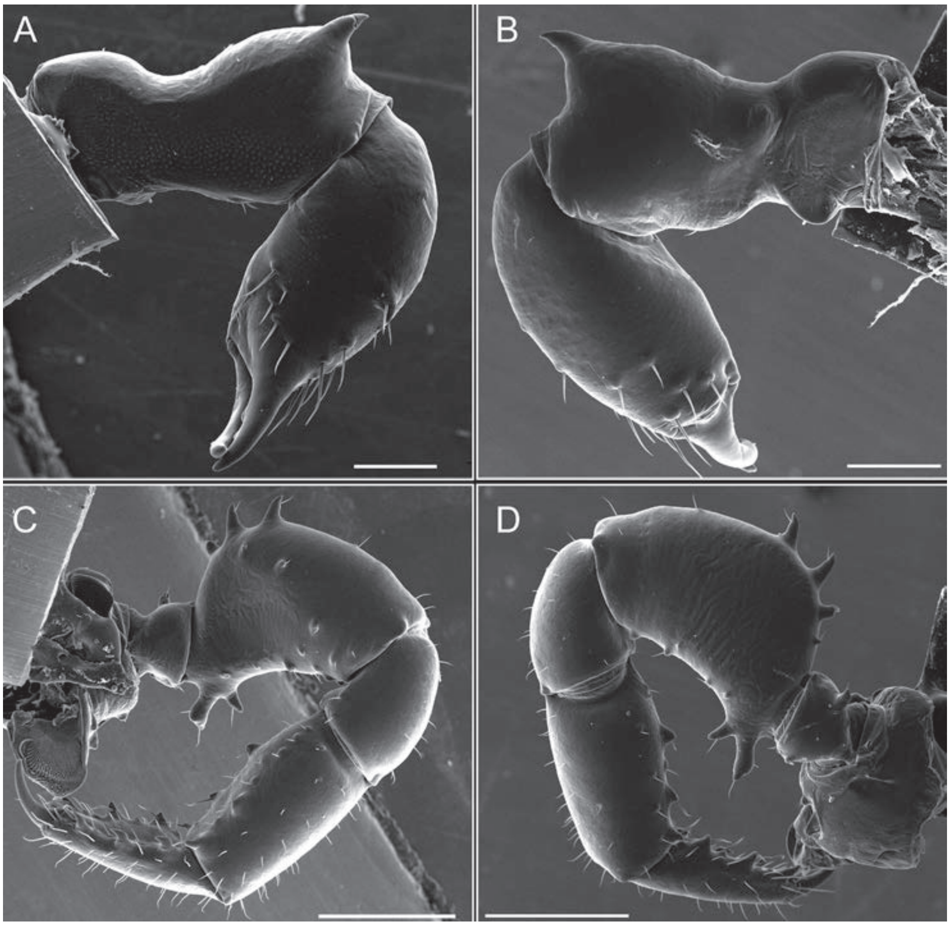

Figure 46. *Chilenuncia chilensis* comb. nov. chelicerae: mesal **A** ectal **B** Pedipalps: mesal **C** ectal **D**. Scale bars: 200 µm (**A, B**); 500 µm (**C, D**).

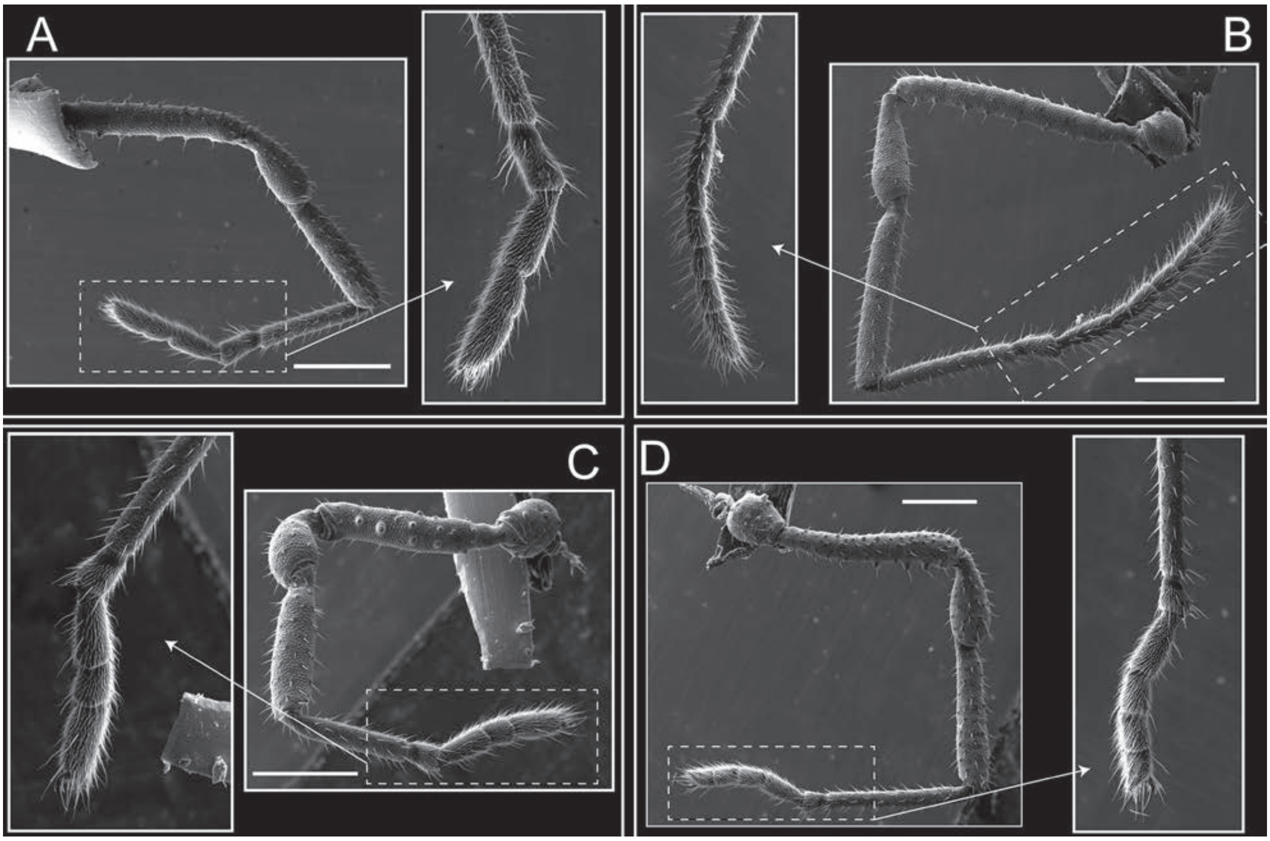

Figure 47. *Chilenuncia chilensis* comb. nov. legs I **A** II **B** III **C** IV **D**. Scale bars: 500 µm.

imm. (MACN). Ñuble: 2 km E de Las Trancas, E. Maury coll., 09.I.1989, 4 ♂ 1 ♀ (MACN). Malleco: Monumento Natural Contulmo, E. Maury coll., 10.I.1987, 3 ♀ (MACN), same collector, 13.I.1989, 2 ♂ 1 imm. (MACN), Parque Nacional Tolhuaca, 2 km E Lago Malleco, A. Newton, M. Thayer coll., 01.I.1983, 1 ♀ (AMNH). Osorno: 36 km W. La Union, L. Peña coll., 25.III.1987, 2 imm. (AMNH). Ñuble: 22.7 km ESE Recinto, site 646, A. Newton, M. Thayer coll., 10.XII.1982, 1 imm. (AMNH). Valdivia: 26 km SE Panguipulli, S. Peck, J. Peck coll., 16.XII.1984, 1 imm. (AMNH). Osorno: Águas Calientes, P. N. Puyehue, N. Platnick, R.Schuh coll., 28.I.1986, 1 imm. (AMNH), Hills of Maicolpue, N. Platnick, P. Goloboff, M. Ramírez coll., 19.II.1992, 1 imm. (AMNH), 10 km E of Bahia Mansa, N. Platnick, O. Francke coll., 30.I.1985, 4 imm. (AMNH); Puyehue, Anticura Sector, Parque Nacional Puyehue, Sendero Pionero, M. Ramírez, F. Labarque coll., 05.II.2005, 10 imm. (MACN); Antillanca road, 6–8 km SE Aguas Calientes, P. N. Puyehue, N. Platnick, R.Schuh coll., 28.I.1986, 3 imm. (AMNH), Termas de Puyehue, N. Platnick, R.Schuh coll., 24.XI.1981, 2 imm. (AMNH). Valdivia: Lago Calafquen, T.Cekalovic coll., 18.II.1977, 2 imm. (MACN). Osorno: Los Derrumbes, 5 km S de Termas de Puyehue, E. Maury coll., 09.I.1988, 5 imm. (MACN). Valdivia: Río Nahuicán, 24 km SE Corral, E. Maury coll., 16.I.1989, 5 imm. (MACN). Osorno: Anticura, E. Maury coll., 09.I.1988, 3 imm. (MACN). Valdivia: Pirehucico, E. Maury coll., 01.XII.1985, 10 imm. (MACN). Osorno: Los Derrumbes, E. Maury coll., 04.XII.1985, 9 imm. (MACN). Valdivia: Niebla, Camping “La Herradura”, 8 km East of Niebla, E. Maury coll., 23.I.1991, 10 imm. (MACN); Pirehucico, E. Maury coll., 18.I.1985, 5 imm. (MACN). Osorno: Los Derrumbes, E. Maury coll., 09.I.1988, 1 imm. (MACN). Termas Puyehue, S. Roig coll., I.1988, 1

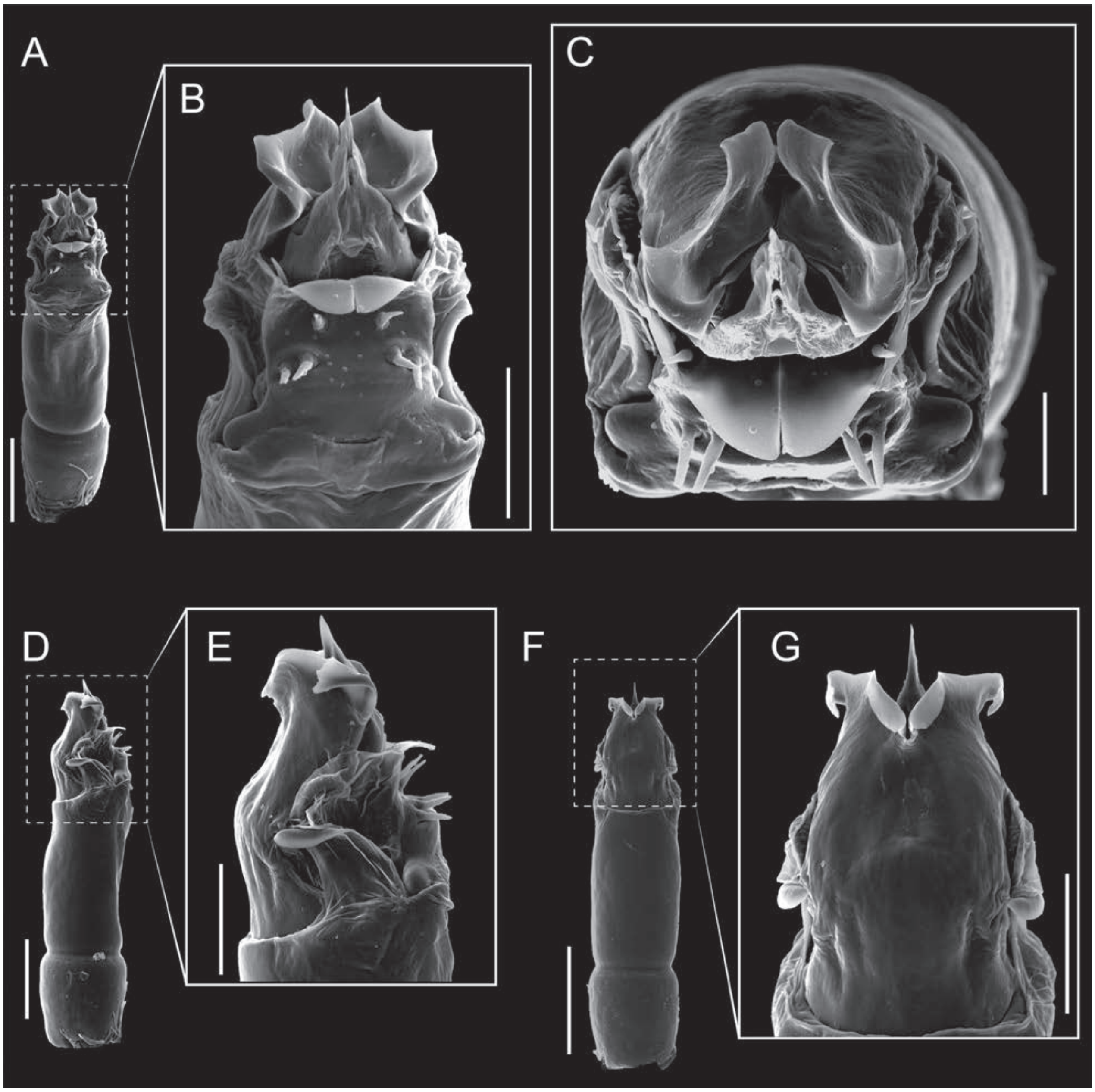

Figure 48. *Chilenuncia chilensis* comb. nov. penis: ventral **A, B** apical **C** lateral **D, E** dorsal **F, G**. Scale bars: 200 µm (**A, D, F**); 100 µm (**B, E, G**); 50 µm (**C**).

imm. (MACN), Arrededores de Puerto Montt, L. Pereira coll., 28.XI.1992, 1 ♀ (MACN). Osorno: Camping "No me olvides", 7 km E de Entrelagos, E. Maury coll., 30.I.1991, 7 imm. (MACN). 3 imm. (MACN), Termas de Río Amarillo, SE de Chaitén, E. Maury coll., 01.XII.1986, 3 imm. (MACN). Los Lagos: Sector Anticura, Parque Nacional Puyehue, Sendero Pionero, G. Giribet, G. Hormiga, A. Pérez-González coll., 17.XI.2014, 1 ♂ (MACN). Cautín: Parque Nacional Villarrica, M. Ramírez, F. Labarque coll., 08.II.2005, 1 imm. (MACN). Malleco: Parque Nacional Nahuelbuta, 2 imm. (MACN). Vilches: Las Tacitas, Bordon coll., II.1972, 1 imm. La Cabaña, T. Cekalovic coll., 01.II.1987, 1 imm. (MACN).

Diagnosis. This species, *C. chilensis*, can be readily distinguished from *C. rostrata* by its much shorter ocular process. Furthermore, it possesses a notch on

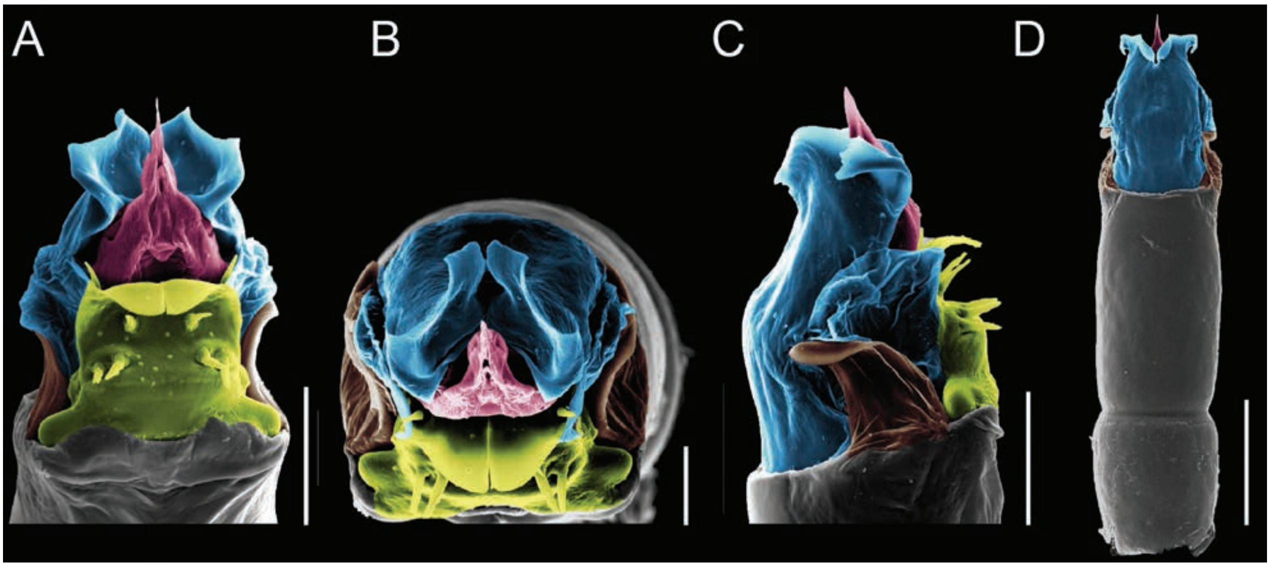

Figure 49. *Chilenuncia chilensis* comb. nov. penis: ventral **A** apical **B** lateral **C** dorsal **D**. Colors: ventral plate (yellow), capsula externa (blue), capsula interna (red). Scale bars: 100 µm (**A, C, D**); 50 µm (**B**).

tarsus I and six tarsomeres on leg II (males), whereas *C. rostrata* exhibits seven tarsomeres on the same leg.

Distribution. Argentina: Provinces of Neuquén and Río Negro. Chile, Metropolitan Region of Santiago, O'Higgins, Maule, Ñuble, Bío-Bío, Araucanía, Los Ríos, and Los Lagos (Fig. 4C).

Redescription male. Measurements: Total length 3.40, carapace length 1.44, dorsal scutum length 2.66, carapace max. width 1.63, mesotergum max. width 2.31. Appendage measurements: Pedipalps. Trochanter length 0.25, femora length 1.32, patella length 0.79, tibia length 1.16, tarsus length 0.91. Leg I: trochanter (tr) 0.25, femora (fe) 1.22, patella (pa) 0.61, tibia (ti) 0.80, metatarsus (mt) 1.08, tarsus (ta) 0.82. II: tr 0.30, fe 1.71, pa 0.69, ti 1.23, mt 1.25, ta 1.37. III: tr 0.36, fe 1.05, pa 0.53, ti 0.83, mt 0.86, ta 0.97. IV: tr 0.41, fe 1.55, pa 0.81, ti 1.24, mt 1.44, ta 1.16.

Dorsum (Fig. 44, 45). Eta (η) hourglass-shaped dorsal scutum. Ocularium elevated and rounded, with a small frontal small apophysis perpendicular to the body. Dorsal scutum microgranulate, without distinct delimitation of areas. Areas I–IV with an arcuate row of small setiferous tubercles; posterior margin with two rows of small setiferous tubercles. All free tergites ornamented with small setae and with two rows of small setiferous tubercles.

Chelicerae (Fig. 46A, B). Segment I with an acute tubercle in the dorso-distal portion, providing a distinctive feature. Segment II with a small frontal tubercle and adorned with only a few setae.

Pedipalps (Fig. 46C, D). Trochanter with a dorsal tubercle adorned with setae and a small ventral spine. Femora with dorsal row of four small spines with subdistal setae, in ventral view with two long proximal spines with subdistal setae and a row of small tubercles. In mesal view, with six low setiferous tubercles. Patella with a smooth surface; tibia with two ectal and mesal tubercles with subdistal setae, a row of four small ventroproximal setiferous tubercles, and a row of three small ectal setiferous tubercles. Tarsus with three mesal and ectal tubercles with subdistal setae, with a few setae.

Legs (Fig. 47). Coxa I with two rows of setiferous tubercles, along two distal setiferous tubercles with subdistal setae. Coxa II with two rows of setiferous tubercles, while coxae III and IV feature only microgranulation. Three bridges between legs II and III, six between III and IV, and 4–8 between leg IV and the opisthosoma, with the distal bridge longer than the others. Spiracles unobstructed by bridges. A smooth surface covers ~ ⅓ of leg II, ¾ of leg III, and < ⅓ of leg IV. Within the smooth area of leg II, there is a small tubercle on each side, accompanied by subdistal setae. Sternum arrow-shaped, with serrated margins, and the posterior area forms a triangle. Segments I–IV covered in setae, tarsal area, and calcaneus densely setose. Tibiae I–III with a ventral and dorsal row of small setiferous tubercles, whereas tibia IV has a row of four distal-ventral tubercles with setae. Calcaneus smaller than astragalus, ≥ 3× smaller in leg I, 4× smaller in legs II–III, and 5× smaller in leg IV. Tarsal count: 4–6–4–4.

Penis (Figs 48, 49). Pars distalis with a large ventral cleft that divides the plate into two lamellae. Each lamella is equipped with three pointed macrosetae on the ventral surface and one macroseta on the dorsal surface. Capsula externa covers dorsal and lateral surfaces and exhibits a V-shaped medial notch, which divides the dorsal fold into two halves. A dorsolateral plate appears attached to the pars basalis. Capsula interna slightly longer than capsula externa and partially covers ventral plate. Capsula interna formed by two parts fused in the apical region and with a visible stylus in its medial portion.

Female. Similar to male, with shorter pedipalpal femora, presence of interocular process and a different tarsal count: 3–6–4–4.

Female measurements: Total length 2.87, carapace length 1.19, dorsal scutum length 2.38, carapace max. width 1.47, mesotergum max. width 2.14. Appendage measurements: Pedipalps. Trochanter length 0.28, femora length 0.96, patella length 0.55, tibia length 0.82, tarsus length 0.75. Leg I: trochanter (tr) 0.20, femora (fe) 1.08, patella (pa) 0.55, tibia (ti) 0.76, metatarsus (mt) 0.89, tarsus (ta) 0.74. II: tr 0.29, fe 1.32, pa 0.66, ti 1.08, mt 1.17, ta 1.30. III: tr 0.26, fe 1.01, pa 0.48, ti 0.69, mt 0.88, ta 0.78. IV: tr 0.32, fe 1.26, pa 0.71, ti 1.17, mt 1.28, ta 1.09.

Chilenuncia rostrata **(Maury, 1990), comb. nov.**

Figs 50–55

Nuncia rostrata Maury, 1990: 110, figs 25–35; Maury 1992: 4; Kury 2003: 22; Pérez-Schultheiss et al. 2019: 20; Pérez-Schultheiss et al. 2021: 412, fig. 3a, d.

Material examined. ***Holotype*****.** ♂ **CHILE.** Llanquihue, Caleta La Arena, 50 km S de Puerto Montt, Carretera Austral, 07–08.XII.1985 (MACN 8703). ***Paratype*** **(allotype ♀). CHILE.** Llanquihue, Caleta La Arena, 50 km S de Puerto Montt, Carretera Austral, 07–08.XII.1985 (MACN 8704). ***Paratypes*****.** CHILE. Llanquihue, Caleta La Arena, 50 km S de Puerto Montt, Carretera Austral, 07–08.XII.1985 (MACN 8705).

Additional material. CHILE. Llanquihue: 35 km W. Río Negro, R.Schuh, N. Platnick coll., 24.I.1986, 1 ♀ (AMNH). Chiloé: Chiloé Island, 5 km N of Quellón,

Figure 50. *Chilenuncia rostrata* comb. nov. habitus, male **A** dorsal view **C** lateral view **E** ventral view. Female **B** dorsal view **D** lateral view **F** ventral view. Scale bars: 1 mm.

R.Schuh, N. Platnick coll., 01.XII.1981, 1 ♀ 1 imm. (AMNH), Isla Chiloé, R.Schuh, N. Platnick coll., 29.XI.1981, 1 ♂ 1 ♀ (AMNH). Llanquihue: P.N. Alerce Andino, N. Platnick, K.Catley, M. Ramírez, T.Allen coll., 23.XI.1993, 1 ♀ 2 imm. (AMNH). Palena: Termas de Pichicolo, 11 km west of Río Negro, Carretera Austral, E. Maury coll., 08.XII.1985, 1 ♀ (MACN 8706). Aysén: 30 km NE de Puerto Cisnes, E. Maury coll., 08.XII.1986, 2 ♀ 3 imm. (MACN 8707).

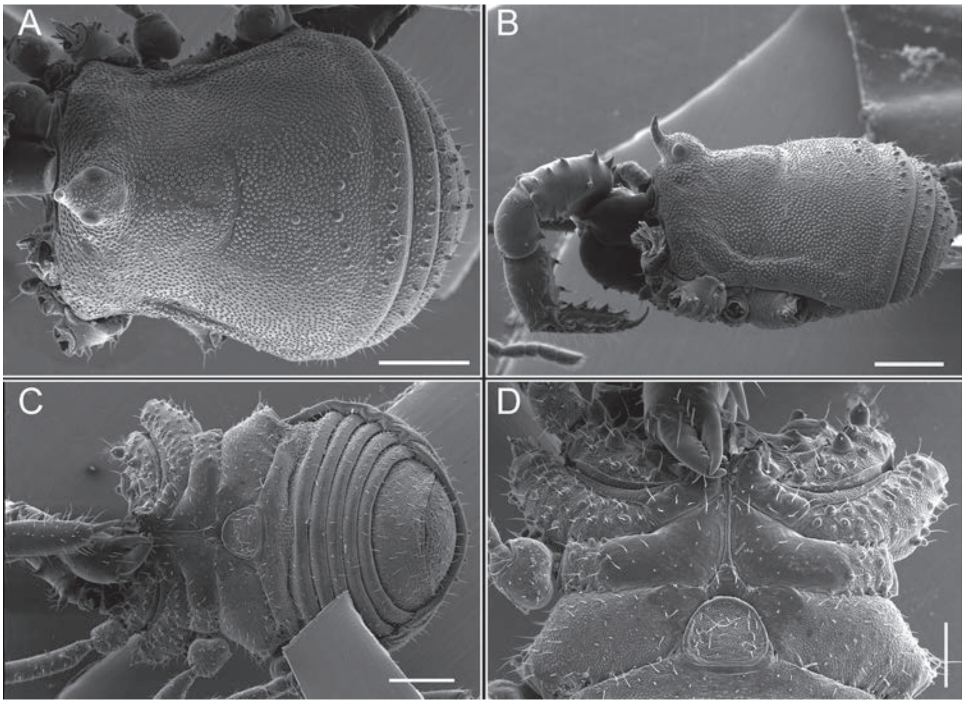

Figure 51. *Chilenuncia rostrata* comb. nov. male, SEM images of habitus **A** dorsal view **B** lateral view **C, D** ventral view. Scale bars: 500 µm (**A, B, C**); 200 µm (**D**).

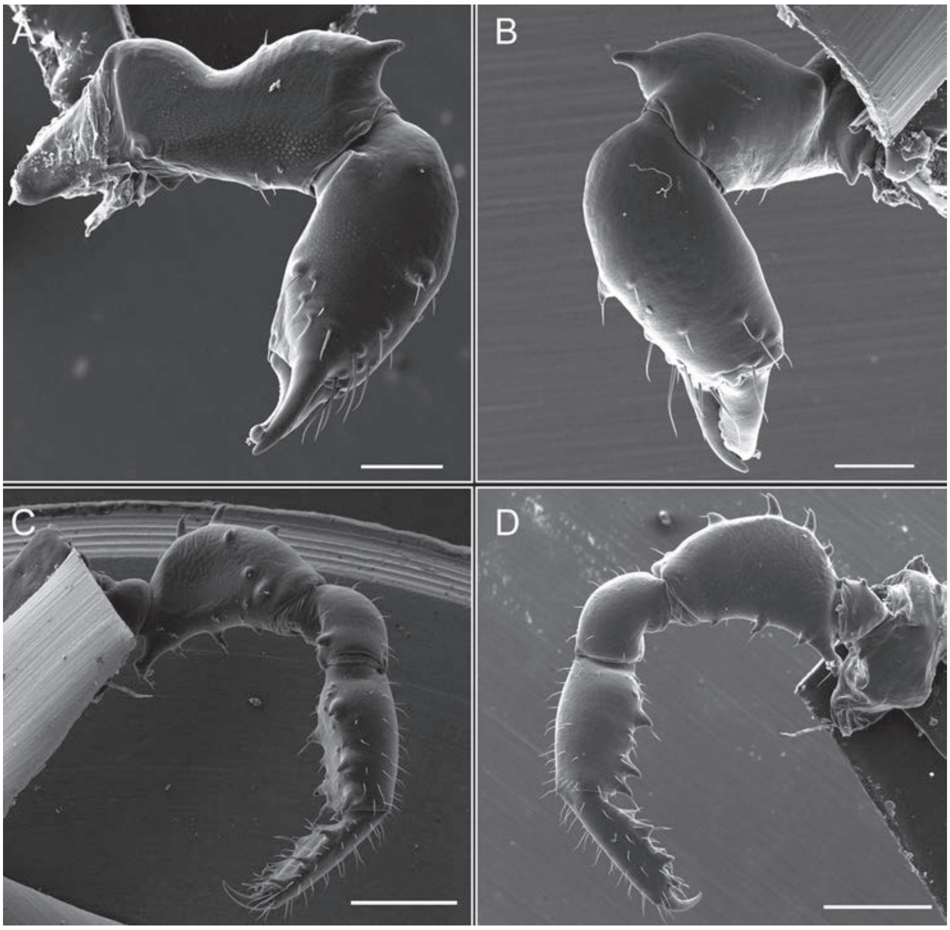

Figure 52. *Chilenuncia rostrata* comb. nov. chelicerae: mesal **A** ectal **B** Pedipalps: mesal **C** ectal **D**. Scale bars: 200 µm (**A, B**); 500 µm (**C, D**).

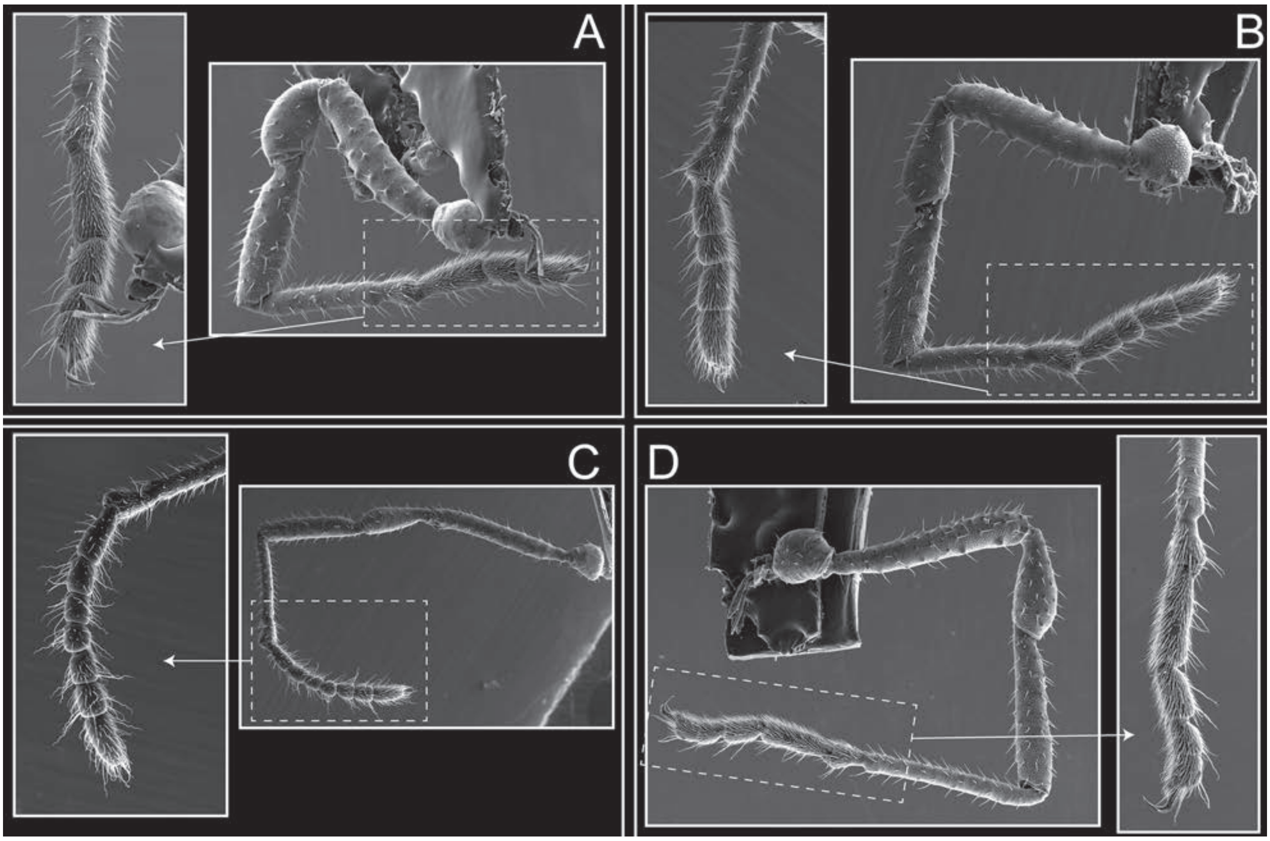

Figure 53. *Chilenuncia rostrata* comb. nov. legs I **A** II **B** III **C** IV **D**. Scale bars: 500 µm (**A, B, D**); 200 µm (**C**).

Diagnosis. This species can be readily distinguished from *C. chilensis* by the prominent interocular apophysis, which is notably longer in *C. rostrata*. Additionally, *C. rostrata* possesses seven tarsomeres on leg II (males), whereas *C. chilensis* has six. These characteristics serve as key distinguishing features between the two species.

Distribution. Chile: Los Lagos and Aysén Regions (Fig. 4C).

Redescription of male (MACN 8705). Measurements: Total length 2.97. Carapace length 1.07, dorsal scutum length 2.09, carapace max. width 1.49, mesotergum max. width 1.94. Appendage measurements: Pedipalps. Trochanter length 0.25, femora length 0.95, patella length 0.55, tibia length 0.68, tarsus length 0.66. Leg I: trochanter (tr) 0.25, femora (fe) 0.87, patella (pa) 0.50, tibia (ti) 0.70, metatarsus (mt) 0.89, tarsus (ta) 0.85. II: tr 0.33, fe 1.28, pa 0.54, ti 0.96, mt 1.08, ta 1.45. III: tr 0.32, fe 0.81, pa 0.43, ti 0.66, mt 0.77, ta 0.85. IV: tr 0.34, fe 1.15, pa 0.61, ti 0.95, mt 1.31, ta 1.03.

Dorsum (Fig. 50, 51). Eta (η) hourglass-shaped dorsal scutum. Ocularium elevated, with a long, backward-curving apophysis. Eyes located laterally in the middle of the ocular structure. Dorsal scutum microgranulate and without clear delimitation of areas. Area I with a pair of setae, while areas II–IV display an arcuate row of small setae tubercles. Posterior margin characterized by a row of small setiferous tubercles. All free tergites with a row of small setiferous tubercles.

Chelicerae (Fig. 52A, B). Segment I with a small tubercle on its dorso-distal surface; segment II with a mesal tubercle and bears a few setae.

Pedipalps (Fig. 52C, D). Trochanter with a small dorsal and ectal tubercle. Femora with two ventroproximal and one ventromedial spine with subdistal se-

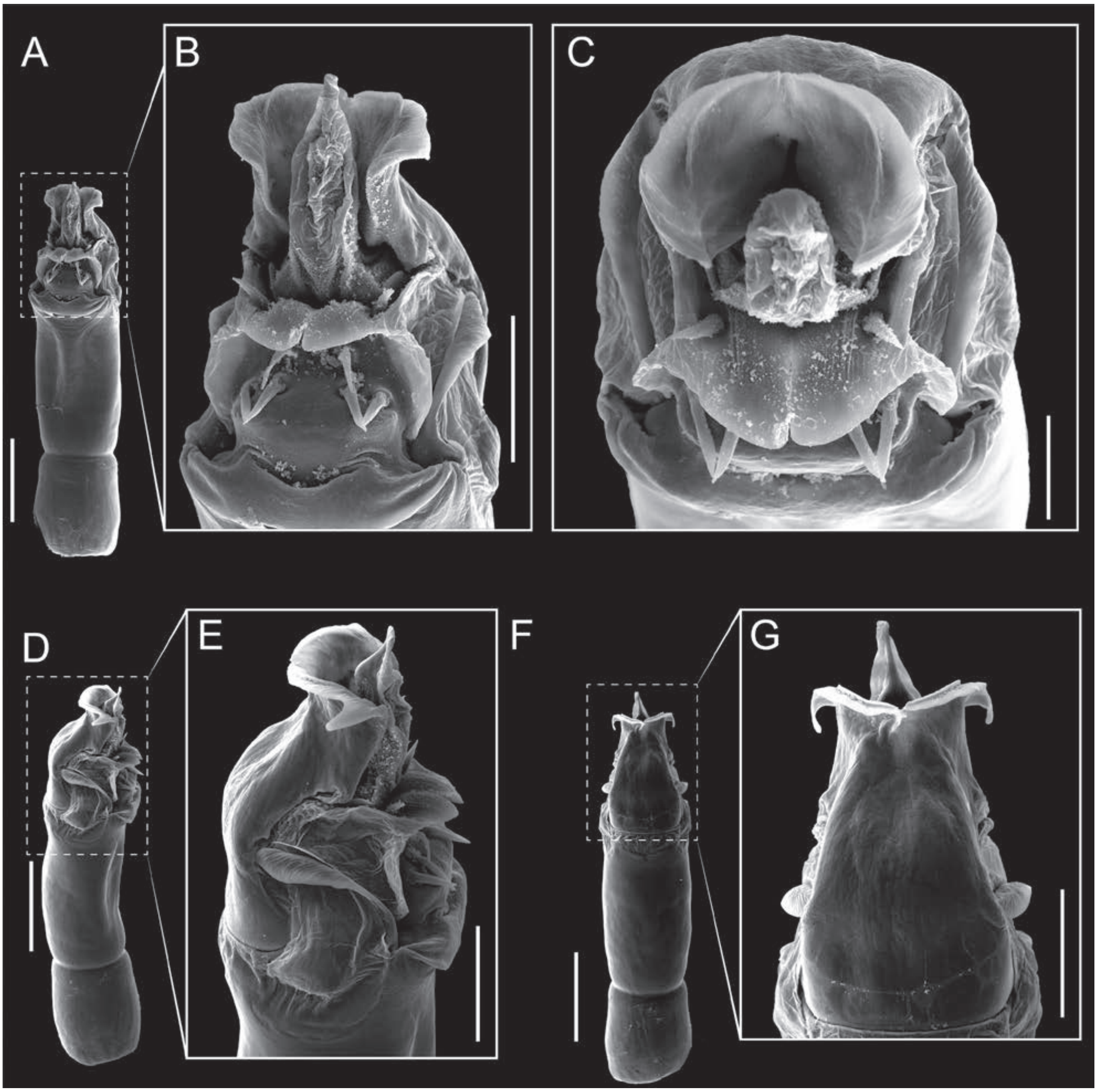

Figure 54. *Chilenuncia rostrata* comb. nov. penis: ventral **A, B** apical **C** lateral **D, E** dorsal **F, G**. Scale bars: 200 µm (**A, D, F**); 100 µm (**B, E, G**); 50 µm (**C**).

tae, with two distal setiferous granules and three dorsoproximal tubercles with subdistal setae. Mesal surface of femora with 2–3 distal setiferous granules. Patella with a ventral setiferous tubercle. Tibia with four ectal and three mesal spines with subdistal setae, while the ventral surface presents small setiferous granules. Tarsus with three mesal and four ectal spines with subdistal setae, as well as a few setae and granules.

Legs (Fig. 53). Coxa I with a row of setiferous tubercles, with two distal setiferous tubercles with subdistal setae. Coxae II–III also with setiferous tubercles, while Coxa IV with only microgranulation. Four bridges between legs II and III, and five or six bridges between legs III and IV. Spiracles not obstructed by bridges. A smooth surface covers ~ ¹⁄₃ of leg II, ¾ of leg III, and < ¹⁄₃ of leg IV. Within the smooth area of leg II, two small tubercles with subdistal

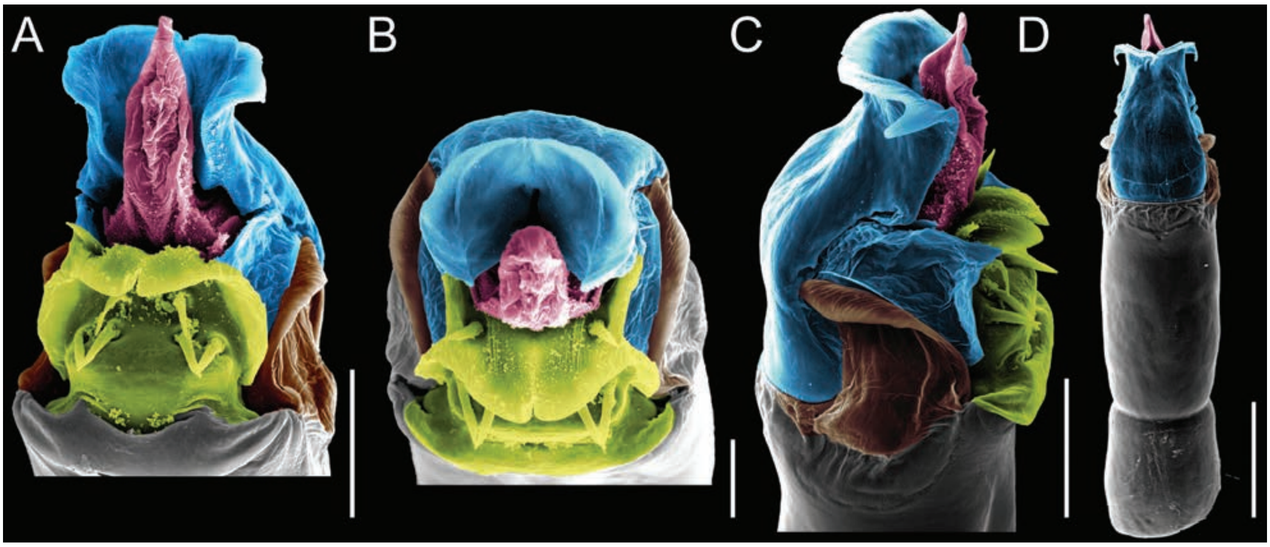

Figure 55. *Chilenuncia rostrata* comb. nov. penis: ventral **A** apical **B** lateral **C** dorsal **D**. Colors: ventral plate (yellow), capsula externa (blue), capsula interna (red). Scale bars: 100 µm (**A, C, D**); 50 µm (**B**).

setae can be observed on each side. Sternum arrow-shaped, with a triangular posterior area. Smooth, covered in setae, without a notch on tarsus I. Tarsal count 4–7–4–4.

Penis (Figs 54, 55). Pars distalis with large ventral cleft that divides the plate into two lamellae. Each lamella with three pointed macrosetae on the ventral surface and one macroseta on the dorsal surface. Capsula externa covers dorsal and lateral surfaces, exhibiting a small medial notch that divides the apical region of the capsula externa. With a dorsolateral plate attached to the pars basalis. Capsula interna slightly longer than capsula externa and partially covers the ventral plate. Capsula interna sac-shaped in appearance.

Female. Similar to male, with shorter pedipalpal femora and interocular apophysis.

Female measurements. Total length 3.17. Carapace length 0.98, dorsal scutum length 2.12, carapace max. width 1.38, mesotergum max. width 2.08. Appendage measurements: Pedipalps. Trochanter length 0.21, femora length 0.83, patella length 0.45, tibia length 0.59, tarsus length 0.62. Leg I: trochanter (tr) 0.23, femora (fe) 0.84, patella (pa) 0.52, tibia (ti) 0.69, metatarsus (mt) 0.82, tarsus (ta) 0.64. II: tr 0.30, fe 1.13, pa 0.52, ti 0.89, mt 0.92, ta 1.23. III: tr 0.30, fe 0.73, pa 0.40, ti 0.72, mt 0.79, ta 0.73. IV: tr 0.30, fe 1.13, pa 0.60, ti 0.90, mt 1.27, ta 0.93. Tarsal count: 3–6–4–4.

Genus *Laftrachia* gen. nov.

https://zoobank.org/4BE5CC16-9A40-4F4C-A0EB-7632F000E1F5
Figs 56–61

Etymology. The specific epithet derives from Laftrache (which in Mapudungun, Mapuche Language, means “little people”) also known as Caftranche, a mythical being present in Mapuche mythology. Feminine grammatical gender.

Diagnosis. This monotypic genus is characterized by its small size, yellow-orange coloration, a prominent ectal-distal process on the pedipalp femora, a low

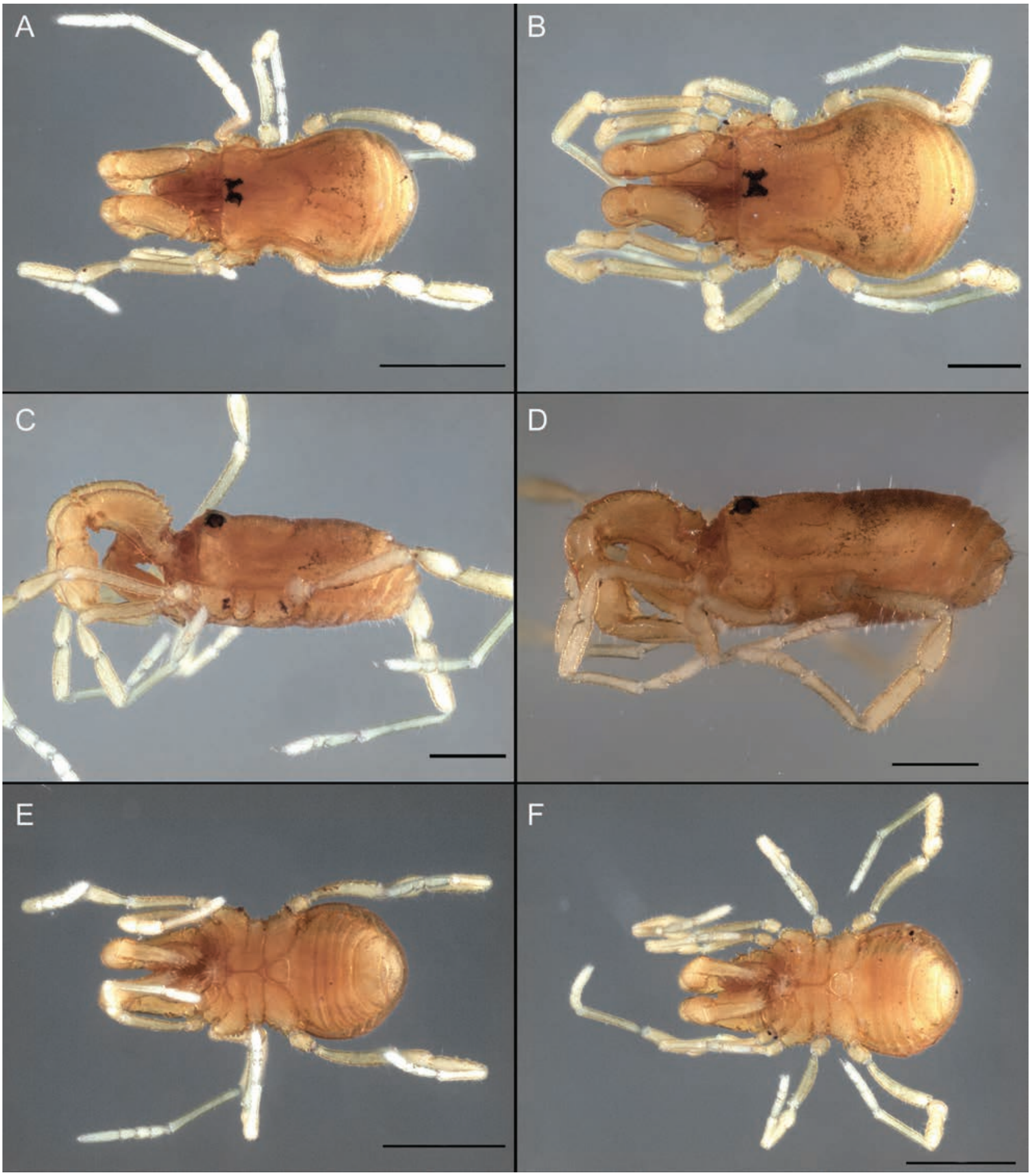

Figure 56. *Laftrachia robin* sp. nov. habitus, male **A** dorsal view **C** lateral view **E** ventral view. Female **B** dorsal view **D** lateral view **F** ventral view. Scale bars: 500 µm. Species of Clade C, see Fig. 3.

ocularium, and distinct male genital morphology. The male genitalia exhibits an arc-shaped ventral plate and a pair of parallel projections within the capsula interna. These distinguishing features differentiate it from other genera within the family Triaenonychidae.

Type species. *Laftrachia robin* sp. nov.

Included species. *Laftrachia robin* sp. nov.

Distribution. Chile: Bío-Bío Region (Fig. 4D).

Laftrachia robin sp. nov.

https://zoobank.org/2BBB0B84-397C-4384-B5A9-3B8A73478123

Figs 56–61

Material examined. ***Holotype*.** ♂ **CHILE.** Arauco: San Alfonso, Quebrada Caramávida, Arauco Reserve, 37.70942°S, 73.17107°W, 750 m, M. Ramírez, A. Ojanguren, A. Pérez-González, G. Azevedo, W. Porto coll., 15.I.2018 (MNHNCL). ***Paratypes*.** **CHILE.** Arauco: San Alfonso, Quebrada Caramávida, Arauco Reserve, 37.70942°S, 73.17107°W, 750 m, M. Ramírez, A. Ojanguren, A. Pérez-González, G. Azevedo, W. Porto coll., 15.I.2018, 1 ♂ 6 ♀ (MACN).

Etymology. The species name, a noun in apposition, is a reference to the DC comics character "Robin" (https://www.dccomics.com/characters/robin). The black pigmentation in the eye region of the species is similar to the mask used by the character in his appearances.

Description of male. Measurements: Total length 1.65, carapace length 0.66, dorsal scutum length 1.28, max. carapace width 0.87, max. dorsal scutum width 1.14. Appendage measurements: Pedipalps. Trochanter length 0.18, femora length 0.88, patella length 0.30, tibia length 0.51, tarsus length 0.50. Leg I: trochanter (tr) 0.16, femora (fe) 0.56, patella (pa) 0.29, tibia (ti) 0.42, metatarsus (mt) 0.37, tarsus (ta) 0.46. II: tr 0.17, fe 0.75, pa 0.32, ti 0.53, mt 0.82, ta 0.57. III: tr 0.18, fe 0.51, pa 0.21, ti 0.27, mt 0.44, ta 0.50. IV: tr 0.22, fe 0.69, pa 0.39, ti 0.57, mt 0.67, ta 0.73.

Dorsum (Fig. 56, 57). Eta (η) hourglass-shaped dorsal scutum. Ocularium low, lacking a medial spine. Carapace covering ~ ½ of the dorsal scutum, displaying furrows on the posterior area and distinct lateral edges. Free tergites with a smooth surface.

Chelicerae (Fig. 58A, B). Segment I characterized by the presence of five ventral tubercles and three dorsal tubercles, all adorned with subdistal setae. Segment II with a total of 11 ectal tubercles, five mesal tubercles, and approximately seven frontal tubercles.

Pedipalps (Fig. 58C, D). Trochanter with a dorsal tubercle. Femora with a row of four ventral tubercles, a row of dorsal tubercles adorned with subdistal setae, and a long distal ectal apophysis. Patella with a pair of small ventral tubercles with setae. Tibia with two ventral rows of tubercles, with three small tubercles and two setiferous tubercles on the mesal side, and a row of six small setiferous tubercles on the ectal side. Tarsus equipped with three tubercles featuring ectal and mesal subdistal setae.

Legs (Fig. 59). Coxa I with four small proximal tubercles, one medial tubercle with subdistal setae, and three distal tubercles (two small and one with subdistal seta). Coxa II with scattered small tubercles with setae. Coxae III and IV smooth, while the cerotegument covers the distal portion of leg III and almost the entire leg IV. Bridge is present. Spiracles visible. Sternum arrow-shaped. Trochanter of leg I and femora of legs I and II covered in small tubercles with setae. Tibia of leg IV covered with small tubercles with setae. Metatarsus-tarsus of all legs densely setose. Tarsus occupies almost the entire length of metatarsus. Tarsal count: 3–4–3–4.

Penis (Figs 60, 61). Pars distalis with an arcuate ventral plate without a cleft, characterized by three ventral and one dorsal macrosetae each side. Capsula

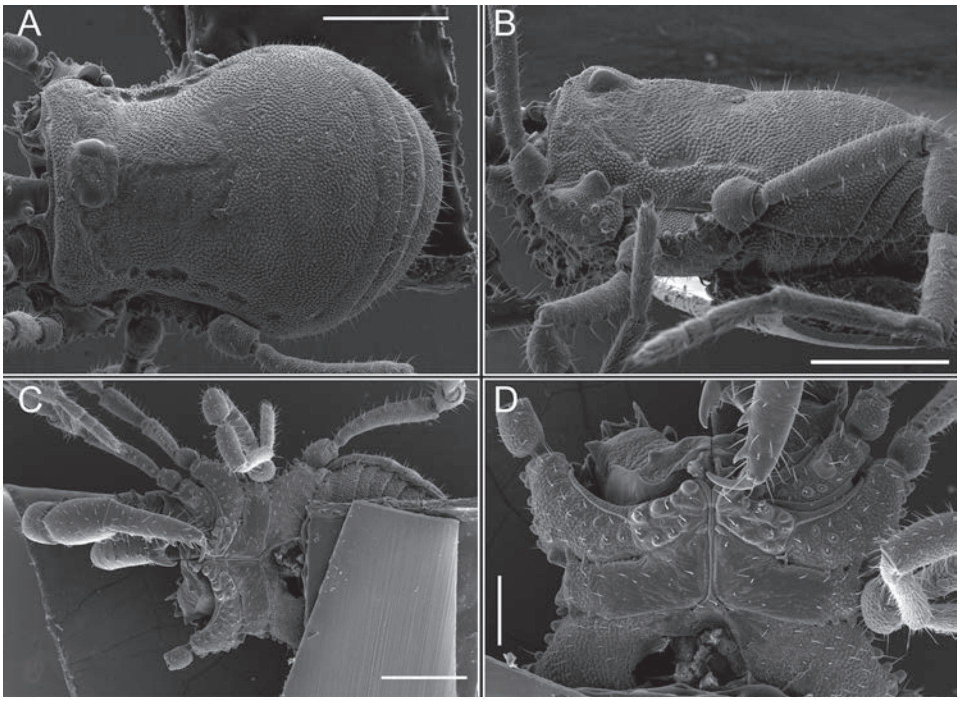

Figure 57. *Laftrachia robin* sp. nov. male, SEM images of habitus **A** dorsal view **B** lateral view **C, D** ventral view. Scale bars: 500 µm.

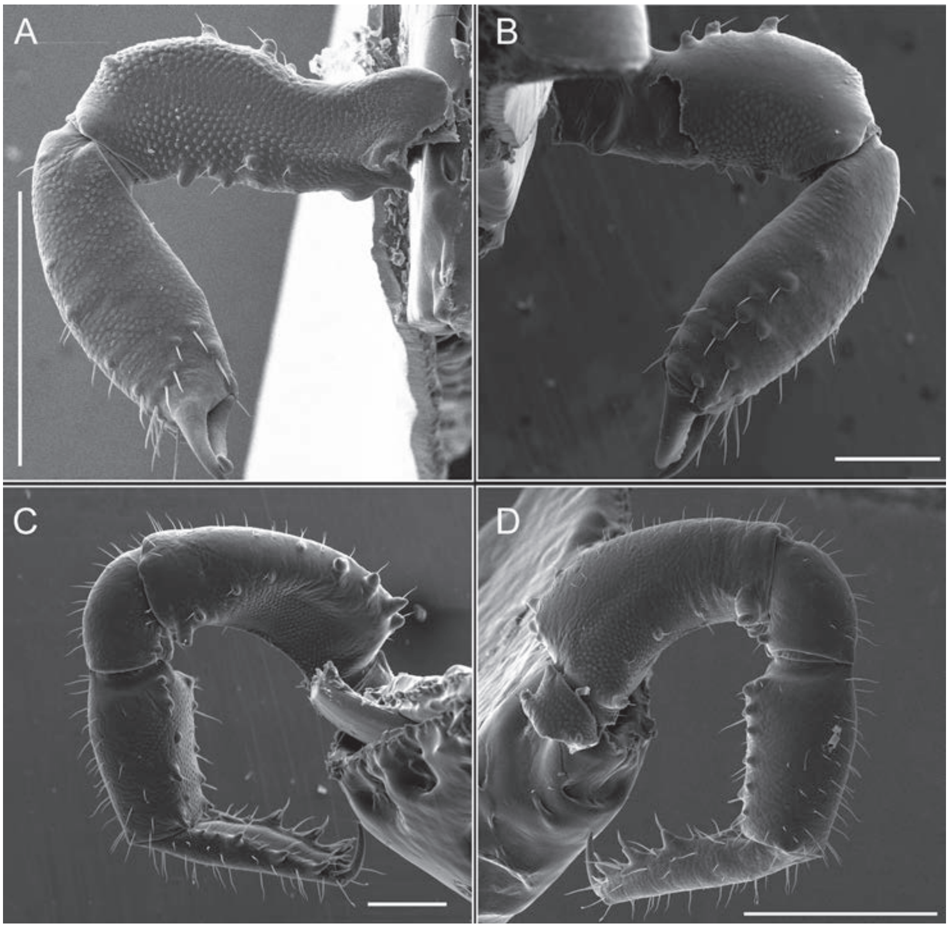

Figure 58. *Laftrachia robin* sp. nov. chelicerae: mesal **A** ectal **B** Pedipalps: mesal **C** ectal **D**. Scale bars: 500 µm.

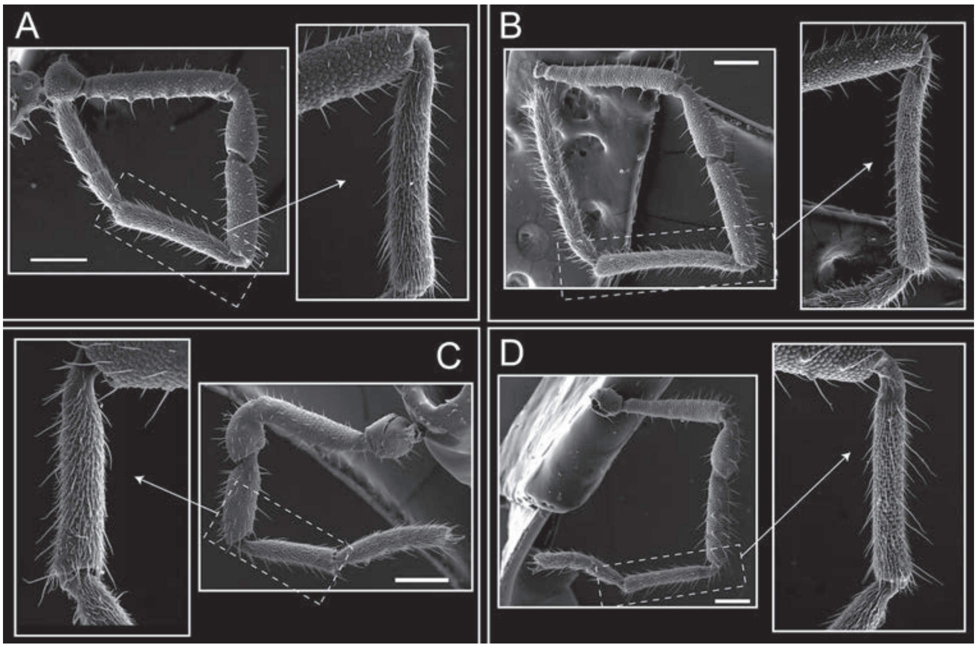

Figure 59. *Laftrachia robin* sp. nov. legs I **A** II **B** III **C** IV **D**. Scale bars: 200 µm.

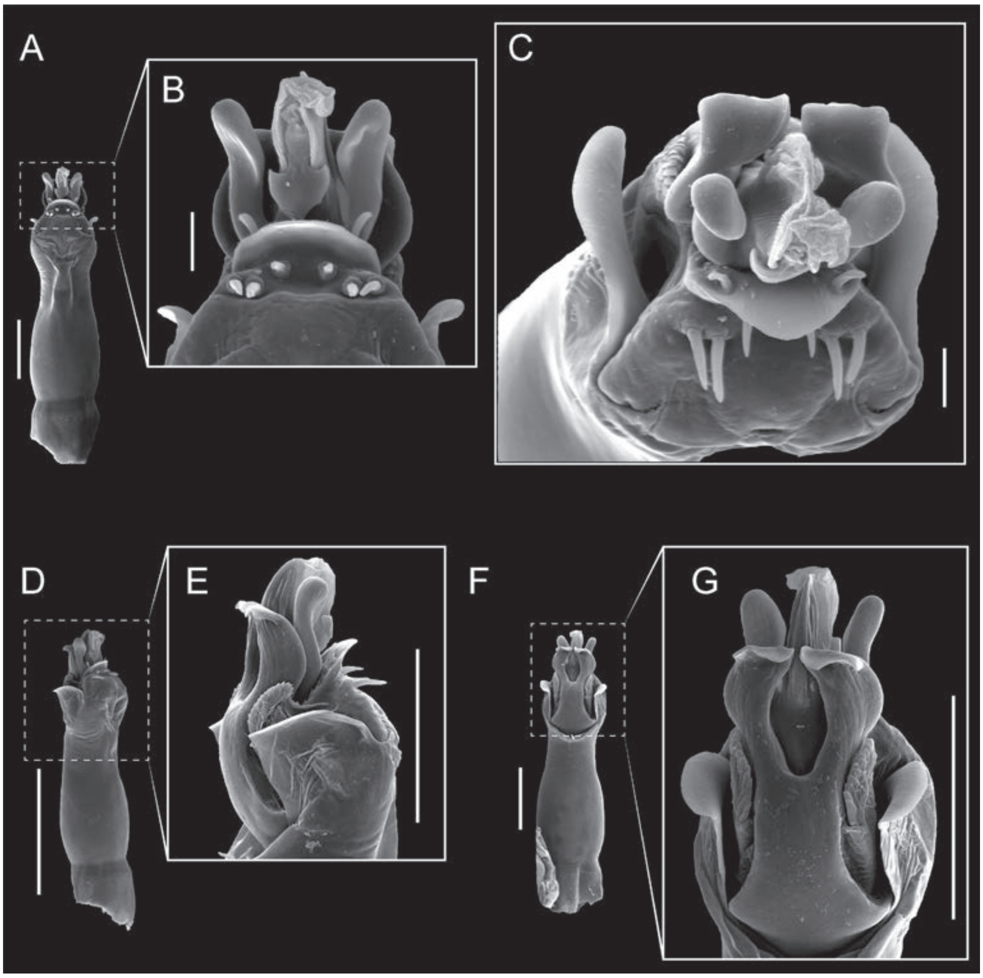

Figure 60. *Laftrachia robin* sp. nov. penis: ventral **A, B** apical **C** lateral **D, E** dorsal **F, G**. Scale bars: 100 µm (**A, D, E, F**); 20 µm (**B, C**); 50 µm (**G**).

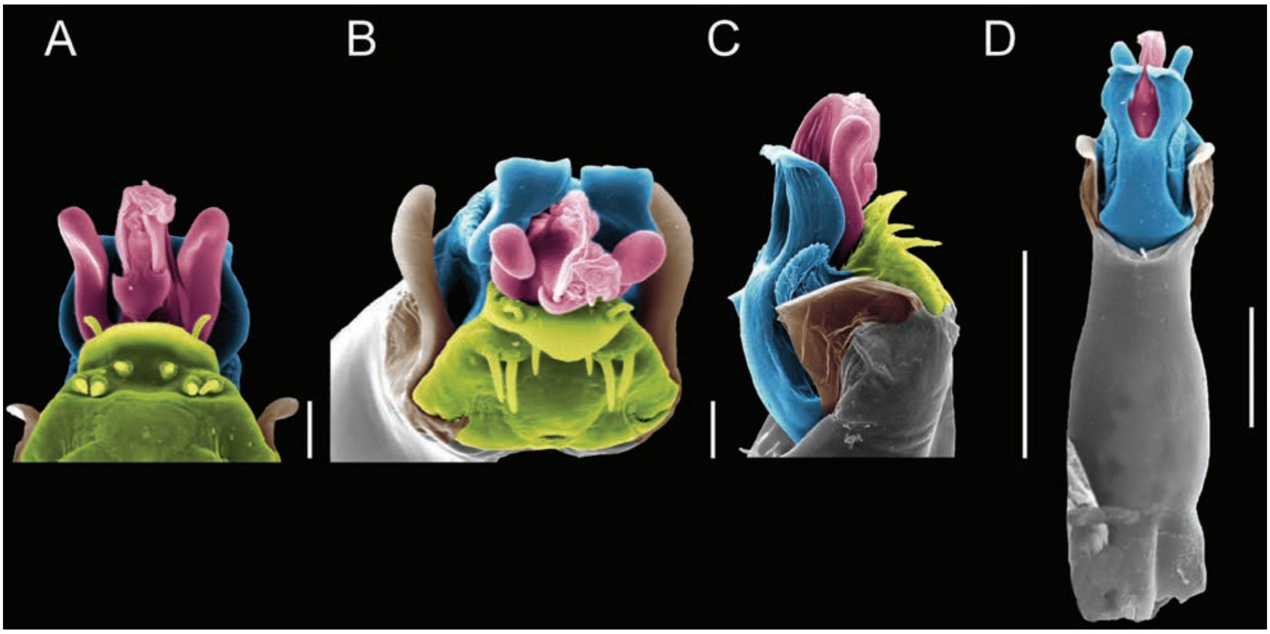

Figure 61. *Laftrachia robin* sp. nov. penis: ventral **A** apical **B** lateral **C** dorsal **D**. Colors: ventral plate (yellow), capsula externa (blue), capsula interna (red). Scale bars: 20 µm (**A, B**); 100 µm (**C, D**).

externa shorter than capsula interna and with a dorsal cleft that divides it into two dorsal halves. Additionally, there are lateral folds present on each side, and a dorsolateral plate surrounds the capsula externa. Capsula interna trifid, with two lateral processes running parallel to stylus. Stylus membranous and shaped like an inflatable bag.

Female. Similar to male, but with certain differences: pedipalps are shorter, lacks ectal-distal apophysis present on pedipalp femora of male.

Female measurements. Total length 1.75, carapace length 0.71, dorsal scutum length 1.46, carapace max. width 0.84, mesotergum max. width 1.23. Appendage measurements: Pedipalps. Trochanter length 0.17, femora length 0.63, patella length 0.34, tibia length 0.46, tarsus length 0.45. Leg I: trochanter (tr) 0.12, femora (fe) 0.57, patella (pa) 0.31, tibia (ti) 0.38, metatarsus (mt) 0.48, tarsus (ta) 0.44. **II**: tr 0.17, fe 0.80, pa 0.35, ti 0.51, mt 0.77, ta 0.80. **III**: tr 0.18, fe 0.47, pa 0.25, ti 0.32, mt 0.44, ta 0.50. **IV**: tr 0.22, fe 0.72, pa 0.38, ti 0.53, mt 0.66, ta 0.60.

Genus *Lautaria* gen. nov.

https://zoobank.org/DBD404FC-68B8-4EE6-8BB9-8E58588C2867
Figs 62–67

Etymology. The genus name honors Lautaro (Leftraru), a renowned toqui (Mapuche military leader) who played a significant role in the Arauco War during the early stages of the Spanish conquest of what is now Chile. The name is derived from Mapudungun, with "lef" meaning "fast" and "traru" or "bald traro." The feminine grammatical gender is used for the generic epithet.

Diagnosis. *Lautaria* can be distinguished from all other genera of Triaenonychidae by the unique male genital morphology (Fig. 66, 67). This

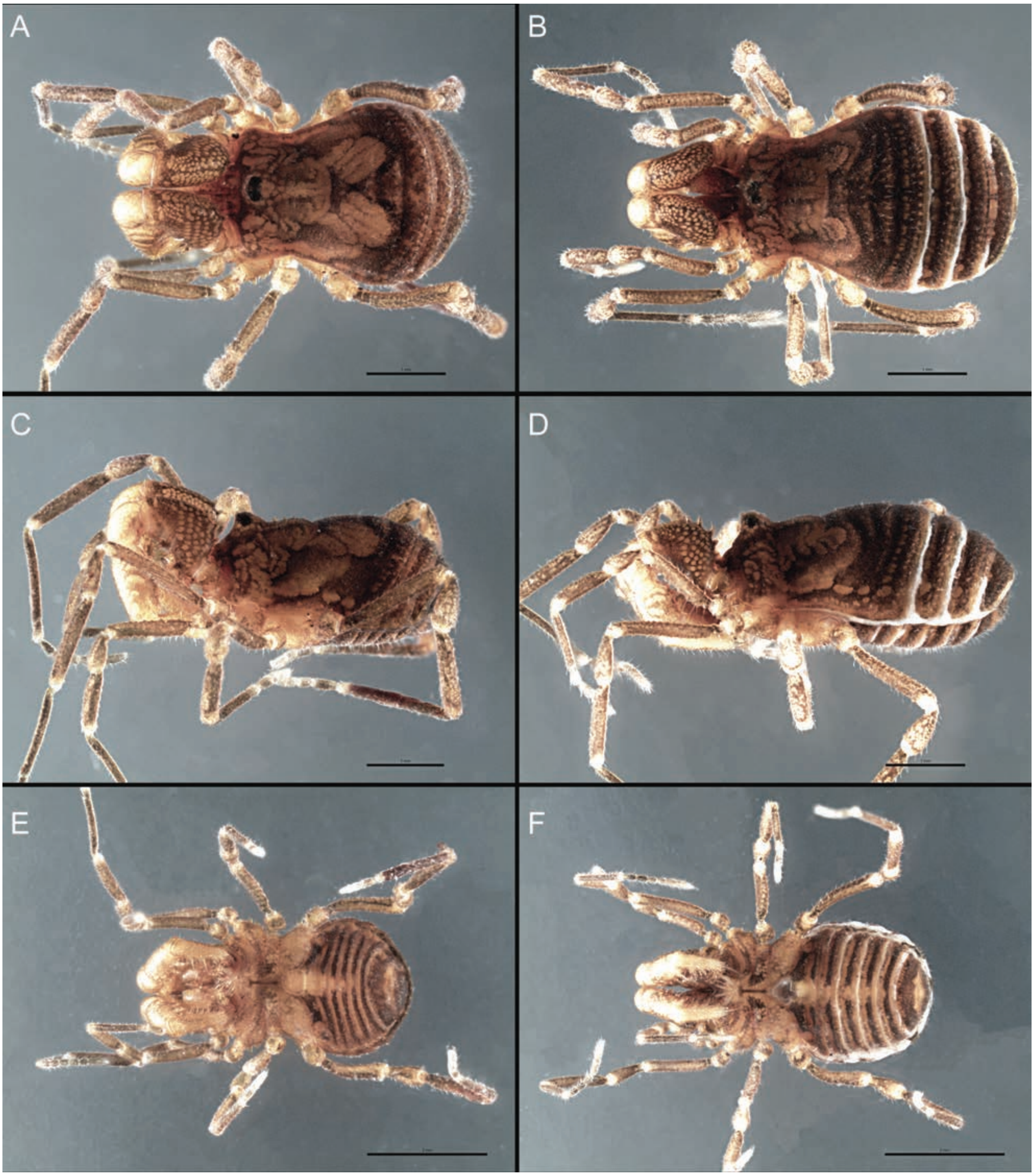

Figure 62. *Lautaria ceachei* sp. nov. habitus, male **A** dorsal view **C** lateral view **E** ventral view. Female **B** dorsal view **D** lateral view **F** ventral view. Scale bars: 500 µm. Species of Clade C, see Fig. 3.

includes a capsula externa with an apical region divided into two halves, forming a 90° angle in relation to the axis of the pars basalis. The external morphology exhibits striking similarities to the genus *Chilenuncia*, and other members of clade C.

Type species. *Lautaria ceachei* sp. nov.

Included species. *Lautaria ceachei* sp. nov.

Distribution. Chile: Ñuble Region (Fig. 4E).

Lautaria ceachei **sp. nov.**
https://zoobank.org/B1D033C3-2192-4672-B2B9-517D1CA30851
Figs 62–67

Material examined. ***Holotype*****.** ♂ **Chile.** Altos del Lircay RN, E Vilches Alto, 35.5987°S, 71.04097°W, 1380 m, M. Ramírez, A. Ojanguren, A. Pérez-González, G. Azevedo, W. Porto coll. (MNHNCL). ***Paratypes*****. Chile.** Altos del Lircay RN, E Vilches Alto, 35.5987°S, 71.04097°W, 1380 m, M. Ramírez, A. Ojanguren, A. Pérez-González, G. Azevedo, W. Porto coll. 15.I.2018, 1 ♂ 4 ♀, 2 imm. (MACN).

Etymology. The specific epithet "ceachei" is derived from the chanted cry "ceacheí," commonly used during sporting events to cheer on Chilean representatives. This Chileanism is created by combining the initial letters of the word "Chile." The epithet serves as noun in apposition, highlighting the connection to Chilean representation and support.

Description of male. Measurements: Total length 2.49. Carapace length 1.14, dorsal scutum length 2.20, carapace max. width 1.63, mesotergum max. width 2.45. Appendage measurements: Pedipalps. Trochanter length 0.30, femora length 0.90, patella length 0.60, tibia length 0.71, tarsus length 0.70. Leg I: trochanter (tr) 0.27, femora (fe) 0.95, patella (pa) 0.54, tibia (ti) 0.83, metatarsus (mt) 1.08, tarsus (ta) 0.61 II: tr 0.32, fe 1.42, pa 0.61, ti 1.10, mt 1.36, ta 0.61. III: tr 0.38, fe 0.95, pa 0.54, ti 0.81, mt 1.02, ta 0.73. IV: tr 0.39, fe 1.41, pa 0.73, ti 1.16, mt 1.49, ta 0.87.

Dorsum (Fig. 62, 63). Eta (η) hourglass-shaped dorsal scutum, characterized by its distinctive form. Ocularium low and rounded, with an acute small apophysis.

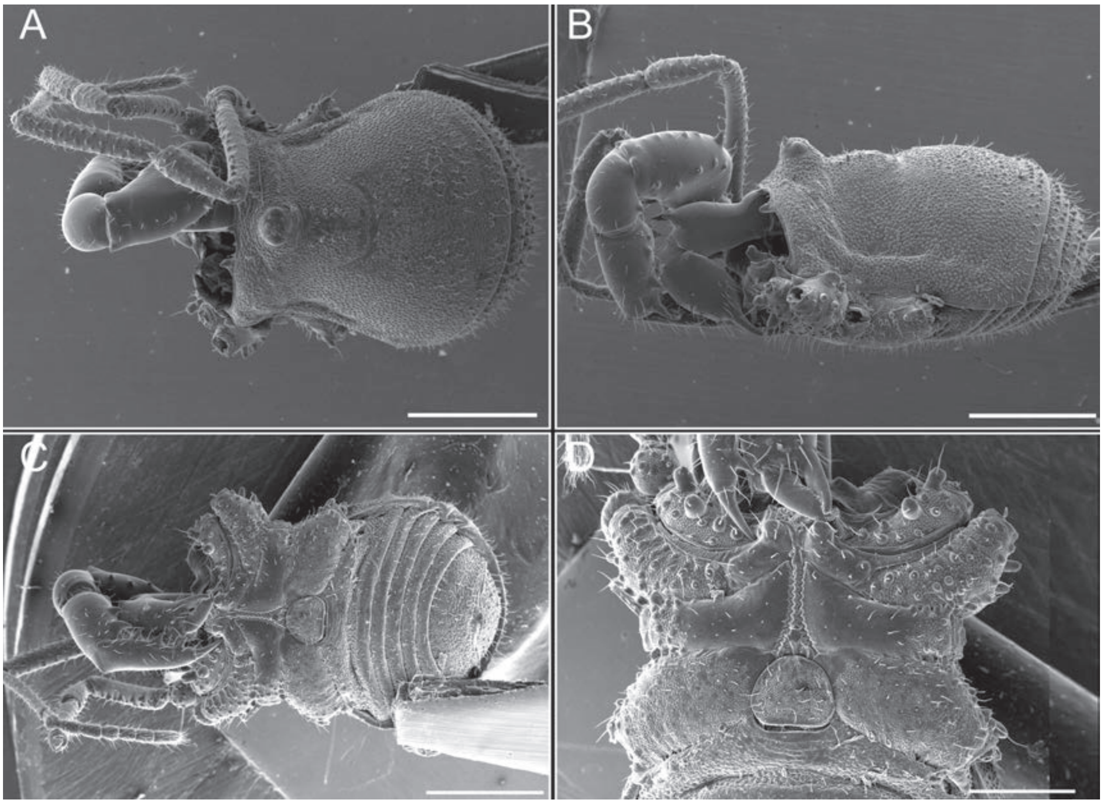

Figure 63. *Lautaria ceachei* sp. nov. male, SEM images of habitus **A** dorsal view **B** lateral view **C, D** ventral view. Scale bars: 1 mm (**A, B, C**); 500 µm (**D**).

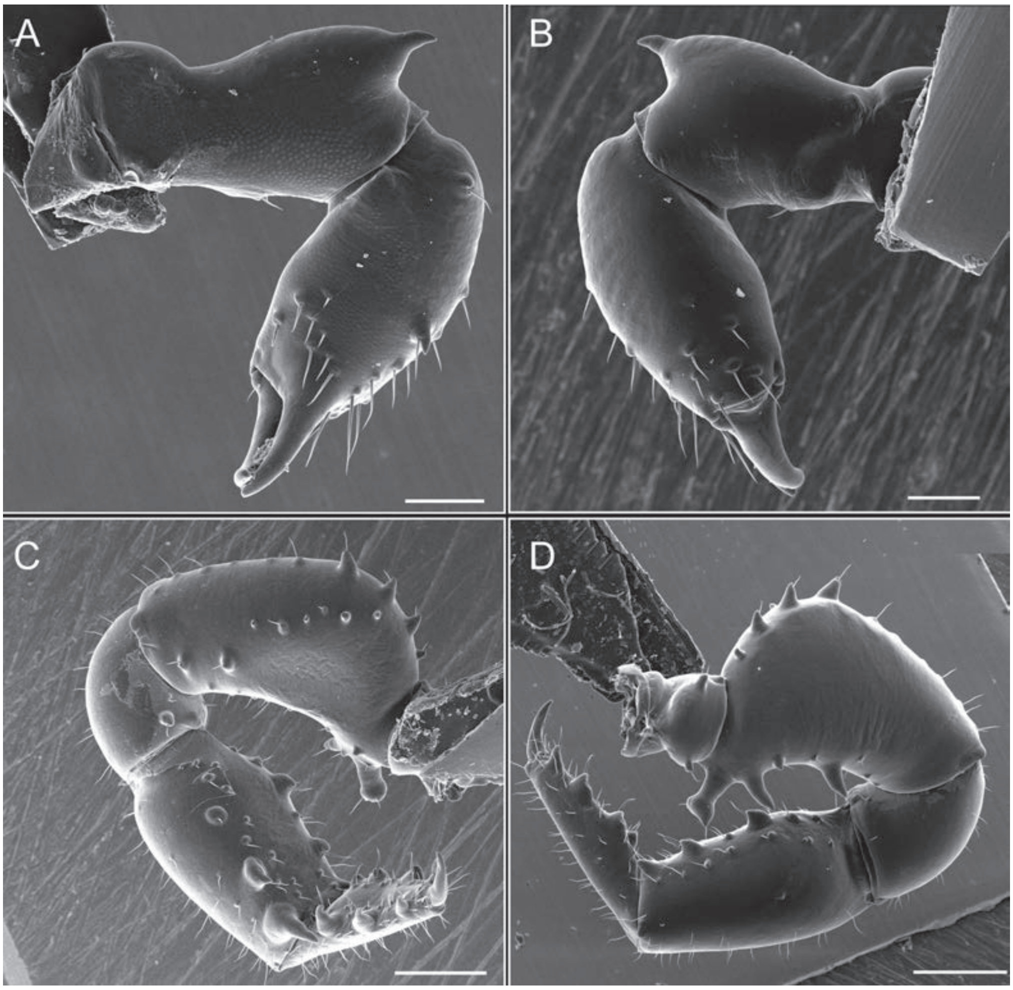

Figure 64. *Lautaria ceachei* sp. nov. chelicerae: mesal **A** ectal **B** Pedipalps: mesal **C** ectal **D**. Scale bars: 200 µm (**A, B**); 500 µm (**C, D**).

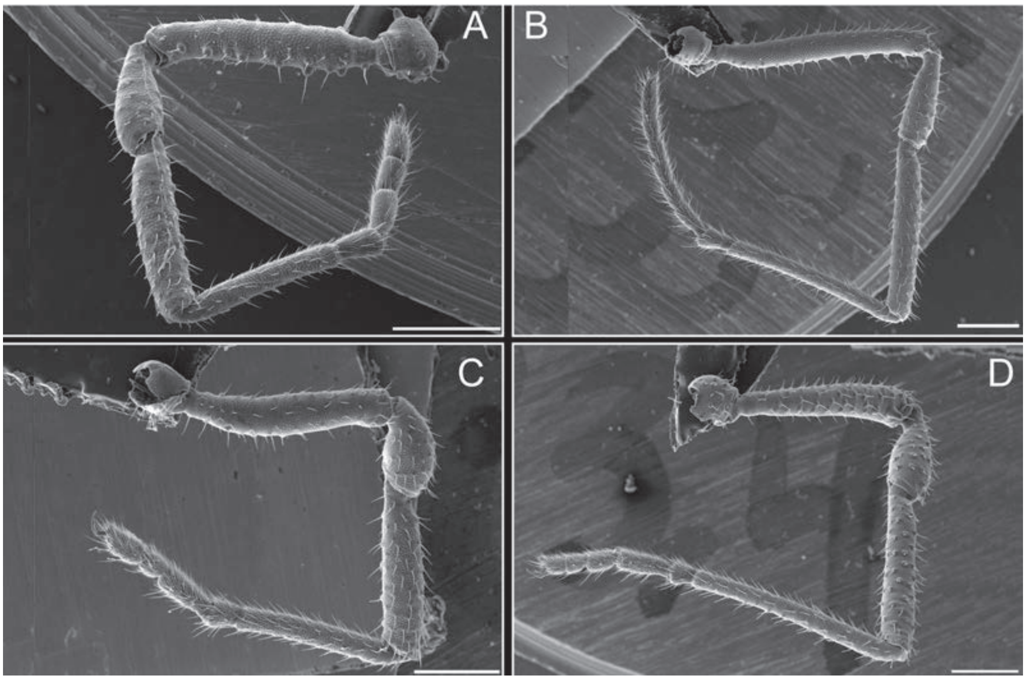

Figure 65. *Lautaria ceachei* sp. nov. legs I **A** II **B** III **C** IV **D**. Scale bars: 500 µm.

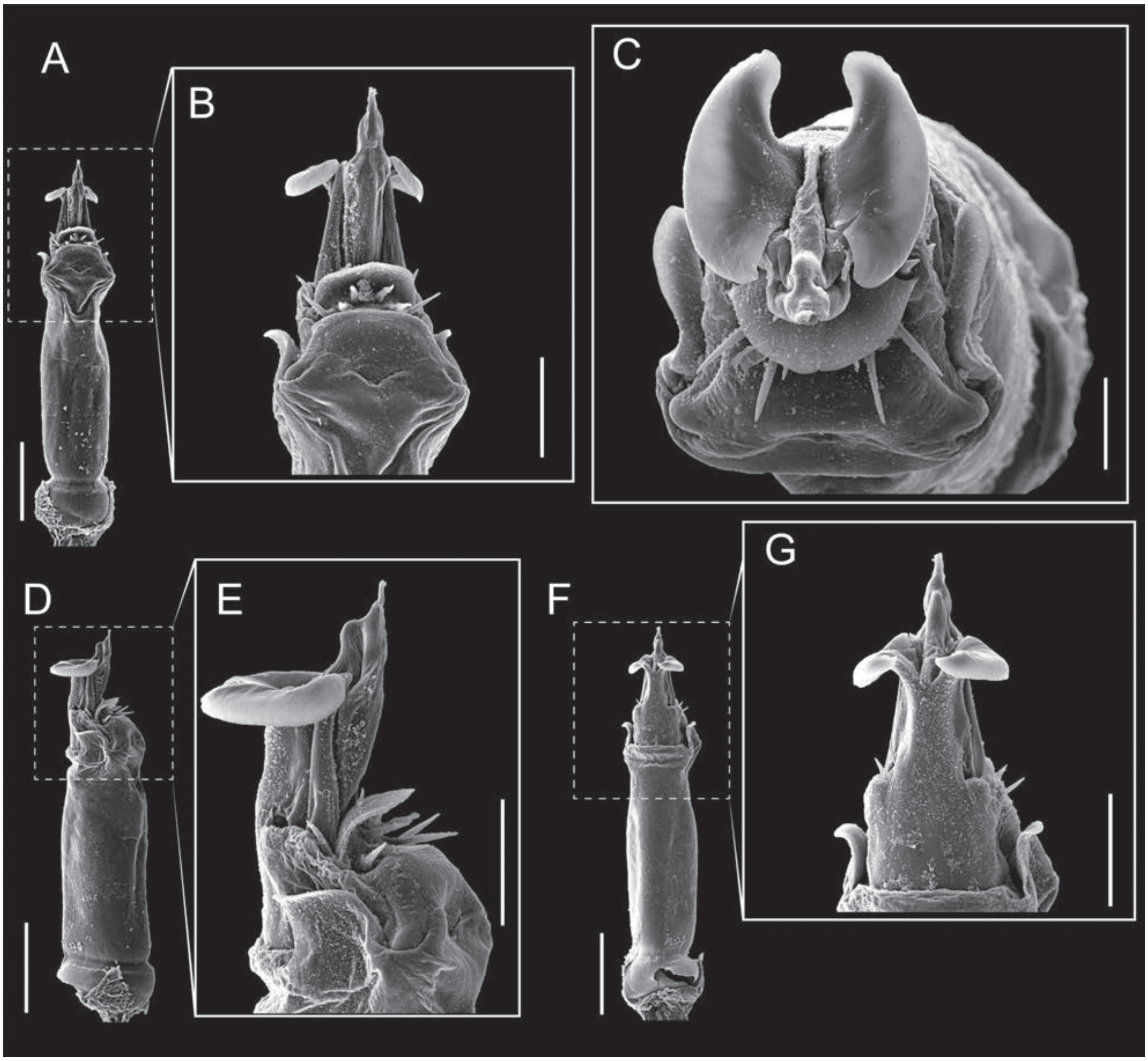

Figure 66. *Lautaria ceachei* sp. nov. penis: ventral **A, B** apical **C** lateral **D, E** dorsal **F, G**. Scale bars: 200 µm (**A, D, F**); 100 µm (**B, E, G**); 50 µm (**C**).

Both the dorsal scutum and free tergites covered with micrgranulation, providing a textured surface. Mesotergal areas without clear separation but with small setiferous tubercles, with a stronger presence in the mesotergum and free tergites.

Chelicerae (Fig. 64A, B). Segment I of with a sharp spine on the dorso-distal surface, with three small ventral-proximal tubercles. Segment II with scattered setae in both ectal and ventral views, and in front view, with a triangular tubercle that stands out from the others.

Pedipalps (Fig. 64C, D). Trochanter with a small dorsal and a ventral tubercle. Femora with two parallel rows of dorso-mesal tubercles, with three ventral spines and a few setiferous tubercles. Patella with a mesal tubercle. Tibia with three ventral-ectal spines, two ventral-mesal spines, and small scattered ventral tubercles.

Legs (Fig. 65). Coxa I characterized by having 9–10 setiferous tubercles, the two apical ones being stronger and more prominent than the others. Coxa II

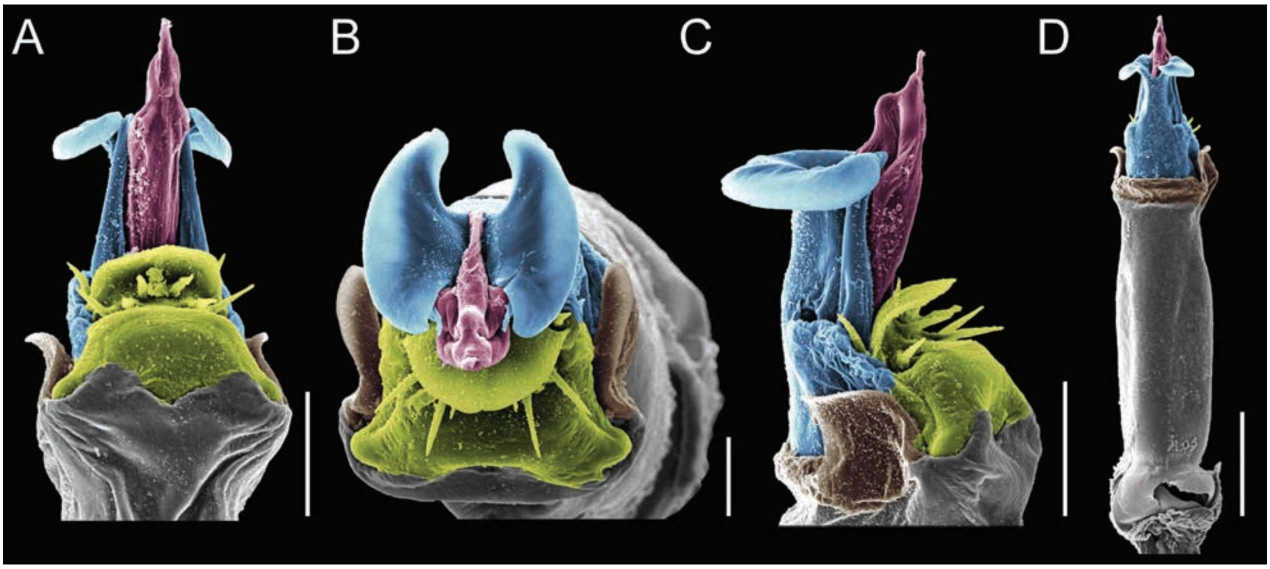

Figure 67. *Lautaria ceachei* sp. nov. penis: ventral **A** apical **B** lateral **C** dorsal **D**. Colors: ventral plate (yellow), capsula externa (blue), capsula interna (red). Scale bars: 1 mm.

with a higher number of setiferous tubercles, ranging from 20 to 25. Coxa III with 12–14 tubercles, while coxa IV has five or six small tubercles. Spiracles not obstructed. A smooth surface covers ~⅓ of leg II, ¾ of leg III, and < ⅓ of leg IV. Sternum arrow-shaped. Legs covered in small tubercles. Astragalus longer than the calcaneus on all legs. Tarsal count: 3–6–4–4.

Penis (Figs 66, 67). Pars distalis with a ventral plate and a small cleft, dividing it into two lamellae. Each lamella with three pointed macrosetae on the ventral surface and one macroseta on the dorsal surface. Capsula externa lower than the capsula interna, with a notch in the apical part, dividing into two lateral apical "wings". With an additional dorsolateral plate. Capsula interna thin and laterally flattened, with a sharp apical area.

Female. Similar to male but with shorter pedipalpal femora and a reduced interocular process.

Female measurements: Total length 2.98. Carapace length 1.11, dorsal scutum length 2.39, carapace max. width 1.66, mesotergum max. width 2.46. Appendage measurements: Pedipalps. Trochanter length 0.33, femora length 1.09, patella length 0.53, tibia length 0.81, tarsus length 1.05. Leg I: trochanter (tr) 0.22, femora (fe) 1.09, patella (pa) 0.50, tibia (ti) 0.86, metatarsus (mt) 1.06, tarsus (ta) 0.63 II: tr 0.24, fe 1.42, pa 0.60, ti 1.12, mt 1.35, ta 1.17. III: tr 0.27, fe 1.06, pa 0.47, ti 0.86, mt 1.01, ta 0.62. IV: tr 0.37, fe 1.43, pa 0.72, ti 1.16, mt 1.42, ta 0.85.

Genus *Nerudiella* gen. nov.

https://zoobank.org/DF572280-150A-44D7-9964-2B1E2749F912
Figs 68–159

Nuncia [part] (references to *Nuncia americana*): Roewer 1961: 102, pl. 19, figs 13–15; Cekalovic 1968: 6; Besch 1969: 733; Muñoz-Cuevas 1971a: 873, fig. 28; Kury 2003: 21.

Nuncia (*Nuncia*) *americana*: Muñoz-Cuevas 1971b: 98, figs 1–17; Cekalovic 1985:11.

Etymology. The generic epithet *Nerudiella* honors renowned Chilean poet and politician Pablo Neruda (1904–1973). Feminine grammatical gender.

Diagnosis. *Nerudiella* species can be easily distinguished from other genera of Triaenonychidae by several notable characteristics. These include a relatively low to medium ocularium, which lacks an interocular apophysis or possesses a reduced apophysis (similar to that of the New Zealand *Nuncia*); a pedipalpal femora typically slightly curved; and presence of a subtle sexual dimorphism. The most salient feature is the male genitalia with a distinctive dorsolateral plate that originates from the genitalia's pars basalis and extends onto the pars distalis. This plate appears wide in its lateral portion but small in dorsal view. These unique genital structures serve as reliable markers for the identification of *Nerudiella* species.

Type species. *Nuncia americana* Roewer, 1961

Included species. *Nerudiella americana* (Roewer, 1961) comb. nov., *Nerudiella cachai* sp. nov., *Nerudiella caramavida* sp. nov., *Nerudiella cautin* sp. nov., *Nerudiella choapa* sp. nov., *Nerudiella curi* sp. nov., *Nerudiella goroi* sp. nov., *Nerudiella jaimei* sp. nov., *Nerudiella malleco* sp. nov., *Nerudiella penco* sp. nov., *Nerudiella pichi* sp. nov., *Nerudiella portai* sp. nov., *Nerudiella quenes* sp. nov., *Nerudiella vilches* sp. nov., *Nerudiella wekufe* sp. nov., *Nerudiella zapallar* sp. nov.

Distribution. Chile: From Coquimbo to Los Lagos Region (Fig. 4F).

Nerudiella americana **(Roewer, 1961), comb. nov.**

Figs 68–73

Nuncia americana Roewer 1961: 102, pl. 19, figs 13–15; Cekalovic 1968: 6; Besch 1969: 733; Muñoz-Cuevas 1971a: 873, fig. 28; Kury 2003: 21.

Nuncia (*Nuncia*) *americana*: Muñoz-Cuevas 1971b: 98, figs 1–17; Cekalovic 1985: 11; Pérez-Schultheiss et al. 2021: 410, fig. 2c, f.

Material examined. ***Paratypes*****. CHILE.** Chepu Peninsula, Chiloé, mixed woodland shrubs, 1 ♂, 1 ♀ (SMF RII/13414).

Additional material. CHILE. Chiloé: Lago Huillinco, M. Ramírez, M. Izquierdo, P. Michalik, C. Wirkner, K. Huckstorf coll., 16.II.2012, 12 imm. (MACN), 5 km of Quellón, N. Platnick, R.Schuh coll., 01.XII.1981, 4 ♂ 8 ♀ 26 imm. (AMNH), Isla Chiloé, R.Schuh, N. Platnick coll., 29.XI.1981, 4 ♂ 3 ♀ 2 imm. (AMNH), Cruce a Coinco, T.Cekalovic coll., 14.II.1983, 3 ♂ 2 ♀ 6 imm. (MACN); Mocopulli, T.Cekalovic coll., 20.II.1986, 1 ♂ 3 ♀ 5 imm. (MACN), Isla Chiloé, T.Cekalovic coll., 02.II.1983, 6 ♂ 5 ♀ 8 imm. (MACN); Isla Chiloé, T.Cekalovic coll., 26.II.1972, 3 imm. (MACN), Piruquina, T.Cekalovic coll., 26.II.1976, 1 ♂ 1 ♀ 1 imm. (MACN), Crossroad to San Pedro, T.Cekalovic coll., 27.II.1976, 4 imm. (MACN), Piruquina, T. Cekalovic coll., 10.II.1981, 2 ♂ 2 ♀ 1 imm. (MACN), same collector, 19.II.1983, 3 imm. (MACN); Chepu, 15 m, N. Platnick, O. Francke coll., 02.02.1985, 1 ♂ 2 imm. (AMNH); 15 km N. Chepu, M. Ramírez coll., 03.02.1991, 3 imm. (MACN), 15 km S de Chepu, M. Ramírez coll., 20.02.1991, 1 imm. (MACN), Lago Huillinco, M. Ramírez, M. Izquierdo, C. Wirkner, K. Huckstorf coll.,

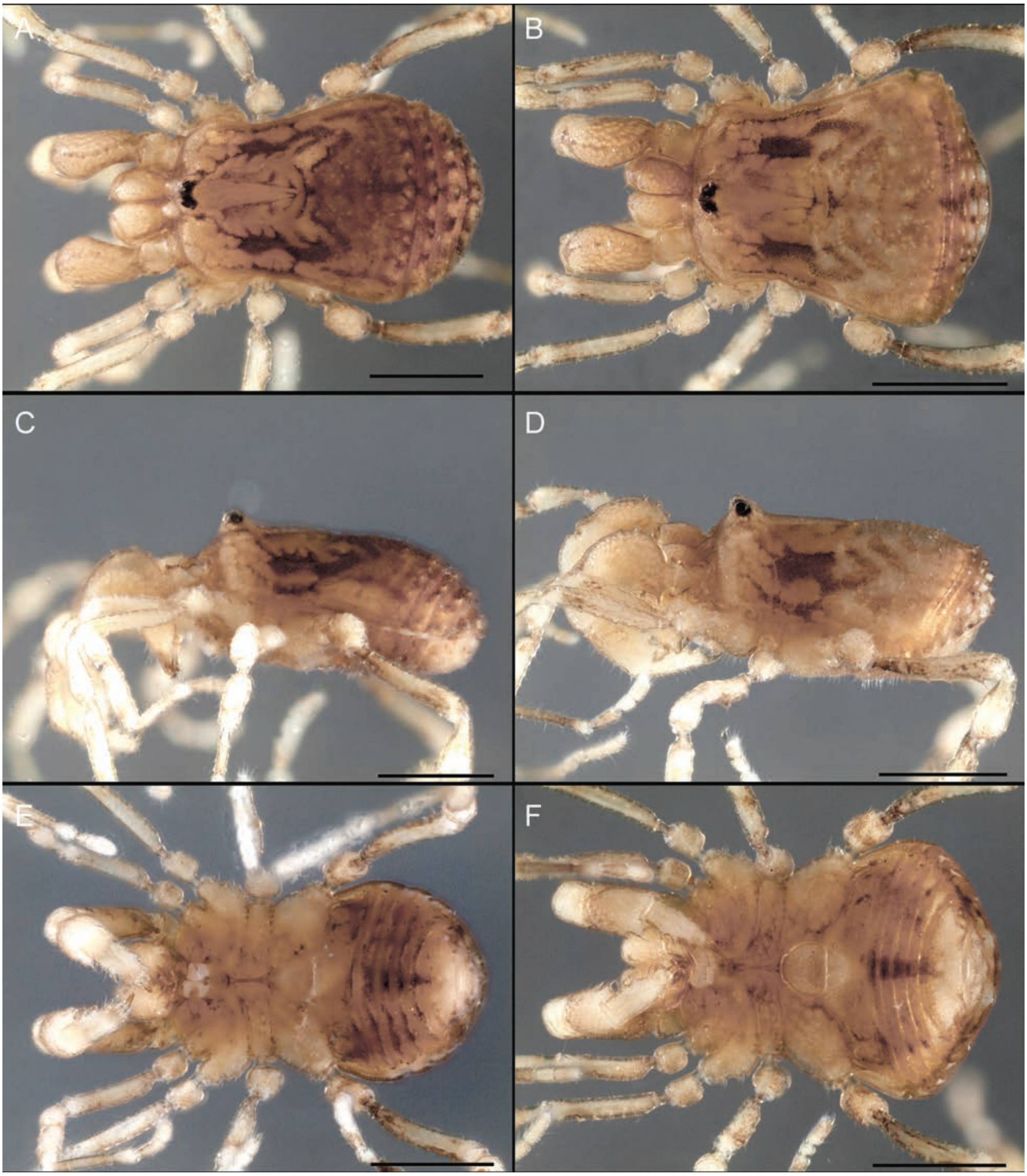

Figure 68. *Nerudiella americana* comb. nov. habitus, male **A** dorsal view **C** lateral view **E** ventral view. Female **B** dorsal view **D** lateral view **F** ventral view. Scale bars: 1 mm. Species of Clade C, see Fig. 3.

15.ii.2012, 1 ♂ (MACN), Chilloé island, 5 km N of Quellón, R.Schuh, N. Platnick coll., 01.12.1981, 1 imm. (AMNH), 8 km Ancud, Isla Chiloé, N. Platnick, O. Francke coll., 01.02.1985, 6 ♀ 22 imm. (AMNH), Isla Chiloé, 8 km S Ancud, S.Peck, J.Peck coll., 01.02.1985, 8 ♂ 5 ♀ 21 imm. (AMNH), 5 km N of Quellón, N. Platnick, R.Schuh coll., 01.12.1981, 1 ♂ 1 ♀ 1 imm. (AMNH); Chepu, E. Maury coll., 29.11.1981, 3 ♂ 1 ♀ 3 imm. (MACN). Llanquihue: Salto Petrohue, S.Peck, J.Peck coll., 23.12.1984, 1 imm. (AMNH).

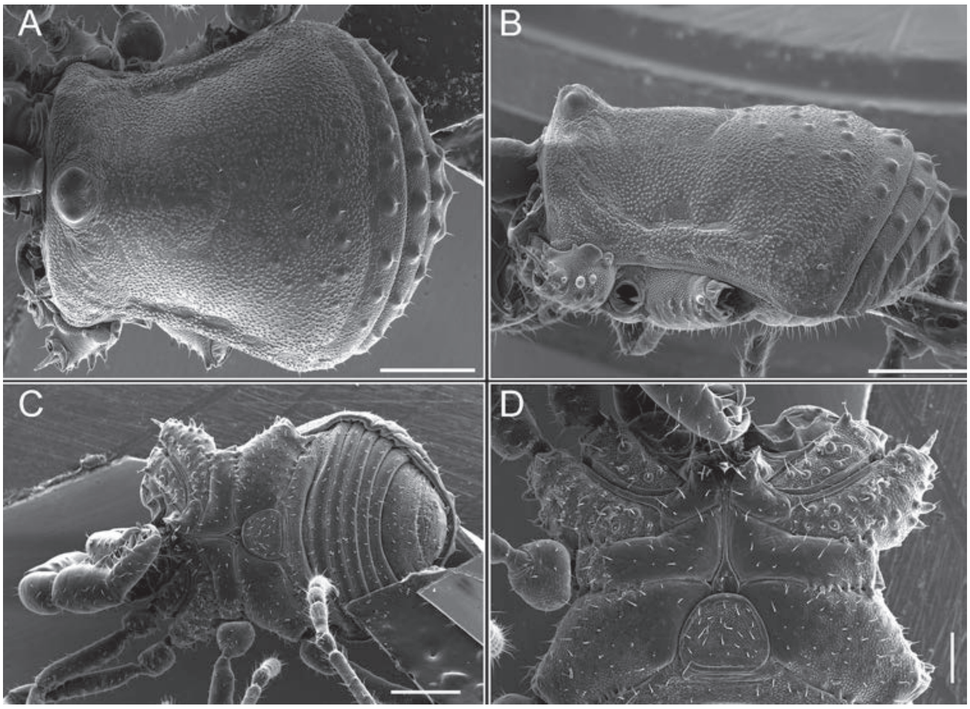

Figure 69. *Nerudiella americana* comb. nov. male, SEM images of habitus **A** dorsal view **B** lateral view **C, D** ventral view. Scale bars: 500 µm (**A, B, C**); 200 µm (**D**).

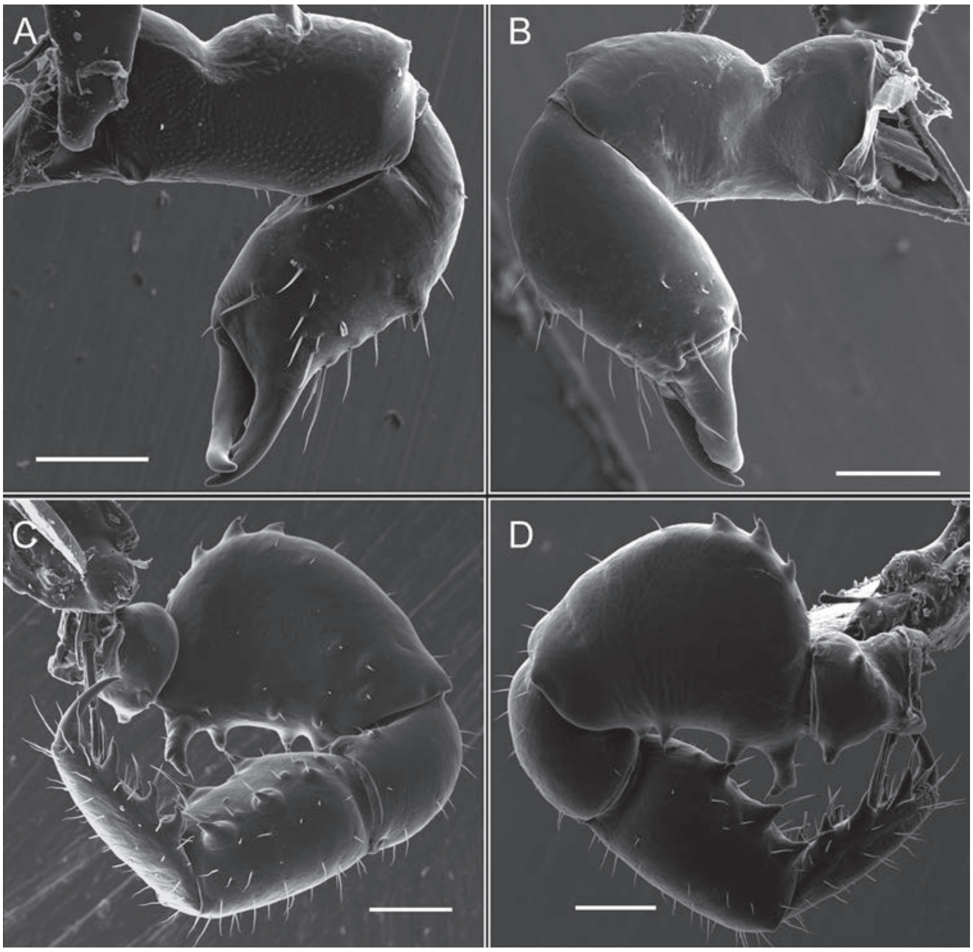

Figure 70. *Nerudiella americana* comb. nov. chelicerae: mesal **A** ectal **B** Pedipalps: mesal **C** ectal **D**. Scale bars: 200 µm.

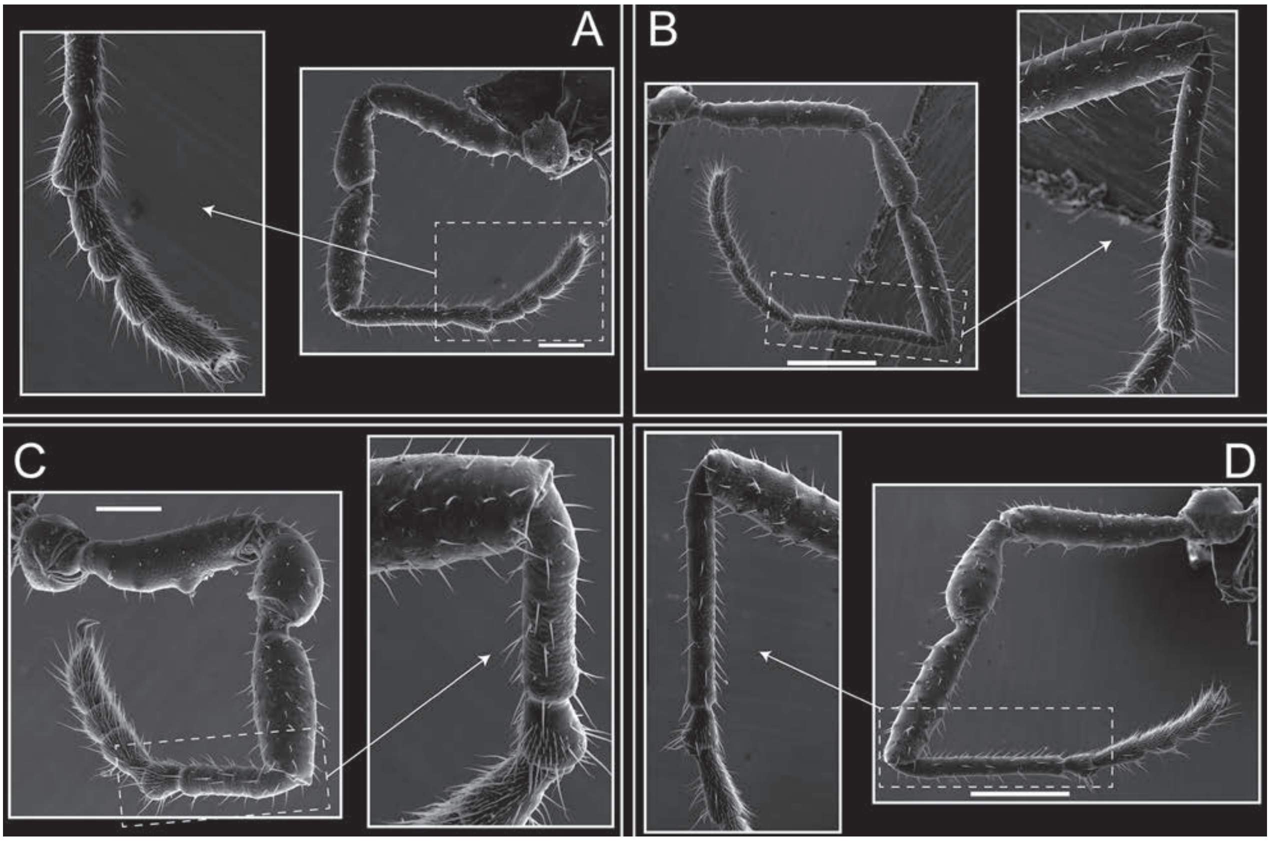

Figure 71. *Nerudiella americana* comb. nov. legs I **A** II **B** III **C** IV **D**. Scale bars: 200 µm (**A, C**); 500 µm (**B, D**).

Diagnosis. This species stands out from the others in the genus due to its sturdy capsula externa and distinctive "T"-shaped dorsal fold. The capsula externa apex is extremely delicate. It can also be differentiated from almost all species of the genus using somatic characters (except from *N. cautin* sp. nov. and *N. jaimei* sp. nov.) by having the dorsal scutum with a low, broad-based tubercles.

Distribution. Chile: Los Lagos Region (Fig. 4F).

Redescription of male paratype SMF RII/13414. Measurements: Total length 2.73, dorsal scutum length 2.21, carapace max. width 1.47, mesotergum max. width 1.95. Appendage measurements: Pedipalps. Trochanter length 0.28, femora length 0.97, patella length 0.61, tibia length 0.74, tarsus length 0.71. Leg I: trochanter (tr) 0.26, femora (fe) 0.92, patella (pa) 0.54, tibia (ti) 0.69, metatarsus (mt) 0.82, tarsus (ta) 0.70. II: tr 0.32, fe 1.16, pa 0.57, ti 0.93, mt 1.07, ta 1.14. III: tr 0.30, fe 0.71, pa 0.43, ti 0.65, mt 0.59, ta 0.72.IV: tr 0.39, fe 1.08, pa 0.70, ti NA, mt NA, ta NA.

Dorsum (Fig. 68, 69). Eta (η) dorsal scutum in the shape of an hourglass. Ocularium slightly elevated. Dorsal scutum microgranulate with a group of low setiferous granules. Areas on scutum not clearly delimited. Along the back margin, with a row of low and broad setiferous granules. Free tergites with a row of low and broad setiferous granules.

Chelicerae (Fig. 70A, B). Segment I smooth in texture without prominent tubercles. Segment II with a small frontal tubercle and covered with scattered setae, giving it a textured appearance.

Pedipalps (Fig. 70C, D). Coxa I with a smooth surface without any notable tubercles. Trochanter with small tubercles on both the dorsal and ventral sides.

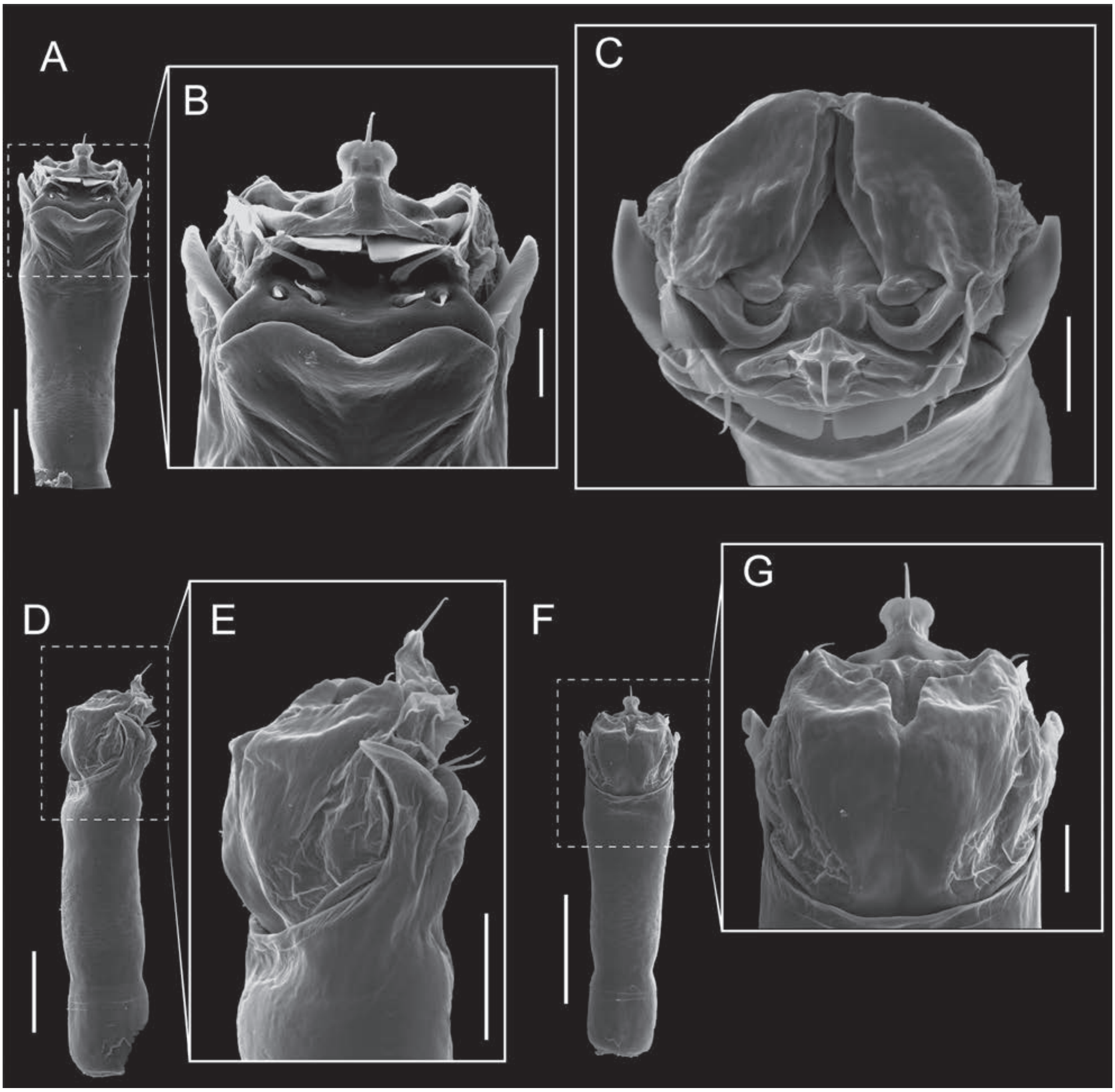

Figure 72. *Nerudiella americana* comb. nov. penis: ventral **A, B** apical **C** lateral **D, E** dorsal **F, G**. Scale bars: 200 μm (**A, D, F**); 50 μm (**B, C, G**); 100 μm (**E**).

In dorsal view, femora with three spines with subdistal setae. In ventral view, with one long bifurcated spine and two spines with subdistal setae. In mesal view, with six low setiferous tubercles on the femora. Patella with a mesal row of setiferous tubercles. Tibia with three ectal and two mesal spines with subdistal setae, and six low setiferous tubercles. Tarsus with three mesal and ectal spines with setae, with a few setae.

Legs (Fig. 71). Leg I with sparse setiferous tubercles. Leg II features two rows of setiferous tubercles, while legs III and IV exhibit only microgranulation without distinct tubercles. With three bridges connecting legs II and III, six bridges between legs III and IV, and four bridges connecting leg IV to the opisthosoma. Distal bridge longer than the others. Bridges do not obstruct the spiracles, although they appear partially covered with a subdistal tubercle. A

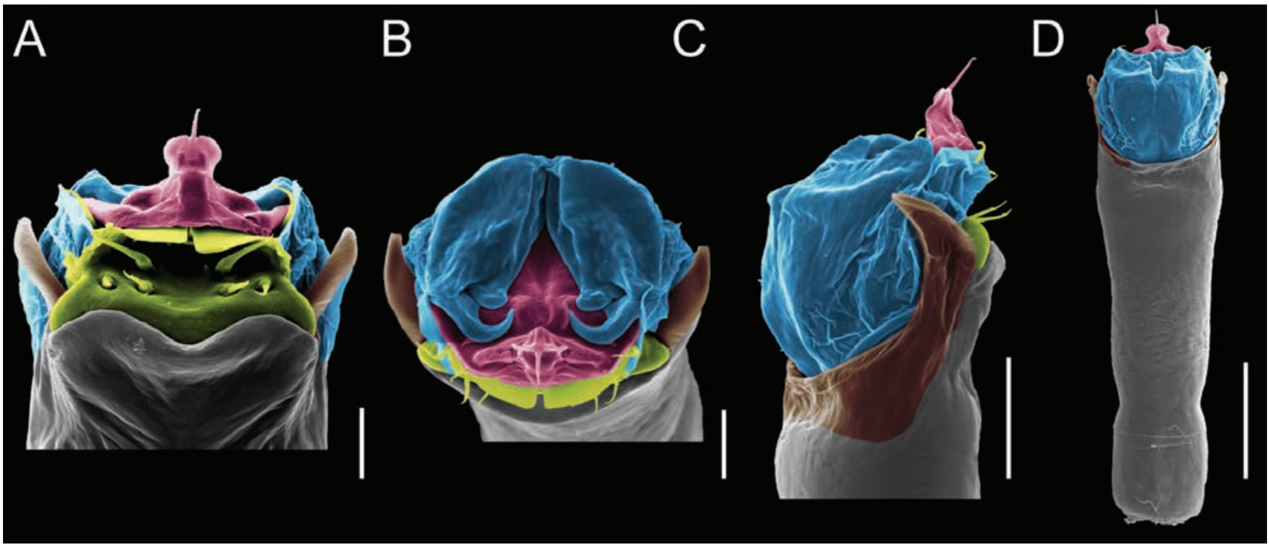

Figure 73. *Nerudiella americana* comb. nov. penis: ventral **A** apical **B** lateral **C** dorsal **D**. Colors: ventral plate (yellow), capsula externa (blue), capsula interna (red). Scale bars: 50 μm (**A, B, D**); 100 μm (**C**).

smooth surface occupies ~ ¼ of leg **II**, ¾ of leg **III**, and ⅓ of leg **IV**. Sternum arrow-shaped. Femora **III** with a remarkable triangular tubercle. Leg **IV** with a row of four subtriangular tubercles. Legs **I**–**IV** covered in setae, with tarsal area and calcaneus densely setose. Calcaneus smaller than astragalus, ~ 3× smaller in legs **I**–**III**, 4× smaller in leg **IV**. Tarsal count: 4–6–4–4.

Penis (Figs 72, 73). Pars distalis with a prominent ventral plate divided into two lamellae by a cleft. Each lamella equipped with three pointed macrosetae on the ventral surface and one on the dorsal surface. Dorsal and lateral surfaces covered by a capsula externa, with a cleft that separates the capsula externa into two halves. With an additional dorsolateral plate attached to the pars basalis. Capsula interna longer than capsula externa and partially covers ventral plate.

Female. Similar to male, with shorter pedipalpal femora.

Female measurements. Total length 2.88, carapace length 1.17, dorsal scutum length 2.21, carapace max. width 1.47, mesotergum max. width 2.07. Appendage Measurements: Pedipalps. Trochanter length 0.23, femora length 0.74, patella length 0.46, tibia length 0.58, tarsus length 0.62. Leg **I**: trochanter (tr) 0.21, femora (fe) 0.88, patella (pa) 0.50, tibia (ti) 0.65, metatarsus (mt) 0.79, tarsus (ta) 0.65. **II**: tr 0.32, fe 1.12, pa 0.56, ti 0.90, mt 0.98, ta 1.18. **III**: tr 0.32, fe 0.81, pa 0.46, ti 0.59, mt 0.67, ta 0.64. **IV**: tr 0.35, fe 1.16, pa 0.70, ti 0.89, mt 1.21, ta 0.87. Tarsal count: 3–6–4–4.

Nerudiella cachai **sp. nov.**

https://zoobank.org/27F81489-12E3-4DC3-858D-5DF1C0ECB048

Figs 74–79

Material examined. ***Holotype***. ♂ **Chile.** Concepción: Estero Nonguén, 36.82106°S, 73.01649°W, T. Cekalovic coll., 21.IV.1976 (MNHNCL). ***Paratypes***. **Chile.** Concepción: Estero Nonguén, T.Cekalovic coll., 13.**III**.1977, 7 ♂ 2 ♀ (MACN). Same locality, T.Cekalovic coll., 16.**IV**.1977, 1 ♀ 1 imm. (MACN). Same

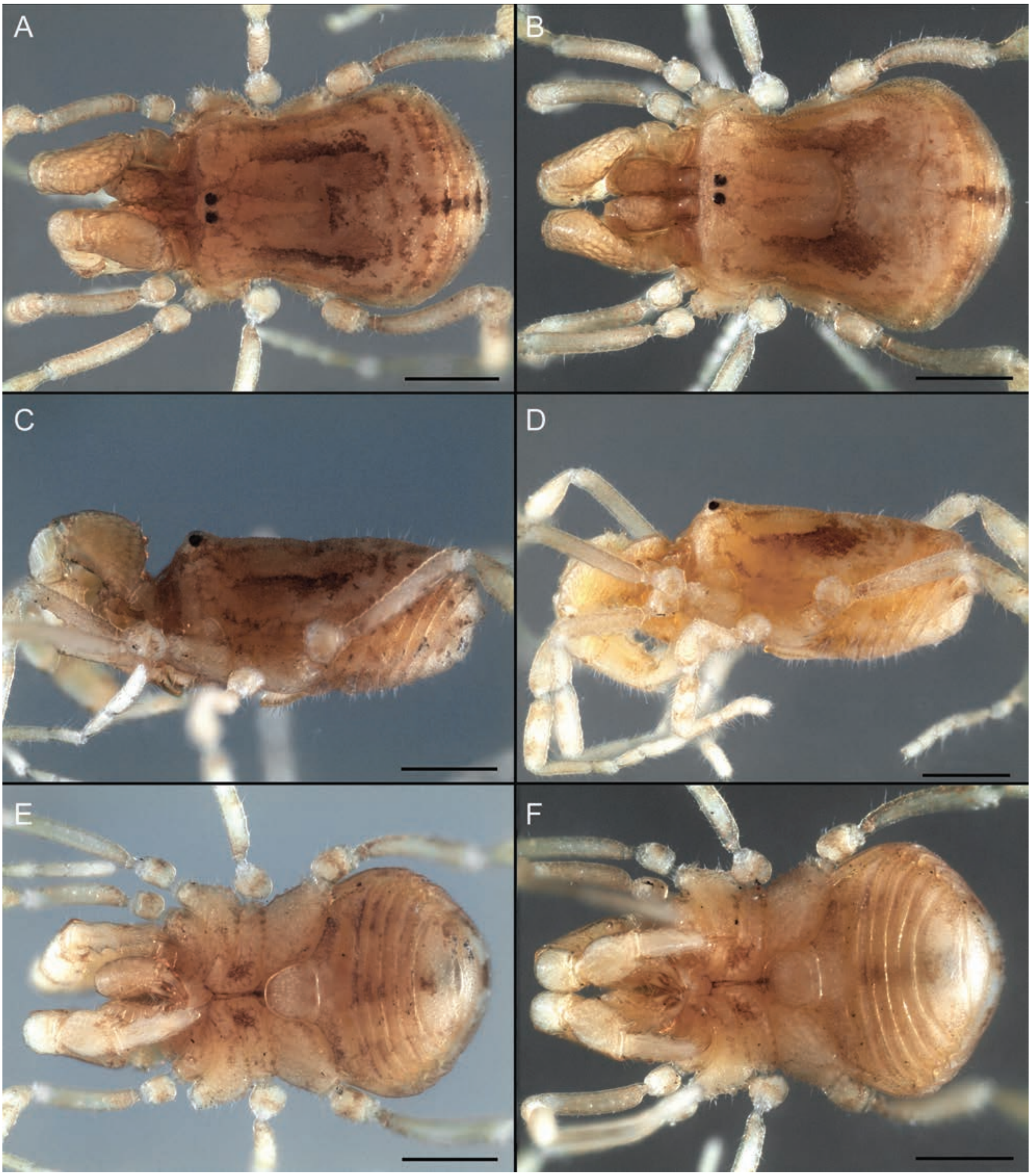

Figure 74. *Nerudiella cachai* sp. nov. habitus, male **A** dorsal view **C** lateral view **E** ventral view. Female **B** dorsal view **D** lateral view **F** ventral view. Scale bars: 500 µm. Species of Clade C, see Fig. 3

locality, 1250 m, N. Platnick, R.Schuh coll., 19.11.1981, 2 ♂ 1 imm. (AMNH). Agua de la Gloria, T.Cekalovic coll., 14.VIII.1978, 1 ♂ (MACN).

Additional material. CHILE. Arauco. Caramávida, San Alfonso, Quebrada Caramávida, San Alfonso, Arauco reserve, 37.70942°S, 73.17107°W, 750 m, A. Ojanguren, P. Goloboff, M. Ramírez, G. Azevedo, W. Porto coll., 15.I.2018, 30 imm. (MACN). 16 km N Tres Pinos, 37.54143°S, 73.41555°W, A. Newton, M. Thayer coll., 12.XII.1982, 2 ♂ (AMNH). Concepción. Penco, 36.734°S, 72.98006°W, T.Ce-

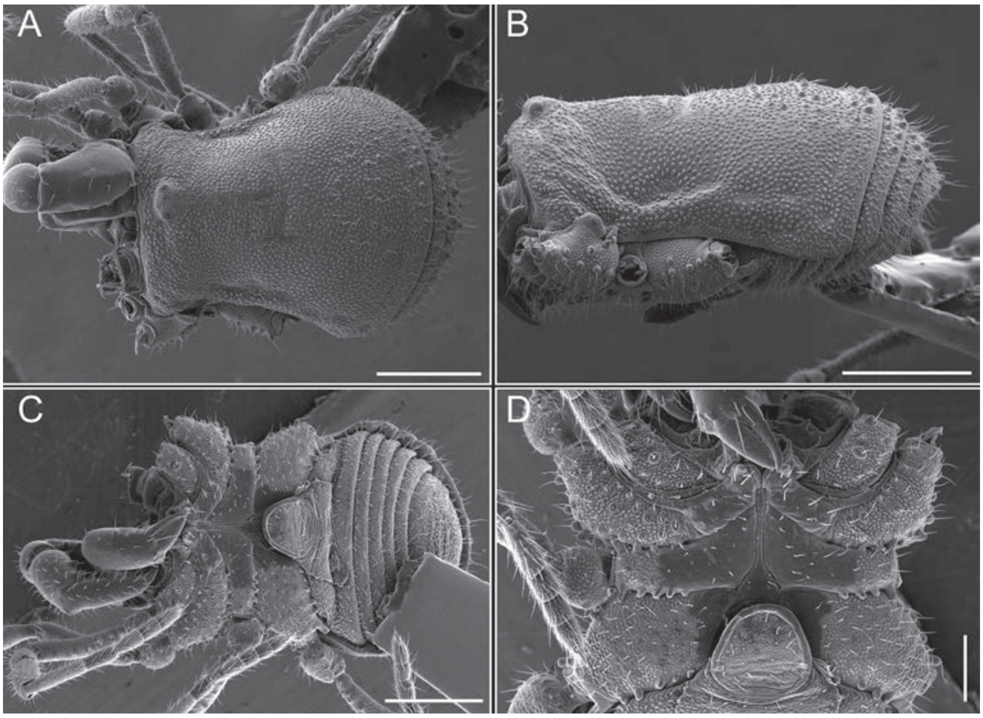

Figure 75. *Nerudiella cachai* sp. nov. male, SEM images of habitus **A** dorsal view **B** lateral view **C, D** ventral view. Scale bars: 500 µm (**A, B, C**); 200 µm (**D**).

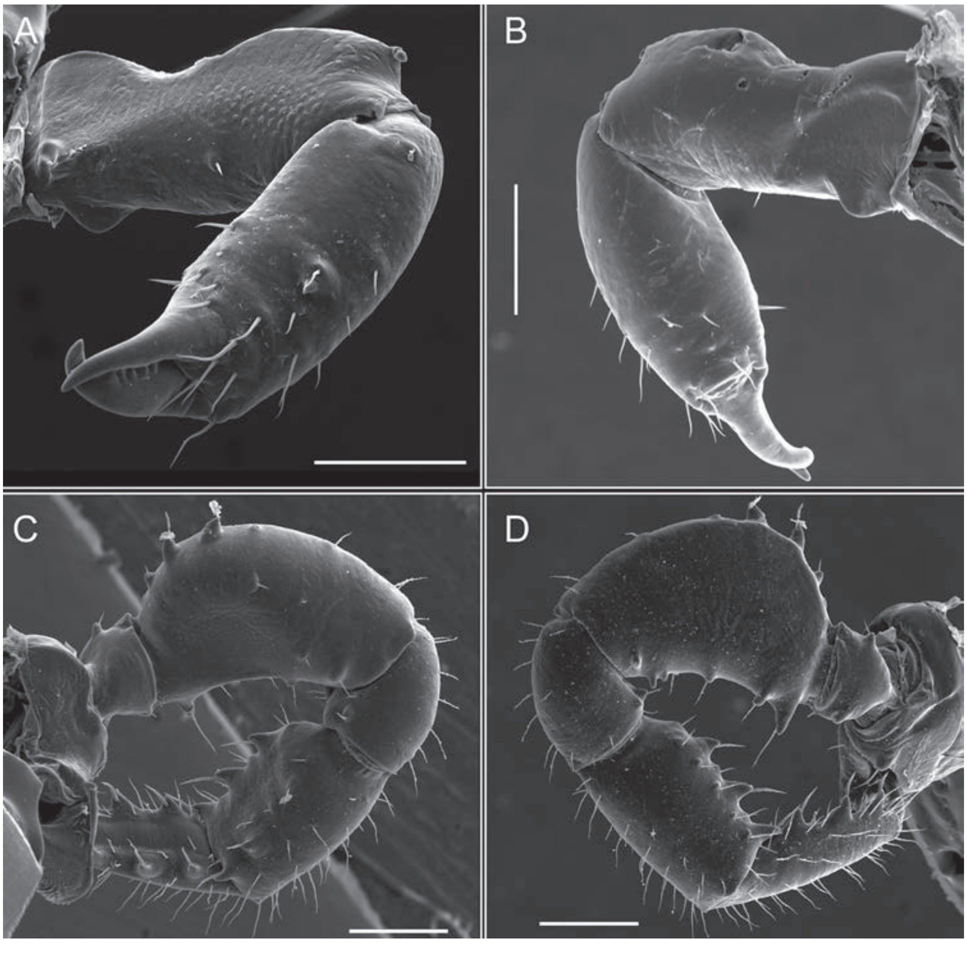

Figure 76. *Nerudiella cachai* sp. nov. chelicerae: mesal **A** ectal **B** pedipalps: mesal **C** ectal **D**. Scale bars: 200 µm.

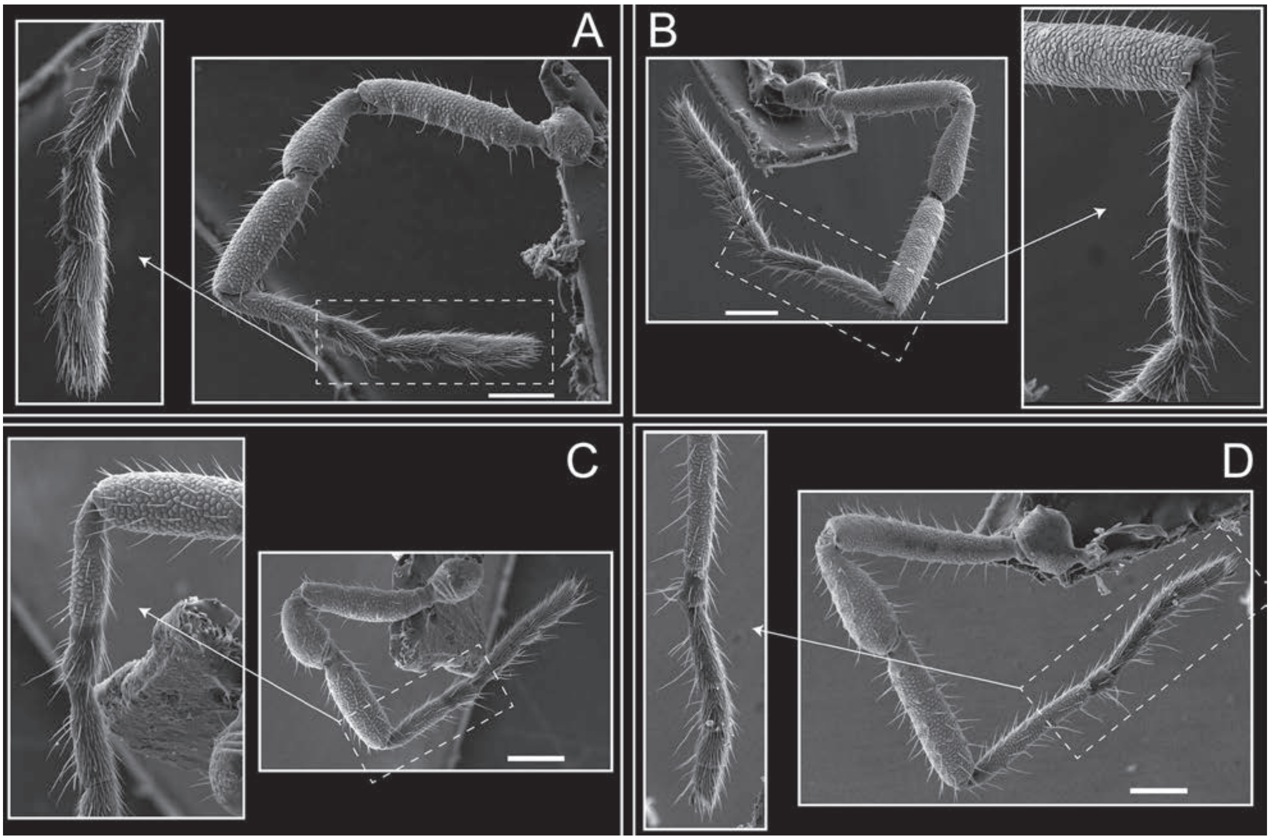

Figure 77. *Nerudiella cachai* sp. nov. legs I **A** II **B** III **C** IV **D**. Scale bars: 200 µm.

kalovic coll., 23.IV.1977, 5 ♂ 5 ♀ 2 imm. (MACN). Cerro Caracol, 36.83465°S, 73.0488°W, T.Cekalovic coll., 10.IV.1977, 6 ♂ 1 ♀ (MACN). Estero Nonguén, 36.82096°S, 73.0164°W, T.Cekalovic coll., 03.XII.1982, 11 imm. (MACN). Esquadrón, 36.9824°S, 73.14165°W, T.Cekalovic coll., 10.08.1978, 1 imm. (MACN). Estero Nonguén, 36.82096°S, 73.0164°W, T.Cekalovic coll., 19.VIII.1978, 2 imm. (MACN). El Manzano, Camino de Santa Juana, 36.86677°S, 72.78498°W, T.Cekalovic coll., 13.I.1985, 1 ♂ (MACN). Colcura, 37.11386°S, 73.14724°W, T.Cekalovic coll., 30.I.1985, 1 imm. (MACN). Hualpén, Terrestrial Biology Station Univ. de Concepción, 36.79821°S, 73.16307°W, 52 m, A. Ojanguren, A. Pérez-González, M. Ramírez, G. Azevedo, W. Porto coll., 14.I.2018, 1 ♀ 3 mm (MACN). Estero Nonguén, 36.82129°S, 73.0164°W, N. Platnick, R.Schuh coll., 16.XI.1981, 6 ♂ 2 ♀ 6 imm. (AMNH). 8.4 km W La Florida, 36.84976°S, 72.78826°W, 170 m, A. Newton, M. Thayer coll., 02.I.1983, 3 ♀ (AMNH). Dichoco. Estero Bellavista, 36.71992°S, 72.91118°W, T.Cekalovic coll., 04.I.1984, 2 ♂ 4 ♀ 4 imm. (MACN). 6 km S San Pedro, 36.90616°S, 73.10894°W, N. Platnick, O. Francke coll., 22.I.1985, 2 ♂ 2 imm. (AMNH). Dichoco. Estero Bellavista, 36.71992°S, 72.91118°W, T.Cekalovic coll., 04.I.1984, 1 ♀ 1 imm. (MACN). Parque Nacional Nahuelbuta, T.Cekalovic coll., 19.XI.1981, 2 ♂ 1 ♀ (MACN). Estero Nonguén, 36.82096°S, 73.0164°W, T.Cekalovic coll., 03.XI.1982, 1 ♂ 4 imm. (MACN).

Etymology. The specific epithet cachai refers to a popular expression in Chile that is roughly translated to “you know what I mean?” “am I right?”, or “get it?”. It is derived from the English term “to catch,” which refers to catching but is also used to mean “understanding or understanding something.” Noun in apposition.

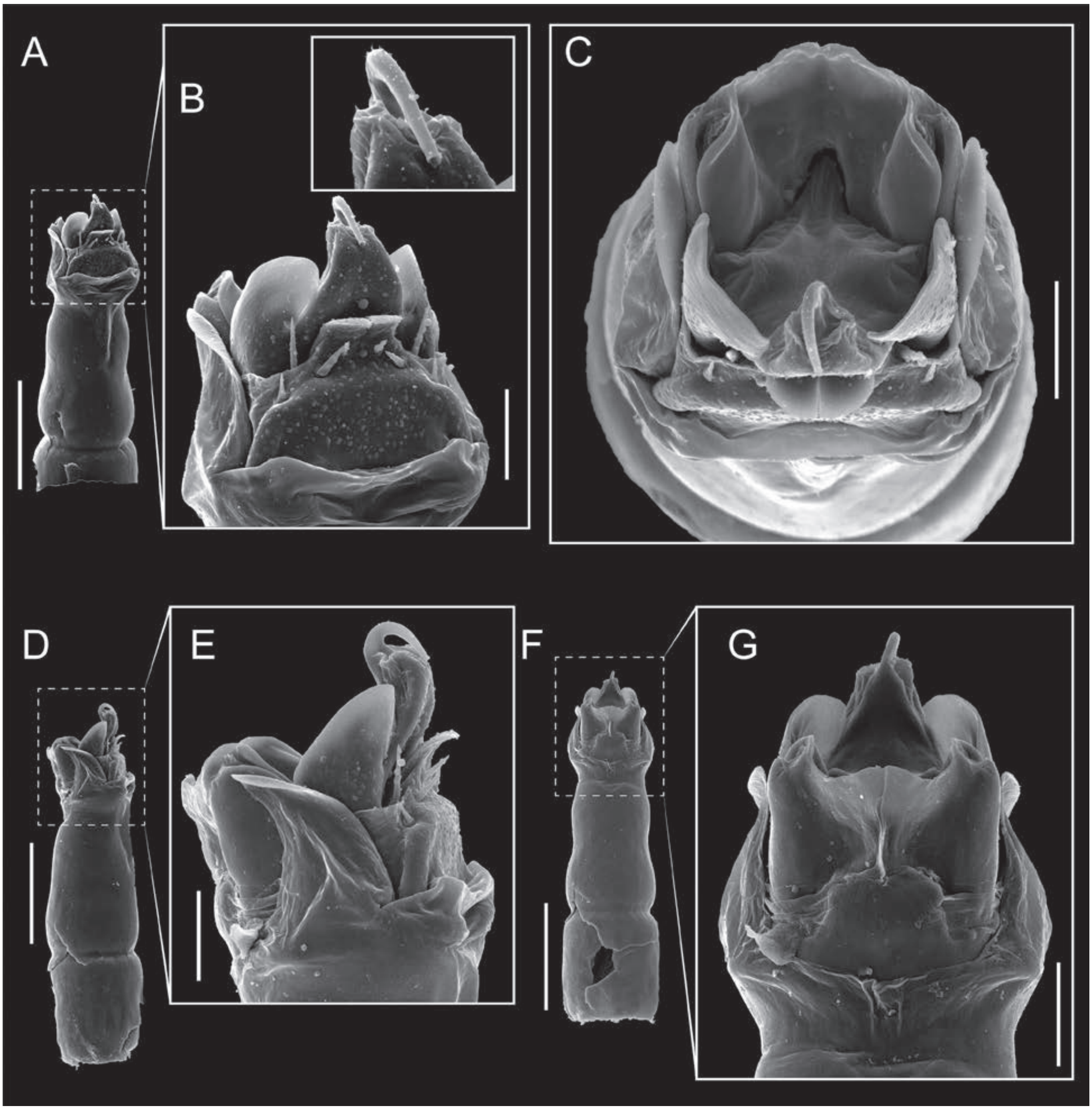

Figure 78. *Nerudiella cachai* sp. nov. penis: ventral **A, B** apical **C** lateral **D, E** dorsal **F, G**. Scale bars: 200 μm (**A, D, F**); 50 μm (**B, C, E, G**).

Diagnosis. This species can be easily distinguished from other species of the genus by its male genitalia, which exhibits a highly reduced ventral plate, with a stylus that is formed by a thin and slender tube.

Distribution. Chile: Bío-Bío Region.

Description of male holotype. Measurements: Total length 2.26, carapace length 0.92, dorsal scutum length 1.84, carapace max. width 1.23, mesotergum max. width 1.70. Appendage measurements: Pedipalps. Trochanter length 0.23, femora length 0.91, patella length 0.44, tibia length 0.68, tarsus length 0.59. Leg **I**: trochanter (tr) 0.22, femora (fe) 1.10, patella (pa) 0.51, tibia (ti) 0.79, metatarsus (mt) 0.92, tarsus (ta) 0.92. **II**: tr 0.27, fe 1.33, pa 0.57, ti 1.00, mt 1.22, ta 1.45. **III**: tr 0.21, fe 0.91, pa 0.31, ti 0.73, mt 0.75, ta 0.74. **IV**: tr 0.32, fe 1.29, pa 0.59, ti 1.04, mt 1.30, ta 0.86.

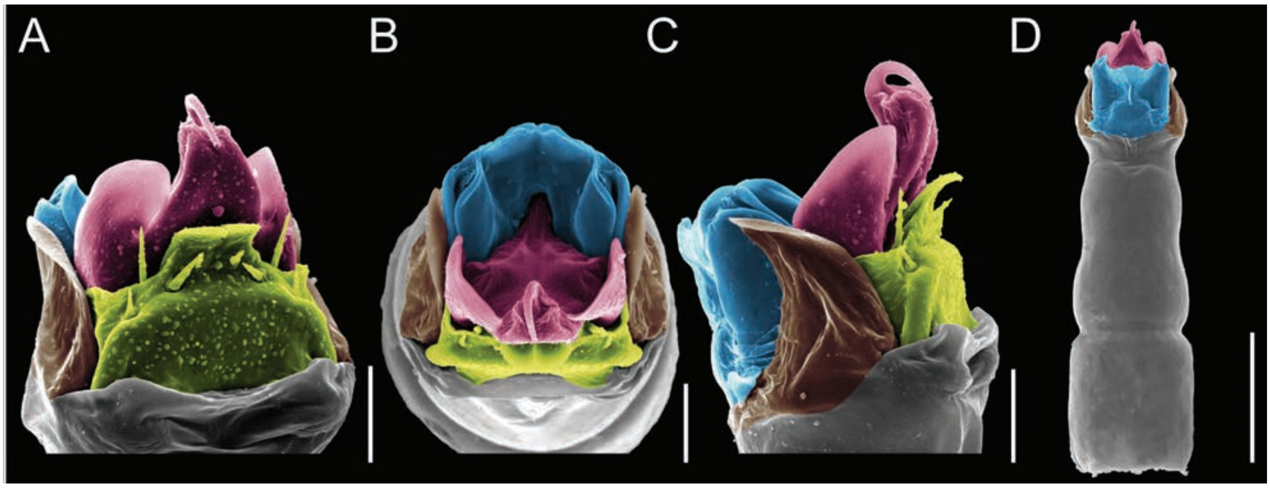

Figure 79. *Nerudiella cachai* sp. nov. penis: ventral **A** apical **B** lateral **C** dorsal **D**. Colors: ventral plate (yellow), capsula externa (blue), capsula interna (red). Scale bars: 50 μm.

Dorsum (Fig. 74, 75). Eta (η) dorsal scutum in the shape of an hourglass. Ocularium low. Dorsal scutum microgranulate, with no clear delimitation of distinct areas. Areas III and IV with irregular rows of small rounded setiferous tubercles; posterior margin with a similar irregular row of small rounded setiferous tubercles. All free tergites covered in small setae and with a row of small rounded setiferous tubercles.

Chelicerae (Fig. 76A, B). Segment I with a small tubercle on its dorso-distal surface. Segment II with a small frontal tubercle and scattered setae.

Pedipalps (Fig. 76C, D). Trochanter characterized by the presence of two small dorsal tubercles and one ventral tubercle. In dorsal view, femora with three spines with subdistal setae; in ventral view, with five tubercles with subdistal setae, with four mesal setiferous tubercles and one ectal setiferous tubercle positioned beneath. Patella with both mesal and ectal setiferous tubercles. Tibia with three ectal and two mesal spines with subdistal setae. Tarsus with three mesal and ectal spines, accompanied by scattered setae.

Legs (Fig. 77). Segments I and II with two rows of setiferous tubercles; segments III and IV microgranulate but without setiferous tubercles. With three bridges connecting legs II and III, six bridges between III and IV, and four bridges between leg IV and the opisthosoma. Distal bridge longer than the others. The bridges do not obstruct the spiracles. The smooth area occupies ~ ¼ of leg II, ¾ of leg III, and < ⅓ of leg IV. Sternum arrow-shaped, with a triangular-shaped posterior margin. Legs I–IV covered with setae, the area of the tarsus and calcaneus are densely setose. Femora I–IV with a ventral row of setiferous granules. Calcaneus smaller than astragalus, ≥ 3× smaller (legs I, III) of the same size (II) and 4× smaller (leg IV). Tarsal count: 3–6–4–4.

Penis (Figs 78, 79). Pars distalis with a small ventral plate divided into two distinct small lamellae by a central cleft. Each lamella adorned with three pointed macrosetae on its ventral surface, with a single macroseta on its dorsal surface. Additionally, there is a capsula externa, characterized by its square shape, which covers the dorsal and lateral surfaces. Attached to the pars basalis is a dorsolateral plate. The capsula interna, longer in length compared to the capsula externa, partially overlays the ventral plate. Apex of the capsula interna with a tubular stylus.

Female. Pedipalp femora noticeably smaller than those of males.

Female measurements. Total length 2.30, carapace length 0.87, dorsal scutum length 1.85, carapace max. width 1.24, mesotergum max. width 1.75. Appendage Measurements: Pedipalps. Trochanter length 0.17, femora length 0.72, patella length 0.35, tibia length 0.54, tarsus length 0.57. Leg I: trochanter (tr) 0.22, femora (fe) 0.73, patella (pa) 0.43, tibia (ti) 0.53, metatarsus (mt) 0.65, tarsus (ta) 0.60. II: tr 0.28, fe 0.97, pa 0.49, ti 0.75, mt 0.82, ta 1.02. III: tr 0.22, fe 0.61, pa 0.38, ti 0.53, mt 0.57, ta 0.56. IV: tr 0.34, fe 0.90, pa 0.55, ti 0.76, mt 0.91, ta 0.75.

Nerudiella caramavida **sp. nov.**

https://zoobank.org/45A9D45E-90CE-43D9-9223-BD691DA31146
Figs 80–85

Material examined. ***Holotype*****.** ♂ **Chile.** Malleco: P.N. Nahuelbuta, M. Ramírez, F. Labarque, 12.II.2005 (MNHNCL). ***Paratypes*****. Chile.** Malleco: P.N. Nahuelbuta, M. Ramírez, F. Labarque, 12.II.2005, 9 ♂ 7 ♀ 3 imm. (MACN), Malleco: P.N. Nahuelbuta, 1250 m, N. Platnick, R.Schuh. 19.XI.1981, 1 ♂ 2 ♀ 6 imm. (AMNH). Ñuble: 2 km E de Las Trancas, E. Maury. 09.I.1989, 1 ♂ 1 ♀ (MACN).

Additional material. Chile. Arauco. Hualpén, Univ. Concepción Terrestrial Biology Station, 36.79821°S, 73.16307°W, 52 m, A. Ojanguren, A. Pérez-González, M. Ramírez, G. Azevedo, W. Porto coll., 14.I.2018, 1 ♂ (MACN). Caramávida, San Alfonso, Quebrada Caramávida, Arauco Reserve, 37.70942°S, 73.17107°W, 750 m, A. Ojanguren, A. Pérez-González, M. Ramírez, G. Azevedo, W. Porto coll., 3 mm. 14.I.2018, 1 ♀, 1 ♂ 3.

Etymology. The specific epithet "*caramavida*" is derived from the type locality of the species, Quebrada Caramávida, located on the western slope of the Cordillera de Nahuelbuta in the Bío-Bío Region. The choice of this name, a noun in apposition, is based on the geographic location where the species was originally discovered.

Diagnosis. This species can be easily distinguished from its congeners by the capsula interna of the male genitalia, which has two long lateral processes.

Distribution. Chile: Bío-Bío Region (Fig. 4F).

Description of male holotype. Measurements: Total length 2.74, carapace length 1.1, dorsal scutum length 2.05, carapace max. width 1.37, mesotergum max. width 1.96. Appendage measurements: Pedipalps. Trochanter length 0.20, femora length 0.92, patella length 0.40, tibia length 0.62, tarsus length 0.83. Leg I: trochanter (tr) 0.20, femora (fe) 0.85, patella (pa) 0.46, tibia (ti) 0.62, metatarsus (mt) 0.78, tarsus (ta) 0.65. II: tr 0.25, fe 1.84, pa 0.57, ti 0.90, mt 1.31, ta 1.29. III: tr 0.31, fe 0.79, pa 0.38, ti 0.64, mt 0.66, ta 0.60. IV: tr 0.31, fe 1.08, pa 0.63, ti 0.88, mt 1.04, ta 0.82.

Dorsum (Fig. 80, 81). Eta (η) hourglass-shaped dorsal scutum. Ocularium low and rounded, pointing a bit forward. Dorsal scutum microgranulate. Mesotergal areas of dorsal scutum not well delimited; with small setiferous tubercles. Free tergites with two rows of small setiferous tubercles.

Chelicerae (Fig. 82A, B). Segment I with an acute tubercle on the dorso-distal surface. Segment II with two mesal setiferous tubercles and 7–8 small se-

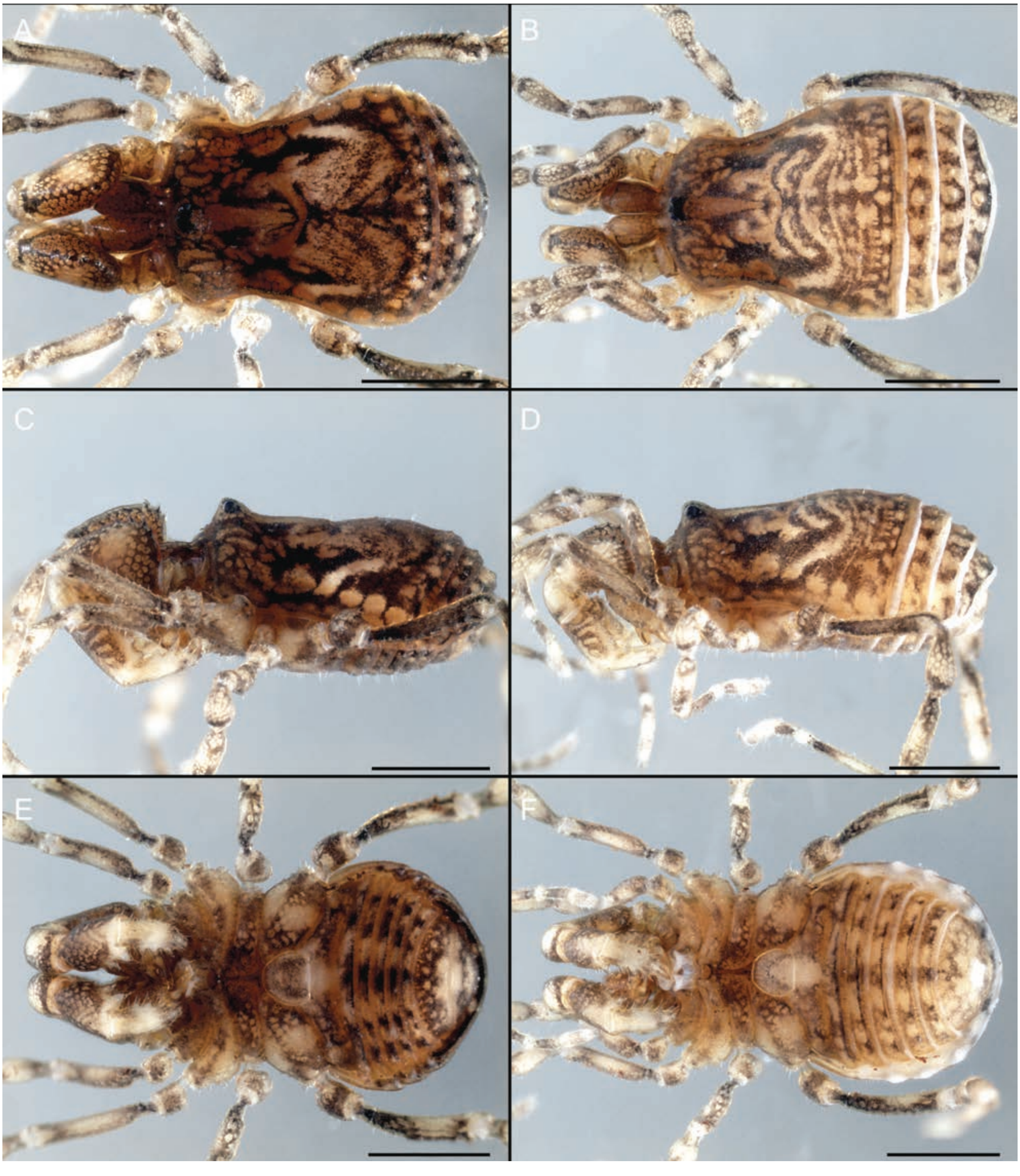

Figure 80. *Nerudiella caramavida* sp. nov. habitus, male **A** dorsal view **C** lateral view **E** ventral view. Female **B** dorsal view **D** lateral view **F** ventral view. Scale bars: 1 mm. Species of Clade C, see Fig. 3.

tiferous tubercles, with one triangular tubercle more prominent than others in frontal view.

Pedipalps (Fig. 82C, D). Trochanter with tiny dorsal and ventral tubercles. Femora with two robust ventral-proximal tubercles and four minor ventral-distal tubercles. Additionally, with a row of setiferous tubercles along dorsal surface of femora, with the three largest tubercles located in the proximal section. Pa-

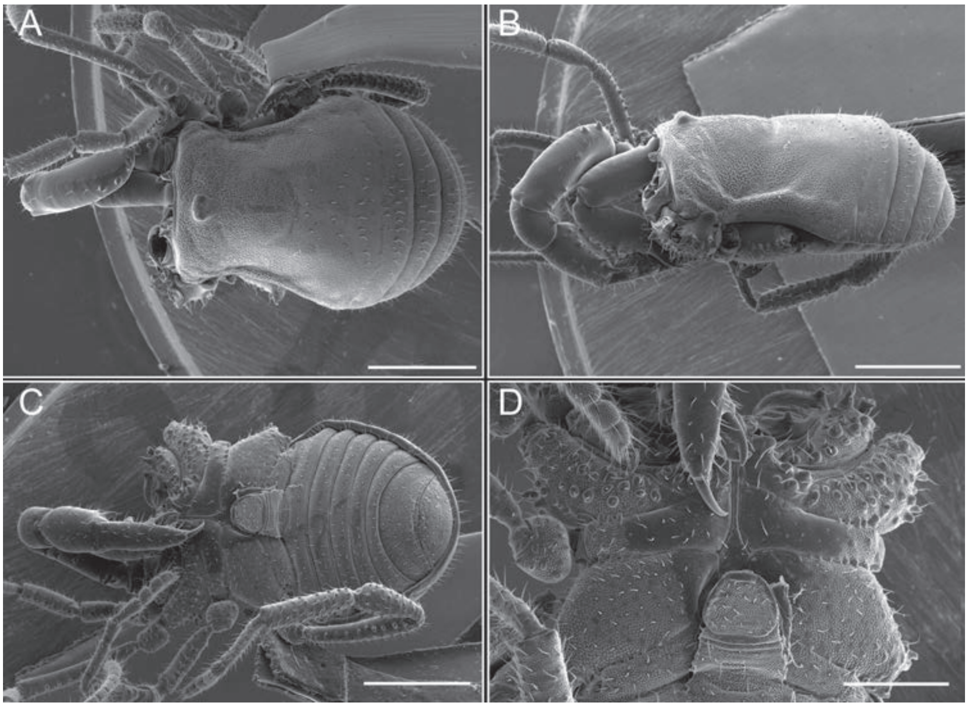

Figure 81. *Nerudiella caramavida* sp. nov. male, SEM images of habitus **A** dorsal view **B** lateral view **C, D** ventral view. Scale bars: 1 mm (**A, B, C**); 500 µm (**D**).

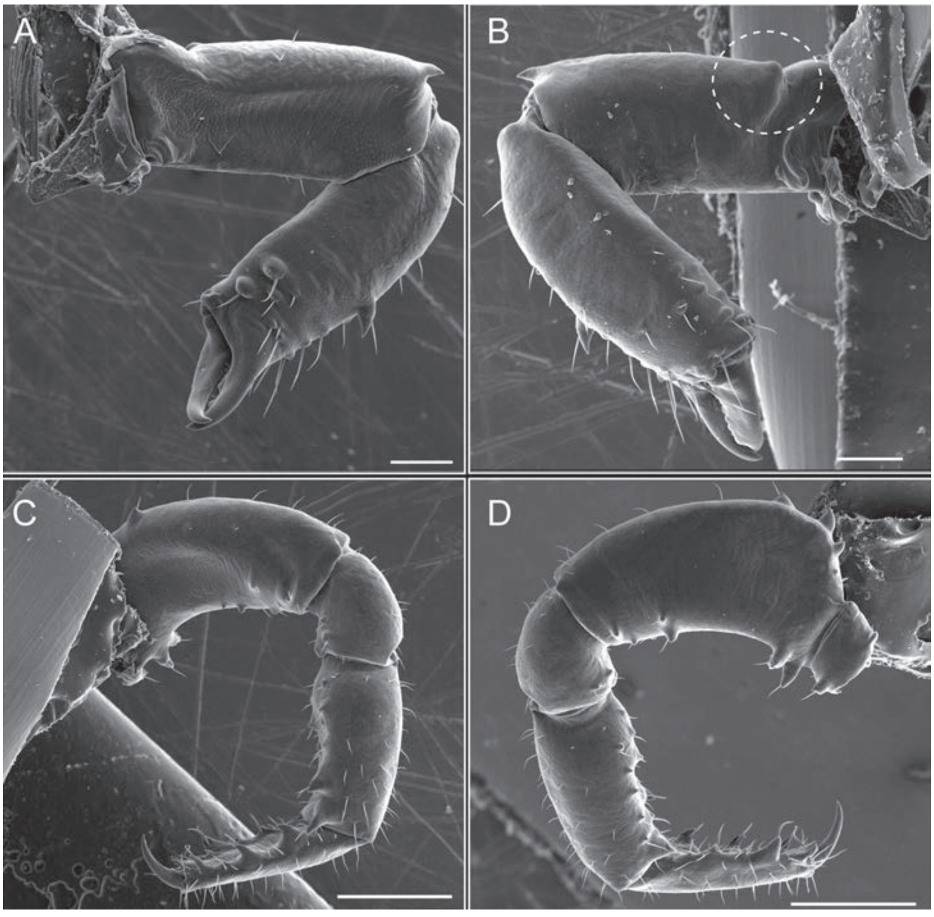

Figure 82. *Nerudiella caramavida* sp. nov. chelicerae: mesal **A** ectal **B** pedipalps: mesal **C** ectal **D**. Scale bars: 200 µm (**A, B**); 500 µm (**C, D**).

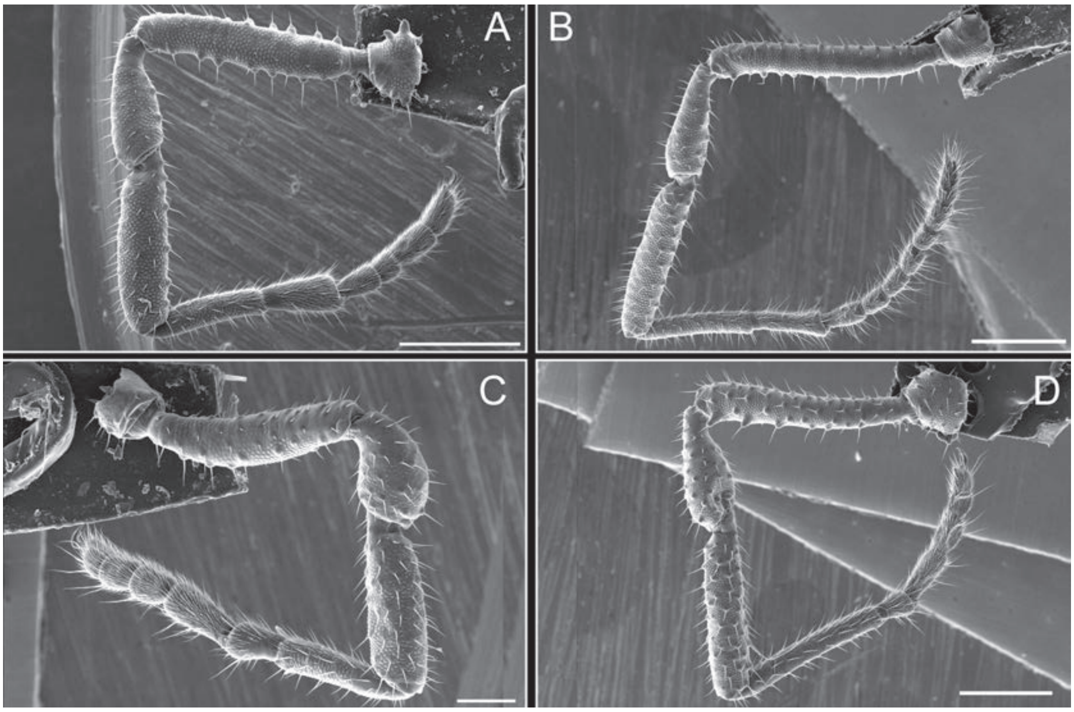

Figure 83. *Nerudiella caramavida* sp. nov. legs I **A** II **B** III **C** IV **D**. Scale bars: 500 µm (**A, B, D**); 200 µm (**C**).

tella with two small ventral-ectal tubercles and two small ventral-mesal tubercles. Tibia with two rows of weaker apical tubercles and two rows of minor ventral tubercles. Tarsus characterized by three mesal and ectal spines; Also, with a few setae and subdistal setae in this region.

Legs (Fig. 83). Segment I with nine or ten setiferous tubercles; segment II with 18–20 setiferous tubercles; segment IV with five or six small tubercles connected to the opisthosoma. Spiracles not obstructed by bridges. Smooth areas with ~ ⅓ of leg II smooth, with two or three small tubercles on each side featuring subdistal setae. The smooth portion extends to ¾ of leg III and < ⅓ of leg IV. Sternum arrow-shaped. Legs smooth, with notch in tarsus I. Tarsal count: 3–6/7–4–4.

Penis (Figs 84, 85). Pars distalis with a large ventral plate bearing a cleft that divides the plate into two halves. Each half with three pointed macrosetae on the ventral surface and one macroseta on the dorsal surface. Capsula externa covering dorsal and lateral surface, its apical region U-shaped. With a dorsolateral plate attached to the pars basalis. Capsula interna longer than the capsula externa, which has a long lateral process, perpendicular to the axis of the genitalia, with a visible stylus in its apical portion.

Female. Similar to male, with shorter pedipalpal femora.

Female measurements. Total length 2.6, carapace length 1.13, dorsal scutum length 2.1, carapace max. width 1.39, mesotergum max. width 1.98. Appendage measurements: Pedipalps. Trochanter length 0.26, femora length 0.99, patella length 0.46, tibia length 0.70, tarsus length 0.87. Leg I: trochanter (tr) 0.24, femora (fe) 1.04, patella (pa) 0.54, tibia (ti) 0.79, metatarsus (mt) 0.94, tarsus (ta) 0.78. II: tr 0.26, fe 1.51, pa 0.64, ti 1.08, mt 1.26, ta 1.44. III: tr 0.31, fe 0.93, pa 0.41, ti 0.69, mt 0.78, ta 0.78. IV: tr 0.32, fe 1.26, pa 0.61, ti 1.09, mt 1.28, ta 0.97.

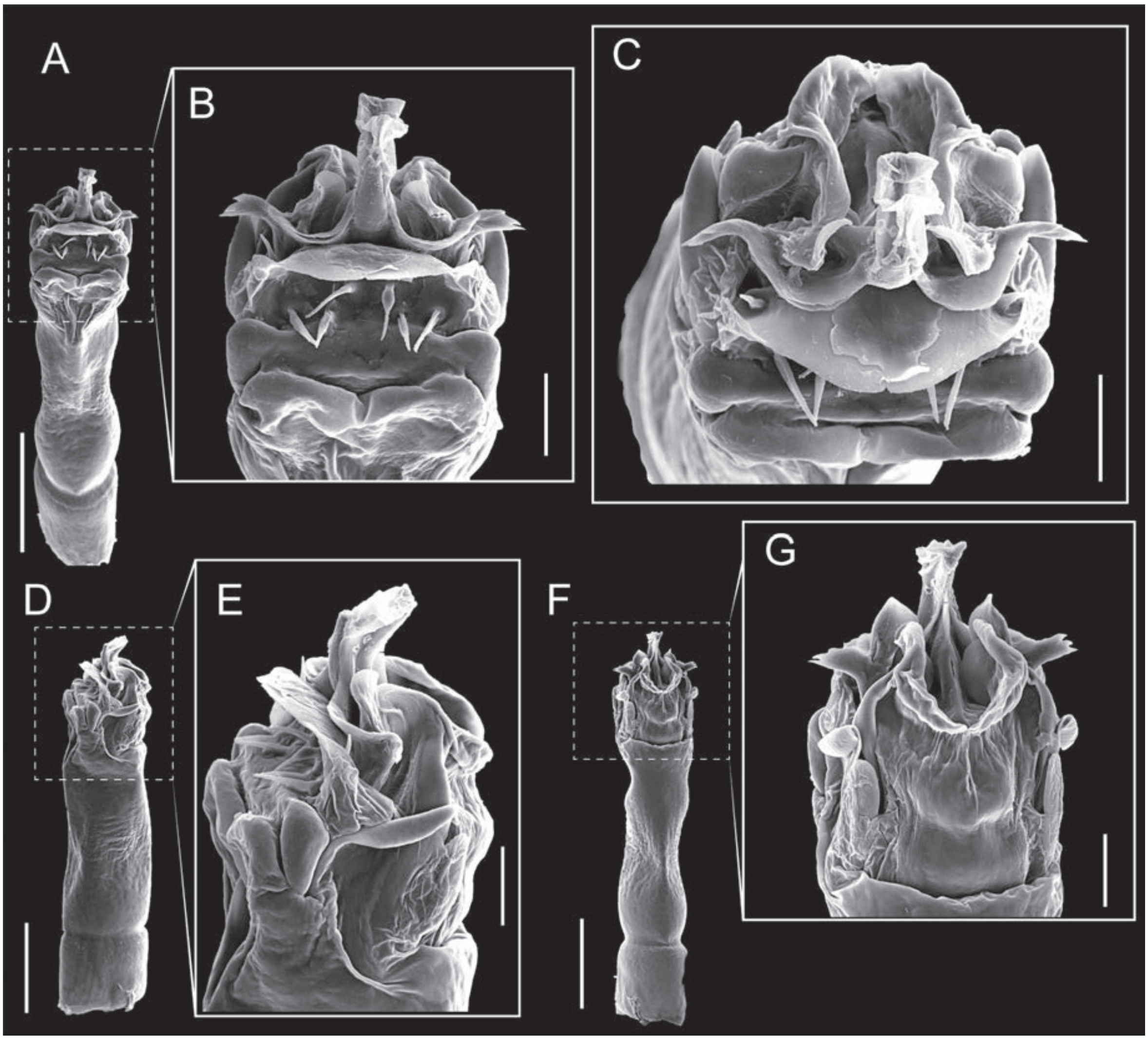

Figure 84. *Nerudiella caramavida* sp. nov. penis: ventral **A, B** apical **C** lateral **D, E** dorsal **F, G**. Scale bars: 200 µm (**A, D, F**); 50 µm (**B, C, E, G**).

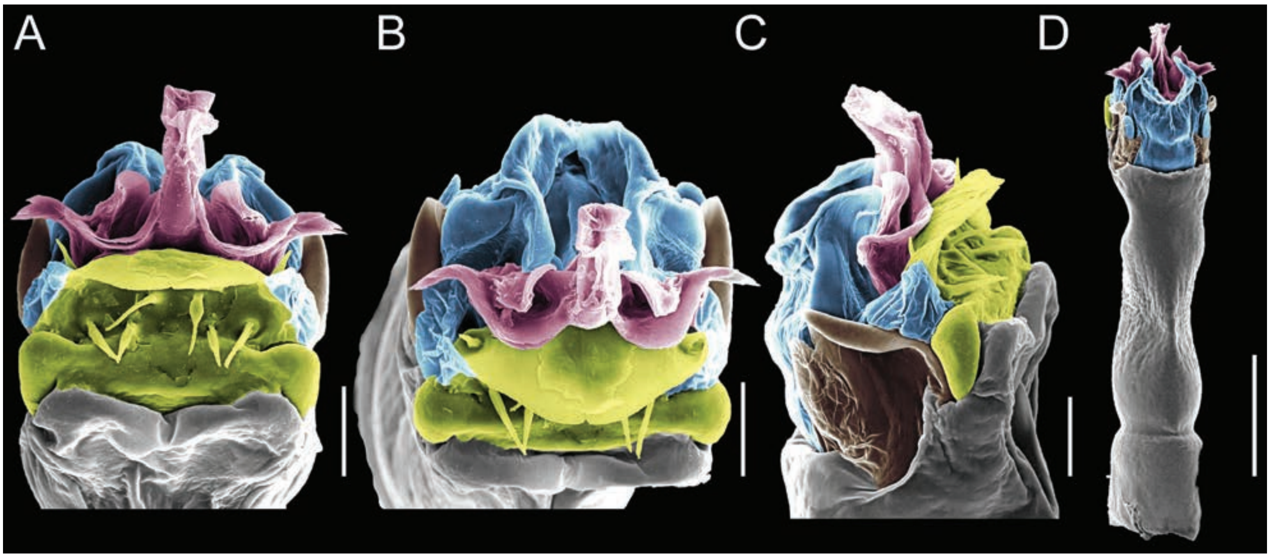

Figure 85. *Nerudiella caramavida* sp. nov. penis: ventral **A** apical **B** lateral **C** dorsal **D**. Colors: ventral plate (yellow), capsula externa (blue), capsula interna (red). Scale bars: 50 µm (**A–C**); 200 µm (**D**).

Nerudiella cautin **sp. nov.**

https://zoobank.org/49BC3855-C82F-42EC-81D3-F4D32C7B23B4
Figs 86–91

Material examined. ***Holotype***. ♂ **Chile.** Región de Los Lagos, Llanquihue, 13 km W Río Negro. Berlese. N. Platnick, R.Schuh coll., coll, 24.I.1986 (AMNH). ***Paratypes***. **Chile.** Palena, Vicinity of Chaitén, 0–100 m. Berlese. N. Platnick, R.Schuh 5–7. XII.1981 2♂ 2♀ 7 imm. (AMNH). Same data, 1♀ 3 imm. (AMNH). Los Lagos, Palena, 25–27 km North Chaitén, 40 m. P. Goloboff, R.Schuh 17.I.1986 2♂ (AMNH). Coihaique, 10 km N Reserva Nacional Coyhaique. S.Peck, J.Peck. 22.I.1985 1♀ (FMNH). Aysén, 30 km N Puerto Cisnes. E. Maury . 09.XII.1986 (MACN).

Etymology. The specific epithet refers to the type locality of the species, the province of Cautín, located in the southern zone of Chile. Noun in apposition.

Diagnosis. The sharp tubercles on the dorsal scutum surface distinguish this species from others its congeners, particularly when observed from a dorsal view. The genitalia shows a unique U-shaped capsula externa (Fig. 91D).

Distribution. Chile: Bío-Bío, Araucanía, Los Ríos, and Los Lagos Regions (Fig. 4F).

Description of male holotype. Total length 4.17, carapace length 1.26, dorsal scutum length 2.64, carapace max. width 1.51, mesotergum max. width 2.06. Appendage measurements: Pedipalps. Trochanter length 0.35, femora length 1.05, patella length 0.58, tibia length 0.79, tarsus length 0.73. Leg I: trochanter (tr) 0.22, femora (fe) 0.83, patella (pa) 0.48, tibia (ti) 0.67, metatarsus (mt) 0.80, tarsus (ta) 0.71. II: tr 0.23, fe 1.17, pa 0.64, ti 0.89, mt 1.03, ta 1.33. III: NA. IV: tr 0.35, fe 1.15, pa 0.64, ti 0.96, mt 1.22, ta 0.98.

Dorsum (Fig. 86, 87). Dorsal scutum microgranulate, without clear delimitation of areas. Area I characterized by a row of three setae, while areas II–III display a row of six low, broad, arch-shaped setiferous tubercles. Area IV and posterior margin with a row of low, broad setiferous tubercles. Free tergites with a row of low, broad setiferous tubercles.

Chelicerae (Fig. 88A, B). Segment I with a small tubercle on the dorso-distal surface. Segment II with a mesal tubercle and bearing few setae.

Pedipalps (Fig. 88C, D). Trochanter with a small dorsal and ectal tubercle. Femora with two ventroproximal tubercles with subdistal setae, four distal setiferous granules, and three dorsoproximal tubercles with subdistal setae. Mesal surface of the femora with two rows of setiferous granules. Patella with ventral setiferous granules. Tibia with three ectal and two mesal spines with subdistal setae, the ventral surface adorned with small setiferous granules. Tarsus with three mesal and ectal spines with subdistal setae, with a few setae and granules.

Legs (Fig. 89). Coxae I–II with setiferous tubercles, with the longest distal tubercle bearing a subdistal seta. Coxae III and IV with microgranulation only, lacking setiferous tubercles. With four bridges between legs II and III, five or six bridges between III and IV, and four bridges between leg IV and the opisthosoma, the distal bridge longer than the others. Spiracles not obstructed by bridges. The smooth surface occupies ~ ¹⁄₃ of leg II, with two small tubercles and two rounded tubercles present. In leg III, the smooth area covers ~ ¾ of the surface, while in leg IV, it occupies < ¹⁄₃ of the surface. Sternum arrow-shaped. Legs smooth, with sparse setae. Tarsal count: 4–7–4–4.

Figure 86. *Nerudiella cautin* sp. nov. habitus, male **A** dorsal view **C** lateral view **E** ventral view. Female **B** dorsal view **D** lateral view **F** ventral view. Scale bars: 1 mm.

Penis (Figs 90, 91). Pars distalis with large ventral plate bearing a cleft dividing the plate into two lamellae. Each lamella with three pointed macrosetae on the ventral surface and one macroseta on the dorsal surface. Capsula externa covering dorsal and lateral surfaces, with a long cleft dividing capsula externa into two parts; with a dorsolateral plate attached to the pars basalis. Capsula interna longer than capsula externa, partially covering the ventral plate, the apical region of the capsula interna thin and sharp, the stylus not visible in its apical portion.

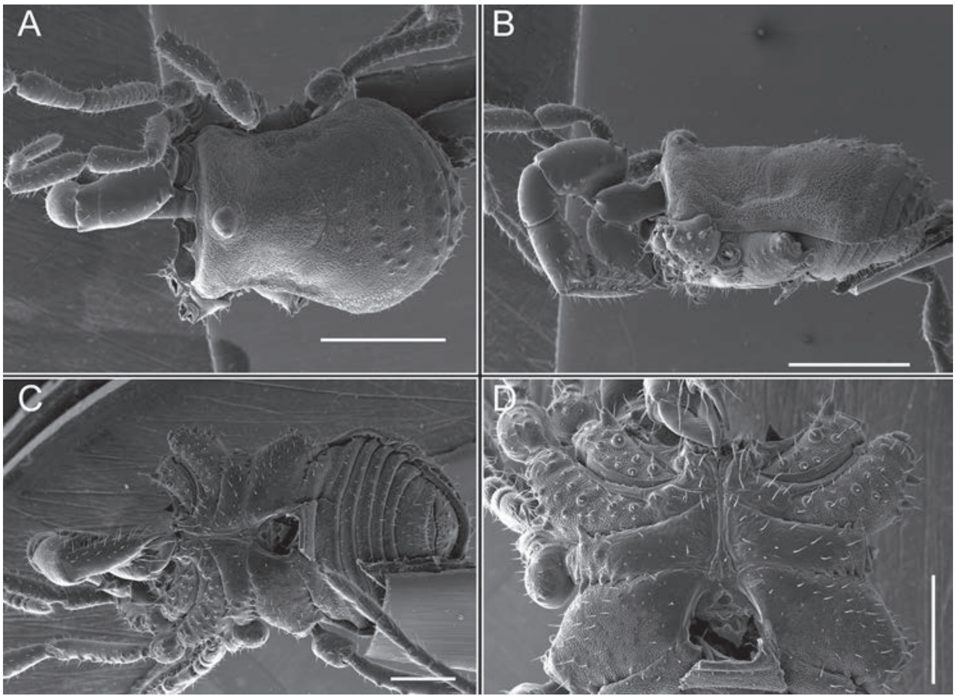

Figure 87. *Nerudiella cautin* sp. nov. male, SEM images of habitus **A** dorsal view **B** lateral view **C, D** ventral view. Scale bars: 500 µm.

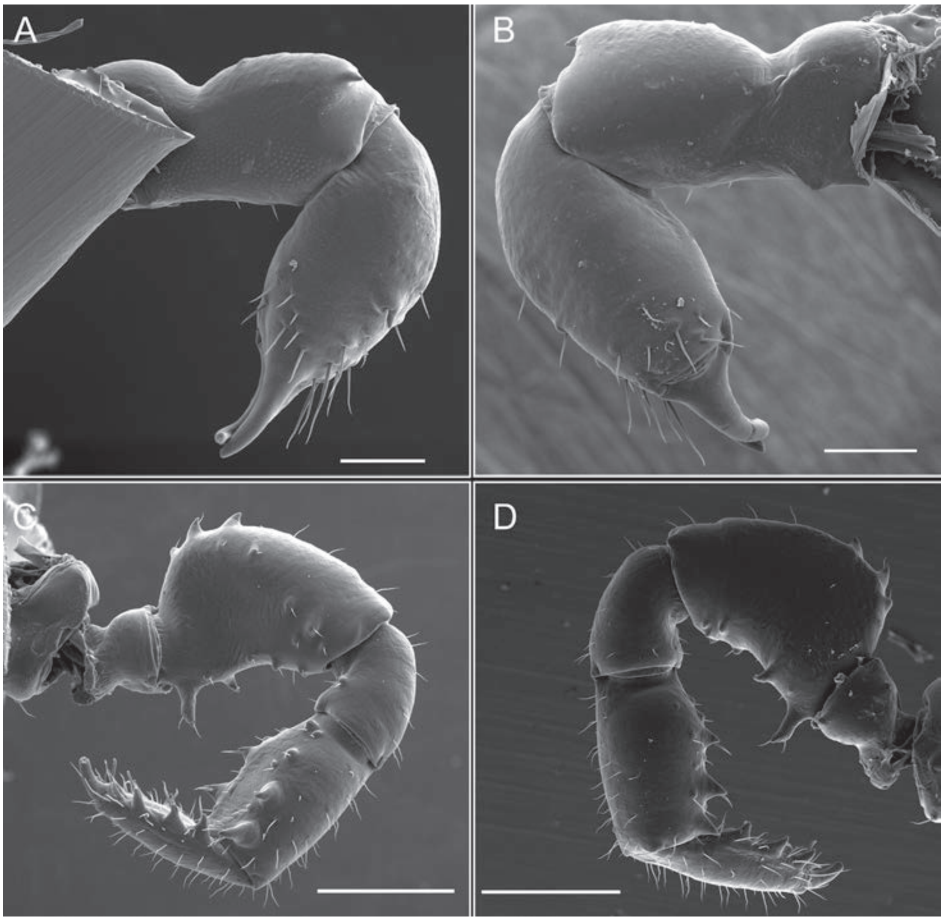

Figure 88. *Nerudiella cautin* sp. nov. chelicerae: mesal **A** ectal **B** pedipalps: mesal **C** ectal **D**. Scale bars: 200 µm (**A, B**); 500 µm (**C, D**).

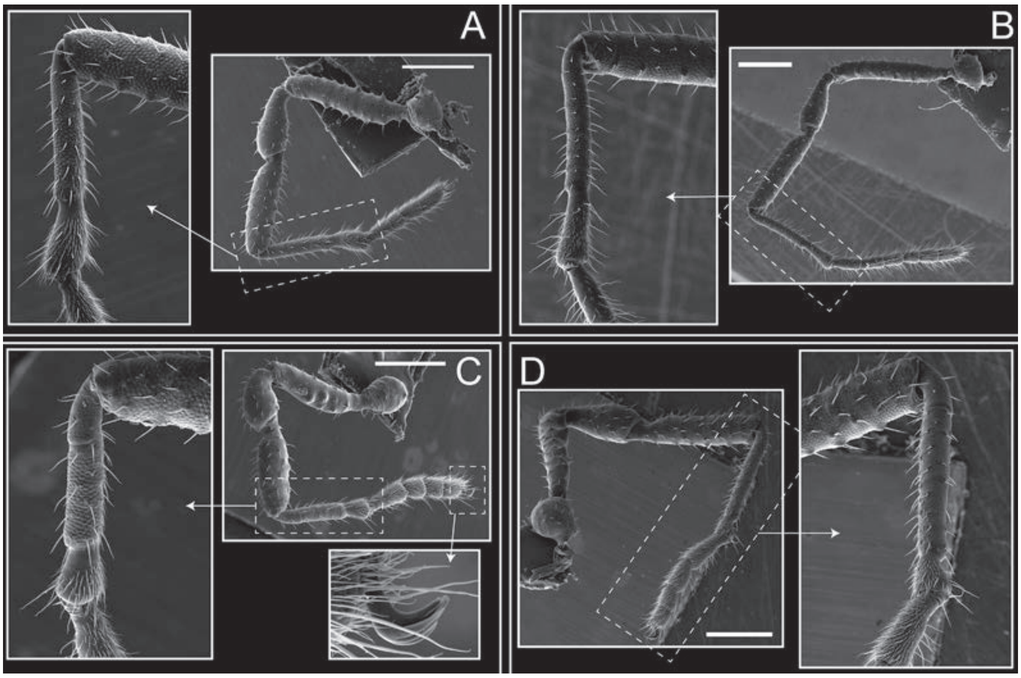

Figure 89. *Nerudiella cautin* sp. nov. legs I **A** II **B** III **C** IV **D**. Scale bars: 500 µm.

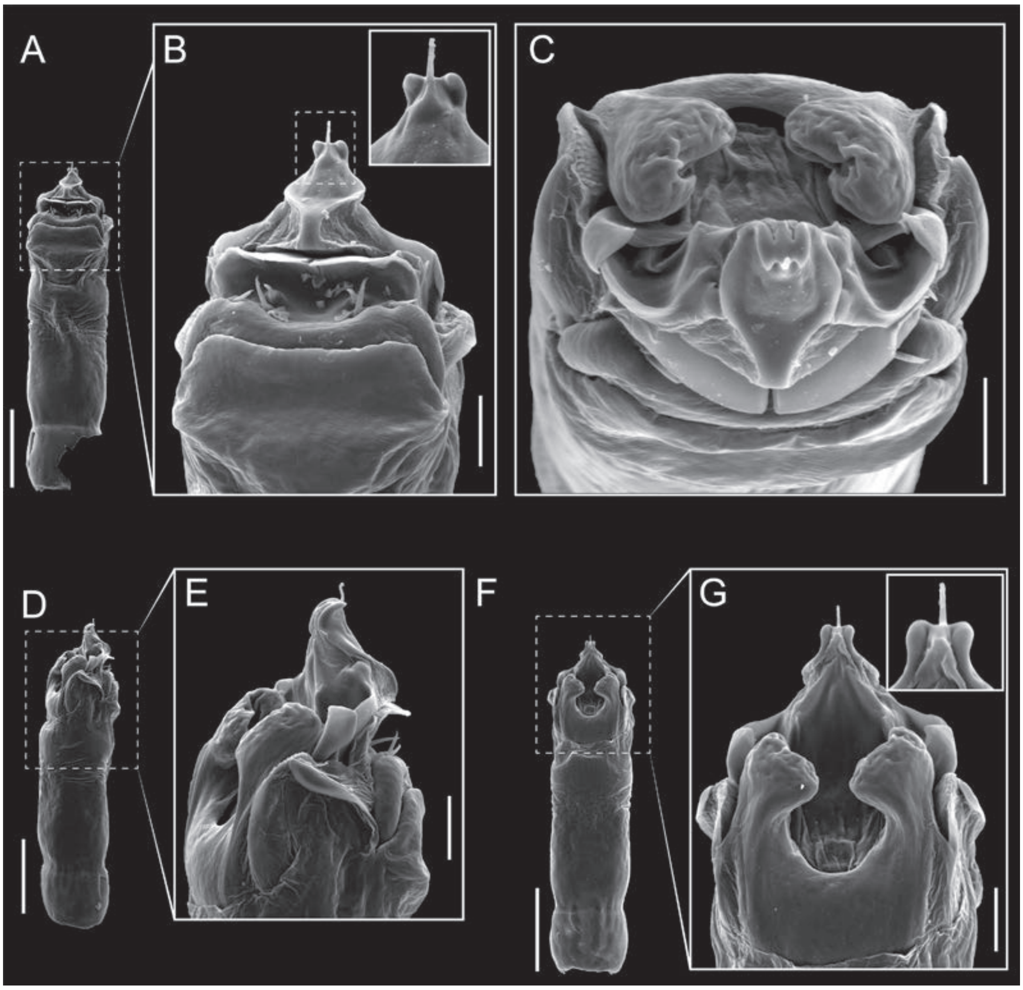

Figure 90. *Nerudiella cautin* sp. nov. penis: ventral **A, B** apical **C** lateral **D, E** dorsal **F, G**. Scale bars: 200 µm (**A, D, F**); 50 µm (**B, C, E, G**).

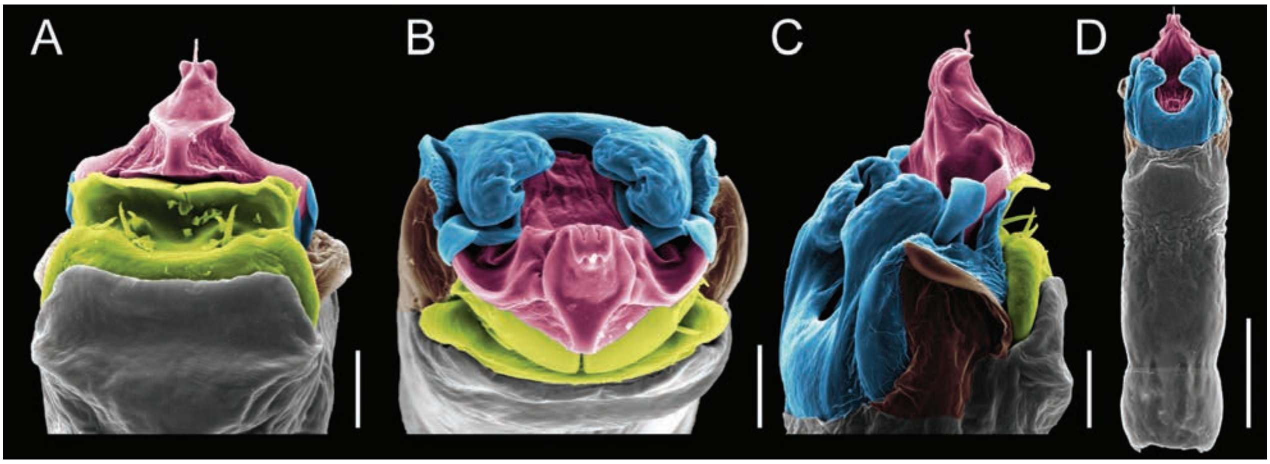

Figure 91. *Nerudiella cautin* sp. nov. penis: ventral **A** apical **B** lateral **C** dorsal **D**. Colors: ventral plate (yellow), capsula externa (blue), capsula interna (red). Scale bars: 50 µm.

Female. Similar to males, but with a noticeable shorter pedipalpal femora.

Female measurements. Total length 2.2, carapace length 1.00, dorsal scutum length 2.1, carapace max. width 1.3, mesotergum max. width 2.0. Appendage measurements: Pedipalps. Trochanter length 0.21, femora length 0.85, patella length 0.50, tibia length 0.50, tarsus length 0.63. Leg **I**: trochanter (tr) 0.22, femora (fe) 0.87, patella (pa) 0.47, tibia (ti) 0.66, metatarsus (mt) 0.76, tarsus (ta) 0.65. **II**: tr 0.25, fe 1.10, pa 0.60, ti 0.89, mt 0.99, ta 1.21. **III**: tr 0.25, fe 0.75, pa 0.36, ti 0.58, mt 0.61, ta 0.67, **IV**: tr 0.33, fe 1.05, pa 0.66, ti 0.89, mt 1.09, ta 0.78. Tarsal count 3–6–4–4.

Nerudiella choapa **sp. nov.**

https://zoobank.org/B4A37CD7-79B1-49D3-9B3C-8ACC7193480E
Figs 92–97

Material examined. ***Holotype*.** ♂ **Chile.** Valparaíso: Pichicuy, Quebrada Huaquén, E. Maury coll., 25.X.1988 (MNHNCL). ***Paratypes*. Chile.** Coquimbo (Choapa province): Pichidangui, Cerro La Silla del Gobernador, E. Maury coll., 31.X.1988, 3 ♂ (MACN). Same data 6 ♀ 2 imm. (MACN).

Etymology. The specific epithet “choapa” is derived from one of the locality where the species was collected, the Choapa province in the Coquimbo region of Chile. It is used as noun in apposition to indicate the association of the species with this specific geographic location.

Diagnosis. This species can be distinguished from its congeners by several key characteristics. Firstly, its dorsal surface and pedipalps are densely setose. Additionally, the femora and tibia of the pedipalp are covered with small tubercles. The unique male genitalia has a capsula externa that covers the dorsal and lateral surfaces. The apical region of the capsula externa is bent at a 90-degree angle in relation to the axis of the genitalia, and there are two small parallel apical structures present. This species shares similarities with *Nerudiella zapallar* sp. nov., particularly in the apical region of the capsula externa, although it is relatively shorter in comparison in the latter species.

Distribution. Chile: Coquimbo and Valparaíso Regions (Fig. 4F).

Figure 92. *Nerudiella choapa* sp. nov. habitus, male **A** dorsal view **B** lateral view **C** ventral view. Scale bars: 1 mm.

Description of male holotype. Measurements: Total length 2.19, carapace length 0.94, dorsal scutum length 1.77, carapace max. width 1.33, dorsal scutum max. width 1.77. Appendage measurements: Pedipalps. Trochanter length 0.21, femora length 0.90, patella length 0.49, tibia length 0.70, tarsus length 0.86. Leg **I**: trochanter (tr) 0.21, femora (fe) 0.86, patella (pa) 0.45, tibia (ti) 0.67, metatarsus (mt) 0.82, tarsus (ta) 0.61. **II**: tr 0.20, fe 1.21, pa 0.53, ti 0.97, mt 1.07, ta 1.23. **III**: tr 0.24, fe 0.83, pa 0.39, ti 0.68, mt 0.77, tr 0.64. **IV**: tr 0.24, fe 1.19, pa 0.57, ti 0.96, mt 1.13, ta 0.75.

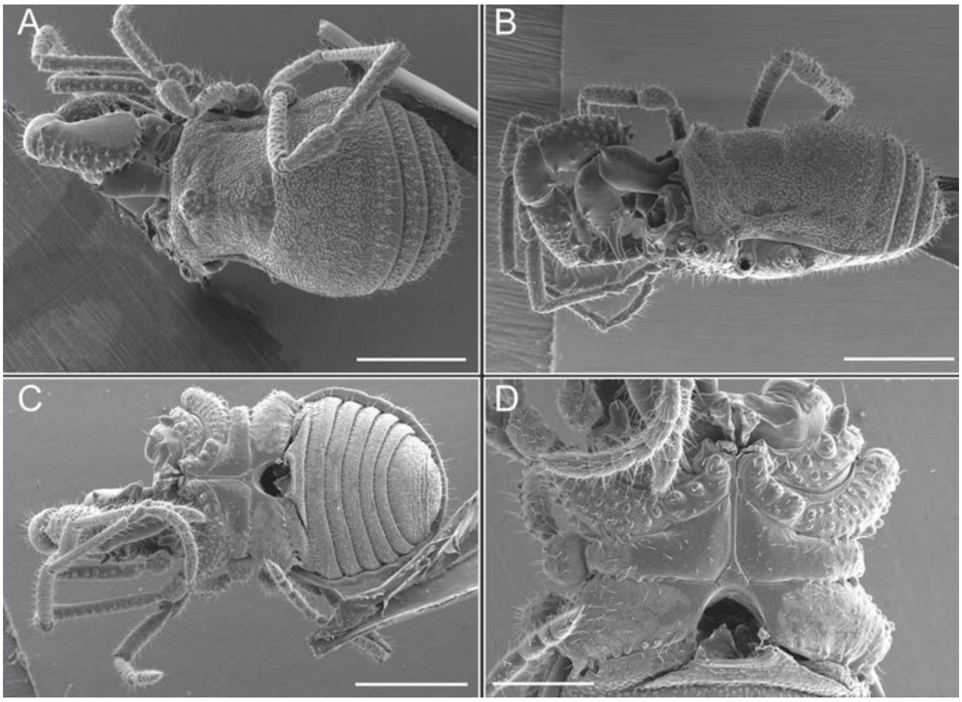

Figure 93. *Nerudiella choapa* sp. nov. male, SEM images of habitus **A** dorsal view **B** lateral view **C, D** ventral view. Scale bars: 1 mm (**A, B, C**); 500 µm (**D**).

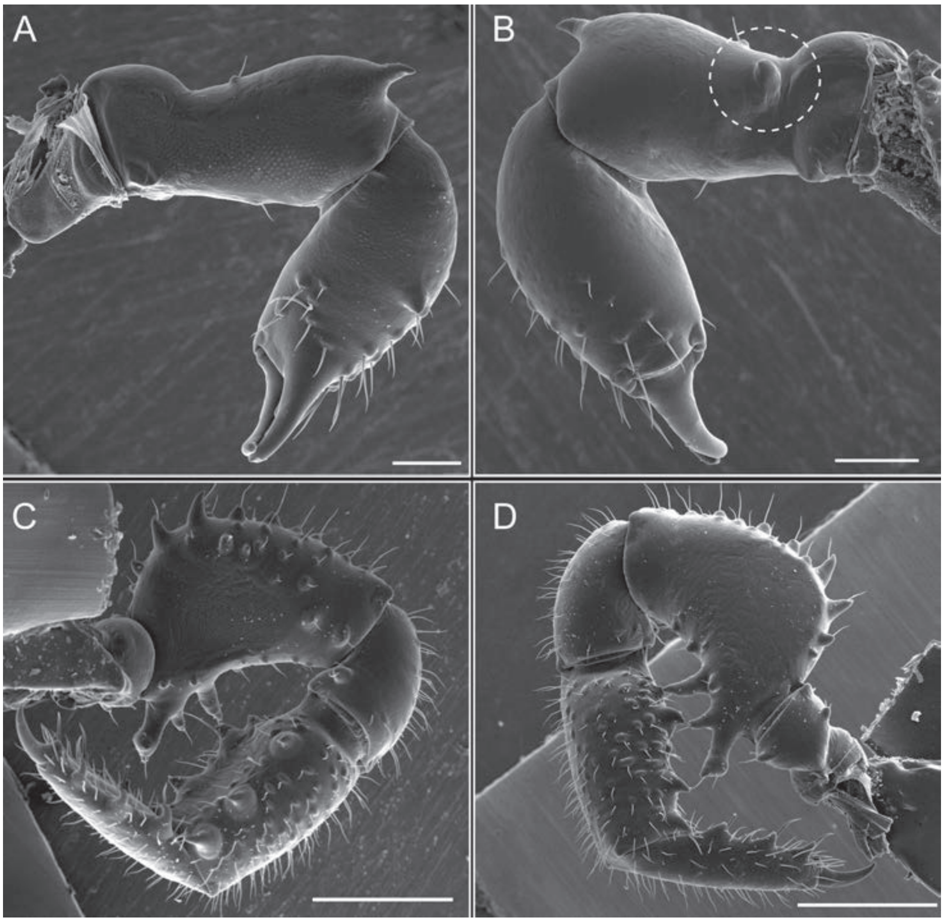

Figure 94. *Nerudiella choapa* sp. nov. chelicerae: mesal **A** ectal **B** pedipalps: mesal **C** ectal **D**. Scale bars: 200 µm (**A, B**); 500 µm (**C, D**).

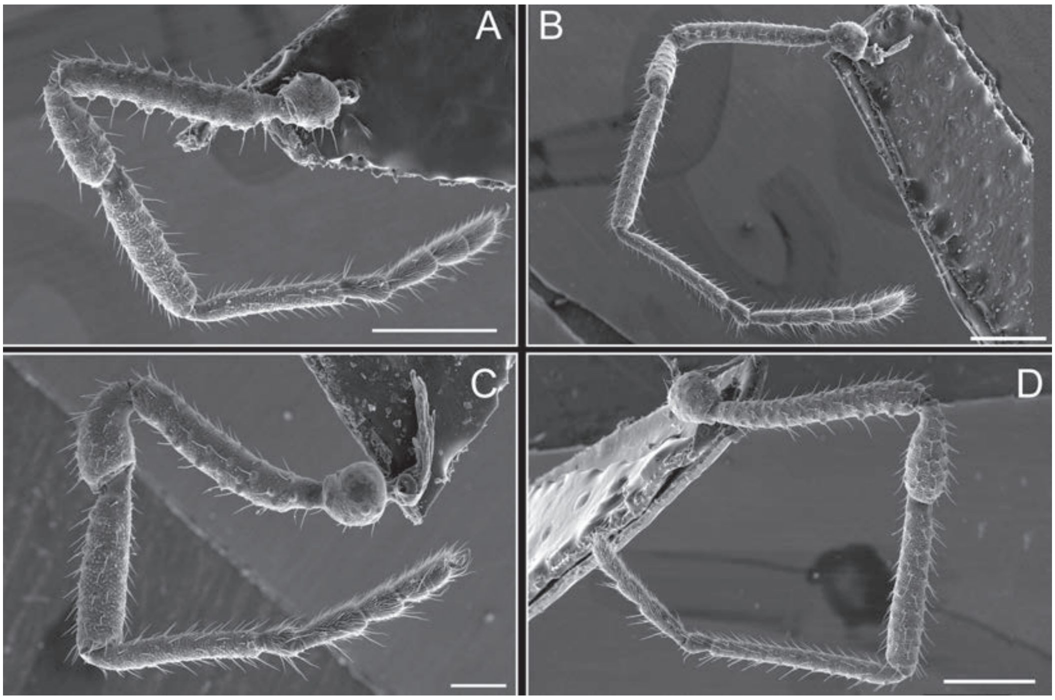

Figure 95. *Nerudiella choapa* sp. nov. legs I **A** II **B** III **C** IV **D**. Scale bars: 500 µm (**A, B, D**); 200 µm (**C**).

Dorsum (Fig. 92, 93). Eta (η) hourglass-shaped dorsal scutum. Ocularium low and rounded, with small tubercles. Dorsal scutum and free tergites with microgranulation. Mesotergal areas lack clear separation but are covered with small setiferous tubercles.

Chelicerae (Fig. 94A, B). Segment I with a sharp tubercle on the dorso-distal surface, with two proximal tubercles. In segment II, there are scattered setae visible in both the ectal and ventral views. In the front view, there is a prominent triangular tubercle that stands out from the others.

Pedipalps (Fig. 94C, D). Trochanter with two small dorsal tubercles and one ventral tubercle. Femora with a dorso-mesal area with setiferous tubercles, including two stronger ones in the proximal region. In the ventral view, there are three prominent proximal spines and a row of small tubercles. Patella with a mesal setiferous tubercle. Tibia with three ventral-ectal spines and two ventral-mesal spines, with the lateral and dorsal areas with small setiferous tubercles. Tarsus with three mesal and ectal spines with subdistal setae, as well as additional setae and a few setae.

Legs (Fig. 95). Coxa I with 11–13 setiferous tubercles, the two apical ones being stronger and more prominent than the others. Coxa II with 18–20 setiferous tubercles, while coxa IV has 5–6 small tubercles. Bridges between legs do not obstruct the spiracles. The smooth surface occupies ~ ⅓ of leg II, ¾ of leg III, and < ⅓ of leg IV. Within smooth area of leg II, there are two small tubercles with subdistal setae on each side. Sternum arrow-shaped. Legs covered in small tubercles, and the astragalus is longer than the calcaneus on all legs (Fig. 95). Tarsal count: 3–5–4–4.

Penis (Figs 96, 97). Genitalia: Pars distalis with a ventral plate bearing a cleft that divides the plate into two lamellae. Each lamella has three pointed macrosetae on the ventral surface and one macroseta on the dorsal surface; cap-

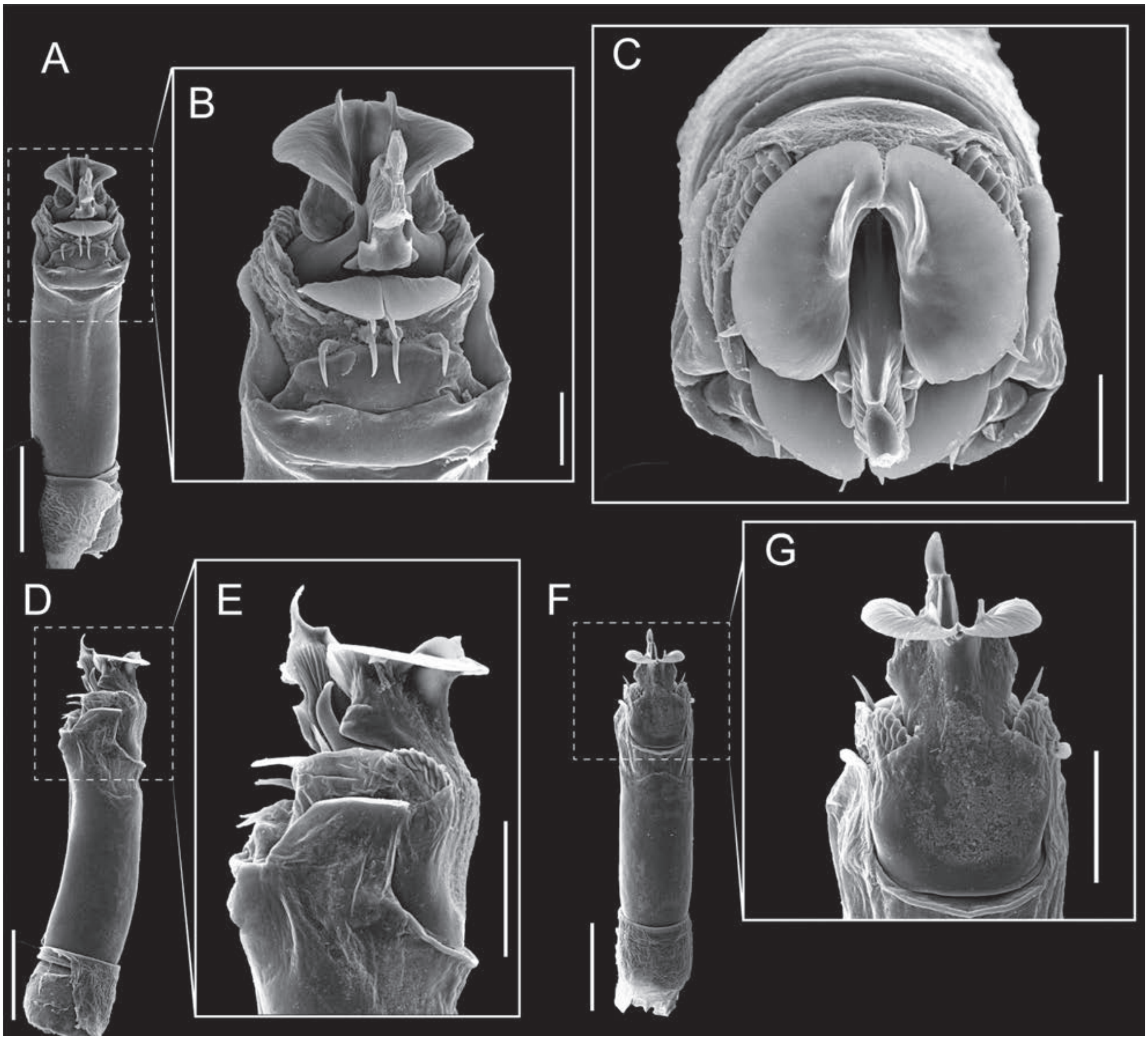

Figure 96. *Nerudiella choapa* sp. nov. penis: ventral **A, B** apical **C** lateral **D, E** dorsal **F, G**. Scale bars: 200 µm (**A, D, F**); 50 µm (**B, C**); 100 µm (**E, G**).

sula externa covering the dorsal and lateral surface, having the apical region bent at an angle of 90 ° in relation to the axis of the genitalia. It includes a pair of small apical processes in the form of small "wings". The capsula interna also has a pair of lateral processes, which are long and ventrally sloping. Capsula interna longer than capsula externa, with its apical portion thinner.

Female. Similar to males, with shorter pedipalpal femora.

Female measurements. Total length 2.63, carapace length 1.0, dorsal scutum length 2.11, carapace max. width 1.47, mesotergum max. width 2.07. Appendage measurements: Pedipalps. Trochanter length 0.27, femora length 0.84, patella length 0.52, tibia length 0.61, tarsus length 0.92. Leg I: trochanter (tr) 0.28, femora (fe) 0.88, patella (pa) 0.48, tibia (ti) 0.68, metatarsus (mt) 0.84, tarsus (ta) 0.63. **II**: tr 0.29, fe 1.16, pa 0.56, ti 0.89, mt 1.05, ta 1.20. **III**: tr 0.28, fe 0.81, pa 0.38, ti 0.64, mt 0.84, ta 0.67, **IV**: tr 0.29, fe 1.18, pa 0.61, ti 0.98, mt 1.25, ta 0.75. Tarsal count 3–6–4–4.

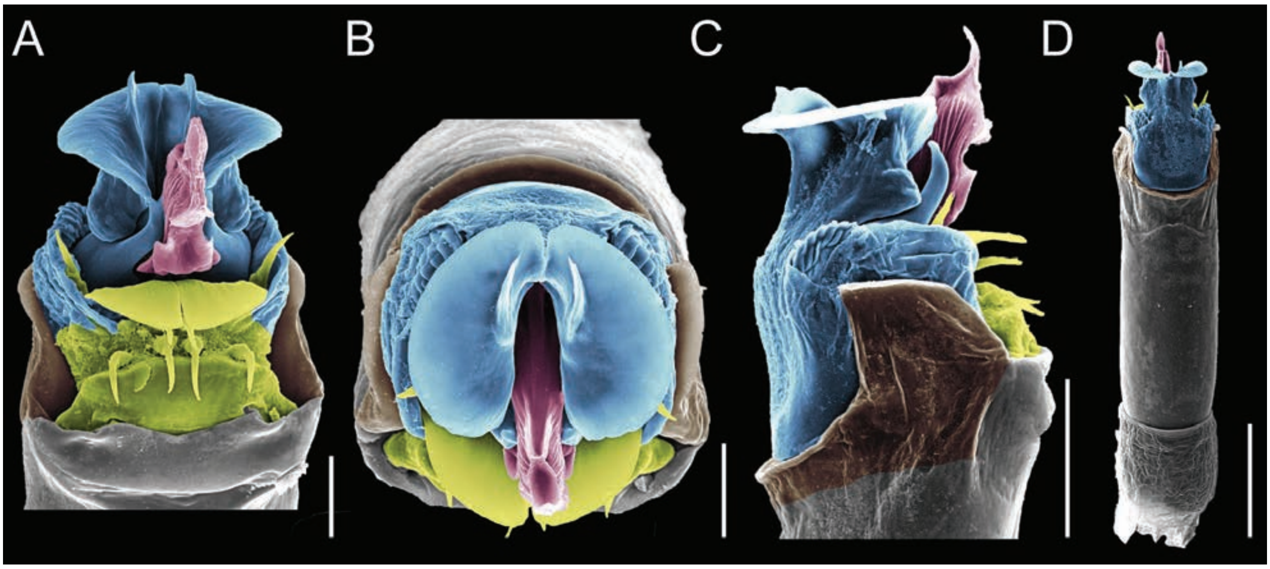

Figure 97. *Nerudiella choapa* sp. nov. penis: ventral **A** apical **B** lateral **C** dorsal **D**. Colors: ventral plate (yellow), capsula externa (blue), capsula interna (red). Scale bars: 50 µm (**A, B**); 100 µm (**C**); 200 µm (**D**).

***Nerudiella curi* sp. nov.**
https://zoobank.org/9F17E25B-8E00-4677-B1C3-9FD8DDAB3731
Figs 98–103

Material examined. ***Holotype*.** ♂ **Chile.** Curicó: Cerro Hueca-Hueca, J. Barriga coll., 10.12.2005 (MNHNCL). ***Paratypes*.** **Chile.** Curicó: Cerro Hueca-Hueca, J. Barriga coll., 10.12.2005, 3 ♂ 5 ♀ (MACN).

Etymology. The specific epithet is a variation of the spelling of "kuri" or "kurü," which is a word in the Mapuche language used to define the color black, which is present in spots on the dorsal surface of individuals of the group. Noun in apposition.

Diagnosis. This species can be readily distinguished from other species in the genus by several characteristics. Firstly, it exhibits a wider genital operculum compared to other species. Additionally, the male genitalia display a distinct morphology, featuring a capsula externa consisting of three lamellae. Furthermore, the ventral plate of the male genitalia is characterized by a row of aligned macrosetae.

Distribution. Chile: Maule Region, Curicó Province (Fig. 4F).

Description of male holotype. Measurements: Total length 2.59, carapace length 0.91, dorsal scutum length 2.03, carapace max. width 1.30, max. mesotergum width 1.77. Appendage measurements. Pedipalps. Trochanter length 0.22, femora length 0.69, patella length 0.37, tibia length 0.52, tarsus length 0.49. Leg I: trochanter (tr) 0.24, femora (fe) 0.89, patella (pa) 0.43, tibia (ti) 0.70, metatarsus (mt) 0.73, tarsus (ta) 0.70. II: tr 0.29, fe 1.11, pa 0.50, ti 0.96, mt 1.05, ta 1.20. III: tr 0.27, fe 0.75, pa 0.36, ti 0.66, mt 0.78, ta 0.63. IV: tr 0.32, fe 1.19, pa 0.63, ti 0.98, mt 1.26, ta 0.77.

Dorsum (Fig. 98, 99). Eta (η) hourglass-shaped dorsal scutum. Ocularium low on the body. Dorsal scutum microgranulate, without clear delimitation of distinct areas. In the anterior region, specifically areas I and II, there are two small setiferous tubercles. In the area III, there is a row of four small setiferous tubercles, while area IV is adorned with a row of eight small setiferous tuber-

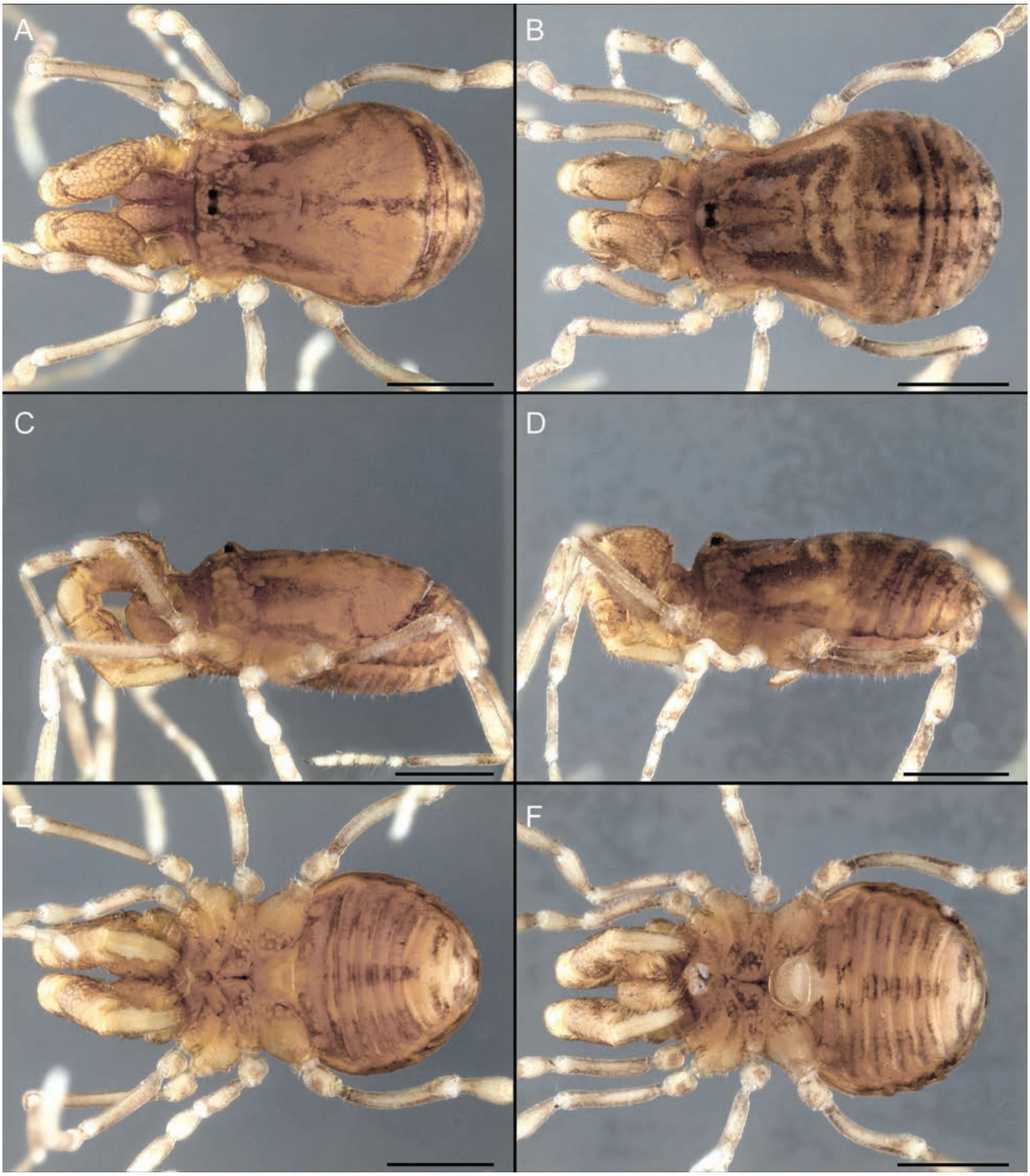

Figure 98. *Nerudiella curi* sp. nov. habitus, male **A** dorsal view **C** lateral view **E** ventral view. Female **B** dorsal view **D** lateral view **F** ventral view. Scale bars: 1 mm.

cles. Posterior margin of dorsal scutum with a row of eight small setiferous tubercles. Free tergites with a row of small setiferous tubercles.

Chelicerae (Fig. 100A, B). Segment I with a small tubercle on the dorso-distal surface. Segment II with a small frontal tubercle and scattered setae.

Pedipalps (Fig. 100C, D). Trochanter with two small dorsal tubercles and one ventral. Femora with a row of three tubercles with subdistal setae on dorsal

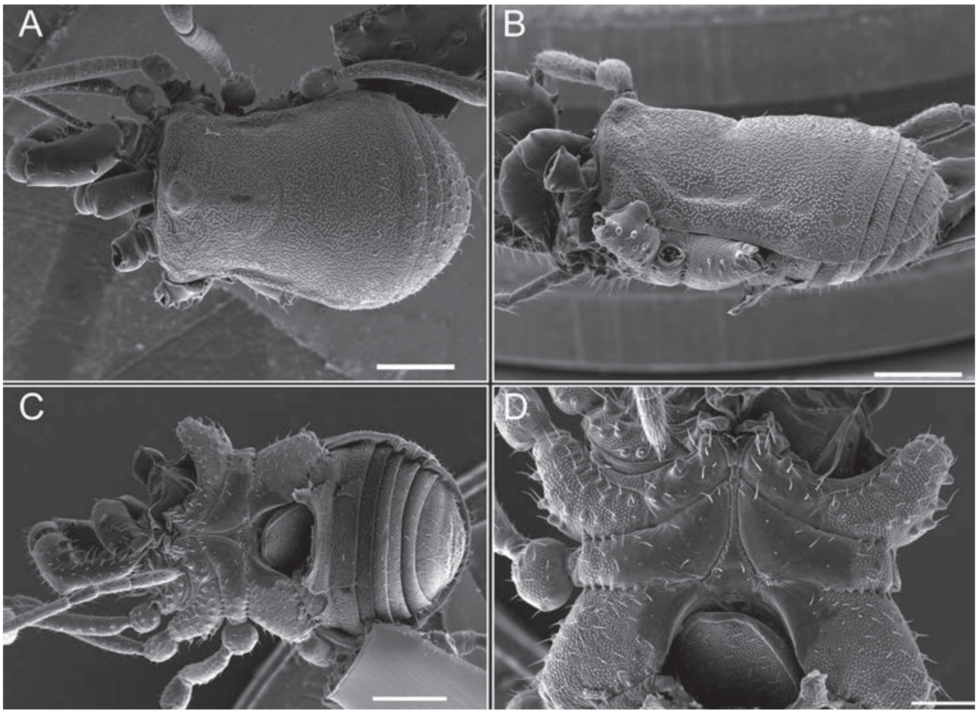

Figure 99. *Nerudiella curi* sp. nov. male, SEM images of habitus **A** dorsal view **B** lateral view **C, D** ventral view. Scale bars: 500 µm (**A, B, C**); 200 µm (**D**).

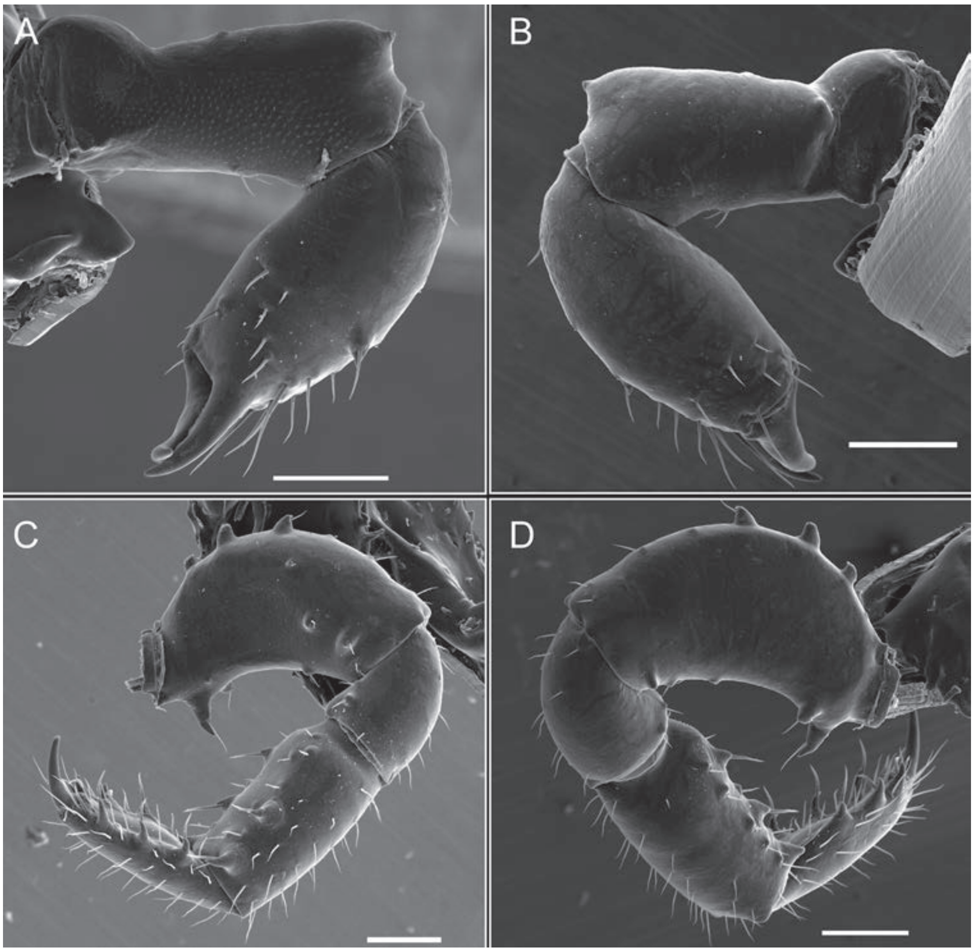

Figure 100. *Nerudiella curi* sp. nov. chelicerae: mesal **A** ectal **B** pedipalps: mesal **C** ectal **D**. Scale bars: 200 µm.

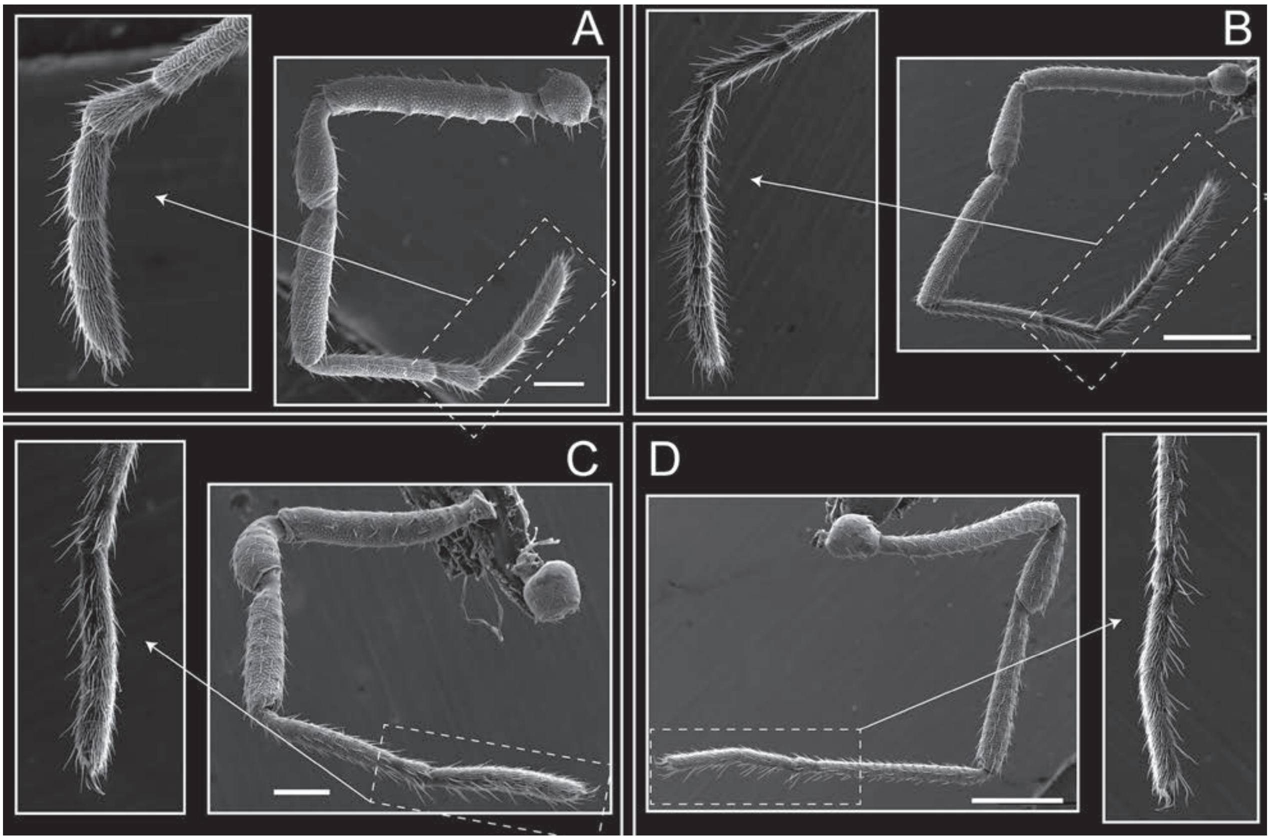

Figure 101. *Nerudiella curi* sp. nov. legs I **A** II **B** III **C** IV **D**. Scale bars: 200 μm (**A, C**); 500 μm (**B, D**).

view, one long and one small spines with subdistal setae on ventral view, six low setiferous tubercles in mesal view, and one in ectal view. Patella with a small mesal and ectal setiferous tubercle. Tibia with a mesal row of five small ectal setiferous tubercles, three ventral ectal spines, and two ventral mesal spines with subdistal setae. Tarsus with three mesal and ectal spines with subdistal setae.

Legs (Fig. 101). Coxa I with two rows of setiferous tubercles and two distal setiferous tubercles with subdistal setae, coxa II with two rows of setiferous tubercles, III and IV only with microgranulation, three bridges between coxa legs II and III, six between coxa legs III and IV, four between leg IV and opisthosoma. Spiracles not obstructed by bridges. Smooth surface that occupies ⅓ of leg II, ¾ of III and ⅓ of IV. Genital operculum larger than other species of the genus. Smooth area of leg II with a setiferous tubercle on each side. Sternum arrow-shaped. Legs I–IV covered in setae, tarsal area, and calcaneus densely setose. Calcaneus smaller than astragalus, ≥ 3× smaller (legs I–III) and 4× (leg IV). Tarsal count: 4–6–4–4.

Penis (Figs 102, 103). Pars distalis with a ventral plate bearing a cleft dividing the plate into two lamellae. Each lamella has a row of three pointed macrosetae on the ventral surface and one macroseta on the dorsal surface. Capsula externa covering the dorsal and lateral surface, divided into three folds, one pair covering the dorsolateral surface and the last one covering the dorsal surface, there is a dorsolateral plate attached to the pars basalis. Capsula interna divided into three parts, two lateral processes and a central process in which it bears an apical stylus. The ventral plate bears a cleft that divides the plate into two

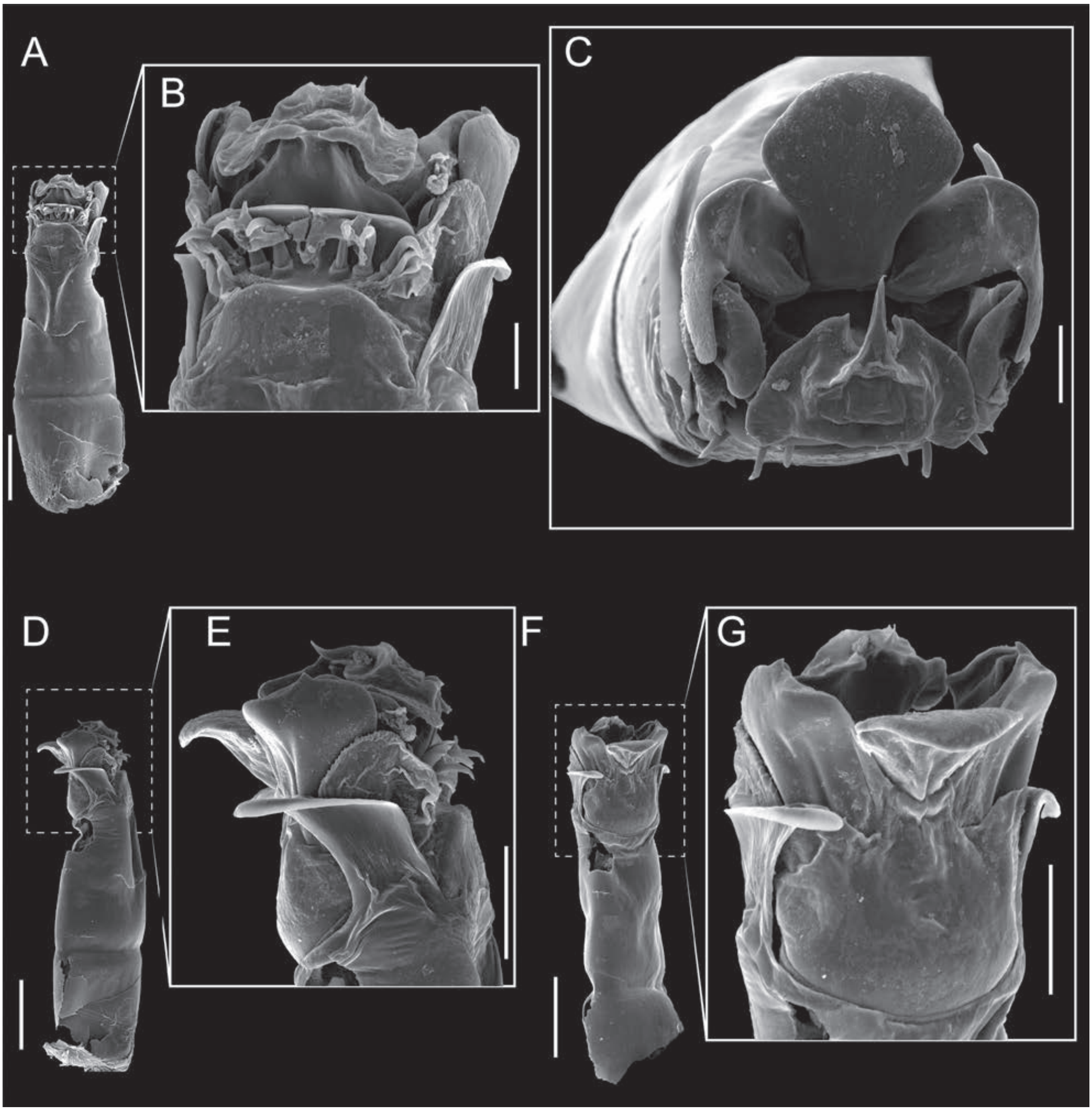

Figure 102. *Nerudiella curi* sp. nov. penis: ventral **A, B** apical **C** lateral **D, E** dorsal **F, G**. Scale bars: 200 µm (**A, D, F**); 50 µm (**B, C**); 100 µm (**E, G**).

halves, each with three ventral and one dorsal macrosetae. Ventral macrosetae arranged in a row.

Female. Similar to males, with shorter pedipalpal femora.

Female measurements. Total length 2.40, carapace length 0.85, dorsal scutum length 1.89, carapace max. width 1.23, mesotergum max. width 1.67. Appendage measurements: Pedipalps. Trochanter length 0.22, femora length 0.69, patella length 0.37, tibia length 0.52, tarsus length 0.49. Leg I: trochanter (tr) 0.14, femora (fe) 0.24, patella (pa) 0.89, tibia (ti) 0.43, metatarsus (mt) 0.70, tarsus (ta) 0.73. **II**: tr 0.70, fe 0.29, pa 1.11, ti 0.50, mt 0.96, ta 1.05. **III**: tr 1.20, fe 0.27, pa 0.75, ti 0.36, mt 0.66, ta 0.78. **IV**: tr 0.63, fe 0.32, pa 1.19, ti 0.63, mt 0.98, ta 1.26, tr 0.77.

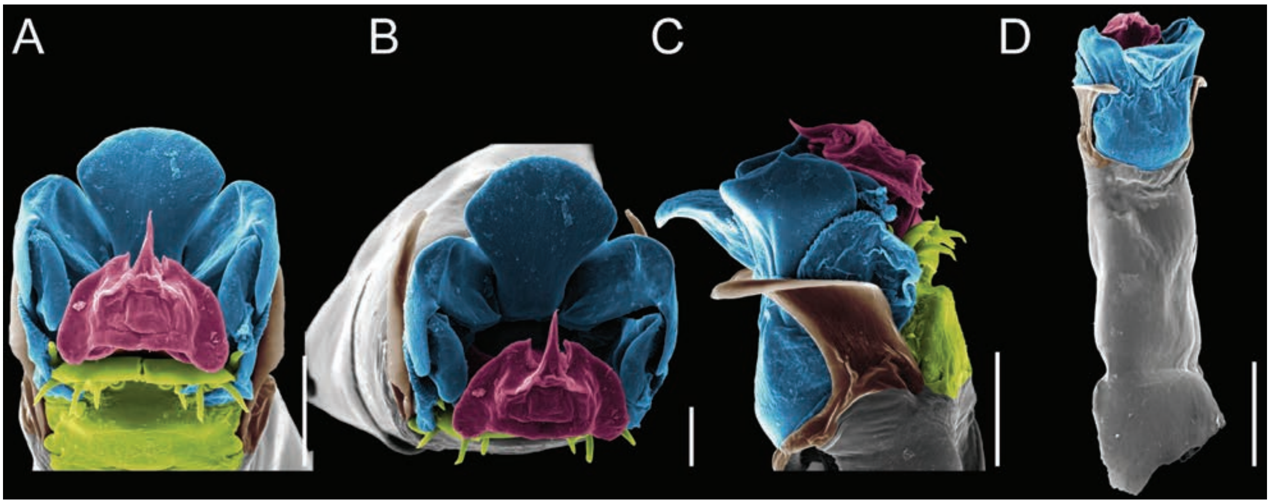

Figure 103. *Nerudiella curi* sp. nov. penis: ventral **A** apical **B** lateral **C** dorsal **D**. Colors: ventral plate (yellow), capsula externa (blue), capsula interna (red). Scale bars: 50 µm (**A, B**); 100 µm (**C**); 200 µm (**D**).

***Nerudiella goroi* sp. nov.**

https://zoobank.org/83521462-412E-44DC-8DEB-07C518E25495
Figs 104–109

Material examined. ***Holotype***. ♂ **Chile.** Concepción: Estero Nonguén, T.Cekalovic coll., 21.IV.1976 (MNHNCL). ***Paratypes***. **Chile.** Concepción: 6 km S San Pedro, 360 m, A. Newton, M. Thayer coll., 12.XII.1982, 1 ♂ (AMNH). Camino a Ramuncho, Cruce Hualpén, T.Cekalovic coll., 02.XI.1986, 4 ♂ 1 ♀ 18 imm. (MACN). Cautín: Ojos del Caburgua, 16 km NE de Pucón, E. Maury coll., 16.I.1987, 1 ♂ 7 ♀ 6 imm. (MACN). Bellavista, Lago Villarrica, 260 m, R.Schuh, N. Platnick coll., 30.I.1986, 1 ♂ 4 ♀ 7 imm. (AMNH). Cautín: Cerro Ñielol Temuco, IX Región (Araucaria), E. Maury coll., 21.I.1991, 1 ♂ 1 imm. (MACN). Cautín: Cerro Ñielol Temuco, IX Región (Araucaria), E. Maury coll., 15.I.1989, 3 ♀ 2 imm. (MACN). Termas de Palguin SE de Pucón, E. Maury coll., 17.01.1987, 1 ♀ 1 imm. (MACN). Estero Chauilco, T.Cekalovic coll., 25.I.1980, 1 ♀ (MACN)

Additional material. Chile. Cautín: Bellavista, Fundo Flor del Lago, 40.6663°S, 72.1733°W, 270 m, M. Ramírez, F. Labarque coll., 09.02.2005, 3 ♂ 5 ♀ 12 imm. (MACN). Same data, 2 ♀ 31 imm. (MACN). Same data 3 ♂ 1 ♀ 2 imm. (MACN). Cautín: Volcán, Villarrica, 1100 m, N. Platnick, O. Francke coll., 28.I.1985, 2 imm. (AMNH). Bellavista, Lago Villarrica, N. Platnick, O. Francke coll., 28.I.1985, 2 ♂ 2 ♀ 4 imm. (AMNH). Bellavista, Lago Villarrica, 260 m, R.Schuh, N. Platnick coll., 30.01.1986, 2 imm. (AMNH). Same locality N. Platnick, K.Catley, M. Ramírez, T.Allen coll., 20.XI.1993, 1 ♂ 1 ♀ 1 imm. (AMNH). Osorno: Pucatrihue, L.Peña coll., 10.II.1985, 2 imm. (FMNH).

Etymology. The specific epithet is bestowed upon the Chilean entomologist Raúl Briones Parra, widely recognized by his nickname “Goro”, in recognition to his significant contributions to the field of entomology and his unwavering dedication to the conservation of the Chilean forests. A noun in apposition.

Diagnosis. This species can be easily distinguished from the other species in the genus by having two sharp tubercles on the ventral-proximal region of the pedipalp femora. The male genitalia has a pair of ventrally curved capsula externa processes.

Figure 104. *Nerudiella goroi* sp. nov. habitus, male **A** dorsal view **C** lateral view **E** ventral view. Female **B** dorsal view **D** lateral view **F** ventral view. Scale bars: 1 mm.

Distribution. Chile: Regions of Bío-Bío, Araucanía, Los Ríos, Los Lagos.

Description of male holotype. Total length 3.9. Carapace length 1.1, dorsal scutum length 2.5, carapace max. width 1.4, mesotergum max. width 1.6. Appendage measurements. Pedipalps. Trochanter length 0.25, femora length 0.94, patella length 0.60, tibia length 0.70, tarsus length 0.68. Leg **I**: trochanter (tr) 0.27, femora (fe) 1.37, patella (pa) 0.59, tibia (ti) 0.90, metatarsus (mt) 1.13, tarsus (ta) 0.83. **II**: tr 0.28, fe 1.75, pa 0.79, ti 1.30, mt 1.50, ta 1.73. **III**: tr 0.32,

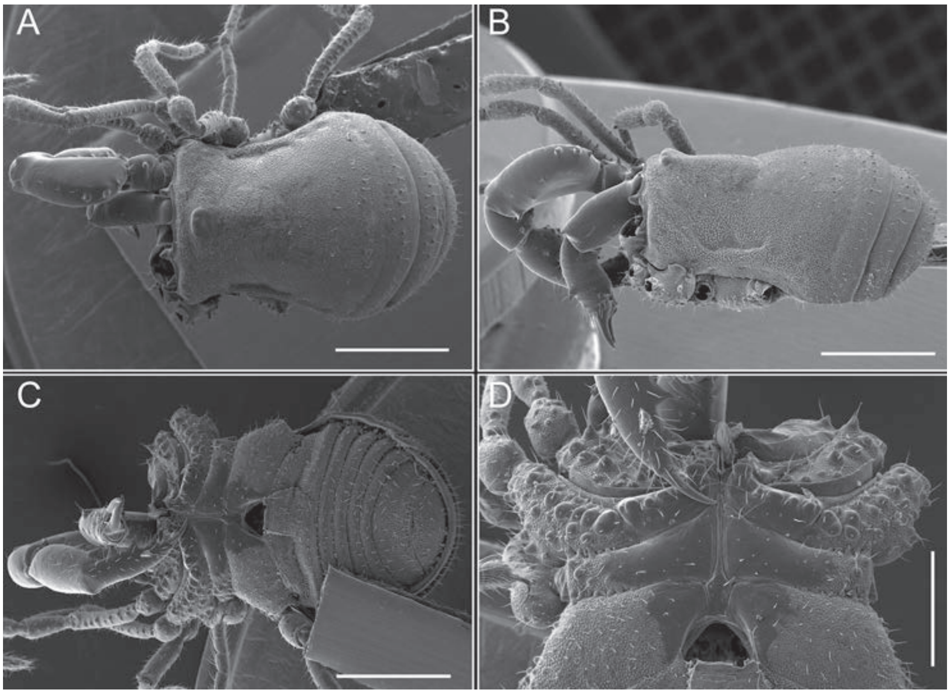

Figure 105. *Nerudiella goroi* sp. nov. male, SEM images of habitus **A** dorsal view **B** lateral view **C, D** ventral view. Scale bars: 1 mm (**A, B, C**); 500 µm (**D**).

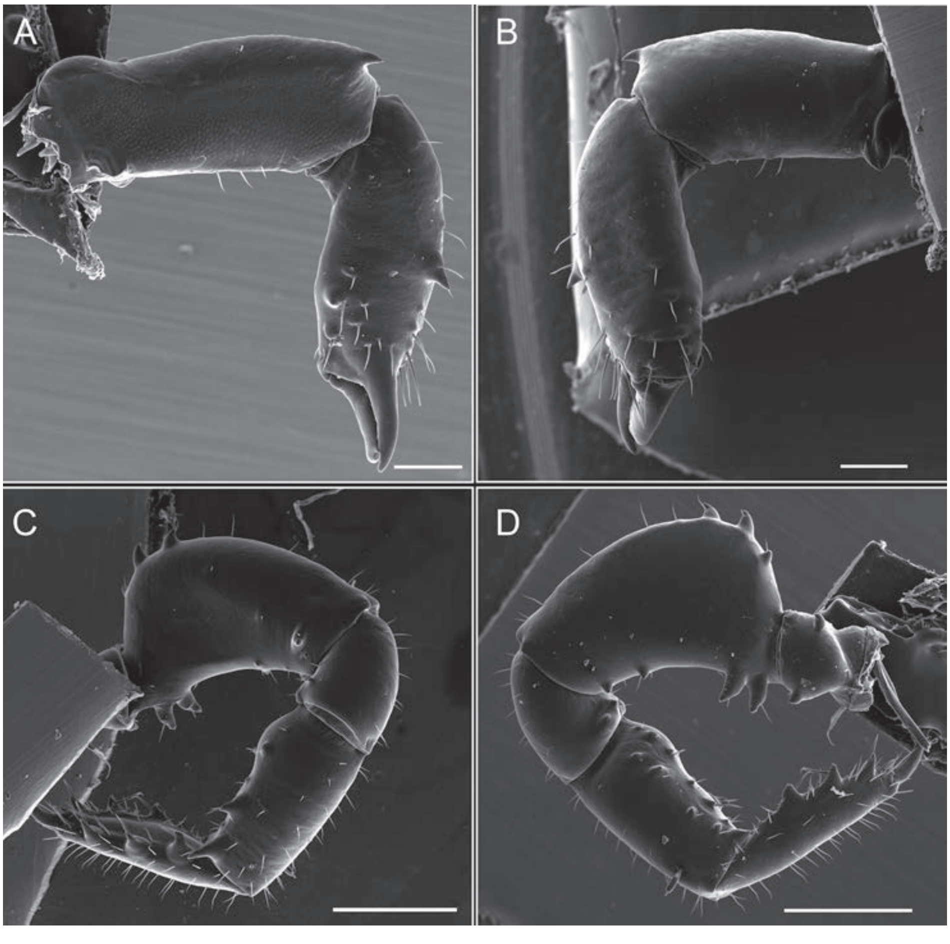

Figure 106. *Nerudiella goroi* sp. nov. chelicerae: mesal **A** ectal **B** pedipalps: mesal **C** ectal **D**. Scale bars: 200 µm (**A, B**); 500 µm (**C, D**).

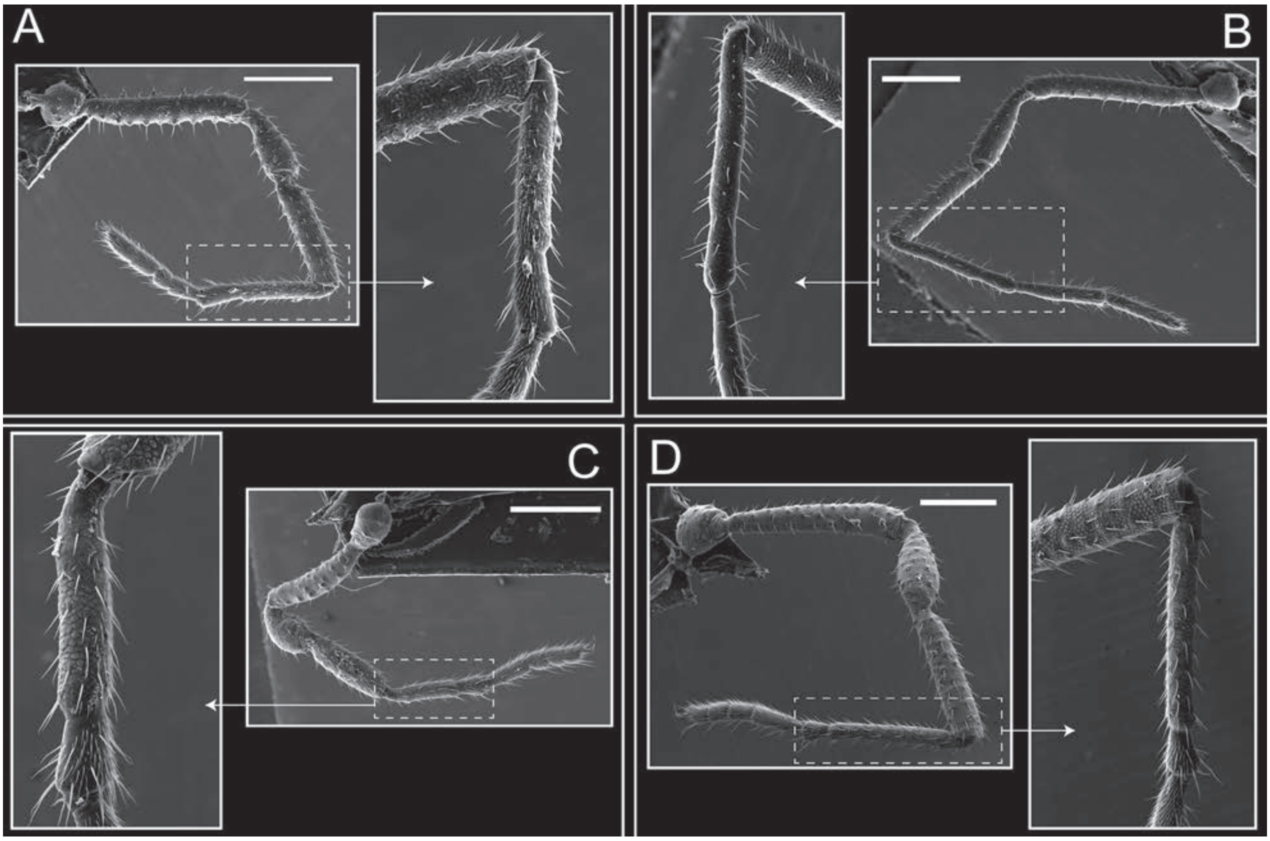

Figure 107. *Nerudiella goroi* sp. nov. legs I **A** II **B** III **C** IV **D**. Scale bars: 500 µm.

fe 1.12, pa 0.50, ti 0.71, mt 0.99, ta 0.86. IV: tr 0.41, fe 1.53, pa 0.84, ti 1.26, mt 1.69, ta 1.04.

Dorsum (Fig. 104, 105). Eta (η) hourglass-shaped dorsal scutum. Ocularium low and rounded. Dorsal scutum microgranulate, with mesotergal areas that lack distinct demarcation but with small setiferous tubercles. Additionally, the mesotergal areas, posterior edge, and free tergites feature a row of small setiferous tubercles.

Chelicerae (Fig. 106A, B). Segment I with an acute tubercle on the dorso-distal surface. Segment II bearing scattered setae in ectal and ventral views, with one triangular tubercle prominent from the others in front view.

Pedipalps (Fig. 106C, D). Trochanter with a small dorsal and ventral tubercle. Femora bearing three dorsoproximal setiferous tubercles; 4–6 small ventral-distal tubercles and two ventral-proximal spines. Patella with 2–3 small ventral tubercles. Tibia possesses two prominent ventral-mesal spines, in addition to small sparse setiferous tubercles. Tarsus with three mesal and ectal spines in addition to setae and sparse setae.

Legs (Fig. 107). Coxa I with 10 setiferous tubercles, II with 18–20 setiferous tubercles, III with three. Spiracles not obstructed by bridges. Smooth surface occupying ⅓ of leg II, ¾ of III and < ⅓ of IV. Smooth area of leg II with 3 tubercles with subdistal setae on each side. Sternum arrow-shaped. Legs covered in small tubercles, astragalus longer than calcaneus on all legs. Tarsal count: 4–8–4–4.

Penis (Figs 108, 109). Pars distalis characterized by a ventral plate divided into two halves by a small cleft. Each half of the plate bears three pointed

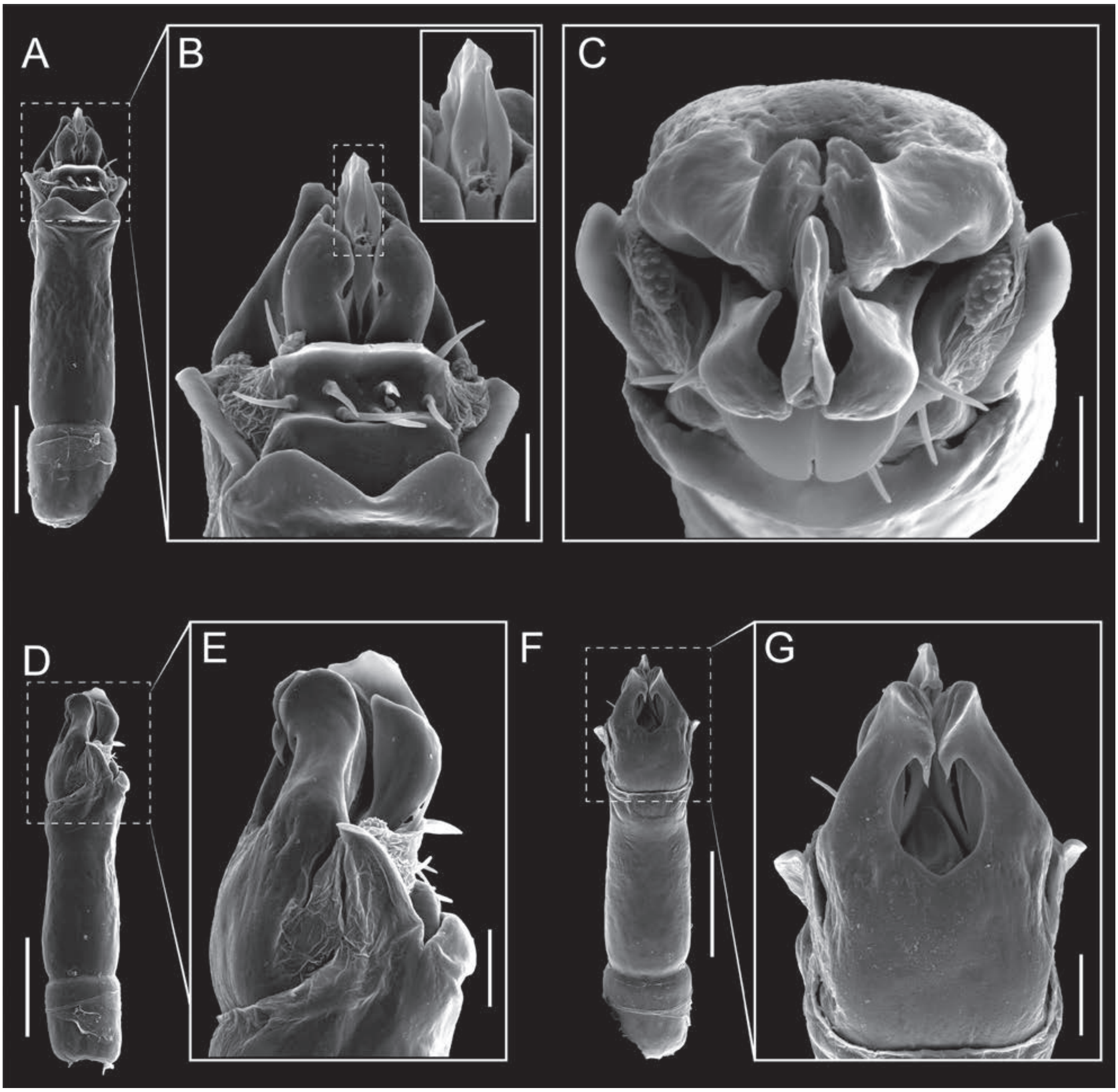

Figure 108. *Nerudiella goroi* sp. nov. penis: ventral **A, B** apical **C** lateral **D, E** dorsal **F, G**. Scale bars: 200 µm (**A, D, F**); 50 µm (**B, C, E, G**).

macrosetae on the ventral surface and one small macroseta on the dorsal surface. The dorsal surface is covered by a capsula externa, with the upper portion of the plate featuring a wide notch that forms a pair of sharp pointed processes at the base of the genitalia. The capsula externa also exhibits a pair of broad lateral processes. It is slightly lower than the capsula interna, which is laterally flattened and compressed between the lateral processes of the capsula externa. The capsula interna does not have a visible stylus. Additionally, there is a dorsolateral plate connected to the pars basalis.

Female. Similar to males, with a shorter pedipalpal femora.

Female measurements. Measurements: Total length 2.50, carapace length 1.1, dorsal scutum length 2.17, carapace max. width 1.55, mesotergum max. width. Appendage measurements: Pedipalps. Trochanter length 0.26, femora

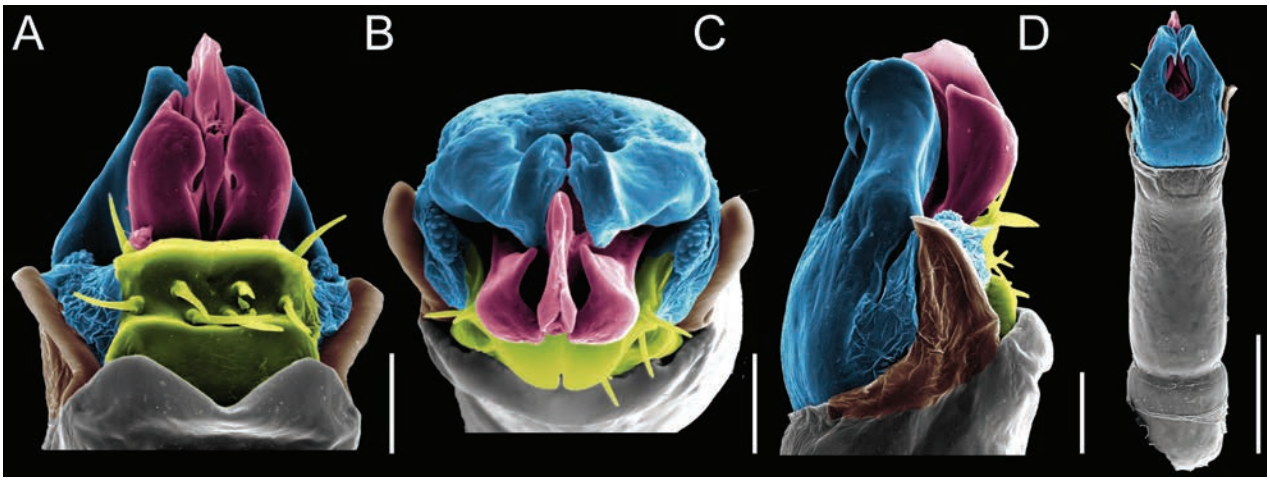

Figure 109. *Nerudiella goroi* sp. nov. penis: ventral **A** apical **B** lateral **C** dorsal **D**. Colors: ventral plate (yellow), capsula externa (blue), capsula interna (red). Scale bars: 50 μm.

length 0.90, patella length 0.55, tibia length 0.57, tarsus length 0.67. Leg **I**: trochanter (tr) 0.25, femora (fe) 0.96, patella (pa) 0.53, tibia (ti) 0.71, metatarsus (mt) 0.84, tarsus (ta) 0.64. **II**: tr 0.24, fe 1.27, pa 0.65, ti 0.98, mt 1.12, ta 1.27. **III**: tr 0.27, fe 0.82, pa 0.41, ti 0.61, mt 0.71, ta 0.69. **IV**: tr 0.31, fe 1.19, pa 0.74, ti 1.03, mt 1.26, ta 0.79. Tarsal count: 4–8–4–4.

Nerudiella jaimei **sp. nov.**

https://zoobank.org/4986C4AB-EB4A-4F3E-86F6-063A7C4604B7
Figs 110–115

Material examined. ***Holotype***. ♂ **Chile.** Malleco. Monumento Natural Contulmo, 350 m, S. Peck, J. Peck coll. (FMNH). ***Paratypes***. **Chile.** Malleco. P.N. Nahuelbuta 1250 m, Berlese, N. Platnick, R. Schuh coll.19.XI.1981. 1 ♂ 2 imm. (AMNH). Same data, 4 ♂ 4 imm. (AMNH). Malleco. Monumento Natural Contulmo, 300 m, N. Platnick, R. Schuh coll.31.1.1986 2 ♀ 4 imm. (AMNH). Malleco. Monumento Natural Contulmo, 350 m, S. Peck, J. Peck coll. 13.II.1985. 5 ♂ 6 ♀ 13 imm. (FMNH). 45 KM W Angol, Nahuelbuta N.P. 1500 m, S. Peck, J. Peck coll. 09.XII.1984. 11 ♂ 6 ♀ 13 imm. (FMNH).

Etymology. The specific epithet is bestowed upon the Chilean entomologist Jaime Pizarro Araya, in recognition to his significant contributions to the field of entomology and his unwavering dedication to the conservation of the Chilean forests. A noun in apposition.

Diagnosis. This species can be distinguished from the other species of the genus by the morphology of the male genitalia, which includes the capsula externa with a robust process, which forms a dorsally curved plate.

Distribution. Chile: Araucanía Region (Fig. 4F).

Description of male holotype. Measurements: Total length 4.0, carapace length 1.0, dorsal scutum length 2.5, carapace max. width 1.2, mesotergum max. width 1.7. Appendage measurements: Pedipalps. Trochanter length 0.26, femora length 0.96, patella length 0.59, tibia length 0.74, tarsus length 0.69. Leg **I**: trochanter (tr) 0.19, femora (fe) 0.70, patella (pa) 0.40, tibia (ti) 0.52, metatarsus (mt) 0.63, tarsus (ta) 0.55. **II**: tr 0.23, fe 0.91, pa 0.50, ti 0.78, mt 0.80, ta

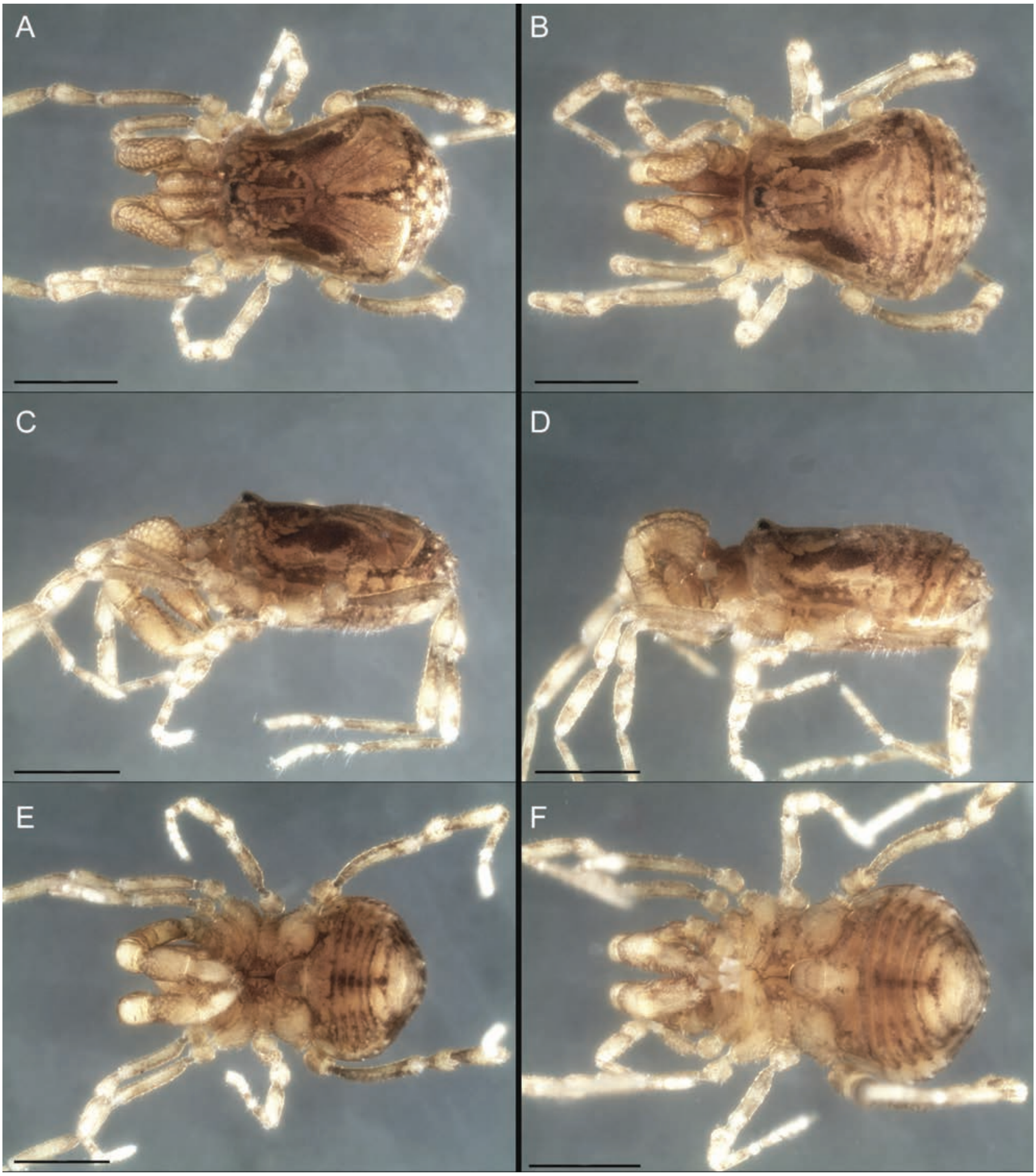

Figure 110. *Nerudiella jaimei* sp. nov. habitus, male **A** dorsal view **C** lateral view **E** ventral view. Female **B** dorsal view **D** lateral view **F** ventral view. Scale bars: 1 mm.

0.92. **III**: tr 0.22, fe 0.58, pa 0.34, ti 0.47, mt 0.50, ta 0.53. **IV**: tr 0.26, fe 0.89, pa 0.51, ti 0.75, mt 0.94, ta 0.63.

Dorsum (Fig. 110, 111). Eta (η) hourglass-shaped dorsal scutum. Ocularium low and rounded in shape. The dorsal scutum microgranulate, and both the opisthosoma and free tergites display rows of small setiferous tubercles. It is worth noting that the tubercle bases of these setiferous tubercles increase in length posteriorly.

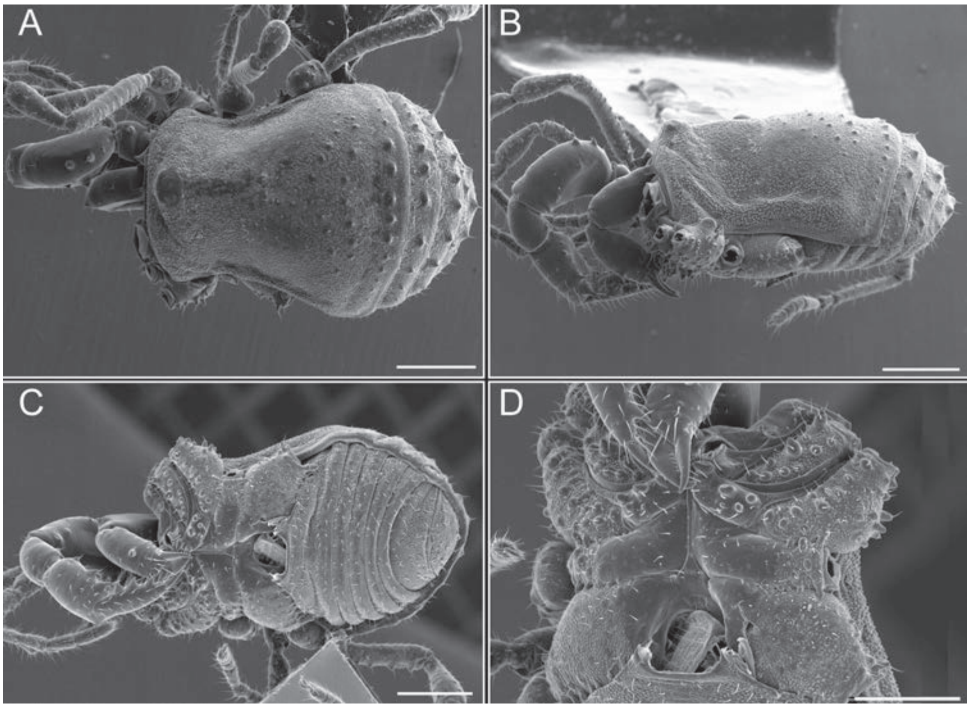

Figure 111. *Nerudiella jaimei* sp. nov. male, SEM images of habitus **A** dorsal view **B** lateral view **C, D** ventral view. Scale bars: 500 µm (**A, B, C**); 200 µm (**D**).

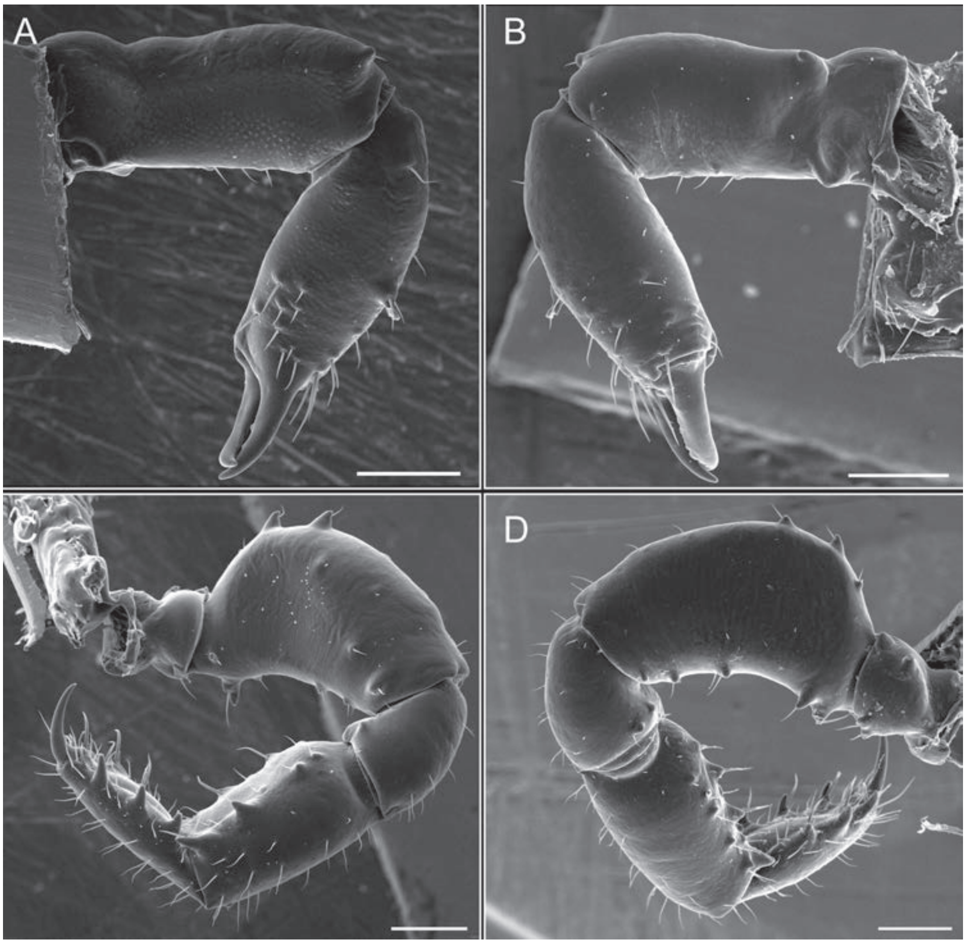

Figure 112. *Nerudiella jaimei* sp. nov. chelicerae: mesal **A** ectal **B** pedipalps: mesal **C** ectal **D**. Scale bars: 200 µm.

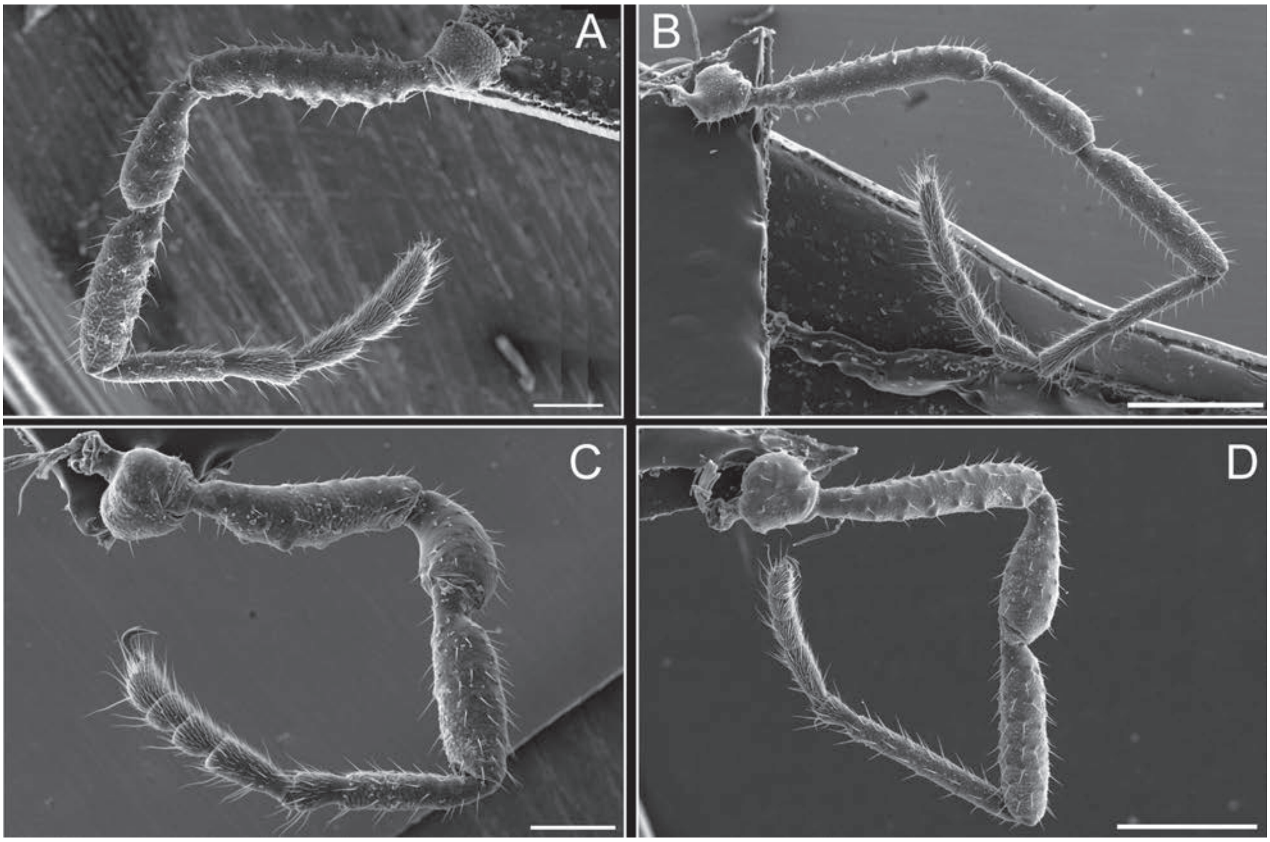

Figure 113. *Nerudiella jaimei* sp. nov. legs I **A** II **B** III **C** IV **D**. Scale bars: 200 µm (**A, C**); 500 µm (**B, D**).

Chelicerae (Fig. 112A, B). Segment I with a small tubercle on the dorso-distal surface. Segment II bearing sparse small setiferous tubercles, with one triangular tubercle prominent from the others in frontal view.

Pedipalps (Fig. 112C, D). Trochanter with two small dorsal and ventral tubercles. Femora bearing three dorsal spines with setae, five ventral-distal and two ventral-proximal. Patella with 2–3 small ventral setiferous tubercles. Tibia covered in small ventral tubercles, with two spines in the ventral-mesal area and three in the ventral-ectal areas. Tarsus with three mesal and ectal spines with subdistal setae in addition to setae and few granules.

Legs (Fig. 113). Coxa I with 9–10 setiferous tubercles (two distal tubercles stronger than the others), II with 12–13, III with six or seven, IV with four or five tubercles connected to the opisthosoma. Spiracles not obstructed by bridges. Smooth surface occupying ⅓ of leg II, ¾ of III and < ⅓ of IV. Leg zone II smooth with two or three small tubercles with subdistal setae on each side. Sternum arrow-shaped. Legs covered with small tubercles, astragalus longer than calcaneus in all legs, in leg II the calcaneus is slightly shorter than the astragalus. Tarsal count: 3–6–4–4.

Penis (Figs 114, 115). Pars distalis with a ventral plate bearing a thin cleft dividing the plate into two lamellae. Each lamella has three pointed macrosetae on the ventral surface and one short macroseta on the dorsal surface; capsula externa covering dorsal surface, with apical part folded dorsally, with a pair of long lateral processes; there is a dorsolateral plate attached to the pars basalis. Capsula externa shorter in length compared to the capsula interna. The capsula interna, on the other hand, is wide in shape, and it features a sharp apical area.

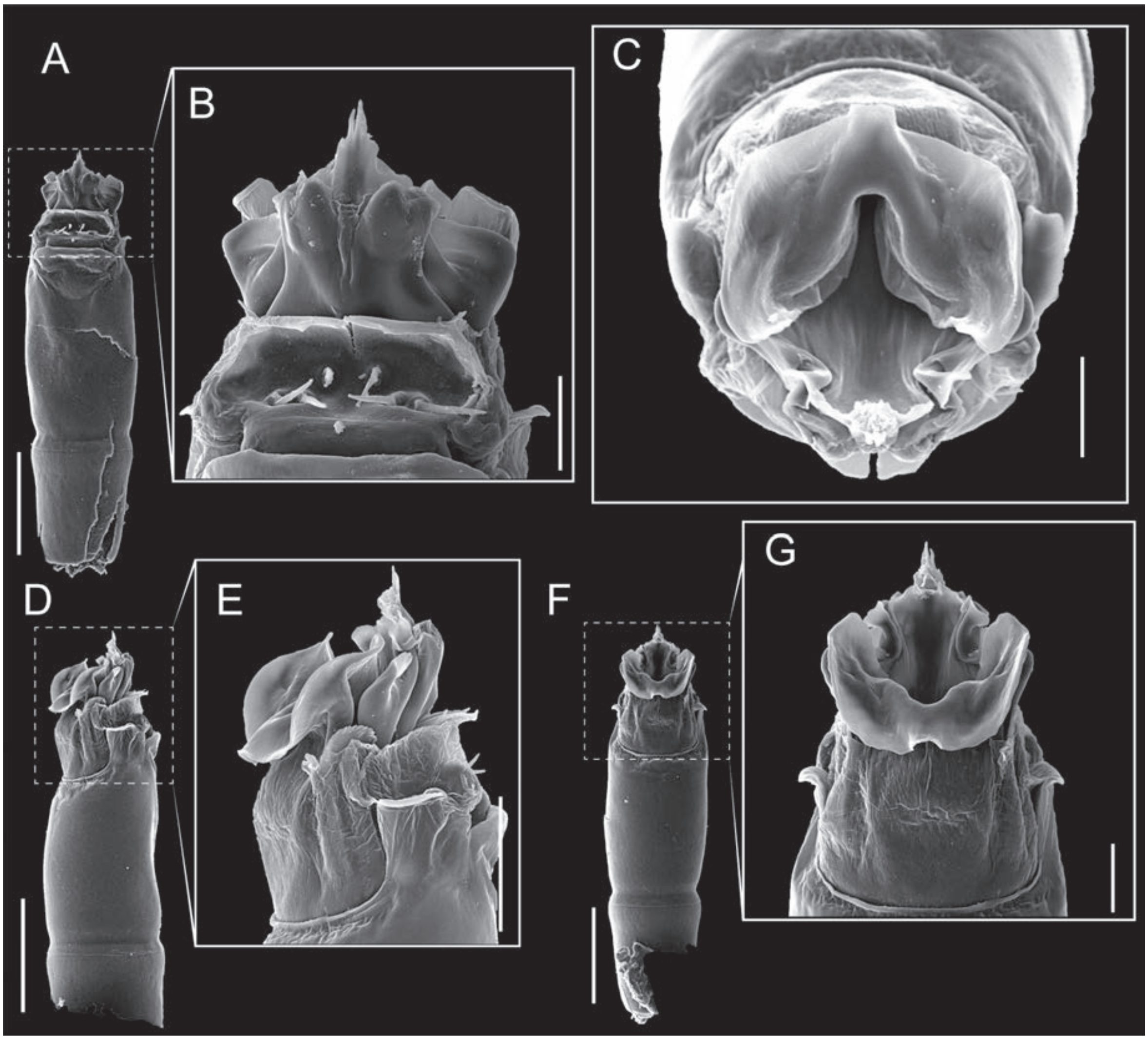

Figure 114. *Nerudiella jaimei* sp. nov. penis: ventral **A, B** apical **C** lateral **D, E** dorsal **F, G**. Scale bars: 200 µm (**A, D, F**); 50 µm (**B, C, G**); 100 µm (**E**).

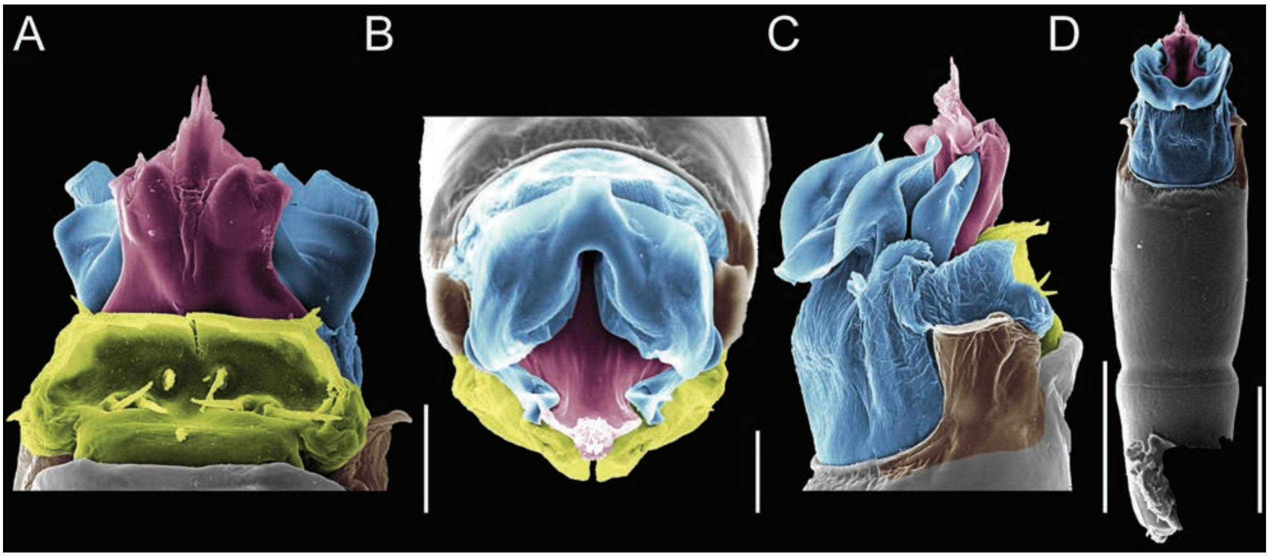

Figure 115. *Nerudiella jaimei* sp. nov. penis: ventral **A** apical **B** lateral **C** dorsal **D**. Colors: ventral plate (yellow), capsula externa (blue), capsula interna (red). Scale bars: 50 µm (**A, B**); 100 µm (**C**); 200 µm (**D**).

Female. Similar to males, with a shorter pedipalpal femora.

Female measurements. Total length 2.39, carapace length 1.1, dorsal scutum length 2.2, carapace max. width 1.57, mesotergum max. width 2.15. Appendage Measurements: Pedipalps. Trochanter length 0.23, femora length 0.77, patella length 0.50, tibia length 0.52, tarsus length 0.65. Leg I: trochanter (tr) 0.18, femora (fe) 0.72, patella (pa) 0.39, tibia (ti) 0.50, metatarsus (mt) 0.57, tarsus (ta) 0.47. II: tr 0.24, fe 0.90, pa 0.48, ti 0.71, mt 0.79, ta 0.87. III: tr 0.22, fe 0.56, pa 0.32, ti 0, 39, mt 0.49, ta 0.47. IV: tr 0.27, fe 0.81, pa 0.51, ti 0.70, mt 0.92, ta 0.59.

Nerudiella malleco **sp. nov.**

https://zoobank.org/18A11F7E-3279-470D-898C-9CB9A84C5599

Figs 116–121

Material examined. ***Holotype*****.** ♂ **Chile.** Malleco: Fundo Maria Esther, 15 km W from Victoria, E. Maury coll., 14.I.1989 (MNHNCL). ***Paratypes*****. Chile.** Malleco: Fundo Maria Esther, 15 km W from Victoria, E. Maury coll., 14.I.1989, 2 ♂ (MACN), 08.I.1987 4 ♂ 1 ♀ 6 imm. (MACN), Monumento Natural Contulmo, E.M coll., 13. I.1989, 2 ♂ 3 ♀ (MACN), 15 km W Victoria, N. Platnick, O. Francke coll., 26.I.1985, 2 ♂ 3 ♀ 7 imm. (AMNH); Malalcahuello, E. Maury coll., 08. I.1987, 1 ♀ (MACN); 17 km E from Curacautín, N. Platnick, R. Schuh coll., 22.XI.1981, 1 ♂ 1 ♀ (AMNH), 1 imm. (AMNH), Monumento Natural Contulmo, E. Maury coll., 19.I.1991, 1 ♂ 4 ♀ (MACN). Same data, 1 imm. (AMNH).

Etymology. The specific epithet refers to the type locality of the species, the Malleco province, located in the Araucanía region of Chile. Noun in apposition.

Diagnosis. This species can be differentiated from other species within the genus by the distinct morphology of the male genitalia. Specifically, the male genitalia feature a robust and V-shaped process on the capsula externa when observed from a dorsal view.

Distribution. Chile: Bío-Bío and Araucanía Regions (Fig. 4F).

Description of male holotype. Measurements: Total length 4.1. Carapace length 1.1, Dorsal scutum length 2.3, Carapace max. width 1.21, Dorsal scutum max. width 1.6. Appendage measurements. Pedipalps. Trochanter length 0.26, femora length 0.98, patella length 0.47, tibia length 0.73, tarsus length 0.71. Leg I: trochanter (tr) 0.21, femora (fe) 0.82, patella (pa) 0.45, tibia (ti) 0.61, metatarsus (mt) 0.67, tarsus (ta) 0.61. II: tr 0.22, fe 1.05, pa 0.53, ti 0.73, mt 0.87, ta 1.03. III: tr 0.22, fe 0.74, pa 0.33, ti 0.55, mt 0.83, ta 0.67. IV: tr 0.25, fe 1.08, pa 0.61, ti 0.83, mt 1.12, ta 0.76.

Dorsum (Fig. 116, 117). Eta (η) hourglass-shaped dorsal scutum. Ocularium low and rounded. The dorsal scutum microgranulate. Mesotergal areas on the dorsal scutum do not have a clear separation but are covered in small setiferous tubercles. Additionally, the free tergites of the species bear a row of small setiferous tubercles.

Chelicerae (Fig. 118A, B). Segment I with an acute tubercle on the dorso-distal surface. Segment II bearing scattered setae in ectal and ventral views, with one triangular tubercle being more prominent than the others in front view.

Pedipalps (Fig. 118C, D). Trochanter with a small dorsal and ventral tubercle. Femora with three dorsoproximal setiferous spines, four small ventral-distal

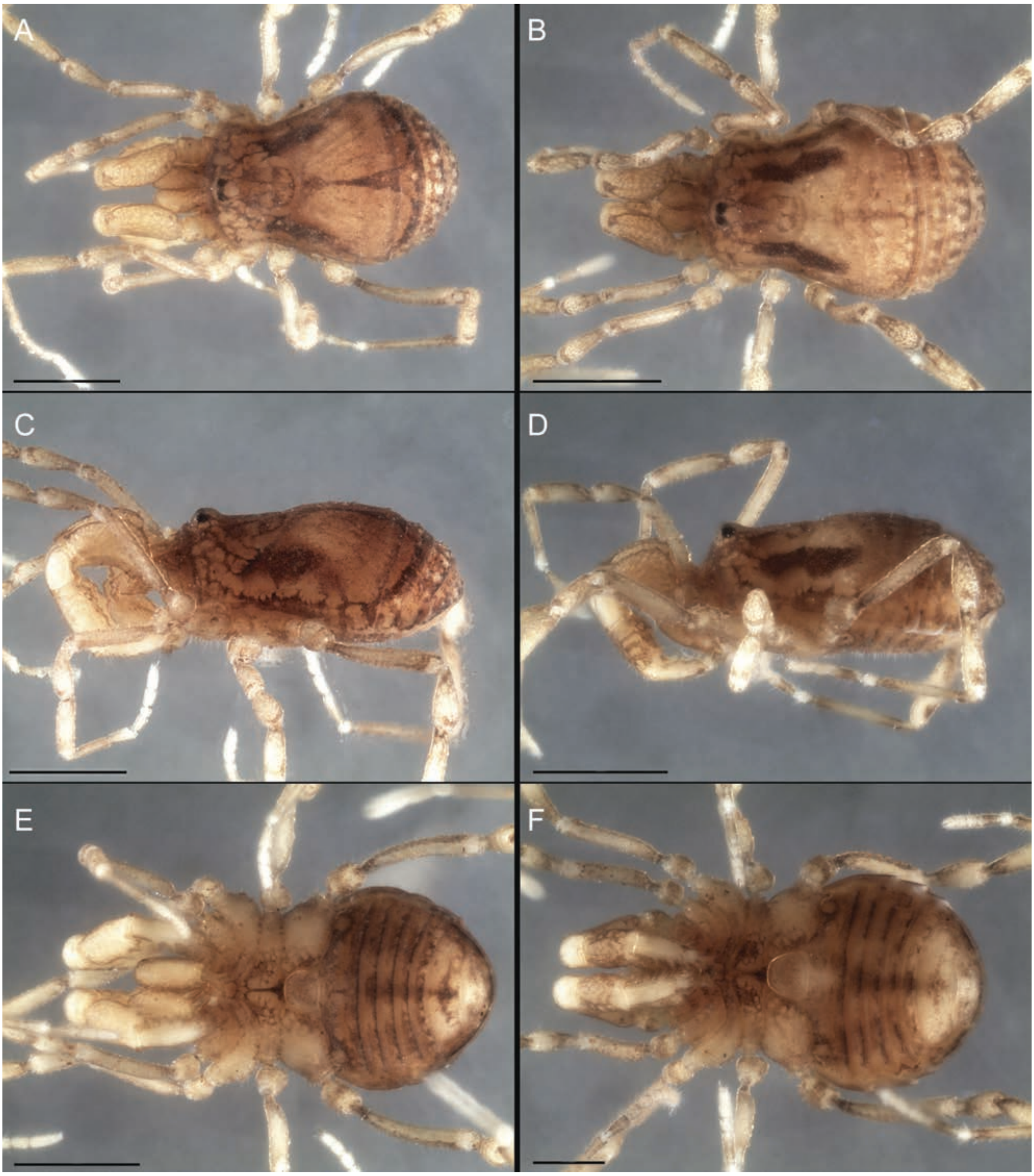

Figure 116. *Nerudiella malleco* sp. nov. habitus, male **A** dorsal view **C** lateral view **E** ventral view. Female **B** dorsal view **D** lateral view **F** ventral view. Scale bars: 1 mm. Species of Clade C, see Fig. 3.

tubercles, and two ventral-proximal spines. Tibia with three ventral-ectal and two ventral-mesal spines. Tarsus with three mesal and ectal spines, accompanied by subdistal setae.

Legs (Fig. 119). Coxa **I** with nine or ten setiferous tubercles, **II** with 18–20 setiferous tubercles, IV with seven or eight small tubercles connected to the opisthosoma. Spiracles not obstructed by bridges. Smooth surface occupying ¹⁄₃ of leg **II**, ¾ of **III** and < ¹⁄₃ of IV. Smooth area of leg **II** with two small tubercles with

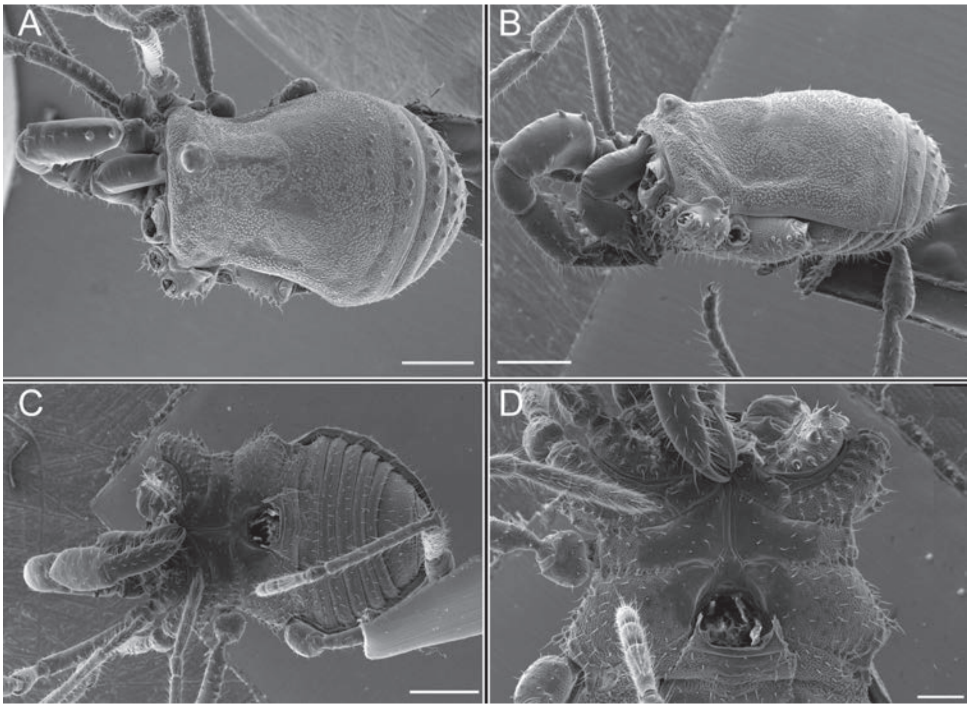

Figure 117. *Nerudiella malleco* sp. nov. male, SEM images of habitus **A** dorsal view **B** lateral view **C, D** ventral view. Scale bars: 500 µm (**A, B, C**); 200 µm (**D**).

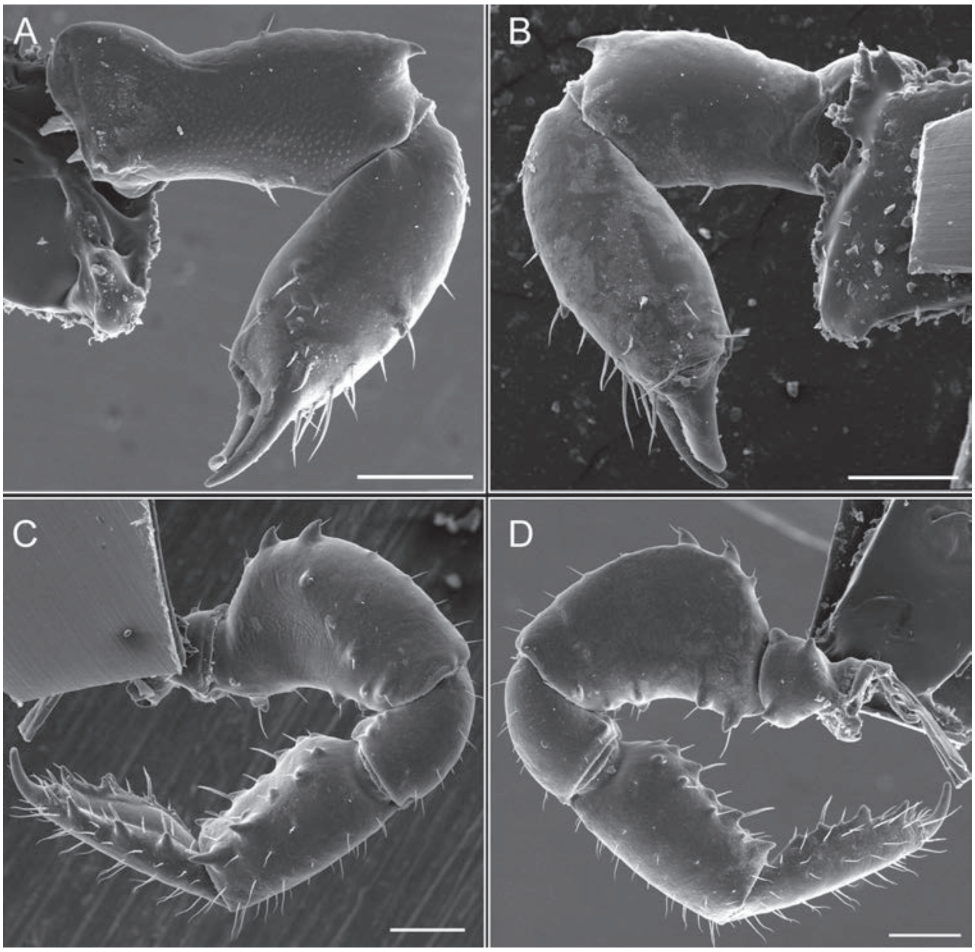

Figure 118. *Nerudiella malleco* sp. nov. chelicerae: mesal **A** ectal **B** pedipalps: mesal **C** ectal **D**. Scale bars: 200 µm.

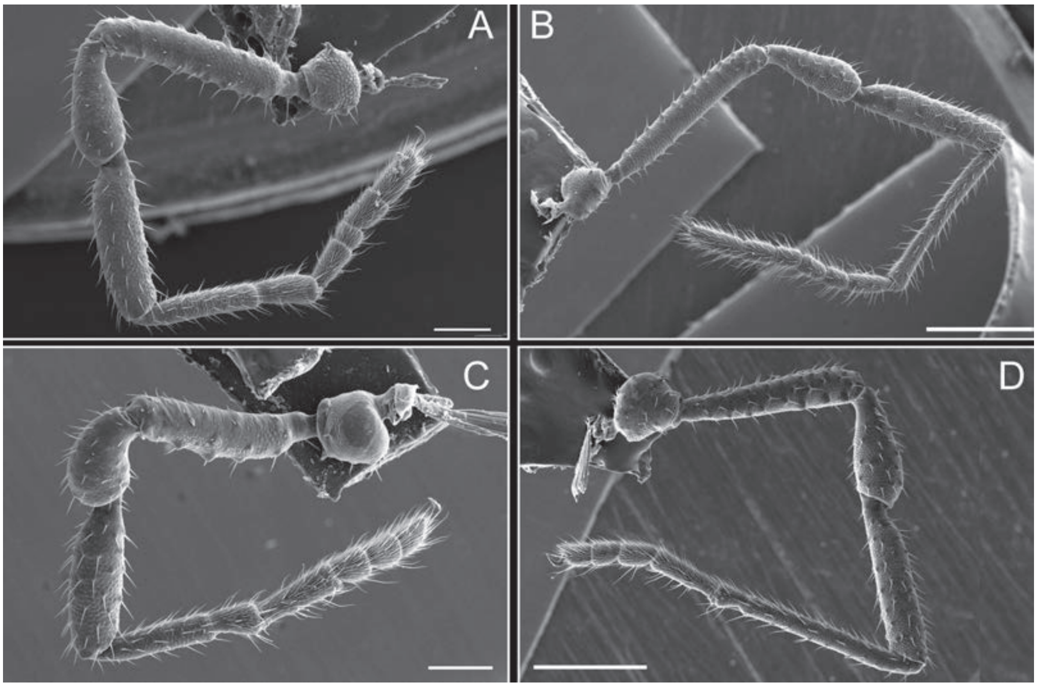

Figure 119. *Nerudiella malleco* sp. nov. legs I **A** II **B** III **C** IV **D**. Scale bars: 200 µm (**A, C**); 500 µm (**B, D**).

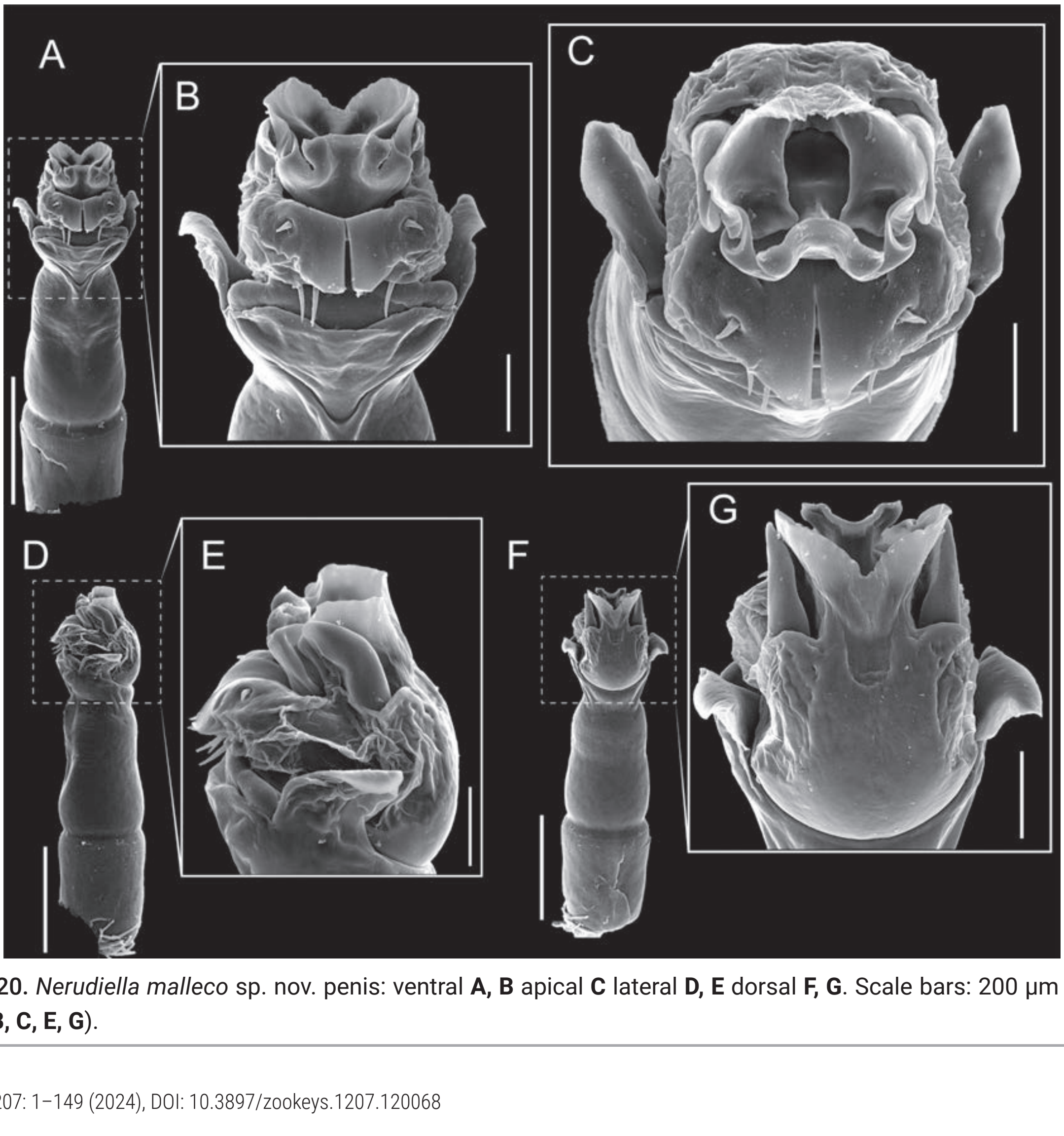

Figure 120. *Nerudiella malleco* sp. nov. penis: ventral **A, B** apical **C** lateral **D, E** dorsal **F, G**. Scale bars: 200 µm (**A, D, F**); 50 µm (**B, C, E, G**).

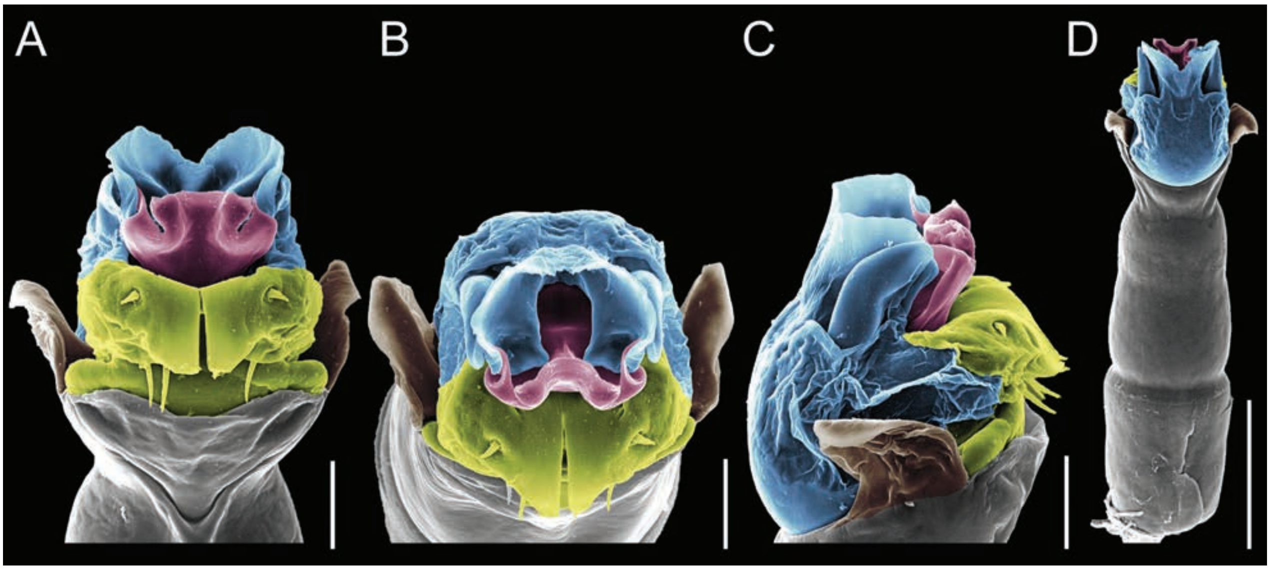

Figure 121. *Nerudiella malleco* sp. nov. penis: ventral **A** apical **B** lateral **C** dorsal **D**. Colors: ventral plate (yellow), capsula externa (blue), capsula interna (red). Scale bars: 50 μm (**A–C**); 200 μm (**D**).

subdistal setae on each side. Sternum arrow-shaped. Legs covered with small tubercles, astragalus longer than calcaneus on all legs. Tarsal count: 3–6–4–4.

Penis (Figs 120, 121). Pars distalis with a ventral plate bearing a fine cleft dividing the plate into two lamellae. Each lamella has three pointed macrosetae on the ventral surface and one small macroseta on the dorsal surface; capsula externa covering dorsal surface, apical area of capsula externa with a V-shaped notch and a pair of lateral processes; there is a dorsolateral plate connected to the pars basalis; dorsolateral plate present. Capsula interna short, with two slits in ventral view, without visible stylus.

Female. Females similar to males, with shorter pedipalpal femora.

Female measurements. Total length 4.07, carapace length 1.16, dorsal scutum length 2.71, carapace max. width 1.41, mesotergum max. width 1.96. Appendage measurements: Pedipalps. Trochanter length 0.26, length of the femora 0.95, length of the patella 0.47, length of the tibia 0.73, length of the tarsus 0.74. Leg **I**: trochanter (tr) 0.28, femora (fe) 0.98, patella (pa) 0.55, tibia (ti) 0.77, metatarsus (mt) 0.85, tarsus (ta) 0.77. **II**: tr 0.31, fe 1.27, pa 0.68, ti 1.06, mt 1.17, ta 1.34. **III**: tr 0.30, fe 0.90, pa 0.41, ti 0.61, mt 0.72, ta 0.76. **IV**: tr 0.37, fe 1.28, pa 0.70, ti 0.99, mt 1.22, ta 0.92.

Nerudiella penco sp. nov.

https://zoobank.org/F00EE6F1-AC0A-4EBE-A71F-D5A7AC8DDD35
Figs 122–127

Material examined. ***Holotype***. ♂ **Chile.** Concepción: Estero Nonguén, N. Platnick, R. Schuh coll., 16.XI.1981 (AMNH). ***Paratypes***. **Chile.** Concepción: Penco, T. Cekalovic coll., 11.II.1979, 1 ♀ (AMNH).

Etymology. The specific epithet refers to the type locality of the species, the commune of Penco, located in the province of Concepción, Chile. Noun in apposition.

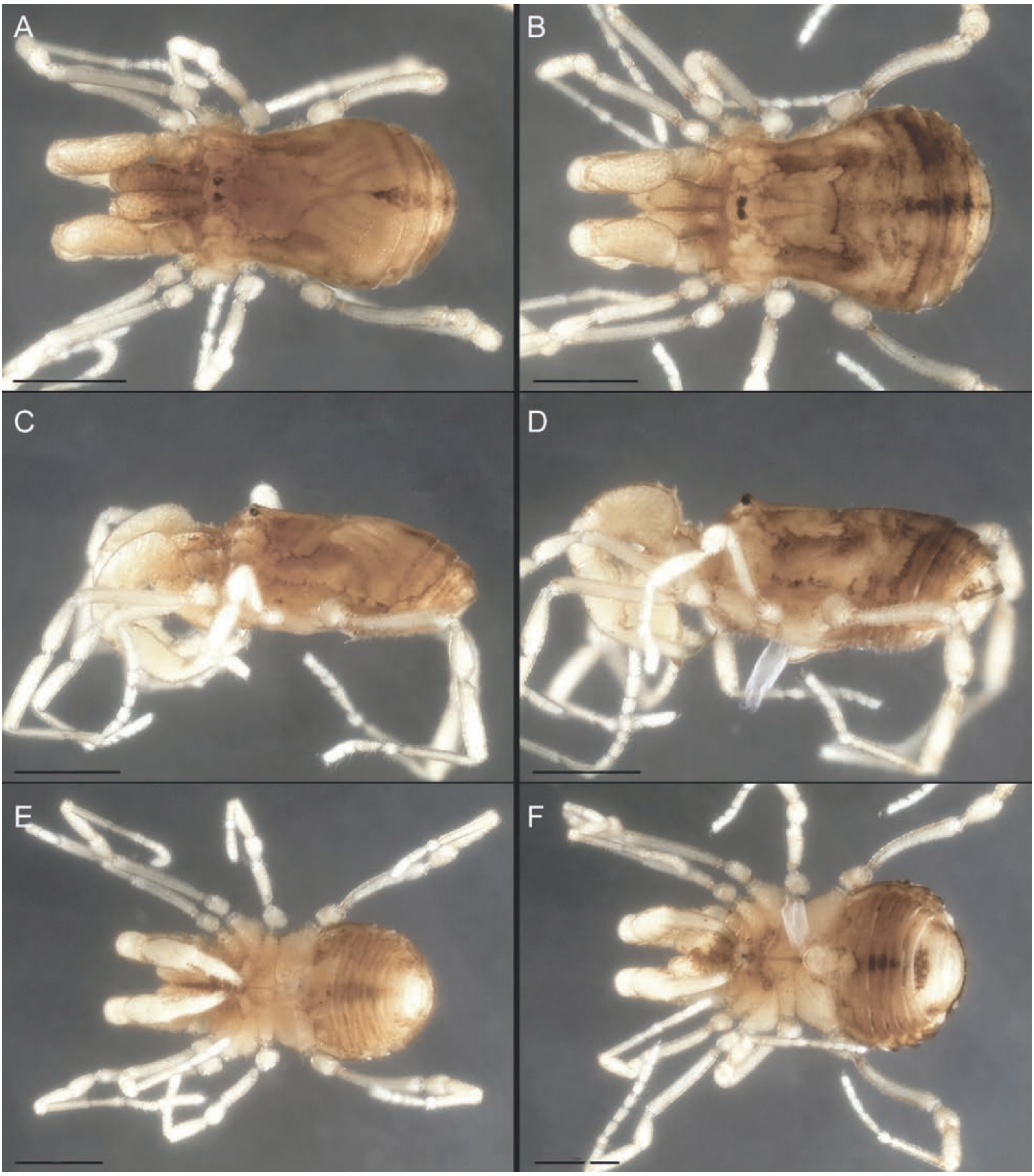

Figure 122. *Nerudiella penco* sp. nov. habitus, male **A** dorsal view **C** lateral view **E** ventral view. Female **B** dorsal view **D** lateral view **F** ventral view. Scale bars: 1 mm.

Diagnosis. This species can be distinguished from the other species in the genus by having the dorsal scutum without tubercles. The male genitalia has longer macrosetae than other species of the genus, capsula externa divided into two halves that touch in the apical portion, leaving a gap between the two halves.

Distribution. Chile: Bío-Bío Region (Fig. 4F).

Description of male holotype. Measurements: Total length 3.67. Carapace length 0.97, dorsal scutum length 1.90, carapace max. width 1.26, mesotergum

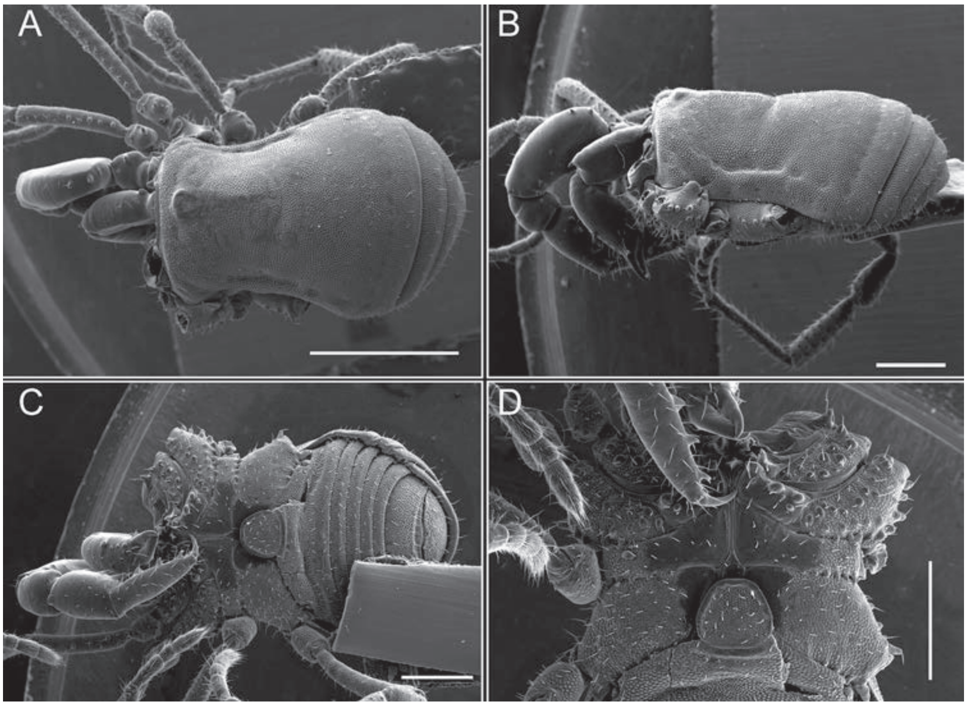

Figure 123. *Nerudiella penco* sp. nov. male, SEM images of habitus **A** dorsal view **B** lateral view **C, D** ventral view. Scale bars: 500 µm.

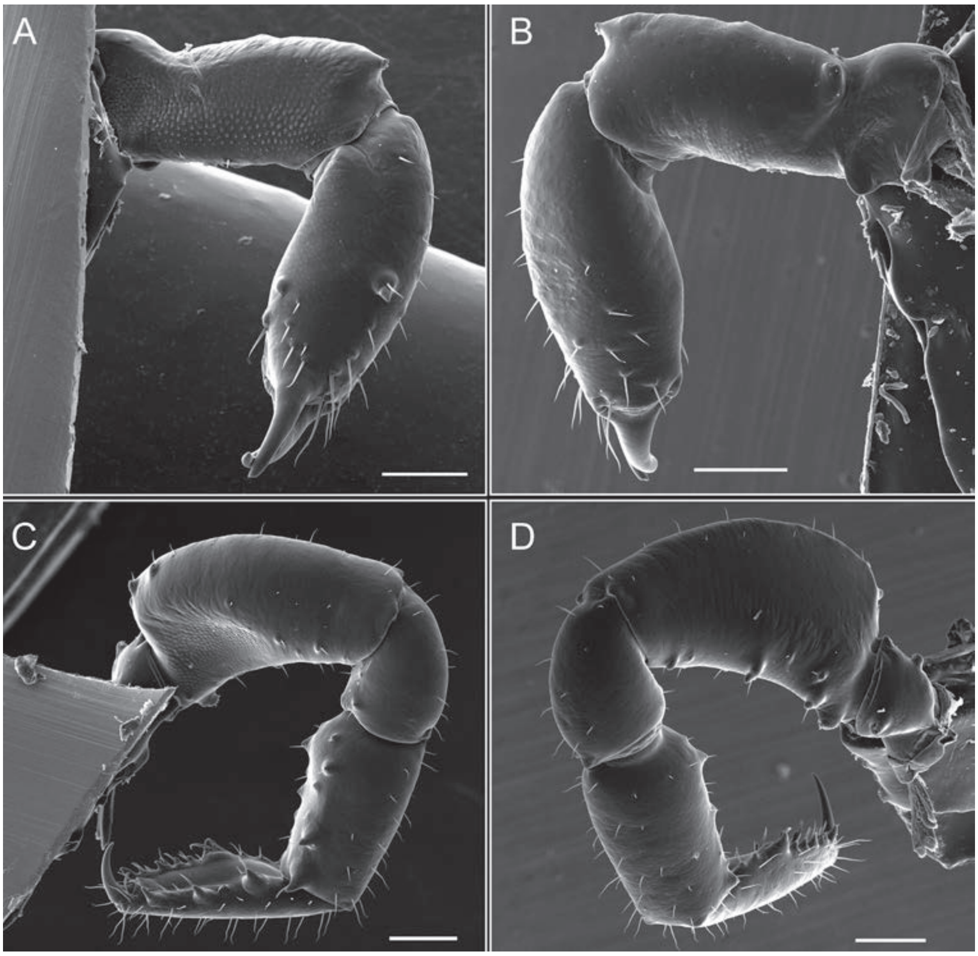

Figure 124. *Nerudiella penco* sp. nov. chelicerae: mesal **A** ectal **B** pedipalps: mesal **C** ectal **D**. Scale bars: 200 µm.

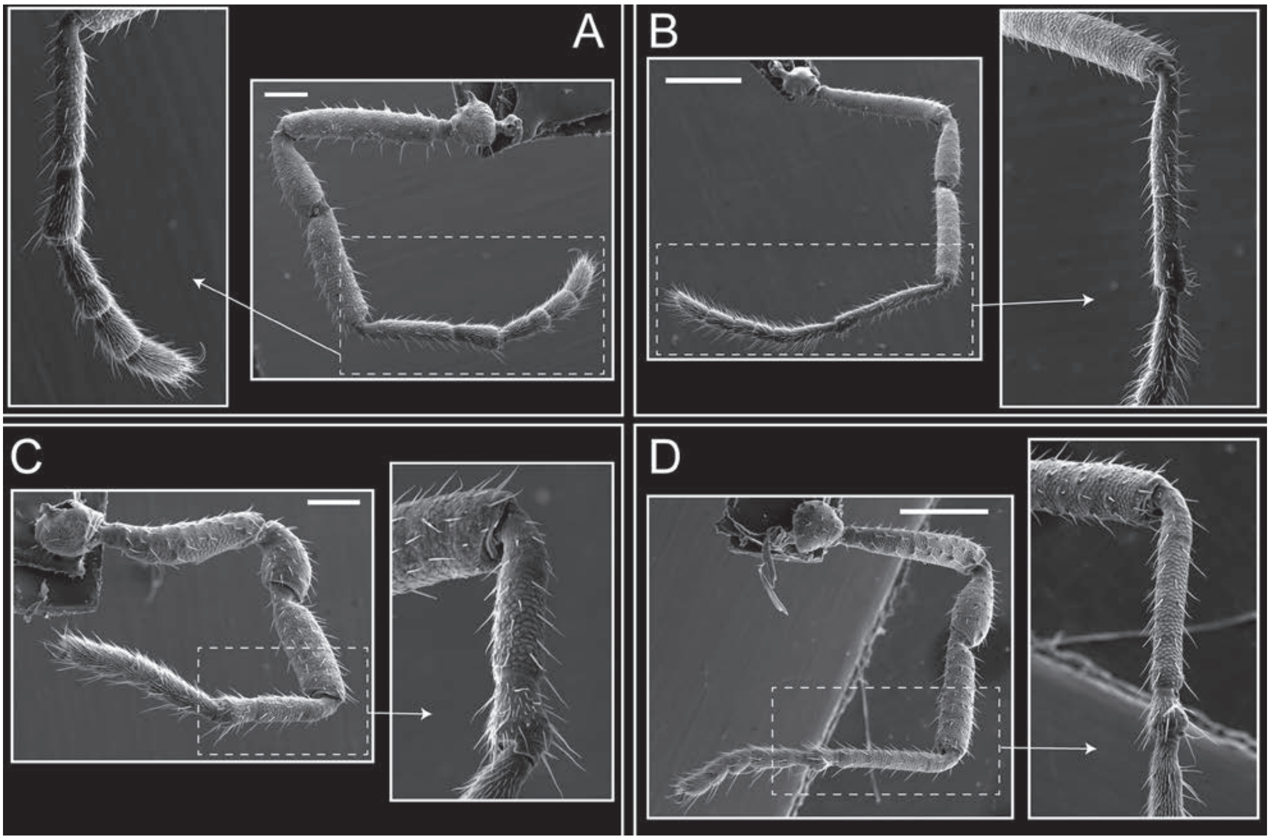

Figure 125. *Nerudiella penco* sp. nov. legs I **A** II **B** III **C** IV **D**. Scale bars: 200 µm (**A, C**); 500 µm (**B, D**).

max. width 1.55. Appendage measurements: Pedipalps. Trochanter length 0.24, femora length 0.98, patella length 0.53, tibia length 0.70, tarsus length 0.71. Leg I: trochanter (tr) 0.19, femora (fe) 0.85, patella (pa) 0.46, tibia (ti) 0.60, metatarsus (mt) 0.70, tarsus (ta) 0.63. II: tr 0.25, fe 1.17, pa 0.56, ti 0.83, mt 0.99, ta 1.27. III: tr 0.26, fe 0.77, pa 0.32, ti 0.55, mt 0.57, ta 0.71. IV: tr 0.30, fe 1.07, pa 0.55, ti 0.85, mt 1.04, ta 0.89.

Dorsum (Fig. 122, 123). Eta (η) hourglass-shaped dorsal scutum. Ocularium low. Dorsal scutum microgranulate, without clear delimitation of areas. Areas III–IV smooth, with few setae; posterior margin with a row of setae. Free tergites have a row of setae.

Chelicerae (Fig. 124A, B). Segment I with a small tubercle on the dorsal-distal surface. Segment II with a mesal tubercle and bearing few setae.

Pedipalps (Fig. 124C, D). Trochanter with a small dorsal and ectal tubercle. Femora with a row of three spines and one setiferous granule on the ventral surface, three small dorsal spines with subdistal setae, and three meso-distal setiferous granules. Patella with 1–2 ventral setiferous granules. Tibia with three ectal and mesal spines with subdistal setae; presence of scant granules in ventral view. Tarsus with an ectal row of two subdistal setiferous spines and 6–8 small setiferous tubercles, there are three spines with subdistal setae on the mesal surface.

Legs (Fig. 125). Coxae I and II covered in setiferous tubercles, III and IV only with the microgranulation, bearing three bridges between legs II and III, five or six between III and IV, four between leg IV and the opisthosoma (the longest being the most distal). Spiracles not obstructed by bridges. Smooth

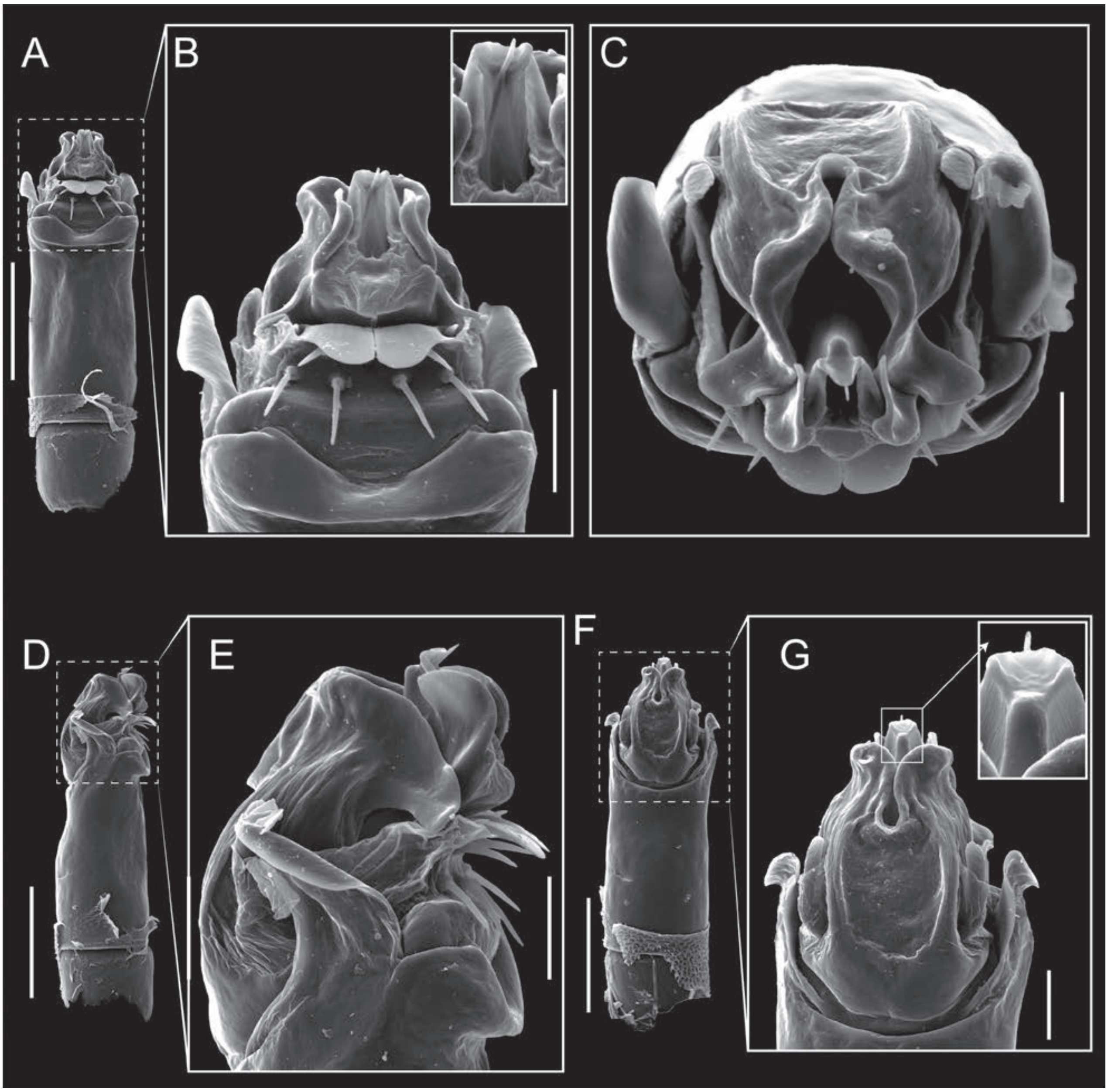

Figure 126. *Nerudiella penco* sp. nov. penis: ventral **A, B** apical **C** lateral **D, E** dorsal **F, G**. Scale bars: 200 μm (**A, D, F**); 50 μm (**B, C, E, G**).

area occupying ¹⁄₃ of leg II (with two small tubercles and two rounded tubercles), ²⁄₃ of III and < ¹⁄₃ of IV. Sternum arrow-shaped. Legs covered in small tubercles, astragalus longer than calcaneus on all legs. Tarsal count: 3–6–4–4.

Penis (Figs 126, 127). Pars distalis with a large ventral plate bearing a cleft that divides the plate into two lamellae. Each lamella has three long pointed macrosetae on the ventral surface and one macroseta on the dorsal surface; capsula externa covering dorsal and lateral surfaces, having a cleft dividing the capsula externa into two halves; there is a dorsolateral plate attached to the pars basalis. Capsula interna longer than the capsula externa, partially covering the ventral plate, with a visible stylus in its apical portion.

Female. Similar to males, with shorter pedipalpal femora.

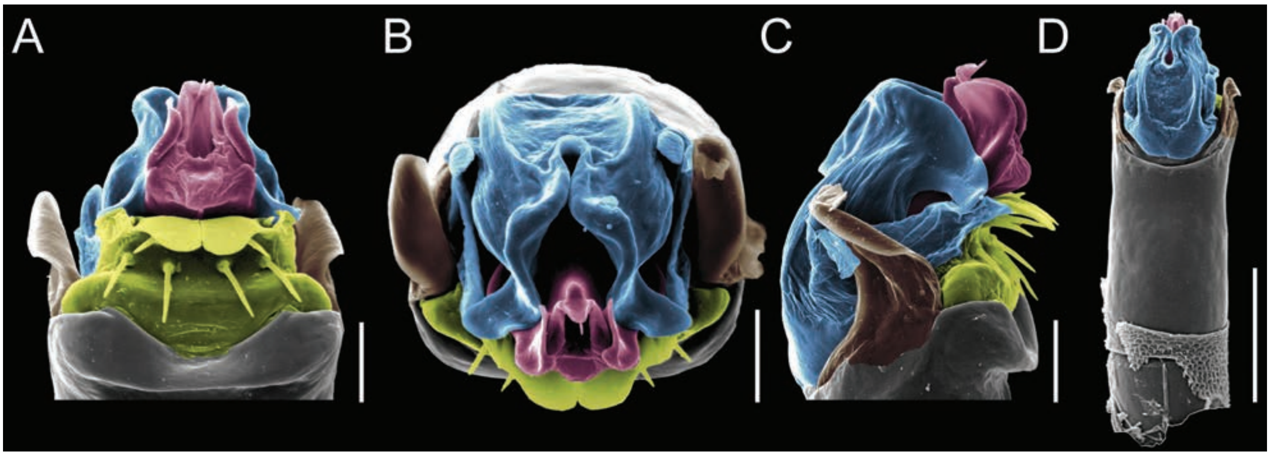

Figure 127. *Nerudiella penco* sp. nov. penis: ventral **A** apical **B** lateral **C** dorsal **D**. Colors: ventral plate (yellow), capsula externa (blue), capsula interna (red). Scale bars: 50 µm.

Female measurements. Total length 4.06, carapace length 1.12, dorsal scutum length 2.16, carapace max. width 1.46, mesotergum max. width 2.04. Appendage Measurements: Pedipalps. Trochanter length 0.27, femora length 0.97, patella length 0.51, tibia length 0.68, tarsus length 0.82. Leg **I**: trochanter (tr) 0.27, femora (fe) 0.99, patella (pa) 0.50, tibia (ti) 0.73, metatarsus (mt) 0.81, tarsus (ta) 0.73. **II**: tr 0.30, fe 1.15, pa 0.65, ti 0.82, mt 1.00, ta 1.00. **III**: tr 0.24, fe 0.81, pa 0.45, ti 0.60, mt 0.68, ta 0.77. **IV**: tr 0.36, fe 1.24, pa 0.69, ti 1.04, mt 1.26, ta 1.20.

Nerudiella pichi **sp. nov.**

https://zoobank.org/7727BE05-A618-4D2A-A79C-291D73318A6D
Figs 128–133

Material examined. ***Holotype***. ♂ **Chile.** Choapa: Pichidangui, Valparaíso, Cerro La Silla del Gobernador, E. Maury coll. 30.X.1988 (MNHNCL). ***Paratypes***. **Chile.** Choapa: Pichidangui, Valparaíso, Quebrada near Puente Totoralillo, 13.XI.1987, E. Maury coll. 1 ♂ (MACN). Los Vilos, Cuesta Caviolén, E. Maury, 12.XI.1987 1 ♂ 2 ♀ (MACN). Valparaíso, 10 km S de Casablanca, E. Maury, 13.I.1984 2 ♀ (MACN). Pichidangui, Valparaíso, Quebrada near Puente Totoralillo, E. Maury coll. 13.XI.1987, 7 ♂ 1 ♀ (MACN). Valparaíso: Quebrada El Tigre 25 km E Zapallar, M. Ramírez, J. Pizarro coll., 12.II.2011, 1 ♀ (MACN).

Etymology. The specific epithet refers to “Pichí” which comes from Mapudungun, the language of the Mapuche (original people of the region), meaning small. Noun in apposition.

Diagnosis. This species can be distinguished from the other species of the genus by having the dorsal microgranulate; Femora and tibia of the pedipalp with small tubercles. The male genitalia have a reduced ventral plate, a very long capsula interna and capsula externa, as well as a long fine structure at the apex of the capsula interna.

Distribution. Chile: Valparaíso Region.

Description of male holotype. Measurements: Total length 2.65, carapace length 1.12, dorsal scutum length 2.21, carapace max. width 1.64, mesotergum

Figure 128. *Nerudiella pichi* sp. nov. habitus, male **A** dorsal view **C** lateral view **E** ventral view. Female **B** dorsal view **D** lateral view **F** ventral view. Scale bars: 1 mm.

max. width 2.02. Appendage measurements: Pedipalps. Trochanter length 0.28, femora length 1.12, patella length 0.73, tibia length 0.77, tarsus length 0.80. Leg **I**: trochanter (tr) 0.20, femora (fe) 1.00, patella (pa) 0.52, tibia (ti) 0.73, metatarsus (mt) 0.90, tarsus (ta) 0.77. **II**: tr 0.27, fe 1.37, pa 0.63, ti 1.03, mt 1.14, ta 1.36. **III**: tr 0.27, fe 0.87, pa 0.40, ti 0.71, mt 0.90, ta 0.76. **IV**: tr 0.35, fe 1.29, pa 0.65, ti 1.05, mt 1.32, ta 0.86.

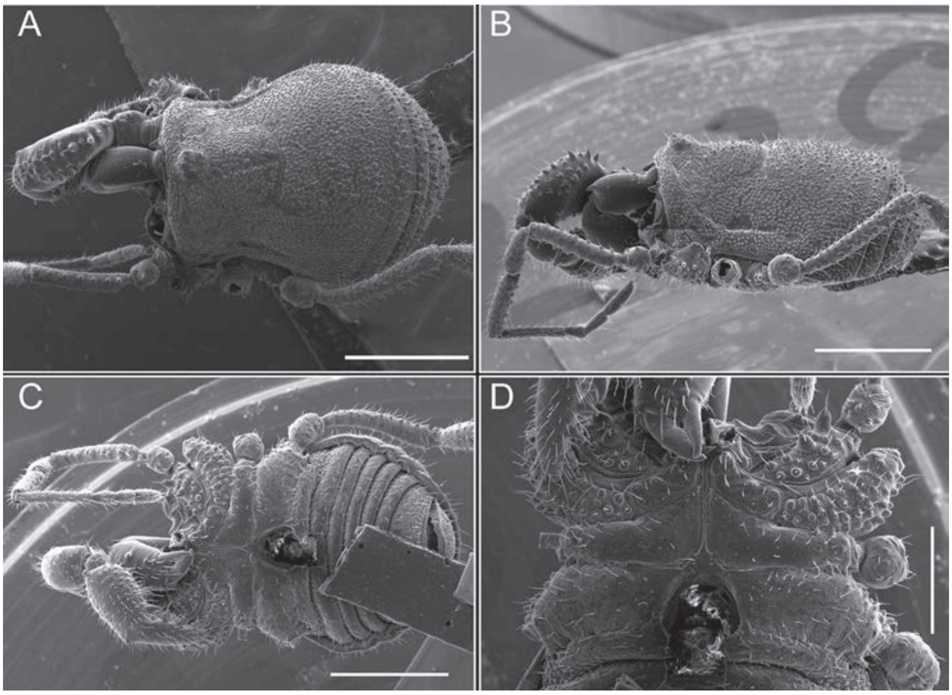

Figure 129. *Nerudiella pichi* sp. nov. male, SEM images of habitus **A** dorsal view **B** lateral view **C, D** ventral view. Scale bars: 500 µm.

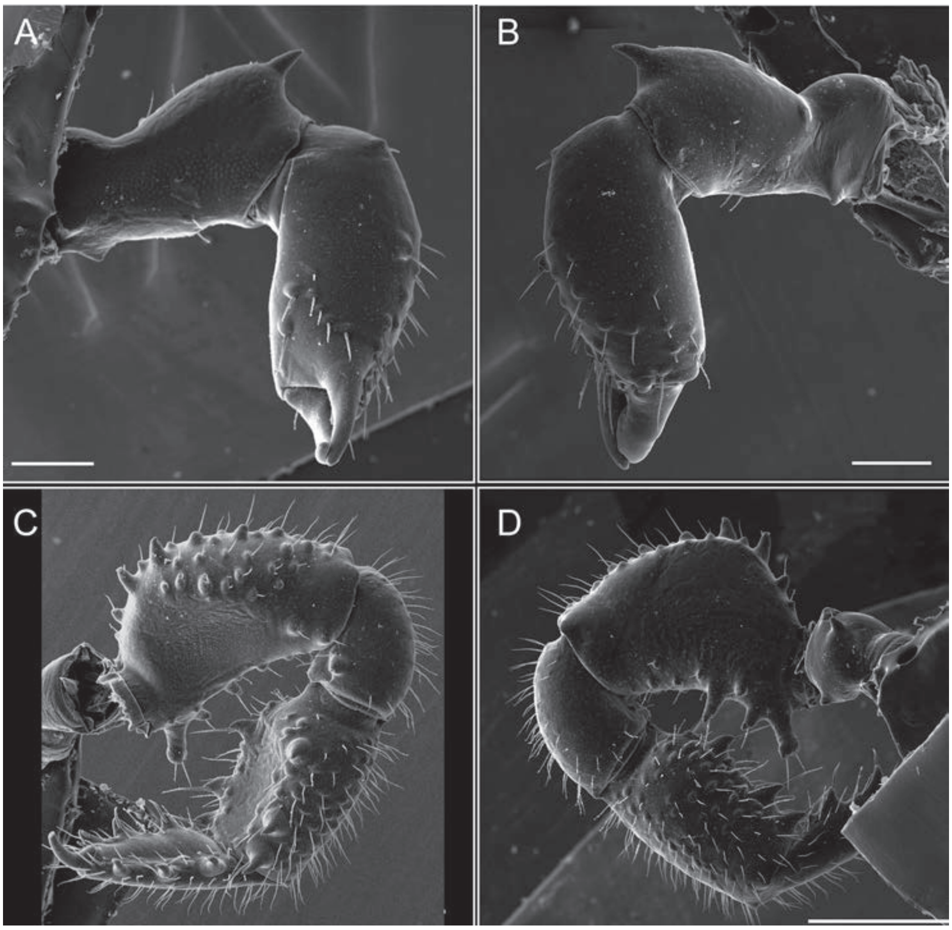

Figure 130. *Nerudiella pichi* sp. nov. chelicerae: mesal **A** ectal **B** pedipalps: mesal **C** ectal **D**. Scale bars: 200 µm (**A, B**); 500 µm (**C, D**).

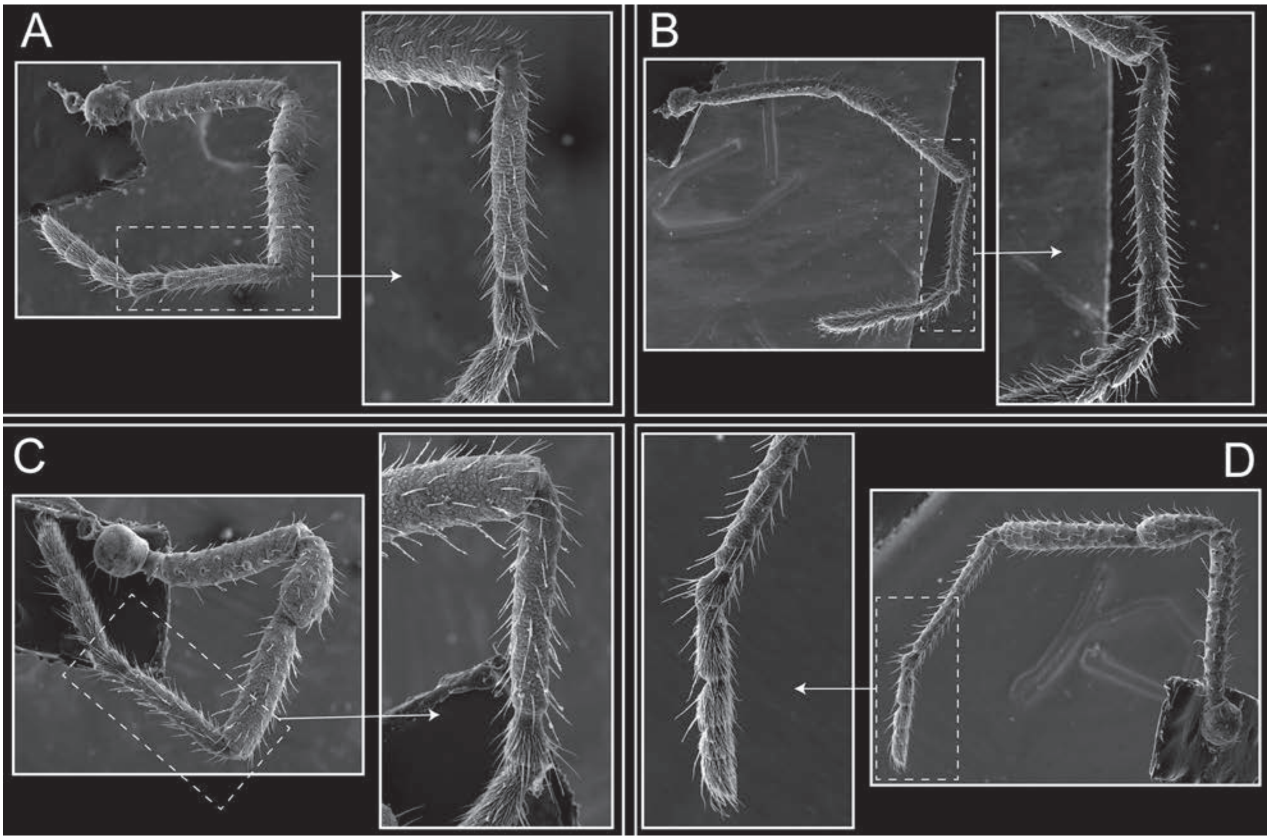

Figure 131. *Nerudiella pichi* sp. nov. legs I **A** II **B** III **C** IV **D**. Scale bars: 200 µm (**A, C**); 500 µm (**B, D**).

Dorsum (Fig. 128, 129). Eta (η) hourglass-shaped dorsal scutum. Low ocularium. Dorsal scutum microgranulate, without clear delimitation of areas. The microgranulation and the setiferous tubercles are almost the same size, so it is difficult to delimit the rows of tubercles that are present in the dorsal scute and free tergites.

Chelicerae (Fig. 130A, B). Segment I with a small tubercle on the dorso-distal surface. Segment II bearing scant setae.

Pedipalps (Fig. 130C, D). Trochanter with a small dorsal and ectal tubercle. Femora bearing an ectal row of setiferous tubercles; dorsal surface with a row of spines and a parallel row of setiferous granules on each side. Patella with a ventral setiferous tubercle, dorsal surface covered with setae. Tibia covered in setiferous granules, with three ectal and mesal spines with subdistal setae on each side. Tarsus with three mesal and four ectal spines with subdistal setae and setae and scant granules.

Legs (Fig. 131). Coxa I with setiferous tubercles, the large one with subdistal setae, II with setiferous tubercles, III and IV only with the microgranulation, three bridges between legs II and III, three between III and IV, five between leg IV and opisthosoma. Spiracles not obstructed by bridges. Smooth surface occupying ¹⁄₃ of leg II, ¾ of leg III and < ¹⁄₃ of leg IV. Sternum arrow-shaped. Legs covered in small tubercles, astragalus longer than calcaneus on all legs. Tarsal count: 3–5–4–4.

Penis (Figs 132, 133). Pars distalis with a ventral plate reduced in its apical portion bearing a cleft that divides the plate into two halves. Each half has three pointed macrosetae on the ventral surface and one macroseta on the dorsal sur-

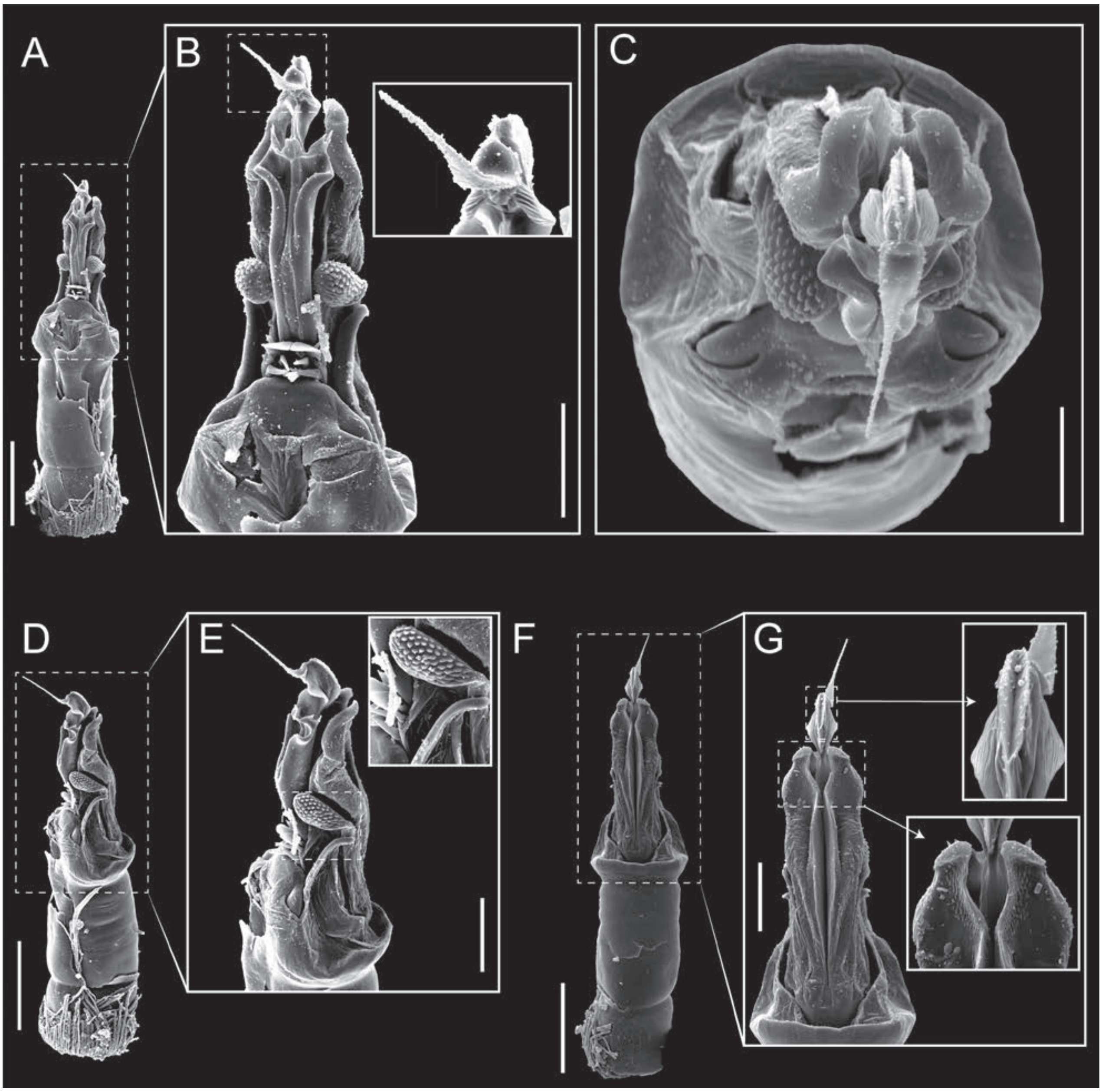

Figure 132. *Nerudiella pichi* sp. nov. penis: ventral **A, B** apical **C** lateral **D, E** dorsal **F, G**. Scale bars: 200 μm (**A, D, F**); 100 μm (**B, E, G**); 50 μm (**C**).

face; capsula externa covering dorsal and lateral surfaces, having a very long cleft dividing the capsula interna into two halves, including two rounded, microsculpted processes; there is a dorsolateral plate attached to the pars basalis. Capsula interna longer than the capsula externa, the apical portion is long and thin.

Female. Similar to male, with shorter pedipalpal femora.

Female measurements. Total length 2.49, carapace length 1.00, dorsal scutum length 2.15, carapace max. width 1.54, mesotergum max. width 2.10. Appendage measurements: Pedipalps. Trochanter length 0.25, femora length 0.89, patella length 0.53, tibia length 0.56, tarsus length 0.67. Leg I: trochanter (tr) 0.24, femora (fe) 0.89, patella (pa) 0.48, tibia (ti) 0.62, metatarsus (mt) 0.82, tarsus (ta) 0.57. **II**: tr 0.28, fe 1.17, pa 0.45, ti 0.90, mt 1.06, ta 1.14. **III**: tr 0.30, fe 0.80, pa 0.38, ti 0.63, mt 0.80, ta 0.67. **IV**: tr 0.33, fe 1.17, pa 0.55, ti 0.96, mt 1.11, ta 0.80.

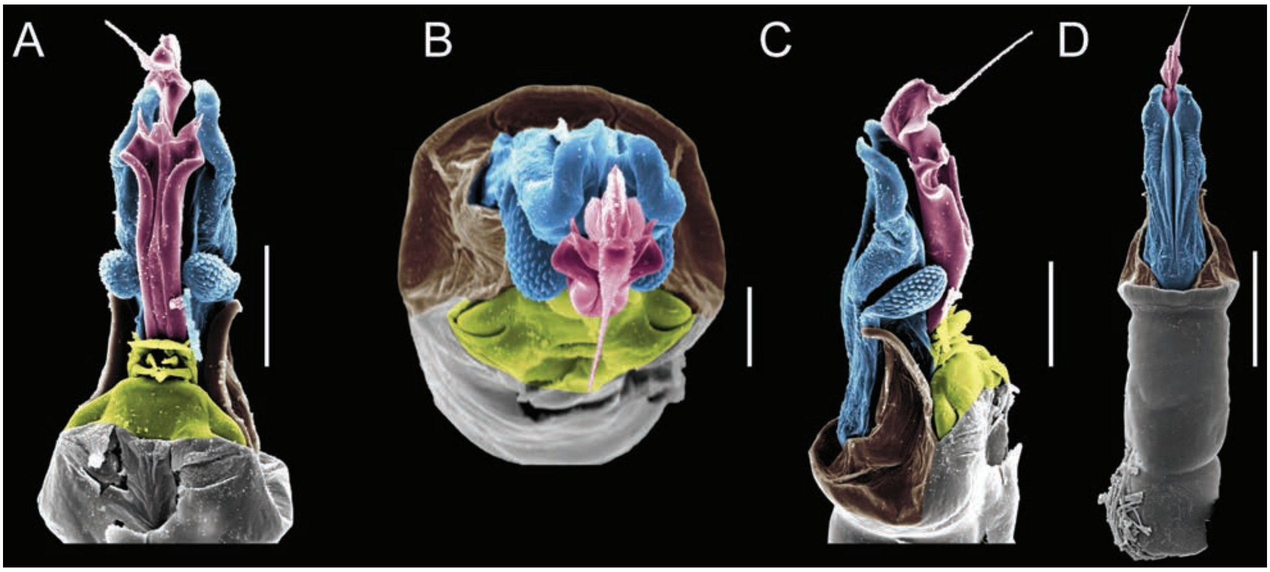

Figure 133. *Nerudiella pichi* sp. nov. penis: ventral **A** apical **B** lateral **C** dorsal **D**. Colors: ventral plate (yellow), capsula externa (blue), capsula interna (red). Scale bars: 100 µm (**A, C, D**); 50 µm (**B**).

***Nerudiella portai* sp. nov.**

https://zoobank.org/A678AF8D-AC23-4F53-95F2-2EA3D2DF35A9
Figs 134–139

Material examined. ***Holotype*.** ♂ **Chile.** Petorca: Cachagua, Quebrada El Tigre, E. Maury coll. 08.XI.1988 (MNHNCL). ***Paratypes*. Chile.** Petorca: Cachagua, Quebrada El Tigre, E. Maury coll., 08.XI.1988, 10 ♂, 12 ♀, 2 imm. (MACN). Same data, 6 ♂ (MACN).

Additional material. Chile. Quillota: Olmue, La Campana, S. Peck, J. Peck coll., 02.XII.1984, 4 ♂ 3 ♀ 4 imm. (FMNH). Valparaíso: Petorca: Zapallar -32.551318°, -71.459492° 200 m (GE), Tullgren Berlese, park bordering the beach, A. Porta coll., 28.XII.2017, 2 ♂, 20 imm. (MACN).

Etymology. Patronym in honor of Argentine arachnologist, acarologist, and mathematician Andrés Porta.

Diagnosis. This species can be distinguished from the other species in the genus by the morphology of the male genitalia, which includes the robust capsula externa with a U-shaped slit in the middle of the capsula externa; and wide capsula interna with an apical constriction.

Distribution. Chile: Valparaíso Region (Fig. 4F).

Description of male holotype. Measurements: Total length 4.00, carapace length 1.05, dorsal scutum length 2.1, carapace max. width 1.34, mesotergum max. width 1.91. Appendage measurements. Pedipalps. Trochanter length 0.18, femora length 0.93, patella length 0.52, tibia length 0.68, tarsus length 0.65. Leg I: trochanter (tr) 0.21, femora (fe) 0.95, patella (pa) 0.52, tibia (ti) 0.70, metatarsus (mt) 0.82, tarsus (ta) 0.69. II: tr 0.20, fe 1.29, pa 0.61, ti 0.88, mt 1.14, ta 1.38. III: tr 0.30, fe 0.75, pa 0.41, ti 0.57, mt 0.68, ta 0.82. IV: tr 0.36, fe 1.18, pa 0.55, ti 1.00, mt 1.025, ta 0.90.

Dorsum (Fig. 134, 135). Eta (η) hourglass-shaped dorsal scutum. Ocularium low, rounded. Dorsal scutum microgranulate, without prominent tubercles.

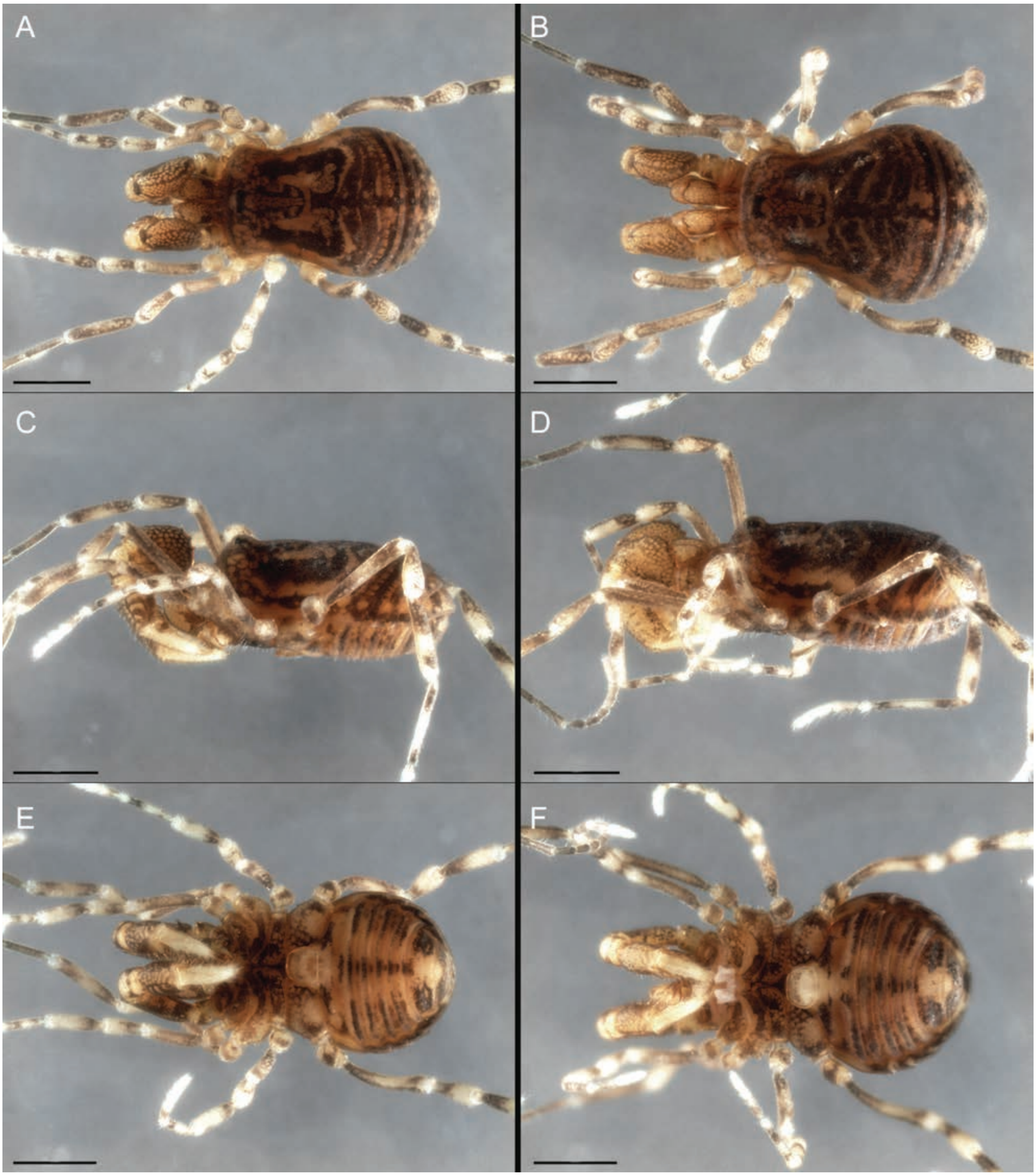

Figure 134. *Nerudiella portai* sp. nov. habitus, male **A** dorsal view **C** lateral view **E** ventral view. Female **B** dorsal view **D** lateral view **F** ventral view. Scale bars: 1 mm. Species of Clade C, see Fig. 3.

Chelicerae (Fig. 136A, B). Segment **I** with a small tubercle on the dorso-distal surface. Segment **II** bearing sparse small setiferous tubercles, with one triangular tubercle prominent from the others in frontal view.

Pedipalps (Fig. 136C, D). Trochanter with a small dorsal and ventral tubercle. Femora bearing two parallel dorsal rows of setiferous spines, the ectal row has stronger spines than the mesal, it also has two proximal spines. Patella with a ventral-ectal setiferous tubercle and two ventral-ectal spines. Tibia covered

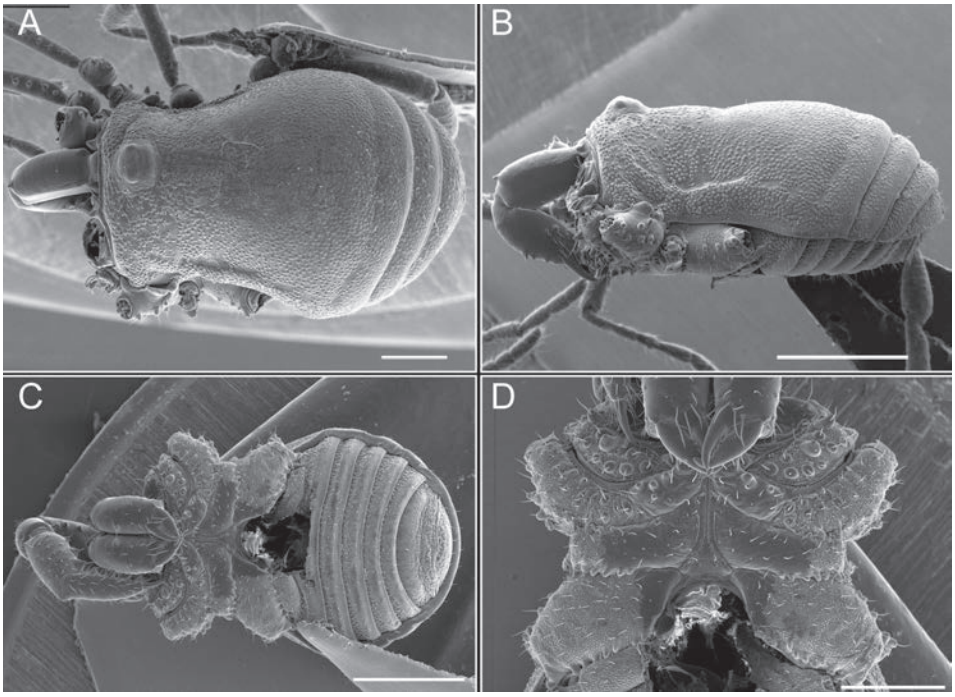

Figure 135. *Nerudiella portai* sp. nov. male, SEM images of habitus **A** dorsal view **B** lateral view **C, D** ventral view. Scale bars: 500 µm.

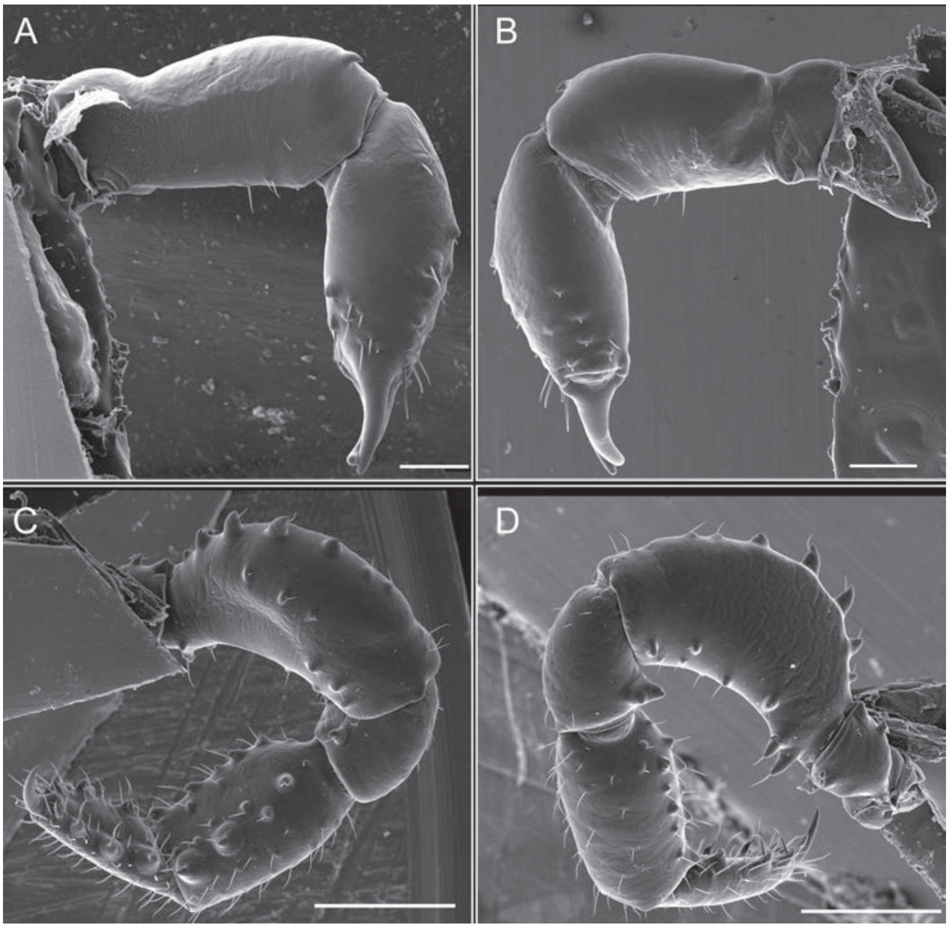

Figure 136. *Nerudiella portai* sp. nov. chelicerae: mesal **A** ectal **B** pedipalps: mesal **C** ectal **D**. Scale bars: 200 µm (**A, B**); 500 µm (**C, D**).

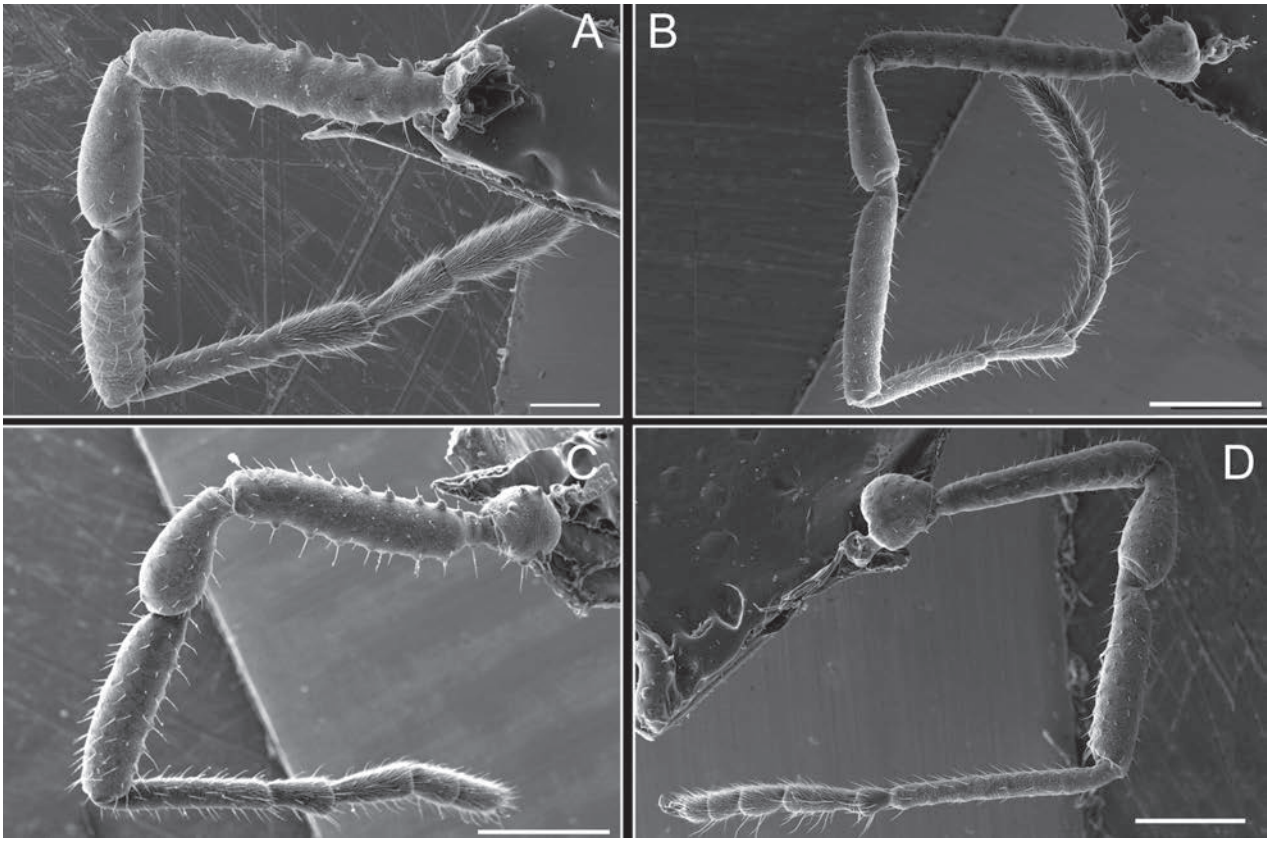

Figure 137. *Nerudiella portai* sp. nov. legs I **A** II **B** III **C** IV **D**. Scale bars: 200 µm (**A**); 500 µm (**B–D**).

in small ventral tubercles and two mesal spines. Tarsus with three mesal and ectal spines with subdistal setae in addition to setae and few granules.

Legs (Fig. 137). Coxa I with nine or ten setiferous tubercles, IV with six or seven tubercles connected to opisthosoma. Spiracles not obstructed by bridges. Smooth surface occupying ⅓ of leg II, ¾ of III and < ⅓ of IV. Leg II smooth with two or three small tubercles with subdistal setae on each side. Sternum arrow-shaped. Legs covered in small tubercles, astragalus longer than calcaneus on all legs. Tarsal count: 3–6–4–4.

Penis (Figs 138, 139). Pars distalis with a ventral plate bearing a cleft dividing the plate into two halves. Each half has three pointed macrosetae on the ventral surface and one macroseta on the dorsal surface; capsula externa covering dorsal surface, bearing a U-shaped slit halfway up plate; there is a dorsolateral plate attached to the pars basalis. Capsula interna slightly longer than the capsula externa, without rigid structures. The apical area of the structure is irregularly shaped and does not have a visible stylus.

Female. Similar to male, with shorter pedipalpal femora.

Female measurements. Total length 4.11, carapace length 1.02, dorsal scutum length 2.15, carapace max. width 1.33, mesotergum max. width 1.99. Appendage measurements: Pedipalps. Trochanter length 0.30. Femora length 0.87, patella length 0.41, tibia length 0.64, tarsus length 0.66. Leg I: trochanter (tr) 0.24, femora (fe) 0.95, patella (pa) 0.54, tibia (ti) 0.59, metatarsus (mt) 0.78, tarsus (ta) 0.71. II: tr 0.27, fe 1.23, pa 0.54, ti 0.93, mt 1.09, ta 1.25. III: tr 0.28, fe 0.75, pa 0.38, ti 0.55, mt 0.71, ta 0.69. IV: tr 0.28, fe 1.28, pa 0.69, ti 0.93, mt 1.25, ta 0.87.

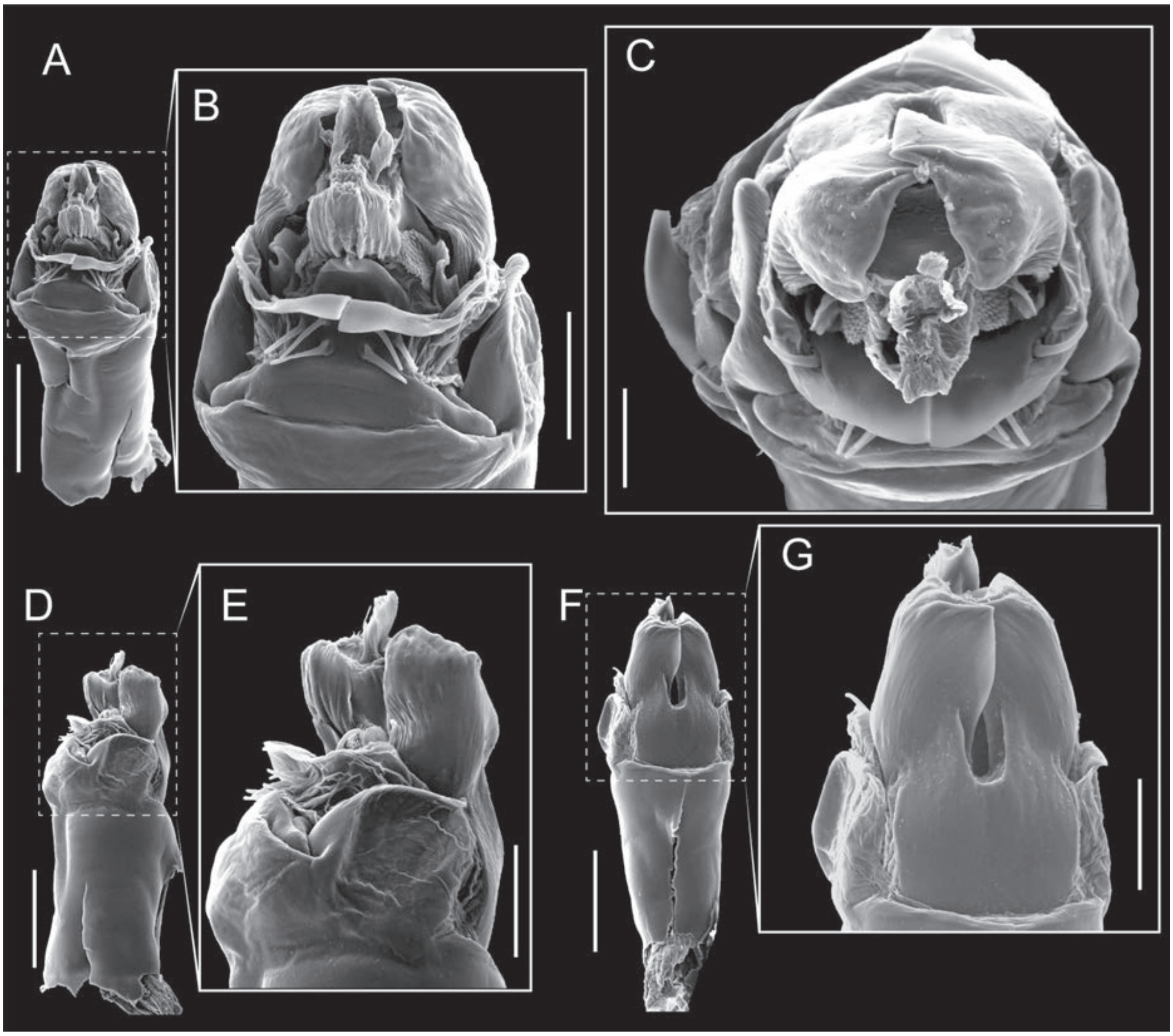

Figure 138. *Nerudiella portai* sp. nov. penis: ventral **A, B** apical **C** lateral **D, E** dorsal **F, G**. Scale bars: 200 µm (**A, D, F**); 100 µm (**B, C, E, G**).

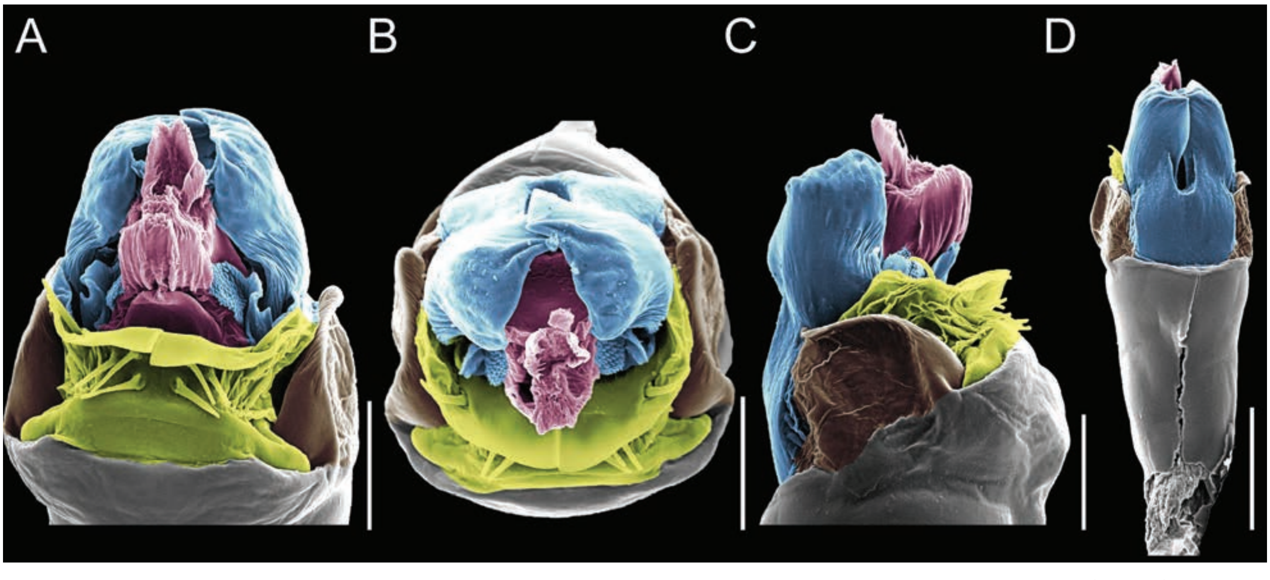

Figure 139. *Nerudiella portai* sp. nov. penis: ventral **A** apical **B** lateral **C** dorsal **D**. Colors: ventral plate (yellow), capsula externa (blue), capsula interna (red). Scale bars: 100 µm (**A–C**); 200 µm (**D**).

Nerudiella quenes **sp. nov.**

https://zoobank.org/5E95016E-5E90-4131-8289-9DA206E43881

Figs 140, 141

Material examined. ***Holotype***. ♂ **CHILE.** Curicó Quebrada in front of Los Queñes, 34.99614°S, 70.80994°W, 665 m A. Ojanguren, A. Pérez-González, M. Ramírez, G. Azevedo, W. Porto coll., 10.I.2018 (MNHNCL). ***Paratypes*. CHILE.** Curicó: Quebrada in front of Los Queñes, gorge in front of Los Queñes, 34.99614°S, 70.80994°W, 665 m, A. Ojanguren, A. Pérez-González, M. Ramírez, G. Azevedo, W. Porto coll.,10. I.2018, 1 ♀ 3 imm.

Etymology. The specific epithet refers to the type locality of the species, the department of Los Queñes, located in the commune of Romeral, province of Curicó, Chile. Noun in apposition.

Diagnosis. This species can be distinguished from the other species in the genus by the morphology of the male genitalia, which includes the robust capsula externa with a "V"-shaped slit and long capsula interna with a triangular apical portion.

Distribution. Chile: Maule Region (Fig. 4F).

Description of male holotype. Measurements: Total length 2.0, carapace length 0.84, dorsal scutum length 1.7, carapace max. width 12, mesotergum max. width 1.6. Appendage measurements: Pedipalps. Trochanter length 0.22, femora length 0.79, patella length 0.43, tibia length 0.56, tarsus length 0.66. Leg I: trochanter (tr) 0.21, femora (fe) 0.87, patella (pa) 0.47, tibia (ti) 0.69, metatarsus (mt) 0.77, tarsus (ta) 0.66. II: tr 0.20, fe 1.1, pa 0.55, ti 0.86, mt 0.96, ta 1.2. III: tr 0.28, fe 0.75, pa 0.34, ti 0.58, mt 0.70, ta 0.60. IV: tr 0.30, fe 1.1, pa 0.53, ti 0.85, mt 1.1, ta 0.66.

Dorsum (Fig. 140). Eta (η) hourglass-shaped dorsal scutum. Low ocularium. Dorsal scutum microgranulate, without clear delineation of areas.

Chelicerae. Segment I with a small tubercle on the dorso-distal surface. Segment II with a frontal tubercle and bearing few setae.

Pedipalps. Trochanter with a small ectal and dorsal tubercles. Femora with two prominent ventroproximal spines and three prominent dorsal spines. Patella with two ventral setiferous granules. Tibia with three ectal and two mesal spines with subdistal setae, with scant granules in ventral view. Tarsus with four ectal and three mesal spines with subdistal setae.

Legs. Coxa II with ~8 rounded setiferous tubercles. Spiracles not obstructed by bridges. Sternum arrow-shaped. Legs I–IV covered in setae, tarsal area, and calcaneus densely setose. Tibiae I–III with a ventral and dorsal row of small setiferous tubercles, IV with a row of four distal-ventral tubercles with setae. Calcaneus smaller than astragalus, ≥ 3× smaller (leg I), 4× (II, III), and 5× (leg IV). Tarsal count: 3–6–4–4.

Penis (Fig. 141). Pars distalis with a large ventral plate bearing a cleft that divides the plate into two lamellae. Each lamella has three pointed macrosetae on the ventral surface and one macroseta on the dorsal surface; capsula externa covering dorsal and lateral surfaces, having a cleft dividing dorsal fold into two halves; there is a dorsolateral plate attached to the pars basalis. Capsula interna longer than the capsula externa, with a visible stylus in its apical portion.

Female. Similar to male, with shorter pedipalpal femora.

Figure 140. *Nerudiella quenes* sp. nov. habitus, male **A** dorsal view **C** lateral view **E** ventral view. Female **B** dorsal view **D** lateral view **F** ventral view. Scale bars: 1 mm. Species of Clade C, see Fig. 3.

Female measurements. Total length 2.07, carapace length 0.89, dorsal scutum length 1.72, carapace max. width 1.24, mesotergum max. width 1.77. Appendage measurements: Pedipalps. Trochanter length 0.19, femora length 0.76, patella length 0.47, tibia length 0.50, tarsus length 0.68. Leg I: trochanter (tr) 0.22, femora (fe) 0.84, patella (pa) 0.44, tibia (ti) 0.65, metatarsus (mt) 0.71, tarsus (ta) 0.64. **II**: tr 0.24, fe 1.09, pa 0.51, ti 0.87, mt 0.95, ta 1.3. **III**: tr 0.23, fe 0.75, pa 0.35, ti 0.60, mt 0.72, ta 0.61. **IV**: tr 0.31, fe 1.08, pa 0.57, ti 0.93, mt 1.16, ta 0.68.

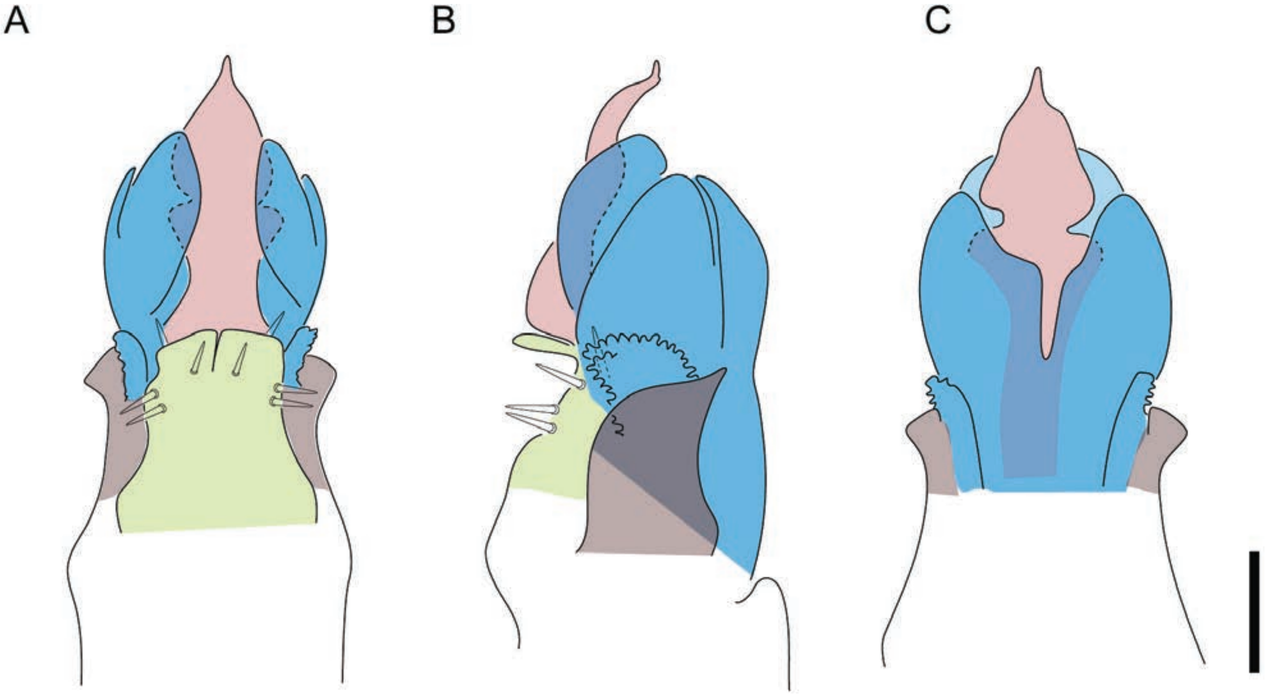

Figure 141. *Nerudiella quenes* sp. nov. Penis ventral **A** lateral **B** dorsal **C** capsula interna (red), Capsula externa (blue), dorsolateral plate (brown), ventral plate (green). Scale bar: 100 µm.

Nerudiella vilches **sp. nov.**

https://zoobank.org/1E1E59C3-6A5F-415A-B640-C49EB3A2AC77

Figs 142–147

Material examined. ***Holotype*****.** ♂ **Chile.** Cachapoal: Río de los Cipreses National Reserve, Near Potrero, A. Ojanguren, A. Pérez-González, M. Ramírez, G. Azevedo, W. Porto coll., 09.I.2018 (MNHNCL). ***Paratypes*****. Chile.** Cachapoal: Río de los Cipreses National Reserve, Near Potrero, A. Ojanguren, A. Pérez-González, M. Ramírez, G. Azevedo, W. Porto coll., 09.I.2018, 1 ♂ 2 ♀ 5 imm. (MACN). Osorno. Talca, Alto de Vilches, N. Platnick, K.Catley, M. Ramírez, T.Allen coll., 14–15/XI/1993, 1 ♂ 2 imm. (AMNH). Talca. Vilches, 132 km E. of Talca, E. Maury coll., 07–08.I.1989, 2 ♂ 1 ♀ (MACN). Alto de Vilches, 70 km E Talca, S.Peck, J.Peck coll., 05.XII.1985, 3 ♂ 3 ♀ 4 imm. (FMNH). Talca. Vilches, A.Roig coll., 17.I.1984, 2 ♂ 1 ♀ (MACN).

Additional material. Chile. RN Altos del Lircay, E Vilches Alto, A. Ojanguren, A. Pérez-González, M. Ramírez, G. Azevedo, W. Porto coll. 11.I.2018 1 ♂ (MACN).

Etymology. The specific epithet refers to the type locality of the species, Vilches, located in the commune of San Clemente, province of Talca, Chile. Noun in apposition.

Diagnosis. This species can be easily distinguished from the other species in the genus by having a projecting process on the ventral femoral region of the pedipalp. The capsula externa of the genitalia does not have dorsal slits but bears a pair of lateral processes.

Distribution. Chile: Maule Region (Fig. 4F).

Description of male holotype. Measurements: Total length 4.12, carapace length 1.05, dorsal scutum length 2.42, carapace max. width 1.33, mesotergum

Figure 142. *Nerudiella vilches* sp. nov. habitus, male **A** dorsal view **C** lateral view **E** ventral view. Female **B** dorsal view **D** lateral view **F** ventral view. Scale bars: 1 mm. Species of Clade C, see Fig. 3.

max. width 1.83. Appendage measurements: Pedipalps. Trochanter length 0.24, femora length 0.94, patella length 0.47, tibia length 0.80, tarsus length 0.71. Leg I: trochanter (tr) 0.30, femora (fe) 0.20, patella (pa) 0.87, tibia (ti) 0.41, metatarsus (mt) 0.69, tarsus (ta) 0.76. II: tr 0.64, fe 0.30, pa 1.13, ti 0.52, mt 0.86, ta 0.94. III: tr 1.24, fe 0.29, pa 0.79, ti 0.32, mt 0.60, ta 0.62. IV: tr 0.68, fe 0.30, pa 1.16, ti 0.55, mt 0.92, ta 1.12, ta 0.74.

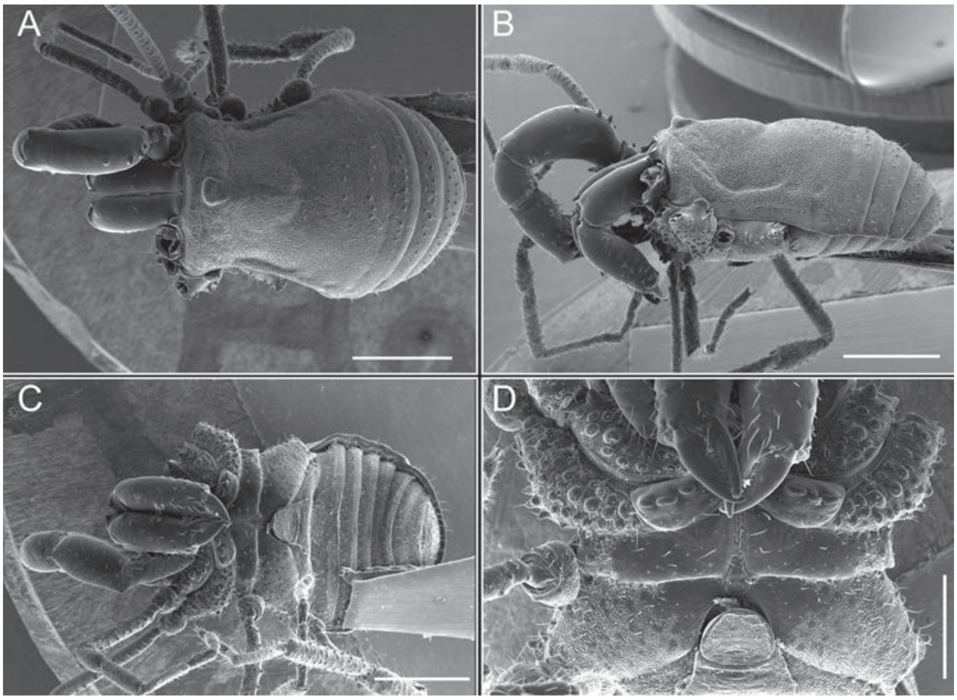

Figure 143. *Nerudiella vilches* sp. nov. male, SEM images of habitus **A** dorsal view **B** lateral view **C, D** ventral view. Scale bars: 1 mm (**A, B, C**); 500 µm (**D**).

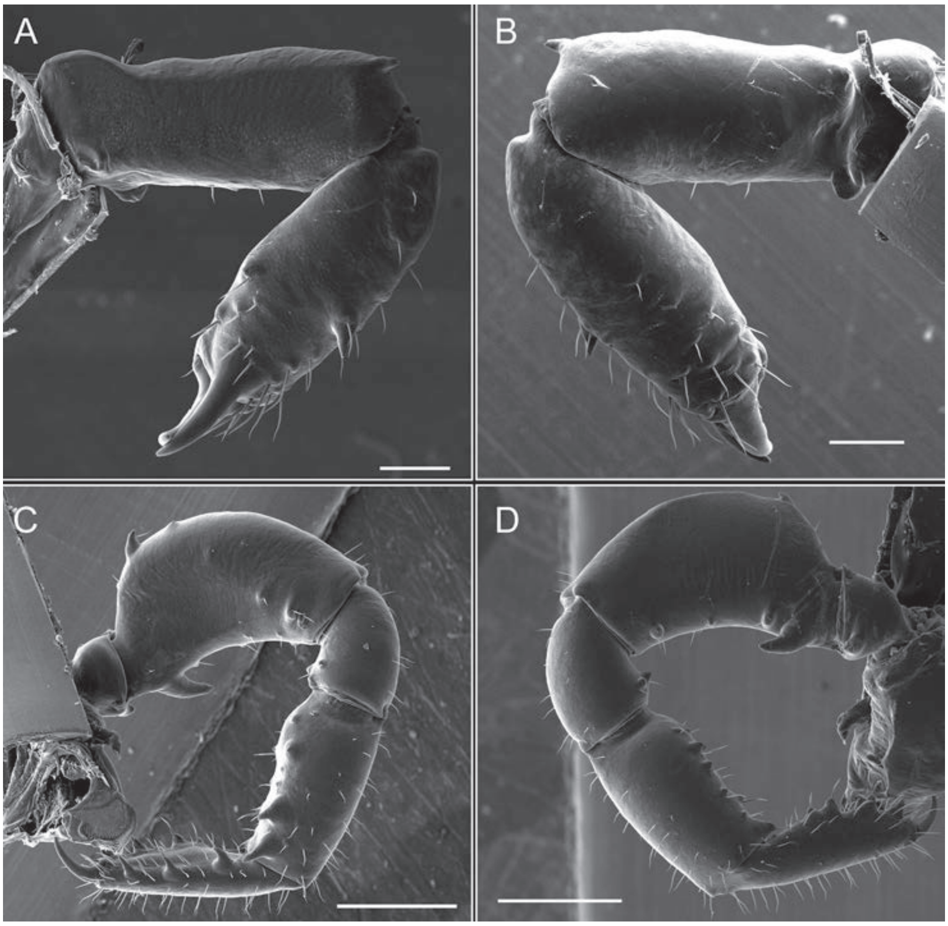

Figure 144. *Nerudiella vilches* sp. nov. chelicerae: mesal **A** ectal **B** pedipalps: mesal **C** ectal **D**. Scale bars: 200 µm (**A, B**); 500 µm (**C, D**).

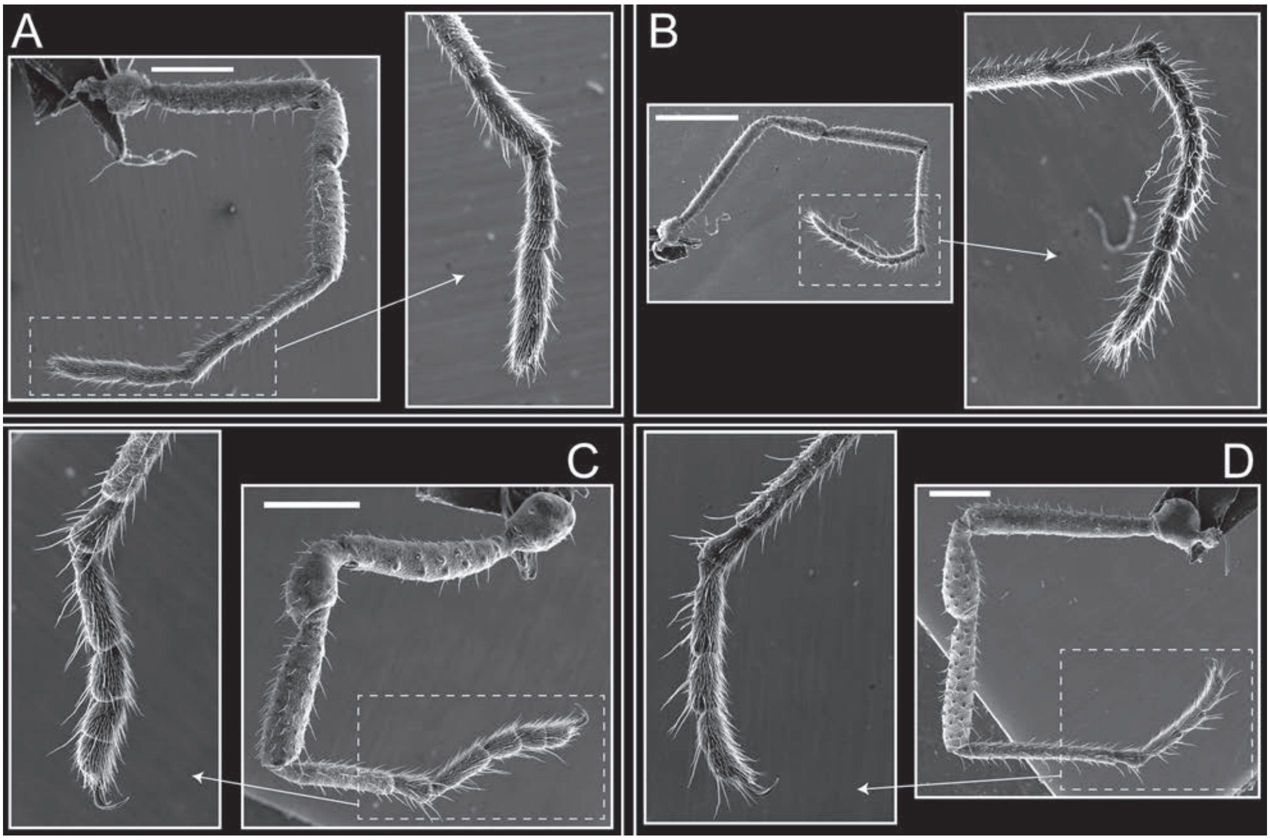

Figure 145. *Nerudiella vilches* sp. nov. legs I **A** II **B** III **C** IV **D**. Scale bars: 500 µm (**A, C, D**); 1 mm (**B**).

Dorsum (Fig. 142, 143). Eta (η) hourglass-shaped dorsal scutum. Low ocularium; dorsal scutum microgranulate, without clear delimitation of areas. Areas III–IV with a row of 6–7 small setiferous tubercles; posterior margin with a row of 12 small rounded setiferous tubercles. All free tergites have two rows of small setiferous tubercles.

Chelicerae (Fig. 144A, B). Segment I with a small tubercle on the dorso-distal surface. Segment II with a frontal tubercle and bearing few setae.

Pedipalps (Fig. 144C, D). Trochanter with a small ectal and dorsal tubercle. Femora bearing a forward-curved proximal ventral spine, a ventral row of three small setiferous granules, a dorsal tubercle with subdistal setae, and three distal setiferous granules. Patella with two ventral setiferous granules. Tibia with three ectal and two mesal spines with subdistal setae, with scant granules in ventral view. Tarsus with four ectal and three mesal spines with subdistal setae.

Legs (Fig. 145). Coxa I–II covered with rounded setiferous tubercles, the distal one is acute and has a subdistal seta, III and IV only with microgranulation. Spiracles not obstructed by bridges. Smooth area occupying ⅓ of leg II (with three tubercles), ¾ of III and ⅓ of IV. Sternum arrow-shaped. Legs I–IV covered in setae. Tibiae I–III with a ventral and dorsal row of small setiferous tubercles, IV with a row of four distoventral tubercles with setae. Calcaneus smaller than the astragalus, ≥ 3× smaller (leg I), 4× (II, III), and 5× (leg IV). Tarsal count: 3–6–4–4.

Penis (Figs 146, 147). Pars distalis with a ventral plate bearing a cleft dividing the plate into two lamellae. Each lamellae has three pointed macrosetae on the ventral surface and one macroseta on the dorsal surface; capsula externa

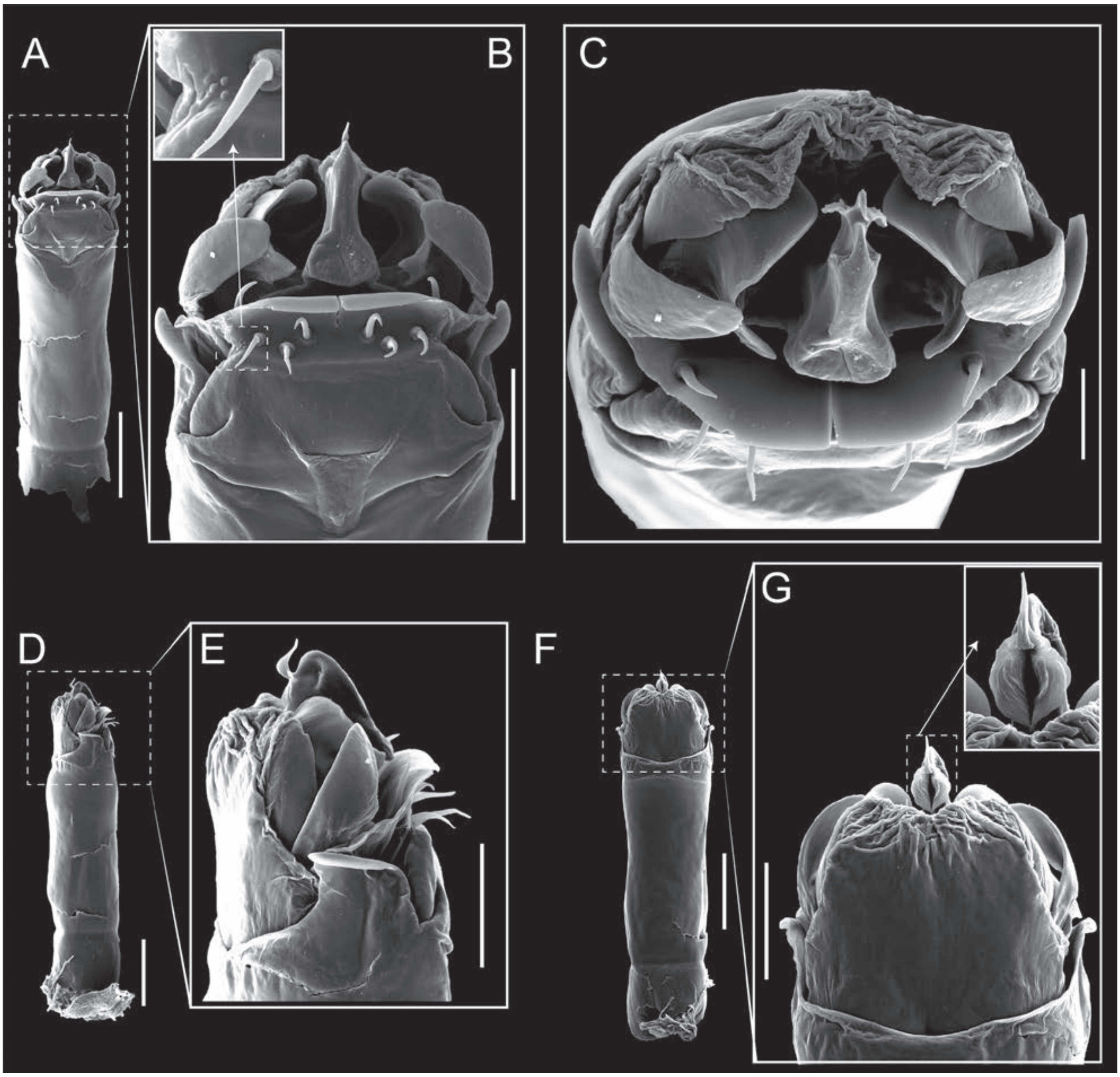

Figure 146. *Nerudiella vilches* sp. nov. penis: ventral **A, B** apical **C** lateral **D, E** dorsal **F, G**. Scale bars: 200 µm (**A, D, F**); 100 µm (**B, E, G**); 50 µm (**C**).

covering dorsal and lateral surfaces, without cleft; it has a pair of lateral processes that are projected ventrally. The capsula interna bears a pair of laminar processes; the apical region has a small dorsal opening and a fine process.

Female. Similar to male, with shorter pedipalpal femora.

Female measurements. Total length 3.67, carapace length 0.93, dorsal scutum length 1.90, carapace max. width 1.16, mesotergum max. width 1.77. Appendage measurements: Pedipalps. Trochanter length 0.22, femora length 0.85, patella length 0.47, tibia length 0.68, tarsus length 0.59. Leg I: trochanter (tr) 0.19, femora (fe) 0.84, patella (pa) 0.46, tibia (ti) 0.63, metatarsus (mt) 0.77, tarsus (ta) 0.67. **II**: tr 0.27, fe 1.12, pa 0.51, ti 0.86, mt 0.97, ta 1.30. **III**: tr 0.27, fe 0.82, pa 0.35, ti 0.55, mt 0.65, ta 0.66. **IV**: tr 0.33, fe 1.20, pa 0.56, ti 0.91, mt 1.07, ta 0.82.

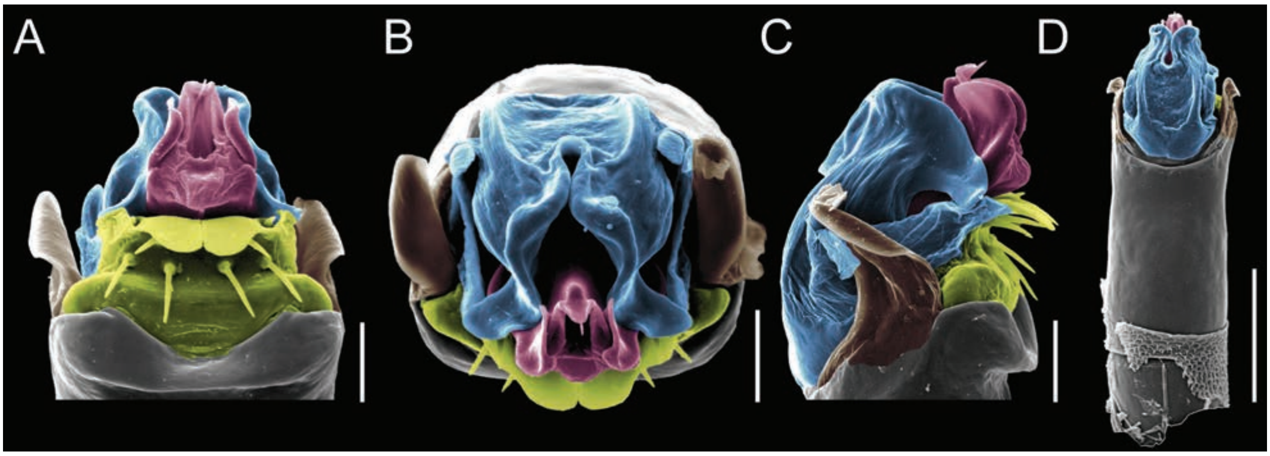

Figure 147. *Nerudiella vilches* sp. nov. penis: ventral **A** apical **B** lateral **C** dorsal **D**. Colors: ventral plate (yellow), capsula externa (blue), capsula interna (red). Scale bars: 100 µm (**A, C, D**); 50 µm (**B**).

Nerudiella wekufe **sp. nov.**

https://zoobank.org/F57E3734-45AE-4AEF-AD70-1A3A27AA7CC7
Figs 148–153

Material examined. ***Holotype*****.** ♂ **Chile.** Concepción: El Manzano, T. Cekalovic coll. 31.III.1984 (MNHNCL). ***Paratypes*****. Chile.** Concepción: El Manzano, T. Cekalovic coll., 03.I.1985, 1 ♂ (MACN). Same data, 03.I.1985, 1 ♀ (MACN). Same locality and collector, 31.III.1984, 1 ♂, 1 ♀, 2 imm. (MACN).

Etymology. The specific epithet refers to the "Wekufe", a spirit and/or harmful force (energy) from Mapuche belief and mythology. Noun in apposition.

Diagnosis. This species can be distinguished from other species in the genus by the presence of an apophysis in the anterior portion of the ocularium. Additionally, in males, the genitalia exhibit a longer capsula externa compared to the capsula interna, providing a distinguishing characteristic.

Distribution. Chile: Bío-Bío Region (Fig. 4F).

Description of male holotype. Measurements: Total length 2.4, carapace length 1.0, dorsal scutum length 1.9, carapace max. width 1.4, mesotergum max. width 1.8. Appendage measurements: Pedipalps. Trochanter length 0.22, femora length 0.8, patella length 0.47, tibia length 0.57, tarsus length 0.76. Leg I: trochanter (tr) 0.25, femora (fe) 0.81, patella (pa) 0.40, tibia (ti) 0.62, metatarsus (mt) 0.73, tarsus (ta) 0.61. II: tr 0.26, fe 1.00, pa 0.54, ti 0.82, mt 0.89, ta 1.2. III: tr 0.28, fe 0.71, pa 0.37, ti 0.56, mt 0.69, ta 0.63. IV: tr 0.29, fe 0.98, pa 0.55, ti 0.85, mt 1.1, ta 0.68.

Dorsum (Fig. 148, 149). Eta (η) hourglass-shaped dorsal scutum. Ocularium low and rounded, with an anterior apophysis. Dorsal scutum and free tergites microgranulate. Although the areas of the dorsal scutum do not exhibit clear separation, they are covered with small setiferous tubercles, which are more prominent on the dorsal scutum and free tergites.

Chelicerae (Fig. 150A, B). Segment I with a sharp tubercle on the dorso-distal surface and three small ventral-proximal tubercles. Segment II with scattered setae in ectal and ventral views, with one triangular tubercle prominent from the others in front view.

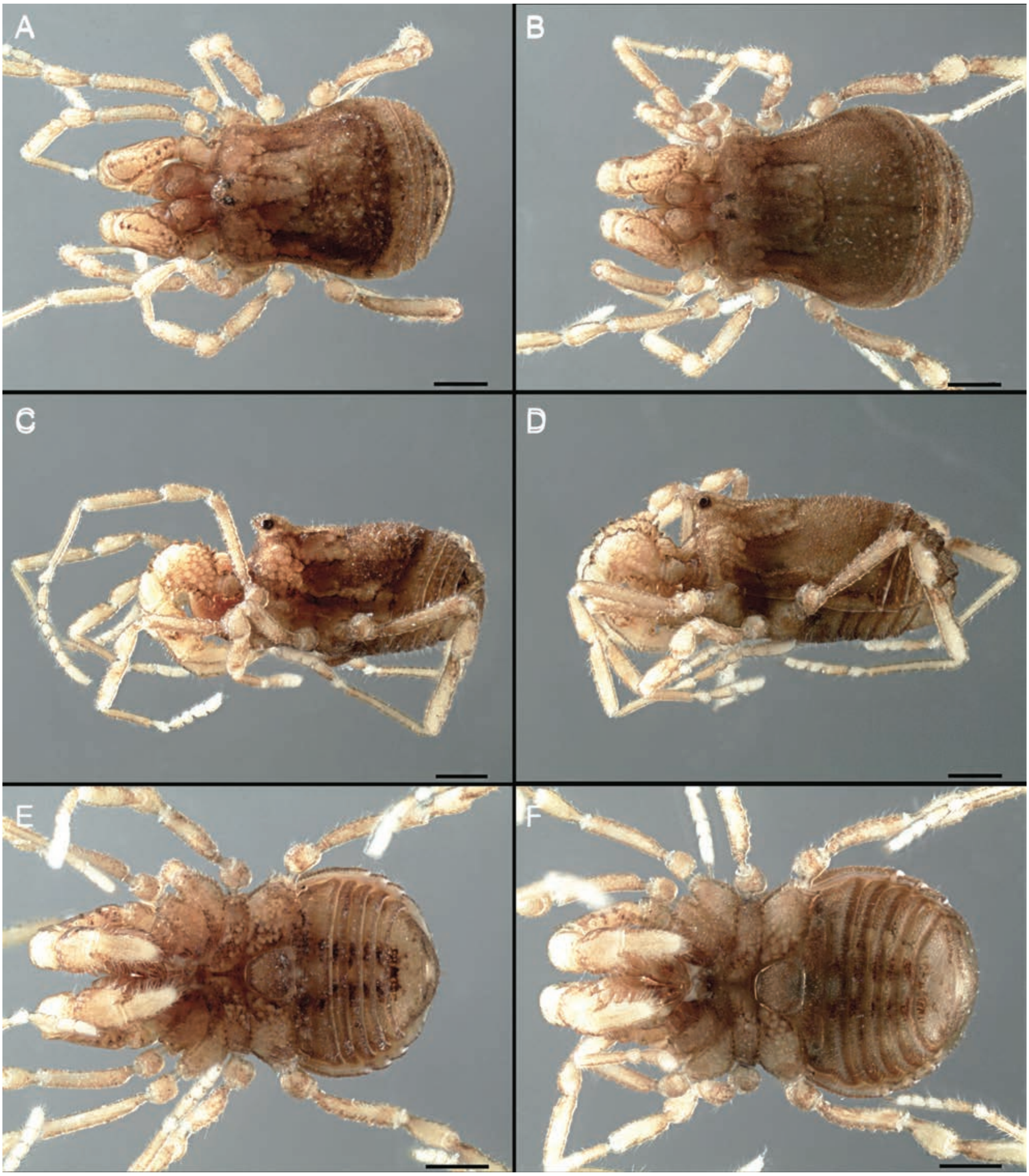

Figure 148. *Nerudiella wekufe* sp. nov. habitus, male **A** dorsal view **C** lateral view **E** ventral view. Female **B** dorsal view **D** lateral view **F** ventral view. Scale bars: 500 µm.

Pedipalps (Fig. 150C, D). Trochanter with two small dorsal tubercles and a ventral one. Femora with two parallel rows of dorsal and spines. Patella with a mesal tubercle and small sparse tubercles. Tibia with three ventral-ectal and two ventral-mesal spines, lateral and dorsal areas with small setiferous tubercles. Tarsus with three mesal and ectal spines with subdistal setae in addition to setae and few setae.

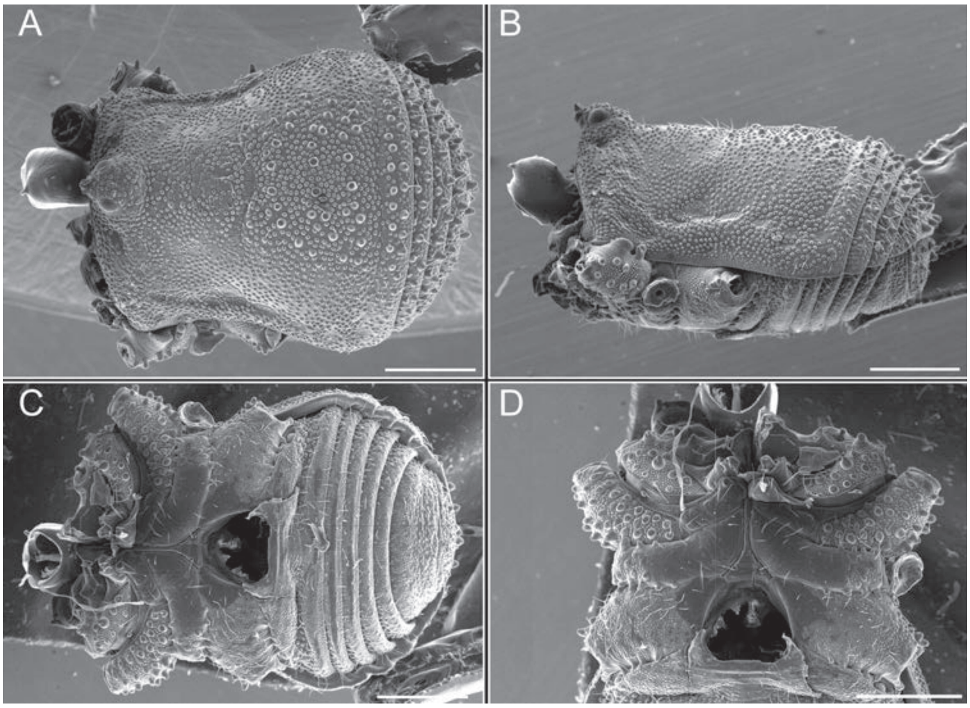

Figure 149. *Nerudiella wekufe* sp. nov. male, SEM images of habitus **A** dorsal view **B** lateral view **C, D** ventral view. Scale bars: 500 µm (**A, B, C**); 1 mm (**D**).

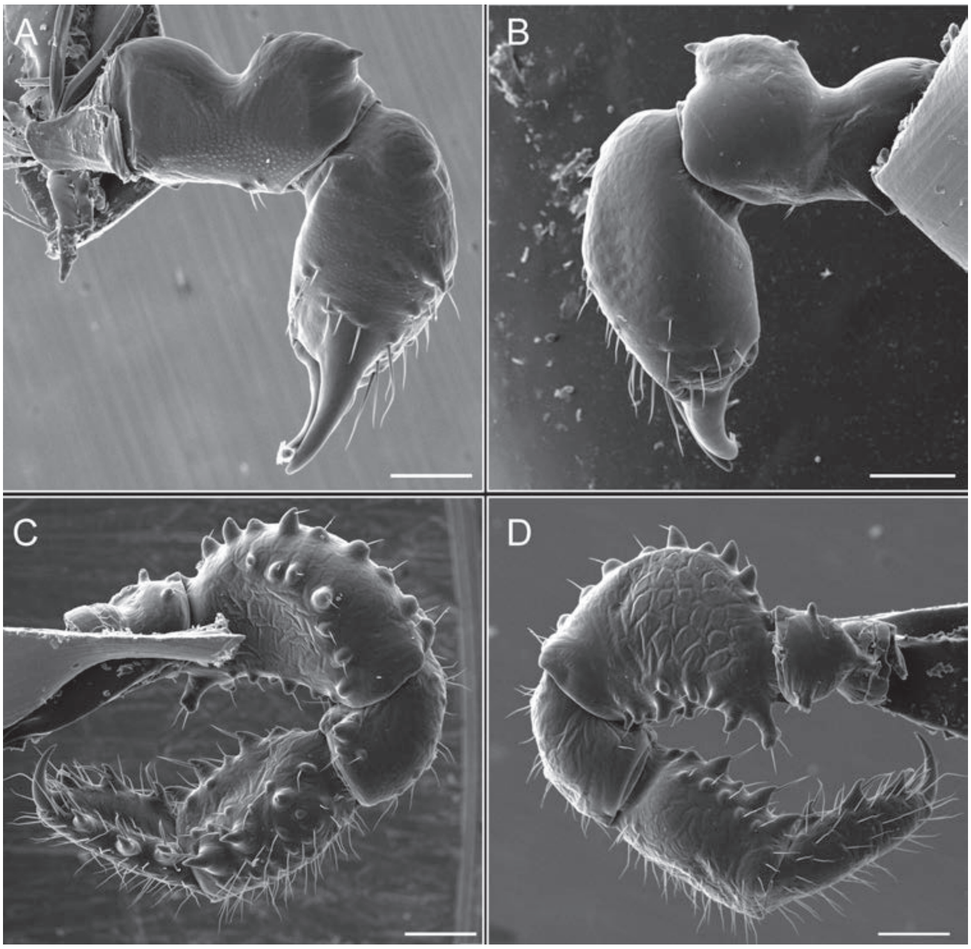

Figure 150. *Nerudiella wekufe* sp. nov. chelicerae: mesal **A** ectal **B** pedipalps: mesal **C** ectal **D**. Scale bars: 200 µm.

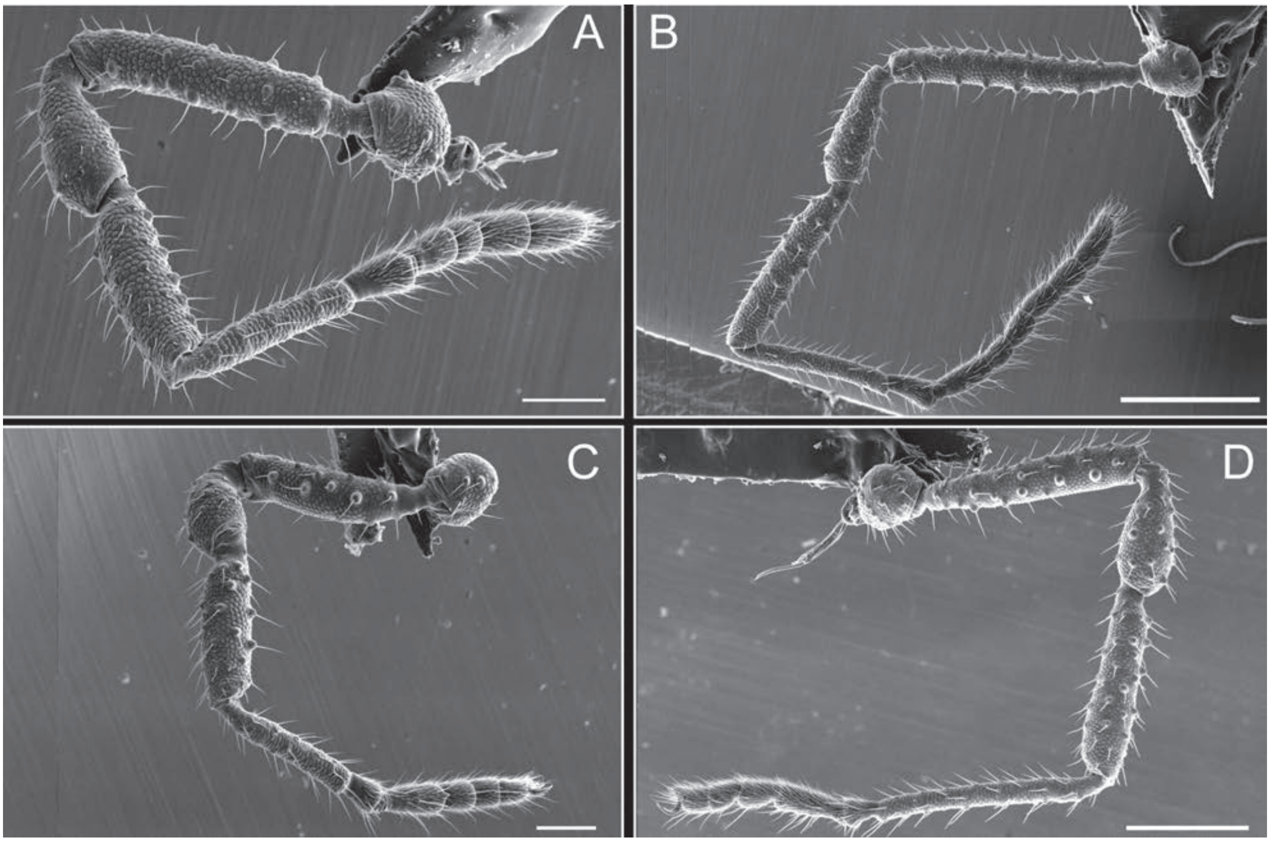

Figure 151. *Nerudiella wekufe* sp. nov. legs I **A** II **B** III **C** IV **D**. Scale bars: 200 µm (**A, C**); 500 µm (**B, D**).

Legs (Fig. 151). Coxa I with 12 or 13 setiferous tubercles the two apical ones are stronger than the others, II with 25–30 setiferous tubercles, III with seven or eight tubercles, IV with five or six small tubercles. Spiracles not obstructed by bridges. Smooth surface occupying ⅓ of leg II, ¾ of III and < ⅓ of IV. Sternum arrow-shaped. Legs covered in small tubercles, astragalus longer than calcaneus on all legs. Tarsal count: 4–6–4–4.

Penis (Figs 152, 153). Pars distalis with a ventral plate that is divided into two halves by a fine cleft. Each half of the ventral plate with three pointed macrosetae on the ventral surface and one macroseta on the dorsal surface. Capsula externa remarkably long, covering the dorsal surface. It is further divided into two halves by a long cleft and possesses a pair of long processes that curve ventrally. Additionally, with a dorsolateral plate attached to the pars basalis. Capsula externa longer than the capsula interna. Capsula interna thin and laterally flattened, with a sharp apical area.

Female. Similar to male, with shorter pedipalpal femora.

Female measurements. Measurements: Total length 2.7, carapace length 1.1, dorsal scutum length 2.1, carapace max. width 1.5, mesotergum max. width 2.0. Appendage measurements: Pedipalps. Trochanter length 0.23, femora length 0.7, patella length 0.47, tibia length 0.58, tarsus length 0.66, leg I: trochanter (tr) 0.25, femora (fe) 0.82, patella (pa) 0.41, tibia (ti) 0.54, metatarsus (mt) 0.74, tarsus (ta) 0.57. II: tr 0.23, fe 1.0, pa 148, ti 0.78, mt 0.83, ta 1.1. III: tr 0.28, fe 0.74, pa 0.37, ti 0.57, mt 0.73, ta 0.65. IV: tr 0.30, fe 0.97, pa 0.54, ti 0.85, mt 1.1, ta 0.7. Tarsal count: 3–6–4–4.

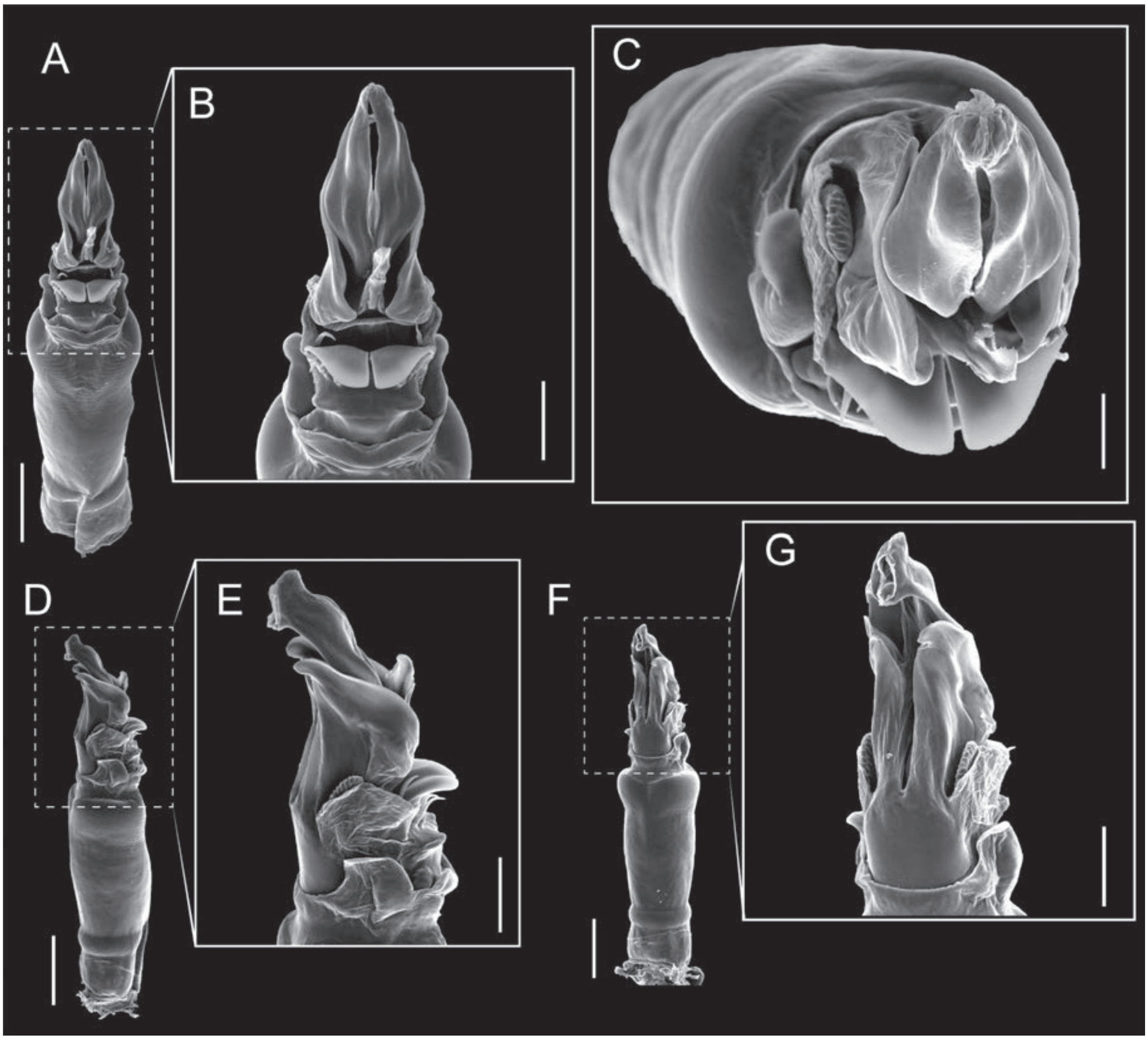

Figure 152. *Nerudiella wekufe* sp. nov. penis: ventral **A, B** apical **C** lateral **D, E** dorsal **F, G**. Scale bars: 200 µm (**A, D, F**); 100 µm (**B, E, G**); 50 µm (**C**).

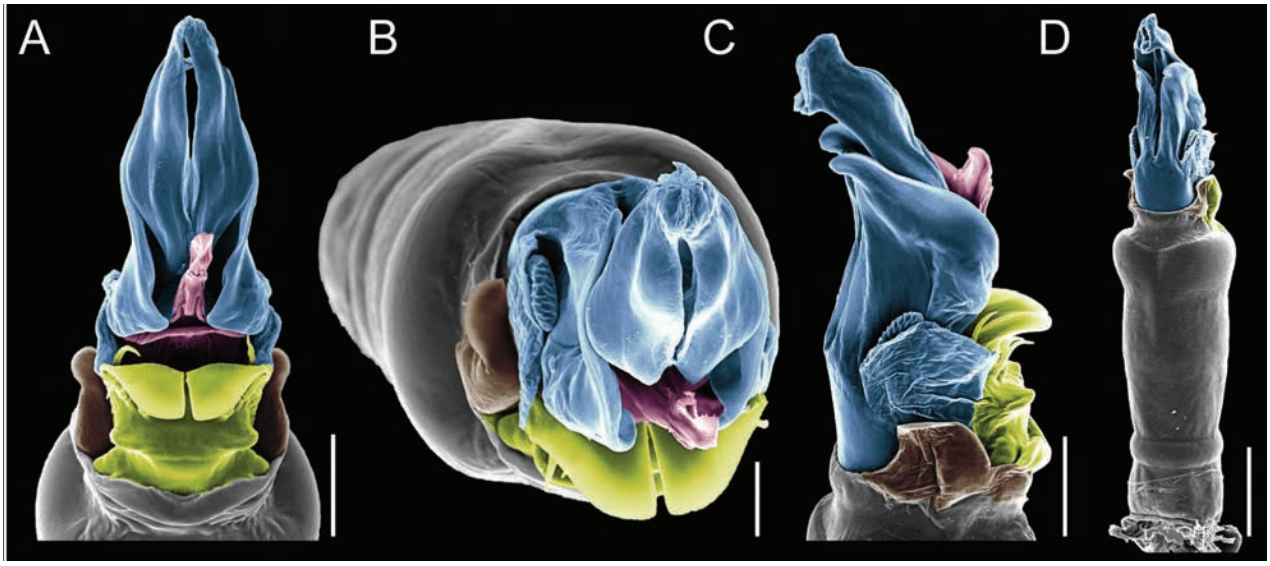

Figure 153. *Nerudiella wekufe* sp. nov. penis: ventral **A** apical **B** lateral **C** dorsal **D**. Colors: ventral plate (yellow), capsula externa (blue), capsula interna (red). Scale bars: 100 µm (**A, C**); 50 µm (**B**); 200 µm (**D**).

Nerudiella zapallar **sp. nov.**

https://zoobank.org/DBDA77EA-D4D0-4AF3-BB05-9B3292CC24C7
Figs 154–159

Material examined. ***Holotype*****.** ♂ **Chile.** Zapallar: E. Ross, A. Michelbacher coll. 27.XI.1950 (CAS).

Etymology. The specific epithet refers to the type locality of the species, the commune of Zapallar, located in the province of Petorca, Region of Valparaíso, Chile. Noun in apposition.

Diagnosis. This species can be distinguished from other species in the genus by a unique combination of features. The dorsal surface and pedipalps exhibit a dense population of setae. Additionally, the femoras and tibiae of the pedipalps are covered with small tubercles. In terms of male genitalia, it features a capsula externa that envelops the dorsal and lateral surfaces. A notable characteristic is the apical region of the capsula externa, which bends at a 90-degree angle in relation to the genitalia's axis. Moreover, two small parallel apical structures are also present. It is worth noting that this species shares some similarities with *Nerudiella choapa* sp. nov., especially in the apical region of the capsula externa. However, it is relatively larger in comparison.

Distribution. Chile: Valparaíso Region (Fig. 4F).

Description of male holotype. Measurements: Total length 2.39. Carapace length 0.94, Dorsal scutum length 1.88, Carapace max. width 1.2, Dorsal scutum max. width 1.8. Appendage measurements. Pedipalps. Trochanter length 0.26, femora length 0.82, patella length 0.43, tibia length 0.65, tarsus length 0.76. Leg I: trochanter (tr) 0.24, femora (fe) 0.85, patella (pa) 0.44, tibia (ti) 0.62, metatarsus (mt) 0.73, tarsus (ta) 0.55. II: tr 0.25, fe 1.27, pa 0.52, ti 0.85, mt 0.85, ta 0.95. III: tr 0.25, fe 0.72, pa 0.35, ti 0.64, mt 0.72, ta 0.57. IV: tr 0.24, fe 1.08, pa 0.52, ti 0.93, mt 1.09, ta 0.68.

Dorsum. (Fig. 154, 155). Eta (η) hourglass-shaped dorsal scutum. Ocularium low, rounded, with small tubercles. Dorsal scutum and free tergites microgranulate, mesotergal areas without clear separation but covered with small setiferous tubercles.

Chelicerae (Fig. 156A, B). Segment I with a sharp tubercle on the dorso-distal surface and three small proximal tubercles. Segment II bearing scattered setae in ectal and ventral views, with one triangular tubercle prominent from the others in front view.

Pedipalps (Fig. 156C, D). Trochanter with a small dorsal tubercle. Femora bearing the dorso-mesal area with setiferous spines, there are three proximal ones that are stronger than the others; in ventral view there are three strong proximal spines, and a row of small tubercles. Patella with a row of setiferous tubercles. Tibia with three ventral-ectal and two ventral-mesal spines, lateral and dorsal areas with small setiferous tubercles. Tarsus with three mesal and ectal spines with subdistal setae.

Legs (Fig. 157). Coxa I with 11–13 setiferous tubercles the two apical ones are stronger than the others, II with 25–30 setiferous tubercles, III with nine or ten tubercles, IV with six or seven small tubercles. Spiracles not obstructed by bridges. Smooth surface occupying ⅓ of leg II, ¾ of III, and < ⅓ of IV. Smooth area of leg II with two small tubercles with subdistal setae on each side. Ster-

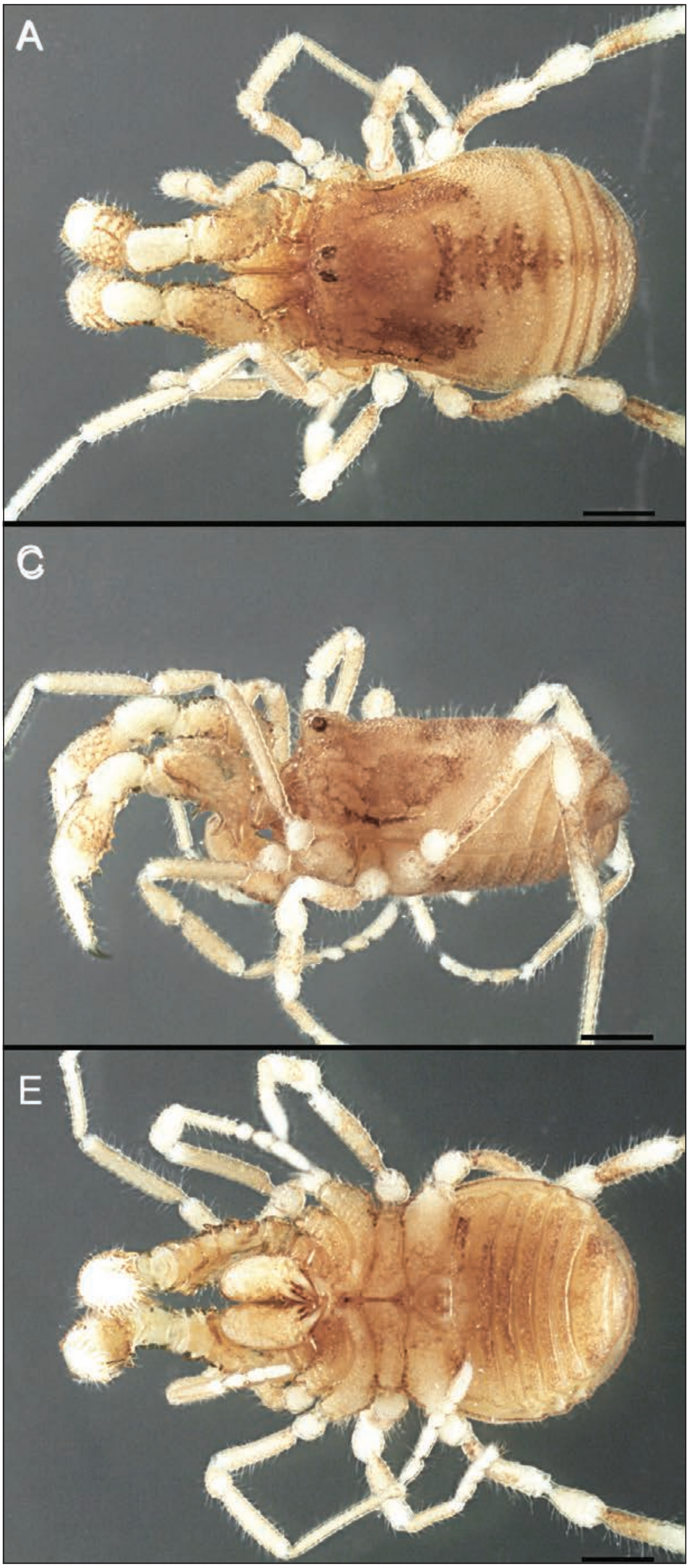

Figure 154. *Nerudiella zapallar* sp. nov. habitus, male **A** dorsal view **B** lateral view **C** ventral view. Scale bars: 1 mm.

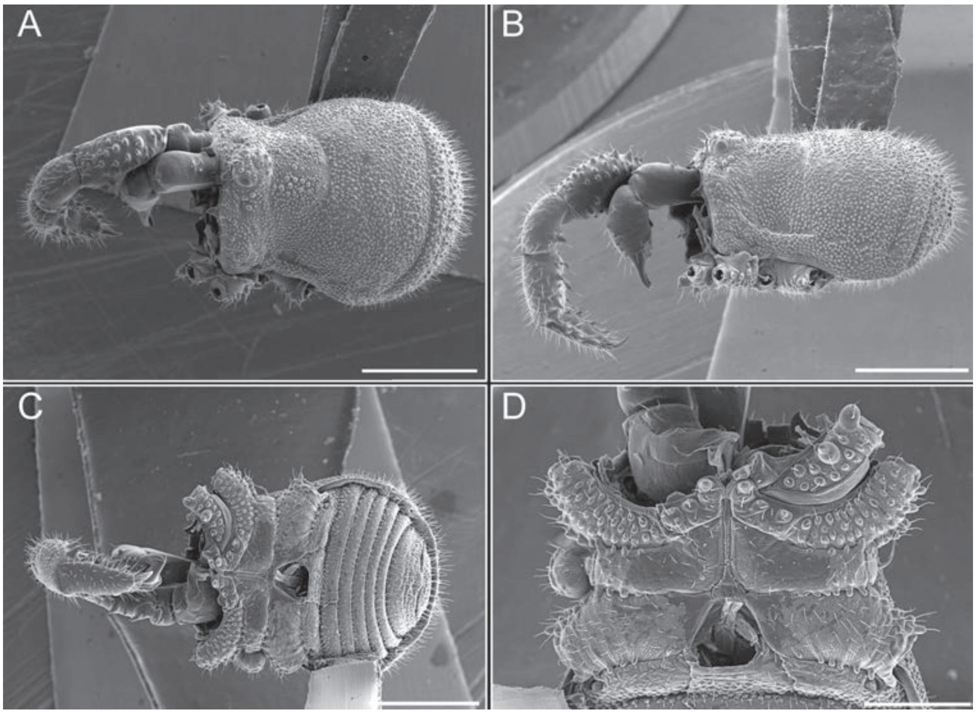

Figure 155. *Nerudiella zapallar* sp. nov. male, SEM images of habitus **A** dorsal view **B** lateral view **C, D** ventral view. Scale bars: 1 mm (**A, B, C**); 500 µm (**D**).

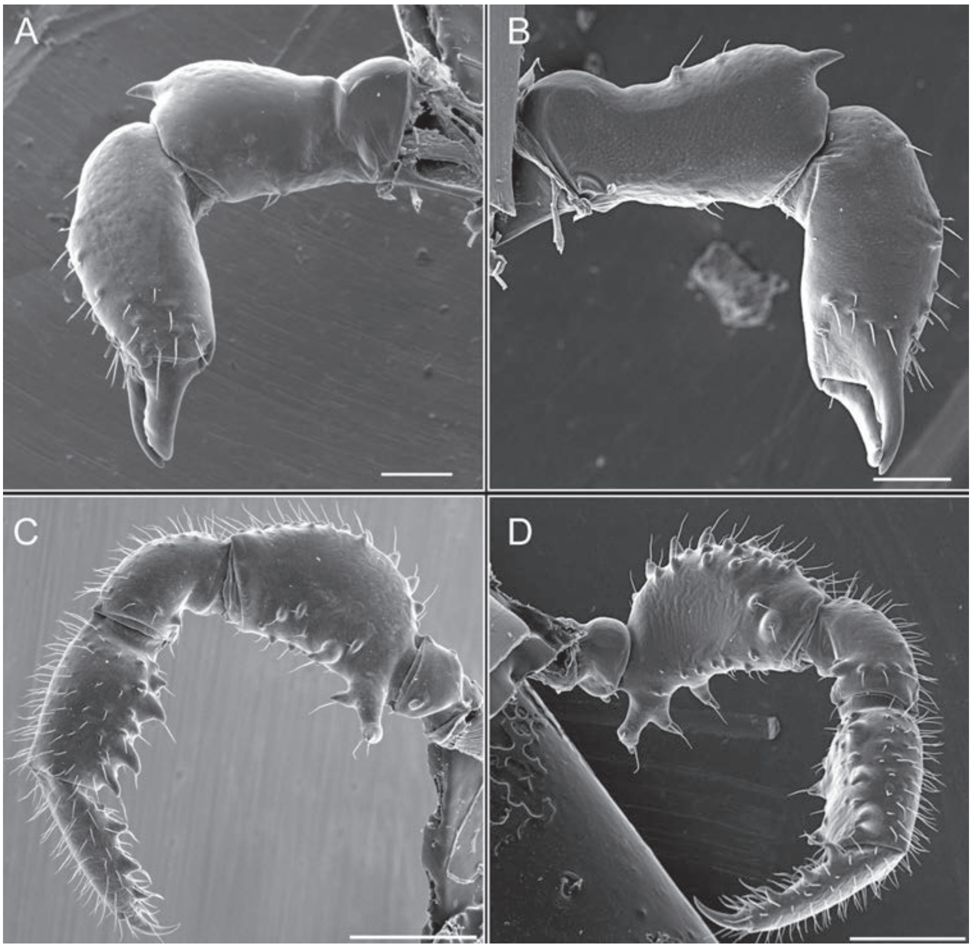

Figure 156. *Nerudiella zapallar* sp. nov. chelicerae: mesal **A** ectal **B** pedipalps: mesal **C** ectal **D**. Scale bars:200 µm.

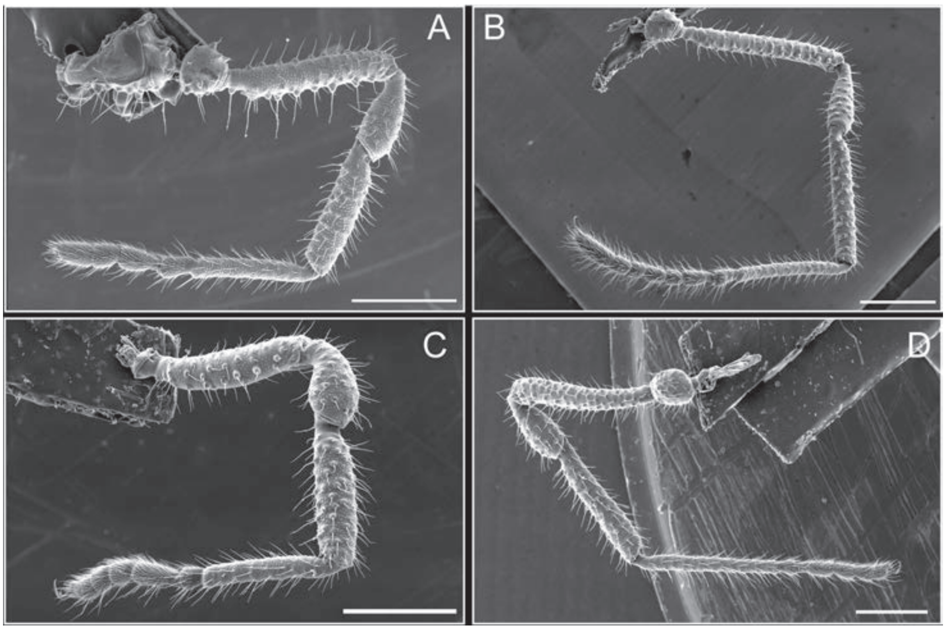

Figure 157. *Nerudiella zapallar* sp. nov. legs I **A** II **B** III **C** IV **D**. Scale bars: 200 µm (**A, C**); 500 µm (**B, D**).

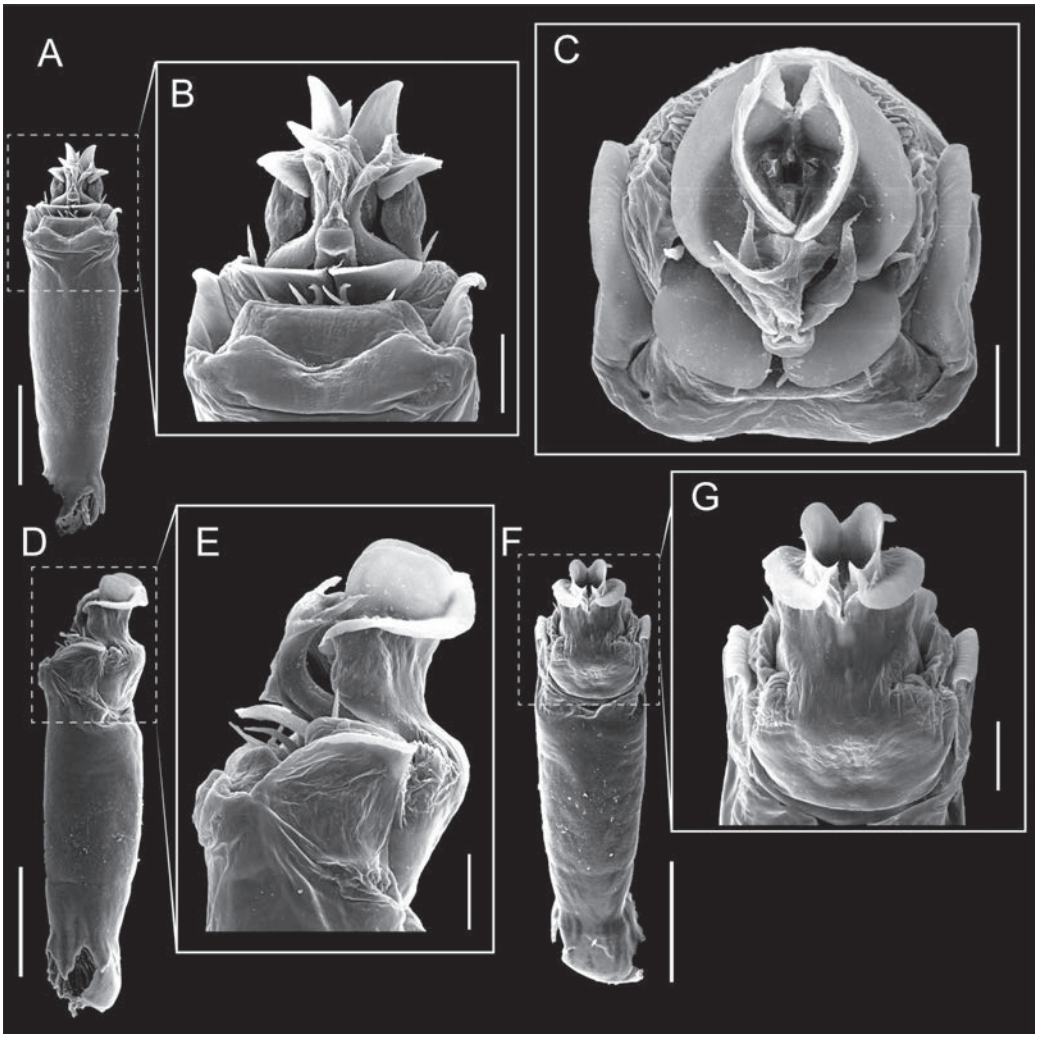

Figure 158. *Nerudiella zapallar* sp. nov. penis: ventral **A, B** apical **C** lateral **D, E** dorsal **F, G**. Scale bars: 200 µm (**A, D, F**); 50 µm (**B, C, E, G**).

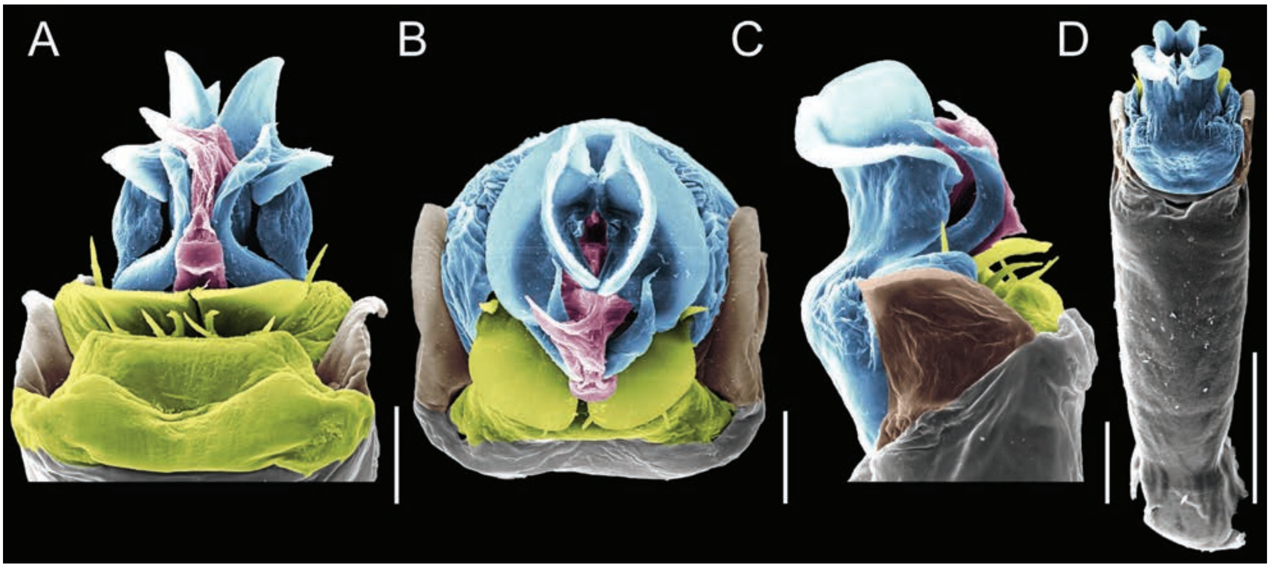

Figure 159. *Nerudiella zapallar* sp. nov. penis: ventral **A** apical **B** lateral **C** dorsal **D**. Colors: ventral plate (yellow), capsula externa (blue), capsula interna (red). Scale bars: 50 µm (**A–C**); 200 µm (**D**).

num arrow-shaped. Legs covered in small tubercles, astragalus longer than calcaneus on all legs. Tarsal count: 3–4/5–4–4.

Penis (Figs 158, 159). Pars distalis with a ventral plate bearing a fine cleft dividing the plate into two halves. Each half with three pointed macrosetae on the ventral surface and one macroseta on the dorsal surface; capsula externa covering the dorsal surface, with the apical part bent at an angle of 90 ° to the axis of the pars basalis of the genitalia, with a pair of long apical processes and a pair of long lateral processes; there is a dorsolateral plate attached to the pars basalis. Capsula externa taller than capsula interna. Capsula interna thin, with a sharp apical area.

Female. Unknown.

Acknowledgments

We thank the Corporación Nacional Forestal (CONAF) for granting collection permits. Jaime Pizarro Araya (Universidad de La Serena), Juan Enrique Barriga Tuñón (Universidad Católica del Maule) and Raúl Briones (Corporación Arauco) provided logistic support for collecting in Chile. Gustavo Hormiga, Facundo Labarque, Peter Michalik, Matías Izquierdo, Christian Wirkner and Katarina Huckstorf assisted with field work. We are also grateful to Fabián Tricarico for his assistance with SEM photographs taken at MACN, and to Ricardo Pinto-da-Rocha their valuable review of the manuscript. Willians Porto thanks the Ernst Mayr Travel Grant for the opportunity to review some of the material used in the phylogenetic analyses at the MCZ (Harvard University).

Additional information

Conflict of interest

The authors have declared that no competing interests exist.

Ethical statement

No ethical statement was reported.

Funding

This work was supported by Consejo Nacional de Investigaciones Científicas y Técnicas, Fondo para la Investigación Científica y Tecnológica, Argentina (projects PICT 2015 -2202, PICT-2019-2745), Museum of Comparative Zoology and Harvard University, U.S.A.

Author contributions

WLP and APG contributed to study conception and design. All authors contributed to data collection, interpretation of results, drafting the manuscript and editing the manuscript. All authors reviewed the results and approved the final version of the manuscript.

Author ORCIDs

Willians Porto https://orcid.org/0000-0002-4209-5664
Shahan Derkarabetian https://orcid.org/0000-0002-9163-9277
Gonzalo Giribet https://orcid.org/0000-0002-5467-8429
Abel Pérez-González https://orcid.org/0000-0002-4245-3302

Data availability

All of the data that support the findings of this study are available in the main text or Supplementary Information.

References

Acosta LE, Maury EA (1998) Opiliones. In: Morrone JJ, Coscarón S (Eds) Biodiversidad de artrópodos argentinos, una perspectiva biotaxonómica. La Plata, 569–580.

Acosta LE, Pérez-González A, Tourinho AL (2007) Methods for taxonomic study. In: Pinto-da-Rocha R, Machado G, Giribet G (Eds) Harvestmen: The Biology of Opiliones. Harvard University Press, Cambridge, 494–510.

Baker CM, Sheridan K, Derkarabetian S, Pérez-González A, Vélez S, Giribet G (2020) Molecular phylogeny and biogeography of the temperate Gondwanan family Triaenonychidae (Opiliones: Laniatores) reveals pre-Gondwanan regionalization, common vicariance, and rare dispersal. Invertebrate Systematics 34: 637–660. https://doi.org/10.1071/IS19069

Besch W (1969) South American Arachnida. In: Fittkau EJ, Illies J, Klinge H, Schwabe GH, Sioli H (Eds) Biogeography and Ecology in South-America. W. Junk, The Hague, 723–740.

Cekalovic T (1968) Conocimiento actual de los Opiliones chilenos. Noticiario Mensual. Museo Nacional de Historia Natural, Santiago 12: 5–11.

Cekalovic T (1985) Catálogo de los Opiliones de Chile (Arachnida). Boletín de la Sociedad de Biología de Concepción 56: 7–29.

Chernomor O, Von Haeseler A, Minh BQ (2016) Terrace Aware Data Structure for Phylogenomic Inference from Supermatrices. Systematic Biology 65(6): 997–1008. https://doi.org/10.1093/sysbio/syw037

Derkarabetian S, Baker CM, Giribet G (2021a) Complex patterns of Gondwanan biogeography revealed in a dispersal-limited arachnid. Journal of Biogeography 48(6): 1336–1352. https://doi.org/10.1111/jbi.14080

Derkarabetian S, Baker CM, Hedin M, Prieto CE, Giribet G (2021b) Phylogenomic re-evaluation of Triaenonychoidea (Opiliones: Laniatores), and systematics of

Triaenonychidae, including new families, genera and species. Invertebrate Systematics 35: 133–157. https://doi.org/10.1071/IS20047

Dunnington D, Thorne B, Hernangómez D (2023) ggspatial: Spatial Data Framework for ggplot2. https://cran.r-project.org/web/packages/ggspatial/index.html [October 3, 2023]

Edgar RC (2004) MUSCLE: Multiple sequence alignment with high accuracy and high throughput. Nucleic Acids Research 32(5): 1792–1797. https://doi.org/10.1093/nar/gkh340

Enderlein G (1909) Die Spinnen der Crozet-Inseln und von Kerguelen. In: von Drygalski E (Ed.) Deutsche Südpolar-Expedition 1901–1903. Druck und Verlag von Georg Reimer, Berlin, 535–540.

Folmer O, Black M, Hoeh W, Lutz R, Vrijenhoek R (1994) DNA primers for amplification of mitochondrial cytochrome c oxidase subunit I from diverse metazoan invertebrates. Molecular Marine Biology and Biotechnology 3: 294–299.

Forster RR (1954) The New Zealand harvestmen (sub-order Laniatores). Canterbury Museum bulletin 2: 1–329.

Forster RR (1965) Harvestmen of the sub-order Laniatores from New Zealand Caves. Records of the Otago Museum 2: 1–18.

Giribet G, Kury AB (2007) Phylogeny and Biogeography. In: Pinto-Da-Rocha AB, Machado G, Giribet G (Eds) Harvestmen: The Biology of Opiliones. Harvard University Press, Cambridge, 62–87. https://doi.org/10.2307/j.ctv322v442.7

Giribet G, Carranza S, Baguna J, Riutort M, Ribera C (1996) First molecular evidence for the existence of a Tardigrada + Arthropoda clade. Molecular Biology and Evolution 13(1): 76–84. https://doi.org/10.1093/oxfordjournals.molbev.a025573

Hickman VV (1939) Opiliones and Araneae. British and New Zealand Antarctic research Expedition 1929–1931 u. command of D. Mawson. Reports - Series B (Zoology and Botany). In: Johnston H (Ed.) Rpts. Br. a. New Zealand Antarctic Research Expedition 1929–1931 4: 159–187.

Hoang DT, Chernomor O, von Haeseler A, Minh BQ, Vinh LS (2018) UFBoot2: Improving the Ultrafast Bootstrap Approximation. Molecular biology and evolution. Molecular Biology and Evolution 35(2): 518–522. https://doi.org/10.1093/molbev/msx281

Kalyaanamoorthy S, Minh BQ, Wong TKF, Von Haeseler A, Jermiin LS (2017) ModelFinder: Fast model selection for accurate phylogenetic estimates. Nature Methods 14(6): 587–589. https://doi.org/10.1038/nmeth.4285

Kassambara A (2023) ggpubr: “ggplot2” Based Publication Ready Plots. https://cran.r-project.org/web/packages/ggpubr/index.html [October 3, 2023]

Kishino H, Hasegawa M (1989) Evaluation of the maximum likelihood estimate of the evolutionary tree topologies from DNA sequence data, and the branching order in hominoidea. Journal of Molecular Evolution 29(2): 170–179. https://doi.org/10.1007/BF02100115

Kishino H, Miyata T, Hasegawa M (1990) Maximum likelihood inference of protein phylogeny and the origin of chloroplasts. Journal of Molecular Evolution 31(2): 151–160. https://doi.org/10.1007/BF02109483

Kumar S, Stecher G, Li M, Knyaz C, Tamura K (2018) MEGA X: Molecular Evolutionary Genetics Analysis across Computing Platforms. Molecular Biology and Evolution 35(6): 1547–1549. https://doi.org/10.1093/molbev/msy096

Kury A (2003) Annotated catalogue of the Laniatores of the New World (Arachnida, Opiliones). Revista Ibérica de Aracnología espec: 325.

Kury AB (2007) Triaenonychidae Sørensen, 1886. In: Pinto-da-Rocha R, Machado G, Giribet G (Eds) Harvestmen: The Biology of Opiliones. Harvard University Press, Cambridge, MA, USA, 239–243.

Kury AB, Medrano M (2016) Review of terminology for the outline of dorsal scutum in Laniatores (Arachnida, Opiliones). Zootaxa 4097(1): 130–134. https://doi.org/10.11646/zootaxa.4097.1.9

Kury A, Mendes AC, Souza D (2014) World Checklist of Opiliones species (Arachnida). Part 1: Laniatores – Travunioidea and Triaenonychoidea. Biodiversity Data Journal 2: e4094. https://doi.org/10.3897/BDJ.2.e4094

Kury AB, Mendes AC, Cardoso L, Kury MS, Granado AA, Giribet G, Cruz-López JA, Longhorn SJ, Medrano M, Oliveira ABR, Kury IS, Souza-Kury MA (2022) WCO: World Catalogue of Opiliones. http://wcolite.com/ [December 2, 2023]

Loman JCC (1902) Neue Aussereuropäische Opilioniden. Zoologische Jahrbücher, Jena. Abteilung für Systematik, Ökologie und Geographie der Tiere 16: 163–216. https://doi.org/10.5962/bhl.part.17151

Maury EA (1990) Triaenonychidae sudamericanos.VI. Tres nuevas especies del género *Nuncia* Loman 1902 (Opiliones, Laniatores). Boletin de la Sociedad de Biologia de Concepción 61: 103–119.

Maury EA (1992) Lista de los ejemplares típicos de “Arachnida” (Opiliones, Scorpiones y Solifugae) depositados en el Museo Argentino de Ciencias Naturales “Bernardino Rivadavia” Suplemento I. Aracanología 6: 1–10.

Mendes AC, Kury AB (2008) Intercontinental Triaenonychidae—The case of *Ceratomontia* (Opiliones, Insidiatores). The Journal of Arachnology 36(2): 273–279. https://doi.org/10.1636/CH07-93.1

Mendes AC, Kury AB (2012) Notes on the systematics of the Triaenonychinae from Madagascar with description of a new species of *Acumontia* Loman (Opiliones: Laniatores). Zootaxa 3593(1): 40. https://doi.org/10.11646/zootaxa.3593.1.2

Muñoz-Cuevas A (1971a) Contribution à la conaissance de la famille des Triaenonychidae du Chili (Opilions Laniatores). Bulletin du Muséum National d’Histoire Naturelle 2: 872–880.

Muñoz-Cuevas A (1971b) Redescription de *Nuncia americana* Roewer et étude de sa morphologie génitale (Opiliones: Laniatores: Triaenonychidae). Seckenbergiana biol. 52: 97–101.

Murphree CS (1988) Morphology of the Dorsal Integument of Ten Opilionid Species (Arachnida, Opiliones). The Journal of Arachnology 16: 237–252.

Nguyen L-T, Schmidt HA, Von Haeseler A, Minh BQ (2015) IQ-TREE: A Fast and Effective Stochastic Algorithm for Estimating Maximum-Likelihood Phylogenies. Molecular Biology and Evolution 32(1): 268–274. https://doi.org/10.1093/molbev/msu300

Olson DM, Dinerstein E, Wikramanayake ED, Burgess ND, Powell GVN, Underwood EC, D’amico JA, Itoua I, Strand HE, Morrison JC, Loucks CJ, Allnutt TF, Ricketts TH, Kura Y, Lamoreux JF, Wettengel WW, Hedao P, Kassem KR (2001) Terrestrial Ecoregions of the World: A New Map of Life on Earth: A new global map of terrestrial ecoregions provides an innovative tool for conserving biodiversity. Bioscience 51(11): 933–938. https://doi.org/10.1641/0006-3568(2001)051[0933:TEOTWA]2.0.CO;2

Pebesma E (2018) Simple Features for R: Standardized Support for Spatial Vector Data. The R Journal 10(1): 439–446. https://doi.org/10.32614/RJ-2018-009

Pebesma E, Bivand R (2023) Spatial Data Science: With applications in R. Chapman and Hall/CRC. 1st edn., 314 pp. https://doi.org/10.1201/9780429459016

Pérez-González A, Werneck RM (2018) A fresh look over the genital morphology of Triaenonychoides (Opiliones: Laniatores: Triaenonychidae) unravelling for the first time the functional morphology of male genitalia. Zoologischer Anzeiger 272: 81–92. https://doi.org/10.1016/j.jcz.2017.12.010

Pérez-Schultheiss J, Urra F, Otárola A (2019) Opiliones Laniatores (Arachnida) de la Cordillera de Nahuelbuta: un desconocido hotspot de diversidad. Boletín Nahuelbuta Natural, 24 pp.

Pérez-Schultheiss J, Urra F, Oyarzún C (2021) Opiliones Laniatores (Arachnida) de Manquemapu, cordillera de la costa de Purranque, Región de Los Lagos, Chile. Revista Chilena de Entomologia 47(2): 405–432. https://doi.org/10.35249/rche.47.2.21.25

Porto W, Pérez-González A (2019) Redescription of the New Zealand harvestman *Nuncia obesa obesa* (Opiliones: Laniatores: Triaenonychidae) and implications for the supposed transcontinental distribution of *Nuncia*. The Journal of Arachnology 47(3): 370–376. https://doi.org/10.1636/0161-8202-47.3.370

Porto W, Pérez-González A (2020) Redescription of *Promecostethus unifalculatus*, the only known harvestman from Crozet Islands (Opiliones: Triaenonychidae). Zootaxa 4861(1): 120–130. https://doi.org/10.11646/zootaxa.4861.1.8

Porto W, Derkarabetian S, Ramírez MJ, Giribet G, Pérez-González A (2022) Notes on South American triaenonychids, with the description of a new genus from Chile (Opiliones: Laniatores: Triaenonychidae). Invertebrate Systematics 36(8): 681–713. https://doi.org/10.1071/IS21080

R Core Team (2022) R: The R Project for Statistical Computing. https://www.r-project.org/ [October 3, 2023]

Roewer C-F (1914) Opilioniden von Neu-Caledonien. In: Sarasin F, Roux J (Ed.) Nova Caledonia Forschungen in Neu-Caledonien und auf den Loyalty-Inseln. Wiesbaden, 439–443.

Roewer C-F (1915) Die Familie der Triaenonychidae der Opiliones - Laniatores. Archiv für Naturgeschichte 80: 61–168.

Roewer C-F (1961) Opiliones aus Süd-Chile. Senckenbergiana Biologica 42: 99–105.

Schwendinger PJ, Giribet G (2005) The systematics of the south-east Asian genus *Fangensis* Rambla (Opiliones: Cyphophthalmi: Stylocellidae). Invertebrate Systematics 19(4): 297–323. https://doi.org/10.1071/IS05023

Shimodaira H (2002) An Approximately Unbiased Test of Phylogenetic Tree Selection. Systematic Biology 51(3): 492–508. https://doi.org/10.1080/10635150290069913

Simon E (1899) Ergebnisse einer Reise nach dem Pacific (Schauinsland 1896–1897). Arachnoiden. Zoologische Jahrbücher, Jena. Abteilung für Systematik, Ökologie und Geographie der Tiere 12: 411–437. https://doi.org/10.5962/bhl.part.2034

Soares HEM (1968) Contribuição ao estudo dos opiliões do Chile (Opiliones: Gonyleptidae, Triaenonychidae). Papéis Avulsos de Zoologia 21(1–28)[1967-1968]: 259–272. https://doi.org/10.11606/0031-1049.1968.21.p259-272

Strimmer K, Rambaut A (2002) Inferring confidence sets of possibly misspecified gene trees. Proceedings. Biological Sciences 269(1487): 137–142. https://doi.org/10.1098/rspb.2001.1862

Vaidya G, Lohman DJ, Meier R (2011) Cladistics multi-gene datasets with character set and codon information. Cladistics 27: 171–180. https://doi.org/10.1111/j.1096-0031.2010.00329.x

Whiting MF, Carpenter JC, Wheeler QD, Wheeler WC (1997) The Strepsiptera problem: Phylogeny of the holometabolous insect orders inferred from 18S and 28S ribosomal DNA sequences and morphology. Systematic Biology 46(1): 1–68. https://doi.org/10.1093/sysbio/46.1.1

Wickham H (2016) ggplot2. Springer International Publishing, Cham. https://doi.org/10.1007/978-3-319-24277-4

Supplementary material 1

Collection information and GenBank accession numbers

Authors: Willians Porto, Shahan Derkarabetian, Gonzalo Giribet, Abel Pérez-González
Data type: docx
Explanation note: Collection information and GenBank accession numbers for specimens used in this study (focus group in red).

Link: https://doi.org/10.3897/zookeys.1207.120068.suppl1

Supplementary material 2

Complete IQ-TREE results

Authors: Willians Porto, Shahan Derkarabetian, Gonzalo Giribet, Abel Pérez-González
Data type: jpg
Explanation note: Results obtained from IQ-TREE, with the SH-aLRT and UFBoot supports indicated at the nodes. The red branches in the illustration represents South American species.

Link: https://doi.org/10.3897/zookeys.1207.120068.suppl2

ZooKeys 1207: 151–165 (2024)
DOI: 10.3897/zookeys.1207.119398

Review Article

Taxonomic considerations of selected Western Palaearctic Mordellidae Latreille, 1802 (Coleoptera, Tenebrionoidea)

Enrico Ruzzier[1,2], Andrea Di Giulio[1,2]

1 *Department of Science, Università Roma Tre, viale G. Marconi 446, 00146 Rome, Italy*
2 *National Biodiversity Future Center (NBFC), 90133 Palermo, Italy*
Corresponding author: Enrico Ruzzier (enrico.ruzzier@uniroma3.it)

Abstract

The present contribution is devoted to the review of some species of Mordellidae belonging to the Italian fauna described by Mariano Zuccarello Patti and Mario Enrico Franciscolo. New taxonomic combinations are proposed: *Mediimorda argyropleura* (Franciscolo, 1942), **comb. nov.**, *Mordella quomoi* Franciscolo, 1942, **comb. rev.**, and *Mordellokoiles grandii* Franciscolo, 1942, **stat. nov.** *Mediimorda argyropleura*, *Mordella quomoi* and *Mordellokoiles grandii* are considered species that are not part of the Italian fauna. In addition, given the impossibility of identifying the species based on its original description and the destruction of type material, *Mordella aradasiana* Patti, 1840 is treated as *nomen dubium*.

Key words: Biodiversity, faunistic, Italy, synonymy

Academic editor: Patrice Bouchard
Received: 23 January 2024
Accepted: 12 June 2024
Published: 12 July 2024

ZooBank: https://zoobank.org/17E116C2-DC4E-4DCB-8910-2D8B939EE446

Citation: Ruzzier E, Di Giulio A (2024) Taxonomic considerations of selected Western Palaearctic Mordellidae Latreille, 1802 (Coleoptera, Tenebrionoidea). ZooKeys 1207: 151–165. https://doi.org/10.3897/zookeys.1207.119398

Introduction

Mordellidae Latreille, 1802, also commonly known as tumbling flower beetles, are members of the rather diverse beetle family that comprises more than 2000 extant species worldwide. This group is notoriously taxonomically complicated due to the great uniformity of species and the fact that some characters have not always been consistently and uniquely applied; this is particularly true for the Western Palaearctic, and Europe in particular, where the great richness in sibling and cryptic species has resulted in high taxonomic productivity as well as increasing difficulty in recognizing species (e.g. Emery 1876; Schilsky 1895; Ermisch 1956, 1962, 1963a, 1963b, 1963c, 1965, 1966, 1969a, 1969b, 1969c, 1977). Therefore, reviewing type material and solving nomenclatural issues (e.g. Kaszab 1979; Horák 1990; Leblanc 2007; Selnekovič and Kodada 2019, Selnekovič and Improta 2020), as well as clarifying the distribution of some species (e.g. Batten 1976a, 1976b; Borowiec 1996; Horák et al. 2012; Ruzzier et al. 2017; Selnekovič and Ruzzier 2019) are essential in this context.

The purpose of this contribution is to review some mordellid taxa described by Mariano Zuccarello Patti and Mario Enrico Franciscolo in order to clarify the identity and assess status of these taxa.

Material and methods

All the material considered in this contribution belongs to the collections of the Museo Civico di Storia Naturale "G. Doria", Genoa, Italy (MSNG).

Measurements are abbreviated in the text as follows: EL, elytral length from scutellar apex to elytral apices along suture; EW, maximum elytral width at humeri; HL, head length from anterior clypeal margin to occipital carina along midline; HpygL, maximum hypopygidial length; HW, maximum head width; PL, pronotal length along midline; PW, maximum pronotal width; PygL, maximum pygidial length; TL, sum of head, pronotal, elytral, and pygidial lengths. Wing venation terminology follows that of Lawrence et al. (2021, 2022).

The morphological study was carried out using an Olympus SZX 16 stereomicroscope. Images were taken with a Visionary Digital LK Lab System (Visionary Digital, Palmyra, VA, USA) equipped with a Canon EOS 6D mark II dSLR camera and an MP-E 65mm f/2.8 1–5× lens (Canon, Tokyo, Japan). Stack images were produced using Helicon Focus v. 7.

Taxonomic treatment

Tribe Mordellini Latreille, 1802

Mediimorda argyropleura (Franciscolo, 1942b), comb. nov.

Mordella argyropleura Franciscolo, 1942b: 18.
Mordella argyropleura: Franciscolo 1949: 52.
Variimorda (*Variimorda*) *argyropleura*: Franciscolo 1995: 11; Horák 2020: 86.
Falsopseudotomoxia argyropleura: Ruzzier 2013: 104.

Material. ***Holotype***, male, labeled "Isola di Capraia, Toscana, S. Rocco, C. Mancini, Giglio, VI.1930 // Olo-Typus // *Mordella argyropleura* n. sp. (handwritten)" (MSNG) (Fig. 1).

Conservation state: state of preservation discreet, left antenna broken, partially missing. The left paramere is damaged and missing the long external branch.

Additional material. 12 exx labeled "Somalia IT. Jach Sciumo (Giuba): 1923, S. Patrizi lg. // *Mediimorda argyropleura* E. Ruzzier det. 2024" (MSNG).

Comments. *Mordella argyropleura* was known to this day exclusively by its type material (Franciscolo 1942b) and the few specimens mentioned in the 1949 contribution (Franciscolo 1949; Ruzzier 2013). The opportunity to review further material in the Genoa Museum's collection, including the former Franciscolo collection, allowed us to identify additional specimens belonging to this "seemingly elusive" species. Interestingly, all the additional specimens studied originated from Somalia, at that time an Italian colony, and collected by Saverio Patrizi (Latella 2009).

Given this latest finding and given the fact that the type of *M. argyropleura* appears to be prepared on the same kind of paper board as the Somali specimens, we consider the locality of the species described by Franciscolo to be the result of a labeling error, and, therefore, *M. argyropleura* should be excluded from the Italian fauna.

Figure 1. *Mordella argyropleura* Franciscolo, 1942, holotype.

Having already had the opportunity to review the type material of *M. argyropleura* (Fig. 1), and after careful consideration based on the comparison of the shape of the paramera (Fig. 2), the general body shape, short antennae, glabrous eyes, presence of a longitudinal dorsal comb on hind tibiae, and small, subtrapezoidal scutellum, we propose *Mediimorda argyropleura* (Franciscolo, 1942b), comb. nov.

The assignment of *Mordella argyropleura* to *Falsopseudotomoxia* Ermisch, 1954 by Ruzzier (2013) is attributable to the need for a redescription and redefinition of *Mediimorda* Méquignon, 1946 and *Falsopseudotomoxia* Ermisch 1954 as possible synonyms and not vicariant genera in the Western Palaearctic and Afrotropical regions. The re-establishment of the taxonomic combination *Variimorda* (*Variimorda*) *argyropleura* (Franciscolo, 1942) by Horák (2020) is to be regarded as an oversight during the process of updating the Palaearctic catalog.

Mordella aradasiana Patti, 1840 *nomen dubium*

Mordella aradasiana Patti, 1840: 292.

Comments. The identity of *M. aradasiana* remains, and will remain, unsolved. The species was described in 1840 by Sicilian amateur naturalist Mariano Zuccarello Patti based on a single specimen he collected in the locality “Praja” (eastern coast of Sicily, between Catania and Agnone Bagni) (Patti 1840). The description, given its year, is rather simple and mostly based on color,

Figure 2. *Mediimorda argyropleura* (Franciscolo, 1942). Holotype of *Mordella argyropleura* Franciscolo, 1942 **A** right paramere and **A'** left paramere; male specimen from Jach Sciumo (Giuba, Somalia) **B** right paramere and **B'** left paramere; male specimen from southern Italy (localities given by Franciscolo 1949, image modified from Ruzzier 2013) **C** right paramere and **C'** left paramere. Scale bar: 0.2 mm.

and the attribution to Mordellidae and the genus *Mordella* Linnaeus, 1758 (the only one uniformly recognized at the time) by the author, who had very little entomological expertise, was made solely because of the presence of an acuminate pygidium.

Based on the scant information provided (e.g., the size and color pattern), it is impossible to assign the species to any Italian and, more generally, circum-Mediterranean mordellid species; in addition, some of the characters provided in the description, such as the occipital part of the head partially covering the pronotum and the elytra not completely covering the wings underneath, would seem to suggest a taxon belonging to *Macrosiagon* Hentz, 1830 (Ripiphoridae Gemminger, 1870), the female of *Macrosiagon meridionalis* (Costa, 1859) in particular. Unfortunately, some of the chromatic elements, such as the red spots on the elytra, a character not observed in any Italian *Macrosiagon*, do not allow us to attribute *M. aradasiana* to the latter taxon with certainty.

The quality of the descriptions, as well as the validity of the species described by Patti, have already been widely criticized and in many cases disavowed by several authors (e.g., Ragusa 1883, 1904, 1924; Luigioni 1929), confirming the uncertainty and impossibility of identifying a species often described as "fictional" (Romano 2006).

It is also exceedingly important to note that the type of *M. aradasiana*, like the entire Patti collection inclusive of other taxa he described, was lost or destroyed (Romano 2006).

Mordella quomoi Franciscolo, 1942, comb. rev.

Mordella quomoi Franciscolo, 1942a: 7.
Mordella cuomoi Franciscolo, 1942b: 22 (subsequent unjustified emendation).
Variimorda (*Variimorda*) *quomoi*: Horák 1985: 11; Ruzzier 2013: 106; Horák 2020: 87.
Variimorda (*Variimorda*) *quomoi* (Franciscolo, 1951 [sic!]): Franciscolo 1995: 11.

Material. ***Holotype*** (by monotypy), male, labeled "Is. Giglio, II.1902. G. Doria // Typus // Mordella Quomoi Franciscolo (handwritten)// Mordella quomoi Francisc. det. M.E. Franciscolo" (MSNG) (Fig. 3A).

Conservation state: modest, antennae and anterior tarsomeres broken, partially missing.

Redescription. ***Measurements.*** HL: 1.0 mm; HW: 1.5 mm; PL: 1.3 mm; PW: 1.9 mm; EL: 3.3 mm; EW: 1.8 mm; PygL: 1.6 mm; HpygL 0.8 mm; TL: 7.2 mm.

Color. General color of the integument dark brown to black, except for the epistoma, mouthparts, palps, and anterior and middle legs which are orange-amber colored (Fig 3B, C). Head uniformly covered with golden recumbent setation. Pronotum on disc covered with recumbent, posteriorly oriented, dark-brown setae; margins and the posterior lobe of the pronotum covered with golden setation as on the head. Scutellum bearing pale-yellowish setae. Elytron covered with dark-brown, recumbent setae as on pronotum, except for a band of yellowish setae, which, starting from the scutellum and following the anterior margin of the elytron, delimits the elytral callus and converges toward the elytral suture, forming a semicircular pattern; in addition, the elytron presents a sub-squared patch of yellowish setae at about three-quarters of its length, close to the elytral suture. Meso and metathoracic ventrites, as well as the basal part of all abdominal ventrites, covered with recumbent, yellowish setae.

Head. Head transverse in dorsal view (1.6× as wide as long), sub-hemispheric in lateral view with the highest point in correspondence to the occiput (3B); occipital margin almost straight in dorsal view (Fig. 3D); integument nearly smooth but densely covered with setigerous punctures. Eyes large, setose, and finely facetted, almost circular in lateral view, extending anteriorly to the antennal insertion and posteriorly to the occiput. Anterior margin of the epistoma straight; exposed part of exposed part of labrum transverse, gently curved at the anterior margin, setose. Maxillary palpus of the *Mordella*-type (*sensu* Franciscolo 1957) (Fig. 4A); first maxillary palpomere flattened, club-shaped, and about 4× its maximum width; second maxillary palpomere short, subconical, 1.7× as long as its maximum width; apical (third) maxillary palpomere securiform, scalene triangular, 2.1× as long as its maximum width, outer margin of the segment (the longest) feebly sinuate. Antennomeres 1–4 subcylindrical, short; antennomeres 1 and 2 stouter than the following two. Antennomeres 6–10 1.9–2.0× longer than wide (the fifth is missing); apical antennomere asymmetrically ellipsoid, 2.6× as long as wide (Fig. 3B).

Prothorax. Pronotum trapezoid in dorsal view, 1.4× as wide as long, widest slightly before middle, moderately convex in lateral view; pronotal disc microreticulate, densely covered with recumbent and posteriorly oriented setae, punctures larger and more impressed than those on head. Anterior margin of the pronotum gently and gradually curved, and the anterior angles curved downward,

Figure 3. *Mordella quomoi* Franciscolo, 1942, holotype **A** original labels **B** dorsal habitus **C** lateral left view **D** detail of head and pronotum in dorsal view. Scale bar: 2.0 mm.

resulting in not being visible in dorsal view. Central lobe of the posterior margin of the pronotum markedly protruding posteriad. Anterior and posterior angles of the pronotum obtuse in lateral view; lateral margins of pronotum gently curved in dorsal view, and straight in lateral view. Profemora and protibia gently but markedly curved dorso-ventrally; tarsomeres subcylindrical, truncate at apex.

Pterothorax. Scutellum triangular, with a broadly rounded apex; integument finely punctured and covered with dense and extremely thin setae.

Elytra subconical in dorsal view, external margins feebly but distinctly curving from the elytral humeri towards the apices; elytra apices rounded, not converging at the suture. Elytra strongly and densely punctate; each puncture bears a spiniform seta, especially on the elytral disc.

Metepisterna of the *Mordellistena*-type (*sensu* Franciscolo 1957), triangular, 2.1× as long as their maximum width; sutures between Metepisterna and metaventrite marked and straight. Coxae (coxal plates) semicircular, 2.1× as wide as their maximum length. Metepisterna, metaventrite, and coxae on their dorsal two-thirds densely covered with setigerous punctures like those on pronotum and elytra. Mesofemora laterally compressed; mesotibia cylindrical and feebly curved; mesotibia as long as the mesotarsus. Metafemora straight, laterally compressed; metatibiae conical, transversely truncate at apex; subapical comb present, short and running parallel to the apical margin of the tibia; dorsal

Figure 4. *Mordella quomoi* Franciscolo, 1942, holotype **A** right maxillary palpus **B** left antennomeres 6–10 **C** 8th sternite **D** paramera, (*R*) right and (*L*) left.

side of metatibia bearing a series of sparsely arranged spines that vaguely resemble a longitudinal comb; metatarsomeres devoid of combs or arranged spinulations. Metatibial spurs slightly asymmetrical with the inner 1.1× as long as the outer.

***Abdomen*.** Abdomen conical, tapered in both lateral and dorsal view; abdominal ventrite 1 longer than ventrites 2 to 4, and 1.25× as long as hypopygidium. Pygidium conical in dorsal view, 2.5× longer than wide at the base; in lateral view the pygidium is conical, slightly bending downward towards the base, 2.4× as long as hypopygidium. Sternite 8 strongly produced in the middle of the posterior edge, 1.7× longer than wide at the base, posterior margin bearing long setae (Fig. 3C).

Paramera asymmetric, of the *Mordella*-type (*sensu* Franciscolo 1957) (Fig. 4D). Right paramere U-shaped, dorsal process longer than the ventral, straight, lanceolate and only weakly sclerotized; ventral process short, strongly sclerotized and pointed at apex, presenting a dentiform process on its internal margin. Left paramere stout, claviform, strongly sclerotized, presenting a pointed straight process at the distal apex.

Comments. The species was originally described as *Mordella* based on a single male specimen, but its diagnosis was based exclusively on its external features, color pattern especially (Franciscolo 1942a). Franciscolo named this new taxon after his high-school teacher Maria Enrichetta Cuomo Ulloa (Franciscolo 1942a, 1942b).

In the same year, Franciscolo renamed the taxon *Mordella cuomoi* (Franciscolo 1942b), whose nomenclatural act constitutes in all respects a subsequent unjustified emendation in accordance with Article 33 of the International Code of Zoological Nomenclature (ICZN 1999). The species was then transferred to *Variimorda* Méquignon, 1946 as *Variimorda* (*Variimorda*) *quomoi* by Horák (1985), without taking into account the nomenclature act (despite being incorrect) proposed by Franciscolo 1942; the fact that Horák referred to the holotype as female, when it is clearly male, suggests that the transfer to *Variimorda* was made solely on the basis of the chromatic pattern. Particularly unusual is the assignment by Franciscolo of *M. quomoi* to *Variimorda* in his checklist of the Italian fauna (Franciscolo 1995); the move to another genus is completely unjustified, given the total lack of footnotes or references in the publication, and completely ignoring the taxonomic change proposed by the same author as many as 50 years earlier. Franciscolo then, without referring to the taxonomic change that had already occurred in Horák (1985), proposed "his" combination *V.* (*V.*) *quomoi*, but mistaking its year of description (1951 instead of 1942). The combination *Variimorda* (*Variimorda*) *quomoi* (Franciscolo, 1942) (*sensu* Horák 1985) was then maintained in the few subsequent references mentioning the taxon (Horák 2008; Ruzzier 2013; Horák 2020). Since the species was originally named after a woman, the correct spelling of the specific epithet should have been "*quomoae*" (feminine) instead of "*quomoi*" (masculine); however, we opt to retain the masculine form to maintain consistency with previous literature.

It is important to point out that the species, since its description, has not been found again despite major sampling efforts (E. Ruzzier pers. comm.), and its real identity has remained somewhat uncertain until now.

The possibility of studying the holotype finally allowed us to produce these considerations: 1) the species has to be treated in its original combination since it does not possess those morphological features typical of *Variimorda*, namely antennal dilatation starting from antennomere 5 (antennal dilatation starting from antennomere 4 in *Variimorda*) and left paramere of the *Mordella*-type, short and claviform (knobbed on the inner margin and provided with a well-developed distal membranous process in *Variimorda*); 2) the species does not belong to the Italian fauna, and the locality is most likely the result of a labeling error. This interpretation is supported by the fact that the original specimen label gives February as the month of collection; winter in Italy does not present the climatic conditions to allow the survival of the adults nor favor the presence of flowering plants that could support its survival. In addition, the fact that the species has not been found again in the *locus typicus*, nor in the biogeographically associated and contiguous areas, further supports the idea that the species is not an element of the Italian fauna. Furthermore, its morphological features and general aspect do not resemble any Western Palaearctic member of the tribe Mordellini, with the only exception of a vague affinity with *Mordellaria aurofasciata* (Comolli, 1837). It is currently impossible to determine a plausible origin of this taxon.

Tribe Mordellistenini Ermisch, 1941

Mordellokoiles grandii Franciscolo, 1942, stat. nov.

Mordellistena (*Mordellokoiles*) *grandii* Franciscolo, 1942: 134; Ruzzier 2013: 111.
Mordellokoiles grandii: Franciscolo 1995: 11.
Mordellistena (*Mordellokoides*) [sic!] *grandii*: Horák 2008: 96 (incorrect subsequent spelling); Horák 2020: 91 (incorrect subsequent spelling).

Material. ***Holotype*** (female, not male as stated in the original description) and two paratypes (both females) labeled "Calabria, V. del Crati, Leoni" (MSNG) (Fig. 5A).

Conservation state: the holotype and one paratype are moderately damaged, missing antennomeres, tarsi, and some legs (including posteriors).

Redescription. ***Measurements*.** Holotype. HL: 1.2 mm; HW: 1.4 mm; PL: 1.5 mm; PW 1.9 mm; EL: 4.6 mm; EW: 1.9 mm; PygL 1.1 mm; HpygL 0.5 mm; TL: 8.4 mm.

***Color*.** Integument reddish brown to brown; head and ventrites darker (Fig. 5B, C). Mouthparts and the first four basal antennomeres reddish brown; antennomeres from the fifth onwards dark brown (visible only in one paratype). Pronotum presenting a faint longitudinal patch of black, thin setae along the midline; elytra pale reddish brown on their basal half but dark brown on the apical half; dark part of the elytra covered with dark setae.

***Head*.** Head moderately transverse in dorsal view (1.2× wider than long), sub-hemispheric but slightly flattened in lateral view (Fig. 5B), with the highest point just behind the middle of the frons; occipital margin almost straight in dorsal view (Fig. 5C); integument smooth and densely covered with setigerous punctures. Eyes small, setose, and finely facetted, broadly ellipsoidal in lateral view, reaching anteriorly the antennal insertion but not reaching posteriorly the occiput. Anterior margin of the epistoma straight; labrum transverse, gently bisinuate on the anterior margin, setose. Maxillary palpus of the *Mordellistena*-type (*sensu* Franciscolo 1957) (Fig. 5D); first maxillary palpomere flattened, conical and oblong, about 3.8× its maximum width; second maxillary palpomere short, subcylindrical, 1.8× longer than its maximum width; apical (third) maxillary palpomere scalene triangular and oblong, 2.7× longer than its maximum width, outer margin of the segment (the longest) straight.

Antennae filiform (missing in the holotype and one paratype); antennomeres 1–4 cylindrical, with 1 and 2 slightly longer and thicker than 3 and 4; antennomeres 5–10 expanded and only slightly serrated, elongated, 1.7–1.9× longer than wide; apical antennomere asymmetrically ellipsoid, slightly impressed on its inner apical side, 1.9× longer than wide (visible only in one paratype).

***Prothorax*.** Pronotum trapezoidal in dorsal view, 1.3× wider than long, widest on its basal third, slightly convex in lateral view, the convexity increases towards the posterior third of the pronotum; pronotal disc smooth but densely covered with impressed setigerous punctures bearing recumbent and posteriorly oriented setae, punctures larger than those on head. Anterior margin not visible from above since the anterior angles curve downward; in dorsal view, lateral margins of the pronotum roundly and gently converge to the neck. Posterior margin of the pronotum irregular, with the central lobe protruding posteriad. Anterior and posterior angles of the pronotum obtuse in lateral view; lateral margins of pronotum straight in lateral view.

Figure 5. *Mordellokoiles grandii* Franciscolo, 1942, holotype **A** original labels **B** dorsal habitus **C** lateral left view **D** left maxillary palpus. Scale bar: 2.0 mm.

***Pterothorax*.** Scutellum triangular, finely punctured, and covered with dense, thin setae.

Elytra 2.4× longer than wide, parallel in dorsal view (Fig. 5C); external margins markedly curving from the 2/3 of the elytral length towards the apices; elytra apices feebly rounded, almost converging at the suture. Elytra strongly and densely punctate; each puncture bears a spiniform seta, especially on the elytral disc.

Hind wing (paratype) of the *Mordellistena*-type (see Fedorenko 2009) (Fig. 6).

Metepisterna of the *Mordellistena*-type (*sensu* Franciscolo 1957), trapezoidal, 2.1× longer than its maximum width; sutures between Metepisterna and metaventrite marked and straight. Coxae (coxal plates) semicircular, and almost as long as wide. Metepisterna, metaventrite, and coxae on their half, densely covered with setigerous punctures like those on pronotum and elytra.

Mesofemora laterally compressed; mesotibia cylindrical and only feebly curved in dorso-lateral view; mesotarsus 1.1× as long as mesotibia. Metafemora straight, laterally compressed; metatibiae conical, transversely truncate at apex; subapical comb present, short and not running parallel to the apical margin of the tibia; dorso-lateral side of metatibia bearing two strongly oblique combs with the proximal longer than the distal. Metatarsomere 1 bearing three oblique, parallel combs, metatarsomere 2 with two, metatarsomere 3 with one

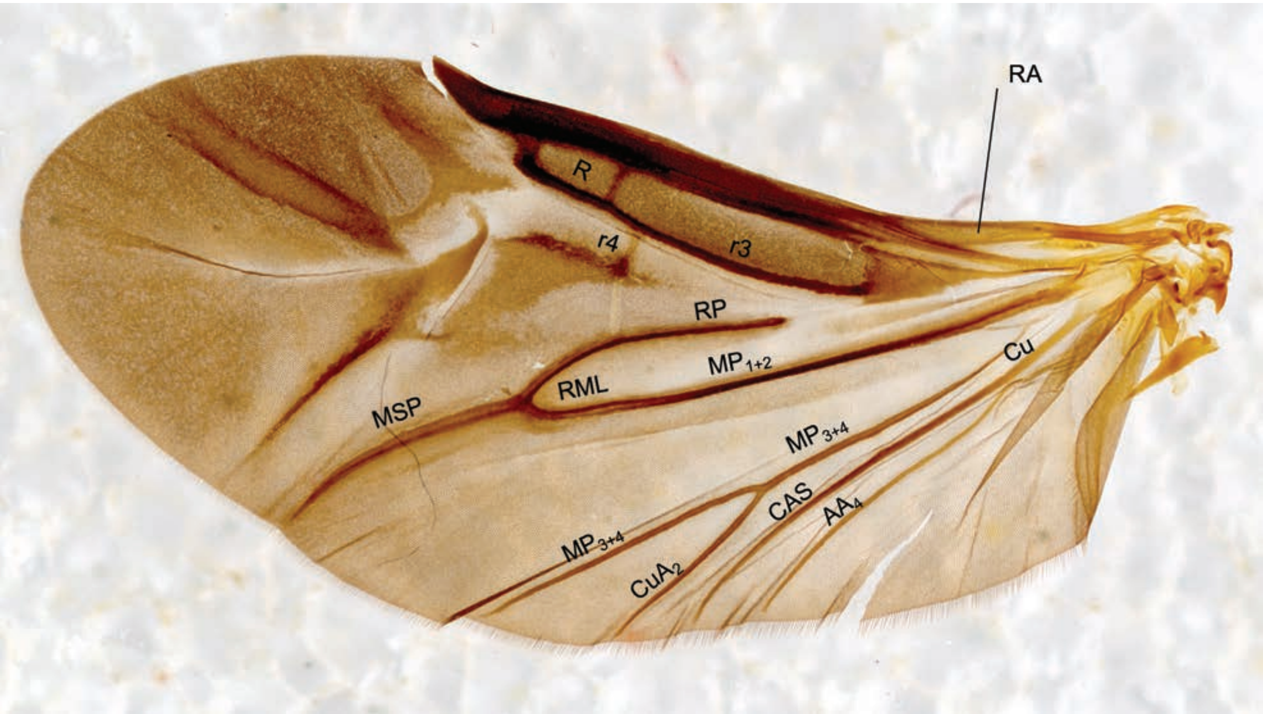

Figure 6. *Mordellokoiles grandii* Franciscolo, 1942., paratype, right wing, in ventral view.

comb, and metatarsomere 4 devoid of any. Metatibial spurs asymmetrical with the inner 2.6× as long as the outer.

Abdomen. Abdomen conical, tapered in both lateral and dorsal view; abdominal ventrite 1 almost of the same length as ventrite 2 and 3, ventrite 4 is the shortest. Pygidium conical in dorsal view, 1.8× longer than wide at the base; in lateral view the pygidium is conical, slightly bending downward towards the base, 2.2× as long as hypopygidium.

Comments. *Mordellokoiles grandii* represents another case of a species described as native to Italy by Franciscolo but never found again since its description. Examination of the type material suggests that this taxon does not belong to the Western Palaearctic fauna and especially poses serious difficulties in framing *Mordellokoiles* with respect to the other genera of Mordellistenini.

As with *Mordella quomoi*, the description of the new taxon is rather synthetic, not accompanied by adequate iconography, the sex of the holotype is clearly mistaken (male instead of female), and the establishment of the subgenus *Mordellokoiles* is based on a sole antennal character of rather dubious validity (shape of the last antennomere). Because *M. grandii* possesses the penultimate tarsomere of the anterior and middle tarsi dilated, it cannot be considered in any way as a subgenus of *Mordellistena* Costa, 1854, a genus that possesses cylindrical and apically truncated pro- and mesotarsomeres. Furthermore, this taxon cannot be assigned to any of the Western Palaearctic Mordellistenini with a similar tarsal character, such as *Tolida* Mulsant, 1856, *Dellamora* Normand, 1916, or *Pseudodellamora* Ermisch, 1942, because it differs from these in its general aspect and other characters. However, *Mordellokoiles* is rather similar to some Oriental and Eastern Palaearctic genera, such as *Falsomordellistena* Ermisch, 1941, *Glipostenoda* Ermisch, 1950 or *Pulchrimorda* Ermisch, 1968. However, it cannot be treated as a synonym of any of these because characters required to identify and separate the genera are almost exclusively sexually dimorphic, and it is the male that usually possess the most informative traits. Consequently, any placements of *Mordellokoiles* in any of the already existing genera could be incorrect, as this taxon establishment was based exclusively on females; therefore, we consider it appropriate to elevate *Mordellokoiles* to a genus rank, pending future reassignment if the male is discovered.

Discussion

The results presented here demonstrate once again how the examination and redescription of type material is a key step in clarifying the identity and distribution of the Western Palaearctic Mordellidae. The assignment of *Mediimorda argyropleura*, *Mordella quomoi*, and *Mordellokoiles grandii* to the Italian fauna by Franciscolo derives most probably from labeling mistakes possibly due to poor management of specimens collected or studied in the early years of his entomological career, as already noted by Magrini and Casale (2015) and Poggi (2023). It is, therefore, possible that the further study of material he has described over the years may result in additional discoveries and corrections in the Italian fauna.

Acknowledgements

The authors would like to thank Roberto Poggi (Museo Civico di Storia Naturale "G. Doria" – Genoa, Italy) for granting the study of the material in his care; and Alberto Ballerio (Brescia), Larry Bezark (California Department of Food and Agriculture), Robert Naczi (New York Botanical Garden), and the anonymous reviewers for providing valuable comments that improved the quality of this manuscript.

Additional information

Conflict of interest

The authors have declared that no competing interests exist.

Ethical statement

No ethical statement was reported.

Funding

The authors acknowledge the support of NBFC to the University of Roma Tre, Department of Science, funded by the Italian Ministry of University and Research, PNRR, Missione 4 Componente 2, 'Dalla ricerca all'impresa', Investimento 1.4, Project CN00000033.

Author contributions

Both authors have contributed equally.

Author ORCIDs

Enrico Ruzzier https://orcid.org/0000-0003-1020-1247
Andrea Di Giulio https://orcid.org/0000-0003-0508-0751

Data availability

All of the data that support the findings of this study are available in the main text.

References

Batten R (1976a) De Nederlandse soorten van de keverfamilie Mordellidae. Zoologische Bijdragen 19: 3–37.

Batten R (1976b) Mordellidae (Coleoptera) from the South of France and the Pyrenees. Entomologische Berichten 36: 164–171.

Borowiec L (1996) Mordellidae, Miastkowate (Insecta: Coleoptera). Fauna Polski, Vol. 18. Muzeum i Instytut Zoologii, Warszawa, 190 pp.

Emery MC (1876) Essai monographique sur les Mordellides de l'Europe et des contrées limitrophes. L'Abeille. Journal d'Entomologie 14: 1–128.

Ermisch K (1956) Mordellidae. In: Horion A (Ed.) Faunistik der mitteleuropäischen Käfer. Band 5: Heteromera. Entomologische Arbeiten aus dem Museum G. Frey Tutzing bei München, München, 269–328.

Ermisch K (1962) 17. *Mordellistena breddini* n. sp. aus dem Siebengebirge und der Eifel. Decheniana 10: 183–186.

Ermisch K (1963a) Die Mordelliden der Insel Cypern (Coleoptera, Heteromera, Mordellidae). Notulae Entomologicae 43: 49–67.

Ermisch K (1963b) Neue Mordelliden (Heteromera, Mordellidae) aus Deutschland und Nachträge zur Faunistik der Mitteleuropaischen Mordelliden. Entomologische Blätter 59: 1–36.

Ermisch K (1963c) Beitrag zur Mordelliden-Fauna Portugals (Coleopt. Heteromera, Mordellidae). Notulae Entomologicae 42: 14–21.

Ermisch K (1965) Neue Mordelliden von der Balkanhalbinsel (Coleoptera, Mordellidae). Reichenbachia 5(30): 251–272.

Ermisch K (1966) Neue westpaläarktische *Mordellistena*-Arten (Coleoptera-Heteromera-Mordellidae). Entomologische Blätter 62(1): 30–39.

Ermisch K (1969a) 79. Familie: Mordellidae. In: Freude H, Harde KW, Lohse GA (Eds) Die Käfer Mitteleuropas. Band 8, Teredilia, Heteromera, Lamellicornia. Goecke & Evers, Krefeld; G. Fischer, Jena, Stuttgart, 160–196.

Ermisch K (1969b) Ergebnisse der Albanien-Expedition 1961 des Deutschen Entomologischen Institutes, 76. Beitrag, Coleoptera: Mordellidae. Beiträge zur Entomologie 19(7/8): 845–859.

Ermisch K (1969c) Neue Mordelliden aus Europa, Nordafrika und dem Nahen Osten. Entomologische Blätter 65(2): 104–115.

Ermisch K (1977) Die *Mordellistena*-Arten Ungarns und benachbarter Gebiete sowie Beschreibung einer neuen *Hoshihananomia*-Art aus Siebenbürgen. Folia Entomologica Hungarica 30: 151–177. [New Series]

Fedorenko DN (2009) Evolution of the beetle hind wing with special reference to folding (Insecta, Coleoptera). Pensoft Publishers, Sofia, 336 pp.

Franciscolo ME (1942a) Mordellidi raccolti dal Marchese G. doria all'isola del Giglio negli anni 1900 - 1902. Materiali per una Fauna dell'Arcipelago Toscano XXI. [Note su Mordellidi italiani] ii. Bollettino della Società Entomologica Italiana 74(1): 6–10.

Franciscolo ME (1942b) Raccolte entomologiche nell'isola di Capraia fatte da C. Mancini e da F. Capra (1927–1931). VII. Mordellidae (Col. Heteromera). Bollettino della Società Entomologica Italiana 74(2–3): 18–23.

Franciscolo ME (1949) Note su alcuni Mordellidi (XII Contributo alla conoscenza dei Mordellidi). Bollettino della Società Entomologica Italiana 79(5–6): 52–58.

Franciscolo ME (1957) Coleoptera: Mordellidae. A monograph of the South African Genera and Species. 1. Morphology, subfamily Ctenidiinae and tribe Stenaliini. South

African Animal Life, Results of the Lund University Expedition in 1950–1951, Uppsala, 1957, 4(V): 207–291.

Franciscolo ME (1995) Fam. Mordellidae. In: Minelli A, Ruffo S, La Posta A (Eds) Checklist delle specie della fauna italiana, fasc. 58. Edizioni Calderini, Bologna, 11–13.

Horák J (1985) Ergebnisse der tschechoslowakisch-iranischen entomologischen expeditionen nach Iran 1970, 1973 und 1977, Coleoptera: Mordellidae 1 (Stenaliini, Mordellini). Entomologische Abhandlungen 49(1): 1–25.

Horák J (1990) Typenrevision einiger wenig bekanntner Arten aus der Gattung *Mordellistena* Costa (Insecta, Coleoptera: Mordellidae). Entomologische Abhandlungen 53(9): 125–142.

Horák J (2008) Family Mordellidae Latreille, 1802. In: Löbl I, Smetana A (Eds) Catalogue of Palaearctic Coleoptera. Vol. 5. Tenebrionoidea. Apollo Books, Stenstrup, 87–105.

Horák J (2020) Family Mordellidae Latreille, 1802. In: Iwan D, Löbl I (Eds) Catalogue of Palaearctic Coleoptera. Vol. 5. Tenebrionoidea, Revised and Updated Second Edition. Apollo Books, Stenstrup, 79–103.

Horák J, Farkač J, Nakládal O (2012) Mordellidae (Coleoptera) from Socotra Island. Acta Entomologica Musei Nationalis Pragae 52(Suppl. 2): 253–268.

ICZN (1999) International Code of Zoological Nomenclature. Fourth edition. London, UK. http://www.iczn.org/iczn/index.jsp

Kaszab Z (1979) Felemás lábfejízes bogarak II. – Heteromera II. Magyarország állatvilága (Fauna Hungariae), IX, 2. Akadémiai Kiadó, Budapest, 105 pp.

Latella L (2009). Le spedizioni zoologiche di Saverio Patrizi, entomologo, biospeleologo e cacciatore. Atti del XVII Congresso ANMS Al di là della Alpi e del Mediterraneo. Verona, 4–7 dicembre 2007. Memorie del Museo Civico di Storia Naturale di Verona. 2. Serie. Monografie Naturalistiche, 4(2009): 53–58.

Lawrence JF, Zhou YL, Lemann C, Sinclair B, Ślipiński A (2021) The hind wing of Coleoptera (Insecta): Morphology, nomenclature and phylogenetic significance. Part 1. General discussion and Archostemata–Elateroidea. Annales Zoologici 71(3): 421–606. https://doi.org/10.3161/00034541ANZ2021.71.3.001

Lawrence JF, Zhou YL, Lemann C, Sinclair B, Ślipiński A (2022) The hind wing of Coleoptera (Insecta): morphology, nomenclature and phylogenetic significance: Part 2. Further discussion, Histeroidea, Bostrichoidea to Curculionoidea. Annales Zoologici 72(3): 433–755. https://doi.org/10.3161/00034541ANZ2022.72.3.004

Leblanc P (2007) Révision des especes oust-paléarctiques du genre *Mediimorda* Méquignon, 1946 et description de deux nouvelles especes d´Afrique du Nord (Coleoptera: Mordellidae). Bulletin Mensuel de la Societe Linneenne de Lyon 76(9–10): 235–250. https://doi.org/10.3406/linly.2007.13665

Luigioni P (1929) I Coleotteri d’Italia. Catalogo sinonimico-topografico- bibliografico. Memorie della Pontificia Accademia dei Nuovi Lincei, ser. II 13: 1–1160.

Magrini P, Casale C (2015) Revisione del genere *Rhegmatobius* Jeannel, 1937, con descrizione di una nuova specifiee una nuova sinonimia (Coleoptera, Carabidae, Bembidiini, Anillina). Annali del Museo Civico di Storia Naturale “G. Doria” 107: 285–325.

Patti MZ (1840) Descrizione di un nuovo coleottero. Giornale di Scienze, Lettere e Arti per la Scilia 72: 292–294.

Poggi R (2023) Descrizione di sette nuove specie di Bythinini italiani, con osservazioni su alcune altre già note. Annali del Museo Civico di Storia Naturale “G. Doria” 116: 279–323.

Ragusa E (1883) Sui *Brachinus joenius* e *siculus* di M. Zuccarello Patti. Il Naturalista Siciliano 3: 13–16.

Ragusa E (1904) Catalogo dei Coleotteri di Sicilia. Il Naturalista Siciliano 17(2–3): 73–80.

Ragusa E (1924) Le Anthocere (Zygaene) della Sicilia. Bollettino del Laboratorio di Zoologia Generale e Agraria della Regia Scuola Superiore d'Agricoltura in Portici 18: 81–94.

Romano M (2006) La ricerca entomologica in Sicilia: Protagonisti, cultori e collezioni a cavallo di tre secoli. Il Naturalista Siciliano 30(2): 151–226.

Ruzzier E (2013) Taxonomic and faunistic notes on Italian Mordellidae (Coleoptera Tenebrionoidea) with redescription of *Falsopseudotomoxia argyropleura* (Franciscolo, 1942) n. comb. Bollettino della Società Entomologica Italiana 145(3): 103–115. https://doi.org/10.4081/BollettinoSEI.2013.103

Ruzzier E, Ghahari H, Horák J (2017) A checklist of the Iranian Mordellidae (Coleoptera: Tenebrionidea). Zootaxa 4320(1): 146–158. https://doi.org/10.11646/zootaxa.4320.1.8

Schilsky J (1895) Die Käfer Europa's. Nach der Natur Beschrieben von Dr. H. C. Küster und Dr. G. Kraatz Fortgesetzt von J. Schilsky, Vol 31. Bauer und Raspe, Nürnberg, 100 pp.

Selnekovič D, Improta R (2020) The type material of Mordellidae described by Achille Costa (Coleoptera: Tenebrionoidea). Zootaxa 4803(1): 42–50. https://doi.org/10.11646/zootaxa.4803.1.2

Selnekovič D, Kodada J (2019) Taxonomic revision of *Mordellistena hirtipes* species complex with new distribution records (Insecta, Coleoptera, Mordellidae). ZooKeys 854: 89–118. https://doi.org/10.3897/zookeys.854.32299

Selnekovič D, Ruzzier E (2019) New distributional records for sixteen Mordellidae species from the Western Palaearctic (Insecta, Coleoptera, Mordellidae). ZooKeys 894: 151–170. https://doi.org/10.3897/zookeys.894.39584

ZooKeys 1207: 167–183 (2024)
DOI: 10.3897/zookeys.1207.116758

Checklist

Amphibian survey of Ko Pha-gnan in Surat Thani Province, Thailand

Dawn R. Cook-Price[1], Sunchai Makchai[2], Sasitorn Hasin[3], Pongthep Suwanwaree[1]

1 *School of Biology, Institute of Science, Suranaree University of Technology, Nakhon Ratchasima, 30000, Thailand*
2 *Thailand Natural History Museum, National Science Museum, Pathum Thani, 12120, Thailand*
3 *Innovation of Environmental Management, College of Innovative Management, Valaya Alongkorn Rajabhat University under the Royal Patronage, Klong Luang, Pathum Thani, 13180, Thailand*

Corresponding author: Pongthep Suwanwaree (pongthep@sut.ac.th)

Abstract

Insular amphibian species are often overlooked, rendering them vulnerable to habitat encroachment and other anthropogenic threats. The aim of this study was to compile a comprehensive list of amphibian species on Ko Pha-ngan in Surat Thani Province, Thailand. Data were collected via transect surveys and drift line fence traps in three different habitat types from February 2021 to September 2023. Our efforts detected 12 unique amphibian species in each of the three habitat types. The highest number of detections was observed in the Ko Pha-ngan-Than Sadet National Park protected areas. The common tree frog (*Polypedates leucomystax*) and the common Asian toad (*Duttaphrynus melanostictus*) were the two most abundantly found species on the island, whereas the Koh Tao caecilian (*Ichthyophis kohtaoensis*) and the newly described false Doria's fanged frog (*Limnonectes pseudodoriae*) where the least commonly found species. In addition, *Microhyla heymonsi* and *Fejervarya limnocharis* tadpoles were observed developing in high-salinity water bodies. Many species have shown a high tolerance in human-dominated landscapes. This study sheds light on the need for additional monitoring to better understand the dynamics of endemic species in addition to the impact tourism-driven development and habitat destruction has on a species with an insularly finite habitat.

Key words: Biodiversity, conservation, insular populations, island biogeography, species list

Academic editor: Annemarie Ohler
Received: 3 December 2023
Accepted: 9 February 2024
Published: 19 July 2024

ZooBank: https://zoobank.org/8E5A11BC-FBC0-46BB-8547-25196080E3D9

Citation: Cook-Price DR, Makchai S, Hasin S, Suwanwaree P (2024) Amphibian survey of Ko Pha-gnan in Surat Thani Province, Thailand. ZooKeys 1207: 167–183. https://doi.org/10.3897/zookeys.1207.116758

Introduction

Amphibians, known for their high sensitivity to environmental changes, play a vital role in ecosystems around the world (Liu et al. 2021). Alarmingly, there has been a global decline in amphibian populations, largely attributed to habitat destruction and fragmentation (Hayes et al. 2010). While the significance of biodiversity data concerns a wide range of research areas, its importance becomes paramount when monitoring declining populations for conservation efforts (National Research Council 1992). This worldwide decline in amphibians is mirrored in Thailand, a country rich in amphibian diversity (Chuaynkern and Duengkae 2014).

Ko Pha-ngan situated in Surat Thani Province in southern Thailand, is one of a trio of islands alongside Ko Samui and Ko Tao. Ko Pha-ngan had a historical link as part of the mainland during the Holocene epoch, as part of the Sunda

Shelf approximately 21,000 years ago (Nutalaya et al. 1979). This might indicate that it was once part of a more diverse ecosystem. Over time, insularization and subsequent separation from the mainland could have gradually eroded this diversity due to limited habitats and exposure to disturbances. Historically, the island was mined for tin along with a significant portion utilized for coconut plantations (Nutalaya et al. 1979), and currently it is a popular tourist destination (Kaewcharoen et al. 2019). Despite being renowned for its bustling party atmosphere, attracting a large fraction of Thailand's tourists, Ko Pha-ngan faces significant environmental challenges. In 2017, the island hosted approximately 1.1 million tourists, accounting for 75% of its total visitors (Kaewcharoen et al. 2019). This surge in tourism, a primary economic driver, has inadvertently propelled development and deforestation on the island. Although it sits approximately 80 km away from the mainland, the biodiversity of Ko Pha-ngan, predominantly shielded by the Ko Pha-ngan-Than Sadet National Park, is both unique and understudied (Department of National Parks, Wildlife and Plant Conservation 2018).

Thailand houses over 170 amphibian species and yet the island amphibians remain enigmatic, with considerable gaps in understanding their ecological significance. This knowledge void is particularly noticeable for Ko Pha-ngan, where the herpetofauna remains unstudied. Most islands in Thailand are understudied, and this island offers a unique opportunity for comparison with the few islands that have been studied in Thailand, such as the pristine Tarutao (Nidup et al. 2013), Phi Phi islands (Milto 2014), and the tourist mecca Phuket (Leong et al. 2003). Those islands are in the Andaman Sea on the opposite side of the peninsula, whereas Ko Pha-ngan is in the Gulf of Thailand. This also allows us to look at the effects that humans have on amphibian habitat.

The infrequency of inventory updates from national parks exacerbates this knowledge gap. This study seeks to bridge this chasm by presenting a detailed amphibian species inventory of Ko Pha-ngan. It is our aspiration that this inventory will catalyze more nuanced conservation efforts on the island, ensuring the survival and thriving of its amphibian inhabitants.

Methods

Situated in the Gulf of Thailand on the east coast of peninsular Thailand, Ko Pha-ngan is 125 km^2 (15 km north to south and 10 km east to west), with the Than Sadet-Ko Pha-ngan National Park occupying a third of the island at 42.9 km^2 and a maximum elevation of 635 m for the entire island (Department of National Parks, Wildlife and Plant Conservation 2018). The island's lower elevation areas are predominantly residential and agricultural, with montane forests in elevated regions (Koh Phangan City 2023).

Surveys were conducted on the island of Pha-ngan between February 2021 and September 2023. The surveys took place twice per week for a total of 78 weeks under a variety of weather conditions and were carried out between the hours of 19:00 and 02:00 for a total of 1,343 hours. This observational study sought out areas with high detectability potential and remote, less traveled regions. The selection of transects was determined by multiple factors including proximity to water, access to private land, and the safety of the terrain and habitat type. Three major habitats were surveyed (Fig. 1): human settlement (HS), human-disturbed forest (HDF), and National Park Forest (NPF). Human-dis-

Figure 1. Habitat types **A, B** human-disturbed forest patch **C** rocky river area inside the national park forested area **D** national park forest area **E** human-disturbed forest area **F, G** human-settlement areas. All photos are where species have been found.

turbed forest is any patch of fragmented forest area near human settlements or witnessing human activity in sections throughout. There were 32 transects utilized on the island spanning all three of the different habitats (Figs 1, 2). This includes seven in HS, 13 in HDF, and 11 in NPF areas. Transect lengths varied between 500 m and 1.5 km with variation in elevation from sea level to 630 m. Over half the island consists of montane forested areas, and most of the flat areas are used for residential and agriculture purposes (Koh Phangan City 2023).

Salinity levels were measured with an EZ-9909A multi-functional meter (Yieryi, China) when frogs or tadpoles were detected in water bodies within 100 m of beach-front areas.

In addition to foot surveys, seven drift-line fence traps were placed strategically across the island. Configured with a single funnel at one end and a double funnel at the other, the trap also incorporated a pitfall trap in the center (Fig. 3).

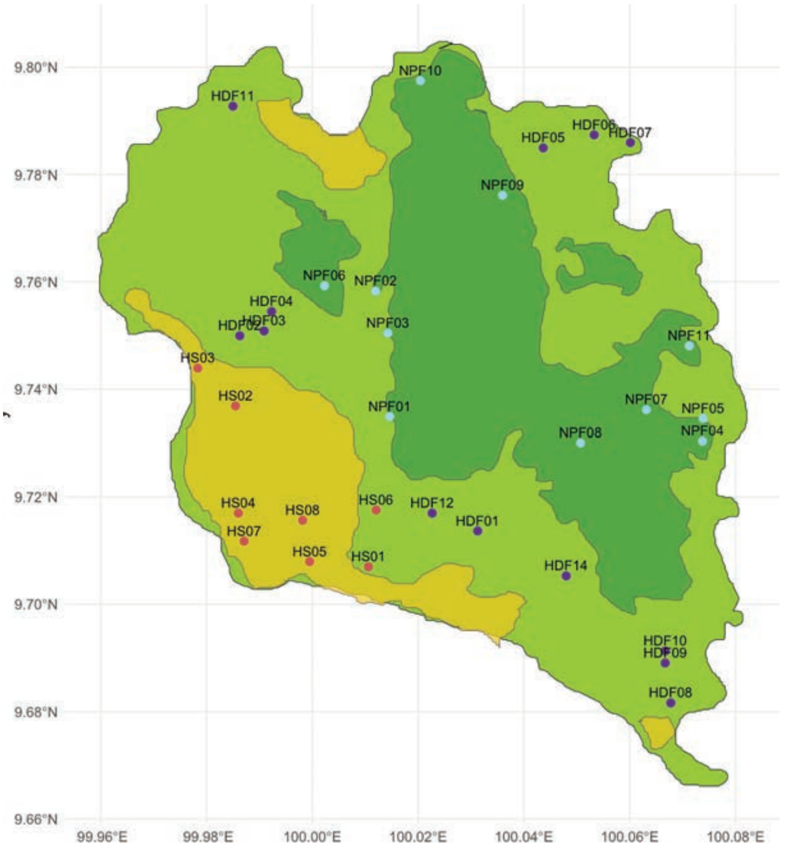

Figure 2. Habitat and transect location map of the island with human settlement (HS) indicated in yellow with red transect points, human-disturbed forest (HDF) areas indicated in light green with purple transect points, and national park forest (NPF) areas indicated in dark green with blue transect points.

Figure 3. A complete view of drift line fence **B** funnel trap used in conjunction with drift line fence.

Configurations were adapted to suit terrain and the length of the funnel trap relative to the available area. The traps, with a 10 m long drift line, offered an alternative means of detection for elusive or reclusive species.

Traps were positioned in the national park forest, human-disturbed forest, and human settlement. They were operational later than foot surveys started as they were open from February 2022 to August 2023, and checked daily for a total of 236 days. A specific trap was open from 7 to 90 days. Each amphibian found was identified in the field when possible before immediate release. The Amphibians of Thailand (Niyomwan et al. 2019) and Thailand's Natural History Museum database (http://nhmsearch.nsm.or.th) were consulted for identification of the amphibians found. To assess species diversity, we employed two ecological indices: the Shannon–Wiener [H' = −∑(pi × ln(pi))] and Simpson's [D=1−∑(pi2]) (Krebs 1989).

Results

Our study documents a total of 12 amphibian species on Ko Pha-ngan, which includes 11 species of anurans from 10 genera and one species of Gymnophiona (Table 1). This study expands the Department of National Park's known records (Department of National Parks, Wildlife and Plant Conservation 2018) by adding five additional anuran species: *Microhyla mukhlesuri*, *Occidozyga martensii*, *Limnonectes pseudodoriae*, *Hoplobatrachus chinensis*, and *Ichthyophis kohtaoensis*. Of the species surveyed, there are no species listed as a concern on the International Union for Conservation of Nature and Natural Resources (IUCN) list (IUCN 2024).

Duttaphrynus melanostictus and *Polypedates leucomystax* were the two most found anuran species on the island, and they were found across all habitats (Table 2). *Duttaphrynus melanostictus* (common Asian toad) was found more frequently in the National Park Forest habitats along the edges of dirt trails whereas the common tree frog was found more evenly through all habitats. *Ichthyophis kohtaoensis* was the least found anuran, likely due to them being fossorial and nocturnal. The newly discovered *Limnonectes pseudodoriae* was found only near or in rocky stream bed areas as described by Yodthong et al. (2021). Though it was found in each habitat, the microhabitat is specialized for this frog as rocky stream areas are the only places they were found. In addition, *Microhyla heymonsi* and *Fejervarya limnocharis* tadpoles were observed in saline water bodies with measured levels of 3–12 parts per thousand (standard saline levels are 10–35 parts per thousand). Due to the island being surrounded by sea water, there are several water bodies that have high saline levels.

The low number of *Ichthyophis kohtaoensis* (caecilians) detected can be attributed to their nocturnal and fossorial lifestyle, making them less likely to

Table 1. Species list and conservation status.

Order	Family	Species	IUCN status
Anura	Microhylidae	*Kaloula pulchra*	LC
		Microhyla heymonsi	LC
		*Microhyla mukhlesuri**	LC
	Dicroglossidae	*Occidozyga martensii**	LC
		Limnonectes blythii	LC
		*Limnonectes pseudodoriae**	LC
		Fejervarya limnocharis	LC
		*Hoplobatrachus chinensis**	LC
	Ranidae	*Hylarana erythraea*	LC
	Rachophoridae	*Polypedates leucomystax*	LC
	Bufonidae	*Duttaphrynus melanostictus*	LC
Gymnophiona	Ichthyophiidae	*Ichthyophis kohtaoensis**	DD

DD = Data Deficient, LC = Least Concern. *New record from the Than Sadet - Ko Pha-ngan National Park checklist.

Table 2. Amphibian detection by habitat and diversity indices.

	Human settlement	Human-disturbed forest	National park forest	Total
Diversity Index				
Shannon-Wiener	2.15	2.17	2.20	
Simpson’s	0.864	0.870	0.870	
Species				
Kaloula pulchra	103	158	212	473
Microhyla heymonsi	72	69	109	250
Microhyla mukhlesuri	14	18	15	47
Occidozyga martensii	88	117	107	312
Limnonectes blythii	48	108	102	258
Limnonectes pseudodoriae	7	45	6	58
Fejervarya limnocharis	39	49	63	151
Hoplobatrachus chinensis	15	16	10	41
Hylarana erythraea	108	136	87	331
Polypedates leucomystax	181	175	179	535
Duttaphrynus melanostictus	167	265	370	802
Ichthyophis kohtaoensis	15	5	18	38
Total	857	1,161	1,278	3,296

be encountered unless conditions are optimal, such as post-rainfall events. This highlights the importance of survey timing and methodology in detecting species with cryptic behaviors. *Hoplobatrachus chinensis* and *Occidozyga martensii* were detected slightly more in human settlement and human-disturbed forest than in the national park forest, possibly due to their preference and tolerance or vernal cow ponds and muddy marshy fields which are not habitats often found in the national park forest.

For diversity analysis, the NPF area has the highest Shannon–Wiener value with HDF and HS closely following in values (Table 2). The Simpson’s Index revealed the same values for both HDF and NPF, and only slightly different for HS. While the differences among these habitats were not statistically significant, the slightly higher diversity indices in NPF regions suggest a slightly more varied amphibian population.

These indices offer complementary insights; Shannon–Wiener places greater emphasis on species richness and evenness. A higher value indicates a more diverse community, where species are not only numerous but also more evenly distributed. The Simpson’s Index focuses more on the dominance of a particular species. A lower value of a Simpson’s Index indicates a higher diversity, meaning that the ecosystem is not dominated by one or a few species but has a more balanced distribution of species. This dual approach allows for a more nuanced understanding of amphibian diversity across different habitats. Though the national park forest habitat had slightly more diversity than the other habitats, the frogs that adapted to human settlement and human-disturbed forests seem to thrive which is consistent with these common species throughout Thailand.

Notably, the national park forest area, while slightly higher in diversity indices, did not differ significantly from human-disturbed forest or human settlement, indicating that amphibian populations are relatively similar across these environments. This similarity is remarkable, considering the varying degrees of human impact, and implies that species such as *Kaloula pulchra* and *Microhyla hemonsi*, which are abundant across all habitats, are the resilient and adaptable to changes in their ecosystems. This indicates a healthier, more balanced amphibian community and a flexibility or resilience among the common species in Thailand.

Taxonomy

Class Amphibia
Order Anura
Family Microhylidae Günther, 1858

Kaloula pulchra **Gray, 1831**
Fig. 4
Banded bullfrog, painted bullfrog

Notes. These fossorial individuals were occasionally observed in tree holes (7), burrows (4), termite mounds (3) and anthropogenic material (3). Once observed in a dirt track puddle of saline water.

Distribution. This species is abundant throughout the island and found in all habitat types. Individuals were observed in all human-settlement transect areas which includes garden areas near homes, fallow fields between human development, edge habitat near human-disturbed forest. This frog was detected in all human-disturbed forest including patches between developed housing areas. Frogs were detected in all national park forest transects. More often detected near water.

Microhyla heymonsi **Vogt, 1911**
Fig. 4
Dark-sided chorus frog

Notes. A total of 250 individuals were observed in a variety of habitat, including near ponds, puddles, grassy areas, streams, and house or garden areas in and around water pots common in garden areas. Found in primarily around freshwater; however, four individuals were also observed in and around brackish and saline water located in human settlement.

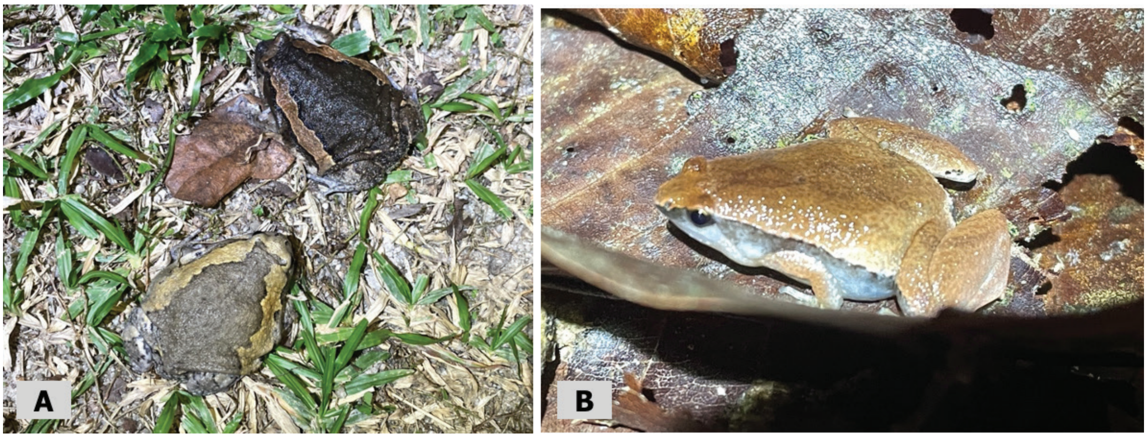

Figure 4. A two color variations of *Kaloula pulchra*, observed in human settlement **B** *Microhyla heymonsi* observed in leaflitter.

Distribution. This species was detected at three of the seven human-settlement areas, six of the 14 human-disturbed forest habitats, and six of the 10 national park forest habitats.

Microhyla mukhlesuri Hasan et al., 2014

Fig. 5

Mukhlesur's narrow-mouthed frog

Notes. Individuals were observed in a variety of habitats. Three individuals were found in a rocky stream bed in national park forest. Eighteen individuals were observed on sandy trails at the edge of both forested and scrub-grassy habitats, five individuals were found in a patch of human-disturbed forest at the edge of human settlement, seven individuals observed in a grassy area in human settlement on the edge of a human-disturbed forest, five individuals observed in a grassy area at the edge of a pond in human settlement, and nine individuals were found in the leaf litter near a pond at the edge of human-disturbed forest. Primarily found around freshwater; however, it was also observed in and around brackish and saline water. Tadpoles observed developing in saline water (August 2023).

Distribution. This species was detected in three of the eight human-settlement transects, three of the 13 human-disturbed forest transects, and seven of the 11 national park forest transects.

Family Rhacophoridae Hoffman, 1932 (1858)

Polypedates leucomystax (Gravenhorst, 1829)

Fig. 5

Southern Clade. Common tree frog or four-lined tree frog

Notes. This species was the second most observed on the island; 535 individuals were commonly observed throughout the island in a variety of habitats including forested areas near water sources such as streams or ponds, grassy plantation areas near water sources, such as overgrown vegetation patches

Figure 5. A *Microhyla mukhlesuri* near a small pond in human-disturbed forest **B** *Polypedates leucomystax* found on low branches near small pond in a marsh area in human-disturbed forest.

near ponds, disturbed forested areas, and human habitat near streams, ponds, or anthropogenic structures holding water. Observed once in a concrete basin of a water fountain in a human-settlement area at the edge of a stream.

Distribution. The common tree frog is distributed throughout peninsular Thailand south of the Isthmus of Kra and is part of the southern clade of this species group (Buddhachat and Suwannapoom 2018). This species is common throughout the island with detection in all 8 of human-settlement transects, 12 of the 13 human-disturbed forest transects, and 10 of the 11 national park forest transects.

Family Ranidae Rafinesque, 1814

Hylarana erythraea **(Schlegel, 1837)**

Fig. 6
Green grass frog

Notes. The 331 individuals detected were commonly observed near ponds and some stream areas. Observations were made on the ground in grass or sandy soil, in water of a pond, on fallen trees, and in low areas on the side of trees. This species was observed in or near fresh, brackish, and saline water.

Distribution. The green grass frog is distributed throughout the island, most commonly near water. Detection occurred in five of the eight human-settlement transects, 13 of the 13 human-disturbed forest transects, and five of the 11 national park forest transects.

Family Dicroglossidae Anderson, 1871

Fejervarya limnocharis **(Gravenhorst, 1829)**

Fig. 6
Pond frog

Notes. We observed 327 individuals near ponds and other water bodies such as puddles or still water near stream areas. Found in fresh, brackish, and saline water habitat. Tadpoles observed through to froglet in saline water puddle.

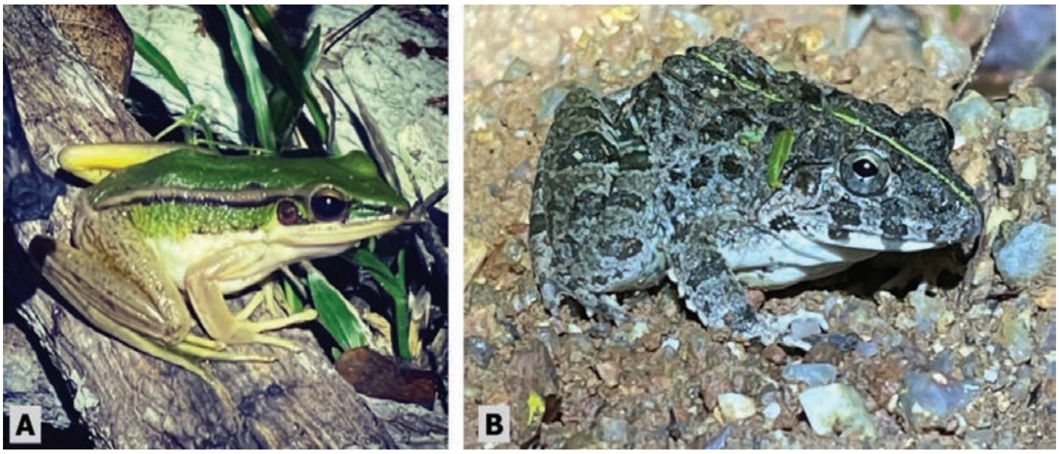

Figure 6. A *Hylarana erythraea* found on a fallen tree branch in a human-disturbed forest patch adjacent to human settlement **B** *Fejervarya limnocharis* on dirt trail between a stream and grassy area at in national park forest area.

Distribution. This species is common throughout the island with detection in six of the eight human-settlement transects, eight of the 13 human-disturbed forest transects, and six of the 11 national park forest transects.

Phrynoglossus martensii Peters, 1867

Fig. 7
Puddle frog

Notes. We observed 151 individuals in puddles situated in dirt track paths in human-disturbed forest and human-settlement areas such as a cement fountain not in use but still retaining water.

Distribution. This species is distributed throughout Thailand but is more prevalent in central and peninsular areas (Köhler et al. 2021). It is common throughout the island near small water bodies such as puddles and small vernal ponds. Individuals were detected in seven of the eight human-settlement transects, 11 of the 13 transects in human-disturbed forest areas, and six of the 11 transects in national park forest areas.

Hoplobatrachus chinensis (Wiegmann, 1834)

Fig. 7
Chinese edible frog

Notes. Individuals were sometimes found in or on the edge of small ponds or vernal water holes used by water buffalo in marshy fallow fields. It is often found in fresh food markets and has been farmed on the island.

Distribution. The species was found near water bodies such as small ponds or standing water areas sporadically throughout the island. Individuals were observed in two of the eight areas in human habitat, two of the 13 areas in human-disturbed forest, and only two of the 11 areas surveyed in national park forest.

Figure 7. A *Phrynoglossus martensii* found in a water fountain at an abandoned party location in human-disturbed forest **B** *Hoplobatrachus rugulosus* at the edge of a small pond in a human-disturbed forest patch in human settlement.

Limnonectes blythii **(Boulenger, 1920)**

Fig 8
River frog

Notes. The 273 individuals detected were primarily observed on the banks of rivers or edges of ponds and rocky riverbeds. The majority (225) were observed in both national park forest and human-disturbed forest areas. The individuals found in human-settlement areas were adjacent or within 25 m of a stream or marshy water source. Fig. 8 shows an individual on a bridge walkway above a stream on dormant party grounds inhabited by villagers.

Distribution. The river frog is distributed throughout the island in or near stream or pond areas with individuals observed in five of the eight human-settlement transects, 10 of the 13 human-disturbed forest transects, and eight of the 11 in national park forest transects.

Limnonectes pseudodoriae **(Yodthong, Rujirawan, Stuart & Aowphol, 2021)**

Fig. 8
False Doria's fanged frog

Notes. This species was observed in or around rocky stream habitat. Eggs were observed on land at the edge of a pool of standing water at a leveled area of a rocky stream wash in national park forest. This newly described species has been documented on only three islands, Ko Pha-ngan, Ko Samui, and Ko Lanta (Yodthong et al. 2021). The individuals observed in the human-settlement area were in a flooded stream area between a house and small pond.

Distribution. This species was detected primarily in rocky river systems. Individuals were detected in one of the eight human-settlement transects, three of the 13 human-disturbed forest transects and five of the 11 national park forest transects.

Figure 8. A *Limnonectes blythii* found on a bridge over a river near human settlement and a small, disturbed forest patch **B** *Limnonectes pseudodoriae* found on a rocky dirt path parallel to a rocky stream wash.

Figure 9. A *Duttaphrynus melanostictus* found on cement patch on a dirt track in humansettlement area in a human-disturbed forest **B** *Ichthyophis kohtaoensis* found under an overturned rock in a garden in human habitat not far from a stream.

Family Bufonidae Gray, 1825

***Duttaphrynus melanostictus* (Schneider, 1799)**
Fig. 9
Asian common toad

Notes. This species was the most observed species on the island; 559 individuals were commonly observed throughout the island on dirt paths, dirt roads, and pooled bodies of water in forested stream areas.

Distribution. The Asian common toad is distributed throughout the island with detection in all eight of the human-settlement transects, all 13 of the human-disturbed forest transects, and all 11 of the national park forest transects.

Family Ichthyophiidae Taylor, 1968

***Ichthyophis kohtaoensis* Taylor, 1960**
Fig. 9
Koh Tao caecilian

Notes. Forty individuals were observed near and around marshy habitat, under anthropogenic items near marshy river overflows, and occasionally under rocks in rocky dirt patches near rivers. Most often detected after or during rain, and commonly found in human-settlement areas after digging or gardening.

Distribution. This caecilian is distributed throughout the island, although it is fossorial and not easily detected. Individuals were detected in two of the eight human-settlement transects, five of the 13 human-disturbed forest transects, and three of the 11 national park forest transects.

Discussion

In more recent history, Ko Pha-ngan's landscape has evolved considerably. Formerly a tin mining hub, it transitioned to a mosaic of plantations with scattered remnants of native forests (Nutalaya et al. 1979). The burgeoning tourism sector compounds these changes by encroaching on essential habitats. Such rampant habitat modifications, while economically justifiable, potentially imperil the island's dwindling biodiversity (Russell and Kueffer 2019), as habitat fragmentation can reduce species diversity (Berger-Tal and Saltz 2019). Such disturbances pose unique challenges for island ecosystems, where specialized species are particularly susceptible (Kanowski et al. 2006).

All the species found are widely distributed across Thailand, demonstrating considerable adaptability to varying habitats. *Polypedates leucomystax* and *Kaloula pulchra*, for instance, are often spotted near human habitations, whereas *Limnonectes blythii* seems to favor riverine environments, indicating specific habitat preferences. This adaptability is evident in the face of rapid environmental changes, hinting at why some species flourish while others are at risk (Liu et al. 2021). This island's species composition can be compared to findings from other regions to gain insights into biodiversity patterns and potential influencing factors. A comparison of our findings with studies from other island regions and mainland habitats might give more insight to the understanding of the diversity observed on Ko Pha-ngan. Tarutao, a protected and more pristine island located in the southern peninsular Satun Province approximately 25 km from peninsular mainland (Cocks et al. 2005), houses 10 amphibian species (Nidup et al. 2013), which is less than the number found on Pha-ngan island. The topography of Tarutao differs slightly from Ko Pha-ngan, as that island has limestone cliffs and is relatively untouched and nestled in the Andaman Sea; however, there are similarities such as size (152 km^2) and elevation (713 m). Four of species on Tarutao, namely *K. pulchra*, *L. blythii*, *P. leucomystax*, and *H. erythraea*, also occur on Ko Pha-ngan. The distinct species on Tarutao suggest regional variations and could be influenced by Tarutao's specific environmental conditions, land protection, and proximity to other biodiversity hotspots.

Phuket, the largest island in Thailand (543 km^2), and the nearby islands of Yao Noi (45 km^2) and Yao Yai (92 km^2) are much closer to the mainland. Phuket is connected by a bridge less than 1 km long, and the two smaller islands are much less developed than Phuket. Phuket has 26 amphibian species (Leong et al. 2003), while Yao Noi and Yao Yai, nestled between Phuket and the mainland, have 19 species each (Visoot et al. 2023). Eleven species on Ko Pha-ngan are also found on these three islands. The only difference was the caecilian which has not been documented on Yao Noi and Yao Yai. Species such as *Leptobrachium smithi* prefer to breed in slow moving river areas or small side pools near riverbeds, and this is not a consistent habitat on Ko Pha-ngan. In addition, species such as *Chalcorana eschatia* and *Phrynoidis asper* prefer river and riverine habitats. Though Ko Pha-ngan has river habitat, during the dry season many of the river systems dry up, which may account for some of the variation in species present. In addition, these species are found in primary or significant secondary forest areas. Despite the tourism similarity, patches of forest differ between the islands.

On the opposite side of the peninsula in the South China Sea, Bidong Island on Malaysia's east coast houses only three amphibian species (*K. pulchra*, *P. leucomystax*, and *M. heymonsi*), likely due to the island's degraded habitat (Fatihah-Syafiq et al. 2020). All these species are found throughout the peninsula, including on Pha-ngan island. The low number of amphibian species can possibly be attributed to areas of the island having not been explored.

On the eastern side of the Gulf of Thailand, the Koh Man Islands are near (7 km) the mainland and only have four anuran species. Three of which are the same as on Ko Pha-ngan (*Fejervarya limnocharis*, *Kaloula pulchra*, and *Duttaphrynus melanostictus*), with only one difference, *Fejervarya cancrivora* (Chan-ard and Makchai 2011).

In the Surat Thani province on the mainland, there are at least 38 amphibian species from Khao Sok National Park (Thai National Parks 2023), and this diversity is much higher than on Ko Pha-ngan. Similar to Surat Thani, the Phang-nga province has 39 species (Pauwels et al. 2002); however, Phuket is much closer to its mainland counterpart (Phang-nga) than Ko Pha-ngan is to Surat Thani. A plausible explanation for these variations in biodiversity is the distance from the mainland of these islands. Tarutao and Ko Pha-ngan, approximately 25 km and 80 km from the mainland, hold fewer species than Phuket, which is just 660 m away and linked by a bridge. Yao Noi and Yao Yai, both within 20 km from the mainland, also support this trend. The MacArthur and Wilson (1967) biogeographical theory suggests that species diversity diminishes with increased isolation. A study in the Yoddom Wildlife Sanctuary in northeastern mainland Thailand further bolsters this claim; it reported a diverse amphibian population of 26 species (Thongproh et al. 2019), which contrasting starkly with the island findings.

While some amphibian species (*Polypedates leucomystax* and *Duttaphrynus melanostictus*) demonstrate adaptability to Ko Pha-ngan's shifting environment, others are at risk, particularly those species endemic to specific habitats such as *Limnonectes pseudodoriae*. River species, such as *Amolops panhai* and *Sylvirana malayana*, found on Phuket and Surat Thani mainland were not detected on Ko Pha-ngan, as they are primarily found in areas with rocky, flowing rivers, and that specific habitat is not consistent on Ko Pha-ngan. In addition, Ko Pha-ngan does not have any *Rhacophorus* (gliding frog) species, which are commonly detected in the tree canopy above or near water sources in the Surat Thani and Phang-nga provinces. The comparative lack of biodiversity can be attributed to factors like distance from the mainland and the island's environmental history. The conspicuous absence of some mainland species might be attributed to historical isolation, compounded by recent human activities, and the limitation of the researchers' observation.

To augment our understanding, in-depth research in the island's remote forested locales is pivotal. Prolonged studies might reveal a more nuanced diversity profile. While the Surat Thani mainland has undergone rigorous examination, its islands remain terra incognita for amphibian research.

Acknowledgements

This work would not be possible without permission from the Department of National Parks, Wildlife and Plant Conservation, and the National Research Council of Thailand. This work would not be possible without the support of the Than Sadet-Ko Pha-ngan National Park staff. All photographs were taken by Dawn Cook-Price.

Additional information

Conflict of interest

The authors have declared that no competing interests exist.

Ethical statement

This study was conducted in strict accordance with the Animals for Scientific Purposes Act B.E. 2558. It received approval from the Ethics Committee at Suranaree University of Technology, ensuring compliance with both local and international standards for ethical wildlife research.

Funding

Funding was provided by Suranaree University of Technology.

Author contributions

Dawn R. Cook-Price and Ponthep Suwanwaree conceptualized and designed the study, performed data analysis and interpretation, and drafted the article. Sunchai Makchai and Sasitorn Hasin assisted with identification and collection of data. Pongthep Suwanwaree provided critical revisions to the article, secured funding, and gave final approval for the version to be published

Author ORCIDs

Dawn R. Cook-Price https://orcid.org/0009-0000-5035-9642
Sunchai Makchai https://orcid.org/0009-0008-4067-7442
Sasitorn Hasin https://orcid.org/0000-0003-0704-2724
Pongthep Suwanwaree https://orcid.org/0000-0002-3047-2717

Data availability

All of the data that support the findings of this study are available in the main text.

References

Berger-Tal O, Saltz D (2019) Invisible barriers: Anthropogenic impacts on inter-and intra-specific interactions as drivers of landscape-independent fragmentation. Philosophical Transactions of the Royal Society of London, Series B, Biological Sciences 374(1781): 20180049. https://doi.org/10.1098/rstb.2018.0049

Buddhachat K, Suwannapoom C (2018) Phylogenetic relationships and genetic diversity of the *Polypedates leucomystax* complex in Thailand. PeerJ 6: e4263. https://doi.org/10.7717/peerj.4263

Chan-ard T, Makchai S (2011) An inventory of reptiles and amphibians on the Koh Man Islands and in the coastal Prasae estuaries, Rayong province, south-eastern Thailand. Thailand Natural History Museum Journal 5: 25–37.

Chuaynkern Y, Duengkae P (2014) Decline of amphibians in Thailand. In: Heatwole H, Das I (Eds) Conservation Biology of Amphibians of Asia. Natural History Publications (Borneo), Kota Kinabalu, 310–336.

Cocks LRM, Fortey RA, Lee CP (2005) A review of Lower and Middle Palaeozoic biostratigraphy in west Peninsular Malaysia and southern Thailand in its context within the Sibumasu Terrane. Journal of Asian Earth Sciences 24(6): 703–717. https://doi.org/10.1016/j.jseaes.2004.05.001

Department of National Parks, Wildlife and Plant Conservation (2018) Than Sadet - Ko Pha-ngan National Park Management Plan 2019–2022, 349 pp. [In Thai]

Fatihah-Syafiq M, Badli-Sham BH, Fahmi-Ahmad M, Aqmal-Naser M, Rizal SA, Azmi MSA, Grismer LL, Ahmad AB (2020) Checklist of herpetofauna in the severely degraded ecosystem of Bidong Island, Peninsular Malaysia, South China Sea. ZooKeys 985: 143–162. https://doi.org/10.3897/zookeys.985.54737

Hayes TB, Falso P, Gallipeau S, Stice M (2010) The cause of global amphibian declines: A developmental endocrinologist's perspective. The Journal of Experimental Biology 213(6): 921–933. https://doi.org/10.1242/jeb.040865

IUCN (2024) The IUCN Red List of Threatened Species. Version 2023-1. https://www.iucnredlist.org

Kaewcharoen R, Aujirapongpan S, Ritkaew S, Ru-Zhe J, Songkajorn Y (2019) Motivation and behavior of international tourists involving the full Moon party at Koh Phangan, Surat Thani province. Dusit Thani College Journal 13(3): 143–162. [In Thai]

Kanowski JJ, Reis TM, Catterall CP, Piper SD (2006) Factors affecting the use of reforested sites by reptiles in cleared rainforest landscapes in tropical and subtropical Australia. Restoration Ecology 14(1): 67–76. https://doi.org/10.1111/j.1526-100X.2006.00106.x

Koh Phangan City (2023) Basic Information. https://www.kohphangancity.go.th/front/menu/2/81 [In Thai]

Köhler G, Vargas J, Than NL, Schell T, Janke A, Pauls SU, Thammachoti P (2021) A taxonomic revision of the genus *Phrynoglossus* in Indochina with the description of a new species and comments on the classification within Occidozyginae (Amphibia, Anura, Dicroglossidae). Vertebrate Zoology 71: 1–26. https://doi.org/10.3897/vz.71.e60312

Krebs CJ (1989) Ecological Methodology. Harper and Row, New York, 654 pp.

Leong TM, Chan-ard T, Chuaynkern Y (2003) Additional anuran and saurian records for Phuket, South Thailand. The Natural History Journal of Chulalongkorn University 3: 17–21.

Liu G, Rowley JJ, Kingsford RT, Callaghan CT (2021) Species' traits drive amphibian tolerance to anthropogenic habitat modification. Global Change Biology 27(13): 3120–3132. https://doi.org/10.1111/gcb.15623

MacArthur RH, Wilson EO (1967) The Theory of Island Biogeography. Princeton University Press, Princeton, 203 pp.

Milto KD (2014) First report of the herpetofauna of Phi Phi Archipelago, Andaman Sea, Thailand. Russian Journal of Herpetology 21: 269–273.

National Research Council (1992) Conserving Biodiversity: a Research Agenda for Development Agencies. The National Academies Press, Washington DC, 127 pp.

Nidup T, Wangkulangkul S, Satasook C, Bates P, Juthong W (2013) Diversity of frog (Amphibia: Anura) and the correlation of habitat heterogeneity in Tarutao Island, Thailand. Proceeding of World Biodiversity Congress, Chiang Mai (Thailand), July 2013, 1–8.

Niyomwan P, Srisom P, Phawangkanan P (2019) Amphibians of Thailand. Parbpim, Bangkok, 487 pp.

Nutalaya P, Campbell KV, Macdonald AS, Aranyakanon P, Suthakorn P (1979) Review of the geology of Thai tin fields. Buletin Persatuan Geologi Malaysia 11: 137–159. https://doi.org/10.7186/bgsm11197906

Pauwels OS, Laohawat OA, Naaktae W, Puangjit C, Wisutharom T, Chimsunchart C, David P (2002) Reptile and amphibian diversity in Phang-nga Province, southern Thailand. The Natural History Journal of Chulalongkorn University 2(1): 25–30.

Russell J, Kueffer C (2019) Island biodiversity in the Anthropocene. Annual Review of Environment and Resources 44(1): 31–60. https://doi.org/10.1146/annurev-environ-101718-033245

Thai National Parks (2023) Wildlife in Khao Sok. https://www.thainationalparks.com/khao-sok-national-park/wildlife

Thongproh P, Duengkae P, Ratree P, Phetcharat E, Kingwongs W, Jaitrong W, Chuaynkern Y, Chuaynkern C, Duengkae P, Ratree P, Phetcharat E, Kingwongsa W, Jaitrong W, Chuaynkern Y, Chuaynkern C (2019) Species diversity and prey items of amphibians in Yoddom Wildlife Sanctuary, northeastern Thailand. Biodiversitas (Surakarta) 20(9): 2718–2732. https://doi.org/10.13057/biodiv/d200937

Visoot Y, Makchai S, Khonsue W, Traijitt T, Srion L, Kitana N, Kitana J, Thammachoti P (2023) Herpetofauna of Yao Islands, Phang-nga Province, Southern Thailand: A list of species and habitat notes. Thailand Natural History Museum Journal 17: 29–43.

Yodthong S, Rujirawan A, Stuart B, Aowphol A (2021) A new *Limnonectes* (Anura: Dicroglossidae) from southern Thailand. Animals (Basel) 11(2): 566. https://doi.org/10.3390/ani11020566

ZooKeys 1207: 185–204 (2024)
DOI: 10.3897/zookeys.1207.120663

Research Article

A new species of *Neotropiconyttus* Kirkaldy (Hemiptera, Reduviidae) in a cacao plantation from the Colombian Napo Province, including a key to species, and taxonomic notes of the genus

Jean Gamboa[1,2], Hélcio R. Gil-Santana[3], Armando Gamboa-Tabares[1], Eidy Martínez-Viuche[1], Francisco Serna[2]

1 *Laboratorio de Entomología Universidad de la Amazonia LEUA, Facultad de Ingeniería, Universidad de la Amazonia, sede Centro, Carrera 11, 5-69, Florencia, Caquetá, Colombia*
2 *Museo Entomológico UNAB, Facultad de Ciencias Agrarias, Universidad Nacional de Colombia, sede Bogotá, Carrera 30, 45-03, Bogotá D.C., Colombia*
3 *Laboratório de Diptera, Instituto Oswaldo Cruz, Av. Brasil, 4365, 21040-360, Rio de Janeiro, Brazil*
Corresponding author: Jean Gamboa (j.gamboa@udla.edu.co)

Abstract

A new species of the genus *Neotropiconyttus* Kirkaldy, 1909 (Hemiptera: Heteroptera: Reduviidae: Harpactorinae: Harpactorini) is described and illustrated. *Neotropiconyttus armandoi* Gamboa & Gil-Santana, **sp. nov.** represents the first record of the genus for the Province of Napo in Colombia, and the first description of a male individual in the genus. The male specimen representing the new species was collected on a leaf of cacao (*Theobroma cacao* L.-Malvaceae). Its remarkable similarity in external coloration and structure with that of the true bug *Monalonion dissimulatum* Distant, 1883 (Hemiptera: Miridae) inhabiting cacao agroforestry systems suggests that the new species could be part of a mimetic complex that incorporates phytophagous and predator bugs. Comments and figures of type specimens of *Neotropiconyttus alboannulatus* (Stål, 1855) and *Neotropiconyttus dama* (Burmeister, 1838), and a key to the species of the genus are also provided.

Key words: Assassin bugs, *Graptocleptes*, Heteroptera, *Hiranetis*, identification, Neotropical

OPEN ACCESS

Academic editor: Jader Oliveira
Received: 9 February 2024
Accepted: 2 April 2024
Published: 19 July 2024

ZooBank: https://zoobank.org/676C9C1D-1D04-4C86-A7B4-8C0A805C5F7A

Citation: Gamboa J, Gil-Santana HR, Gamboa-Tabares A, Martínez-Viuche E, Serna F (2024) A new species of *Neotropiconyttus* Kirkaldy (Hemiptera, Reduviidae) in a cacao plantation from the Colombian Napo Province, including a key to species, and taxonomic notes of the genus. ZooKeys 1207: 185–204. https://doi.org/10.3897/zookeys.1207.120663

Introduction

In the Neotropics, the tribe Harpactorini of the subfamily Harpactorinae is the most diverse group within Reduviidae, with approximately 53 genera in the Neotropics (Forero 2011; Gil-Santana 2015; Gil-Santana et al. 2015, 2017; Gil-Santana and Oliveira 2023). Different species of bugs (Hemiptera: Harpactorini), with bees and wasps, have been recognized as being involved in mimicry systems regarding the general body form, wing coloration, and characteristics concerning physical proportions (e.g., Champion 1899; Elkins 1969; Maldonado and Lozada 1992; Hogue 1993; Gil-Santana 2008, 2015, 2016, 2022; Gil-Santana et al. 2013, 2015, 2017; Castro-Huertas and Forero 2021). Maldonado and Lozada (1992) presented a key to Neotropical wasp-mimicking Harpactorinae genera, which, in their view, helps to quickly sort out specimens from unidentified material, although this is a somewhat artificial way of grouping genera. The most updated version of their key was published by Gil-Santana and Oliveira (2023), where they included the following genera: *Acanthischium* Amyot & Serville, 1843, *Coilopus* Elkins, 1969, *Graptocleptes* Stål, 1866, *Hiranetis* Spinola, 1837, *Myocoris* Burmeister, 1835, *Neotropiconyttus* Kirkaldy, 1909, *Parahiranetis* Gil-Santana, 2015, *Quasigraptocleptes* Gil-Santana & Oliveira, 2023, and *Xystonyttus* Kirkaldy, 1909. Gil-Santana and Oliveira (2023) also summarized the literature regarding these genera.

Maldonado and Lozada (1992) recognized *Neotropiconyttus* (Hemiptera, Heteroptera, Reduviidae, Harpactorinae, Harpactorini) among these genera when they described *N. heminigra* Maldonado & Lozada, 1992 and presented a table with a set of color characters to differentiate the species of *Neotropiconyttus*. However, the herein second author (HRG-S) examined the type specimens of *N. dama* (Burmeister, 1838) currently deposited at the Museum für Naturkunde Berlin, Leibniz Institute for Evolution and Biodiversity Science, Berlin, Germany (**MFNB**), and concluded that there were some errors in Maldonado and Lozada´s table, compromising the recognition of *N. dama*. For example, they recorded the pronotum and mesosternum as blackish instead of reddish. Therefore, in this study, a key based on the table published by Maldonado and Lozada (1992) was elaborated on the species of the genus, allowing a clearer-cut recognition of them.

On the other side, Kirkaldy (1909) created *Neotropiconyttus* as a new name for "*Amaurosphodrus* Stål, 1872" with [*N.*] *alboannulatus* as the type species of the genus, even though *Myocoris dama* had been described earlier (Burmeister, 1838). It is uncertain who first established the combination *Neotropiconyttus dama*, but the earliest reference to this combination is found in the catalog of Wygodzinsky (1949).

Descriptions of *N. dama* and *N. alboannulatus* were based on color features alone, and those of *N. heminigra* on color, shape, and measurements of various anatomical structures (Burmeister 1838; Stål 1855; Maldonado and Lozada 1992). Both male and female genitalia have remained undescribed for all species.

General appearance and coloration make the species of assassin bugs belonging to *Neotropiconyttus* mimetic to the true bugs *Monalonion* spp. (Hemiptera: Miridae), as well as with wasps belonging to Ichneumonidae and Braconidae (Hymenoptera). Moreover, some species of *Graptocleptes* and *Neotropiconyttus* are highly similar in shape and color. As to the living habitats of *Neotropiconyttus*, no details are included in their species descriptions.

Seeking to recognize the natural insect enemies of *Monalonion* spp. and their corresponding natural biology in cacao (*Theobroma cacao* L., Malvaceae) plantations in Southeastern Colombia, the research project "Study of diversity, population dynamic and biotic potential of predators and parasitoids controlling true bugs of the genus *Monalonion* Herrich-Schäffer, 1850 in cacao plantations in the states of Huila and Caquetá, Florencia" was carried out. In this work, the first record of the genus *Neotropiconyttus* for the Napo province in Colombia and the description of a new species of the genus are included.

Besides describing *Neotropiconyttus armandoi* sp. nov. and improving the knowledge of the species of *Neotropiconyttus*, photographs deploying the diverse coloration of the syntypes of *N. alboannulatus* and *N. dama*, are provided.

The female holotype of *N. heminigra* was not located in any collection. All information about the species is considered, following the original description by Maldonado and Lozada (1992).

Materials and methods

In 251 farms with cacao plantations in the states of Huila and Caquetá, Colombia, 5,401 Reduviidae specimens were collected, of which only one specimen matched the description of the genus *Neotropiconyttus*. The single specimen was collected on a leaf of a *T. cacao* tree. The individual was collected employing an entomological net, then placed into a 30 ml plastic bottle containing ethyl alcohol 96% and transported to Laboratorio de Entomología Universidad de la Amazonia (LEUA) in Florencia (Caquetá, Colombia). Curatorship of the specimen, which was point-mounted, was carried out following the protocols established in the LEUA insect collection.

Images of a female syntype of *Neotropiconyttus alboannulatus* (Stål, 1855) (Figs 1–4), deposited in the Swedish Museum of Natural History, Stockholm, Sweden (**NHRS**) were provided by Gunvi Lindberg with the copyright belonging to the NHRS. Three female syntypes of *Neotropiconyttus dama* (Burmeister, 1838), deposited in the Hemimetabola Collection of the MFNB, were directly examined and photographed by HRG-S (43–51) in 2015. The images were taken utilizing a Nikon D5200 digital camera with a Nikon Macro lens of 105 mm.

The identification of the specimen into the genus *Neotropiconyttus* was carried out employing the taxonomic keys proposed by Maldonado and Lozada (1992), Gil-Santana (2015), and Gil-Santana and Oliveira (2023). Additionally, comparisons of the specimen found in the current study with photographs of the female syntype of *N. alboannulatus* (Figs 1–4), available on the website of the NHRS (http://www2.nrm.se/en/het_nrm/a/neotropiconyttus_alboannulatus.html), and examination of female syntypes of *N. dama* deposited in the MFNB (Figs 43–51) by the second author (HRG-S) allowed confirm this finding.

Images and measurements of the type-specimen of *N. armandoi* sp. nov. described in this work were taken using a LEICA M205A stereomicroscope (Figs 5–16, 40–42, 56) and a HITACHI TM4000Plus II environmental scanning electron microscope (Figs 17–32). A distribution map of the species of the genus *Neotropiconyttus* was designed using of the software QGIS v. 3.26.2 (Fig. 52). Pygophore and aedeagus were drawn using the software CorelDRAW v. 2022 (Figs 33–39). All figures were prepared utilizing the software Photoshop 2023 v. 24.0.

For the morphological description, an Olympus SZ51 stereomicroscope was utilized. The pygophore was extracted employing forceps and pins and placed into a NaOH 20% solution for 24 hours. Dissected structures were then studied immersed in glycerol. After all dissections and imaging of the male genitalia portions, they were placed into a microvial attached to the bottom of the specimen pin. General terminology follows Schuh and Weirauch (2020). Male genitalia terminology follows Gil-Santana et al. (2013, 2017), Gil-Santana (2016), and Gil-Santana and Oliveira (2023). The holotype was housed in the LEUA Collection.

When describing label data, a slash (/) separates the lines, and a double slash (//) separates different labels. Comments or translations of label data into English are provided in square brackets ([]).

Results

Taxonomy

Subfamily Harpactorinae
Tribe Harpactorini

Genus *Neotropiconyttus* Kirkaldy, 1909

Neotropiconyttus Kirkaldy, 1909: 388 [as a new name for *Amaurosphodrus* Stål, 1872]; Wygodzinsky 1949: 42 [catalog]; Putshkov and Putshkov 1985: 53 [catalog]; Maldonado 1990: 241 [catalog]; Maldonado and Lozada 1992: 162 [comments on diagnostic characteristics], 165 [in key]; Gil-Santana 2015: 30 [citation as a wasp-mimetic genus], 37 [in key]; Gil-Santana 2016: 92 [citation as a wasp-mimetic genus]; Gil-Santana et al. 2017: 41 [citation as a wasp-mimetic genus]; Gil-Santana and Oliveira 2023: 164 [citation as a wasp-mimetic genus], 200 [in key].

Type species. [*Zelus*] *alboannulatus* Stål, 1855 by original designation, Kirkaldy, 1909: 388.

Diagnosis. *Neotropiconyttus* may be separated from other wasp-mimicking genera by the following set of characters: Head fairly setose to very densely setose, especially on ventral and postocular portions, postantennal spines curved and directed forward; pronotum not inflated; scutellum visible from above; fore femora thicker only basally; fore tibiae straight.

Description. Integument smooth. ***Head*:** gibbous, large, approximately as long as wide across eyes (neck excluded); with sparse long and short, straight or somewhat curved blackish setae; the latter much denser, forming pubescence of long blackish thick setae on postocular portion and gula. Clypeus straight in dorsal view, curved in lateral view. Antennal insertion at level of upper 1/3 of eye; scape straight, shiny; pedicel straight or somewhat curved; basiflagellomere slightly curved or straight; in [known] males somewhat thickened in basal ~ 1/2; distiflagellomere slightly curved and thinner than the other segments. Postantennal spines strongly curved and directed forward. Eyes globose, glabrous, projecting laterally, prominent in dorsal view, close to dorsal margin of head; reaching or not reaching ventral margin of head. Interocular sulcus thin and shallow, curved laterally. Just anterior to it, on midline, a small oval fossa followed anteriorly by a very short thin shallow median sulcus, which sometimes is not evident. Ocelli and portion between them elevated, the former somewhat closer to eyes than to each other. Labium stout, curved, reaching prosternum approximately at proximal part of its distal 1/3; segment II (first visible) thickest and longest, straight, reaching level of distal 1/3 of eye or its posterior margin; segment IV shortest, triangular, tapering. Neck thin. ***Thorax:*** Anterior collar narrow; anterolateral angles prominent, subtriangular. Transverse sulcus not deep, interrupted before middle by a pair of submedian shallow carinae; slightly curved laterally. Mid-longitudinal sulcus on fore lobe of pronotum moderately deep; disc of hind lobe smooth; lateral longitudinal sulci well marked at posterior 1/2 to posterior 2/3 of hind lobe of pronotum. Humeral angle slightly or not elevated, rounded at lateral margin. Scutellum with margins elevated, apex rounded. Legs: coxae globose; femora and tibiae slender, elongated, and generally straight. Fore femur shorter than head and pronotum together, thickened at basal portion and somewhat curved at midportion; middle and hind femora slightly thickened basally, sometimes dilated subapically and slightly narrower approximately at median portion where distal pale annuli may be located; apices of all femora with a pair of lateral small tubercles. Fore tibiae thickened apically, where there is a dorsal spur and a mesal comb. Hemelytra long, surpassing abdomen by ~ 1/2 length of membrane. ***Abdomen*:** elongated; spiracles rounded.

Neotropiconyttus alboannulatus **(Stål, 1855)**

Figs 1–4

Zelus alboannulatus Stål, 1855: 189 [description].

Amaurosphodrus albo-annulatus; Stål 1867: 297 [description], 1872: 82 [catalog]; Lethierry and Severin 1896: 178 [catalog]; Champion 1899: 283 [citation, comments], tab. XVII, figs 15, 15a.

Zelus albo-annulatus; Walker 1873: 136 [catalog].

Neotropiconyttus alboannulatus; Kirkaldy 1909: 388 [as the type of *Amaurosphodrus* Stål, 1872 in the new combination]; Wygodzinsky 1949: 42 [catalog]; Maldonado 1990: 241 [catalog]; Maldonado and Lozada 1992: 165 [comparison with other species of the genus based on color characteristics]; Froeschner 1999: 207 [catalog].

Distribution. Colombia.

Notes. *Neotropiconyttus alboannulatus* was described based on (a) female specimen (s) from Colombia (Stål 1855) (Figs 1–3). The female “Typus” currently deposited in NHRS is considered a syntype, according to Art. 73.2 of the ICZN (1999). This specimen has a label with the locality “Remedios”, written by Stål (1855) as the original information. Therefore, according to Art. 76.1 of the ICZN (1999), “Remedios” is considered the type locality of *N. alboannulatus*. Further, the species was also recorded in Mexico (Walker 1873) and Panama (Champion 1899). The latter author observed only females similar to the type specimen.

Morphological remarks. Length ~ 9.5 mm. The so far recorded specimens are generally blackish with small whitish annuli on median portion of femora, somewhat larger on hind legs, and the anterior ~ 1/2 of the ventral surface of the abdomen reddish.

Neotropiconyttus armandoi **Gamboa & Gil-Santana, sp. nov.**

https://zoobank.org/E42F47F0-E9D1-492D-9D88-9E02163BA2D5

Figs 5–42

Type material examined. *Male Holotype*. Colombia: Caquetá, Morelia, Vda. Caldas, Fca. El Porvenir; 01°29'57"N, 75°44'03"W, 272 m, 05-Dec.-2021, A. Gamboa// Captura con jama entomológica en dosel (hoja) de [Collected with entomological net in canopy (leaf) of] *Theobroma cacao* (Malvaceae)-cacao//LEUA-42920//[red printed label:] HOLOTYPE (LEUA).

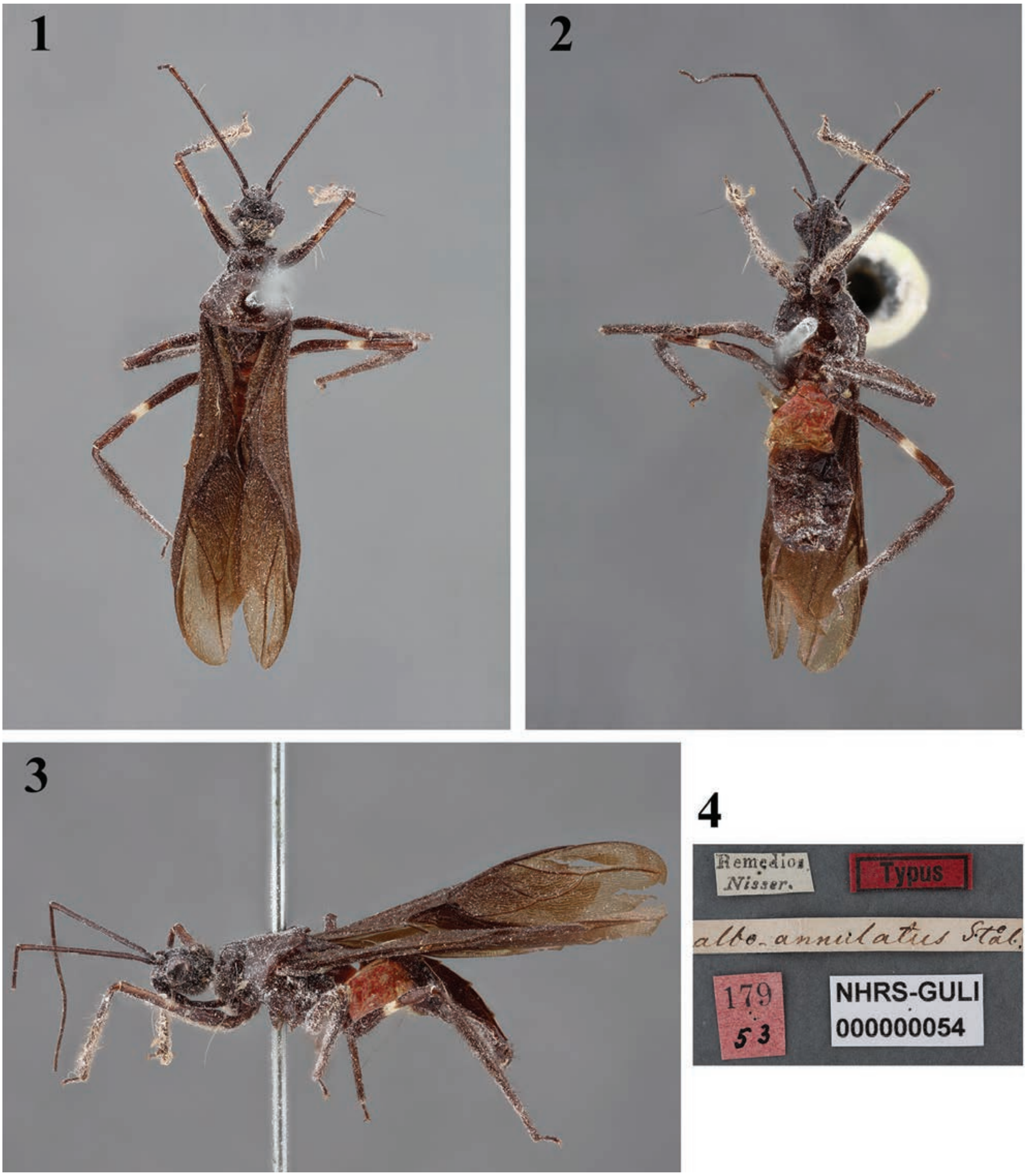

Figures 1–4. *Neotropiconyttus alboannulatus* (Stål, 1855), syntype, female, deposited in NHRS, catalog number NHRS-GULI000000054, photographs provided by Gunvi Lindberg, 2023 of Naturhistoriska Riksmuseet [Swedish Museum of Natural History] and made available by this institution under the Creative Commons Attribution 4.0 International Public License, CC-BY 4.0, https://creativecommons.org/licenses/by/4.0/legalcode **1** dorsal view **2** ventral view **3** lateral view **4** labels.

Diagnosis. *Neotropiconyttus armandoi* sp. nov. can be distinguished from the congeneric species by the orange pronotum with darker orange symmetrical spots on the anterior lobe (Fig. 10).

Description. Male. Measurements (mm): Body length: from frons to tip of hemelytra 11.52; to tip of abdomen 8.42. ***Head:*** length 1.74; anteocular portion

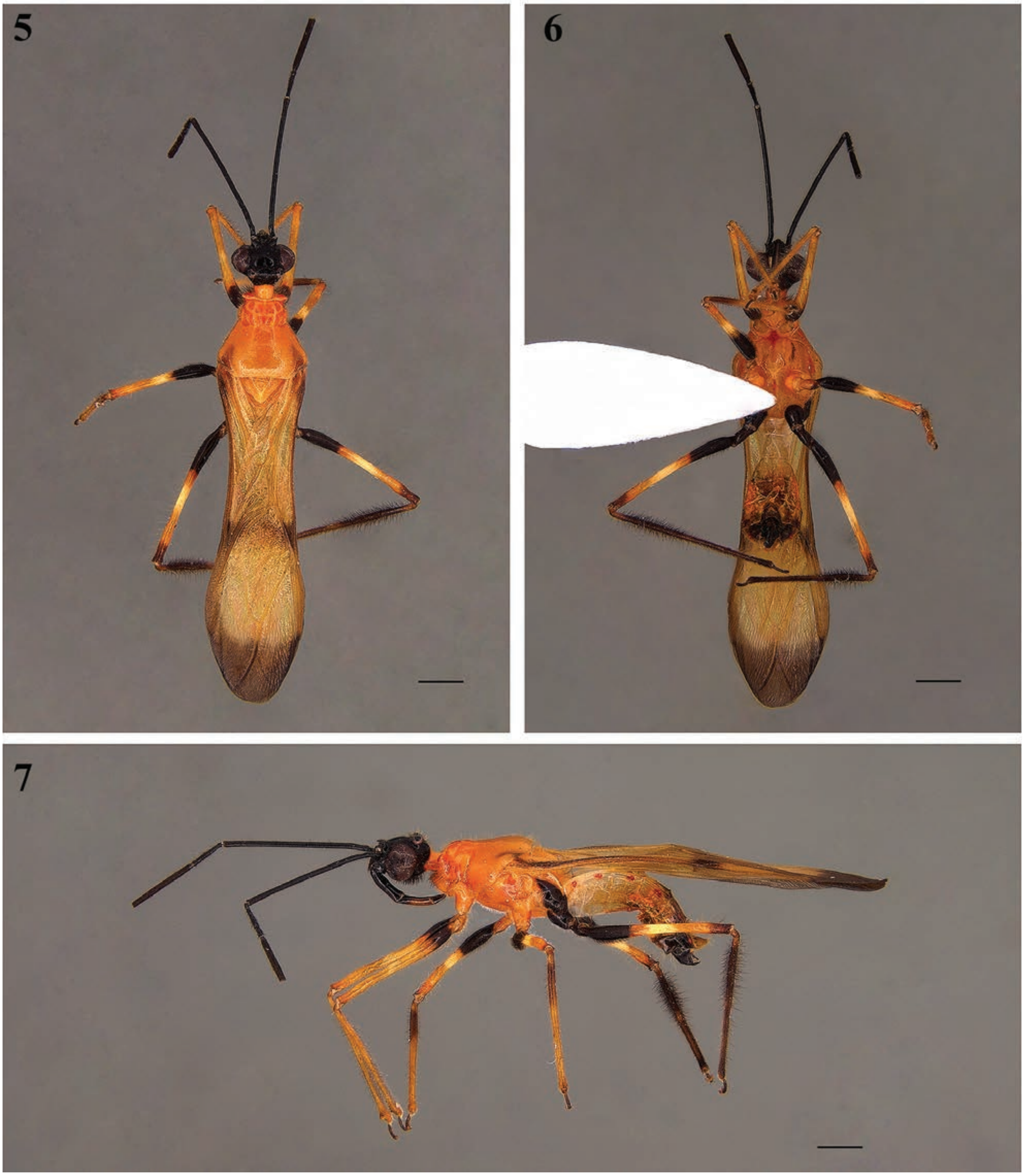

Figures 5–7. *Neotropiconyttus armandoi* sp. nov., holotype, male habitus **5** dorsal view **6** ventral view **7** lateral view. Scale bars: 1.0 mm.

(lateral view) 0.39; postocular portion (lateral view) 0.49; head width across eyes 1.56; interocular distance 0.76; eye width 0.41; eye length 0.71; ocellar tubercle width 0.26. Antenna: scape length 3.52; pedicel length 0.86. Labium (lateral view): visible segment II length 0.98; labial segment length III 0.68; labial segment length IV 0.40. ***Thorax:*** pronotum length (at midline) 1.95; pronotum maximum width 2.23; scutellum length (at midline) 0.59. Hemelytron: total length 8.28; membrane 4.79. Legs (lateral view): foreleg: coxa 0.64; trochanter 0.12;

femur 3.31; tibia 3.41; tarsus 0.42; middle leg: coxa 0.26; trochanter 0.21; femur 2.76; tibia 3.32; tarsus 0.45; hind leg: coxa 0.27; trochanter 0.17; femur 3.74; tibia 4.73; tarsus 0.51. ***Abdomen:*** total length (ventral view, at midline, from anterior margin of sternite II to posterior border of genitalia): 3.88; maximum width 1.49.

Coloration: *Head:* mostly black; neck orange; ocellar tubercle paler around each ocellus; eyes dark brown (Figs 5–9); antenna [distal portion absent]: scape, pedicel, and basal portion of first flagellomeres black (Figs 5–7); labium: visible segments: II black, III mostly pale brownish, blackish basally and slightly darker at apex, IV dark brown (Fig. 9). ***Thorax:*** mostly orange, somewhat paler at pleural and sternal areas; pronotum, collar, anterior lobe of pronotum with faint reddish tinge; darker orange symmetrical spots (dorsal part) and small reddish dots (lateral and ventral) on anterior lobe; posterior lobe of pronotum orange with inner portions of humeral areas pale brown; scutellum pale orange; mesepisternum orange with small lateral reddish dots and long reddish spot anteroventrally; metepisternum orange anteriorly and black posteriorly, above the hind coxa (Figs 10, 11). Hemelytron: generally orange, somewhat translucent, with anterobasal angle, costal margin and a narrow transversal stripe, fainter at median portion and approximately apical ~ 1/4 of membrane pale blackish (Figs 5–7). Legs: fore and middle coxae orange and trochanters orange basally and darker distally; hind coxae and trochanters blackish. Femora generally orange; from fore to hind femora basal portion progressively more extensively dark brown to blackish; approximately at middle, a submedian ill-defined narrow pale annulus; apices somewhat darkened, more extensively on hind femora. Fore and middle tibiae orange, the former with small basal and distal dark markings, latter with extreme base and a large subbasal portion dark; hind tibiae pale blackish, apex paler; tarsi dark (Figs 7, 14–16). ***Abdomen*:** pale orange (sternites II–IV), darker orange (sternites V and VI), and blackish (sternite VII), spiracles with the area surrounding them reddish, pygophore blackish (Figs 12, 13).

Structure: *Head*: 1.10× as long as wide, labrum triangular 1.38× as long as wide, postclypeal suture deep, frons 0.51× as wide as head width (anterior view), antennal sclerite slightly raised, postantennal spine curved forward, small, apex acute. Eyes large, protruding, glabrous, rounded, and ellipsoid in dorsal and lateral views, respectively, reaching closer and beyond dorsal and ventral margins of the head; postocular region short; ocelli and area between them elevated, the former much closer to eyes than to each other; ellipsoid on tubercles, tubercles anteriorly bounded by postocular suture, which is thin and shallow, curved laterally; just anterior to it, on midline, a small oval fossa; mandibular plate triangular, maxillary plate slightly bulged, postgena reduced, flat posteriorly, gula slightly swollen (Figs 8, 9); antenna: scape cylindrical, long, somewhat curved; 2.02× as long as head length, base flattened; pedicel 0.24× as long as scape, short, thinner basally; basal portion of basiflagellomeres [the portion still present in the holotype] cylindrical, straight, slightly thicker than scape; remaining portions of basiflagellomere and both distiflagellomeres absent. Labium: [visible] segment II cylindrical, basally curved, 0.47× as long as labium; III slightly curved and reduced, 0.33× as long as labium; IV conical, 0.19× as long as labium. ***Thorax*:** collar, 0.02× as long as pronotum at midline, lateral areas longer, subtriangular, in dorsal view; pyramid-shaped in lateral view; anterior lobe of pronotum 0.30× as long as pronotum total length, with mesial longitudinal suture deep, absent on hind lobe; lateral portions of anterior lobe

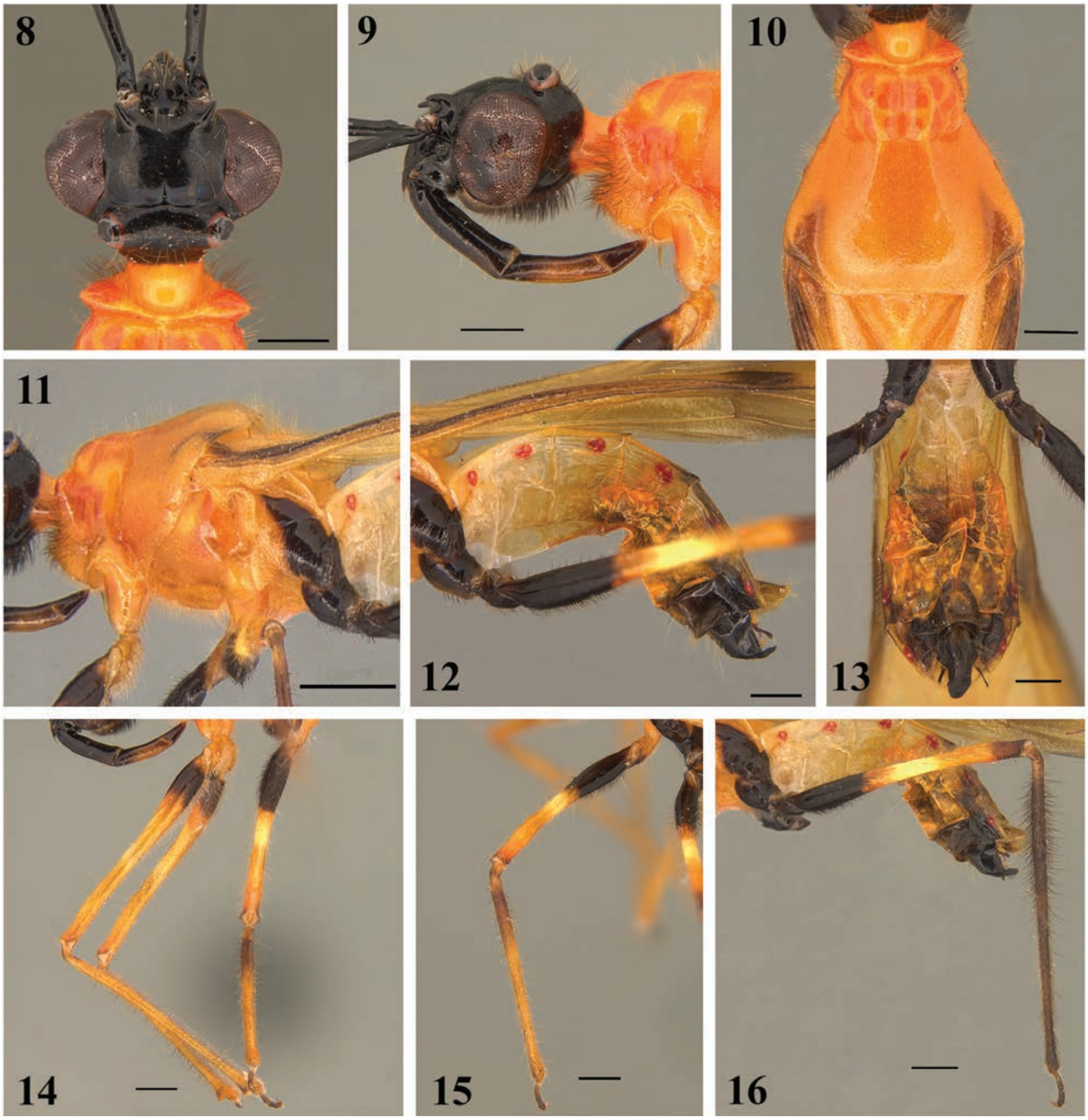

Figures 8–16. *Neotropiconyttus armandoi* sp. nov., holotype, male **8, 9** head **8** dorsal view **9** lateral view **10, 11** thorax **10** dorsal view **11** lateral view **12, 13** abdomen **12** lateral view **13** ventral view **14** foreleg and a middle leg **15** middle leg **16** hind leg. Scale bars: 1.0 mm (**11**); 0.5 mm (**8–10**, **12–16**).

slightly swollen; transverse sulcus of pronotum not deep, interrupted submedially by a pair of shallow carinas straight and curved between and laterally to the latter, respectively. Hind lobe with disc smooth, lateral longitudinal sulci well marked at posterior 1/2 to 2/3; humeral angle moderately elevated, rounded at lateral margin. Scutellum with margins elevated, apex thin, acutely pointed. Pleural suture long; epimeron concave; mesoepisternum swollen; metaepisternum rhomboid (lateral view); metepimeron medial lobe narrowing posteriorly (Figs 10, 11). Hemelytron: 2.13× as long as total abdomen length; membrane ellipsoid, reaching 0.57× hemelytron length total, 2.21× as long as width. Legs: coxa truncated cone-shaped; trochanters, slightly curved; femora enlarged at

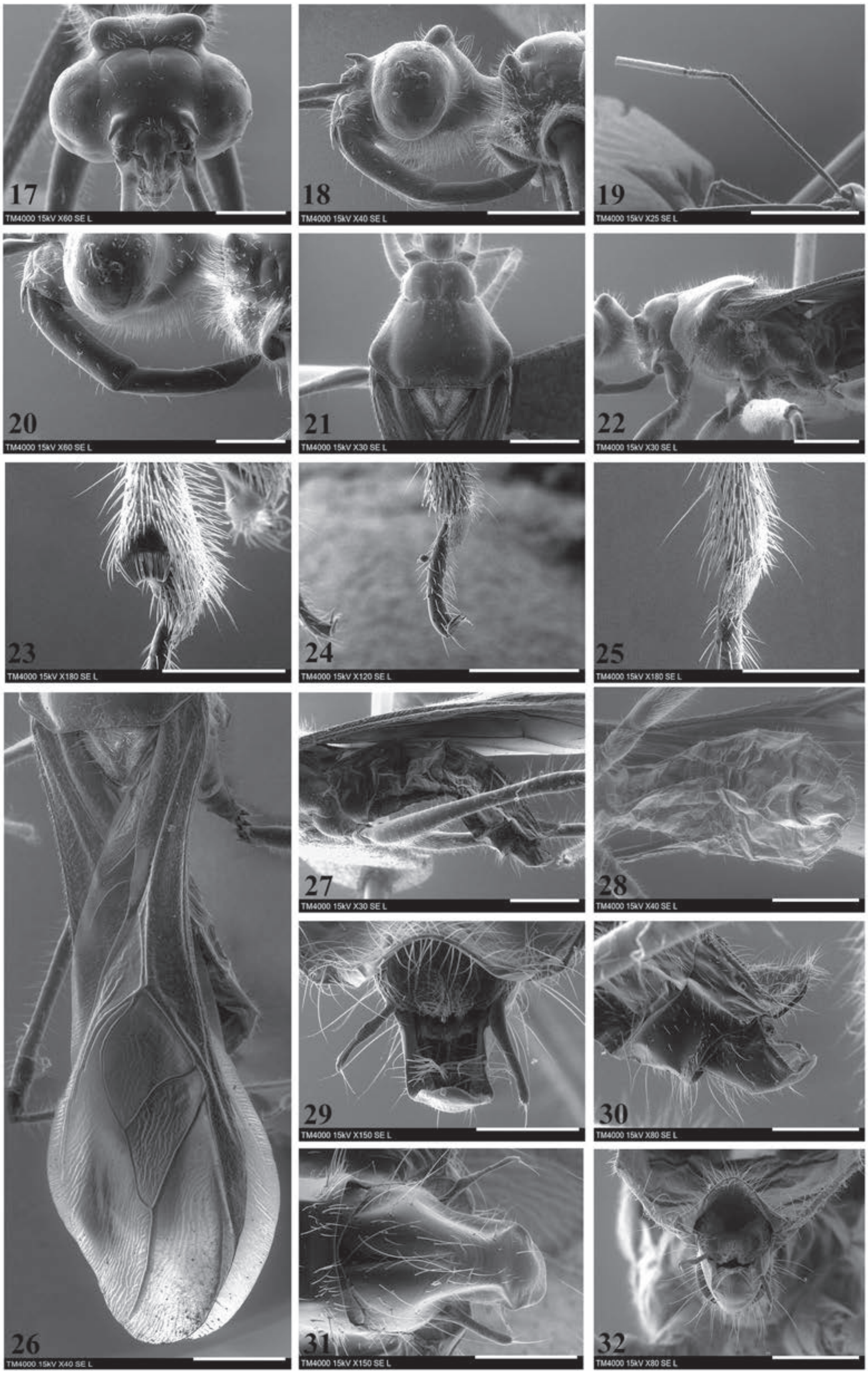

Figures 17–32. *Neotropiconyttus armandoi* sp. nov., holotype, male **17** dorso-anterior view head **18** lateral view head **19** antenna **20** labium and ventral portion of head and, lateral view **21, 22** thorax **21** dorsal view, **22** lateral view **23–25** inner surface of apical portion of tibiae **23** fore tibia **24** middle tibia **25** hind tibia **26** posterior margin of pronotum scutellum and hemelytra **27** lateral view abdomen **28** ventral view abdomen **29–32** pygophore **29** dorsal view **30** lateral view, including the VII and posterior margin of VIII abdominal segments **31** ventral view **32** posterior view, including the dorsal portion of VII abdominal segment. Scale bars: 300 µm (**23, 25, 29, 31**); 400 µm (**24**); 500 µm (**17, 20, 30, 32**); 1.0 mm (**18, 21, 22, 26–28**); 2.0 mm (**19**).

basal portion and slightly thickened distally, apices with short anterior and posterior projections; tibia generally cylindrical; fore tibia slightly curved basally, enlarged apically where there is a small spur and a mesial comb; middle tibiae straight, slightly thickened at apex; hind tibiae somewhat enlarged at subbasal 1/3; tarsi thickening distally towards the apex (Figs 14–16). ***Abdomen*****:** 1.98× as long as pronotum total length. Dorsal aspect, segments II–VII, each from 0.12× to 0.17× as long as abdomen total length, and pygophore 0.09× as long as abdomen total length. Posterior margin of segment VIII exposed ventrally, wider laterally, and shorter at median portion (Figs 12, 13).

Vestiture: ***Head*****:** labrum glabrous; clypeus, gena, mandibular plate, maxillary plate, and buccula with suberect and slightly pale curved setae, on clypeus distributed on the lower 2/3; frons mostly glabrous with three setae between postantennal spines; vertex mostly glabrous with very few pale setae near margins surrounding eyes; ocellar tubercles with suberect, slightly curved pale and some darkened setae; postocular region with few erect and curved pale and some darkened setae on dorsal and lateral areas; neck glabrous; gula with thick and curved and denser blackish setae on median portion, forming a pubescence (Figs 17, 18). Antenna: scape with few slightly curved, suberect setae, shorter than scape width; pedicel, except the glabrous base, covered by numerous erect and suberect, short and long, straight and curved dark setae, length subequal to pedicel diameter, one seta longer and thinner than others on apex (Fig. 19). Labium: segment II (first visible) with few curved pale setae, on anterior portion, although variable in their length, all shorter than segment diameter; III and IV with very few curved, short, pale setae (Fig. 20). ***Thorax*****:** anterior margin of prothorax, including collar, propleura and sternal portion, densely setose, forming a pubescence of long, thin, somewhat darkened setae; midline of collar with long sparser pale setae; remaining portions of pronotum generally covered by scattered thin, moderately long, curved or straight pale setae, somewhat more numerous on posterior margin; anterior portions of propleura with numerous long, thin, darkened setae; proepimeron setose; mesoepisternum with setae, denser and longer mesially; mesepimeron covered with very dense short setae; metepisternum with denser setae ventrally (Figs 21, 22). Hemelytron: clavus with short, pale, decumbent, curved setae, which are more numerous on basal portion; corium with similar setae more numerous over veins; membrane glabrous (Fig. 26). Legs: coxae: setae suberect, curved, at least with three different sizes, maximum length 1/2 of coxa diameter in lateral view, on foreleg very numerous on posterior surface, on middle and hind legs very numerous on anterior and posterior surface; trochanter with numerous setae on anterior, mesial, and posterior surfaces, maximum length subequal to coxa diameter in lateral view. Femora, with setae of at least three lengths, some longer than femur width; on basal portion, they are more numerous, forming a pubescence of dense, erect, brush-like setae ventrally; laterally few setae. Tibia covered by many suberect, subdecumbent, and decumbent setae, except basally; setae longer and more abundant proximally, fore, middle, and hind tibiae with long setae densely packed on the tibia apex in medial surface (Figs 23–25). Setae on tarsi suberect, several of which longer than twice tarsus diameter. ***Abdomen*****:** lateral margin of tergites II–VI with very few, short, curved, and suberect setae; tergite VII with numerous setae of different sizes; sternites II–VII with setae on ventral side of different sizes, curved, and suberect, some setae slightly shorter than parameres length, sternite VIII glabrous (Figs 27–32).

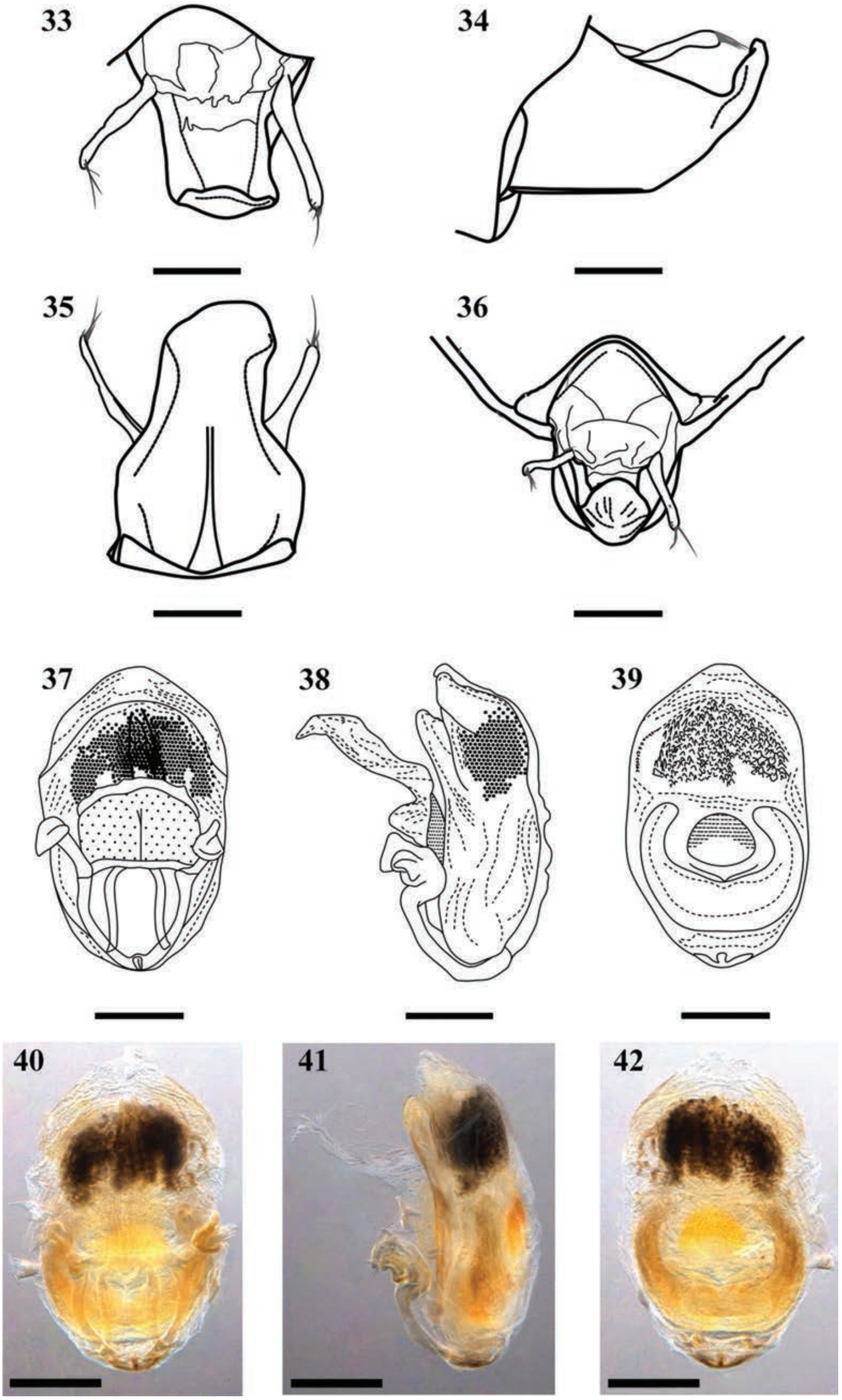

Figures 33–42. *Neotropiconyttus armandoi* sp. nov., holotype, male genitalia **33–36** pygophore and parameres, general outline **33** dorsal view **34** lateral view **35** ventral view **36** posterior view **37–39** aedeagus **37** dorsal view **38** lateral view **39** ventral view **40–42** aedeagus with endosoma completely inflated **40** dorsal view **41** lateral view **42** ventral view. Scale bars: 0.3 mm (**36**); 0.2 mm (**33–35, 37–42**).

Genitalia: Pygophore: mostly black, in dorsal view: 1.12× as long as maximum (anterior) width, concave, slightly narrower in middle and posterior portions; in ventral view wider anteriorly, anterior surface 0.67× as wide as total length, ventrally swollen, with anterior mesial folds extending posteriorly for 0.43× the total length of pygophore; in lateral view, scalene-triangle-shaped, subtrapezoidal, posterior margin upwards. Vestiture: setae yellowish orange, curved, subdecumbent, and with different lengths, several slightly longer than 0.75× pygophore length (lateral view), more numerous on ventral surface (Figs 29–36). Parameres: dark brown and black, symmetrical, elongated; right paramere broad basally, cylindrical both proximal and distally, rounded apically, apex with erect and slightly curved setae (~ 8) of different lengths, distal 1/2 with a dorsal seta decumbent and short; left paramere slightly warped from drying (Figs 29–36). Phallus: flat dorsoventrally. Articulatory apparatus (dorsal view): basal plate, in dorsal and lateral views, with subrounded arms and with 1/2 to 1/3 of the length in comparison of that of the phallus, inflected distally, basal plate bridge 0.58× as long as right arm of the articulatory apparatus (Figs 37–42). Dorsal phallothecal plate: elongated, weakly sclerotized, subrectangular in dorsal view, elongated posteriorly, slightly curved anteriorly, proximal part with punctures, distal part smooth, laminate and translucent, and with wrinkled margins; struts with subparallel arms slightly curved, joined distally (Figs 37–42). Endosoma: endosoma wall translucent, faintly rugous, slightly wrinkled apically. Three processes of endosoma: a large pale U-shaped to subrounded basal process formed by diffuse thickening; a median subspherical process lying between the lateral arms of the U-shaped basal process and formed by a grouping of small thickenings and a subdistal large darkened endosoma process formed by numerous small acute processes (Figs 37–42).

Etymology. *Neotropiconyttus armandoi* sp. nov. is named in memory of Armando Gamboa Torres (1955–2007), father of the first and third authors herein. Armando was a primary and secondary school teacher who, every day after his long working hours, devoted his time to agriculture. As time went by, he gathered an important set of empirical knowledge of crops in traditional agroecosystems of the Amazon region, such as banana (*Musa* spp. - Musaceae), cassava (*Manihot esculenta* Crantz - Euphorbiaceae), sugarcane (*Saccharum officinarum* L. - Poaceae), and corn (*Zea mays* L. - Poaceae). Thereby, Armando ingrained his interest in agriculture throughout his life in all “his” kids.

Distribution. Colombia (Caquetá).

Type locality. COLOMBIA, Caquetá, Morelia, Vda. Caldas, Fca. El Porvenir, 01°29'57"N, 75°44'03"W 272 m.

Neotropiconyttus dama **(Burmeister, 1838)**

Figs 43–51

Myocoris dama Burmeister, 1838: 105 [description]; Walker 1873: 130 [catalog].

Amaurosphodrus dama; Stål 1872: 82 [catalog]; Lethierry and Severin 1896: 178 [catalog].

Neotropiconyttus dama; Wygodzinsky 1949: 42 [catalog]; Maldonado 1990: 241 [catalog]; Maldonado and Lozada 1992: 165 [comparison with other species based on color characteristics].

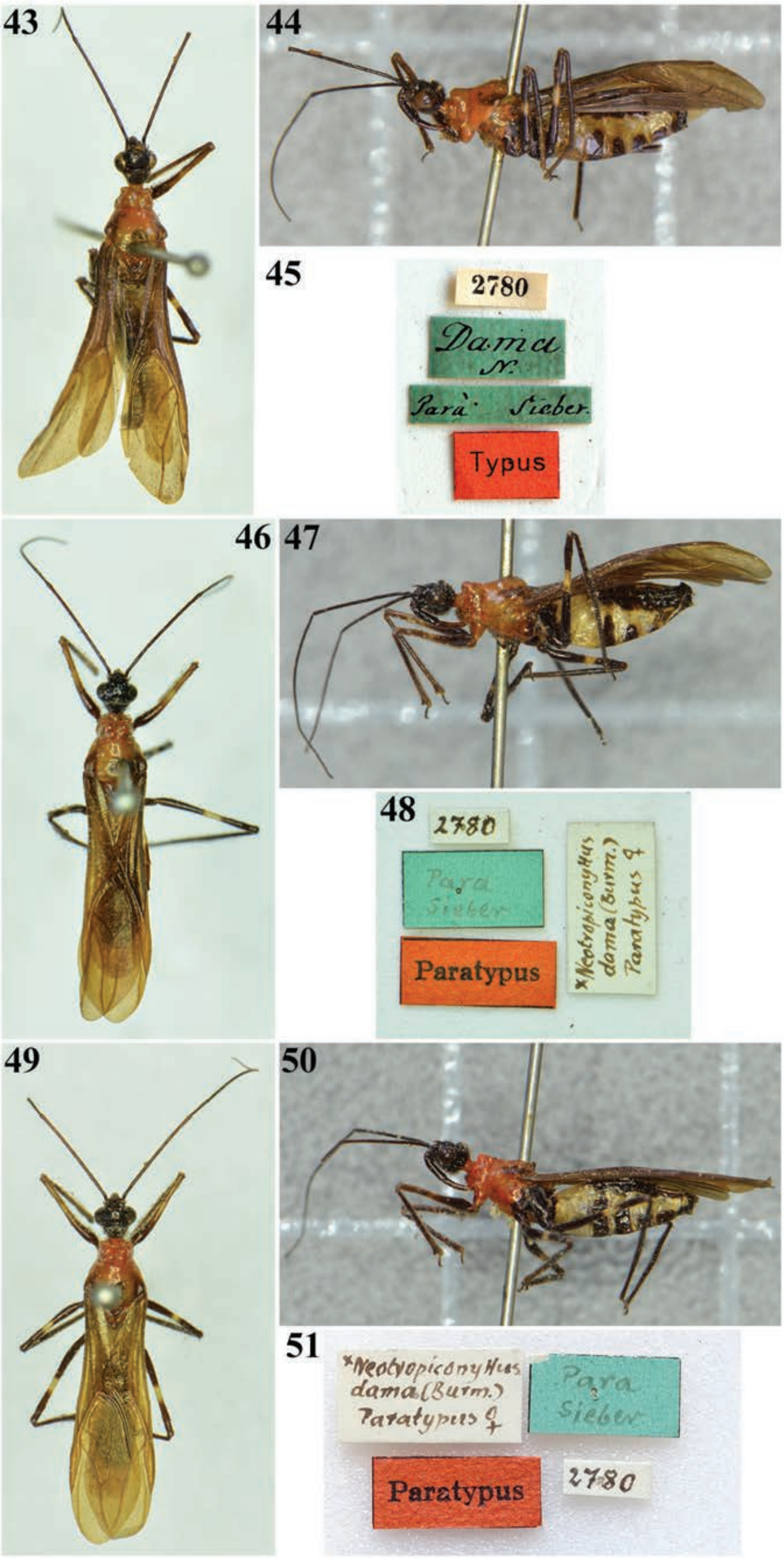

2780
Dama
N.
Parà · Sieber
Typus

2780
Para
Sieber
Paratypus
×Neotropiconyttus
dama (Burm.)
Paratypus ♀

×Neotropiconyttus
dama (Burm.)
Paratypus ♀
Para
Sieber
Paratypus
2780

Figures 43–51. *Neotropiconyttus dama* (Burmeister, 1838), syntypes, females **43–45** specimen labeled as "Typus" **43** dorsal view **44** lateral view **45** labels **46–51** specimens labeled as "Paratypus" **46** dorsal view **47** lateral view **48** labels **49** dorsal view **50** lateral view **51** labels.

Distribution. Brazil.

Type material examined. *Myocoris dama* Burmeister, 1838. Brazil: three female syntypes: [printed label] 2780 // [handwritten green label] *Dama* / *N*. // [handwritten green label] Parà [Pará] Sieber // [printed red label] Typus; [handwritten] 2780 // [handwritten] ^{x}*Neotropiconyttus* / *dama* (Burm.) / Paratypus ♀ // [handwritten green label] Para / Sieber // [printed red label] Paratypus; [handwritten] 2780 // [handwritten] ^{x}*Neotropiconyttus* / *dama* (Burm.) / Paratypus ♀ // [handwritten green label] Para / Sieber // [printed red label] Paratypus (MFNB).

Neotropiconyttus dama was described based on specimens from the State of Pará, Brazil (Burmeister 1838). In the MFNB, there are three female type specimens of *N. dama*. One specimen is labeled as "Typus" (Figs 43–45); the others are labeled as "Paratypus" (Figs 46–51). All of them are considered as syntypes in this work, following Art. 73.2 of the ICZN (1999). Notably, all the syntypes have a green label stating, besides the name of the Brazilian state of Pará, the name of "Sieber." Friedrich Wilhelm Sieber was a servant and preparator of Johann Centurius Count von Hoffmannsegg, who obtained permission from the King of Portugal to visit Brazil to collect insects. Leaving Lisbon in 1801, Sieber went to the Province of Pará, where he stayed for 12 years, collecting not only in the vicinity of Belém but also in different areas of the provinces of Pará and Rio Negro (currently, state of Amazonas) (Papavero 1971). Therefore, the precise type locality of the species in this large region remains uncertain.

Morphological remarks. General length 12–12.5 mm. General color blackish; labium with distal 1/2 of second and third visible labial segments variably paler; neck, prothorax, and mesothorax mostly reddish; humeral angles, posterior margins of mesopleura and mesosternum, and most of metapleura dark to blackish. Legs: except for fore coxae and a portion of fore trochanters, which are reddish, the remaining portions of the legs mostly dark to blackish; dorsal portion of distal ~ 2/3 of fore femora paler, and ill-defined pale yellowish annuli; middle and hind femora with submedian distal pale whitish to yellowish annuli; hemelytra darkened. Abdomen: sternites mostly yellowish with the following portions or markings blackish: narrowly basally on sternite II and adjacent connexival portion; on segments IV–VII: connexivum and shortly adjacent portion, median markings of variable extension on respective sternites, and genitalia.

Key to species of *Neotropiconyttus*

1 Anterior lobe of pronotum orange with darker orange symmetrical spots (Fig. 5) .... ***N. armandoi* sp. nov.**
– Anterior lobe of pronotum black or reddish (Figs 1, 43, 44, 46, 47, 49, 50)... **2**
2 Posterior lobe of pronotum black and ivory white .... ***N. heminigra***
– Posterior lobe of pronotum entirely black or reddish with humeral angles dark to blackish (Figs 1, 43, 44, 46, 47, 49, 50) **3**
3 Pro- and mesothorax mostly reddish or orange, abdomen mostly yellow to pale whitish, segments IV–VII with connexivum, large median dark markings on sternites, and genitalia blackish (Figs 43, 44, 46, 47, 49, 50) .... ***N. dama***
– Thorax entirely black, abdomen entirely reddish at anterior ~ 1/2 and posteriorly blackish (Figs 1–3) .... ***N. alboannulatus***

Discussion

Identification

Neotropiconyttus, *Myocoris*, *Xystonyttus*, *Graptocleptes*, *Hiranetis*, *Parahiranetis*, and *Quasigraptocleptes* can be recognized by following the wasp-mimic Harpactorini key of Gil-Santana and Oliveira (2023). The remarkable similarity in shape, coloration, size, and setosity among the specimens representing the genera mentioned above has led to errors in the identification and cataloging at several entomological collections (personal observation of the first two authors), and unexpected synonymies, such as that recorded by Gil-Santana et al. (2013).

The three previously recognized species of *Neotropiconyttus* differ in coloration on the pronotum, mesosternum, mesopleuron, fore trochanter, hemelytron, and abdomen (Maldonado and Lozada 1992). A taxonomic revision of the genus based on more anatomical characters would be necessary to delimit the species better. We suggest exploring a new set of characters that could be employed to describe or redescribe the species, including measurements, detailed coloration, and genitalia traits.

All species of *Neotropiconyttus*, including *N. armandoi* sp. nov., were described based on specimens from a single locality and few additional specimens were observed after the original descriptions (e.g., *N. alboannulatum* by Champion 1899). This circumstance adds some taxonomic issues since population variation could not be recorded. The scarce data regarding the distribution of *Neotropiconyttus* species (Fig. 52) is due to sampling bias. More collecting effort is necessary to better understand the distribution and dispersion of the species.

Habitat

Neotropiconyttus armandoi sp. nov. is only known from the type locality in Morelia, Caquetá, Colombia, in the transition zone between Cordillera Oriental (eastern mountain range) and the Amazonian basin, corresponding to the Napo province of Colombia. The previous three recognized *Neotropiconyttus* species are recorded from localities in Brazil (Pará), Perú (Iscozacin), and Colombia (Remedios, Antioquia). Morelia, Pará, and Iscozacin correspond to localities in the provinces of Napo, Tapajós-Xingú, and Yungas, respectively, in the Amazonian subregion; and Remedios corresponds to the Magdalena province, in the Caribbean subregion (Fig. 52) (Morrone 2014).

The type locality of *Neotropiconyttus armandoi* sp. nov. is part of one of the ecoregions with the highest deforestation areas, in which the forest is felled and burned to establish introduced pastures for livestock. In this ecoregion, there is a prevailing need to recognize insect diversity, understand the impacts of anthropic activities on this biological group, and design and implement environmental conservation strategies.

The only known individual of the species was associated with an agroforestry system that includes trees and bushes, such as *Theobroma cacao* L. (Malvaceae), *Eugenia stipitata* McVaugh (Myrtaceae), and *Musa paradisiaca* L. (Musaceae), bordered by crops of *Saccharum officinarum* L. (Poaceae) and *Brachiaria decumbens* Cv. Basilisk (Poaceae) (Figs 53, 54). This ecosystem has

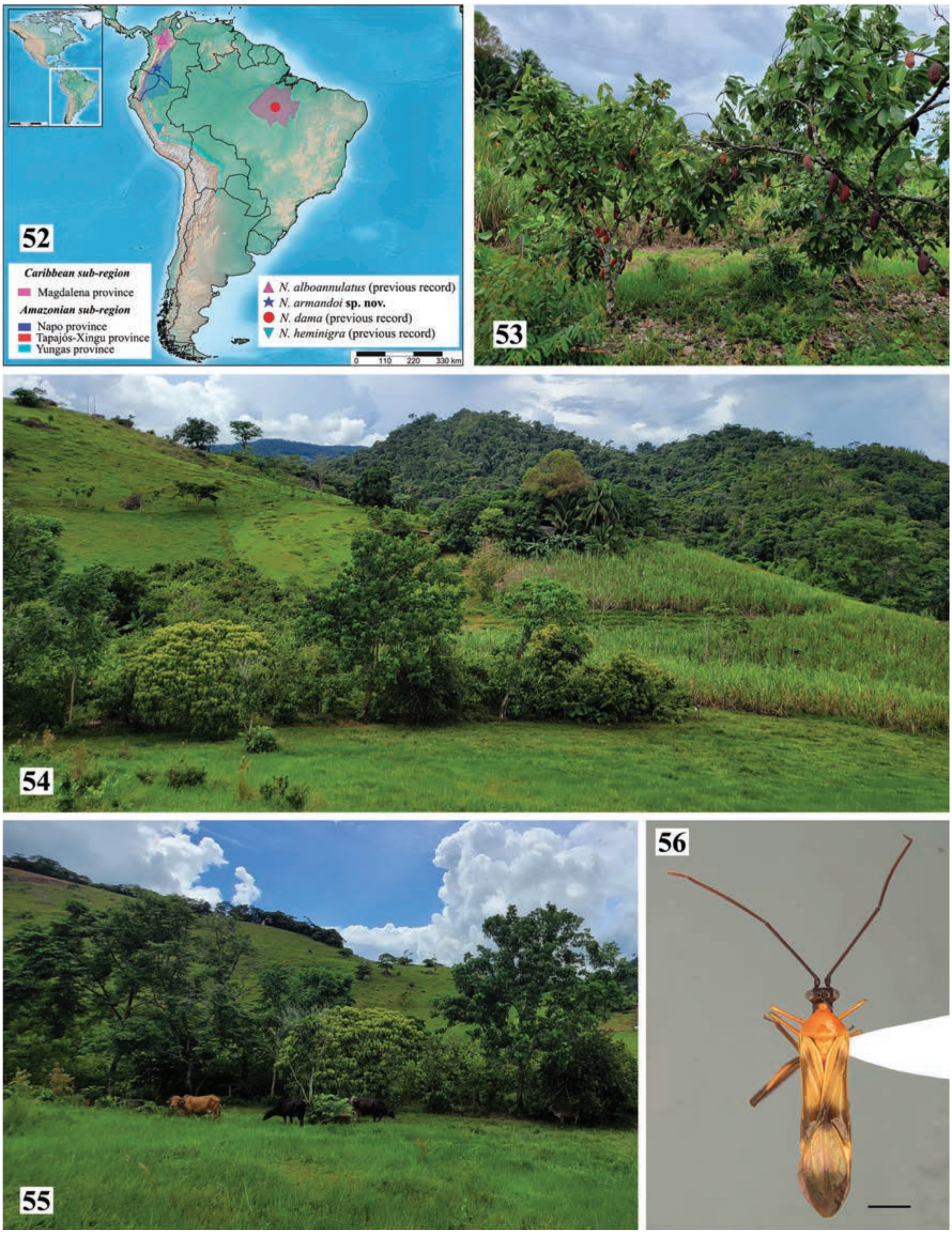

Figures 52–56. *Neotropiconyttus armandoi* sp. nov., habitat **52** geographical distribution of *Neotropiconyttus* species **53** cacao agroecosystem (type locality) **54** adjacent agroecosystems of *Saccharum officinarum* (Poaceae) and *Brachiaria decumbens* (Poaceae) **55** live fence with native trees and shrubs **56** *Monalonion dissimulatum* Distant, 1883, male habitus. Scale bar: 2.0 mm.

ecological connectivity through living fences in riparian vegetation (native trees and shrubs) of a lotic ecosystem (Quebrada La Sardina) (Fig. 55).

The *Neotropiconyttus armandoi* sp. nov. individual was collected inside an agroforestry system, standing on a *T. cacao* tree leaf near the fruits of this crop, in which individuals of the true bugs of the genus *Monalonion* feed, with a predominance of the species *Monalonion dissimulatum* (Fig. 56). The astonishing similarities between the two species regarding size, shape, and coloration characters prompted the inference of mimicry between *Neotropiconyttus armandoi* sp. nov. and *M. dissimulatum*.

Acknowledgements

To Yennifer Carreño, Mauricio Parada, Juan Arcos, and Éric Córdoba for their support in taking photographs and preparing the images for publication. To Lizeht Gamboa for the administrative support during the execution of the Research Project. To the Supervision Support Group of the Research Project, including Juan Suárez, Karen Obregón, Paulo Murcia, Olga González, and Diego Vega. We also especially thank Gunvi Lindberg (NHRS) for the photographs she provided.

Additional information

Conflict of interest

The authors have declared that no competing interests exist.

Ethical statement

No ethical statement was reported.

Funding

We thank the Ministry of Science, Technology and Innovation (Ministerio de Ciencia, Tecnología e Innovación) – MINCIENCIAS and the General Royalty System (Sistema General de Regalías) – SGR for funding the Research Project “Study of the diversity, population dynamic and biotic potential of predators and parasitoids that control true bugs of the genus *Monalonion* in cacao plantations of the states of Huila and Caquetá Florencia (estudio de la diversidad, dinámica poblacional y potencial biótico de depredadores y parasitoides controladores de chinches verdaderas del género *Monalonion* en plantaciones de cacao de los departamentos de Huila y Caquetá Florencia)” [code BPIN 2020000100513], approved by Agreement Number 100 of November 24, 2020, from which this study has derived.

Author contributions

Conceptualization: JG, HRG-S, FS. Data curation: JG, AG-T, EM-V. Investigation: JG, HRG-S, AG-T, EM-V, FS. Methodology: JG, HRG-S, AG-T, EM-V, FS. Project administration: JG. Writing - original draft: JG, HRG-S, FS. Writing - review and editing: JG, HRG-S, FS.

Author ORCIDs

Jean Gamboa https://orcid.org/0000-0002-8783-0175
Hélcio R. Gil-Santana https://orcid.org/0000-0002-0544-348X
Armando Gamboa-Tabares https://orcid.org/0000-0001-5777-8495
Eidy Martínez-Viuche https://orcid.org/0009-0001-6558-6482
Francisco Serna https://orcid.org/0000-0002-6143-9821

Data availability

All of the data that support the findings of this study are available in the main text.

References

Burmeister H (1838) Some account of the genus *Myocoris*, of the family Reduvini. Transactions of the Royal Entomological Society of London 2(2): 102–107. https://doi.org/10.1111/j.1365-2311.1836.tb00303.x

Castro-Huertas V, Forero D (2021) Revision and phylogenetic analysis of the genus *Acanthischium* Amyot & Serville, 1843 (Hemiptera: Reduviidae: Harpactorinae). Insect Systematics & Evolution 52(5): 524–574. https://doi.org/10.1163/1876312X-bja10018

Champion GC (1899) Insecta Rhynchota. Hemiptera-Heteroptera, Vol II. In: Godman FD, Salvin O (Eds) Biologia Centrali Americana. Taylor and Francis, London, 193–304.

Elkins JC (1969) A new genus of hemipteran wasp mimics (Reduviidae, Harpactorinae). Journal of the Kansas Entomological Society 42: 456–461.

Forero D (2011) Classification of Harpactorinae, assassin bugs Hemiptera: Heteroptera: Reduviidae. Boletín del Museo Entomológico Francisco Luís Gallego 1: 9–24.

Froeschner RC (1999) True bugs (Heteroptera) of Panama: A synoptic catalog as a contribution to the study of Panamanian biodiversity. Memoirs of the American Entomological Institute 61: 1–393.

Gil-Santana HR (2008) New records, and nomenclatural and biological notes on Reduviidae (Hemiptera: Heteroptera) from Bolivia and Brazil. Zootaxa 1785(1): 43–53. https://doi.org/10.11646/zootaxa.1785.1.2

Gil-Santana HR (2015) *Parahiranetis salgadoi*, a new genus and species of Harpactorini (Hemiptera: Heteroptera: Reduviidae), with a key to Neotropical wasp-mimicking harpactorine genera. Acta Entomologica Musei Nationalis Pragae 55(1): 29–38.

Gil-Santana HR (2016) First description of the male of *Hiranetis atra* Stål and new country records, with taxonomic notes on other species of Hiranetis Spinola (Hemiptera, Heteroptera, Reduviidae, Harpactorinae). ZooKeys 605: 91–111. https://doi.org/10.3897/zookeys.605.8797

Gil-Santana HR (2022) New records, taxonomic notes, and the description of a new species of Harpactorinae (Hemiptera: Heteroptera: Reduviidae) from French Guiana. Zootaxa 5105(3): 381–400. https://doi.org/10.11646/zootaxa.5105.3.3

Gil-Santana HR, Oliveira J (2023) A new genus and a new species of wasp-mimicking Harpactorini (Hemiptera, Heteroptera, Reduviidae, Harpactorinae), with an updated key to the Neotropical genera. ZooKeys 1152: 163–204. https://doi.org/10.3897/zookeys.1152.96058

Gil-Santana HR, Davranoglou L-R, Neves JA (2013) A new synonym of *Graptocleptes bicolor* (Burmeister), with taxonomical notes (Hemiptera: Heteroptera: Reduviidae: Harpactorini). Zootaxa 3700(3): 348–360. https://doi.org/10.11646/zootaxa.3700.3.2

Gil-Santana HR, Forero D, Weirauch C (2015) Assassin bugs (Reduviidae excluding Triatominae). In: Panizzi AR, Grazia J (Eds) True bugs (Heteroptera) of the Neotropics, Entomology in Focus 2. Springer Science+Business Media, Dordrecht, 307–351. https://doi.org/10.1007/978-94-017-9861-7_12

Gil-Santana HR, Salomão AT, Oliveira J (2017) First description of the male and redescription of the female of *Parahiranetis salgadoi* Gil-Santana (Hemiptera, Reduviidae, Harpactorinae). ZooKeys 671: 19–48. https://doi.org/10.3897/zookeys.671.11985

Hogue CL (1993) Latin American Insects and Entomology. University of California Press, Los Angeles, 536 pp.

ICZN [International Comission on Zoological Nomenclature] (1999) International code of zoological nomenclature. 4th edn. The International Trust for Zoological Nomenclature, London. https://www.iczn.org/the-code/ [accessed 20 oct 2023]

Kirkaldy GW (1909) Hemiptera, old and new, No. 2. Canadian Entomologist 41(11): 388–392. https://doi.org/10.4039/Ent41388-11

Lethierry L, Severin G (1896) Catalogue général des Hémiptères. Tome III. Hétéroptères. R.Friedländer & Fils, Libraires-Éditeurs, Berlin, 275 pp.

Maldonado CJ (1990) Systematic catalogue of the Reduviidae of the World. Caribbean Journal of Science, Special publication No. 1, University of Puerto Rico, Mayagüez, 694 pp.

Maldonado CJ, Lozada RPW (1992) Key to the group of neotropical wasp-mimetic harpactorine genera and the description of a new species (Hemiptera: Reduviidae). Proceedings of the Entomological Society of Washington 94(1): 162–165.

Morrone JJ (2014) Biogeographical regionalisation of the Neotropical region. Zootaxa 3782(1): 1–110. https://doi.org/10.11646/zootaxa.3782.1.1

Papavero N (1971) Essays on the history of Neotropical Dipterology, with special reference to collectors (1750–1905). Vol. 1. Universidade de São Paulo, São Paulo, 216 pp. https://doi.org/10.5962/bhl.title.101715

Putshkov VG, Putshkov PV (1985) A catalogue of the Assassin-bugs genera of the World (Heteroptera, Reduviidae). Published by the authors, Kiev, 137 pp.

Schuh RT, Weirauch C (2020) True Bugs of the World (Hemiptera: Heteroptera). Classification and natural history, 2nd ed. Siri Scientific Press, Manchester, 767 pp.

Stål C (1855) Nya Hemiptera. Öfversigt af Kongliga Vetenskaps-Akademiens Förhandlingar 12: 181–192.

Stål C (1867) Bidrag till Reduviidernas kännedom. Öfversigt af Kongliga Vetenskaps-Akademiens Förhandlingar 23(9): 235–302.

Stål C (1872) Enumeratio Hemipterorum. Bidrag till en företeckning öfver alla hittils kända Hemiptera, jemte systematiska meddelanden. 2. Kongliga Svenska Vetenskaps-Akademiens Handlingar 10(4): 1–159.

Walker F (1873) Catalogue of the specimens of Hemiptera Heteroptera in the Collection of the British Museum (Part VIII). Printed for the Trustees of the British Museum, London, 220 pp.

Wygodzinsky P (1949) Elenco sistematico de los reduviiformes americanos. Instituto de Medicina Regional de la Universidad Nacional de Tucumán. Monografia 1: 1–102.

ZooKeys 1207: 205–299 (2024)
DOI: 10.3897/zookeys.1207.117225

Monograph

Towards a revision of the Palaearctic species of *Aphodius* Hellwig, 1798, subgenus *Liothorax* Motschulsky, 1860 (Coleoptera, Scarabaeidae, Aphodiinae)

Robert B. Angus[1], Jason F. Maté[2], Elizabeth M. Angus[3], David Král[4]

1 Department of Life Sciences (Insects), The Natural History Museum, Cromwell Road, London SW7 5BD, UK
2 c/Henares 16, Velilla de San Antonio, Madrid, 28891, Spain
3 Biomedical Imaging Unit, Level B South Block, Mail point 12, General Hospital, Southampton SO16 6YD, UK
4 Department of Zoology, Faculty of Science, Charles University, Viničná 7, CZ-128 00, Praha 2, Czech Republic
Corresponding author: Robert B. Angus (r.angus@rhul.ac.uk)

Academic editor: Andrey Frolov
Received: 11 December 2023
Accepted: 6 May 2024
Published: 22 July 2024

ZooBank: https://zoobank.org/94F18819-5AF5-4100-AB35-AA3C3976EE80

Citation: Angus RB, Maté JF, Angus EM, Král D (2024) Towards a revision of the Palaearctic species of *Aphodius* Hellwig, 1798, subgenus *Liothorax* Motschulsky, 1860 (Coleoptera, Scarabaeidae, Aphodiinae). ZooKeys 1207: 205–299. https://doi.org/10.3897/zookeys.1207.117225

Abstract

The Palaearctic species of *Aphodius* Hellwig, 1798, subgenus *Liothorax* Motschulsky, 1860 are revised using a combination of chromosome analysis, molecular phylogenetics and morphological statistical analysis. Sixteen species are recognised, one of which is shown to comprise two subspecies. Based mainly on the morphology of the aedeagal endophallus and the phylogenetic analysis, they are placed in two groups: the. *niger* group, apparently monophyletic, comprising *Aphodius* (*Liothorax*) *niger* Illiger, 1798, *A.* (*L.*) *muscorum* (Ádám, 1994), **stat. rest.**, *A.* (*L.*) *felix* **sp. nov.**, *A.* (*L.*) *bellumgerens* **sp. nov.**, *A.* (*L.*) *bameuli* **sp. nov.**, *A.* (*L.*) *krelli* **sp. nov.**, *A.* (*L.*) *isikdagensis* (Balthasar, 1953), *A.* (*L.*) *alberti* **sp. nov.** and *A.* (*L.*) *wilsonae* Maté et Angus, 2005, **stat. rest.**; and the *plagiatus* group, almost certainly paraphyletic, comprising *A.* (*L.*) *plagiatus* (Linnaeus, 1767), including *A.* (*L.*) *p. plagiatus* and *A.* (*L.*) *p. sinoplagiatus* **subsp. nov.**, *A.* (*L.*) *rodrigoi* **sp. nov.**, *A.* (*L.*) *discoides* A. Schmidt, 1916, **stat. rest.**, *A.* (*L.*) *rutilipennis* (Baudi di Selve, 1870), **stat. rest.**, *A.* (*L.*) *chellala* **sp. nov.**, *A.* (*L.*) *kraatzi* Harold, 1868, and *A.* (*L.*) *rusakovi* Gusakov, 2004. A key to the species is given as well as details of their morphology, distributions, and habitats.

Key words: Chromosomes, distribution, habitats, morphology, mtDNA, new species, Scarabaeidae, taxonomy

Introduction

Aphodius Hellwig, 1798 subgenus *Liothorax* Motschulsky, 1860 species are elongate parallel-sided beetles, to some extent hemicylindrical in shape though occasionally less elongate and more rounded. The head nearly always lacks any trace of tubercles on the frontoclypeal suture, the anterior margin of the clypeus is emarginate over its median third and the lateral angles of this emargination are bluntly rounded. The lateral area of the frons, between the frontoclypeal suture and the eyes, bulges outwards as a pair of rounded genae whose outer margin may be either a simple continuation of that of the clypeus or distinctly angled outwards. The adult beetles typically inhabit mud at the edges of pools and epipharynx is of the type mainly adapted for saprophagy. Only very rarely do the beetles inhabit and eat dung.

At present five species of *Liothorax* are listed from the Palaearctic (Dellacasa et al. 2016), and a further five from the Nearctic (Dellacasa et al. 2007). No species is recorded as Holarctic.

In recent years, a large amount of chromosomal, molecular, and morphological data, not congruent with the current classification of the Palaearctic members of the group, has been accumulated by the authors, necessitating a taxonomic revision. The present revision is based on a combination of different methodologies – morphology, morphometrics, molecular phylogenetics and chromosomal studies – a rare example of truly integrative taxonomy.

The initial motivation of the present work stems from total disbelief that the distinctive features of *Aphodius* (*Liothorax*) *wilsonae* Maté & Angus were merely traits of intraspecific variation, as claimed by Dellacasa and Dellacasa (2005). In 2005 Maté and Angus (2005) described a new species of *Liothorax* as *Aphodius* (*Liothorax*) *wilsonae*, clearly related to *L. niger* Illiger, 1798 but differing significantly from it on several aspects, not just on external morphology but also in its chromosomes, mtDNA, and in the morphology of the aedeagus and particularly the endophallus, with strikingly smaller endophallic teeth.

Maté and Angus (2005) regarded *A. wilsonae* as widely distributed in southern Europe and extending into Asia as far as Iran, although they noticed that the specimens from outside the Iberian Peninsula were quite different, and therefore all material outside Iberia was left out of the type series pending additional data. Furthermore, the authors also lacked sufficient *A. niger*-like material from much of its range in Central and Eastern Europe, and as such left these specimens labelled as *A.* cf. *niger*. In spite of these limitations, the evidence for *niger* and *wilsonae* being distinct species was highly supportive. Nevertheless, and in spite of this suite of characters, Dellacasa and Dellacasa (2005) placed *A. wilsonae* as a synonym of *A.* (*L.*) *niger*, stating that the characters used to characterise the new species were the traits of intraspecific variation. Furthermore, in their 2007 review of *Liothorax*, Dellacasa et al. (2007) maintained this view, and it persists in Volume 3 of the revised edition of the Catalogue of Palaearctic Coleoptera (Dellacasa et al. 2016).

Since Dellacasa and Dellacasa (2005), Dellacasa et al. (2007) provided neither data nor a detailed explanation of why they considered characters of *A. wilsonae* to be within intraspecific variation of *A. niger*, we can only speculate that it was based solely on gross (dorsal) morphological, aedeagal, and epipharyngeal characters (but not, surprisingly, the endophallus), whilst completely ignoring the morphological, karyological, and molecular evidence which was impossible to reconcile with both lineages being conspecific. In order to counter the claim that the character variation was mere “intraspecific variation” it was necessary to examine a much larger sample of specimens. In April 2009 RBA collected a small sample of a black *Aphodius* (*Liothorax*) on the Campo Felice of the Abruzzo mountains of Italy and, assuming it to be *A. wilsonae*, remarked that we now had the species in Italy, so it would have to be taken more seriously (Angus 2010: 3). However, subsequent study of the chromosomes by RBA and of the DNA by JFM showed that the animal was not *L. wilsonae* but an undescribed species. In the light of this discovery, RBA and JFM embarked on a study of *L. niger*-like material from as wide an area as possible, and it is this project which lies at the heart of the current revision.

Materials and methods

Material

The museums from which material has been borrowed for study, and in which material has been deposited, are as follows:

The Linnean Society, Burlington House, London, UK (**LSCL**) (Susan Ryder); The Natural History Museum, London, UK (**NHMUK**) (Max Barclay); Oxford University Museum, Oxford, UK (**OUM**) (Darren Mann); Muséum d'histiore naturelle, Genève, Switzerland (**MNHG**) (Giulio Cuccodoro); Muséum national d'Histoire naturelle, Paris, France (**MNHN**) (Mlle Nicole Berti); Humboldt Museum, Berlin, Germany (**ZMB**) (Johannes Frisch); Zoologische Staatsammlung München, Germany (**ZSM**) (Michael Balke); Hungarian Museum of Natural History, Budapest, Hungary (**MNHB**) (Ottó Merkl); Museo Nacional de Ciencias Naturales, Madrid, Spain (**MNCN**) (Mercedes París); Naturhistorisches Museum, Wien (**NMW**) (Harald Schilhammer); Zoological Institute, Russian Academy of Sciences St Petersburg, Russia (**ZIN**) (Andrey Frolov); Steinhardt Museum of Natural History, Tel Aviv, Israel (**IL-SMNH**) (Laibale Friedman); National Museum Prague, Czechia (**NMP**) (Jiří Hájek); Denver Museum of Nature and Science, Denver, Colorado, USA (**DMNS**) (Frank Krell); Alberto Ballerio Collection, Brescia, Italy (**AB**); Stefano Ziani Collection, Imola, Italy (**SZ**); Axel Bellmann Collection, Bremen, Germany (**ABC**); Carsten Zorn Collection, Gnoien, Germany (**CZC**); Jason Maté Collection, Madrid, Spain (**JFMC**).

Details of the material from which successful chromosome preparations have been obtained are given in Table 1 and of that sequenced for DNA, comprising ten ingroup and three outgroup species, are given in Table 2.

Morphological data were obtained from 209 specimens (183 ingroup and 26 outgroup taxa) from several collections and from field-collected specimens (Table 3). Only specimens that could be identified with certainty a priori were used with the exception of the *niger-muscorum* complex. For this latter group there were a number of specimens from Czechia that could not be unambiguously categorised and so they were identified as "*A. niger* cf." as a way to compare them with the unambiguously identifiable *A. niger* and *A. muscorum* (Ádám, 1994) material. These *A. niger* cf. specimens were used only in the principal component analyses to explore their relation within the morphospace, but not for other analyses as they did not represent a proper category. Although we aimed to sample at least six specimens per taxon, a few species were represented by only a few historical specimens. Due to the limited availability of material for some species and the low sexual dimorphism in the group (Dellacasa and Dellacasa 2005) male and female specimens were used together. The linear measurements used here are not affected by sexual dimorphism.

Methods

Habitus photographs of whole beetles and parts of the external structures were taken with a Leica M125 stereomicroscope + Canon EOS 550D digital camera, and of uninflated aedeagi and mouthparts mounted on slides in dimethyl hydantoin formaldehyde (DMHF) resin with a Zeiss Axioskop + Canon EOS 450D digital camera, in the Sackler Bioimaging Laboratory of the Natural History Museum, London. Both were stacked using Helicon Focus software.

Table 1. Details of the material from which successful preparations have been obtained.

Species	Locality of origin	Specimens
A. plagiatus	England: Norfolk, Hunstanton 52.968°N, 0.525°E	1♂
	Dorset, Studland Heath 50.654°N, 1.955°W	3♂♂, 3♀♀
	China: Qinghai, Gangca 37.3°N, 100.183°E	1 ♂
A. kraatzi	Slovakia: Chl'aba 47.823°N, 18.849°E	1♀
A. rutilipennis	Cyprus: Limassol district, Zakaki marshes 34.644°N, 30.001°E	1♂, 1♀
A. niger	Sweden: Södermanland, Hölö, Tullgarn, Näsudden 58.95°N, 17.62°E	3♂♂, 3♀♀
	England: Hampshire, New Forest, Brockenhurst district, Balmer Lawn 50.830°N, 1.57°W	2♂♂, 3♀♀
	White Moor 50.821°N, 1.607°W	5♂♂
	Long Slade Bottom 50.800°N, 1.620°W	2♂♂, 3♀♀
A. bameuli	France, Corsica: Haute-Corse, by Lac de Melo 42.212°N, 9.025°E	6♂♂, 12♀♀
A. bellumgerens	Italy, Sicily: Provincia di Palermo, Parco delle Madonie, Piano Battaglia 37.880°N, 14.073°E	5♂♂, 1♀
	Provincia di Messina, Parco dei Nebrodi Monte Soro 37.529°N, 14.693°E	12♂♂, 5♀♀
A. felix	Italy: Provincia di L'Aquila, Campo Felice 42.215°N, 13.445°E	2♂♂, 3♀♀
A. krelli	Italy, Sardinia: Provincia di Nuoro, Badde Salighes 40.343°N, 8.902°E	3♂♂, 3♀♀
A. muscorum	Hungary:Hajdú-Bihar, Hortobágyi National Park, Kis-Kecskés area 47.677°N, 21.061°E	10♂♂, 10♀♀
	Jasz-Nagykun-Szolnok, Kisújszállás 47.216°N, 20.713°E	2♀♀
A. wilsonae	Spain: Provincia de Burgos, near Balneario de Corconte 43.009°N, 3.859°W	5♂♂, 6♀♀
	Provincia de Cantabria, Areños 43.112°N, 4.729°W	2♂♂
	Provincia de Madrid: Manzanares el Real 40.725°N, 3.860°W	2♂♂, 2♀♀
	Near El Vellón 40.76°N, 3.620°W	2♂♂, 2♀♀
	Provincia de Guadalajara, Matarrubia 40.852°N, 3.295°W	1♀

Where aedeagi were partly inflated as a result of the hypotonic potassium chloride treatment for chromosome preparation the endophallus was further extruded by gentle squeezing with forceps. Detailed methods are given by Angus et al. (2000). The preparations were viewed uncoated for scanning electron microscopy in the Natural History Museum, London and the Biomedical Imaging Unit of Southampton General Hospital. Occasionally the endophallus of old, mounted specimens had been extruded as a result of partial decomposition. In these cases the aedeagi were transferred to a 5% solution of potassium hydroxide to soften them, and the aedeagus was squeezed very gently to further inflate the extruded endophallus. Inflated aedeagi were transferred to alcohol for critical-point drying. They were then photographed as for other external structures, and, in some cases scanning electron micrographs (SEMs) of uncoated aedeagi were taken. They were viewed in low vacuum mode using secondary electrons on a FEI Quanta 200 SEM. This work was carried at the Biomedical Imaging Unit in Southampton. Endophallus teeth were normally measured from SEM images, usually at 1200× magnification but sometimes at 600 or 300×. The teeth of *A. isikdagensis* Balthasar, 1953 were measured from a photograph.

Pronotal bases were also viewed as SEM images, to show the varying development of the border. In this case the whole beetle was mounted and the pronotal bases were viewed uncoated in low vacuum mode using secondary electrons on a FEI Quanta 250 SEM. This work was also carried at the Biomedical Imaging Unit in Southampton General Hospital.

Table 2. Species sequenced in the present study with their locality data. Those belonging to subgenus *Liothorax* are considered as "ingroup" (IG) and the rest used to root the phylogeny as "outgroup" (OG). Last two columns show the GenBank submission codes for the successfully amplified sequences.

CODE	IG/ OG	Subgenus	Species	Locality Data	COX1	CytB
AALioBam21	IG	*Liothorax*	*bameuli*	FRANCE, Corsica, Lac de Melo, above Corte, 19–25.vi.2011 short turf. Leg. R.B & E.M Angus	PP788597	PP791934
AApLioBam66	IG	*Liothorax*	*bameuli*	FRANCE, Corsica, Lac de Melo, above Corte, 19–25.vi.2011 short turf. Leg. R.B & E.M Angus	PP788594	PP791932
AApLioBam77	IG	*Liothorax*	*bameuli*	FRANCE, Corsica, Lac de Melo, above Corte, 19–25.vi.2011 short turf. Leg. R.B & E.M Angus	PP788595	PP791933
AApLioBam573	IG	*Liothorax*	*bameuli*	FRANCE Corsica Plateau d´Alzo 1500 m, 42°16'N, 9°04'E 21V1994 leg C. Zorn	PP788593	
AApLioBel125	IG	*Liothorax*	*bellumgerens*	ITALY, Sicily, Parco delle Madonie, Piano Battaglia, At deges of pool 1 MAY2013 Leg. R.B. & E.M. Angus	PP788596	PP791935
AApLioBel343	IG	*Liothorax*	*bellumgerens*	ITALY, Sicily, Parco delle Madonie, Piano Battaglia, At deges of pool 1 MAY2013 Leg. R.B. & E.M. Angus	PP788598	PP791936
AApLioBel593	IG	*Liothorax*	*bellumgerens*	ITALY, Sicily, Monte Soro 25APRIL2018 chromosome 4 27APR2018	PP788599	PP791958
AALioBel594	IG	*Liothorax*	*bellumgerens*	ITALY, Sicily, Parco delle Madonie, Piano Battaglia, #2, edge of pool 1 MAY2013 Leg. R.B. & E.M. Angus	PP788600	PP791937
AApLioFx22	IG	*Liothorax*	*felix*	ITALY. Abruzzo. Campo Felice. Washed into pool. 1.vi.2009. R. B. Angus	PP788601	PP791938
AApLioRu91	IG	*Liothorax*	*rutilipennis*	CYPRUS, Limassol Distrc, Zakaki, Rain puddle in lorry park, at edge of reedbed; 3/3/2005. R.B.Angus	PP788621	PP791940
AApLioRu110	IG	*Liothorax*	*rutilipennis*	CYPRUS, Limassol Distrc, Zakaki, Rain puddle in lorry park, at edge of reedbed; 3/3/2005. R.B.Angus mounted spec	PP788620	PP791939
AApLioKz236	IG	*Liothorax*	*kraatzi*	RUSSIA, Astrakhan P, Dosang env. (46°54'N, 47°55'E) 1–5/v/2014 cattle dung. A. Frolov & L. Akhmetova	PP788605	PP791944
AApLiKz270	IG	*Liothorax*	*kraatzi*	RUSSIA, Astrakhan P, Dosang env. (46°54'N, 47°55'E) 1–5/v/2014 cattle dung. A. Frolov & L. Akhmetova	PP788606	PP791945
AApLiKz272	IG	*Liothorax*	*kraatzi*	SLOVAKIA, S., E of Chlaba, 11.vi. 2014, 47°49'24.01"N, 18°50'56.23"E, 107 m a.s.l. Sandy place S of railway, at light, Leg. D. Král	PP788607	
AApLiKz273	IG	*Liothorax*	*kraatzi*	SLOVAKIA S., E of Chlaba, 11.vi. 2014, 47°49'24.01"N, 18°50'56.23"E, 107 m a.s.l. Sandy place S of railway, at light, Leg. D. Král	PP788608	
AApLioKr83	IG	*Liothorax*	*krelli*	ITALY, Sardinia, Nuoro Prov., Badde Salighes, 1 April 2012 R.B. & E.M. Angus unsexed	PP788604	PP791941
AApLioKr165	IG	*Liothorax*	*krelli*	ITALY, Sardinia, Sassari, La Ciaccia, Valledoria, 17 Feb 2008, old sheep dung, R.B.Angus	PP788603	PP791943
AApLioKr155	IG	*Liothorax*	*krelli*	ITALY, Sardinia, Nuoro, Altopiano della Campeda, 40°21.245'N, 8°47.044'E 580 m 18 MAY 2005 leg. Starke	PP788602	PP791942
AApLioMu59	IG	*Liothorax*	*muscorum*	HUNGARY. Jász-Nagykun-Szolnok kisújszállás. Mud in drying ditch. 14.iv.2011. R. B. Angus.	PP788612	PP791946
AApLioMu60	IG	*Liothorax*	*muscorum*	HUNGARY. Jász-Nagykun-Szolnok Kisviszalas. Mud in drying ditch. 14.iv.2011. R. B. Angus.	PP788613	PP791947
AApLioMu68	IG	*Liothorax*	*muscorum*	HUNGARY. Jász-Nagykun-Szolnok kisújszállás. Mud in drying ditch. 14.iv.2011. R. B. Angus.	PP788614	PP791948
AApLioMu299	IG	*Liothorax*	*muscorum*	HUNGARY, Hortobagy, 3;7/5/2011, R.B. & E.M. Angus	PP788609	PP791949
AApLioMu417	IG	*Liothorax*	*muscorum*	HUNGARY, Hortobagy, 5;7/5/2011, R.B. & E.M. Angus	PP788610	
AALioMu559	IG	*Liothorax*	*muscorum*	CZECH REPUBLIC, Bohemia, Hradec Kralove -16.4.2011 "Na Plachte", lgt P. Kylies	PP788611	PP791955
AApLioNgSE	IG	*Liothorax*	*niger*	SWEDEN: Södermanland, Hölö: Tullgarn, Näsudden, 58.953788°N, 17.616277°E,15.v.2011. Hans-Erik & Livia Wanntorp	PP788615	PP791950
AApLioNgUK1	IG	*Liothorax*	*niger*	U.K., Hants. New Forest Long Slade Bottom 30.v.2002 R.B.Angus	PP788616	PP791963
AApLioPl37	IG	*Liothorax*	*plagiatus*	U.K., Norfolk, Hunstunton, 27/9/2001, R.B.Angus	PP788619	PP791951
AApLioPl131	IG	*Liothorax*	*plagiatus*	CHINA, Qinghai, N. Qinghai Hu, Gangca. Roadside pool 37°18'N, 100°11'E, 3370 m. 5.vi.2013,R.B. Angus, F.L. Jia & Y. Zhang	PP788618	PP791964
AApLioPl1	IG	*Liothorax*	*plagiatus*	UK, England, Norfolk, Hunstunton, 27/9/2001, R.B.Angus	PP788617	

CODE	IG/ OG	Subgenus	Species	Locality Data	COX1	CytB
AApLioW86	IG	*Liothorax*	*wilsonae*	SPAIN, Burgos, Balneario de Corconte, 12/03//2011 Leg R. Angus	PP788626	PP791952
AApLioW1	IG	*Liothorax*	*wilsonae*	SPAIN, Provincia de Burgos, Balneario de Corconte, 40.031°N, 3.884°W, 26.iv.2001. leg. R.B. Angus. (BMNH).	PP788622	PP791959
AApLioW248	IG	*Liothorax*	*wilsonae*	SPAIN, Burgos, Balneario de Corconte, 12/03/2011 Leg R. Angus	PP788623	PP791965
AApLioW264	IG	*Liothorax*	*wilsonae*	SPAIN, Burgos, Balneario de Corconte, 26.iv.2001 R.B. Angus	PP788624	PP791953
AApLioW606	IG	*Liothorax*	*wilsonae*	SPAIN, Burgos, Valle de Valdebezana, 42.993512, -3.831779, Virtus R. Angus leg	PP788625	PP791954
AApNiaVarMD53	OG	*Nialus*	*varians*	SPAIN, Madrid, Alcalá de Henares, 15/4/2008, lg J.F.Maté	PP788627	PP791960
AApNialVarAz208	OG	*Nialus*	*varians*	AZERBAIJAN, 4.v.2014 fish pond btw Kalageyli & Xalilli 40°36'55.8"N, 48°12'37.5"E 220 m lg Faille, Fresneda, Ribera & Rudoy	PP788628	PP791957
AApSubSt1	OG	*Subrinus*	*sturmi*	SPAIN, Madrid, La Acebeda, 41.091714, -3.627400 01/08/1999 1375 m lg. J.F.Maté	PP788629	PP791962
AApLabPseu1	OG	*Labarrus*	*pseudolividus*	NAMIBIA, Mukwe Dist., W. Capriva Pk Divvju; 18°04'04"S, 21°28'51"E 31/xii/1998 campsite at U.V. D Mann Leg.	PP788630	PP791961

Table 3. List of species and number of specimens used in the morphometric part of the study.

Subgenus	Species	# Specimens
Liothorax	*alberti*	12
Liothorax	*bameuli*	11
Liothorax	*bellumgerens*	9
Liothorax	*chellala*	7
Liothorax	*discoides*	8
Liothorax	*felix*	7
Liothorax	*isikdagensis*	4
Liothorax	*kraatzi*	13
Liothorax	*krelli*	7
Liothorax	*muscorum*	16
Liothorax	*niger*	20
Liothorax	*niger cf*	6
Liothorax	*plagiatus*	23
Liothorax	*rodrigoi*	3
Liothorax	*rusakovi*	6
Liothorax	*rutilipennis*	13
Liothorax	*sinoplagiatus*	4
Liothorax	*wilsonae*	14
Labarrus	*lividus*	6
Nialus	*varians*	9
Subrinus	*sturmi*	11
Total specimens measured		**209**

SEMs were also used to check the nature of the surface reticulation of elytra and metasterna. For this, back-scattered electrons were used for imaging, as these categorically show only the surface sculpture. Images were taken in the Electron Microscope Unit of the Natural History Museum, London, using a Zeiss Leo 1455VP SEM in low vacuum mode on uncoated specimens.

Chromosome preparations were made from dividing cells in testes and midguts of adult beetles, using the methods described by Shaarawi and Angus

(1991) and Angus (1982). In brief, living beetles are placed in watch glasses of 0.1% colchicine solution in insect saline buffered to pH6.8 with Sörensen's phosphate buffer, and the abdomen is partially detached. After ca 12 min the beetle is transferred to a watch glass of ½-isotonic (0.48% KCl) at pH 6.8. The abdomen is fully detached and the mid gut and testes are dissected out. After 12 min the midgut and testes are transferred to a watch glass of fixative (3:1 absolute ethanol: glacial acetic acid). The fixative is changed 3× and the tissue left for at least 1 h. At this stage, the beetle is killed with boiling water and either mounted on a card or placed in absolute ethanol for DNA analysis. Small pieces of tissue are then transferred to clean microscope slides, excess fixative is removed and a small drop of 45% acetic acid is dropped on to the tissue, to dissociate the cells. The tissue is pulled apart in this drop with fine pins. A small drop of fixative causes the cell suspension to spread over the slide where it is allowed to dry. It is then stained with 1% Giemsa stain at pH 6.8. The dry slide is then examined under a microscope and suitable chromosome spreads are photographed under oil immersion. After this the oil is removed using two changes of xylene and one of absolute ethanol, in Coplin jars, and the slide is once more allowed to dry. At this stage C-banding is attempted, ideally on two-day-old slides. The slides are immersed in a saturated solution of barium hydroxide at room temperature (ca 23 °C), initially for 3 min. They are then rinsed in three changes of distilled water at pH 6.8 and placed in a Coplin jar of 2× SSC (0.3 M NaCl + 0.03 M trisodium citrate) at 55–60 °C and left for 1 h. They are then rinsed in 3 changes of distilled water at pH 6.8 and stained for 10 min in 1% Giemsa, as before. If C-banding has not developed the C-banding procedure can be repeated (any immersion oil being removed as before) and the slide the slide can be restained. This cycle can be repeated as often as is found necessary – each repeat usually involves an additional 1 min in barium hydroxide. Meiosis metaphase I chromosomes usually require more treatment than mitotic ones.

Preparations were photographed onto high-contrast microfilm and printed at a magnification of 3000×. They were than scanned into a computer and the chromosomes arranged using Adobe Photoshop. Chromosomes were measured once arranged as karyotypes, and Relative Chromosome Lengths (RCL, the length of each chromosome expressed as a percentage of the total haploid autosome length in the nucleus) and Centromere Indices (CI, the length of the short arm of a chromosome expressed as a percentage of the total length of the chromosome) were calculated. These terms and calculations are as recommended by the Paris Conference (1971). In practice CI measurements are subject to considerable variation and are best expressed as a limited number of categories. Based on Sumner (2003) these are metacentric, CI 50–46; submetacentric, CI 45–26; subacrocentric, CI 25–5, and acrocentric (including telocentric), CI < 15. RCL data are given in Table 4 and a summary of chromosome characters, including CI, is given in Table 5.

For molecular analysis all collected specimens were taken back alive to the lab by RBA for karyological work. After dissection of the abdomen, the specimens were stored in 95% ethanol until DNA extraction. Isolation of DNA from specimens followed a modified protocol of the "salting out" method of Miller et al. (1988). Briefly, whole specimens were air dried in 1.5 ml microcentrifuge tubes, after which a mix of proteinase K (5 µl, 10 mg/ml) in lysis buffer (300 µl TNES buffer, pH 7.5, 10% SDS) was added and the samples incubated for 6–8 h at

Table 4. Relative Chromosome Lengths, mean, 95% confidence limits, number measured. Important distinctive values shown in cells with yellow background.

	1	2	3	4	5	6	7	8	9	X	Y
A. niger S + NF	17.68 17.09–18.27 N=12	16.23 15.53-16.92 N=12	12.71 11.83–13.59 N=12	12.32 11.72–12.92 N=12	11.40 10.88–12.12 N=11	9.49 8.82–10.17 N=12	8.03 7.76–8.30 N=12	7.37 6.94–7.81 N=12	6.32 5.84–6.81 N=11	15.55 13.46–17.64 N=7	13.88 12.03–15.72 N=5
A. muscorum Hortobágyi	14.5 14.2–14.83 N= 59	16.78 16.46–17.09 N=60	12.92 12.67–13.17 N=60	12.71 12.41–13.02 N=59	10.82 10.55–11.11 N=60	9.65 9.35–9.95 N=60	8.83 8.59–9.06 N=60	7.46 7.26–7.67 N=60	6.29 6.09–6.5 N=60	18.33 17.63–19.03 N=44	5.95 5.15–6.75 N=16
A. muscorum Kisújszállás ♀♀	13.41 12.13–14.69 N=4	17.19 16.31–18.07 N=4	11.63 10.36–12.91 N=4	12.75 11.88–13.62 N=4	11.00 10.40–11.60 N=4	10.31 9.56–11.05 N=4	9.00 8.09–9.91 N =4	7.19 5.94–8.45 N=4	6.74 6.24–7.24 N=4	18.92 17.09–20.76 N=4	
A. felix	13.39 12.93–13.86 N=14	13.48 13.12–13.84 N=14	12.84 12.22–13.45 N=14	12.21 11.86–12.56 N=14	11.57 11.19–11.95 N=14	10.61 10.2–11.02 N=14	9.54 9.23–9.85 N=14	9.29 8.88–9.71 N=14	7.66 7.16–8.16 N=14	10.76 9.97–11.55 N=8	2.42 2.0–2.84 N=6
A. bellumgerens	16.95 15.95–17.94 N=12	15.43 14.78–16.08 N=12	11.96 11. 40–12.52 N=12	10.59 9.93–11.25 N=12	10.19 9.62–10.75 N=12	9.93 9.59–10.27 N=6	9.17 8.64–9.69 N=12	8.80 8.22–9.38 N=12	7.40 6.83–7.97 N=12	19.64 18.09–21.18 N=9	8.71 5.17–12.25 N=3
A. bameuli	13.16 12.45–13.87 N=12	12.82 12.24–13.42 N=12	13.19 12.49–13.89 N=12	11.97 11.48–12.46 N=12	11.31 10.95–11.67 N=12	11.14 10.24–12.04 N=11	9.59 8.96–10.22 N=12	9.3 9.01–9.59 N=12	8.96 8.5–9.41 N=11	13.74 12.2–15.28 N=7	3.61 1.89–5.34 N=5
A. krelli	13.57 12.9–14.25 N=16	12.88 12.35–13.42 N=16	12.76 12.11–13.42 N=16	11.89 11.4–12.39 N=16	11.49 11.15–11.82 N=16	10.91 10.61 - 11.21 N=16	10.09 9.18–11 N=11 5.22 4.63–5.8 N=5 Short form	9.68 9.14–10.21 N=16	9.5 9.07–9.92 N=16	15.09 14.08–16.1 N=12	3.61 2.98–4.24 N=4
A. wilsonae	14.74 14.11–15.37 N=16	12.16 11.59–12.73 N=16	12.97 12.51–13.44 N=16	11.63 11.29–11.98 N=16	10.89 10.6–11.19 N=16	10.07 9.68–10.49 N=16	9.81 9.52–10.11 N=16	9.22 9.02–9.41 N=16	8.26 7.96–8.56 N=16	11.53 10.71–12.35 N=10	3.5 3.14–3.84 N=6

37–40 °C to ensure complete tissue digestion. Tubes were shaken every hour to ensure that the lysis solution could access the whole specimen. Afterwards the specimens were chilled to 4 °C for 1 h before the next step. Once chilled, 85 µl of saturated NaCl solution (> 5M) was added to each vial for a total volume of 390 µl. The tubes were shaken for 15 sec to ensure mixing and spun for 5 min at 14k rpm. The supernatant was removed to a new set of 1.5-ml vials containing 400 µl of 100% EtOH. They were shaken for 15 sec and spun at 14k rpm for five minutes. The supernatant was discarded and the DNA pellet washed with 500 µl of ice cold 70% EtOH. After discarding the supernatant the pellets were allowed to air dry before resuspending in 20–50 µl of TE buffer (pH 8.0) and storage at -20 °C.

Sequencing. PCR reactions were carried out using PCR beads (GE27-9557-01, Illustra™ PuReTaq RTG PCR, 0.2 ML, Cytiva, Buckinghamshire, U.K.) to which 0.2–0.5 µl of genomic DNA suspension was added to an overall reaction volume of 25 µl. Typical conditions were as follows: 1 cycle of denaturation at 94 °C for 2 min as an initial step followed by 35–40 amplification cycles at 94 °C for 30 sec for denaturing, 47–49 °C for 30 sec, 68–72 °C for 30 sec for extension, and a final extension step at 72 °C for 5 min. PCR products were cleaned via sodium acetate/ethanol precipitation. Once dried, products were sent to an outside sequencing lab (SECUGEN S.L., Madrid, Spain) for final Sanger sequencing.

Table 5. Summary of the major features of the karyotypes.

Chromosome	*A. plagiatus*	*A. kraatzi*	*A. rutilipennis*	*A. niger*	*A. muscorum*	*A. felix*	*A. bellumgerens*	*A. bameuli*	*A. krelli*	*A. wilsonae*
1	m	m. hs	sm	m.hl	sm.hl(part)	m-sm hl weak	m.hl	m.hl	m.hl	m.hl
2	m	m.hs	m	m	sm	m	m	m	m	sm
3	m	sm.hs	sm.hl	m.	sa.hs	m.hs	m	sm.hl	sm.hl	sm.hl
4	m.**2c?**	sm.hs	sm	sm	sm	m	m	sm.hl	sm.hl	sm.hl
5	sm/sa	sm.hs	sm.hl	sm	sa.hs	m	m	sm.hl	sm.hl	sm.hl
6	m	sm.hs	m	sm.hs	sa.hs	m.hl	sm	sm	sm.hl	sm.hl
7	sm **2c?**	sm.hs	m.hl	sm	sm	m	m	sm	sm.hl/sa	sm.hl
8	sm **2c?**	sa	sm.hl	sm	sa	m/sa	sm	m.hl	m.hl	sm.hl
9	sm/sa	sa	m	sa	sm-sa	sm	sm	m/sa	m/sa	sm
X	sm/sa	[10] sa	sm.hl	m.hl	m-sm.hl	sm hl	m.hl	sm.hl	sm.hl	sm.hl
y	sm(dot)	-	m(dot)	m	m(dot)	m(dot)	m (small, h)	sa (small)	m(dot)	m(dot)
B		1.h		1–3.sa.h						
Distinctive features	No hl or hs	8 hs	5 hl	y long m	C1 shorter than C2	C1 hl weak	2 hl, including C1	6 hl not C6,7	8 hl C7 &9 polymorphic	8 hl No polymorphisms

C-chromosome; m-metacentric; sm-submetacentric; sa-subacrocentric; hl-heterochromatic long arm; hs-heterochromatic short arm; h-heterochromatic; /- either borderline or alternative (polymorphic). **2c?**-possible secondary constriction.

Two mtDNA regions were sequenced, the 39 end of cox1 (Pat [5’TCCAATGCACTAATCTGCCATATTA] and Jerry [5’CAACATTTATTTTGATTTTTTGG]), and cytochrome b (cb-1 [5’ TATGTACTACCATGAGGACAAATATC] and cb-2 [5’ATTTACACCTCCTAATTTATTAGGAAT]) (Simon et al. 1994). DNA chromatographs were visually checked in Chromas (v. 2.6.6.) for ambiguous or erroneous base readings. Final sequences were exported into AliView (v. 1.28; Larsson 2014) for editing and alignment of sequences. Aligned datasets were exported as fasta files into MEGA11 (MEGA11: Molecular Evolutionary Genetics Analysis v. 11; Koichiro et al. 2021) for concatenation and analysis.

Phylogenetic analysis

Parsimony analysis was run in MEGA 11, which was also used to run the 1000 bootstrap replications (50% character removal). The parsimony search employed the Tree-Bisection-Regrafting (TBR) algorithm (Nei and Kumar 2000) with search level 3 in which the initial trees were obtained by the random addition of sequences (100 replicates). All positions with less than 95% site coverage were eliminated (i.e., fewer than 5% alignment gaps), missing data and ambiguous bases were allowed at any position (partial deletion option). Bootstrapping was run concurrently with the parsimony tree search using the default conditions in Mega11. Jackknife support was estimated in PAUP (v. 4.0a169: Swofford 2003) using default conditions. For decay indices, one of the trees of the parsimony search was used to generate a search file in TreeRot (v. 3.0; Sorenson and Franzosa 2007). The settings for the decay index file were Branch-and-bound search, gaps treated as missing, with addition sequence set to furthest “Maxtrees” set at 500 (no automatic increase), “Multrees” on and branch collapse on and trees unrooted.

For the Maximum Likelihood method, the model implemented was the General Time Reversible model. A discrete Gamma distribution was used to model evolutionary rate differences among sites (5 categories (+G, parameter = 1.2620)). The rate variation model allowed for some sites to be evolutionarily invariable ([+I], 62.14% sites). All positions with less than 95% site coverage were eliminated, i.e., fewer than 5% alignment gaps, missing data, and ambiguous bases were allowed at any position (partial deletion option).

Genetic distances were calculated to quantify sequence divergences within species and between species using p-distance and using Kimura's (Kimura 1980) two-parameter (K2P) models as implemented in MEGA 11. The p-distance is the most commonly reported genetic distance method whereas K2P distance is preferred if genetic divergence is low (Hebert et al. 2003). Interspecific distances were calculated for those species with at least two sequences; hence no intraspecific divergence could be reported for *A.* (*L.*) *felix* sp. nov. (intraspecific cell labelled n/c).

For the multivariate analysis fifteen linear measurements were collected for each specimen pertaining to the body and legs (Table 6). These measurements were selected based on the discriminatory potential as evidenced by previous work on *Aphodius* taxa (Maté 2003) as well as on the observations made on the tarsal characters of *A. wilsonae* (Maté & Angus, 2005). The measurements (Fig. 1) were made on stacked images of the specimens as well as mounted material. For the material that was imaged, specimens were mounted and at least three perspectives were captured per specimen (dorsal, lateral, and ventral) to ensure that the anatomical features of interest were properly oriented. Images were taken wither with a Nikon D40 camera mounted on a Wemacro rig and aligned using Zerene Stacker (Zerene Systems LLC, WA, USA), or when photographed in the Sackler imaging laboratory of the Natural History Museum, London, a Leica MZ 125 stereomicroscope equipped with a Cannon DSLR camera, and the images stacked using Helicon Focus 7. All images were size-calibrated using a reference measure, and the features of interest were measured either in ImageJ (Schneider et al. 2012) or in Photoshop (Photoshop CS5.1). Each measurement was taken twice to the nearest hundredth of a millimetre and averaged for each feature/specimen. A random subsample of specimens was remeasured to check for repeatability. Measurements were taken, when possible, from the same side to minimise the effects of asymmetry. All measurements were curated for outliers that could indicate input or measurement errors.

Statistical analyses

Prior to all analyses, measurements were size corrected using total body length (TBL) as the size correction. Although most previous studies have used a ratio of each linear measure against TBL, aphodiine scarabs show allometric body size variation (Maté 2003) which cannot be completely removed by performing a ratio, making it difficult to accurately discriminate taxa using morphometric techniques (Sidlauskas et al. 2011). To correct for allometric size effects, the GroupStruct (v. 0.1.0) R-package was used (Chan and Grissmer 2022). After extracting size, the measurements were cross checked against total length to ensure that the size correction procedure was effective and the new data matrix

Table 6. Tabulated list of the fifteen morphological linear measurements collected in the present study with their acronyms.

Code	Description
EL	Elytral length, from base of elytra at corner of scutellum to apex measured dorsally.
PL	Pronotal length, measured dorsally.
PW	Pronotal width, the widest distance across the pronotum as measured dorsally.
EW	Elytral width, the widest distance across combined elytra as measured dorsally.
MTTIB L	Metatibial length, distance from joint to apex of tibia.
DV HEIGHT	Dorsoventral height, highest point from dorsum to ventrum as measured laterally (not illustrated).
ScL	Scutellar length, medial length from apex to inflexion point at base.
MT TARS L	Metatarsal length, combined length of all metatarsi.
1MT TARS L	Length of first metatarsal segment as measured between joints.
MTSPINE	Metattibial spine length, distance from joint to apex.
MSTIB L	Mesotibial length, distance from joint to apex of tibia.
MSTARS L	Mesotarsal length, combined length of all five mesotarsi.
1MSTARS L	Length of first mesotarsal segment as measured between joints.
MSSPINE	Mesotibial spinal length
TL	Total length

was used for all further analyses. All statistical analyses were performed in the RStudio (v. 1.2.5033; RStudio Team 2020) platform using the packages tidyverse (v. 1.3.0; Wickham et al. 2019), tibble (v. 3.1.6; Müller and Wickham 2023), dplyr (v. 1.0.7; Wickham et al. 2021) and yarr (v. 0.1.5; Phillips 2017) as well as others that are individually mentioned below.

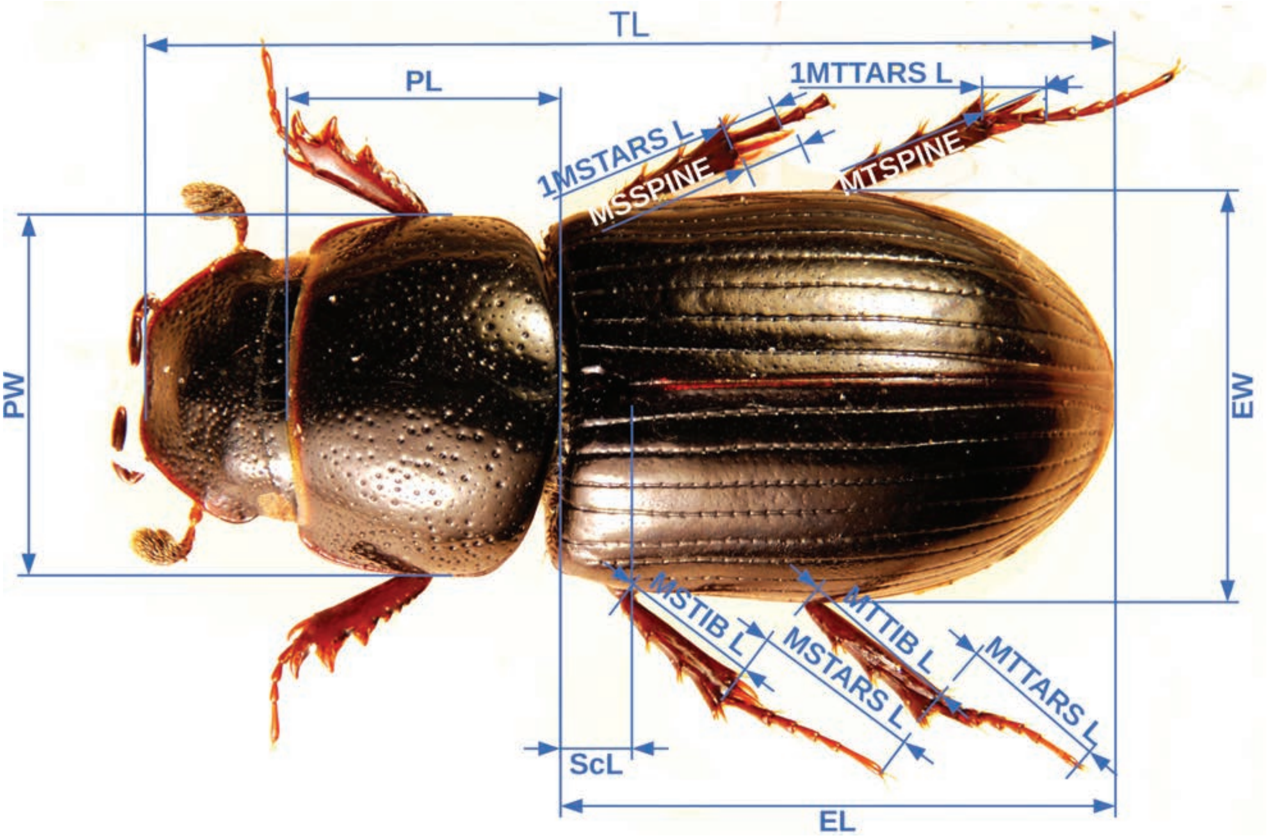

Figure 1. Linear morphological measurements collected in this study. For definitions refer to Table 6.

Principal component analyses

We derived the orthogonal morphological axes using principal component analysis (PCA) on a matrix of the allometrically corrected linear measurements, computed using the packages Psych (v. 1.9.12.31; Revelle 2021) and nFactors (v. 2.4.1). Prior to analysis the data was tested for suitability via several indicators (Bartlett's test for sphericity, Bartlett Test of Homogeneity of Variances, and KMO [Kaiser, Meyer and Olkin Measure of Sampling Adequacy]). The number of components to extract was estimated examination of a scree plot, parallel analysis and VSS [Very Simple Structure]. Different rotation methods were performed to better load each variable to the components. The resulting factors were used to generate the bivariate plots.

Morphological divergence

Divergence between groups and within groups was assessed by measuring the morphological divergence across all the measurements as well as individual morphological parameters. Euclidian and Manhattan distances were computed and compared, with both methods giving the same results, hence subsequent analyses used only Euclidian distances. Significance between groups was tested via the pairwise Wilcoxon Test and Tukey's Test with the *p*-values adjusted using the Bonferroni method.

Results

Taxonomy

Treatment of *Liothorax* as a genus or as a subgenus of *Aphodius*

Motschulsky (1860) erected the genus *Liothorax* for three species, including *Scarabaeus plagiatus* Linnaeus, 1767, the only one of the trio still included in *Liothorax*, and which G. Dellacasa (1983) designated as the type species. Following Bedel (1911) most authors, including Baraud (1992) have regarded *Liothorax* as a subgenus of *Aphodius* Hellwig, 1798. However, Dellacasa et al. (2001a) proposed the elevation of all the subgenera of *Aphodius* to generic level, and this arrangement is used in Volume 3 of the latest Catalogue of Palaearctic Coleoptera (Dellacasa et al. 2016). Nevertheless, in the absence of phylogenetic research demonstrating the need to change the rank of *Liothorax* we follow majority of authors and treat it as a subgenus of *Aphodius* in this revision, as recommended by two referees and with the support of the editor.

Subgeneric characters

In this illustrated account of the genus the two-letter abbreviations of countries from where material was obtained are those used in the Catalogue of Palaearctic Coleoptera. *Liothorax* species are elongate parallel-sided beetles, to some extent hemicylindrical in shape (Figs 2–4) though occasionally less elongate and more rounded (*A. rodrigoi* sp. nov., Fig. 2d; *A. krelli* sp. nov. and *A. wilsonae*, Fig. 4e, g). The head nearly always lacks any trace of tubercles on the frontoclypeal suture, although there can be a very slight medial one in some male specimens of *A. rusakovi* Gusakov, 2004, just visible by the lighting in the whole beetle (Fig. 2i) but not in the enlarged view (Fig. 5m) and with no trace in the female, and the clypeus is elevated medially. The anterior margin of the clypeus is emarginate over its median 1/3 and the lateral angles of this emargination are bluntly rounded (Figs 5, 6). The lateral area of the frons, between the frontoclypeal suture and the eyes, bulges outwards as a pair of rounded genae whose outer margin may be a simple continuation of that of the clypeus, but may be distinctly angled outwards, as in female *A. isikdagensis* (Fig. 6b) The epipharynx (Figs 7–9) is of the type mainly adapted for saprophagy (Dellacasa et al. 2010), but retaining some features of the coprophagous type. The acropariae are sparse but fine, more extensively developed in some species (e.g., *A. plagiatus* (Linnaeus, 1767) (Fig. 7a–f) and almost absent in others (e.g. *A. isikdagensis*, Fig. 8c, d), the chaetopariae are stout but are fairly long and closely set, the prophobae and apophobae are present – the apophobae as lines of dense fine bristles lateral to the chaetopariae and the prophobae concentrated in the posterior part of the pedia generally clustered at the edges of the mesoepitorma. The number and position of the chaetopedia varies, both between and within species and may differ on the two sides of the same specimen (e.g., *A. wilsonae*, Fig. 9i). The pariae are rounded laterally and the clithra is emarginate either side of the median tylus, which has the corypha distinctly protruding. For morphology of the epipharynx see Dellacasa et al. (2010).

The mandibles (Fig. 10) conform to the typical structure of most Aphodiini adapted to a soft saprophagous diet (sensu Stebnicka 1985), being triangular in shape and equally as long as they are wide, with a well-developed, flattened incisor lobe which extends over the apex of the callum laterale. The lateral edge of the mandible is strongly developed and sclerotised basally and can be regularly convex or almost (*A. niger* group, except for *wilsonae*, Fig. 10h), or sinuate (*A. plagiatus* group) depending on the width of the incisor lobe which varies in width and is much smaller in the *plagiatus* group taxa. The incisor lobe is broadly concave medially with pectinated edge and is clothed in long setae both in the distal end (pecten distalis) as well as the medial edge (pecten medialis) and ventral side of the apex of the callum laterale (pecten ventralis). In common with other closely related taxa in the "*Nialus* Mulsant & Rey, 1870" complex (sensu Rakovič 1991) their mandibles have well sclerotised basis and callum laterale with abundant and large glandular pores as well as a strong apical pore on the callum laterale that sits at the distal end of a strengthening ridge running more or less parallel to the medial edge of the callum. The length of this ridge is variable intra-specifically, from strong and well developed in the niger group (except *L. wilsonae*), to much reduced (*rodrigoi* crown group) or even absent (*plagiatus* group). The setae on the pecten distalis are particularly strong and well sclerotised compared to most other Aphodiini species and the pectination along the medial edge is also stronger than other groups of Aphodiini. The prostheca is reduced in length and it falls well short of the middle of the medial edge. Compared to other species in the *Nialus* complex, *Liothorax* has a well-developed molar lobe with rather pronounced tritors (sensu Hata and Edmonds 1983), and the prostheca can be much shorter than typical, barely reaching less than a 1/3 of the medial edge (*plagiatus* group) and with a poorly developed prosthecal comb. The conjuncta (filtrum) is much coarser, with wider and reduced number of ridges than in other groups, ranging from five to six in the *plagiatus* group and seven to nine in the *niger* group, with the highest number of ridges being found in the *niger*-crown group (*A. niger* Illiger, 1798, *A. muscorum* (Ádám, 1994), *A. felix* sp. nov., and *A. krelli* sp. nov.). For definitions of the morphology of the mandibles please refer to Nel and De Villiers (1988) and Hata and Edmonds (1983).

The maxillae (Figs 11, 12) of the *plagiatus* group are generally narrower than those of the *niger* group, and with the galeae generally smaller, barely produced laterally and with hooked setae on apex and medio-apical area and less dense setation.

The pronotum is hemicylindrical, highly arched transversely but generally only weakly so longitudinally, and more or less parallel-sided (Figs 5, 6). The surface of the pronotum has a double punctation whose strength and density are very variable. The lateral margins are bordered and this border extends inwards round the hind angles to a variable extent. Thus, the hind margin may be entirely bordered, or the border may be narrowly or widely interrupted medially, or there may be an unbordered section either side of the bordered median area (Figs 13–16).

The scutellum is pentagonal, with the sides more or less parallel over their basal 1/2, then tapered to a point apically (Figs 5, 6).

The elytra are finely but distinctly striate with the interstices 6–10× wider than the striae, normally flat but sometimes weakly convex. The interstices may be distinctly but finely reticulate, in some species giving a slightly dull appearance (in contrast to the glossy striae), while in other species the elytra appear glossy black. The underlying reticulation in all cases is small-meshed isodiametric, but its strength varies both within and between species, and has caused considerable confusion (Fig. 17). Thus, in Britain at least, *A. plagiatus* has been distinguished from *A. niger* by its more obviously reticulate elytra, giving a somewhat matt appearance. While this is true of some populations of *A. plagiatus* e.g., from England and Moravia (Fig. 17a), in other populations (e.g. from Hungary and the St Petersburg district of Russia) the elytra are glossy black with the reticulation less prominent, while material from the Tibetan plateau has the elytra glossy with reticulation visible only under intense illumination and at high magnification (Fig. 17b, c). This necessity for high intensity illumination to reveal the reticulation suggested that perhaps the transparent epicuticle was smooth, with the reticulation a feature of the underlying exocuticle. However, scanning electron (SEM) micrographs show that the reticulation is in fact present on the epicuticle (Fig. 17a”, c”).

The raised bead round the apex of the elytra is well developed (Fig. 19a), comparable with that of *Aphodius* (*Nialus*) *varians* Duftschmid, 1805 (Fig. 19b), slightly narrower than the apical section of stria 2, clearly narrower than those of *Aphodius* (*Calamosternus*) *granarius* (Linnaeus, 1767) and *A.* (*C.*) *hyxos* (Petrovitz, 1962) where the bead is at least as wide as the stria and may be ca 2× its width (Fig. 19c, d). The bead is clearly wider than in species such as *A.* (*Agoliinus*) *lapponum* Gyllenhal, 1806 (Fig. 19e) and *A.* (*Agrilinus*) *constans* Duftschmid, 1805 (Fig. 19f).

The elytra have clearly angulate, rounded shoulders with a more or less developed denticle which can be variable in development.

The small spines at the apex of the mid- and hind tibiae are short and fairly even in length (Fig. 18w, x). The apical spurs of the mid and hind tibiae are of varying length between the species and can be helpful in species identification, in particular in separating members of the *A. plagiatus* group of species, in which the basal segment of the mid tarsus is always clearly shorter than the longer tibial spur from the *A. niger* group of species in which the basal tarsal segment in some species is longer than the longer tibial spur, while in others the segment may be either shorter than or ca the same length as the spur (Fig. 18a–t). This character was first used by Ljungberg and Hall (2009) for separating Swedish *A. niger* and *A. plagiatus*.

The sculpture of the metaventrites (Figs 20, 21) may be helpful in recognising species. Particularly striking is the ventrite of male *A. plagiatus*, closely and heavily punctate with the punctures bearing yellow setae. Otherwise, the extent of any reticulation over the median part of the ventrite can be useful.

Following the account of aedeagal structure given by Lawrence and Ślipiński (2013: 61) the phallobase is sclerotised ventrally, and the parameres in the *A. niger* group are turned upwards at the apex. However, for practical purposes it seems more useful to refer to the orientation of the aedeagus when extruded backwards from the apex of the abdomen, with the parameres downturned apically in the *A. niger* group, and with the phallobase sclerotised on its upper surface (Fig. 23f). This means that the right and left sides refer to their positions within the abdomen.

The aedeagus has its endophallus armed with teeth, spines, and bristles, both on the neck of the endophallus (which in inflated specimens never protrudes beyond the paramere apices), and on the main section. The armature of the main section may be used to divide the genus into two sections, the *plagiatus* group with various spines and bristles and the *niger* group with an area of strong recurved thorn-like teeth on its right side. The main field of bristles in *A. rutilipennis* Baudi di Selve, 1870 also lies on the upper right side of the endophallus but the inflated endophallus of *A. chellala* sp. nov. is too damaged for this to be ascertained, and the location of the spines and bristles on the endophalli of *A. plagiatus* and *A. discoides* (A. Schmidt, 1916) is not clear from these rumpled endophalli (Figs 22–24). The parameres of the two sections are also shaped differently. In the *plagiatus* group the parameres are more or less straight and in dorsoventral view of cleared preparations there is a sclerotised strut running to the inner apical corner, lateral to which is a soft sensory area whose shape can be informative (Fig. 22). In the *niger* group the parameres are downturned apically and in dorsoventral view the sensory area is generally not visible, though it is visible in lateral view (Fig. 23) In some species this down-turning is weak and if the parameres are flattened, either by squashing on a slide, or by collapse on drying, the sensory area may become visible in dorsoventral view as a curved band across the parameres apex (Fig. 24).

The sternite of the aedeagal encasement (Fig. 25) shows variation in the central spike, which tends to be narrower in the *A. plagiatus* group.

The spermathecae (Fig. 26) have a simple curved (comma-shaped) form and their sizes may be useful in species (or subspecies) recognition.

Secondary sexual characters are variable and generally only weakly developed. The metaventrite may be flattened or concave medially in males, as against more rounded in females, but this is not always the case (Figs 20, 21). In *L. plagiatus* the metaventrite is flat and rather strongly punctate and bears well-developed yellowish setae in males while in females it is more arched medially and the punctures and setae are finer and the setae are often lost (Fig. 20a, b). Males may have the apical spur of the fore tibiae stronger than in females, and sometimes curved (Fig. 18u, v).

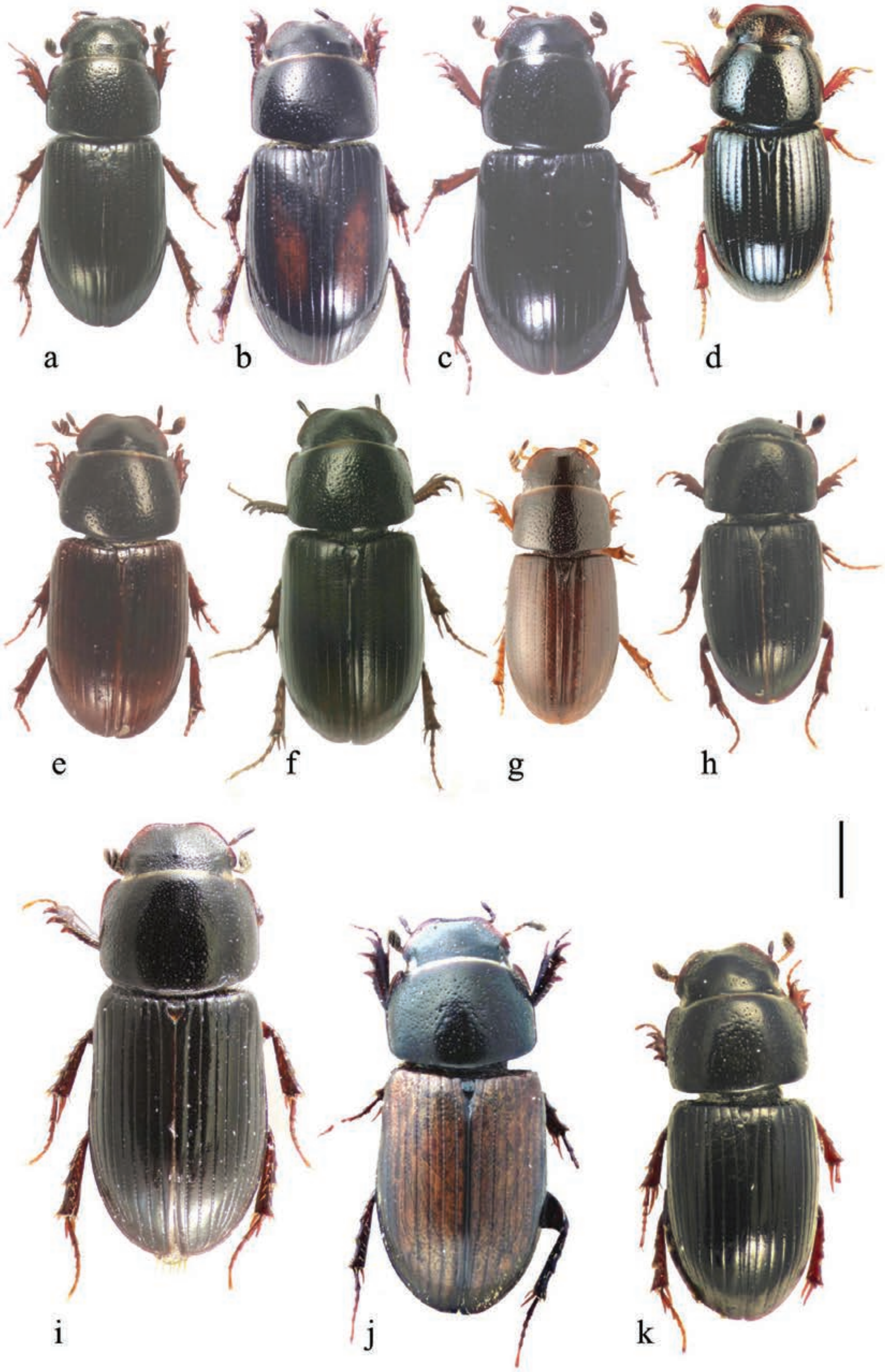

Figure 2. a–k whole beetles **a** *A. plagiatus*, CZ, Moravia **b** *A. plagiatus*, MG, Mongolia **c** *A. jakutorum*, holotype, RU, East Siberia **d** *L. rodrigoi* sp. nov., holotype SP, Aranjuez **e** *A. rutilipennis* (*A. ressli*, holotype) TR, Hatay, Iskenderun **f** *A. rutilipennis*, large ♀, CY, Akrotiri **g** *A. rutilipennis* (*A. cypricola*, holotype) CY **h** *A. chellala* sp. nov., holotype, AG, Chellala **i** *A. rusakovi*, ♂ paratype, RU, Orenburg **j** *A. discoides*, neotype (*A. bytinskisalzi,* holotype) IS, Kuneitra **k** *A. discoides*, black form from TR, Karakurt. Scale bar: 1 mm.

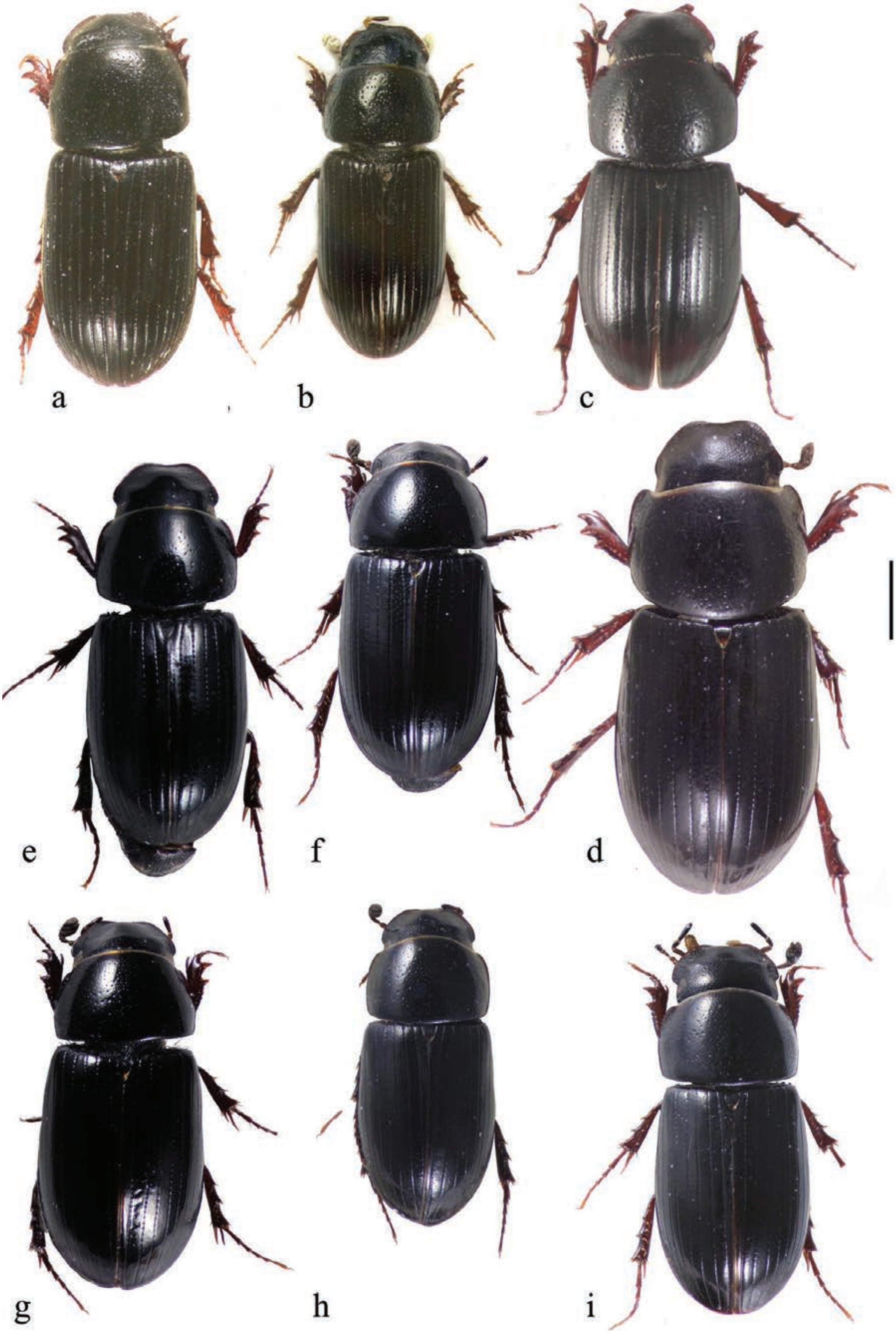

Figure 3. a–i whole beetles **a**, **b** *A. kraatzi* **a** AF, Kabul, ♀ **b** KZ, Kyzil Kum **c**, **d** *A. isikdagensis*, TR, Ḉamildere **c** ♂ paratype **d** ♀ paratype **e**–**g** *A. alberti* sp. nov., TR. Rize, Ovitdagi **e** holotype ♂ **f** paratype ♂ **g** paratype ♀ **h** *A. alberti*?, ♂, AR, Armenia **i** *A. isikdagensis*?, ♂, TR, Artvin. Scale bar: 1 mm.

Figure 4. a–g whole beetles **a** *A. niger*, SV, Tullgarn **b** *A. muscorum*, holotype HU, Vörös tó **c** *A. felix* sp. nov., holotype, IT, Campo Felice **d** *A. bameuli* sp. nov., holotype, Corsica, by Lac de Melo **e** *A. krelli* sp. nov., holotype, IT, Sardinia **f** *A. bellumgerens* sp. nov., holotype, IT, Sicily, Piano Battaglia **g** *A. wilsonae*, holotype, SP, Provincia de Burgos, Balneario de Corconte. Scale bar: 1 mm.

Figure 5. a–p *A. plagiatus* group, heads and pronota **a–c** *A. plagiatus plagiatus* **a** GB, Norfolk **b** CZ, Moravia, Dobre Pole **c** RU, St Petersburg **d** *A. p. sinoplagiatus* ssp. nov., paratype, CH, Qinghai, Gangca **e–g** *A. discoides* **e** neotype IS Kuneitra **f** TR, Kyzil Dag **g** Turkey Muş **h** *A. discoides, black* ♂, TR, Karakurt **i–k** *A. rutilipennis* **i** *A. ressli*, holotype, TR, Hatay **j** CY, Akrotiri **k** *A. cypricola*, holotype, CY **l** *A. chellala* sp. nov., holotype, AG, Chellala **m** *A. rusakovi*, paratype ♂, RU, Orenburg **n** *A. ballerioi* sp. nov., paratype ♂, TR, Rize **o, p** *L. kraatzi* **o** RU, Astrakhan **p** SR. Scale bar: 1 mm.

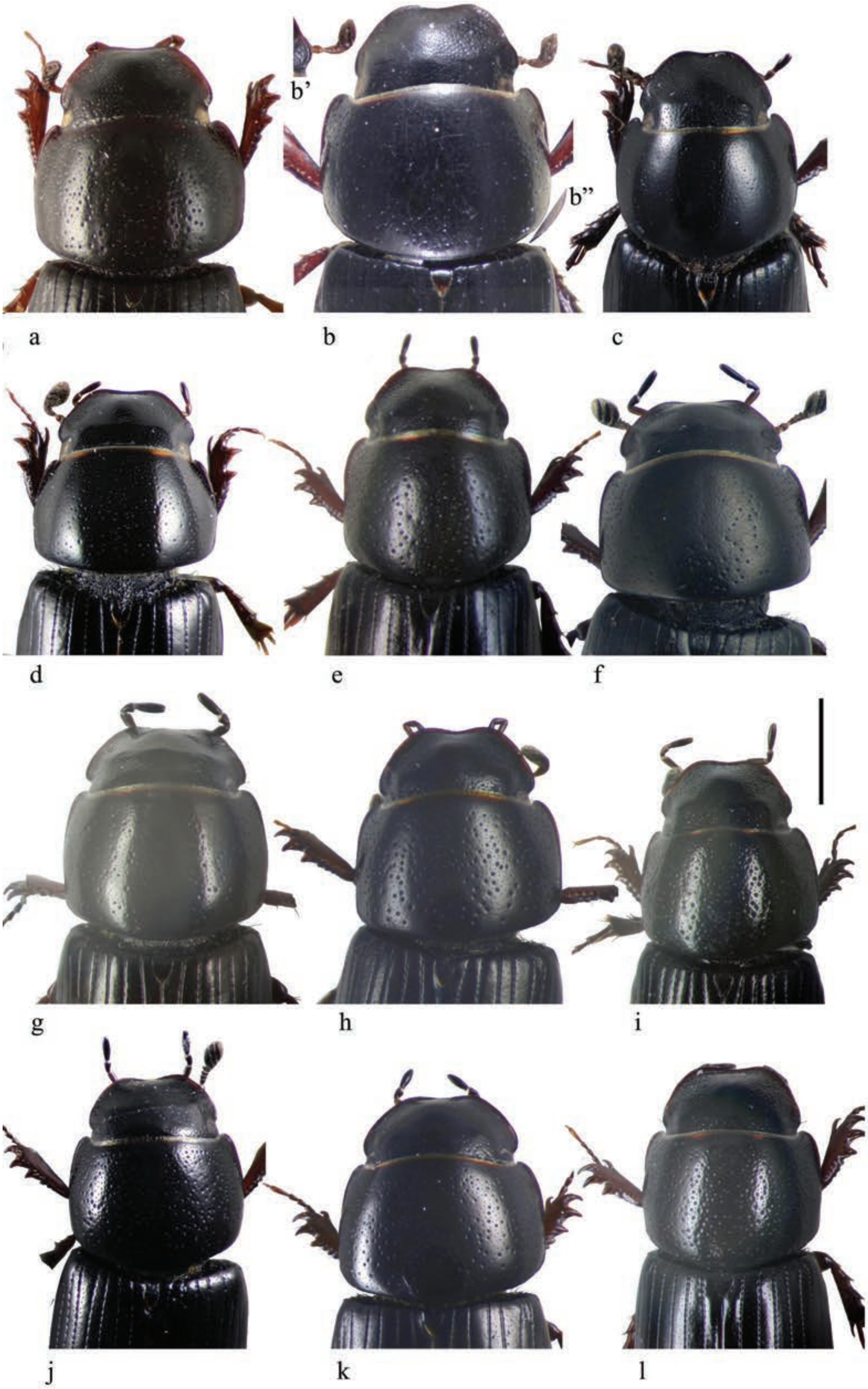

Figure 6. a–**l** *A. niger* group, heads and pronota **a**, **b** *A. isikdagensis*, paratypes, TR Ḉamildere **a** ♂ **b** ♀ **b'** detail of right lateral part of frons and gena, different orientation **b''** detail of right posterior of pronotum, different orientation **c**, **d** *A. alberti* sp. nov., TR, Rize, Ovitdagi **c** holotype **d** ♀paratype **e** *A. niger*, GB, Hampshire, New Forest **f** *A. muscorum*, HU, Hortobágyi **g** *A. bameuli* sp. nov., holotype, FR, Corsica, by Lac de Melo **h** *A. krelli* sp. nov., holotype, IT, Sardinia **i** *A. felix* sp. nov., holotype, IT, Campo Felice **j** *A. bellumgerens* sp. nov., holotype, IT, Sicily, Piano Battaglia **k**, **l** *A. wilsonae*, SP **k** holotype, Provincia de Burgos, Balneario de Corconte **l** paratype, Provincia de Madrid, Manzanares el Real. Scale bar: 1 mm.

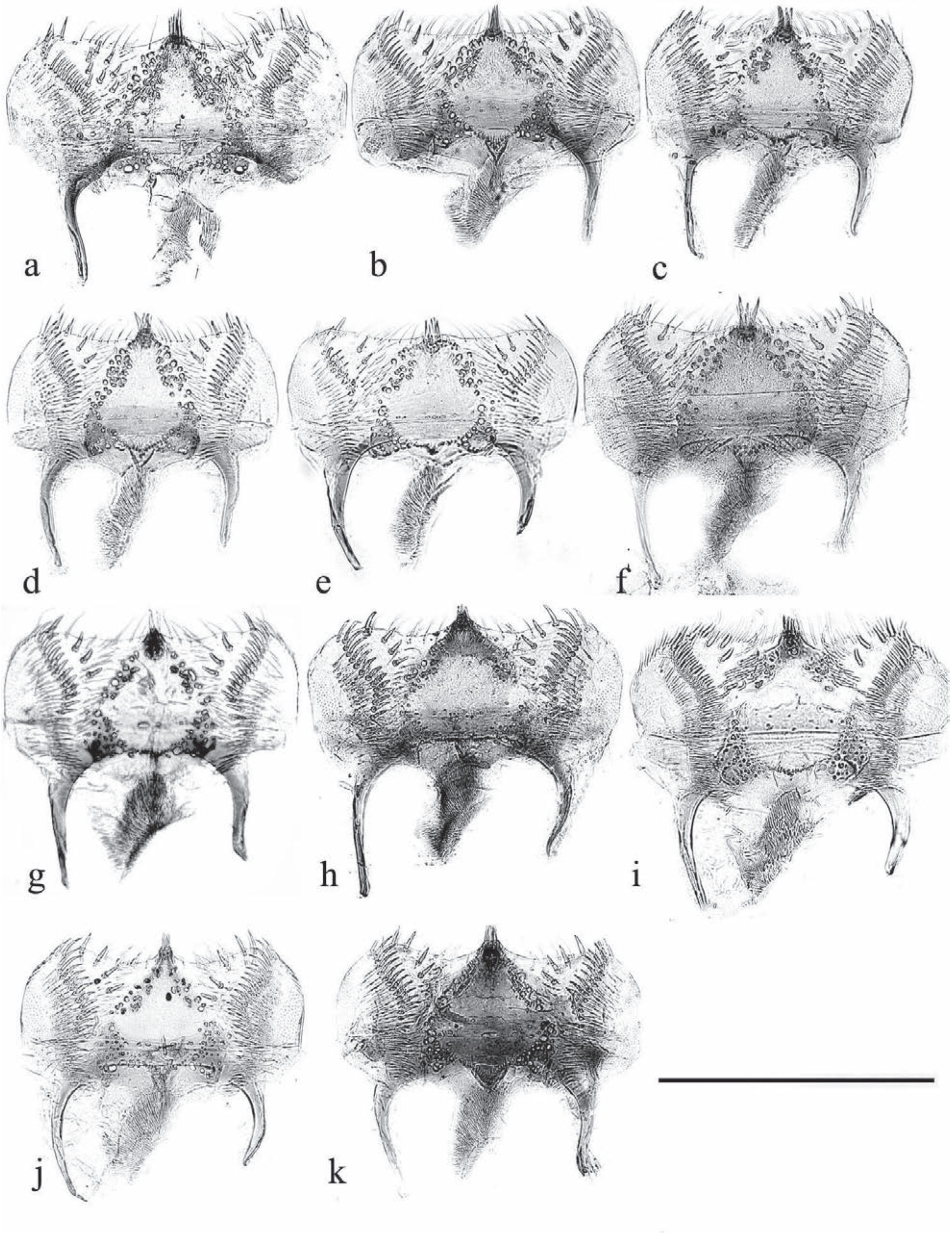

Figure 7. a–k epipharynxes **a– f** *A. plagiatus plagiatus* **a**, **b** GB, Hunstanton, Norfolk **c** CZ, Moravia, Dobré Pole **d** RU, Pavlovsk, St Petersburg **e** *A. p. sinoplagiatus* ssp. nov., paratype, CH, Gangca, Qinghai **f** *A. p. sinoplagiatus*?, CH, "Pekin, coll. Fry" **g** *A. rodrigoi* sp. nov., holotype, SP **h** *A. discoides*, TR **i** *A. rusakovi*, paratype, RU, Orenburg **j** *A. rutilipennis*, CY, Akrotiri **k** *A. chellala*, sp. nov., paratype, AG, Chellala. Scale bar: 0.5 mm.

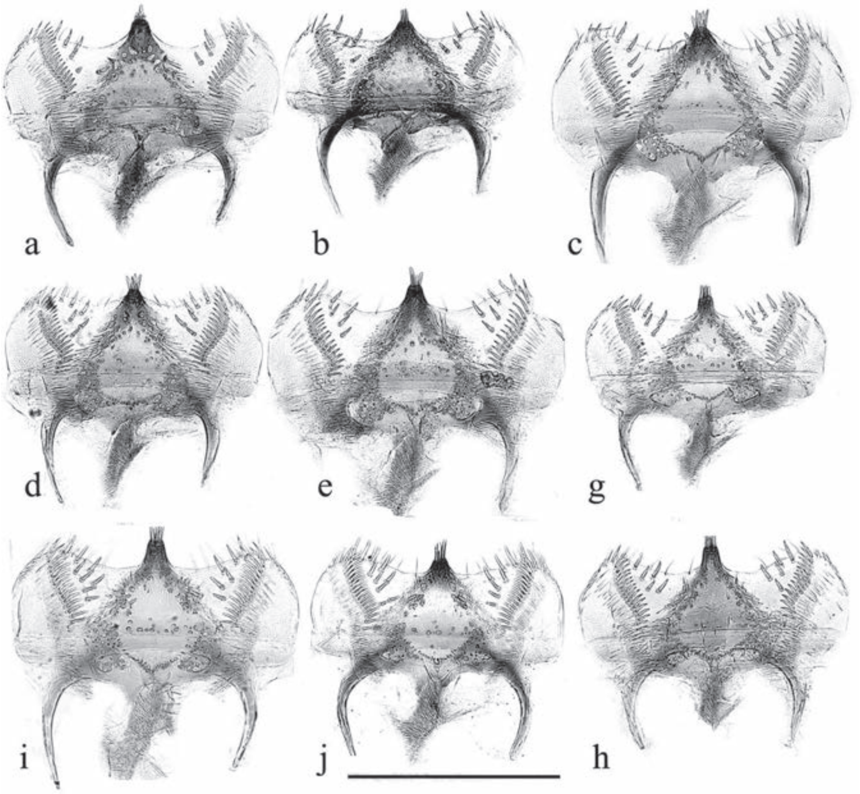

Figure 8. a–k epipharynxes **a**, **b** *A. kraatzi*, SV **c**, **d** *A. isikdagensis* paratypes, TR, Ḉamildere **e**, **f** *A. felix* sp. nov., paratypes **g**, **h** *A. bameuli* paratypes **i** *A. alberti*?, AR **j** *A. krelli* sp. nov., paratype **k**, **l** *A. alberti* sp. nov., paratypes. Scale bar: 0.5 mm

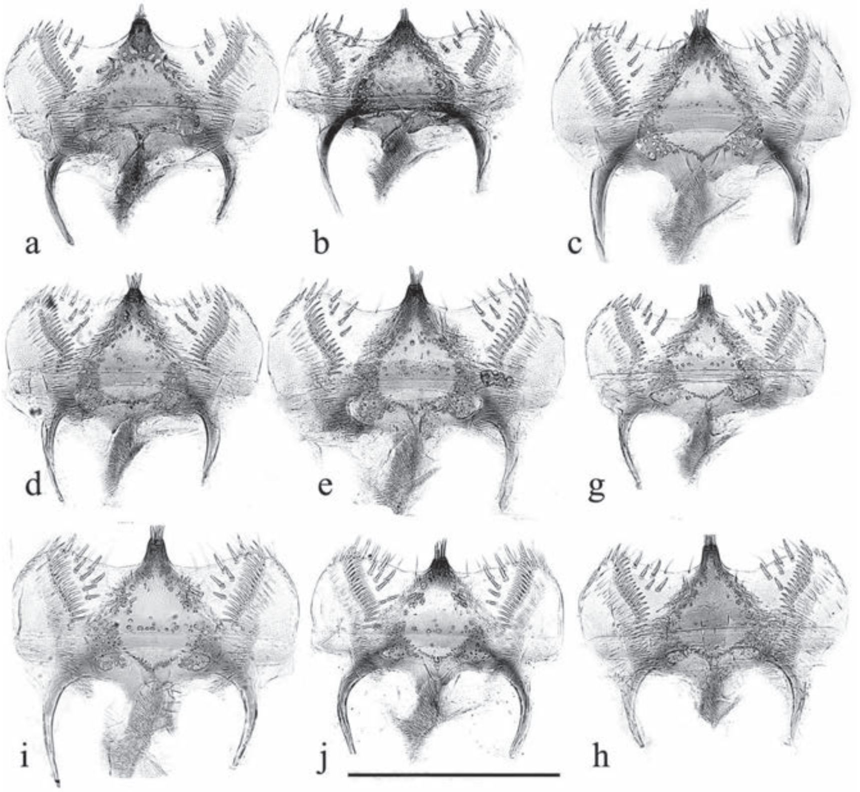

Figure 9. a–i epipharynxes **a**–**c** *A. niger* **a** SV, Tullgarn **b**, **c** GB, Hampshire, New Forest **d** *A. niger*?, CZ, Hradec Králové **e** *A. muscorum*, HU, Hortobagyi **f**, **g** *A. bellumgerens* sp. nov., IT Piano Battaglia, paratypes **h**, **i** *A. wilsonae* paratypes, SP **h** El Vellón **i** Manzanares el Real. Scale bar: 0.5 mm.

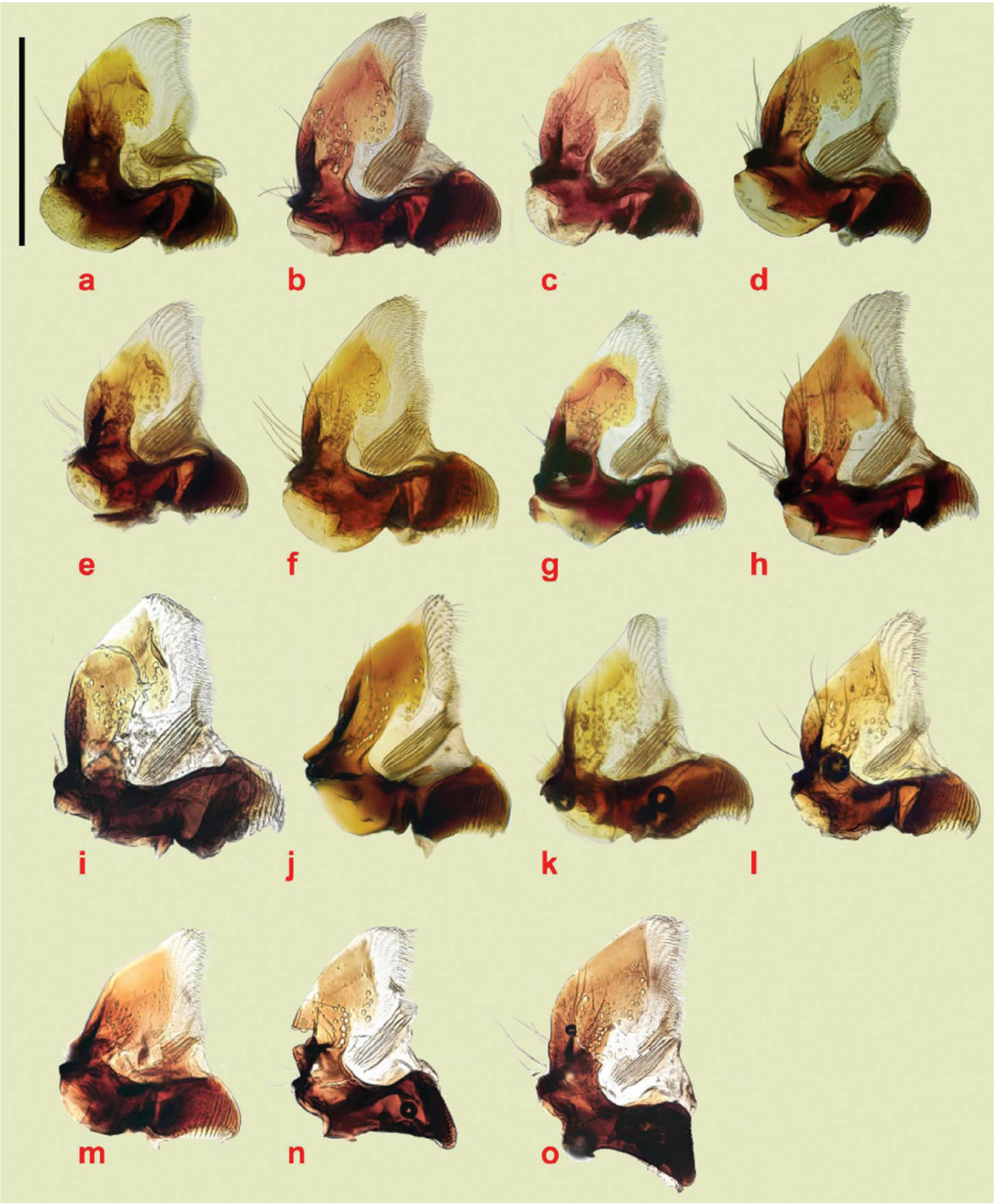

Figure 10. Mandibles **a** *A. niger,* GB, Hampshire, New Forest **b** *A. muscorum*, HU, Hortobagyi **c** *A. felix* sp. nov., IT, Campo Felice **d** *A. krelli* sp. nov., IT, Sardinia, Badde Salighes **e** *A. alberti* sp. nov., TU, Ovit Dağı **f** *A. bellumgerens* sp. nov., IT, Sicily, Piano Battaglia **g** *A. bameuli* sp. nov., FR, Corsica, Haute-Corse **h** *A. wilsonae*, SP, Cantabria, Corconte **i** *A. rusakovi*, RU **j** *A. kraatzi*, SK, Chlaba **k** *A. plagiatus*, GB, Norfolk, Hunstanton **l** *A. rodrigoi* sp. nov., SP, Madrid, Aranjuez **m** *A. chellala* sp. nov., AG, Chellala **n** *A. rutilipennis* sp. nov. **o** *A. discoides* sp. nov. Scale bar: 0.5 mm.

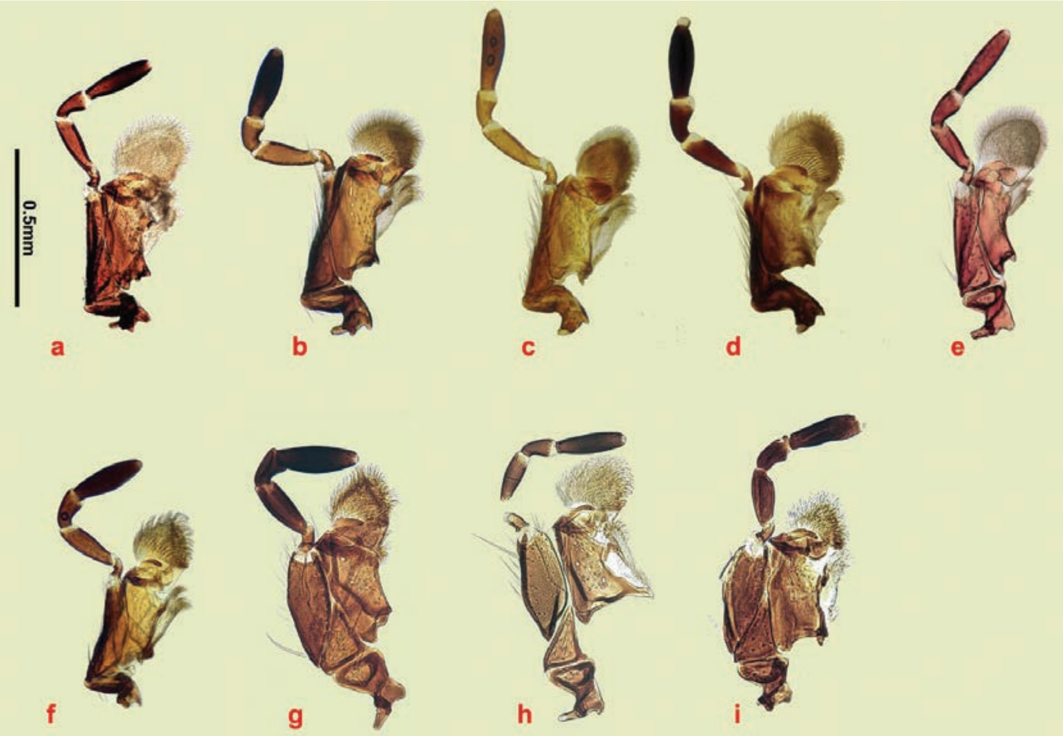

Figure 11. *Aphodius plagiatus* group, maxillae **a** *A. rusakovi*, KZ, Syr-Darja **b**, **c** *A. kraatzi* **b** CZ **c** RU **d** *A. plagiatus plagiatus*, GB, Norfolk **e** *A. p. sinoplagiatus* ssp. nov., paratype, CH, Qinghai, Gangca **f** *A. rodrigoi* sp. nov. paratype SP Madrid, Aranjuez **g** *A chellala*, paratype, AG, Chellala **h** *A. rutilipennis* CY **i** *A. discoides*, TR, Karacadag. Scale bar: 0.5 mm.

Figure 12. *Aphodius niger* group, maxillae **a** *A. niger*, GB, Hampshire, New Forest **b** *A. muscorum* HU, Hortobagy **c** *A. felix* sp. nov., paratype, IT, Campo Felice **d** *A. krelli*, paratype, IT, Sardinia *A. muscorum*? CZ, Břeclav, Pohansko **e** *A. isikdagensis*, paratype, TR, Ҫamildere **f** *A. alberti*, sp. nov., paratype, TR *A. niger*? CZ, Hradec Králové **g** *A. bellumgerens* sp.nov., paratype IT, Sicily *A. felix* sp. nov., paratype, IT, Sardinia **h** *A. bameuli* sp. nov., paratype, FR, Corsica Sicily **i** *A. wilsonae*, SP. Scale bar: 0.5 mm.

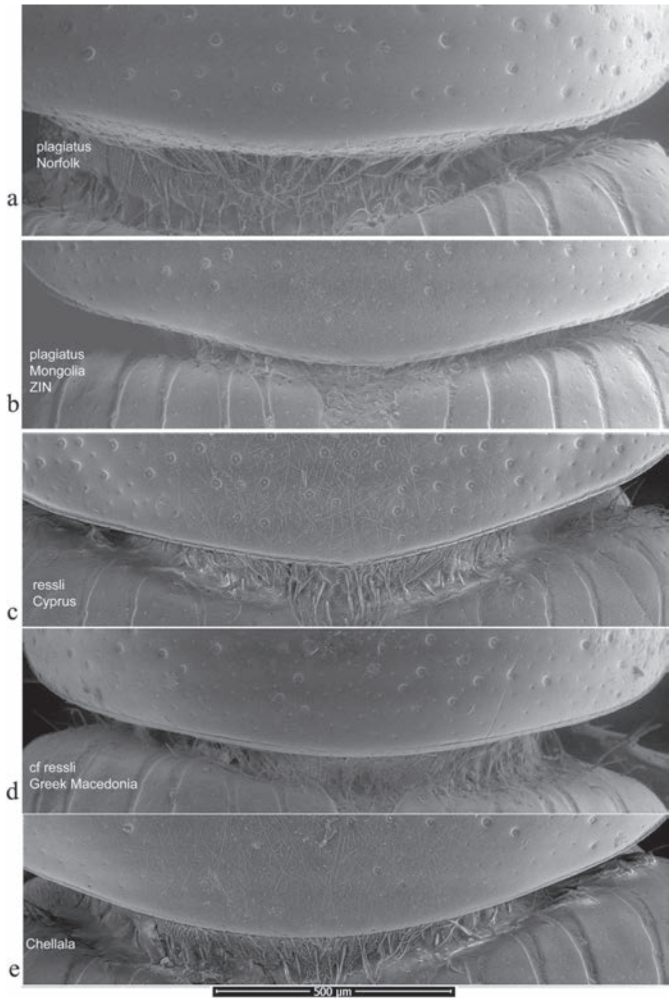

Figure 13. *Aphodius plagiatus* group, pronotal bases 1 **a**, **b** *A. plagiatus* **a** GB, Norfolk **b** MG **c** *A. rutilipennis*, CY **d** *A.* cf. *rutilipennis*, GR, Thessaloniki **e** *A. chellala* sp. nov., paratype, AG.

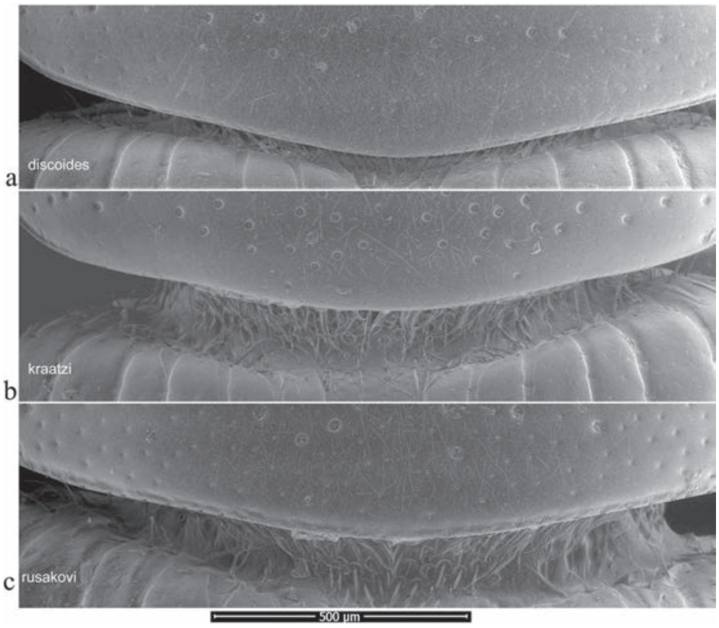

Figure 14. *Aphodius plagiatus* group, pronotal bases 2 **a** *A. discoides*, TR **b** *A. kraatzi*, SK **c** *L. rusakovi*, paratype, RU, Volgograd oblast'.

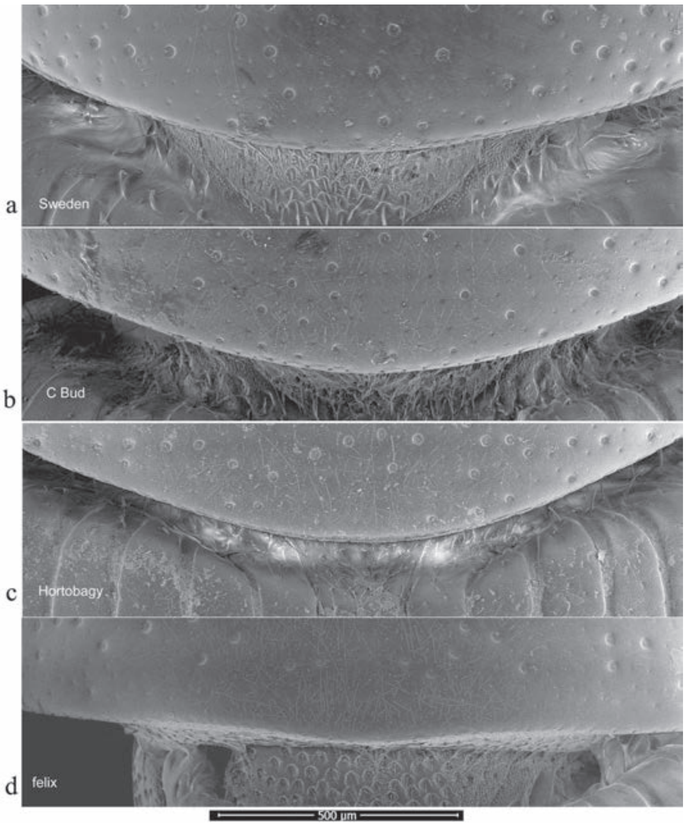

Figure 15. *Aphodius niger* group, pronotal bases 1 **a** *A. niger*, Sweden, Södermanland, Tullgarn **b** *A.* cf. *niger*, CZ, České Budějovice **c** *A. muscorum*, HU, Hortobágyi **d** *A. felix* sp. nov., paratype.

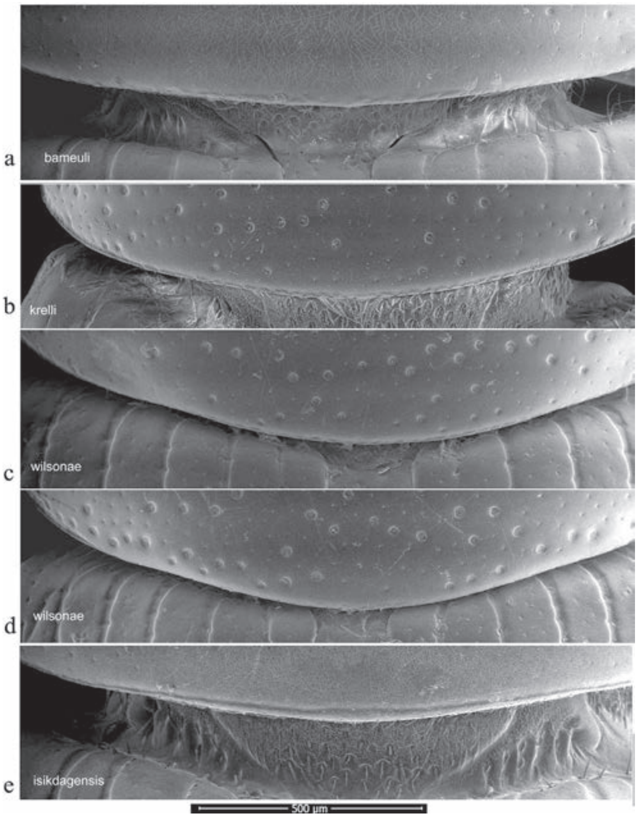

Figure 16. *Aphodius niger* group, pronotal bases 2 **a** *A. bameuli* sp. nov., paratype, FR, Corsica **b** *A. krelli* sp. nov., paratype, IT, Sardinia **c**, **d** *A. wilsonae*, paratypes, SP, Manzanares el Real **e** *A. isikdagensis*, paratype, TR, Ḉamildere.

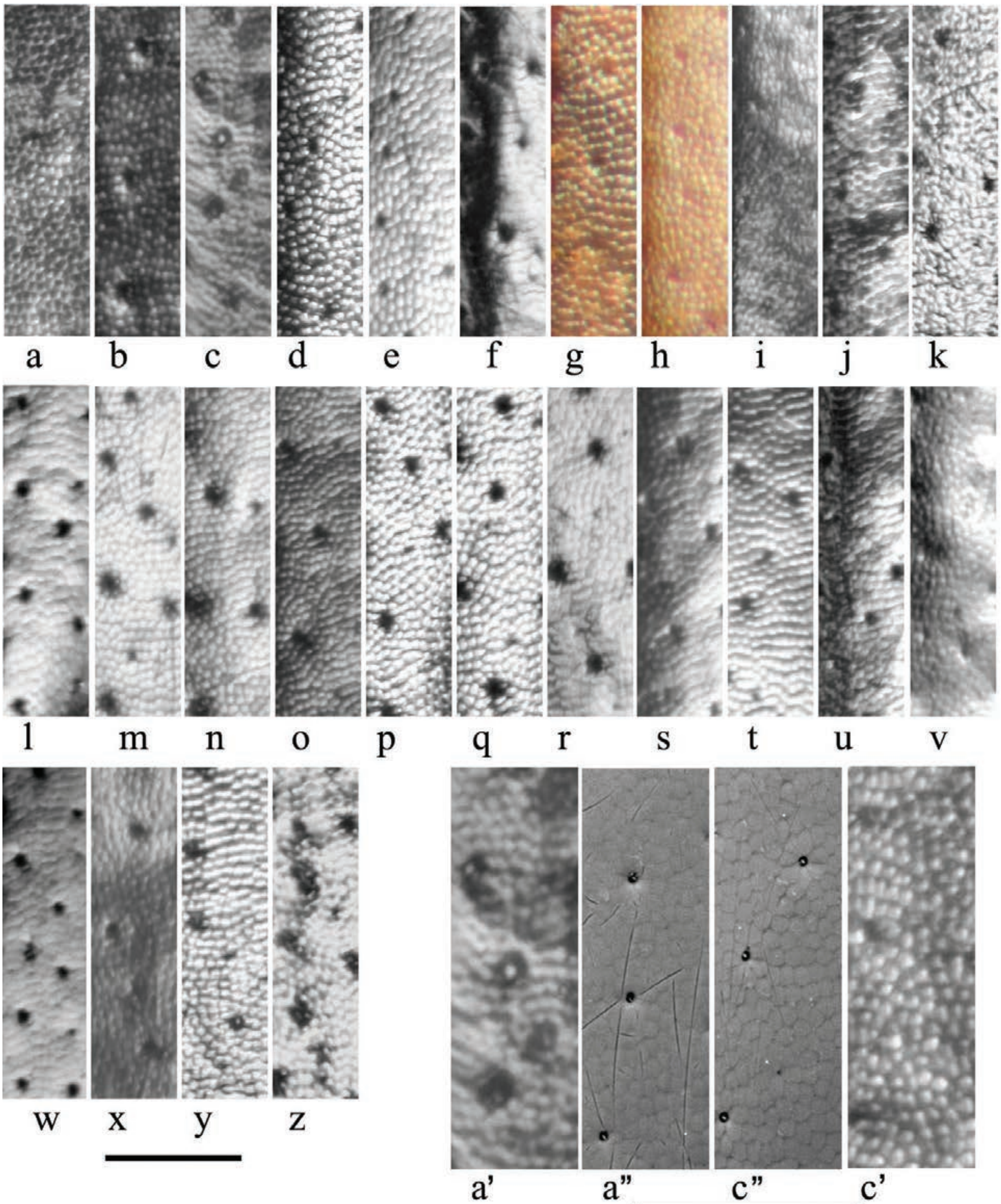

Figure 17. Elytral sculpture of interstices 2 or 3 **a**–**z** stacked photographs **a** *A. plagiatus plagiatus*, CZ, Moravia **b**, **c** *A. p. sinoplagiatus* ssp. nov., paratypes, CH **b** Gangca, Qinghai **c** Gansu **d** *A. rutilipennis* (*A. ressli*, holotype), TR, Hatay **e** *A. chellala* sp. nov., holotype **f** *A. rusakovi*, paratype, RU, Orenburg **g**, **h** *A. discoides* **g** neotype, IS, Kuneitra **h** TR, Kizildag **i** *A. discoides*, black specimen, TR, Karakurt **j** *A. kraatzi*, SK **k** *A. isikdagensis*, paratype, TR, Ḉamildere **l**, **m** *A. niger*, Sweden, Södermanland, Tullgarn **n–q** *A. muscorum*, HU **n** holotype, Vörös-tó **o** Hortobágyi **p**, **q** Kisjúszállás **r, s** *A. niger*? **r** CZ, Hradec Králové **s** CZ, České Budějovice **t** *A. muscorum*? SK, Bol **u** *A. bellumgerens* sp. nov., paratype, IT, Sicily **v** *A. felix* sp. nov., paratype, IT **w** *A. wilsonae*, paratype, SP **x** *A. bameuli* sp. nov., paratype, FR, Corsica **y** *A. krelli* sp. nov., paratype, IT, Sardinia **z** *A. alberti* sp. nov., paratype, TR, Rize, Ovitdag. **a’–c’** *A. plagiatus*, at higher magnification **a’**, **c’** stacked photographs **a”**, **c”** SEM images **a’**, **a”** *A. p. sinoplagiatus* ssp. nov., CH, Gansu **c”**, **c’** *A. p. plagiatus*, CZ, Moravia. Scale bars: 0.1 mm.

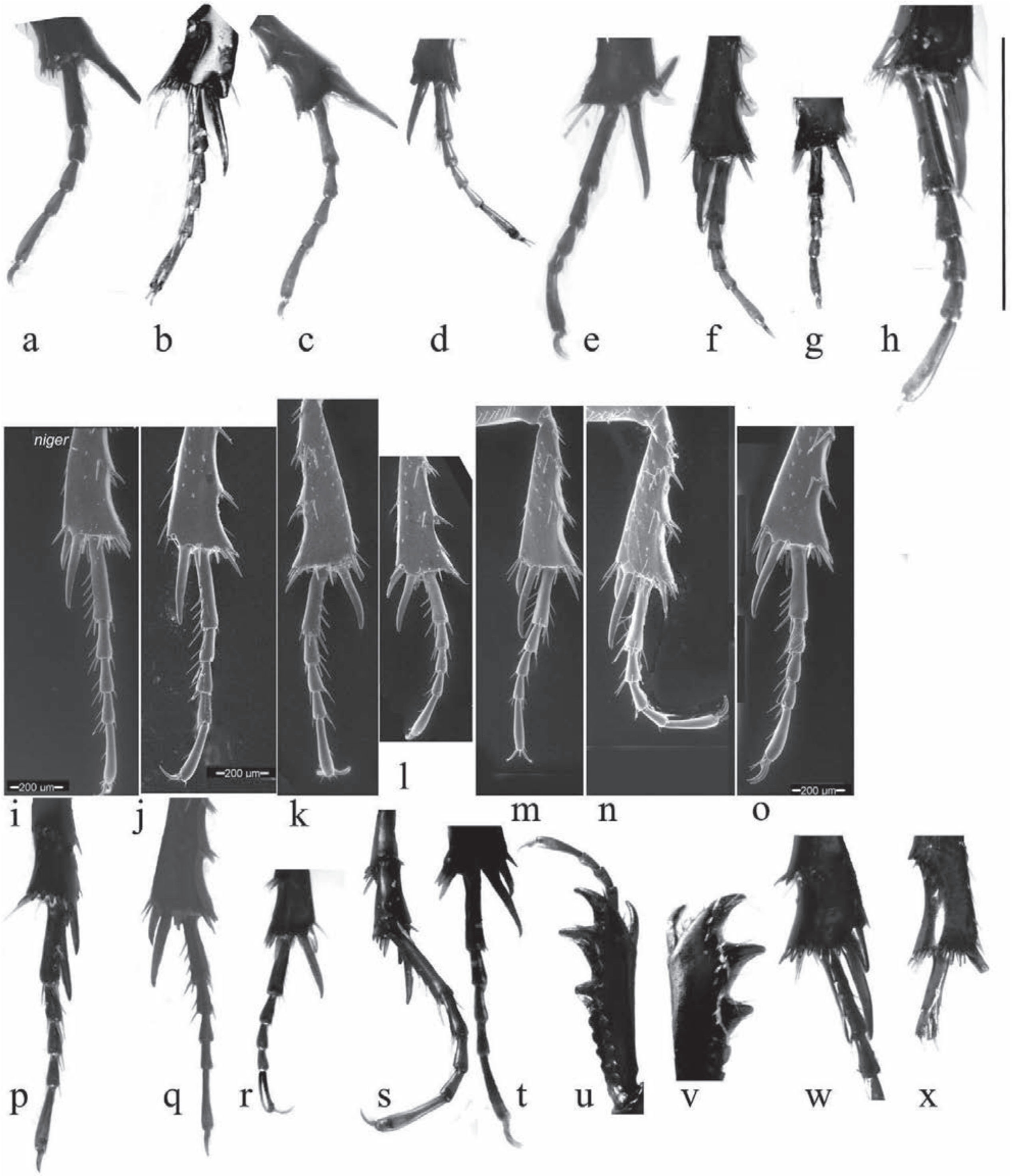

Figure 18. Legs **a–h** *A. plagiatus* group, stacked photographs mid tarsi and apical portions of tibiae **a** *A. plagiatus sinoplagiatus* ssp. nov., paratype, CH, Gangca, Qinghai **b** *A. rodrigoi* sp. nov. holotype, SP, Aranjuez **c** *A. rutilipennis* (*A. ressli*, holotype), TR, Hatay **d** *A. chellala* sp. nov., holotype, AG, Chellala **e** *A. discoides*, neotype, IS, Keneitra **f**, **g** *A. kraatzi* **f** SV **g** RU, Karasuk, W. Siberia **h** *A. rusakovi*, paratype ♂, RU, Orenburg **i–t** *A. niger* group, mid tarsi, and tibial apices **i–o** SEM images **p–t** stacked photographs **i** *A. niger*, Sweden, Södermanland, Tullgarn **j** *A. muscorum*, HU, Hortobágyi **k**, **l** *A. bameuli* sp. nov., paratypes, FR, Corsica **m**, **n** *A. krelli* sp. nov., paratypes, IT, Sardinia **o** *A. wilsonae*, paratype SP **p, q** *A. felix* sp. nov, IT, Abruzzo, Campo Felice **p** paratype **q** holotype **r** *A. bellumgerens* sp. nov., paratype, IT, Sicily **s** *A. isikdagensis*, paratype, TR, Ḉamildere **t** *A. alberti* sp. nov., holotype, TR, Rize, Ovitdag **u**, **v** fore tibiae and tarsi of ♂♂ to show the spur. **u** *A. bameuli* sp. nov., paratype, FR, Corsica **v** *A. rusakovi*, paratype, RU, Orenburg **w**, **x** apex of hind tibia to show the short spines **w** *A. muscorum*, HU **x** *A. wilsonae*, paratype, SP. Scale bar: 1 mm.

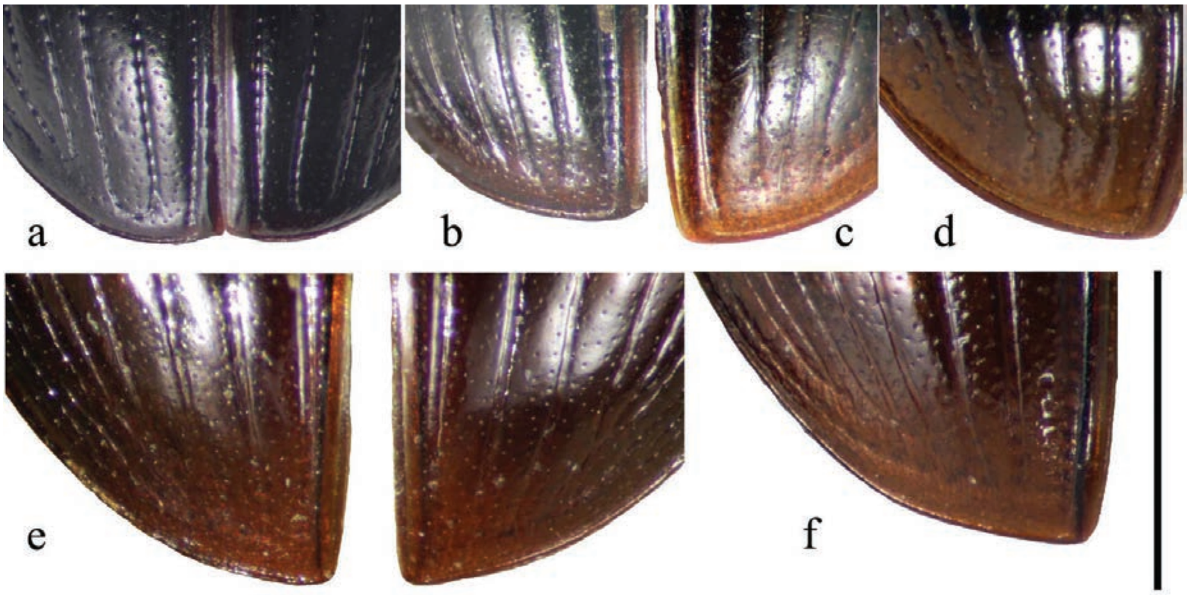

Figure 19. Elytral apices **a** *A.* (*L.*) *niger*, SV, Södermanland, Tullgarn **b** A. (*Nialus*) *varians*, FR, left elytron **c** *A.* (*Calamosternus*) *granarius*, CY, right elytron **d** *A.* (*C.*) *hyxos*, CY, left elytron **e** *A.* (*Agoliinus*) *lapponum*, GB, Cumbria, both elytra **f** *A.* (*Agrilinus*) *constans*, IT, Sardinia, left elytron. Scale bar: 1 mm.

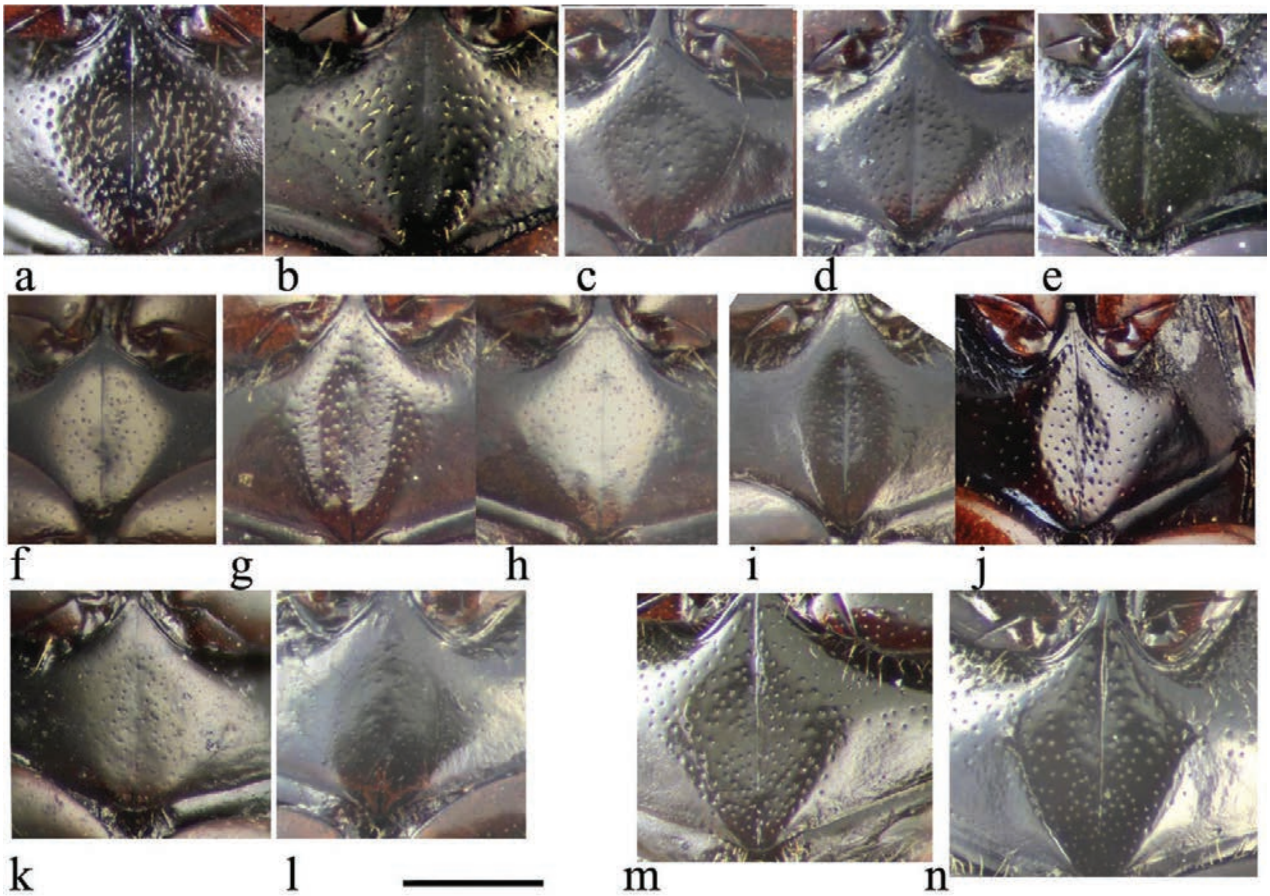

Figure 20. Metaventrites, *A. plagiatus* group **a** *A. plagiatus plagiatus*, GB, Studland, ♂ **b** *A. p. sinoplagiatus* ssp. nov., paratype, CH, Gansu, ♀ **c**, **d** *A. rutilipennis*, CY **c** ♂ **d** ♀ **e**, **f** *A. chellala* sp. nov., paratypes, AG **e** ♂ **f** ♀ **g**, **h** *A. kraatzi*, RU, Orenburg, ♂ **i** *A. kraatzi*, SK, ♀ **j** *A. rodrigoi* sp. nov., holotype, ♂, SP, Provinicia de Madrid, Aranjuez **k**, **l** *A. discoides* **k** neotype ♂, IS, Kuneitra **l** TR, ♀ **m**, **n** *A. rusakovi* **m** paratype, ♂, RU, Orenburg **n** ♀ RU, Volgograd oblast'. Scale bar: 0.5 mm.

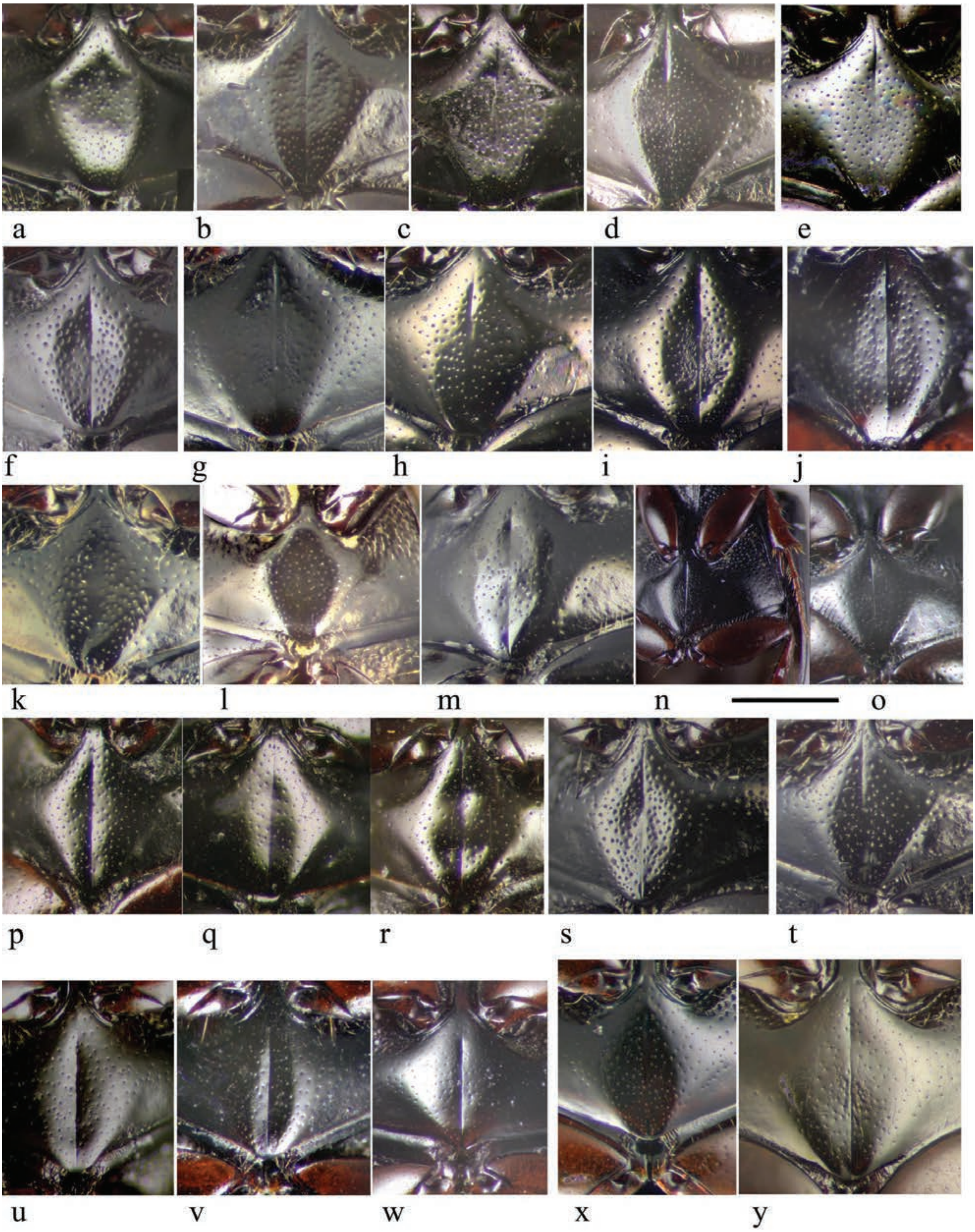

Figure 21. Metaventrites, *A. niger* group **a–d** *A. niger* **a**, **c**, **d** SV, Södermanland, Tullgarn **b** GB, Hampshire, New Forest **a**, **b** ♂ **c**, **d** ♀ **e**, **g–j** *A. muscorum* **e** holotype ♀, HU, Vörös-tó **f** *A. felix* sp. nov., paratype ♂, IT, Campo Felice **g** ♂, HU, Hortobágyi **h**, **i** ♀♀, HU, Kisujszallas **j** ♀, HU, Josvafo **k** *A. felix* sp. nov. paratype ♀, IT, Campo Felice **l**, **m** *A. bellumgerens* sp. nov., paratypes, IT, Sicily, Piano Battaglia **l** ♂ **m** ♀ **n**, **o** *A. alberti* sp. nov., paratypes, TR, Rize, Ovitdag **n** ♂, **o** ♀ **p**–**r** *A. bameuli* sp. nov., paratypes, FR, Corsica **p** ♂ **q**, **r** ♀ **s**, **t** *A. krelli* sp. nov., paratypes, IT, Sardinia **s** ♂ **t** ♀ **u**–**w** *A. wilsonae*, paratypes **u**, **v** SP, Manzanares el Real **u** ♂ **v** ♀ **w** ♀, SP, El Vellon **x**, **y** *A. isikdagensis*, paratypes, TR, Ḉamildere **x** ♂ **y** ♀. Scale bar: 0.5 mm.

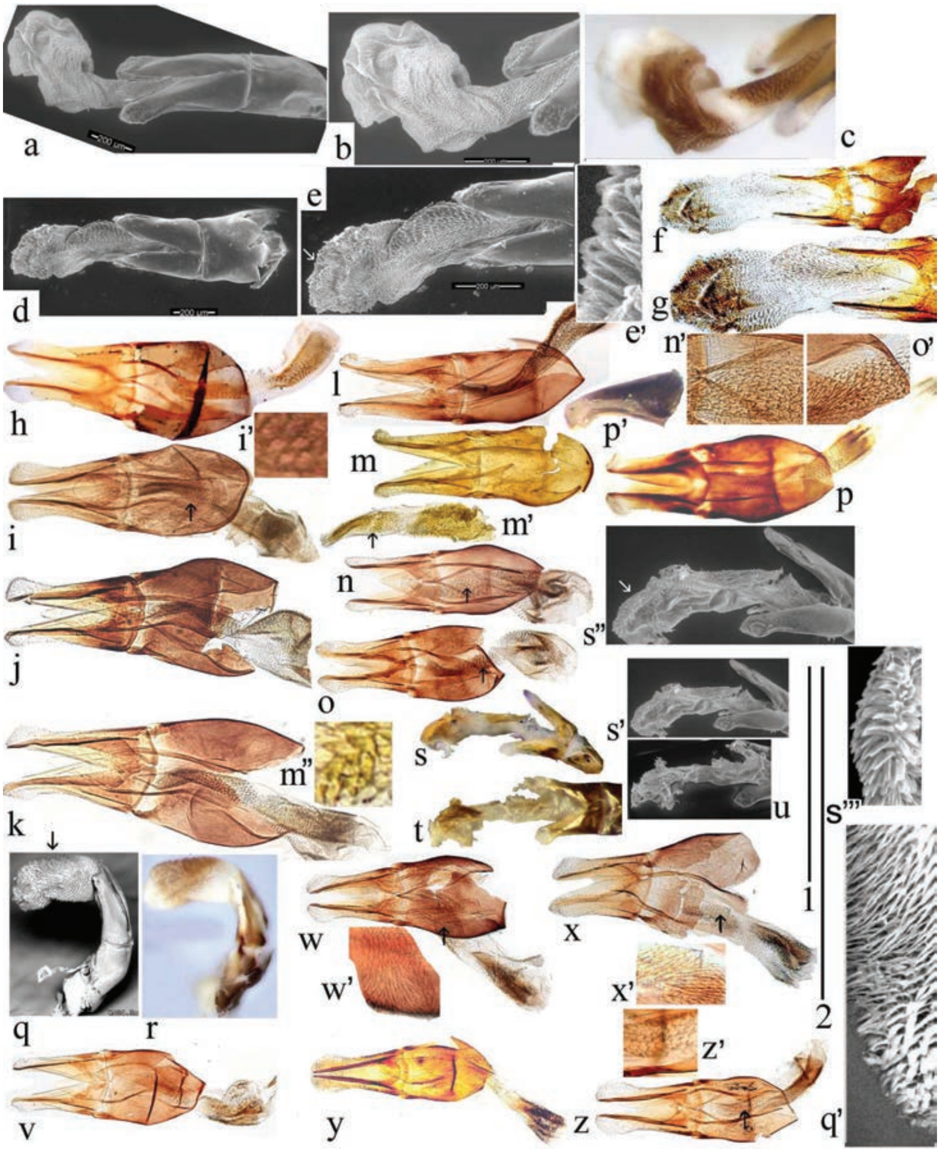

Figure 22. *Aphodius plagiatus* group aedeagi **a–c** *A. plagiatus plagiatus*, GB, Studland, Dorset, aedeagus with extruded endophallus **a**, **b** SEM images **a** whole aedeagus **b** endophallus in more detail **c** stacked photograph of endophallus **d–g** *A. discoides*, neotype (*Aphodius bytinskisalzi*, holotype, IS, Kuneitra) **d**, **e**, **e’** SEM images **f**, **g** stacked photographs **h–n** cleared preparations mounted on slides **h** *A. p. plagiatus*, GB, Norfolk **i** *A. p. sinoplagiatus*? “China, Pekin”, Fry collection **i’** teeth on neck of endophallus in the region marked with an arrow in **i j**, **k** *A. plagiatus sinoplagiatus* ssp. nov., paratypes **j** CH, Gangca **k** CH, Tsaidam **l** *Aphodius jakutorum* Balthasar, lectotype, RU, East Siberia **m** *A. rodrigoi* sp. nov., holotype, SP, Aranjuez, dissected aedeagus **m’** endophallus **m”** endophallic teeth in area indicated by arrow in **m’** at higher magnification **n** *A. discoides*, TR, Karacadag **n’** teeth on neck of endophallus, in area indicated by arrow in **n** at higher magnification **o** *A. discoides,* black specimen from TR, Karakurt, **o’** teeth on neck of endophallus, in area indicated by arrow in **o** at higher magnification **p**, **p’** *A. rusakovi* **p** paratype, RU, Orenburg **p’** RU Volgograd obl. Fastov, paramere, lateral **q–v** SEM images and stacked photographs **q**, **r** *A. rutilipennis*, CY, with endophallus inflated **q** SEM image **q’** (bottom right of plate) dorsal surface of endophallus in area indicated by arrow in **q** at higher magnification, to show the hair-like setae **r** stacked photograph of the same specimen **s**, **s’** *A. chellala* sp. nov., paratype with endophallus extruded **s** stacked photograph **s’**, **s”**, **s”’** SEMs of the same specimen **s”**, **s”’** at higher magnifications **t**, **u** *L. chellala* sp. nov., holotype with the endophallus extruded **t** stacked photograph **u** SEM image **v**–**z** photographs of cleared specimens mounted in DMHF on slides **v**, **w** *A. rutilipennis* **v** CY **w** TR **w’** teeth on neck of endophallus, in area indicated by arrow in **w** at higher magnification **x** *A. chellala* sp. nov., paratype, AG, Taguin (La Smala) **x’** teeth on neck of endophallus, in area indicated by arrow in **x** at higher magnification **y**, **z** *A. kraatzi* **y** KZ, Syr Darya **z** AF, Kabul **z’** teeth on neck of endophallus, in area indicated by arrow in **z** at higher magnification Scale bar 1: 1 mm (**a**, **d**, **f**–**t**, **v**–**z**); 0.4 mm (**n’**, **o’**, **s”**, **w’**, **x’**, **z’**); 0.17 mm (**e’**, **m”**, **q’ s”’**). Scale bar 2: 1 mm (**b**, **c**, **e**, **g** and **s”**).

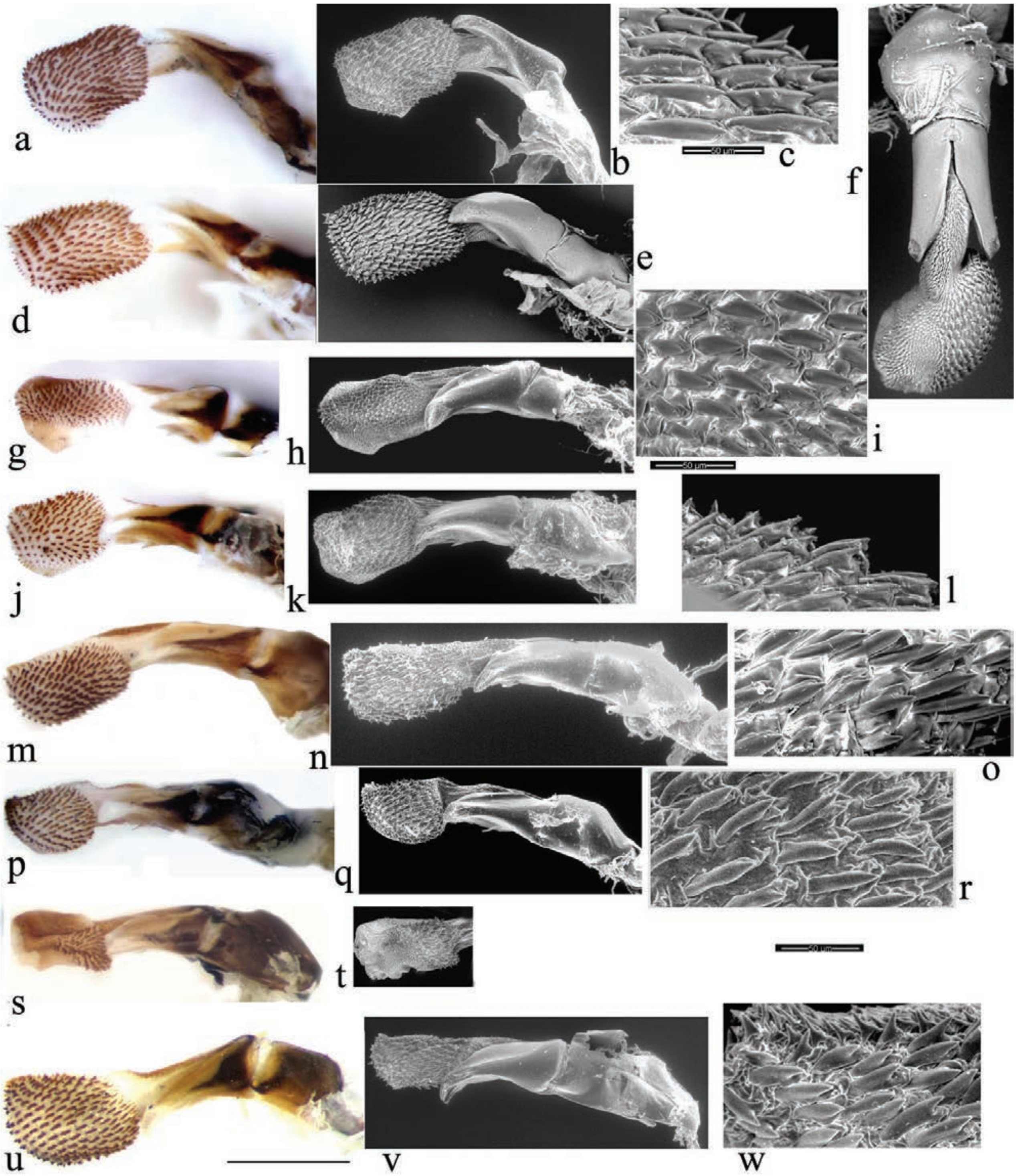

Figure 23. *A. niger* group, aedeagi with inflated endophalli, stacked photographs and SEM images **a–e, g–w** right lateral view **f** viewed from above **a–c** *A. niger*, SV, Södermanland, Tullgarn **a** stacked photograph **b** the same aedeagus, SEM image **c** detail of endophallic teeth **d–f** *A. niger*, GB, Hampshire, New Forest **d** stacked photograph **e**, **f** SEM images **g–i** *A. wilsonae*, SP, Areños **g** stacked photograph **h** SEM image, **i** detail of endophallic teeth **j–l** *A. bameuli* sp. nov., holotype **j** stacked photograph **k** SEM image **l** detail of endophallic teeth **m–o** *A. krelli* sp. nov., holotype **m** stacked photograph **n** SEM image **o** detail of endophallic teeth **p–r** *A. bellumgerens* sp. nov., paratype **p** stacked photograph **q** SEM image **r** detail of endophallic teeth **s**, **t** *A. bellumgerens* sp. nov., holotype **s** stacked photograph **t** SEM image of endophallus **u** *A. muscorum*, HU, Hortobágyi, stacked photograph **v**, **w** *A. felix* sp. nov., holotype, SEM images **v** aedeagus **w** detail of endophallic teeth. Black Scale bar: 0.5 mm for aedeagi and endophallus, white SEM scale on black background: 50 µm for details of endophallic teeth.

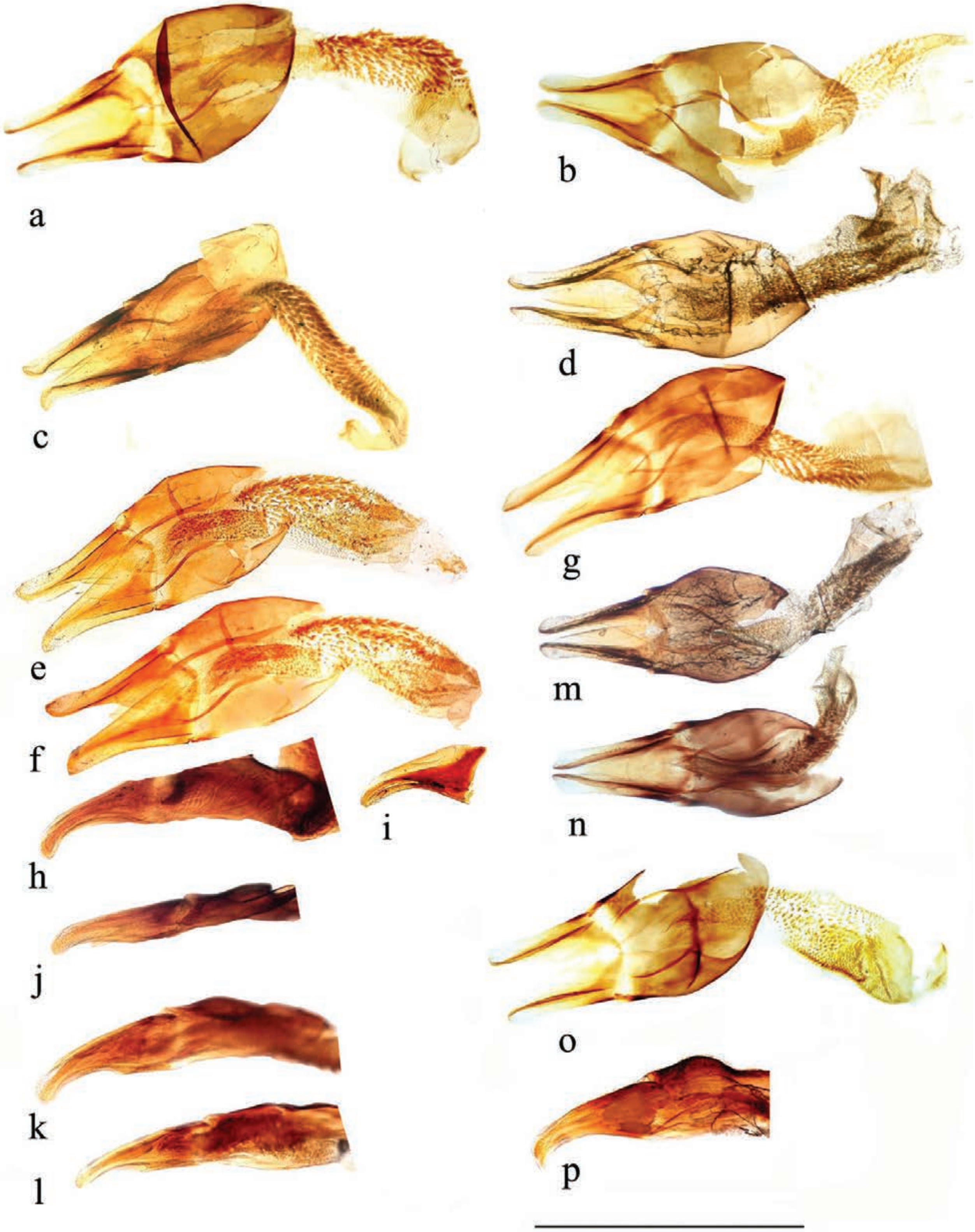

Figure 24. *A. niger* group aedeagi, cleared preparations mounted in DMHF on slides **a–g**, **m–o** dorsoventral view **h–l**, **p** right lateral view **a** *A. niger*, SV, Södermanland, Tullgarn **b** *A. bameuli* sp. nov., paratype **c** *A. isikdagensis*, paratype, TR, Ḉamildere **d** *A. krelli* sp. nov., paratype, IT, Sardinia **e**–**f** *A. alberti* sp. nov., TR, Rize, Ovitdag **e** paratype, after squashing **f** the same specimen, before squashing **g**, **h**, **j** *A. alberti* sp. nov., different paratypes **i** *A. alberti* sp. nov., paratype, paramere **k** *A. isikdagensis*?, TR, Artvin **l** *A. alberti*?, Armenia **m** *A. bellumgerens* sp. nov., paratype, IT, Sicily, Piano Battaglia **n** *A. bellumgerens*, paratype IT, Sicily, Nebrodi **o** *A. wilsonae*, paratype, SP, Manzanares el Real **p** *A. muscorum*, HU, Hortobági. Scale bar: 1 mm.

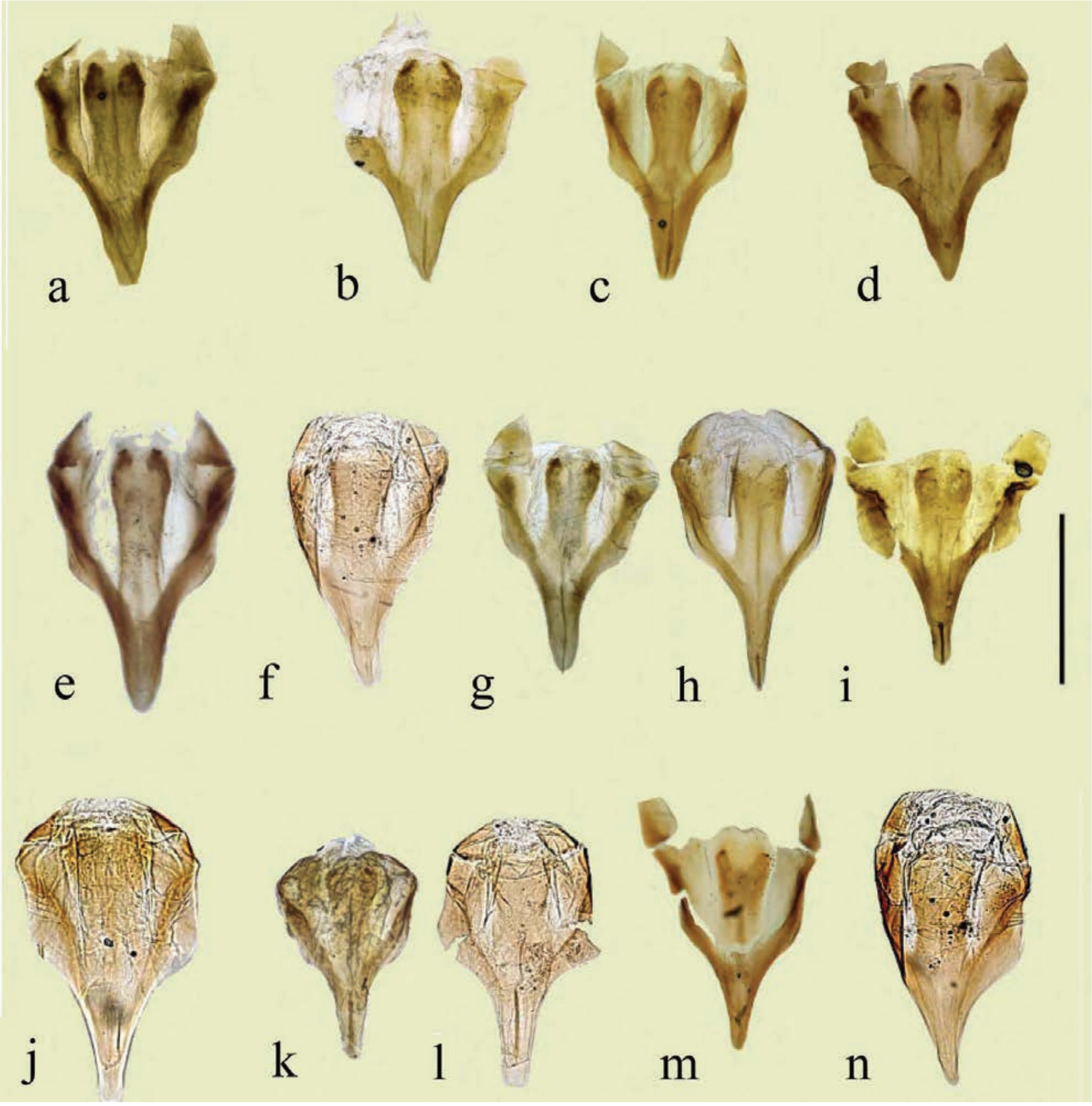

Figure 25. Aedeagal encasements (9th abdominal sternite) **a** *A. niger,* GB, Hampshire, New Forest **b** *A. muscorum*, HU, Hortobagyi **c** *A. felix* sp. nov., IT, Campo Felice **d** *A. alberti* sp. nov., TU, Ovit Dağı **e** *A. bellumgerens* sp. nov., IT, Sicily, Piano Battaglia **f** *A. bameuli* sp. nov., FR, Corsica, Haute-Corse **g** *A. wilsonae*, SP, Cantabria, Corconte **h** *A. kraatzi*, RU, Chita Reg. **i** *A. plagiatus*, UK, Norfolk, Hunstanton **j** *A. plagiatus*, CN, Beijing **k** *A. rodrigoi* sp. nov., SP, Madrid, Aranjuez **l** *A. chellala* sp. nov., AG, Chellala, paratype **m** *A. rutilipennis* sp. nov., CY, Konakli, paratype **n** *A. discoides* sp. nov., paratype. Scale bar: 0.5 mm.

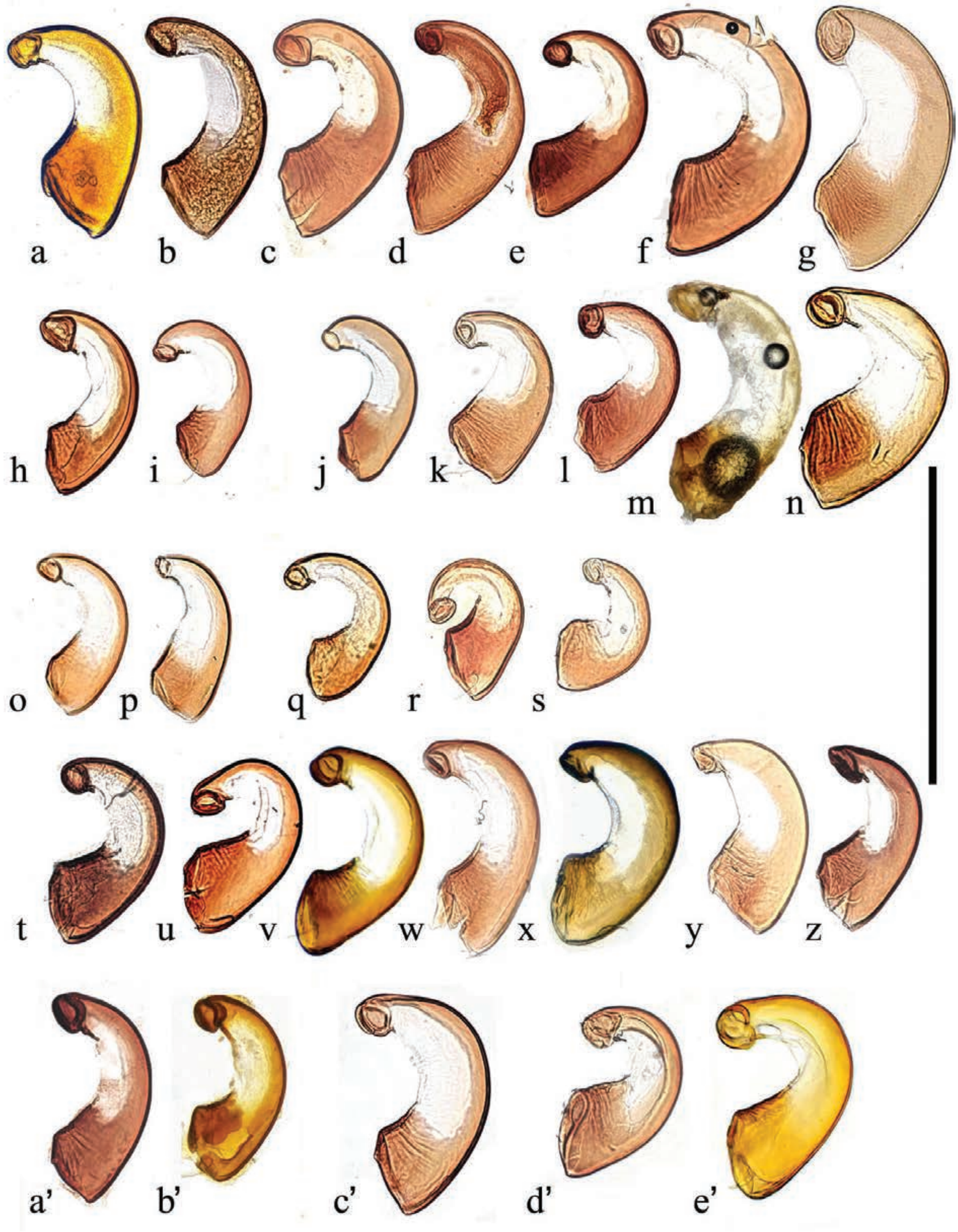

Figure 26. Spermathecae **a–e** *A. plagiatus plagiatus* **a** CZ, Dobre Pole **b** GB, Norfolk **c** KZ, Karaganda **d**, **e** RU, Transbaikal, Ulan Ude **f**, **g** *A. p. sinoplagiatus*, CN **f** Gansu **g** holotype, CN, Qinghai **h**, **i** A. discoides, TR **h** Kizil dag, **i** Muş **j** *A. rutilipennis* CY, Limassol distr **k** *A. rutilipennis*?, GR Thesaloniki **l** *A. chellala*, paratype, AG, Chellala **m**, **n** *A. rusakovi* **m** paratype, RU, wet but not covered **n** KZ, Syr-Darja **o–s** *A. kraatzi* **o**, **p** SK **q** RU, Astrakhan **r** RU, Lenkoran **s** AF, Kabul **t** *A. niger*, GB, Hampshire, New Forest **u** *A. muscorum* HU, Hortobágyi **v** *A felix*, paratype, IT **w**, **x** *A. bameuli*, paratypes, FR **y** *A. krelli*, sp. nov., IT **z** *A. bellumgerens* sp. nov., paratype, IT **a'**, **b'** *A. alberti* sp. nov., TR paratypes **c'** *A. isikdagensis*, paratype, TR Çamildere **d'**, **e'** *A. wilsonae*, SP **d'** paratype, SP, Madrid **e'** SP, Soria. Scale bar: 0.5 mm.

Species recognised in this revision

The *A. plagiatus* group

A. (*L.*) *plagiatus* (Linnaeus, 1767)
plagiatus plagiatus (Linnaeus, 1767)
= *jakutorum* Balthasar, 1938)
= *hungaricus* Endrődi, 1955
plagiatus sinoplagiatus subsp. nov.
A. (*L.*) *rodrigoi* sp. nov.
A. (*L.*) *discoides* A. Schmidt, 1916, stat. rest.
= *discus* Reitter, 1892
= *bytinskisalzi* Petrovitz, 1971
A. (*L.*) *rutilipennis* Baudi di Selve, 1870, stat. rest.
= *ressli* Petrovitz, 1962
= *cypricola* Balthasar, 1971
A. (*L.*) *chellala* sp. nov.
A. (*L.*) *kraatzi* Harold, 1868
A. (*L.*) *rusakovi* Gusakov, 2004

The *A. niger* group

A. (*L.*) *niger* Illiger, 1798
A. (*L.*) *muscorum* Ádám, 1994, rest.
A. (*L.*) *felix* sp. nov.
A. (*L.*) *bellumgerens* sp. nov.
A. (*L.*) *bameuli* sp. nov.
A. (*L.*) *krelli* sp. nov.
A. (*L.*) *isikdagensis* Balthasar, 1953
A. (*L.*) *alberti* sp. nov.
A. (*L.*) *wilsonae* Angus & Maté, 2005, stat. rest.

Key to the *Liothorax* species included in this paper

The key is suitable for males and series including both sexes. It is not suitable for females only because females of some species cannot be separated by morphological features.

1 Parameres downturned apically, viewed from above either not showing the apical sensory area (Fig. 23a, b, d, g, m–o) or with it extending over the apical margin from the tip of the dark strut to the outer margin of the apex (Fig. 24c, e), Endophallus with strong recurved teeth (Figs 23, 24). Basal segment of mesotarsus either longer or ca the same length as the longer mesotibial spur (Fig. 18i–t) (the *niger* group)..**2**

– Parameres not downturned apically, viewed from above with more or less transparent sensilla-rich pads running along the apical 1/3 to 1/2 of their outer margins (Fig. 22h–n, v–z). Endophallus with various hairs and bristles, never with strong recurved teeth (Fig. 22). Basal segment of mesotarsus always clearly shorter than the longer mesotibial spur (Fig. 18a–h) (the *plagiatus* group) .. **10**

2 Specimens from Anatolia and the Trans Caucasus. Parameres in lateral view often only weakly downturned (Fig. 24h–l, p), and, viewed from above, with the apical sensory area often running across the apex, from the tip of the darkened strut to the outer apical angle (Fig. 24c, e) **3**

– Specimens from Europe, Kazakhstan, or western Siberia. Parameres in lateral view generally more strongly downturned (Fig. 24p) and, viewed from above, with a darkened strut running along their inner margins to the apex, their apices lateral to this transparent, not showing the sensilla-rich pads (Fig. 24a, b, d, g, m-o) **4**

3 Larger species, length 4.5–5.8 mm. Legs mid brown (Fig. 3c, d). Epipharynx (Fig. 8c, d), with apophobae arranged in narrow bands ca 2 bristles wide. Turkey, Çamildere, Isik Dag mountain ....***A* (*L.*) *isikdagensis***

– Smaller species, length 4.1–4.9 mm. Legs very dark brown to glossy black (Fig. 3e–h). Epipharynx (Fig. 8k, l) with the median darkened area narrowed over basal 1/4 and apophobae arranged in single rows. Turkey...................
....***A.* (*L.*) *alberti* sp. nov.**

4 Basal segment of mesotarsus always distinctly longer than longer mesotibial spur. Length of longest teeth of endophallus ca 55–65 µm...................**5**

– Basal segment of mesotarsus usually slightly shorter than longer mesotibial spur. Length of longest teeth of endophallus ca 35–55 µm. Y chromosome short, dot-like. If slightly longer, largely heterochromatic..................**6**

5 Y chromosome long, metacentric, euchromatic (Fig. 31a, b, d, e). Elytra glossy black, though interstices have fine reticulation. Central part of metaventrite without reticulation (Fig. 21a–d)............................***A.* (*L.*) *niger***

– Y chromosome short, almost dot-like (Fig. 31f–h). Elytral interstices often with fine but distinct reticulation, giving the surface a leaden-grey silky sheen. Metaventrite of females variously depressed medially, depressed area often partly reticulate (Fig. 21e, g–j). Hungary ....
....***A.* (*L.*) *muscorum***

6 Endophallic teeth conspicuously shorter than in all other species, ca as high as long. Length of longest teeth ca 35 µm (Fig. 23g–i, 24o). Iberian Peninsula..***A.* (*L.*) *wilsonae***

– Endophallic teeth clearly longer than high. Length of longest endophallic teeth at least 40 µm **7**

7 Pronotal punctation generally rather sparse and fine (Fig. 6g). Median plate of metaventrite more finely and sparsely punctured (Fig. 21p–r). Corsica...
.... ***A.* (*L.*) *bameuli* sp. nov.**

– Pronotal and/or metaventral punctation stronger....................................... **8**

8 Tooth-field of endophallus approximately as long as parameres (Figs 23p–t, 24m, n). Pronotal punctation generally strong, that of metaventrite strong or weak. Sicily ....***A.* (*L.*) *bellumgerens* sp. nov.**

– Endophallic tooth-field longer than parameres. Pronotal and metaventral punctation generally strong **9**

9 Lateral near vertical area of pronotal surface bulging in posterior 1/3, so lateral margins in this area not visible from above (Fig. 6i). Central Apennines (Campo Felice) .... ***A.* (*L.*) *felix* sp. nov.**

– Lateral near vertical area of pronotal surface less bulging, lateral margins entirely visible from above (Fig. 6h). Sardinia................ ***A.* (*L.*) *krelli* sp. nov.**

10 Median plate of metaventrite more or less flat in males, weakly arched in females, strongly punctate, the punctures bearing yellow recurved setae, these particularly conspicuous in males. In some females the punctures are a bit weaker, and in females the setae seem more easily lost (Fig. 20a, b). (Caution: these setae are easily lost, especially through attempts to clean dried specimens). Most specimens (from Europe, Siberia, and Mongolia) with the elytral interstices distinctly but finely reticulate, often giving a leaden-grey sheen, and with the pronotal base bordered by a more or less continuous fine impressed line, but some (subspecies *L. p. sinoplagiatus* from the Tibetan Plateau) with the elytra glossy black with the reticulation difficult to see, and the basal pronotal impressed line broadly interrupted medially. Elytra slightly rounded at sides. The most widespread species, from Europe to eastern Siberia and China .... ***A.* (*L.*) *plagiatus***

– Median plate of metaventrite without yellow setae, usually more finely punctured **11**

11 Rather elongate beetles with the outer margins of the elytra, viewed from above, rather straight and parallel-sided (Figs 2i, 3a, b) **12**

– Less elongate beetles with the outer margins of the elytra more rounded (Fig. 2a–h, j, k) **13**

12 Larger, length 4.5–6.5 mm. Base of pronotum completely bordered by a fine impressed line, this sometimes weaker medially (Fig. 14c). Protibial spur of male strongly incurved apically (Fig. 18v). ♀ with spermatheca larger (Fig. 26m, n), length ca 0.35 mm. Russia, Orenburg and Volgograd districts, eastern Ukraine .... ***A.* (*L.*) *rusakovi***

– Smaller, length 3.7–4.8 mm. Basal line of pronotum completely effaced over middle 1/3 (Fig. 14b). Beetles often appearing very narrow. ♀ with spermatheca smaller (Fig. 26o–s), length ca 0.25 mm. Dry sandy areas eastwards from southern Slovakia to Middle Asia, Transbaikal, and Afghanistan.......... .... ***A.* (*L.*) *kraatzi***

13 Base of pronotum with a continuous fine but distinct groove (Fig. 2d). Metaventrite with median diamond-shaped area moderately punctate, depressed medially (Fig. 20j). Aedeagus (Fig. 22m, m', m'') with the scales of the basal portion longer than in any other member of the *L. plagiatus* group (length 19–26 µm in *rodrigoi* vs 14–21 µm in the others.) Central Spain. ....***A. (L.) rodrigoi* sp. nov.**

– Base of pronotum with fine groove interrupted by at least the width of one larger pronotal puncture (Fig. 13c, d), but frequently more widely interrupted **14**

14 Width of median interruption of basal pronotal groove normally ca equal to diameter of one larger pronotal puncture, but occasionally wider, equal to ca 5 of the larger punctures (Fig. 13c, d). Cyprus, southern Anatolia, Greece, Albania. ....***A.* (*L.*) *rutilipennis***

– Basal groove of pronotum broadly interrupted medially............................**15**

15 Small black species from Algeria. Aedeagus with endophallus with some elongate scales (aedeagus Fig. 22s–u, x) ....***A.* (*L.*) *chellala* sp. nov.**

– East Mediterranean species. Elytra usually dirty yellowish on disc, but may be black. Aedeagus with endophallus without bristles or elongate scales (aedeagus Fig. 22d–g, n, n') ....***A. (L.) discoides***

Figure 27. Habitat pictures **a** *A. niger,* GB, Hampshire, New Forest **b** *A. muscorum*, HU, Hortobagyi **c** *A. niger,* SW, Tullgarn **d** *A. krelli* sp. nov., IT, Sardinia, Badde Salighes **e** *A. bameuli* sp. nov., FR, Corsica, Haute-Corse, Lac de Melo **f** *A. wilsonae*, SP, Cantabria, Corconte **g** *A. bellumgerens* sp. nov., IT, Sicily, Nebrodi.

Figure 28. Habitat pictures **a** *A. plagiatus*, RU, Pavlosk Park **b** *A. rodrigoi* sp. nov., SP, Toledo, Quero **c** *A. p. sinoplagiatus*, CN, Tibet, Ganca **d** *A. kraatzi*, RU, Astrakhan oblast' **e** *A. alberti* sp. nov., TU, Ovit Dağı (photograph Copyright Yunus Yasuv) **f** *A. felix* sp. nov., IT, Campo Felice.

The *plagiatus* group

Species of the *plagiatus* group are characterised by the aedeagal endophallus bearing fields of scales, hairs, or bristles, but never strong recurved teeth (Fig. 22). The basal segment of the mesotarsi is always shorter than the longer mesotibial spur (Fig. 18a–h).

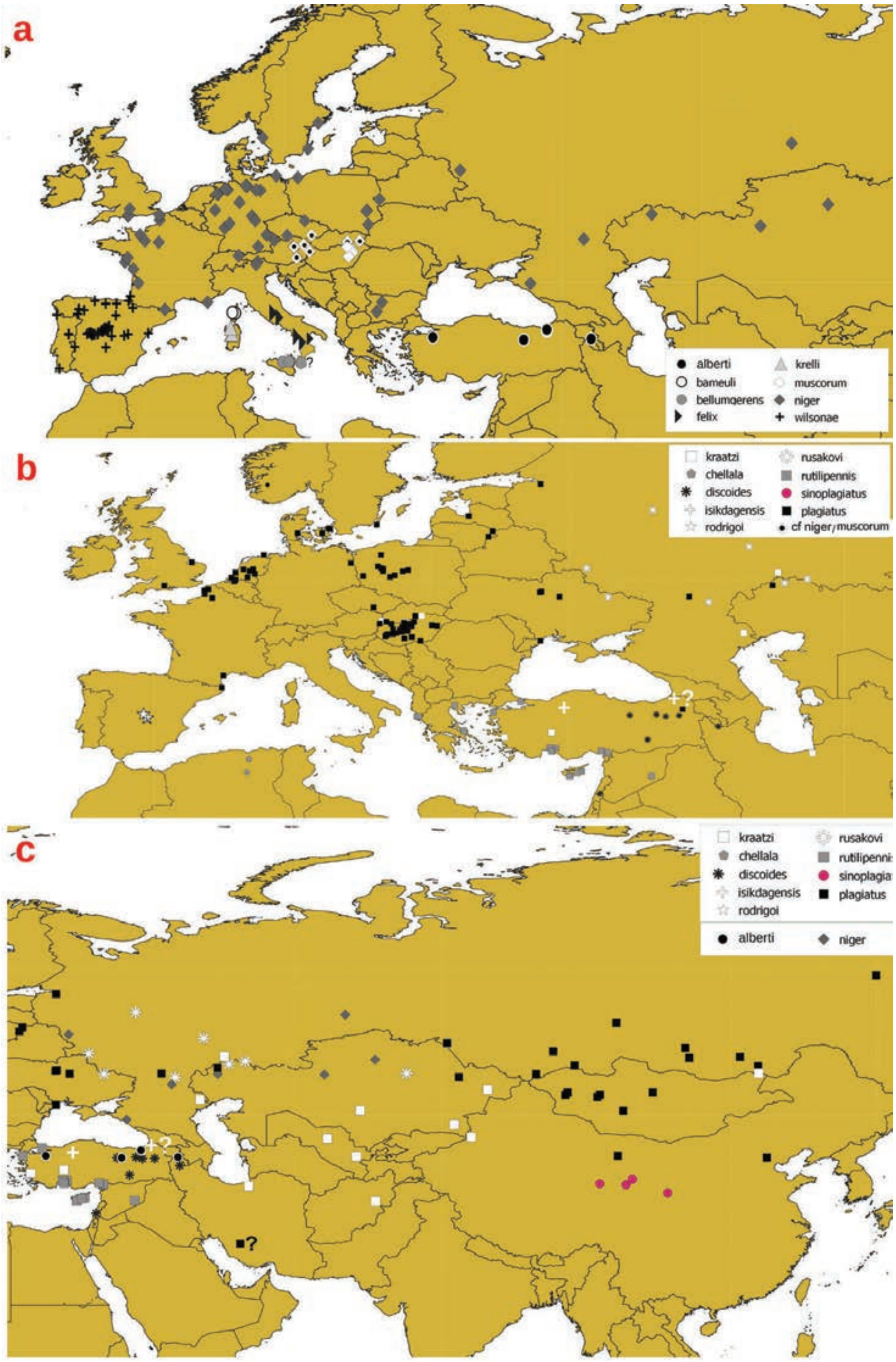

Figure 29. a distribution of *niger*-group taxa in Western and Central Europe **b** distribution of *Liothorax* species in Central and Eastern Palearctic **c** distribution of *plagiatus*-group species in Central and Eastern Palearctic. The record of *isikdagensis* with the question mark indicates a doubtful specimen from Artvin Çam, TR (Ziani Coll).

***Aphodius* (*Liothorax*) *plagiatus plagiatus* (Linnaeus, 1767)**
Figs 2a–c , 5a–d, 7a–f, 13a, b, 17 a–c", 18a, 20a, b, 22h–l, 25i, j, 26a–g , 30a, b

Type material examined. *Scarabaeus plagiatus* Linnaeus, 1767 (image examined on linnean-online.org/20869/#?s=0&cv=0). Designated lectotype by Krell (1995) (LSCL).

Aphodius hungaricus Endrődi, 1955. Type series examined (MNSB).

Aphodius jakutorum Balthasar, 1938. Holotype ♂ (NMP).

Additional material examined. SP: Aiguamolls de l'Empordà, Urbanización Ampuriabrava, 42.225°N, 3.089°E. spec 5445, 1♀ (MNCN).

GB: Norfolk, Hunstanton, 52.9638°N, 0.5168°W. At edge of lake after flood. 27.x.2001, R.B. Angus. 6 ♂♂, 4 ♀♀, 5 unsexed (NHMUK). Dorset, Studland Heath, 50.455°N, 1.954°E. Buried in sand by damp path. 17.v.2002, C. J. Wilson & R.B. Angus. 3 ♂♂, 1♀ (NHMUK).

LI: Litauen, Nowe Święciany, 4–20.6.1916, leg. P. Salchert, 1 unsexed; Livind, Smolwy, Sudl, Dünaburg, 16.6.1916, leg. Selchert, 1 unsexed (ABC).

HU: Hungria, *Aphodius* (*Liothorax*) *plagiatus* var *immaculatus*, 201539 (MNCN).

CZ: Dobré Pole, 48.824°N, 16.533°E, 30.iv.2011, Martinů Ivo. 1 ♂, DNA (1) (62) JFM, 4 unsexed (NHMUK);

SK: E of Chlaba, 11.vi.2014, sandy place S of railway, 47.823°N, 18.846°E, 107 m a.s.l., at light, D. Král lg. 1♂(JFMC).

RU: Pavlovsk Park, St Petersburg, 59.694°N, 30.476°E, at edge of snow-melt pool. v.1982, R.B. Angus. 1♂ (NHMUK); Yaroslavl, Berditsino, 57.454°N, 40.1108°E. leg. Yakovlev. 1♂ (ZIN); Novosibirsk oblast', Sorochicko env. 116 m. 53.285°N, 77.887°E. Waterside litter. 9.v.2012. D.J. Mann & J. Cooter. 1♂, 2♀♀ (OUM); Tuapse, Chernomorsk oblast', 44.098°N, 39.090°E. 1, unsexed (ZIN); Minusinsk distr. Shushenskoe, 53.324°N, 91.946°E. 1, unsexed (ZIN); Chuyskaya steppe, Kosh Agach, 49.991°N, 88.657°E. 1 ♀ (ZIN); Bunbui, Kansk neighbourhood, Yenisei government, 56.382°N, 99.025°E, 1 unsexed, black (ZIN); Transbaikal, Berezovka near Ulan Ude, 51.9320°N, 107.2400°E. 1, unsexed (JFMC).

TR: Bozkale near Kars, 40.587°N, 42.980°E (ZIN).

IN: Shiraz, Lake Maharlou, 29.450°N, 52.759°E, 1♀ (MNHP).

KZ: Yanvartsevo, right bank of the Ural River, 51.424°N, 52.239°E, leg. L. Arnoldi, 1 unsexed, black (ZIN); Koksengir S of Zhana-arka, Karaganda. 49.44°N, 79.44°E. leg. Logonova, 22.v.1958. 1 ♀ (ZIN)

MG: 40 KM Bayanbulag 45.083°N, 98.583°E. 16.vii.2005, leg. A, Mikyška. 1 ♂, elytra with red flashes (NMP); Mongolia west, 50 KM SW Uliastay. 16.vii,2005, leg. A. Mikyška, 1 ♂, elytra with red flashes (NMP); Right bank of R. Kerulen (Herlen) near the Prikhity mountains. 1 unsexed, black (ZIN)

CH: "Pekin", Fry coll. 2♂♂, 1♀ (NHMUK).

Differential diagnosis. *Aphodius plagiatus* is recognisable by the basal segment of the mesotarsi being shorter than the longer mesotibial spur, and the heavily punctured metaventrite, especially in males. The aedeagus is distinctive, with the parameres not decurved apically and the endophallus lacking recurved teeth.

Redescription. General appearance (Fig. 2a–c). Length: 3.6–4.9 mm (♂), 4.0–4.8 mm (♀); width: 1.6–2.0 mm (♂), 1.8–2.0 mm (♀). Black, head, pronotum, and scutellum glossy (pronotum sometimes less so) (Fig. 5a–d), elytra black, sometimes with a dull red streak over the middle part (Fig. 2b), interstices with very fine reticulation often giving a silky grey sheen.

Head glossy black with a diffuse dull brown area along the outer margins of the clypeus and genae, Frons with moderately strong punctation, the punctures separated by ca 1.5× their diameters, and with some sparse very fine punctures between them. Frontoclypeal suture often very fine, straight over median 2/3, then angled obliquely forward at each side, reaching the margin at the front of the genae. Occasionally the suture is more distinct. Clypeus bulging upwards medially, this bulge with fine sparse punctation which becomes coarser and rather rugose anterolaterally. Most European material has this rugose area fairly extensive and well-developed, but a male from St Petersburg (Russia) has the rugosity weaker and less extensive, and in material from the Tibetan Plateau (Qinghai and Gansu) the rugosity is further reduced (Fig. 5a–d). The genae protrude laterally at an angle of ca 45° in front of eyes, then curve inwards to meet the frontoclypeal suture ca 1.5× eye-diameter in front of eyes. Clypeal margin obtusely angled outward from this point, then curved inwards to the median excision. Genae laterally with a narrow raised margin, this continued across the clypeus, becoming weaker medially. Antennae and maxillary palpi black to blackish brown. Epipharynx (Fig. 7a–f) with the clithra generally only weakly sinuate either side of the tylus, but more strongly so in one Chinese specimen (Fig. 7f). Chaetopedia 2–6.

Pronotum glossy black, hemicylindrical, highly arched transversely, weakly so longitudinally. Lateral area of surface bulging outwards, almost obscuring the lateral margins (viewed from above) in basal 1/2. Surface with double punctation, the larger punctures heavy, twice the diameter of those on the head, separated from one another by 1–4× their diameter, and with very fine dot-like punctures scattered among them. The larger punctures are very sparse on the disc, denser laterally. Basal margin of pronotum varying from being entirely bordered to having the middle 1/2 unbordered (Fig. 13a, b).

Scutellum pentagonal, elongate, the sides more or less parallel in basal 1/2, then convergent apically to rounded apex. Surface glossy black with a few very fine punctures medially

Elytra black, sometimes with an oblique reddish streak over their middle parts. Interstices generally with a greyish silky sheen, contrasting with the glossy striae, but sometimes glossy black, as in the type material of *L. hungaricus* (Endrődi, 1995) (MNSB), the St Petersburg specimen already mentioned, and in material from the Tibetan Plateau. The interstices have a fine isodiametric reticulation, easily seen in most European and Mongolian material, but less so in the St Petersburg specimen, and almost invisible in the Tibetan material where the elytra appear very highly polished. Nevertheless, if the elytra are viewed with strong light and at high magnification the reticulation is always present (Fig. 17a–c). Scanning electron microscopy (Fig. 17a”, c”) confirms that this reticulation is on the elytral surface rather than being buried under the epicuticle. In most specimens the fine punctures of the interstices are very faint, though with some variation, but in the Tibetan material they are considerably stronger (Fig. 17a, a’, a”, c, c’, c”). Interstices flat, ca 8–10× wider than the striae. Striae narrow, vertical-sided, their bottoms glossy. Strial punctures in single rows, small, separated by ca 5× their diameter, and scarcely indenting the strial margins. Lateral margins of elytra gently rounded and slightly divergent over their basal 1/2, then tapered to the bluntly rounded apex.

Metaventrite median diamond-shaped plate in males flat and heavily punctate, the punctures bearing distinct yellowish setae (Fig. 20a) which may be lost, especially if an attempt is made to clean dead specimens. In females the median plate is less flat, generally depressed medially and the punctation is finer, ca 2/3 the strength of that in males, and the setae are more frequently lost, even in living material (Fig. 20b).

Legs dark brown to black, tarsi dark brown, and tibial spurs a slightly paler brown. Basal segment of mid tarsi clearly shorter than the longer tibial spur (Fig. 18a).

Aedeagus (Fig. 22a–c, h–k) ca 1.1 mm long in *A. p. plagiatus*, 1.25–1.4 mm in *A. p. sinoplagiatus* ssp. nov., the parameres widened apically and the endophallus bearing fields of small scales but no hairs or bristles. The expanded apical area of the parameres is more abruptly widened in Chinese material, giving a square-ended appearance (Fig. 22i, j, k), than in European where it is more oblique (Fig. 22h) and the holotype of *A. jakutorum* (Balthasar, 1938) (Fig. 22l) appears to match European material in this character. However, some caution is needed as this part of the parameres tends to shrivel when dried and exposed and often does not fully expand when wetted out. Note that the aedeagus of the Peking specimens shown in Fig. 22i is ca 1.1 mm long, matching *A. p. plagiatus* rather than *A. p. sinoplagiatus* ssp. nov.

Spermatheca (Fig. 26a–g) ca 0.36 mm long in *A. p. plagiatus*, but clearly longer in *A. p. sinoplagiatus* ssp. nov., length ca 0.42 mm.

Remarks. *Aphodius plagiatus* is the most widely distributed of all the Palaearctic *Liothorax*, with its range extending from England in the west to east Siberia (Yakutia) and China (Qinghai, Gansu, and the Beijing area) in the east (Fig. 29b, c). The southern limits of its range are unclear. There are no confirmed records from the Iberian Peninsula and the Catalogue of Palaearctic Coleoptera gives no records from Italy. Records from the Balkans require confirmation because of confusion with *A. rutilipennis*. All material from Syria examined in this study has been determined to be *L. discoides* and not *L. plagiatus* as reported by Baraud (1992). The only (doubtful) record of *L. plagiatus* from the Middle East is a female from Iran (Shiraz) found in the collections of the Paris Museum by one of the authors (JFM) which was collected during the 1965 Mission Franco-Iranienne and was identified by Baraud as *L. niger*. This specimen was not mentioned by him in his Coléoptères Scarabaeoidea d´Europe (1992) nor, to our knowledge, by any other author, and, apart from *A. kraatzi* from Ashooradeh Island is the only specimen of *Liothorax* known for Iran. This specimen was examined in 2004 and tentatively identified as a form of *wilsonae* or *plagiatus* based on a strongly punctured metaventrite, shortened tarsi, and a surface finish notably different from *niger*, but due to its divergent morphology was not included in the type series. In light of the work done since, we suspect that it is a member of the *plagiatus* group, but requiring additional material, in particular males. As such this record has been labelled on the distribution maps (Fig. 29c) with a black question mark and a black square.

One of the peculiarities of *A. plagiatus* is the existence of two distinct colour forms, one plain black and the other, exemplified by the lectotype presumably from Sweden, with a red longitudinal-oblique flash over the central area of each elytron. One of us (RBA) has noted the red-streaked form in England, Ukraine (Kiev and Odessa), and Mongolia. The red form appears to be absent from the Czech Republic and Hungary as well as from Russia. As far as is known, this red-streaked form does not occur in *A. plagiatus sinoplagiatus*.

Aphodius plagiatus is normally found at the roots of vegetation in damp places and is often found washed up among strandline detritus at the edge of pools (Fig. 28a, c). It is generally associated with salinity, as in the Qinghai pool shown in Fig. 28c, but there did not appear to be any trace of salinity in Pavlovsk Park near St Petersburg where RBA collected one specimen at the edge of a snowmelt pool in April 1982 (Fig. 28a).

***Aphodius* (*Liothorax*) *plagiatus sinoplagiatus* subsp. nov.**

https://zoobank.org/4ADB8359-223B-4AFA-B942-510A6EF9C63C
Figs 22j, k, 26f, g, 30c

Type material examined. ***Holotype*** ♀ Amdo/1884/Przevalsky (printed label), Zaidam/ Burch Budde/1-11-000 // *Aphodius*/*plagiatus*/var. (handwritten) (ZIN). ***Paratypes***: 1 ♂, data as holotype (originally on the same pin) (ZIN); 1♂ China Qinghai/N. Qinghai Hu/Gangca. Roadside/pool Printed label and a further label with the same data in Chinese. 37°18'N, 100°11'E/3370 m. 5.vi.2013,/R.B. Angus, F.L. Jia & Y. Zhang.// *A. plagiatus* (L.)/ Chromosome prep./6.vi2013./R.B. Angus //JFM 130815017 (printed labels) (NHMUK); 1♀ Cina-Gansu/Dingxi/7.8 – 12.8 1996/E. Kučera leg.//Ex coll. David Král/(NMP).

Differential diagnosis. *Aphodius* (*L.*) *plagiatus sinoplagiatus* differs from *A.* (*L.*) *p. plagiatus* by its very glossy varnished appearance, the slightly larger aedeagus (length ca 1.25–1.4 mm) with abruptly widened paramere apices (Fig. 22j, k), and above all by the strikingly larger spermatheca, length ca 0.42 mm (Fig. 26f, g), as against ca 0.36 mm in *A.* (*L.*) *p. plagiatus* (Fig. 26a–e).

Description. Length: 4.1–4.4 mm (♂), 4.1–4.6 mm (♀), width 1.8–2.0 mm (♂), 1.8–2.0 mm. Head: glossy black, sparsely double punctate, clypeus bulging upwards, frontoclypeal suture without tubercles, straight over middle ¾, effaced laterally. Outer angles of anterior emargination rounded.

Pronotum: highly arched transversely, lateral margins not visible from above medially. Surface sparsely double punctate, the larger punctures slightly stronger than on head, the Gansu male more heavily punctate. Basal margin largely unbordered, the raised margin extending ca ¼ of the way in from the hind angles.

Elytra black, highly polished (varnished), as scutellum. Metaventrite (♂ and ♀) as in the nominal subspecies. Legs mid- to dark brown, longer mesotibial spur longer than basal segment of mesotarsus.

Aedeagus (Fig. 22j, k) length 1.25–1.4 mm, outer apical membranous part abruptly widened.

Spermatheca (Fig. 26f, g) length ca 0.42 mm.

Etymology. *sinoplagiatus* is an adjective indicating its Chinese distribution.

Remark. The aedeagus of 2 ♂♂ from near Beijing (Fig. 22i) resembles that of *L. p. sinoplagiatus* in its widened paramere apices, but is smaller, length ca 1.1 mm.

***Aphodius* (*Liothorax*) *rodrigoi* sp. nov.**

https://zoobank.org/ABCB9508-F963-4C3D-ACDA-CEB4642AC551
Figs 2d, 7g,11f, 20j, 22 m, m', m'', 25k

Type material examined. ***Holotype*** ♂: Spain: Madrid Aranjuez F. Morüder // Aphodius plagiatus det C.M. Veiga 1990 (MNCN). ***Paratypes***: 4 ex ♀ Aranjuez F. Morüder // DA 251 F.J.Cabrero // DG 251 F.J.Cabrero // AP Bucal 206 F.J. Cabrero // Aphodius plagiatus det C.M.Veiga 1990; 1 ex; ♂ Quero Prov Toledo Lauffer // DG 178 F.J.Cabrero // DA 249F.J.Cabrero // Aphodius plagiatus det C.M.Veiga 1990; 1 ex; ♀ Quero v.1908 Molina // AP Bucal 56 F.J.Cabrero // DG 174 F.J.Cabrero // Aphodius plagiatus det C.M.Veiga 1990; 1ex; ♂ Villacañas (TOLEDO) C. Bolívar // Hoyer C.M.Veiga // AP Bucal 205 F.J.Cabrero // DA 250 F.J.Cabrero // Aphodius plagiatus det C.M.Veiga 1990 1 ex. (MNCN).

Differential diagnosis. *Aphodius* (*L.*) *rodrigoi* resembles a small highly-polished somewhat rounded *A.* (*L.*) *plagiatus*. The metaventrite is slightly less strongly punctate and with the median diamond-shaped area depressed to mid-line. Aedeagus: (Fig. 22m, m', m") general size and shape of parameres similar to *A. plagiatus*, not turned downwards apically, but with the following differences: apices of parameres less produced laterally, parameres narrower and more converging towards apex, in lateral view parameres gradually curved towards apex and narrowest towards apex compared to *L. plagiatus* which is narrowest 1/3rd towards apex.

The apical segment of the maxillary palpi is slightly longer (10%) than the 2nd segment: terminal segment slightly longer (10%) than 2nd segment (Fig. 11f), as against 15–20% longer in *A. plagiatus* (Fig. 11d, e).

Description. General appearance (Fig. 2d). Length: 3.5–4.0 mm (♂) (HT 3.75 mm), 4.0–4.23 mm (♀); width: 1.4–1.6 mm (♂ and ♀).

Glossy black throughout except clypeal and elytral apical edges which are fuscous red. Legs and maxillary palps reddish yellow to maroon, antennae tan except for last three segments which are darker and clothed in off-white setae.

Head: frons strongly convex, clypeus flat to slightly concave. Frontoclypeal suture weak, widely interrupted in the middle. Clypeal edge truncated to slightly emarginate, impressed medially; side angles rounded with edge widely elevated. Sides of head almost straight and continuously merging with genae. Genae produced beyond eyes, rounded, strongly bordered and with some short yellowish setae.

Surface shiny with residual reticulation and strongly punctured. Punctation double, the larger punctures regularly dispersed on the clypeal sides and frons, absent from genae and anterior clypeus. Larger punctures 2–3× diameter of the smaller ones and strongly impressed, particularly on the sides where the surface almost appears wrinkled and closely spaced (1–1.5× their diameter). Anterior edge of clypeus very finely and regularly punctured, completely devoid of larger punctures.

Maxillary palp: terminal segment slightly longer (10%) than 2nd segment (Fig. 11f) (in *A. plagiatus* the terminal segment is longer, 15–20% longer than the 2nd segment) (Fig. 11d, e). Galeal patch armed with five or six strong galeal chaetae (7–9 in *A. plagiatus*). Galea smaller, similar in dimensions to the Tibetan ssp. of *A. plagiatus* but not to European populations in which it is larger.

Epipharynx (Fig. 7g) corypha small and only slightly produced (somewhat similar to the Tibetan populations of *A. plagiatus*), with the chaetae (celtes) much reduced in size. Fenestrae on zygum (angustofenestrae) and chaetae (heli) less numerous than in *A. plagiatus* and limited to the edge against pedia. Chaetopaedia as in *A. plagiatus*. Chaetopariae noticeably stronger than in *A. plagiatus*.

Pronotum subquadrate, sides slightly rounded, subparallel, and widest towards base. Regularly convex longitudinally and transversely. Base completely and distinctly bordered, border strong but fine. Anterior edge not bordered at all. Lateral margins visible dorsally in the apical 1/3 only. Sides strongly bordered throughout, anteriorly going around corner up to the middle of the eye. Lateral margins with short yellowish hairs barely visible dorsally in apical 1/2.

Surface of pronotum black and shiny, not at all alutaceous with only some residual superficial shagreen. Punctation double, larger punctures regularly distributed throughout but densest on the sides and anterolateral corners. Large punctures flat bottomed and umbilicated. Diameter 4–5× that of the smaller ones and spaced 1–3× their diameter.

Scutellum elongate, sides rounded, convergent throughout (only slightly pentagonal), length 1/11 elytral length. Glossy black, unpunctured, basally impressed, disk convex.

Elytra black, intervals convex, surface strongly glossy and slightly alutaceous under high magnification. Intervals with double row of very fine and faint punctures. Striae fine, 1/8× width of intervals, with sides crisp and right-angled. Regularly punctured, punctures wider than the striae and separated by 2× diameter (first 2 striae) or 3–4× (remainder). Elytral epipleura strong, gradually convergent towards apex, and at humeri forming a small but distinct tooth.

Underside black with yellowish pubescence on the abdomen.

Metaventrite (Fig. 20j): median diamond-shaped area rather strongly punctate, glabrous, its mid-line distinctly impressed. Surface regularly heavily punctate, the punctures with one end somewhat pointed, shiny, and not alutaceous. Sexual dimorphism subtle, female flatter than male.

Legs reddish to dark brown, tarsi and tibial spurs red to tan, rather long and slender. Protarsal spur regularly acuminate and curved in both sexes, reaching to apex of second tarsal segment. Metatarsal segments short. Basotarsomere slightly shorter than upper metatibial spine as long as segments 2 + 3. Fimbrial setae short and of unequal length. Longer spur of mid tibiae as long as first two tarsal segments.

Aedeagus: (Fig. 22 m, m’, m”) general size and shape of parameres similar to *A. plagiatus*, not turned downwards apically, but with the following differences: apices of parameres less produced laterally, parameres narrower and more convergent towards apex, in lateral view parameres gradually curved towards apex and narrowest nearer apex (ca ¼ of the paramere length as against ca 1/3 in *L. plagiatus*).

Endophallus typical of other members of the *A. plagiatus* species group, with two patches of elongate triangular scales or bristles. Those in basal patch longer and more elongate than any member of the *plagiatus* group (19–26µm in *A. rodrigoi* vs 14 –21µm), similar to those of *A. wilsonae* (22–32µm), those in the apical patch like *A. plagiatus*.

Etymology. The name is derived from the surname of the name Joaquín Rodrigo Vidre, a Spanish composer whose most famous work, “Concierto de Aranjuez”, refers to the geographical area from which the species hails.

Remarks. All the known specimens are from the south of Madrid (Aranjuez) and the adjacent areas of Toledo (Fig. 29b) The localities are associated with temporary endorheic saline lagoons and lakes (Fig. 28b) One of the authors (JFM) made repeated visits to several of the localities during late winter over several years (January and April of 2015–2017), but no specimens were found. Although it is possible that the species was missed due to its ecology or time of emergence, it is also possible that the species is very rare or has been extirpated from much of its former distribution. The known localities are part of an extensive system of aquifer-fed saline lagoons encompassing much of La Mancha and collectively known as “La Mancha Húmeda” (Wet La Mancha). Many of these lagoons are degraded or lost to agriculture but almost 1/2, including several visited for this study, are protected and in apparently good ecological condition (Florín-Beltrán 2001). Hence, it would be hasty to declare this interesting Iberian endemic extinct without carrying out extensive sampling across the area and in particular within the protected lagoons which might still host it.

***Aphodius* (*Liothorax*) *discoides* A. Schmidt, 1916, stat. rest.**

Figs 2j, k, 5e–h, 7h, 14a, 17g–i, 18e, 20k, l, 22d–g, e’, n’, o’, 25n, 26h, i

Aphodius (*Nialus*) *plagiatus* var. *discus* Reitter 1892: 204.
Aphodius (*Nialus*) *plagiatus* var. *discoides* Schmidt, 1916: 96 (new name for *Aphodius discus* Reitter 1892, not *Aphodius discus* Wiedemann, 1823).
Aphodius (*Nialus*) *bytinskisalzi* Petrovitz, 1971: 219.

Note. Reitter described *Aphodius plagiatus* “var. *discus* m” as having the elytra yellow with only the wide margins black, and gave the locality “Araxes, Syria” (now Aras). Schmidt (1916) proposed the replacement name *A. discoides* as Reitter’s *Aphodius discus* is a junior homonym of *Aphodius discus* Wiedemann, 1823. Dellacasa et al. (2007) dismiss these names as unavailable as they refer to colour variants, but this is incorrect, as it would be the case only if the name was “infrasubspecific”. For names published before 1961, the International Code of Zoological Nomenclature (1999, 4th edition) states that a name “is subspecific if first published before 1961 and the author expressly used one of the terms “variety” or “form” (including the use of the terms “var.”, “forma”, “v” and “f”), unless the author also expressly gave it infrasubspecific rank, or the content of the work unambiguously reveals that the name was published for an infrasubspecific entity”. Reitter clearly stated that his name referred to a variety from a known locality, meaning that the taxon concerned was subspecific rather than infra-subspecific. This name is therefore available and, in the form of Schmidt’s replacement name (*discoides*) is the oldest known name for this species. We have been unable to locate any type material of Reitter’s *A. discus* and therefore here designate a neotype. The specimen chosen is the holotype of *A. bytinskisalzi*, a male whose aedeagus has the endophallus extruded, from the same general area as Reitter’s material.

Type material examined. *Holotype*. *Aphodius bytinskisalzi* ♂ ISRAEL, Kuneitra. 6.iv.1968. Leg Bytinski-Salz Tel-Aviv. This specimen is here designated as the neotype of *L. discoides* Schmidt. 33.12657°N, 35.8586°E (IL-SMNH.)

Additional material examined. TR:1 ♂, “Turkei leg Schönmann et Schilhammer” “Prov. Diyarbakir Karacadag 28.5.1987. “*Aphodius* (*Liothorax*) *plagiatus* det Pittino 1989” (NMW); 1 ♂, Turkey Karacadag In coll. D. Král (NMP); 1♀, Turkey, 24.vi.1993, Kizildag env. Klíma leg. In coll. D. Král (NMP); 1 unsexed, Turkey, 1.v.1998, Erzincan 8 km Askale. Leg Sama (SZ); 1 ♀, Turkey, 17.v.2011, Muş 1400 m Buǵlan geçidi G. Sama leg. (SZ); 1 black ♂, Turkey or. Karakurt env. In coll. D. Kràl (NMP).

Differential diagnosis. This species agrees with *A. plagiatus* in the general form of the aedeagus, and in particular the absence of any bristles on the endophallus, which distinguishes it from all other known species. The lightly punctate central area of the metaventrite gives a clear separation from *A. plagiatus*. Most of the studied material has the elytra largely yellow, unique among the known Palaearctic *Liothorax*, but recognition of black specimens requires study of the aedeagus.

Redescription. General appearance (Fig. 2j, k). Length: 3.8–4.8 mm (♂), 3.4–4.5 mm (♀), width 1.65–2.1 mm (♂), 1.5–2.0 mm (♀).

Head black, finely and sparsely double punctate, with small punctures and minute dots, the punctures separated by ca 2× the diameter of the larger punctures, punctation slightly rugose towards the anterior margin, especially either side of the median emargination of the clypeus. Sides of clypeal emargination rounded. Frontal suture almost invisible, but median transverse portion present, with a small vague elevation medially, just behind median bulge of clypeus, in males, and weakly raised at ends, just mediad of inner margins of eyes, where it would be expected to angle forwards to anterior margin of genae. However, this part of the suture is effaced. Centre of clypeus raised. Maxillary palpi blackish brown, antennae mid brown, clubs darker. Epipharynx (Fig. 7h) with the anterior margin of the clithra only weakly emarginated either side of the tylus, and the apophobae rather stout and the prophobae restricted to areas close to the edges of the basal 1/2 of the mesoepitorma.

Pronotum black with anterior and lateral margins vaguely browned. Hemicylindrical, strongly arched transversely, scarcely at all longitudinally. Punctation double, sparse, stronger than on head, punctures separated by at least 2× the diameter of the larger punctures. The larger punctures more developed posteriorly and laterally, almost absent from the anterior-median 1/3. Pronotal surface with a fine weak isodiametric reticulation (viewed at ×80). Sides of pronotum almost straight, parallel, incurved anteriorly. Pronotal surface bulges out laterally in basal 1/4, but the basal 1/4 of the lateral margins is still just visible from above. Head and pronotum (Fig. 5e–h): basal margin of pronotum unbordered in middle 1/3 (Fig. 14a).

Scutellum elongate, glossy dark brown, pentagonal, sides parallel in basal 1/2, then convergent to bluntly pointed tip.

Central area of elytra typically dull yellowish brown, semi-transparent so that the folded wings are visible, suggesting a vague darker pattern over this part of the elytra. Sutural interstice darker, as are the outer interstices (interstice 7 to the edge), with the darkening of interstice 7 sometimes confined to the outer edge just behind the humeral callus, then expanding over the entire interstice to the apex. Interstice 6 may be darkened in apical 1/2, and the apical 1/3 of the elytra is darkened throughout. Striae narrow, shallow, strial punctures scarcely encroaching on the strial edges. Interstices flat, sparsely and very finely punctate, ground with a fine isodiametric reticulation giving a silky sheen, though the strength of the reticulation varies (Fig. 17g–i). In the black male listed above the elytra and scutellum are entirely black. This specimen agrees with *A. discus* in the shape and sculpture of the head and pronotum and in the endophallus with scales only, lacking any hairs or bristles.

Median diamond-shaped plate of metaventrite (Fig. 20k, l) weakly depressed to mid-line, finely punctate, the surface with fine isodiametric reticulation.

Legs: dark brown, tarsi a little paler. Longer spur of mid tibiae clearly longer than basal segment of tarsus, extending to ca the middle of segment 2 (Fig. 18e).

Aedeagus (Fig. 22d–g) similar to that of *A. plagiatus*, but smaller, length ca 0.85 mm. Endophallus with short fine scales and with a field of densely packed columnar bristles at its apex (Fig. 22e’). The scales of the basal section of the aedeagus are the same size and shape in the black specimen as in the ones with paler elytra (Fig. 22n’, o’).

Remarks. *Aphodius discoides* appears to have a rather restricted distribution in Anatolia, Syria and Israel (Fig. 29b). It appears to be a rather rare species. We have no habitat information.

***Aphodius* (*Liothorax*) *rutilipennis* Baudi di Selve, 1870, stat. rest.**

Figs 2e–g , 5i–k , 7j, 13c, d, 18c, 20c, d, 22q, q', r, v, w, 25m, 26j, k, 30d, e

Aphodius (*Liothorax*) *plagiatus* var *rutilipennis* Baudi di Selve,1870: 64.
Aphodius ressli Petrovitz, 1962: 126
Aphodius cypricola Balthasar, 1971: 57.
Aphodius isikdagensis Balthasar 1952, sensu Dellacasa et al. 2001b: 6 (misidentification).

Note. Baudi di Selve (1870) described a variety of *A. plagiatus* in which the elytra were brownish bronze ("brunneo-subaeneis") and said that this variety was less rare (on Cyprus) than the black form. He added that, among other things, the mesosternum (sic) was more delicately and less densely punctate than in European *A. plagiatus*. Dellacasa et al. (2007) stated that the name *A. rutilipennis* Baudi di Selve was unavailable as it was simply a colour variant, but that would only be the case if the name was "infrasubspecific". For names published before 1961, the International Code of Zoological Nomenclature (1999, 4th edition), states that a name "is subspecific if first published before 1961 and the author expressly used one of the terms "variety" or "form" (including the use of the terms "var.", "forma", "v" and "f"), unless the author also expressly gave it infrasubspecific rank, or the content of the work unambiguously reveals that the name was published for an infrasubspecific entity". Baudi makes no reference to infrasubspecific status, nor does his description imply that it was such. This name is therefore available and is the oldest known name for this species.

Type material examined. *Aphodius plagiatus* var *rutilipennis* Baudi di Selve,1870. Type material in the Museo Civico di Storia Naturale Giacomo Doria, Genova (MCSNGDG) – not examined (not available for study).

Aphodius ressli Petrovitz, 1962. Holotype ♀ (MNHG);

Aphodius cypricola Balthasar, 1971. Holotype ♂ (NMP).

Additional material examined. GR: Corfu, 39.6°N, 19.8°E. Reitter, Nevinson coll. 1♂ (NHMUK). Evia, Chalcis, 36.463°N, 26.635°E, 1932, leg. J. Fodor. 1 unsexed (MNHB). Macedonia, Langassa Göll. 40.464°N, 32.147°E. 1♀ (MNHB).

AL: Albania mer. Butrint, 39.754°N, 20.021°E. Smetana, 1958, l♀ (NMP).

TR: Besika (Beşik) Bay, 40.274°N, 26.459°E. 2 ♂♂, 5 unsexed. Ex C.G. Champion (NHMUK). Turkey mer. Devecusagi, Yumurtalik env., 36.884°N, 36.039°E. 14.iv.1992. leg. O. Hovorka. 1 unsexed (NMP) prov. Antalya, Manavgat. 36.763°N, 31.437°E. leg. A. Bellmann 13.iii.2000. 1♂ (ABC). Antalya, Manavgat. 36.763°N, 31.437°E. leg. A. Bellmann 13.iii.2000. 1♂ (ABC). Antalya, 5Km nördi, Sagirin, Köprülu kanyon, 19.03.2002, leg. A. Bellmann, 1 unsexed (ABC); same data, 22.03.2002, 1 unsexed (ABC); Antalya, Akseki, 1300 m a.s.l., 19March2002, leg. Bellmann 1 unsexed (ABC); Alanya, Konakli; 13.03.2000 leg. A.Bellmann, 1 unsexed (ABC). Istanbul Halkali 28.vii.1968 Cl. Besuchet, 1 unsexed (MHNG).

CY: Akrotiri, 34.634°N, 32.991°E. G. Mavromoustakis 2♂♂ (NHMUK); Limassol distr. Zakaki marshes, puddle in lorry park at edge of reedbed, 3.iv.2005.

R.B. Angus. 3 ♂♂, chromosome prep. 4: 7.iv.2005 R.B Angus, DNA extracts 110 & 91, J.F. Maté 2013, 1♀, chromosome prep. 5: 7.v.2005 (NHMUK); "Insel Cypern" ex coll, Fodor. 2♂♂, 1♀ (MNHB); Zypern, Sotira (Salzee), 6.4.2010, W. Ziegler leg., 1 unsexed (ABC).

Differential diagnosis. A small black *A. plagiatus* group species, occasionally with dull reddish elytra, immediately distinguished from *A. plagiatus* by its clearly more lightly sculptured metaventrite and the bristles on the endophallus. Black specimens are distinguished from *A. chellala* sp. nov. by the narrower gap in the basal border of the pronotum.

Redescription. General appearance (Fig. 2e–g). Head and pronotum (Fig. 5i–k). Length: 3.1–4.1 mm (♂), 3.9–4.2 mm (♀); width: 1.4–1.8 mm (♂), 1.7–1.9 mm (♀).

Head black, anterolateral margins of clypeus and genae with a vague dull yellowish brown strip, and actual margins narrowly raised. Frontoclypeal suture more or less straight over median 1/3 but middle part effaced, laterally angled to anterior edge of genae, but this part scarcely traceable. Frons with moderate double punctation which is effaced on the middle 1/4. Disc of clypeus bulges upwards, this bulge with only very fine sparse dot-like punctation, surface away from the bulge with moderate double punctation and the surface becoming weakly wrinkled towards the anterior and lateral margins. Front of clypeus weakly excised over middle 1/3, recurved either side of this excision. Antennae and maxillary palpi dull yellowish brown antennal clubs and apical segments of palpi darker. Epipharynx (Fig. 7j) with the anterior margin if the clithra excised either side of the median tylus, and the prophobae and apophobae quite extensively developed and with 3 or 4 chaetopedia each side.

Pronotum hemicylindrical, highly arched transversely, weakly so longitudinally. Lateral margins bordered but basal 1/2 not visible from above because of the outwardly bulging lateral parts of the pronotal surface in this area. Posterior margin of the pronotum usually with an almost continuous border, this with a small median interruption whose width is approximately the same as the diameter of the larger pronotal punctures (Fig. 13c). In the holotype of *A. cypricola* and a female from Greek Macedonia (Langasa-Göl, now Lagkadas near Thessaloniki) the median gap in the basal border of the pronotum is rather wider (Fig. 13d), but the aedeagal characters are the same as in other material. Pronotal surface with moderate double punctation, the larger punctures separated by 1–2× their diameter, becoming sparser medially. Smaller punctures dot-like and all punctures absent from a median longitudinal strip.

Scutellum elongate, pentagonal, glossy reddish brown with a few punctures medio basally.

Elytra maroon-bronze or black, interstices with a silky sheen due to the fine reticulation on their surfaces. Striae narrow, shallow and glossy, with punctures separated by ca 2× their diameter and indenting the strial margins. Interstices ca 6× as wide as the striae, flat and with a very fine reticulation and scattered very fine punctures separated from one another by ca 1/3 of the width of the interstices. Lateral margins of elytra slightly rounded to widest point just behind the middle, then rounded to the blunt apex.

Metaventrite: (Fig. 20c, d) grey-bronze with maroon reflections, median diamond-shaped plate depressed medially. Surface reticulate, the reticulation effaced in the middle of the median depression. Punctation fine and sparse, becoming stronger over the outer part of the median depression, but absent from its centre.

Legs: mid brown, basal segment of mid tarsi clearly shorter than the longer tibial spur (Fig. 18c).

Aedeagus (Fig. 22q, q' r, v, w) small, length ca 0.7 mm with the endophallus bearing a dense field of bristles dorsally and the apices of the parameres membranous, expanded and obliquely truncate.

Remarks. *Aphodius rutilipennis* is distributed in mainly lowland coastal areas of southeast Europe and Asiatic Turkey (Anatolia) from Corfu and southern Albania (Butrint) in the west, via Evia and Macedonia (Greece), Besika Bay (Turkey), Cyprus (Limassol and Larnaca districts) to Hatay (Iskenderun) (Turkey: the type locality of *L. ressli*) in the east (Fig. 29b, c) On Cyprus it appears to be mainly winter-active. RBA collected it at the edge of a muddy pool in the Zakaki marshes (Limassol) and C. Makris (Limassol, Cyprus) collected it from under a discarded piece of carpet lying on the mud in the same area (pers. comm. to RBA, April 1985). This whole area is slightly saline.

***Aphodius* (*Liothorax*) *chellala* sp. nov.**

https://zoobank.org/D293FE92-32FA-4B73-8FB6-15CE48B7D55C
Figs 2h, 5l, 7k, 13e, 17e, 18d, 20e, f, 22s–s''', t, u, 25l, 26l

Type material examined. ***Holotype*** ♂: Chellala, ALGERIA (33.074°N, 0.123°W) De Vauloger. Nevinson coll. 1918 – 14 (NHMUK). ***Paratypes*****:** 8 ♂♂, 14 ♀♀, 1 unsexed (lacking head), data as holotype. 1 ♂ and 2 ♀♀ have the labels "Prov. D'Alger. Chellala 1895 de Vauloger", these presumably the basis of the English labels on the other specimens. 9 ♂♂, 3 ♀♀, Taguin (near Zmalet El Emir Abdelkader, 35.221°N, 1.402°W), Algeria, De Vauloger. Nevinson coll. 1918 –14. NHMUK. As with the Chellala material, 2 ♂♂ have the French label "Prov. D'Alger Taguin 1895 de Vauloger" (NHMUK).

Differential diagnosis. Closely resembling dark specimens of *A. rutilipennis* but basal margin of pronotum (Fig. 13e) more broadly interrupted than in *A. rutilipennis* (Fig. 13c, d). Endophallus of aedeagus, when extruded, with the scale-patches (Fig. 22q', s''') clearly different from the dense bristle-field of *A. rutilipennis* (Fig. 22q, q').

Description. General appearance (Fig. 2h). Length 3.6–4.5 mm (♂), 3.7–4.5 mm (♀), width 1.5–1.8 mm (♂), 1.6–1.9 mm (♀). Black, antennae, maxillary palpi and legs dark brown. Head: glossy black with anterior from in front of the genae dull brown, this colour merging into the general black ground colour. Anterior margin of clypeus emarginate medially, sides of the emargination rounded. Surface glossy with no trace of reticulation but with sparse double punctation, the larger punctures scarce medially. Disc of clypeus raised as a hump. Frontoclypeal suture fine, without tubercles, complete, angled forward just mediad of the inner margin of the eyes, running to anterior end of genae. Genae protruding in front of eyes, rounded, no angle between anterior end of genae and clypeus. Head and pronotum (Fig. 5l): epipharynx (Fig. 7k) similar to that of *A. rutilipennis*, but, at least in the specimen figured, more heavily sclerotised medially. Pronotum: hemicylindrical, highly arched transversely and weakly so longitudinally in mid-line. Sides of pronotum weakly curved, somewhat convergent anteriorly. Lateral margins in basal 1/4 not visible from above, concealed by lateral bulging of pronotal surface. Surface glossy, with no trace of reticulation but with sparse large punctures interspersed with much finer ones, these ca 1/5 of the diameter of the larger ones. In some specimens the punctation is a little stronger and closer. Anterior margin of pronotum not bordered, lateral margins bordered from just mediad of anterior angles to base, this border extending (as a very fine impressed line) over the lateral 1/3 of the hind margin. Median 1/3 of hind margin without any trace of an impressed line (Fig. 13e). Scutellum pentagonal, sides parallel in basal 1/2, the convergent to blunt apical point. Surface glossy black, impunctate. Elytra black, not quite parallel-sided, widest just behind middle then sides convergent to bluntly rounded apex. Interstices wide and almost flat, ca 5× the width of the striae, silky black due to fine indistinct reticulation, and with sparse fine punctures, these separated by ca 8× their diameters. Elytral sculpture: Fig. 17e. Striae narrow, vertical-sided, glossy, strial punctures encroaching on their margins. The striae stop short of the elytral apex on the inner 1/2 of the elytra, leaving a smooth glossy apical field. Metaventrite (Fig. 20e, f) fairly finely punctate, median furrow of central diamond-shaped plate flattish. No consistent sexual dimorphism. Legs dull mid- to dark brown. Long spur of mid tibiae clearly longer than the basal segment of the tarsi (Fig. 18d). Hind tibiae with apical spines fairly long and unequal on dorsal/external edge, shorter and of even length along ventral/internal edge.

Aedeagus (Fig. 22s–s‴, t, u) small, length ca 0.6 mm. Apex of parameres membranous, obliquely truncate, often distorted in dried specimens, even when they are soaked again. Endophallus with scales, some of which are elongate, when not everted indistinguishable from that of *A. rutilipennis* (Fig. 22v, x). However, the everted endophallus shows a clearly different arrangement of scale-patches (Fig. 22q’, s‴). The two specimens with the endophallus everted were the only ones where it had become extruded by partial decomposition of the specimen. These endophalli were softened in dilute potassium hydroxide, transferred to alcohol and then critical-point dried. Unfortunately the better of the two (Fig. 22s–s‴) disintegrated when removal from the SEM stub was attempted. For this reason, the specimen with the less good endophallus is chosen as the holotype.

Etymology. The specific name *chellala* is a feminine noun, the name of the type locality.

Remarks. So far known only from North Africa (Fig. 29b). We have no information about the habitat.

Aphodius (*Liothorax*) *kraatzi* Harold, 1868

Figs 3a, b, 5o, p, 8a, b, 14b, 17j, 18f, g, 20g–i , 22y, z, 25h, 26o–s , 30f–h

Aphodius kraatzi Harold, 1868: 84.

Type material examined. (MNHP), seen but not studied in detail by DK.

Additional material examined. SK: S. Slovakia, E. of Chlaba, sandy place S of the railway. 47.842°N, 18.844°E. 107 m a.s.l.. 11.vi.2014. leg. D. Král. 1♂, 5♀♀ (NHMUK). Martovce. 47.858°N, 18.127°E. 2 ♀♀ (NHMUK). Velké Kosíhy. 47.734°N, 18.127°E. 1♀ (NHMUK). Virt. 47.742°N, 18.324°E. 31.vii – 2.viii.2012. Martinů Ivo leg. 2, unsexed (NMP).

GR: Lesbos, Petra. 39.399°N, 26.181°E. 2, unsexed (NMW).

RU: Astrakhan obl. Dosang. 46.904°N, 47.916°E. Cattle dung. A. Frolov & L. Akhmetova. 2♀♀, 4 unsexed, 23.v.2007, 1 ♀, 1–3.v.2004 (NHML). Novosibirsk obl. Karasuk. 53.5°N, 78°E. vi–vii.1982. R.B. Angus. 1♀ (NHMUK). SE Siberia, S Chita reg. 50.071166°N, 115.663446°E. Zun Tore Lake. 30.v.2002. 1 ♂ (JFMC)

IN “O. Ashur-ade” (Ashooradeh Island). 36.91°N, 53.96°E. Solovkin 1.v.1913. 4, unsexed (ZIN)

KZ: Dzhulek, Orenburg – Tashkent railway, Syr Darja (Taken as Zholek near Baigakum, 44.314°N, 66.466°E), 3♂♂, 3 ♀♀, 9, unsexed (NHML). Kozakhit, Almaty obl. Altyn Emel NP Ul;ken Kalkan. 43.874°N, 78.749°E. N bank of R. Ile, at light, 5.v.2012. D.J. Mann & J. Cooter. 1♂, 3 unsexed (OUM).

UZ: Kyzylkum desert Baymachan distr. 11.v.1995. 2, undissected (NHMUK).

AF: Kabul. 34.548°N, 69.213°E. 1 ♂, 1♀ (NMP), 1♀, 1 unsexed (NMW).

Differential diagnosis. A conspicuously narrow elongate black beetle, with the scutellum wide, generally wider than elytral interstice 2. Elytral interstices weakly raised, not flat as in most other species. Smaller, length 3.7–4.8 mm. Basal line of pronotum completely effaced over middle 1/3 (Fig. 14 b). ♀ with spermatheca smaller (Fig. 26o–s), length ca 0.25 mm.

Redescription. General appearance (Fig. 3a, b). Black, elongate, parallel-sided, and conspicuously narrow. Length: 3.4–4.8 mm, width 1.5–1.9 mm.

Head black with anterior and lateral margins of the clypeus narrowly brown. Anterior margin of clypeus emarginated, the sides of this emargination bluntly rounded. Central part of clypeus bulging upwards, frontoclypeal suture occasionally slightly raised medially but without any trace of a real tubercle, straight or slightly curved backwards over middle 1/2, angled forward to run to the junction of the clypeus and genae laterally. Punctation double, varying from close and strong to rather sparse, generally weaker and sparser in the central area of the frons and becoming rugose anteriorly and laterally (head and pronotum: Fig. 5o, p) Maxillary palpi dark brown, the apical segment blackish. Antennae brown, the clubs darker. Epipharynx (Fig. 8a, b) with the anterior margin of the clithra almost straight either side of the median tylus and the acropariae very well-developed. The prophobae are well-developed on each side of the mesoepitorma and there are three or four chaetopedia on each side. Pronotum black, hemicylindrical, highly arched transversely, only weakly so longitudinally. Entire lateral margins visible from above. Surface with double punctation of variable strength, generally weaker medially. Hind margin bordered only in lateral 1/4s (Fig. 14b). Scutellum rather wide, generally wider than elytral interstice 2, pentagonal, moderately elongate, sides parallel in basal 1/2, then angled to apical convergence. Metaventrite variable. Median diamond-shaped plate sometimes excavated and quite strongly punctured (Fig. 20g), or flatter and more finely punctured (Fig. 20h, i). Legs brown, longer spur of mid tibiae clearly longer than the basal segment of the tarsus (Fig. 18f, g). Elytra glossy black, interstices very weakly convex, finely reticulate and with sparse fine punctation, and 6–8× width of the striae (Fig. 17j).

Aedeagus (Fig. 22y, z) ca 0.8 mm long, apical 1/3 of parameres slightly more expanded than in A. *rutilipennis* and *A. chellala* sp. nov., its outer margin more rounded. Endophallus with fine bristles.

Remarks. *Aphodius kraatzi* is widely distributed in the drier regions of the western and central Palaearctic, from southern Slovakia to Kazakhstan, Uzbekistan, Afghanistan, and the Chita region of Transbaikal in Russia (Fig. 29b, c).

Most specimens are taken at light but Andrey Frolov (St Petersburg) mentions that it can sometimes be found at the roots of grass and other herbaceous plants, as in the area of the Astrakhan oblast' (Russia) shown in Fig. 28d. He adds that material flying to light often arrives from the direction away from neighbouring water (pers. comm. to RBA, April 2015). In 1982 RBA took one specimen in a water-filled ditch at Karasuk on the Kulundinskaya Steppe in Western Siberia.

***Aphodius* (*Liothorax*) *rusakovi* Gusakov, 2004**

Figs 2i, 5m, 14c, 17f, 20m, n, 18h, v, 22p, p', 26m, n

Aphodius (*Liothorax*) *rusakovi* Gusakov, 2004: 6.

Type material examined. 2 paratypes from the Orenburg oblast', Russia (NHMUK).

Additional material examined. RU: 1 ♀, Ulyanovsk, 54.056°N, 48.519°E (ZIN); 1 ♂, Volgograd oblast', 48.7°N, 44.5°E, Fastov. leg. Grebennikov.(ZIN).

KZ or UZ 1♀ "Syr-Darja./ B. v. Bodemeyer." (NMP).

Differential diagnosis. A conspicuously narrow parallel-sided species, comparable with *A. kraatzi* but larger, length 4.5–6.5 mm and base of pronotum completely bordered by a fine impressed line, this sometimes weaker medially (Fig. 14c). Protibial spur of male strongly incurved apically (Fig. 18v). ♀ with spermatheca larger (Fig. 26m, n).

Redescription. General appearance (Fig. 2i). Glossy black, length 4.7–5.5 mm, width 1.9–2.2 mm. Head fairly closely punctate, sometimes slightly rugose on the frons and anterolateral parts of the clypeus, and occasionally rugose over all except the central part of the clypeal bulge. Double punctation scarcely apparent except when the punctation is sparser on the clypeal bulge. Clypeus emarginated anteriorly, edges of this emargination bluntly rounded (head and pronotum: Fig. 5m). Frontoclypeal suture interrupted medially in ♀, in ♂ sometimes with a very weak tubercle, viewed with suitable lighting (Fig. 2i). Epipharynx (Fig. 7i) with anterior margin of clithra almost straight either side of the median tylus and the mesoepitorma scarcely darkened. Prophobae rather strong, grouped towards the margins of the mesoepitorma. Chaetopedia three or four each side. Pronotum highly arched transversely, weakly so longitudinally. Entire lateral margins visible from above (Figs 2i, 5m). Surface with double punctation, this often close though sometimes sparser on the disc. In some specimens the punctures are deeply impressed, so the pronotal surface does not appear smooth. Basal margin entirely bordered, the border rather heavy (Fig. 14c). Elytra noticeably elongate, parallel-sided. Striae narrow but rather deep, strial punctures separated by ca 4× their diameters. Interstices 6–8× the width of the striae, with distinct sparse fine punctation and fine reticulation (Fig. 17f). Apex bluntly rounded. Metaventrite (Fig. 20m, n) with median diamond-shaped plate fairly strongly punctate and no obvious sexual dimorphism. Legs with longer spur of mid tibiae slightly longer than the basal segment (Fig. 18h), and in males the spur of the anterior tibiae is distinctly hooked (Fig. 18v).

Aedeagus (Fig. 22p, p') length ca 1.1 mm, parameres relatively short and blunt-ended, somewhat downturned apically. Endophallus with scales but no hairs or bristles.

Remarks. Distributed mainly in southern Russia, Ukraine, and Kazakhstan (Fig. 29b, c). Gusakov (2004) lists the holotype and 14 paratypes as having been collected in a dried-out rivulet at Ilek, 120 km SSW of Orenburg on the southern Urals, with two further paratypes from the Rostov and Kharkov districts of Ukraine and four more from the Temirsky region and Uralsk oblast' in Kazakhstan The Ulyanovsk specimen (ZIN) is labelled as having been taken in a damp saline area (solonchak).

The *niger* group

Species of the *niger* group are characterised by the aedeagal endophallus bearing a field of large recurved teeth (Figs 23, 24), clearly visible in cleared preparations where the endophallus is retracted as well as in specimens with the endophallus everted. The apices of the parameres are downturned, though sometimes only weakly so (Figs 23, 24). The basal segment of the mesotarsi may be longer than the longer mesotibial spur, but it is often more or less the same length of the spur or, in some species, clearly shorter than the spur, as in species of the *plagiatus* group (Fig. 18). The *niger* group comprises nine species, of which five are here described as new.

Aphodius (*Liothorax*) *niger* Illiger, 1798

Figs 4a, 6e, 9a–c, 15a, b, 17l, m, 18i, 19a, 21a–c, 23a–f, 24 a, 25a, 26t, 31a, b, d, e, 34a–d

Aphodius niger Illiger, 1798: 24. Conserved as valid name: International Commission for Zoological Nomenclature Opinion 2009 (2005: 45).

Type material examined. ***Lectotype***, unsexed, “Suec”, designated by Krell et al. (2003) (ZMB).

Additional material examined. SV: Sodermanland, Holo, Tulgarn, Nasuden. 58.95°N, 17.62°E. Trampled bare organic mud. 15.v.2011. Hans-Erik & Livia Wanntorp. 4♂♂, chromosome preps 2: 24.v.2001, 1:25.v.2011, 2: 25.v.2011, 1: 31.v.2011, R.B. Angus; 7♀♀, chromosome preps 3: 24.v.2011, 4: 24.v.2011, 9: 25.v.2011, 2: 31.v.2011, 3: 31.v.2011, 4: 31.v.2015, 5: 31.v.2011, R.B. Angus (NHMUK); 1 ♂ same data, chromosome prep. 2: 24.v.2011 (NMP).

GB: Hampshire, New Forest. Long Slade Bottom. 50.801°N, 1.619°W. Temporary pool after heavy rain. 30.v.2002, R.B. Angus. 4 ♂♂, 4 ♀♀, 5 unsexed. Chromosome preps 1–3: 31.v., 2: 1.vi, 4: 1.vi.2011, R.B. Angus (NHMUK); 1 ♂, same data.(NMP); New Forest, White Moor Pond. 50.820°N, 1.607°W. 2.x.2015, 2.v.2016, R.B. Angus. 8 ♂♂, 7 ♀♀, 3 unsexed. Chromosome preps: 3:x.2015, 5: v.2016. New Forest, Balmer Lawn. 50.828°N, 1.567°W. At edges of pond and ditch. V.2002. R.B. Angus (NHMUK). Inkpen Common, Berkshire 51.375°N, 1.453°W (fide Mann and Garvey (2014), not examined) 1 unsexed (OUM).

RU: Yaroslavl oblast', Berditsino, 57.454°N, 40.1108°E. leg. Yakovlev. 1♂ (NMW).

Differential diagnosis. *Aphodius niger* is immediately distinguished from all other *Liothorax* species (and all Aphodiinae whose chromosomes are known) by its long, almost entirely euchromatic, Y chromosome (Fig. 31a, b, d, e). The basal segment of the mesotarsus is always clearly longer than the longer mesotibial spur (Fig. 18i). Elytra glossy black, though interstices have fine reticulation. Central part of metaventrite without reticulation (Fig. 21a–d). Endophallic teeth clearly longer than high. Length of longest endophallic teeth at least 40 µm.

Redescription. General appearance (Fig. 4a). Length 4.2–4.5 mm (♂), 4.1–5 mm (♀), width 1.8–2 mm (♂), 1.8–2.2 mm (♀) (Swedish material), 4.4–4.8 mm (♂), 4.4–5.1 mm (♀), width 2.0–2.2 mm (♂ and ♀) (English Material).

Head black, without obvious brownish margin. Anterior margin of clypeus excised over middle 1/3, the lateral edges of this excision bluntly rounded. Frontoclypeal suture very fine, without any trace of a tubercle, straight-transverse over middle 1/2, angled forward to run to the clypeo-genal junction laterally. The lateral parts of the suture may be almost completely effaced. Clypeus raised in a rounded bulge medially. Surface moderately strongly punctate with double punctation. Larger punctures separated by ca their own diameter over most of the head, but sparser on clypeal bulge. Antennae and palpi blackish brown. Epipharynx (Fig. 9a–c) with the anterior margin of the clithra strongly excised either side of the median tylus and with a few fine acropariae. Chaetopedia stout, 3–6 each side. Chaetopariae ca as stout as chaetopedia, forming a close-set line each side. Apophobae very fine, arranged in a line outside that of the chaetopariae; prophobae vine, quite long, arranged against the sides of the mesoepitorma. Pronotum (Fig. 6e) hemicylindrical, black, highly arched transversely, weakly so longitudinally, lateral parts of surface bulging outwards so that the lateral margins are often not visible from above in their basal 1/3. Surface glossy black, with double punctation, the larger punctures separated by 1–2× their diameter, sparser medially and sometimes petering out in anterior 1/8 where only the fine punctures are present. Scutellum elongate, pentagonal, glossy black with a few sparse punctures. Elytra black, interstices flat, 6–8× the width of the striae, finely reticulate and with sparse fine punctures (Fig. 17l, m), the reticulation stronger towards the apex (Fig. 19a). Striae glossy, without reticulation, with a single row of punctures separated by ca 2× their diameter and excising the strial margins. Metaventrite moderately punctate, the median plate not reticulate, sometimes distinctly concave in males Fig. 21a but sometimes almost flat with a median impressed line, as in females (Fig. 21b, c). Legs blackish brown, mesotarsi always with basal segment longer than longer mesotibial spur (Fig. 18i).

Aedeagus (Figs 23a–f, 24a) length ca 1.2 mm, paramere length ca 0.48 mm, basal piece length ca 0.69 mm, tooth-field length ca 0.67 mm (measurements from the cleared preparation; Fig. 24a). Length of longest teeth on endophallus 54–65 µm. Parameres with the sclerotised strut running from the base just mediad of the outer lateral margin to the inner apical angle. Apical soft pad of parameres rounded apically, not widened.

Remarks. Chromosomally verified material is from the New Forest, England and Södermannland, Sweden. Material from Berditsino, Russia (NMW) is taken to belong to this species. In the New Forest *A. niger* is typically taken at the edges of pools and ditches in April-May, but when large numbers are taken it is almost always due to inwash from the surrounding grassland after heavy rain (Fig. 27a). In Britain, outside of the New Forest, *A. niger* has recently been found at Inkpen Common near Hungerford in Berkshire (Mann and Garvey 2014). In the Swedish locality the beetles were burrowing in trampled organic mud (H.-E. Wanntorp, pers. comm., April 2011) (Fig. 27c). Very occasionally *A. niger* is taken in dung, as by J. Bergsten in the New Forest in 1999, and sometimes in dry areas of the Swedish island of Öland (H. Lundqvist, pers. comm., April 2011). These are rare, random occurrences and may sometimes result from the beetle taking shelter from drought. One further feature of the occurrence of *A. niger* is worthy of comment – it shows dramatic fluctuations in abundance. Thus, in 2002 it was very abundant in its New Forest localities whereas more recently RBA has taken it only in low numbers. Similarly, H.-E. Wanntorp describes the species as being in very high numbers in the locality where he usually only took a few specimens (Fig. 29a).

***Aphodius* (*Liothoxax*) *muscorum* Ádám, 1994**

Figs 4b, 6f, 9e, 15c, 17n-q, 18j, 21e, g, i, j, 23u, 25b, 26u, 31f–l, 34e–g

Aphodius (*Liothorax*) *muscorum* Ádám, 1994: 6.

Type material examined. The holotype (Fig. 4b) has five labels: 1: Hung. Borsod-Abaúj-Zemplén m., Aggtelek Vörös-tó, 350 m. 2: Typhetum angustifoliae-latifoliae. 3: iszapból (= from mud) 1989.v.19., leg Ádám L. 4: Paratypus *Liothorax muscorum* Ádám, 1994 (A red label, incorrect because Adam mentioned only a single holotype with these data). 5: HOLOTYPE *A.* (*Liothorax*) *muscorum* Adam. R. B. Angus det. 2017. It is a female, so only somatic characters are available for assessment (MNSB).

Additional material examined. HU: Kisújszállás, 47.212°N, 20.700°E, iv.2012, R.B. Angus, 2 ♀♀(NHMUK). Hortobagy National Park, Kis-Kecskés area, 47.67721˚N, 21.06067˚E. Washed from mud at edge of a lake, and swarming in mud at edge of lake, 47.67772˚N, 21.07451˚E. 24.iv.2015, 16♂♂, 18♀♀. R. B. Angus (NHMUK, JFM). Aggteleki NP, Josvafö, Szelce-völgy 1♀, 1 unsexed (MNSB). Aggteleki NP, Josvafö, Menes-völgy. 1 unsexed (MNSB). Bukk NP 1♂, 2 ♀♀, 3 unsexed (MNSB). Hortobágyi N.P., 3.vi.1980, leg. U. Göllner, 2 unsexed (ABC).

Differential diagnosis. Closely resembling *A. niger* but clearly distinguished as a separate species by the short, almost dot-like, Y chromosome (Fig. 31f–h). Elytral interstices often with fine but distinct reticulation, giving the surface a leaden-grey silky sheen. Metaventrite of females variously depressed medially, depressed area often partly reticulate (Fig. 21e, g–j).

Redescription. General appearance (Fig. 4b). Length: 4.2–5.2 mm (♂), 4.3–5.2 mm (♀). Width: 1.85–2.35 mm (♂), 1.9–2.3 mm (♀). Black, head, pronotum and scutellum glossy (pronotum sometimes less so), elytra with interstices distinctly reticulate, giving a silky lead-grey sheen. Head: glossy black, rather finely punctate, the punctures separated by 2–3× their diameter. Some slightly larger punctures are present. Frontoclypeal suture very fine, with a glossy impunctate area either side of it. Median 2/3 almost straight, its mid-point and lateral ends slightly raised. Suture angled forward outside the lateral elevations, reaching the margin of the head at the front of the genae. Genae (preocular lobes) protrude laterally at an angle of ca 45˚ in front of eyes, then curve inwards to meet the frontoclypeal suture ca 1.5× eye-diameter in front of eyes. Clypeal margin obtusely angled outward from this point, then curved inwards to the median excision. Median area of clypeus bulging upwards. Genae laterally with a narrow raised margin, this continued across the clypeus, becoming weaker medially. The punctation of the frons is sometimes stronger, with a clear distinction between larger punctures and fine dot-like ones. Antennae and maxillary palpi black to blackish brown. Epipharynx (Fig. 9e) similar to that of *A. niger* (Fig. 9a–c). Head and pronotum (Fig. 6f). Pronotum: hemi-cylindrical, glossy black and with double punctation. The intensity of the punctation is variable, with the larger punctures in some specimens confined to the lateral and posterior 1/4s of its surface, while in others it extends over the whole surface and in some cases both the large and small punctures are heavily impressed, giving a roughened appearance to the surface. There is often an ill-defined narrow median band more or less free of punctures, extending from behind the middle of the disc almost to the hind margin. Lateral margins with a distinct raised bead, this either black or dark brown and extending round the hind corners often giving a continuous narrow raised border over the entire basal margin. It is necessary to tilt the specimen to trace the full course of this border, which is sometimes absent either side of the median 1/3, or from the middle 1/3 of the margin (Fig. 15c). Lateral margins visible from above over the anterior 1/2, behind this varying from being completely visible to totally obscured by the bulging pronotal surface. Scutellum: elongate, sides parallel in basal 1/2, then angled inwards to bluntly rounded apex. Surface glossy black, with sparse fine punctures. Elytra: black but with lead-grey silky sheen resulting from fine but distinct reticulation on the interstices. The strength of the reticulation varies from very weak in the holotype (Fig. 17n) to rather stronger in some Hortobágyi material (Fig. 17o) and stronger still in the two females from Kisújszállás (Fig. 17p, q). This reticulation may be obscured if the specimen is at all greasy. Interstices flat, ca 6× wider than the striae, with very fine punctures, these ca the same size as the meshes of the reticulation. Striae narrow, vertical-sided, their bottoms glossy. Strial punctures in single rows, small, separated by ca 3× their diameter, and excising the strial margins.

Metaventrite: median diamond-shaped plate in male finely and sparsely punctate, concave, depressed to median longitudinal groove (Fig. 21g); in female variable, sometimes median longitudinal groove flattened, but with the median area depressed anteriorly and sometimes with some reticulate sculpture (Fig. 21i, j).

Legs dark brown, often blackish, basal segment of mesotarsi normally longer than longer mesotibial spur (Fig. 18j) but sometimes equal in length or slightly shorter.

Aedeagus: Fig. 23u. Endophallus with heavy recurved teeth. Length ca 1.06 mm, paramere length ca 0.54 mm, basal piece length ca 0.69 mm. Length of tooth-field ca 0.57 mm, of longest teeth on endophallus 47–58 µm.

Remarks. As already mentioned, Ádám described *A. muscorum* as a new species, intending it to be the valid name for the species then known as *Aphodius* (*Liothorax*) *niger* (Panzer,1797). However, chromosomal research by RBA has shown that Hungarian material is in fact different from true *A. niger*, so Ádám's *Liothorax muscorum* must be regarded as a valid species. Ádám gives a description which, from its reference to variation in the strength of the elytral sculpture, is based on a fairly wide selection of Hungarian material. However, he lists only one type specimen, the holotype from the lake Vörös-tó in the Aggteleki national park in NE Hungary, adding that he took the unsexed specimen from mud in a drying out *Typha* bed. Vörös-tó is now a fairly deep lake with limited development of *Phragmites* round its edge. It was dredged out when the nearby entrance to the Baradla Barlang (cave) was developed (Sandor Rozsa, Chief Warden of the National Park, pers. comm. to RBA, April 2012). The nearby Aggteleki-tó has extensive development of mud and *Typha*, but though RBA has taken *A*. (*Nialus*) *varians* in both lakes he failed to find the *Liothorax*. It is therefore necessary to rely on the holotype and a limited amount of material from the neighbourhood, in the MNSB, for comparison with extensive material from the Hortobágyi National Park, from which chromosomes and DNA are available.

Aphodius muscorum stat. nov. is at present reliably identified only from Hungary. It appears to be a steppe species which may have a wider distribution eastwards but this needs to be verified with *A. niger* s.l. material from adjacent areas further east (Fig. 29a). RBA took the species abundantly in lakeside mud in the Hortobágy National Park in April 2015 (Fig. 27b), and 2 specimens in the mud of a drying out ditch near Kisújszállás in April 2012.

Aphodius "cf *A. niger*": species resembling *A. niger* and *A. muscorum*, but of uncertain identity

Material examined. RU: Volgograd, 48.739°N, 44.529°E. 1♂ (NMP). Tyumen. 57.215°N, 65.574°E. 1♂.(NMP).Tuyanso, Chernomorsk oblast'. 44.310°N, 30.517°E. 1915. 1♂ (ZIN)

KZ: 10 KM SE of Akmolinsk (Astana) 51.085°N, 71.720°E. Under detritus by the water. 5.v.1957. E. L. Gurjeva. 1 ♀ (ZIN). Akmola obl. Kokshipan. By R. Tirs, Marsh on floodplain with *Ranunculus* and *Fritillaria*. 13.v.1957. E.L. Gurjeva. 1♂ (ZIN). Akmola oblast', dolina Basaga-ozik., 49.840°N, 65.991°E. In a Solonchak (saltmarsh). L. Arnoldi, 27,v.1957.(ZIN); Uralsk 51.214°N, 51.271°E. 1♂ (NMP).

CZ: Hradec Králové, Na Plachtě. 50.186°N, 15.859°E. 1♂, 1 unsexed (NHMUK). České Budějovice, Hosín aerodrome. 2 unsexed (NHMUK). Břeclav Pohansko 48.73°N, 18.918°E. Martinů Ivo leg. 20.iv.2008. 1♂, 4 ♀♀, 4 unsexed (NHMUK).

SK: Bol. 48.494°N, 21.949°E. 2 unsexed (NHMUK).

AU: Feldkirch Moosbrugger Vbg. 47.258°N, 9.581°E. 1♂, 1♀(JHMC). Purgstall a. E. Austria inf. 48.063°N, 15.132°W & 48.064°N, 15.133°E. 2, unsexed. Leg. Ressi (JFMC). Umgebung Wien Mauerbach, 48.246°N, 16.165°E & 48.264°N, 16.354°E. 2, unsexed (JFMC). Wien Umgebung, 48.209°N, 16.392°E. 1, unsexed (JFMC). Neusiedler See. 47.712°N, 16.16.804°E 1, unsexed (JFMC). Ullig Hart bei Graz, 47.082°N, 15.440°E. 1, unsexed (JFMC).

GE: Masselund, Emsland, 8.5.1969, Kerstens 1 unsexed; Hasslünne, Emsland, 8.5.59, Kerstens, 1 unsexed (ABC); Garz Dr Minarz, "594 niger", 1 unsexed; c. Epplsh Steind. d., 1♂, 6 unsexed (NMW).

PL: Hinter Pommern Kołobrzeg (Zieleniewo), 1 unsexed (MNCN).

RU: Yaroslavl oblast', Berditsino, 57.454°N, 40.1108°E. leg. Yakovlev. 1♂ (NMW).

Remarks. Material from France, Italy, Bosnia, and Turkey is listed by Maté and Angus (2005). It is not listed here but is mapped (Fig. 29).

Material from coastal or near-costal localities from Poland, Germany, and France is likely to be *A. niger*. The Yaroslavl specimen is taken as *A. niger* because locality seems to be ecologically similar to the English and Swedish ones. This might also be true of the Tyumen male.

The specimens from Břeclav Pohansko and Bol are likely to be *A. muscorum* because these lowland localities are on the edge of the Hungarian plain, and the same is true of all the eastern Austrian material.

The outstanding problem with Central European material is the identity of the "*A. niger*" from the German Mittelgeberge and the northern and central parts of

Czechia, as well as the French Massif Central. The map given by Rößner (2012) shows German records, mainly pre-1950, concentrated either in coastal regions or somewhat further inland (the Mittelgeberge) with few records connecting the two areas. Rößner et al. (2016) give updated records, with some west German localities in the Mittlegeberge post 1950. Costessèque (2005) records it from all the Départements of the Massif Central, but RBA failed to find it in the southern Auvergne (Cantal, Haute-Loire) in April 2017. While all the material may be *A. niger*, there remains the possibility that a further, as yet unknown species may be present. We have, unfortunately, not been able to obtain living material from this inland area.

The material from Astana and the Akmola oblast and Uralsk may include a new species characterised by a reticulate metaventrite in the males, but a male from a saline depression (Solonchak) by the river Basaga-ozik lacks any trace of reticulation. The Volgograd male also lacks any trace of reticulation on the central portion of the metaventrite. The males from the Chernomorsk oblast' and Volgograd also lack any reticulation on the metaventrites and their identities are unclear.

Aphodius **(*Liothorax*)** ***felix*** **sp. nov.**

https://zoobank.org/79A36FAF-5DDF-45AC-99BB-A9BC5CDBEC67
Figs 4c, 6i, 8e, f, 15d, 16v, 18p, q, 21f, k, 23v, w, 25c, 26v, 32a–e

Type material examined. ***Holotype*** ♂: Italy, Abruzzo, Campo Felice. Washed into pool. 1.vi.2009. R. B. Angus. Chromosome prep. 4, 7.vi.2009. R. B. Angus (NHMUK). ***Paratypes*****:** 1♂, data as holotype, chromosome prep. 3, 7.vi.2009. R. B. Angus; 3♀♀, data as holotype, chromosome preps 1 – 3, 9.vi.2009. R. B. Angus (NHMUK); 1♀, data as holotype, 1.vi.2009 (sequenced) (JFMC); Basilicata, M. Sirino (PZ) XI.1997 1400–1700m Leg. F. Angelini (JFMC).

Differential diagnosis. *Aphodius felix* sp. nov. was the first new species to be recognised, after *A. wilsonae*, initially because of its small y chromosome. The endophallic teeth are large, as in *A. niger*, and the basal segment of the mesotarsi is not longer than the longer mesotibial spur. The pronotum is fairly strongly punctate and the sides bulge outwards so that the lateral margins are not visible from above either all the basal 1/2 or visible again in the basal 1/6 (Fig. 6i), a character shared with Sicilian *A. bellumgerens* (Fig. 6j). Chromosomally, these two species are clearly distinguished by their X chromosomes, the X being clearly the longest in the nucleus in *A.* (*bellumgerens* Fig. 32f–i), but clearly shorter than autosome pairs 1–3 in *A. felix* (Fig. 32a–e).

Redescription. General appearance (Fig. 4c). Length: 4.4–4.5 mm (♂), 4.2–5.0 mm (♀); width: 1.9–2.0 mm (♂), 1.6–2.3 mm (♀). Glossy black, tarsi, and tibial spurs dark brown, tibiae with a hint of brown-bronze reflections.

Head with dorsal surface domed, flatter behind frontoclypeal suture. Frontoclypeal suture distinct, completely non-tuberculate but with smooth elevated areas each side of the median straight section and a weaker elevation medially. Genae rounded, strongly protuberant laterally in front of eyes. Clypeus with rounded median emargination, angles either side of this rounded. Clypeus and genae with strong raised margin, this slightly brownish. Surface strongly and more or less evenly punctuate, the punctures separated by ca 1.5× their diameter, and finer medially. Antennae and palpi more or less black. Epipharynx

(Fig. 8e, f) clithra evenly excised either side of the median tylus, chaetopedia with four or five rather stout spines and spines of chaetopariae mainly shorter than chaetopedia. Head and pronotum as in Fig. 6i.

Pronotum hemicylindrical, highly arched transversely but more or less flat longitudinally, lateral margins more or less parallel, but slightly convergent anteriorly, weakly and very evenly curved. Pronotal surface bulging outwards from the general curvature over all or part of the basal 1/2 of the pronotum, ca 1/4 of the way in from each side, so that the lateral margins are not visible from above either in all of the basal 1/2 of the pronotum, or visible in the basal 1/6 (Fig. 6i). Lateral margins with distinct raised border, this continued very finely over the lateral 1/3 of the basal margin, the median 1/3 of which normally lacks any border Occasionally the median 1/4 of the basal margin is bordered but on either side of this is an unbordered section amounting to one 1/4 of the length of the basal margin (Fig. 15d). Anterior margin without any trace of a raised border. Surface with double punctation of variable strength. Larger punctures separated by 2–4× their diameter, sometimes very strongly impressed and with the pronotal surface depressed immediately round their edges, but sometimes more moderate and with the pronotal surface evenly curved around them. Finer punctures dot-like, in some specimens separated from one another by ca 2× their diameter but in other specimens much sparser, separated by 4–6× their diameter. Pronotal surface between the punctures smooth, glossy. Scutellum: elongate, pentagonal, ca 10% of elytral length, glossy black with brownish lateral and apical edges, and with sparse punctures medially. Elytra: glossy black but the interstices slightly duller than head and pronotum and with fine isodiametric reticulation (visible at × 40 magnification with bright diffuse illumination) (Fig. 16v). Striae narrow (ca 1/5 the width of the interstices), vertical sided and with punctures separated by ca 2× their diameter. In the two ♂♂ the punctures bulge into the interstices but in the three ♀♀ they hardly deflect the strial margins. Lateral margins of the elytra distinct, at base strongly upcurved in front of the humeral bulges; stronger basally and at apex ca as wide as stria 2. Interstices 4× as wide as striae, with fine sparse punctation, this a bit stronger in the humeral area in front of abbreviated stria 9.

Metaventrite: median diamond-shaped plate fairly strongly punctate, concave to the depressed mid-line (2 ♂♂) (Fig. 21f, k), flat with faint median impressed line to median concavity over middle 1/3 of the diamond-shaped area (3 ♀♀). Legs: black with dark brown tarsi and tibial spurs, rather long and slender, basal segment of hind tarsi as long as segments 2 + 3 + 1/2 of segment 4. Longer spur of mid tibiae longer than basal segment of mid tarsi, though sometimes the segment is almost as long as the spur (Fig. 18p, q).

Aedeagus (Fig. 23v, w): size and shape of parameres as *A. niger*, and spines of endophallus strong as in *A. niger*. Longest teeth on endophallus 45 μm long.

Etymology. *felix* – Latin, happy, named from the type locality, Campo Felice.

Remarks. As yet this species is known only from the type series. The beetles were taken at the edge of a pool below a grassy slope on Campo Felice (Fig. 29a) in the Abruzzo mountains (Fig. 28f) after a day of continuous heavy rain. A return visit a day or so later, after better weather, yielded no further specimens, so that it seems that this species lives at the roots of the grass and other herbs rather than in the mud at the water's edge. Specimens from northern and central Italy mentioned in Maté and Angus (2005) are most likely *A. felix*. See Remarks after *A. bellumgerens*.

***Aphodius* (*Liothorax*) *bellumgerens* sp. nov.**

https://zoobank.org/892D4998-D52B-4B6B-BF0D-ADA21A086F2F

Figs 4f, 6j, 9f, g, 16d, 17u, 18r, 21l, m, p–t, 24m, n, 25e, 26z, 32f–i

Type material examined. ***Holotype*** ♂: Sicily. Parco delle Madonie. Piano Battaglia. At edges of pool. 1.v.2013. R.B. & E.M. Angus. Chromosome prep. 7: 8.v.2013 (NHMUK). Length 3.9 mm, width 1.8 mm. ***Paratypes*****:** 7♂♂, 8♀♀, same data as holotype. Chromosome preparations 1–8, 7.v.2012, 1–6 and 8, 8.v.2012 (NHMUK). 7♂♂, 5♀♀, same data as holotype but 23.iv.2018 (NHMUK), 1♂, 1♀, same data (NMP); 12♂♂, 6♀♀, Sicily, Nebrodi, Monte Soro, 1600m a.s.l. 25.iv.2018. R.B. & E.M. Angus. Chromosome preparations 1–4, 27.iv.2018, 1–5, 1.v.2018, 1–5, 2.v.2018, 1–4, 10.v.2015 (NHMUK). 1♂, Sicily, Nebrodi, leg F. Krell (DMNS). 3, data as holotype (sequenced) (JFMC); 1 SICILY, Nebrodi, Monte Soro, 1600m a.s.l. 25.iv.2018. R.B. & E.M. Angus. Chromosome preparation 4, 27.iv.2018 (Sequenced) (JFMC).

3♂♂, 4♀♀, 37 unsexed: ITALY, Sicily, Monte Soro, Tumpelufer, welkes Laub. 1800 m NN 30.5.1993 leg. U Schaffrath (ABC & JFMC).

Differential diagnosis. Most similar to *A. felix*, from which it is shown to be different because of its clearly larger X chromosome (Fig. 32f–i, a–e). The slightly smaller aedeagus, with the endophallic tooth-field clearly shorter than the parameres (Figs 23p–t, 24m, n) is also distinctive.

Description. General appearance (Fig. 4f). Length: 3.6–4.4 mm (♂), 4.0–4.8 mm (♀), width: 1.65–1.95 mm (♂), 1.7–2.0 mm (♀). Glossy black, apical segments plus claws of tarsi dark brown.

Head with no trace of reticulation but with sparse double punctures, the punctures separated by ca 2× the diameter of the larger punctures. Fronto-clypeal suture indistinct but present, without tubercles but slightly raised at ends of median section, before turning to run to the anterior margins of the genae. Anterior margin of clypeus emarginated medially, rounded at sides of the emargination. Antennae and palpi black. Epipharynx (Fig. 9f, g) with anterior margin of clithra emarginate each side of projecting median tylus, with a few fine acropariae. Chaetopedia 4 or 5 each side, stout. Chaetopariae forming a single line each side, closely set, stout. Apophobae forming a narrow band of fine setae outside the chaetopariae, prophobae in a narrow field each side of the mesoepitorma. Head and pronotum (Fig. 6j): pronotum: surface either smooth and glossy as head or slightly dull, with double punctation, size of the large punctures stronger than on head, but variable, these punctures separated by ca 2× their diameter. Small punctures tiny dots. Mid-line impunctate or with very fine punctures. Pronotum more or less hemicylindrical, highly arched transversely, in mid-line weakly arched longitudinally. Sides of pronotum bulging outwards in basal 1/3, so that the basal 1/3 of the lateral margins is not visible from above. Lateral margins completely bordered, this border extending along lateral 1/3 of basal margin as a very fine impressed line. Median 1/3 of basal margin without an impressed border, as in the *A. wilsonae* shown in Fig. 16d. Scutellum pentagonal, sides parallel in basal 1/2, then converging to blunt apical point. Elytra: sides either almost parallel over basal 2/3 or more distinctly rounded to widest point 2/3 of the way from the base, bluntly rounded to apex. Interstices flat, ca 6× the width of striae, glossy black, sometimes with very fine reticulation, especially over basal 1/4 (Fig. 17u). Sutural interstices weakly raised to suture. Striae narrow, shallow, the strial punctures scarcely impinging on their margins. Median diamond-shaped plate of metaventrite with sparse fairly fine punctures, sometimes flattened in males or with a median depression in females (Fig. 21l, m).

Legs: Long spur of mid tibiae clearly longer than basal segment of tarsi, exceeding it by a distance approximately equal to the width of the basal margin of the second tarsal segment (Fig. 18r). Spines on apical margin of posterior tarsi short and even on outer/ventral face, longer, sparser, and more irregular on inner/dorsal face.

Aedeagus (Figs 23p–t, 24m, n) Length ca 0.9–1.1 mm, paramere length ca 0.43–0.47 mm, basal piece length ca 0.5–0.6 mm, tooth field length ca 0.3–0.4 mm. This is one of the few species in which the length of the endophallic tooth-field is less than that of the parameres. Longest teeth on endophallus ca 47 µm long.

Etymology. *bellumgerens* – Latin, waging war, adjective, named for the type locality, Piano Battaglia (the battlefield).

Remarks. So far known only from Sicily (Fig. 29a). Many of the types were taken by swishing the water at the edges of the pool on the Piano Battaglia, washing the beetles from the banks so that they floated on the water. This pool dries out completely in the summer. The Monte Soro specimens were floating and clinging to plants in a shallow pool, following recent rain (Fig. 27g). We have seen specimens from Calabria (Sta Christina, Cippo di Garibaldi) which are apparently morphologically identical but have not been included in the type series due to the scarcity of material and lack of karyological or molecular data. RBA has recently received living material from Calabria: Villaggio Mancusa, 39.10727°N, 16.64085°E, from which chromosomes indicating *A. felix*, not *A. bellumgerens* have been obtained. These data will be published in due course.

***Aphodius* (*Liothorax*) *bameuli* sp. nov.**

https://zoobank.org/F188AEBA-0E15-4EB4-B1AD-A1A49DBBA81E

Figs 4d, 6g, 8g, 16a, x, 18k, l, u 21p–r, 23j–l, 24b, 25f, 26w, x, 33a–d, 34h

Type material examined. *Holotype* ♂: Corsica, Haute-Corse, pelouse (lawn) grassland by the Lac de Melo. Cow dung. 19.vi.2011. R. B. and E. M. Angus. Chromosome prep. 2, 29.vi.2011. R. B. Angus (NHMUK). ***Paratypes*:** 2♂♂, data as holotype, 1 labelled Chromosome prep. 1, 29.vi.2011. R. B. Angus; 4♂♂, data as holotype but 24.vi.2011; 14♀♀, data as holotype, including Chromosome preps 1–4, 28.vi.2011, 6–9, 28.vi.2011 and 1–3, 1.vii.2011, R. B. Angus; 1♀, data as holotype (NMP); 11♀♀, data as holotype but 24.vi.2011; 2♂♂, 5♀♀, data as holotype but 30.vi and 1.vii.2009, R. B. and E. M. Angus. ♂ Chromosome preps 1 and 2, 6.vii.2009, ♀ Chromosome preps 3–5, 5.vii.2009 (NHMUK). 1♂ data as previous (NMP); 1♂, data as holotype but 24.vi.2011, in F. Krell collection (DMNS). 3 Corsica, Haute-Corse, pelouse (lawn) grassland by the Lac de Melo. Cow dung. 19.vi.2011. R. B. and E. M. Angus (sequenced) (JFMC); 7 ♂♂, 23 unsexed, "18.vii.1983. Corse. Lac de Nino 1743 m. Rinderkot. Leg. H. Fery". In H. Fery collection (ZSM); 2 unsexed, "France Corse Nino-See 1730 m. 12.vii.1987. Leg H. Hirschfelder." In H. Fery collection (ZSM). In CZC and JFMC: 1♂ 1♀, 1 unsexed France: Corsica Plateau d´Alzo 1500m 42°16'N, 9°04'E 21/V/1994 leg. C. Zorn.

Differential diagnosis. The parallel-sided, hemicylindrical, lightly sculptured appearance (Fig. 4d) is distinctive. The pronotal sides bulge outwards laterally so that the lateral margins are not visible from above in basal 1/2 of the pronotum. The lateral margins themselves are parallel, only very slightly convergent anteriorly. The general shape of the beetles and their pronotal configuration resembles those of *A. niger* and *A. muscorum* (Fig. 4a, b), but these species are more heavily sculptured.

Description. General appearance (Fig. 4d). Length: 4.0–4.6 mm (♂), 3.9–4.8 mm (♀); width: 1.7–1.9 mm (♂), 1.6–2.0 mm (♀). Glossy black, tarsi, tibial spurs dark brown, femora and tibiae dark brown with black-bronze reflections. Head: dorsal surface domed, flatter behind frontoclypeal suture. Medial area of clypeus more demarcated as a dome than in *A. felix*. Frontoclypeal suture distinct, completely non-tuberculate but with distinct smooth elevated areas each side of the median straight section and a weaker elevation medially. Genae rounded, strongly protuberant laterally in front of eyes. Clypeus with rounded median emargination, angles either side of this rounded. Clypeus and genae with strong raised margin, this slightly brownish. Surface strongly and more or less evenly punctuate, the punctures separated by ca 1.5× their diameter, and finer medially. Antennae and palpi more or less black. Epipharynx (Fig. 8g) clithra evenly excised either side of the median tylus, chaetopedia with 4–6 spines, these slightly less robust than those of *A. felix* and spines of chaetopariae as long as or longer than chaetopedia. Head and pronotum as in Fig. 6g. Pronotum hemicylindrical, highly arched transversely but more or less flat longitudinally, lateral margins more or less parallel, but very slightly convergent anteriorly, weakly and very evenly curved. Pronotal surface bulging outwards from the general curvature over the basal 1/2 of the pronotum, ca 1/4 of the way in from each side, so that the lateral margins are not visible from above in the basal 1/2 of the pronotum (Fig. 6g). Lateral margins with distinct raised border that continued very finely over the lateral ca 1/3 of the basal margin, at least the median 1/3 of which lacks any border (Fig. 16a). Anterior margin without any trace of a raised border. Surface with double punctation of variable strength, but in general weaker than in *L. felix* sp. nov., though the strength of the punctation of the two species overlaps. Larger punctures separated by 2–4× their diameter, sometimes very strongly impressed and with the pronotal surface depressed immediately round their edges, but sometimes more moderate and with the pronotal surface evenly curved around them. Finer punctures dot-like, in some specimens separated from one another by ca 2× their diameter but in other specimens much sparser, separated by 4–6× their diameter. Pronotal surface between the punctures with a silky sheen and a very fine, generally indistinct, small, isodiametric reticulation.

Scutellum elongate, pentagonal, ca 10% of elytral length, glossy black with brownish lateral and apical edges, and with sparse punctures medially.

Elytra glossy black but the interstices slightly duller than head and pronotum, appearing slightly silky and with a very fine indistinct isodiametric reticulation sometimes visible. Striae narrow (ca 1/5 the width of the interstices), vertical sided and with punctures separated by ca 2× their diameter. In the two ♂♂ the punctures bulge into the interstices but in the 3 ♀♀ they hardly deflect the strial margins. Lateral margins of the elytra distinct, at base strongly upcurved in front of the humeral bulges; stronger basally and at apex ca as wide as stria 2.

Interstices 4× as wide as striae, with fine sparse punctation (Fig. 16x), which is a bit stronger in the humeral area in front of abbreviated stria 9.

Legs (Fig. 18k, l, u) dark brown with bronze-black reflections and tarsi and tibial spurs brown, rather long and slender, basal segment of hind tarsi as long as segments 2 + 3 + 1/2 of segment 4. Longer spur of mid tibiae longer than basal segment of mid tarsi.

Metaventrite (Fig. 21p–r): median diamond-shaped area rather lightly punctate, without pubescence, its mid-line either almost indistinguishable or variably depressed, sometimes forming a distinct longitudinal furrow up to 1/3 as wide as the median point of the diamond. There is no sexual dimorphism.

Aedeagus (Figs 23j–l, 24b) Length ca 1.2 mm, paramere length ca 0.45 mm, basal piece length ca 0.76 mm, length of endophallic tooth-field ca 0.4 mm. Length of longest teeth on endophallus ca 44 μm.

Etymology. Named after our good friend Dr Franck Bameul of Bordeaux, who accompanied RBA and EMA to the Lac de Melo on the 24.vi.2011 and was with us as we all endured a prolonged and spectacular thunderstorm.

Remarks. *Aphodius bameuli* sp. nov. is endemic to Corsica (Fig. 29a) and, as far as we know, is the only *Liothorax* definitely associated with dung. On the Melo lawns (Fig. 27e) it occurred in cow pats, avoiding the more liquid regions towards the centre of the dung. It ate the dung, which filled the guts of specimens used for chromosome work. Hans Fery (pers. comm. ix.2015) told us that when he collected it by the Lac de Nino the water was very high, covering the lakeside lawns but that the cow pats protruded above the water surface and that is where the beetles were found. RBA and EMA failed to find it in the cow dung on the lawns in the valley of Pozzi (Ghisoni), further south.

It is an elongate, parallel-sided, and lightly sculptured species.

***Aphodius* (*Liothorax*) *krelli* sp. nov.**

https://zoobank.org/40001D30-4534-4350-97CB-5E286675ADC8

Figs 4e, 6h, 8j, 16b, 17y, 18m, n, 23m, o, 26y, 33e–l, 34i, j

Type material examined. ***Holotype*** ♂: Sardinia, Nuoro Province, Badde Salighes 3.iv.2012. R. B. & E. M. Angus. L 5.0 mm, b 2.1 mm. Chromosome prep. 2, 5.iv.2012 (NHMUK). ***Paratypes*:** 4♂♂, 4♀♀, data as holotype, but 1♂ taken on 1.iv.2012. ♂ paratypes with chromosome preparation data prep. 5: 5.iv.2012 and prep. 1: 10.iv.2012, ♀ paratypes with data preps 3, 4, 6–8: 5.iv.2012 (NHMUK); 1♀, data as holotype (NMP) 1♀, data as holotype (JFMC); 1♂, chromosome prep 5, 5.iv.2012, data as holotype (DMNS); 1♀, Sardinia, Sassari, Ciaccia, 17.VII.2008, old sheep dung, R. B. Angus (JFMC); 2 unsexed, ITALY, Sardegna, Nuoro, Altopiano della Campeda, 40°21.245'N, 8°47.044'E, 580m, 18.5.2005 leg. Starke (ABC); 1 unsexed, [ITALY], Badde Salighes Sardegna [Nuoro Pr], *Aphodius* (*Nialus*) *niger* Carpaneto det. 1982 (MNHG).

Differential diagnosis. Sardinian *A. krelli* differs from Corsican *A. bameuli* in being less parallel-sided (Fig. 4e, d) and with the pronotum more heavily punctate (Fig. 6h, g). The karyotypes of the two are very similar in the sizes and shapes of their chromosomes (Fig. 33e–l) but the long arm of autosome 7 in *A. krelli* is heterochromatic and is polymorphic for a deletion – it may be present (Fig. 33f, i–l) or absent (Fig. 33g, h).

Description. General appearance (Fig. 4e). Length: 4.4–5.0 mm, width: 2.0–2.1 mm (♂), 4.1–4.5 mm, width 1.7–2.0 mm (♀). Head: glossy black with no trace of reticulation, anterior margin vaguely browner. Sculpture of double punctation, the fine punctures separated by ca 2× their width, the coarser punctures ca 3× the diameter of the fine ones, distributed over the anterior and lateral parts of the head and on the frons. Frons elevated in a vague hump on disc. Frontoclypeal suture very fine but distinct and complete. Anterior margin of clypeus emarginated medially, the margin rounded either side of this emargination. Anterior and lateral margins of head bordered, the border extending from the back of the genae. Genae distinct, fairly abruptly divergent anteriorly from anterior margin of the eyes, widest point behind middle of genae, in front of which the genal margins curve more gently to the clypeus, which they meet at a slight angle. Epipharynx (Fig. 8j) with anterior margin of clithra strongly emarginate each side of the median tylus, and with a few fine acropariae. Chaetopedia stout and long, four or five each side; chaetopariae closely set, fairly stout, forming a line each side. Prophobae very fine, clustered along the edges of the mesoepitorma; apophobae fine and long, arranged in a line outside the chaetopariae. Antennae and palpi blackish brown. Head and pronotum as in Fig. 6h. Pronotum: hemicylindrical, highly arched transversely but very weakly so longitudinally in the mid-line. Lateral margins entirely visible from above. Lateral margin bordered, basal margin with very fine border, this sometimes complete but usually absent from the median 1/2 to 1/3 of the margin. Surface glossy black with no hint of reticulation but with double punctation. Fine punctures dot-like, extending over the whole surface, coarser punctures ca 4–8× the diameter of the dots, sparser and tending to be smaller on the disc. Fine punctures separated by ca 4–6× their diameter, coarse ones by 1.5–2.5× their diameter.

Scutellum: narrow, pentagonal, sides parallel in basal 1/2 then convergent to a blunt point apically. Surface glossy black with a few punctures in basal 1/2.

Elytra: elongate, not quite parallel-sided, widest just behind middle, then tapered to bluntly rounded apex. Ground colour of interstices silky black with very fine faint isodiametric reticulation (Fig. 17y). Striae glossy black. Interstices flat, ca 10× the width of the striae, with scattered fine punctures separated by ca 4–5× their width. Sutural interstices weakly raised longitudinally from their external margins to ca 1/3 of the way to the suture, then depressed to the suture. Striae narrow, with vertical sides, with a single row of punctures separated by ca 3× their diameter, the sides of these punctures encroaching into the strial margins. Metaventrite with median diamond-shaped area fairly strongly punctate, the punctures larger than in *A. bameuli*, in males concave to median impressed furrow, in females often flatter.

Legs: dark brown, longer spur of mid tibiae clearly longer than basal segment of tarsus, although sometimes only slightly so (Fig. 18m, n). Post tibiae with apical fringe of spines short and of even-length ventrally, longer, sparser and of uneven lengths dorsally.

Aedeagus: Fig. 23m–o. Length ca 1.1 mm, length of parameres ca 0.5 mm, of basal piece ca 0.6 mm, of endophallic tooth-field ca 0.6 mm. Length of longest endophallic teeth 56–58 μm.

Etymology. This species is named after Dr F.-T. Krell of the Museum of Nature and Science, Denver, Colorado.

Remarks. *Aphodius krelli* sp. nov. is endemic to Sardinia (Fig. 29a). Pittino (2010) lists various Sardinian localities, including Badde Salighes, but all the analysed material is from Badde Salighes (Fig. 27d). *Aphodius krelli* sp. nov. is described as a new species despite the fact that its karyotype is similar to that of *A. bameuli* sp. nov. from Corsica. In spite of the karyological similarities, it is genetically divergent from *A. bameuli*, from which it differs by 4.7%, and instead clusters with *A. bellumgerens* sp. nov., forming a strongly supported clade. In addition the morphometric study clusters *A. krelli* sp. nov. between the *niger*-crown group and the 3B group, from which it differs in being significantly more convex. Morphologically it differs from *A. bameuli* sp. nov. in being generally more heavily sculptured and more rounded. Its habitat is also different – whereas *A. bameuli* sp. nov. is a dung-inhabiting species, *A. krelli* sp. nov., like most *Liothorax*, is found at the edge of water. The type material, brought home alive for laboratory studies, was divided into two lots. One was given organic detritus from where it was collected while the other was given damp fibrous cow-dung of the sort eaten by *A. bameuli* sp. nov. The beetles given detritus continued feeding on the journey home but those given dung did not feed at all.

***Aphodius* (*Liothorax*) *isikdagensis* (Balthasar, 1952)**

Figs 3c, d, 6a, b, 16e, 18s, 24c, 26c’

Aphodius (*Ataeniomorphus*) *isikdagensis* Balthasar, 1952: 22.

Type material studied. ***Holotype*** (labelled as ♂, undissected), with the locality data as given above and a label “*Aphodius* (*Ataeniomorphus*) *isikdagensis* n. sp., Dr V. Balthasar”. At present *A. isikdagensis* is known only from the type series, the holotype and seven paratypes, one labelled as ♀ allotype, with the locality data Çamlidere, Isik d., Anat. 23.vi.47. Exp. N. Mus. ČSR. ***Paratypes*:** 1 labelled as ♀ allotype and 6 paratypes, noted by Balthasar as 4♂♂ and 2♀♀. Thus 1 paratype is unaccounted for. Balthasar does not appear to have dissected any of the types (though a male paratype had been dissected) and apparently distinguished the sexes on the degree of clypeal bulging and the degree to which the genae were angled out at their junction with the clypeus. Both these characters are clear in two of the paratypes (Figs 3c, d, 6a, b) the largest of the ♂♂ and ♀♀, but not in two other ♀♀ where the reduced clypeal bulging is clear, but not the outward angling of the genae. Assuming 1 ♂ paratype is elsewhere, the 6 paratypes noted by Balthasar comprise 2♂♂ and 4♀♀. It may be that Balthasar inadvertently switched the numbers of males and females. Balthasar gives the length range as 4.5–5.5 mm. Our measurements are based on stacked images.

Additional material studied. One male, Turkey, Artvin Çam gec. 2000 m, coll. Ziani, shown by its aedeagus (Fig. 24k) to belong to the *A. niger* section, may belong here. Its length is 4.64 mm, width 1.89 mm, so it is within the size range of *A. isikdagensis*, with which it also agrees in the brown, not blackish, legs, though the maxillary palpi are black. The aedeagus (Fig. 24k) in lateral view is shown to have the parameres only weakly downturned apically.

Differential diagnosis. The larger of the two known Turkish species, identified as a member of the *A. niger* group by the large recurved endophallic teeth

(Fig. 24c). Maxillary palpi mid-brown. Epipharynx (Fig. 8c, d) with apophobae arranged in narrow bands ca two bristles wide.

Redescription. General appearance (Fig. 3c, d). Length 4.6–5.8 mm, width 1.9–2.5 mm. Head black, browner towards the anterior and lateral margins, no tubercle on frontoclypeal suture. Frontoclypeal suture fine and straight-transverse over middle 1/3, at either end of this either effaced or angled forward to reach the edge of the head at the junction of the clypeus and genae. Outer margin of genae more or continuous with that of the frons in male, distinctly angled outwards in female (Fig. 6a, b). Clypeus moderately bulging upwards medially in male, weakly so in the female, anterior margin broadly excised medially, the sides of this excision bluntly rounded. Punctation rather weak, sometimes stronger and tending to be rugose towards the anterior and lateral margins. Epipharynx (Fig. 8c, d) with the central tylus strongly projecting and the anterior margin of the clithra clearly excised either side. Central darkened sclerotised epitorma broadly triangular, the whole median darkened region appearing widest at base (Fig. 8c) or narrowed basally (Fig. 8d). Acropariae virtually absent, chaetopedia strong, six or seven each side. Surface of gymnopedia covered with small tooth-like asperities. Prophobae quite strong, clustered at the edges of the sclerotised mesoepitorma, apophobae fine, arranged in a narrow slightly irregular band ca two bristles wide, outside the chaetopariae. Antennae and palpi mid brown. Pronotum (Fig. 6a, b) hemicylindrical, highly arched transversely, scarcely at all longitudinally. Entire lateral margins visible from above. Surface with double punctation, male paratype with the larger punctures separated by at least twice their diameter, sparser on disc. The female paratype has the punctation sparser and finer. Posterior margin completely bordered (Figs 6a, b, 16e), the border wider medially, narrowed but continuous round the posterior corners.

Scutellum pentagonal, elongate, glossy, sometimes with a few punctures medio-basally. Elytra black, interstices flat, 6–8× width of the striae, with fine isodiametric reticulation and sparse fine punctures (Fig. 17k).

Metaventrite (Fig. 21x, y) moderately punctured, flattened over median diamond-shaped plate, sometimes with an impressed median line. Legs mid brown, basal segment of mesotarsi elongate, either clearly longer than the longer tibial spur, or ca the same length (Fig. 18s).

Aedeagus (Fig. 24c): total length ca 1.1 mm, parameres length ca 0.48 mm, basal piece length ca 0.64 mm, length of endophallic tooth-field ca 0.70 mm. Length of longest tooth on endophallus (measured from photograph) ca 60 μm. Parameres with darkened sclerotised strut running from near the outer margin at the base to the inner margin at apex, where the apical sensory pads run round the apex from the tip of the oblique strut to the outer edge, almost to its outer apical angle.

Remarks. This species is identified as a member of the *Aphodius niger* group by the large, recurved teeth on its endophallus (Fig. 24c), and the parameres with the apical sensory pads running round the apex from the tip of the oblique strut to the outer edge. This may be the result of collapse of only weakly downturned apically parameres as a result of drying.

Dellacasa et al. (2001b) regarded this species as conspecific with *A. rutilipennis*, at that time known as *A. ressli* (Petrovitz, 1962). They figure the aedeagus (without the endophallus in its sac), but the parameres do not really match those of the paratype shown in Fig. 24c. Dellacasa et al. (2007), in their revision of the world species of *Liothorax*, show the same figure of the aedeagus.

At present *A. isikdagensis* is known only from the type series, the holotype and seven paratypes, one labelled as ♀ allotype, with the locality data Çamlidere, Isik d., Anat. 23.vi.47. Exp. N. Mus. ČSR (Fig. 29b, c). Other Turkish material (Vilayet Rize, Ovitdagi gecidi m 2600, coll. Balerio; Kizildag Gecidi 2290 m, coll. Král; Artvin Çam gec. 2000 m, coll. Ziani) is shown by its parameres to belong to the *A. niger* species complex, and this is also true of a male from central Armenia, Selim Pass 2350 m, coll. Ziani. See discussion of *L. alberti* sp. nov.

***Aphodius* (*Liothorax*) *alberti* sp. nov.**

https://zoobank.org/EB4FACD0-EC1A-40A1-9DFB-EB3418C749F6
Figs 3e–g, 5c, d, 6c, d, 8k, l, 18t, 20o, 21n, o, 24e–j 25d, 26b’, c’

Type material examined. ***Holotype***: ♂, “Turchia – Vil. Rize, Ovitdagi gecidi mt 2600,18-jun-1992. leg. A. Ballerio.” (NHMUK). ***Paratypes***: 4♂♂, 7♀♀, 17 unsexed, data as holotype. 1♂, 1♀, 1 with mouthparts dissected (NHMUK), 1♂, 2♀♀, 14 unsexed (AB). 5♀♀, data as holotype (JFMC).

Other material examined. Four specimens, unsexed, Ulu Dag b. Bursa As. M. occ. V:1968 Schweiger, MNHG, may belong to this species. A male from central Armenia, Selim Pass 2350 m, coll. Ziani is shown by its parameres to belong to the *A. niger* species complex, and it agrees with *A. alberti* in its black to blackish-brown appendages and its small size, length 3.9 mm. The epipharynx of this specimen has the apophobae less regular but the darkened area is narrowed in its basal 1/4.

Differential diagnosis. *Aphodius alberti* sp. nov. is the second *A. niger* group species recognised in Turkey, and as such requires comparison with *A. isikdagensis*. The most striking distinctions are the size ranges: in *A. alberti* sp. nov. 4.1–4.9 mm, in *A. isikdagensis* 4.5–5.8 mm and the colour of the appendages: in *L. alberti* sp. nov. the legs are blackish brown to very dark brown (Fig. 3e–g), in *A. isikdagensis* mid brown (Fig. 3c, d). The maxillary palpi are metallic black to very dark blackish brown in *A. alberti* sp. nov. as against mid brown in *A. isikdagensis* (metallic black in the Artvin specimen). In *A. isikdagensis* there is a sexual dimorphism in the head: the males with the central area of the clypeus clearly more strongly bulging upwards than in females, and the outer margin of the genae almost continuous with the clypeal margin in the male, but distinctly angled outwards in the female. In *A. alberti* sp. nov. the central area of the clypeus of both sexes bulges upwards strongly, and the outer margin of the genae is almost continuous with that of the clypeus. The epipharynxes of the two species show some clear differences: in *A. isikdagensis* the median darkened area is broadly triangular, widest at its base, there are six or seven chaetopedia each side, and the rows of apophobae are arranged in narrow bands, ca two bristles wide, while in *A. alberti* sp. nov. the darkened area is narrowed over its basal 1/3, there are four chaetopedia each side and the rows of apophobae are as single lines (Fig. 8c, d, k, l).

Description. General appearance (Fig. 3e–g). Length 4.1–4.5 (♂), 4.1–4.9 mm (♀), width 1.9–1.95 mm (♂), 1.9–2 mm (♀). Head (Figs 3e–g, 6c, d) black, anterior clypeal margin narrowly dark brown, excised medially, angles at sides of excision bluntly rounded. Central area of clypeus bulging upwards in both sexes, punctation fine, moderately dense, with some variation in strength, this not dependant on the sex of the specimen. Frontoclypeal suture fine and straight-transverse over central 1/2, with no trace of a median tubercle, then angled forward to meet the sides just anterior to the genae. Lateral margins of genae either continuous with those of clypeus or with a very slight outward angle, without sexual dimorphism. Maxillary palpi glossy blackish brown, antennae dark brown. Epipharynx (Fig. 8k, l) with the central tylus strongly projecting anteriorly and the anterior margin of the clithra clearly excised either side. Central darkened sclerotised epitorma triangular in apical 2/3, then the sides curved inwards so that the width at the base of the darkened region is ca 3/4 of its maximum width. Acropariae virtually absent, chaetopariae well-spaced, four each side. Surface of gymnopedia covered with small tooth-like asperities. Prophobae fairly strong, clustered at the edges of the median sclerotised mesoepitorma, apophobae fine, arranged in a single line outside the chaetopariae.

Pronotum hemicylindrical, highly arched transversely, scarcely at all longitudinally. Entire lateral margins visible from above. Surface with double punctation, some specimens (male and female) have the punctation heavier with the larger punctures separated by at least twice their diameter, sparser on disc (Figs 3e, g, 6d), in others the punctation is sparser and finer (Figs 3f, 5c, d). Posterior margin completely but narrowly bordered (Figs 3e–g, 6c, d), the border not widened medially, continuous round the posterior corners. Scutellum pentagonal, elongate, glossy, sometimes with a few punctures medio-basally.

Elytra black, interstices flat, 6–8× width of the striae, with fine isodiametric reticulation and sparse fine punctures. Metaventrite (Fig. 21n, o) rather finely punctured in both sexes, flattened over median diamond-shaped plate, sometimes with an impressed median line. Legs dark blackish brown (Fig. 3e–g), basal segment of mesotarsi elongate, slightly longer than the longer tibial spur (Fig. 18t). The legs and metaventrite Fig. 20o appear unnaturally pale brown due to the intense lighting.

Aedeagus (Fig. 24e–j) Aedeagus length ca 1.1 mm, parameres length ca 0.44 mm, basal piece length ca 0.59 mm. Length of tooth-field ca 0.58 mm, length of longest teeth ca 54μm. Parameres in lateral view weakly to moderately downturned apically (Fig. 24h–j). In dorsoventral view sensory area either not visible (Fig. 24g, the holotype), or visible after squashing as a curved band round the paramere apex (Fig. 24e, f, a paratype). The parameres struts are clearly less darkened in the paratype, suggesting that the aedeagus is less fully hardened, which would render it more prone to squashing.

Remarks. Apparently widespread on high ground in Anatolia and possibly extending into Armenia (Fig. 29a). According to A. Ballerio (pers. comm., 16.vi.2023) the *Liothorax* were found on snow patches and in puddles at the sides of the road passing through Ovit pass, a typical alpine prairie (Fig. 28e). They were mixed with fewer *Aphodius* (*Neagolius*) *ovitensis* Pittino & Ballerio, 1994.

Aphodius (*Liothorax*) *wilsonae* Maté & Angus, 2005, stat. rest.

Figs 4g, 5k, 6k, l, 9h, i, 16c,d, 17w, 18o, 21u–w, 23g–i, 24o, 26d’, e’, 33m-p, 34k, l

Aphodius (*Liothorax*) *wilsonae* Maté & Angus, 2005: 329.

Type material examined. ***Holotype*** ♂, SP Provincia de Burgos, Balneario de Corconte, 40.031°N, 3.884°W, 26.iv.2001. leg. R.B. Angus (NHMUK). ***Paratypes***: SP: Provincia de Madrid, Manzanares el Real, Embalse de Santillana, 40.720°N, 3.857°W, 1.iv.2003, sieving detritus from edge of water, leg. R.B. Angus & G.I. Aradottir, 1♂, 1♀, 1 unsexed (NHMUK).

Other material examined. SP Provincia de Cantabria, Areños, 43.112°N, 4.724°W, 5.vi.2012.By digging mud under dried-out pool. 1♂. Leg. R.B & E.M. Angus; Provincia de Burgos, S of Balneario de Corconte, strandline detritus. 1.iv.2014. leg. R.B. Angus. 1♂ (NHMUK); Provincia de Álava, Vittoria au Mt Gorbea, 34.634°N, 2.782°W, Juin 1879. 1♀ (MNHG); Provincia de Madrid, Puerto de la Morcuera, 40.828°N, 3.399°W. 15.1v.1997. 2, unsexed (NMP).

P: Monchique, Algarve, 37.317°N, 8.557°W. 6–13.v.1910, leg. K. Jordan. 3♂♂, 1♀ (NHMUK); Serra de Estrela, 40.326°N, 7.708°W. leg. H. Fery. 2♂♂, 1 unsexed (ZSM).

Differential diagnosis. Endophallic teeth conspicuously shorter than in all other species, ca as high as long. Length of longest teeth ca 35 µm (Fig. 23g–i, 24o), as against at least 40 µm in other species.

Redescription. General appearance (Fig. 4g). Length 3.3–4.8 mm (♂), 3.8–5 mm (♀), width 1.6–2.1 mm (♂), 1.7–2.2 mm (♀). Black without obvious paler edges to head, antennae, palpi, and legs black to very dark brown. Head with the frontoclypeal suture very fine, often more or less effaced, laterally almost always so, and without tubercles. Clypeus bulging upwards medially, with double punctation, this finer on disc. Epipharynx (Fig. 9h, i) with anterior margin of clithra strongly emarginate either side of the projecting median tylus, with a few very fine acropariae. Chaetopedia well-developed, stout, 6–8 each side. Chaetopariae shorter and thinner than chaetopedia, forming a closely-set line each side. Apophobae forming a line of very fine hairs outside the chaetopariae, prophobae lying in small inconspicuous groups near the sides of the mesoepitorma.

Head and pronotum (Fig. 6k, l): pronotum highly arched transversely and generally distinctly arched longitudinally, giving a somewhat domed appearance, the hemicylindrical appearance less usual than in other *Liothorax* species. Surface of pronotum bulging outwards laterally so that the lateral margins are sometimes not visible from above in their basal 1/3s. Surface with double punctation, the strength of this variable, from rather fine (Fig. 5k) to distinctly coarser.

Scutellum elongate, pentagonal, glossy with a few punctures medially.

Elytra black, interstices with very fine reticulation (Fig. 17w) and widely separated fine punctures, ca 8× the width of the striae. Striae glossy, vertical-sided, with punctures separated by ca 2× their diameter and encroaching on the vertical sides of the striae (Fig. 16w). Metaventrite (Fig. 21u–w) with central diamond-shaped area bearing sparse fine or moderate punctures and often small patches of reticulation. No obvious sexual dimorphism. Legs dark brown, longer spur of mesotibiae clearly slightly longer than basal segment of mesotarsus (Fig. 18o).

Aedeagus (Figs 23g–i, 24o). Length ca 1.1 mm, paramere length ca 0.43 mm, basal piece length ca 0.69 mm, length of endophallic tooth-field ca 0.37 mm, length of longest teeth ca 35 µm.

Remarks. *Aphodius wilsonae* stat. rest. is widely distributed mainly on higher ground in the northern half of Spain and Portugal, but with some material from the Algarve (this location needs to be verified by future sampling; Fig. 29a). It is generally taken in the spring and early summer, either in detritus at the edges of water bodies (Fig. 27f), or at the roots of vegetation where pools have dried out. It is sometimes very abundant.

Chromosomes

Details of the material from which successful preparations have been obtained are given in Table 1, Relative Chromosome Length in Table 4, and a summary of the major features of the karyotypes in Table 5.

***Aphodius plagiatus*.** Published information: Maté and Angus (2005). 2n = 18 + Xy. Mitotic chromosomes, arranged as karyotypes, are shown in Fig. 30a, b, male from England (Studland), Giemsa-stained and C-banded *L. p. plagiatus*, and Fig. 30c, *L. p. sinoplagiatus* ssp. nov., male from Tibet (Qinghai, Gangca), Giemsa-stained. Heterochromatin is confined to pericentromeric C-bands. There is a distinct step-decrease in size between autosomes 1 and 2. Autosome pairs 5 and 9 are more of less acrocentric, while the others are more or less metacentric, but pairs 4, 7, and 8 have the short arm prone to being less condensed, suggesting a secondary constriction. The X chromosome is a small subacrocentric and the y a very small (dot-like) submetacentric. Qinghai material matches that from Studland and Hunstanton, but C-banding failed (the only nucleus obtained apparently disappeared as a result of the treatment). None of the chromosomes has a heterochromatic long arm.

Aphodius rutilipennis. Published information: none. 2n = 18 + Xy. Mitotic chromosomes, arranged as a karyotype, are shown Fig. 30d, e, Giemsa-stained and C-banded. Autosomes 1, 3, 5, 7, 8, and the X chromosome have heterochromatic long arms. The y chromosome is a dot-like metacentric.

Aphodius kraatzi. Published information: none. 2n = 20 including the sex chromosomes, + B-chromosomes. Karyotypes have been obtained from only 1 ♀, which means the X chromosome cannot be identified. Fig. 30f, g shows the chromosomes from one nucleus, Giemsa-stained and C-banded, while Fig. 30h, i shows a second nucleus, this time with one B-chromosome. Chromosomes 1–3, 5, and 6 have the shorter arms heterochromatic, chromosome 4 is subacrocentric with a heavy pericentromeric C-band, and chromosomes 8–10 are distinctly shorter than the others, subacrocentric and with only small pericentromeric C-bands. The B-chromosome is entirely heterochromatic.

***Aphodius niger*.** Published information: Maté and Angus (2005). 2n = 18 + XY_p (♂), XX (♀) + B-chromosomes. *Aphodius niger* differs from all other Aphodiinae whose chromosomes are known in the large, mainly euchromatic (and therefore gene-carrying) Y chromosome. First metaphase of meiosis (Fig. 34a–d) shows that the Y chromosome is strongly condensed and forms a typical "parachute" association with the X chromosome. C-banding (Fig. 34b, d) shows that the C-banding region of the Y chromosome is smaller than the condensed chromosome visible in unbanded preparations (Fig. 34a, c). Mitotic chromosomes, arranged as karyotypes, are shown in Fig. 31a–f, and RCLs are given in Table 2. *Aphodius niger* is one of four known species in which only one pair of autosomes, in addition to the X chromosome, has a consistently heterochromatic long arm, although the long arm of autosome 3 may be extensively heterochromatic as well (Fig. 30b). The remaining chromosomes have fairly heavy centromeric C-bands. The other species in this group are *A. muscorum* Adam, *A. felix* sp. nov., and *A. bellumgerens* sp. nov. *Aphodius niger* has autosome pair 2 metacentric, pairs 1 and 3–6 submetacentric and pairs 7–9 subacrocentric. The X chromosome is submetacentric and the Y is metacentric. The B-chromosomes are metacentric and heterochromatic (Fig. 31b, e).

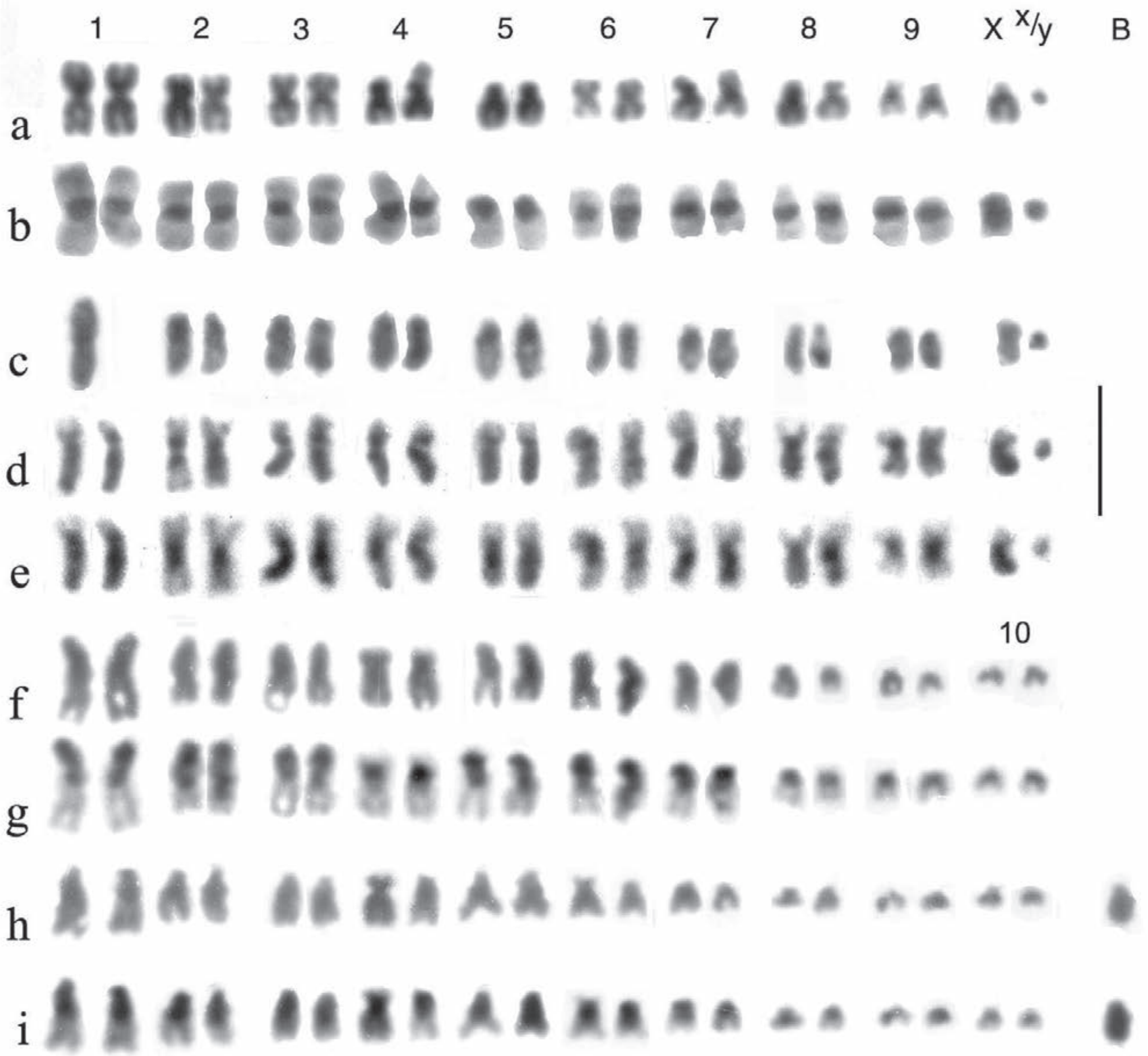

Figure 30. Mitotic chromosomes, arranged as karyotypes **a**, **b** *A. plagiatus plagiatus*, ♂, GB, Dorset, Studland **a** plain (Giemsa stained) **b** the same nucleus C-banded **c** *A. plagiatus sinoplagiatus*, ♂, CH, Qinghai, Gangca, plain **d**, **e** *A. rutilipennis*, ♂, CY, Zakaki Marshes **d** plain **e** C-banded **f**–**h** *A. kraatzi* ♀, SK **f**, **g** nucleus without B-chromosomes **f** plain **g** C-banded **h**, **i** nucleus with 1 B-chromosome **h** plain **i** C-banded. Scale bar: 5 µm.

***Aphodius muscorum*.** Published information: none. 2n = 18 + Xy_p (♂), XX (♀). Mitotic chromosomes, arranged as karyotypes, are shown in Fig. 31f–l, and RCLs are given in Table 2. The y chromosome is a small submetacentric, smaller than autosome pair 9 and largely heterochromatic (Fig. 31g). Metaphase I of meiosis shows the Xy_p bivalent with the y far smaller than in *A. niger*, and in one case only revealed after C-banding (Fig. 34e–g). The X chromosome and one pair of autosomes have a heterochromatic long segment, but in this case the autosome, although placed as pair 1, is slightly shorter than pair 2. This arrangement is because pair 2, metacentric and with a heavy but discrete centromeric C-band, appears to be the same as in *A. niger*. Autosome pairs 1 and 3–7 are submetacentric, with pair 8 being borderline submetacentric-subacrocentric, and only pair 9 clearly subacrocentric. The RCL table shows pair 1

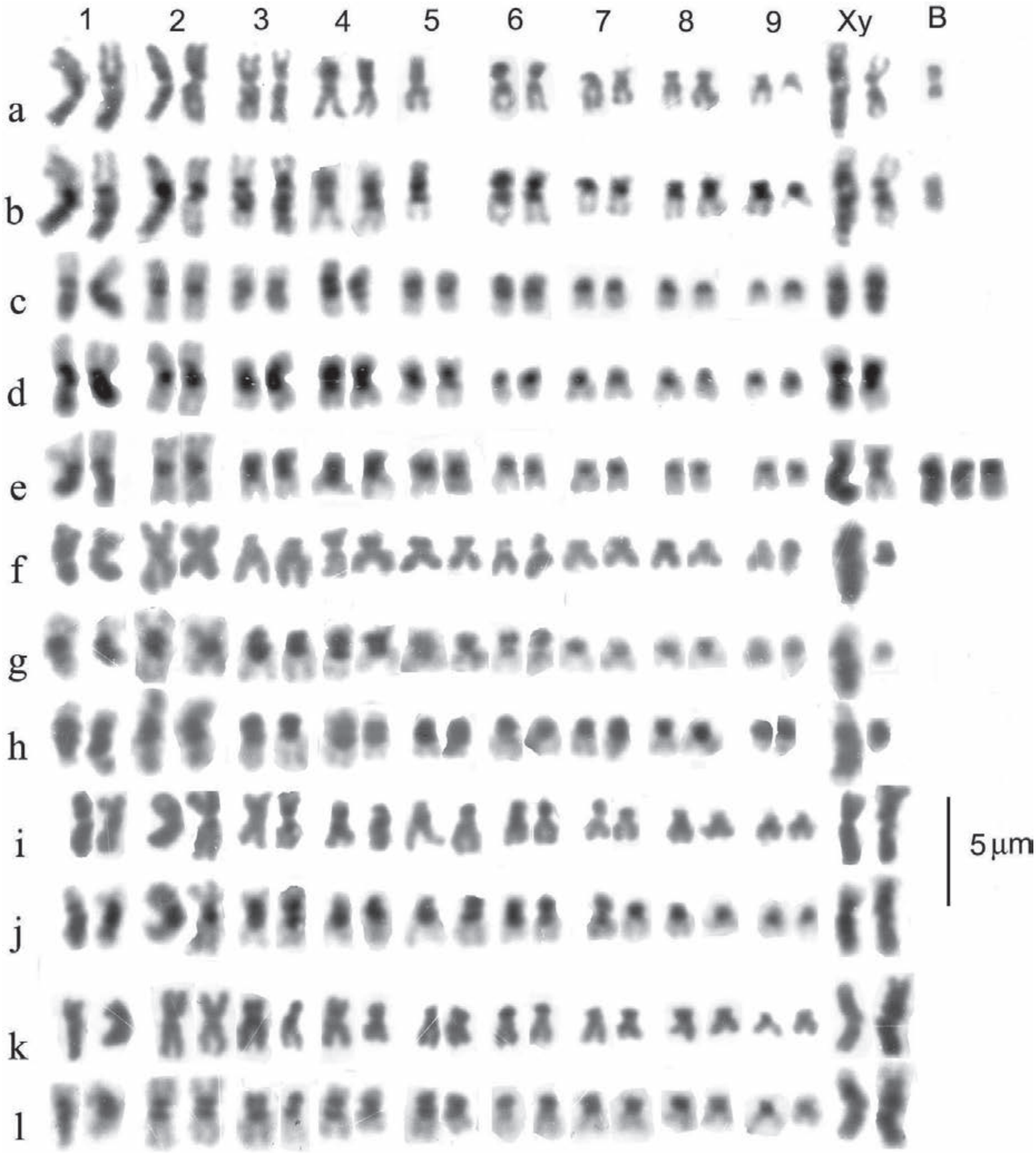

Figure 31. Mitotic chromosomes, arranged as karyotypes **a**, **b** *A. niger*, ♂, SV, Tullgarn **a** plain **b** the same nucleus C-banded (1 replicate of autosome 5 missing) **c** *A. niger* ♀, SV, Tullgarn, C-banded **d**, **e** *A. niger*, ♂♂, GB, Hampshire, New Forest, C-banded **e** with 3 B-chromosomes **f**, **g** *A. muscorum*, ♂, HU, Hortobágyi **f** plain **g** the same nucleus C-banded **h** *A. muscorum*, ♂, HU, Hortobágyi, C-banded **i**, **j** *A. muscorum*, ♀, HU, Kisújszállás **i** plain **j** C-banded **k**, **l** *A. muscorum*, ♀, HU, Kisújszállás **k** plain **l** the same nucleus C-banded. Scale bar: 5 µm

to be significantly shorter than in *A. niger* and pair 7 to be significantly longer. The RCL values are clearly the same in the sample from the Hortobágyi and the two females from Kisújszállás, though here the sample size is too small for the larger autosome 7 to appear significantly different from that of *A. niger*. The extent of the heterochromatin on the long arm of autosome 1 shows some variation (Fig. 31) but the heterochromatic region is not sufficient to account for the smaller size of this autosome than that of *A. niger*.

Figure 32. Mitotic chromosomes arranged as karyotypes **a–e** *A. felix* sp. nov. IT, Abruzzo. Campo Felice **a**, **b** holotype ♂ **a** plain **b** the same nucleus C-banded **c** holotype ♂ C-banded, autosome 8 polymorphic, 9 subacrocentric **d** paratype ♂, C-banded, autosomes 8 and 9 metacentric **e** paratype ♀ **f–i** *A. bellumgerens* sp. nov., paratypes, IT, Sicily **f**, **g** *A. bellumgerens* sp. nov., ♂, paratype **f** plain **g** C-banded **h**, **i** *A. bellumgerens* sp. nov., ♀, paratype **h** plain **i** C-banded. Scale bar: 5 µm

***Aphodius felix* sp. nov.** Published information: none. 2n = 18 + Xy (♂), XX (♀). Mitotic chromosomes, arranged as karyotypes, are shown in Fig. 32a–e, and RCLs are given in Table 2. No preparation of meiosis is available. Autosome 1 and the X chromosome have the long arm heterochromatic and the long arms of autosome pairs 4, 5, 6, and 8 may also be heterochromatic, with the heterochromatin staining less densely than that of the centromeres. Autosome 8 is polymorphic for a pericentric inversion and may be either metacentric or subacrocentric. Autosome pairs 2 and 3 are metacentric, 4 – 7 and the X chromosome are submetacentric, and pair 9 is subacrocentric. The y chromosome is a very small, almost dot-like, metacentric. Autosomes 1 and 2 are ca the same size and pairs 3–9 show a progressive decrease. The X chromosome is ca the same size as pair 6.

Figure 33. Mitotic chromosomes arranged as karyotypes **a–d** *A. bameuli* sp. nov., ♂ paratypes, FR, Corsica, by the Lac de Melo. Autosome 9 polymorphic in **a**, **b** homozygous submetacentric in **c**, **d**. **a**, **c** plain **b** and **d** the same nuclei C-banded **e–l** *A. krelli* sp. nov., types, IT, Sardinia **e**, **f** paratype ♂ with the heterochromatic long arm of autosome **1** weakly developed **e** plain **f** the same nucleus C-banded **g**, **h** holotype with the heterochromatic long arm of autosome **1** fully developed **g** plain **h** the same nucleus C-banded **i**, **j** paratype ♂ with both replicates of autosome 7 lacking the heterochromatic long arm **i** plain **j** the same nucleus C-banded **k**, **l** paratype ♀ with autosome 9 heterozygous for an inversion polymorphism **k** plain **l** the same nucleus C-banded **m–p** *A. wilsonae* SP **m**, **n** holotype ♂ **m** plain **n** the same nucleus C-banded **o**, **p** paratype ♀ from Balneario de Corconte **o** plain **p** the same nucleus C-banded. Scale bar: 5 µm.

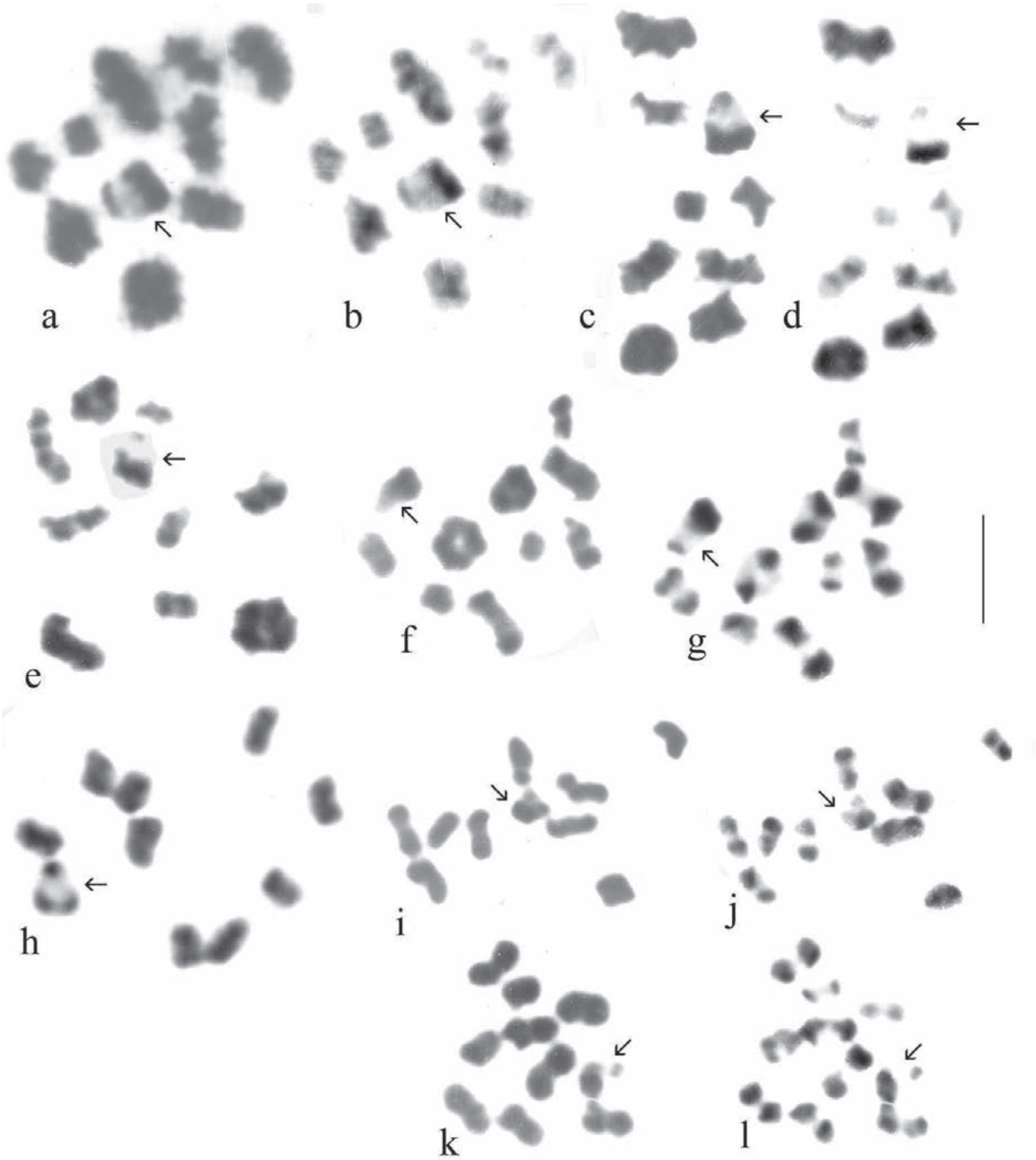

Figure 34. Meiotic chromosomes, metaphase I from testis **a–d** *A. niger*, GB, Hampshire, New Forest, White Moor **a**, **c** plain **b**, **d** the same nuclei C-banded **e–g** *A. muscorum*, HU, Hortobágyi **e** plain **f**, **g** the same nucleus **f** plain **g** C-banded **h** *A. bameuli* paratype, FR, Corsica, by Lac de Melo, plain **i**, **j** *A. krelli* IT, Sardinia, paratype **i** plain **j** the same nucleus C-banded **k**, **l** *A. wilsonae*, SP, Areños **k** plain **l** the same nucleus C-banded. The sex bivalent is indicated by an arrow. Scale bar: 5 µm.

***Aphodius bellumgerens* sp. nov.** Published information: none. 2n = 18 + Xy (♂), XX (♀). Mitotic chromosomes, arranged as karyotypes, are shown in Fig. 32f–i, and RCLs are given in Table 2. No preparation of meiosis is available. Autosome 1 and the X chromosome have their long arms clearly heterochromatic, and the X chromosome is the longest in the nucleus. Autosomes 1–5, 7, and 8 are submetacentric, and 5 and 9 are subacrocentric. The y chromosome is a small submetacentric, but not dot-like and in fact only slightly shorter than pair 9. It is largely heterochromatic (Fig. 32g).

Aphodius bameuli **sp. nov.** Published information: none. 2n = 18 + Xy_p (♂), XX (♀). Mitotic chromosomes, arranged as karyotypes, are shown in Fig. 33a–d, metaphase I of meiosis is shown in Fig. 34h and RCLs are given in Table 2. Autosome pairs 1, 2, 6–8, and the X chromosome are submetacentric, with heterochromatic long arms. Autosome 2 is metacentric, with a heavy centromeric C-band, autosome 8 is submetacentric with the centromeric C-band sometimes extending on to the basal part of the long arm, and autosome 9 has a heavy centromeric C-band and is polymorphic for a pericentric inversion and may be either metacentric or subacrocentric. The X chromosome is the longest in the nucleus and the y chromosome is a small subacrocentric, ca 1/3 of the length of autosome 9.

Aphodius krelli **sp. nov.** Published information: none. 2n = 18 + Xy_p (♂), XX (♀). Mitotic chromosomes, arranged as karyotypes, are shown in Fig. 33e–l, metaphase I of meiosis is shown in Fig. 34i (Giemsa-stained), j (the same nucleus, C-banded), and RCLs are given in Table 2. The RCLs of the chromosomes, as well as their configurations and distribution of heterochromatin show almost no differences from the karyotype of *L. bameuli*, including the inversion polymorphism of autosome pair 9. Autosome pair 7 has the long arm heterochromatic and is polymorphic for a deletion of its heterochromatic long (Fig. 33k, l). This polymorphism has not been detected in *A. bameuli* and the arm concerned has not been found to be heterochromatic.

***Aphodius wilsonae*.** Published information: Maté and Angus (2005). 2n = 18 + XY_p (♂), XX (♀) + B-chromosomes. Mitotic chromosomes, arranged as karyotypes, are shown in Fig. 33m–p, metaphase I of meiosis is shown in Fig. 34k (plain), l (the same nucleus, C-banded), and RCLs are given in Table 2. Autosome pair 2 is metacentric with a heavy centromeric C-band autosome 9 is submetacentric with a heavy centromeric C-band. The remaining autosomes, and the X chromosome, are submetacentric, sometimes almost subacrocentric, with heterochromatic long arms. The X chromosome is of the same size range as pairs 2–5, clearly smaller than those of *A. bameuli* sp. nov. and *A. krelli* sp. nov. (Table 2). The y chromosome is a very small metacentric, less than 1/2 the length of autosome 9. The B-chromosome, figured by Maté and Angus (2005), is a small submetacentric, similar in size to autosome 9. It has not been C-banded.

Molecular analysis

Thirty-eight specimens were sequenced (Table 4): ten ingroup species (34 specimens in total) and three outgroup species (four specimens) representing three of the assumed most closely related subgenera (*Labarrus* Mulsant & Rey, 1870, *Subrinus* Harold, 1870 and *Nialus*, sensu Rakovič, 1981). Of the 34 ingroup specimens 29 were sequenced successfully for both genes, whilst five *Liothorax* specimens (*A. bameuli* sp. nov. (573), *A. kraatzi* (272 and 273), *A. muscorum* (417), and *A. plagiatus* (1)) failed to produce usable cytochrome-b (cyt-b) sequences despite repeated attempts. Once aligned the sequence ends were trimmed to eliminate primer binding sites and reduce missing data, resulting in a combined dataset 1210 base pairs (bp) long (430 bp for cytochrome b and 780 bp for cytochrome oxidase I), of which 380 bp were variable and 277 bp parsimony informative. The parsimony search found 28 equal length most parsimonious trees (length = 220). The consensus tree (Fig. 35, majority consensus 80%) was well resolved with high consistency (CI, 0.623 [0.568]) and retention indices (RI, 0.842 [0.842]; reported numbers are for all sites first and parsimony-informative sites only second). Node support for most of the species' groups was strong on all three measures (support is reported for the main nodes only, with decay indices above and bootstraps and jackknife values below, in that order). Within the *niger* clade (*niger* crown+*bameuli-bellumgerens*+ *wilsonae*), the data strongly supported all the species outside the *niger*-crown clade (*A. niger*, *A. felix* sp. nov., *A. muscorum*, and *A. krelli* sp. nov.) which was largely unresolved, due to the placement of some specimens of *A. muscorum*, although there was support for the split between *A. felix* sp. nov. and the other three taxa. Support for the *niger*-crown group was high. The maximum likelihood tree search (log-likelihood -1497.25, tree not shown) resulted in a similar topology albeit with some minor differences in the *niger*-crown clade. The *niger* clade was highly supported and all three groups within it showed deep and well supported splits. The *plagiatus* group (*A. kraatzi*, *A. plagiatus* and *A. rutilipennis*) was paraphyletic, with *A. plagiatus*+*A. rutilipennis* forming a clade basal to all the other *Liothorax* species. Within it, *A. plagiatus* and *A. rutilipennis* were deeply split, as were the Asian (Qinghai, specimen 131, subspecies *A. p. sinoplagiatus*) and European *A. plagiatus* species (1 and 37). Similarly *A. kraatzi* had a deep split between the Western European (236 and 270) and Eastern Russian (272 and 273) *A. kraatzi*.

Molecular divergences. The interspecific p-distances are shown in Table 7 and range from > 17% (K2P) between subgenera to 0% within species. These distances are comparable to other studies and congruent with the often-quoted interspecific gap of 2–4%. These distances were further analysed by comparing the distributions of the intraspecific (IS), interspecific (ES) and within *niger*-crown group (NG) distances, as shown in Fig. 36. The distance distributions for all three groups showed little overlap, with the intraspecific and interspecific distance distributions being highly significantly different (Wilcoxon's rank test [< 2e-16], Kruskal-Wallis [< 0.000001]), whereas the NG and IS distance distributions overlapped slightly more (Wilcoxon [0.0073], Kruskal-Wallis [n.s.]). Much of the overlap within the IS-ES and NG-IS was due to two species: *A. plagiatus*, where there

Table 7. Intergroup (below diagonal), (diagonal, grey) p-distances and Kimura two-parameter (above diagonal) intra group distances for combined molecular dataset.

	OUTGROUP	***A. (L.) bameuli***	***A. (L.) bellumgerens***	***A. (L.) felix***	***A. (L.) krelli***	***A. (L.) kraatzi***	***A. (L.) muscorum***	***A. (L.) niger***	***A. (L.) plagiatus***	***A. (L.) rutilipennis***	***A. (L.) wilsonae***
OUTGROUP	0.1353	0.1592	0.1647	0.1733	0.1697	0.1604	0.1707	0.1730	0.1571	0.1508	0.1608
A. (L.) bameuli	0.1279	0.0038	0.0287	0.0509	0.0466	0.1026	0.0471	0.0525	0.1064	0.0908	0.0453
A. (L.) bellumgerens	0.1315	0.0273	0.0051	0.0563	0.0500	0.0970	0.0508	0.0528	0.1089	0.0871	0.0413
A. (L.) felix	0.1367	0.0466	0.0513	n/c	0.0119	0.1059	0.0142	0.0147	0.1162	0.0911	0.0521
A. (L.) krelli	0.1347	0.0430	0.0460	0.0116	0.00	0.1051	0.0040	0.0077	0.1161	0.0958	0.0463
A. (L.) kraatzi	0.1293	0.0885	0.0843	0.0905	0.0901	0.0209	0.1060	0.1047	0.1163	0.1080	0.0963
A. (L.) muscorum	0.1351	0.0435	0.0467	0.0138	0.0039	0.0909	0.0057	0.0101	0.1161	0.0987	0.0478
A. (L.) niger	0.1367	0.0480	0.0484	0.0143	0.0076	0.0898	0.0099	0.0017	0.1186	0.0985	0.0491
A. (L.) plagiatus	0.1262	0.0901	0.0921	0.0966	0.0967	0.0983	0.0968	0.0984	0.0203	0.0953	0.1036
A. (L.) rutilipennis	0.1227	0.0791	0.0764	0.0793	0.0830	0.0925	0.0851	0.0850	0.0824	0.00	0.08696
A. (L.) wilsonae	0.1289	0.0419	0.0386	0.0476	0.0429	0.0837	0.0442	0.0452	0.0878	0.0762	0.0047

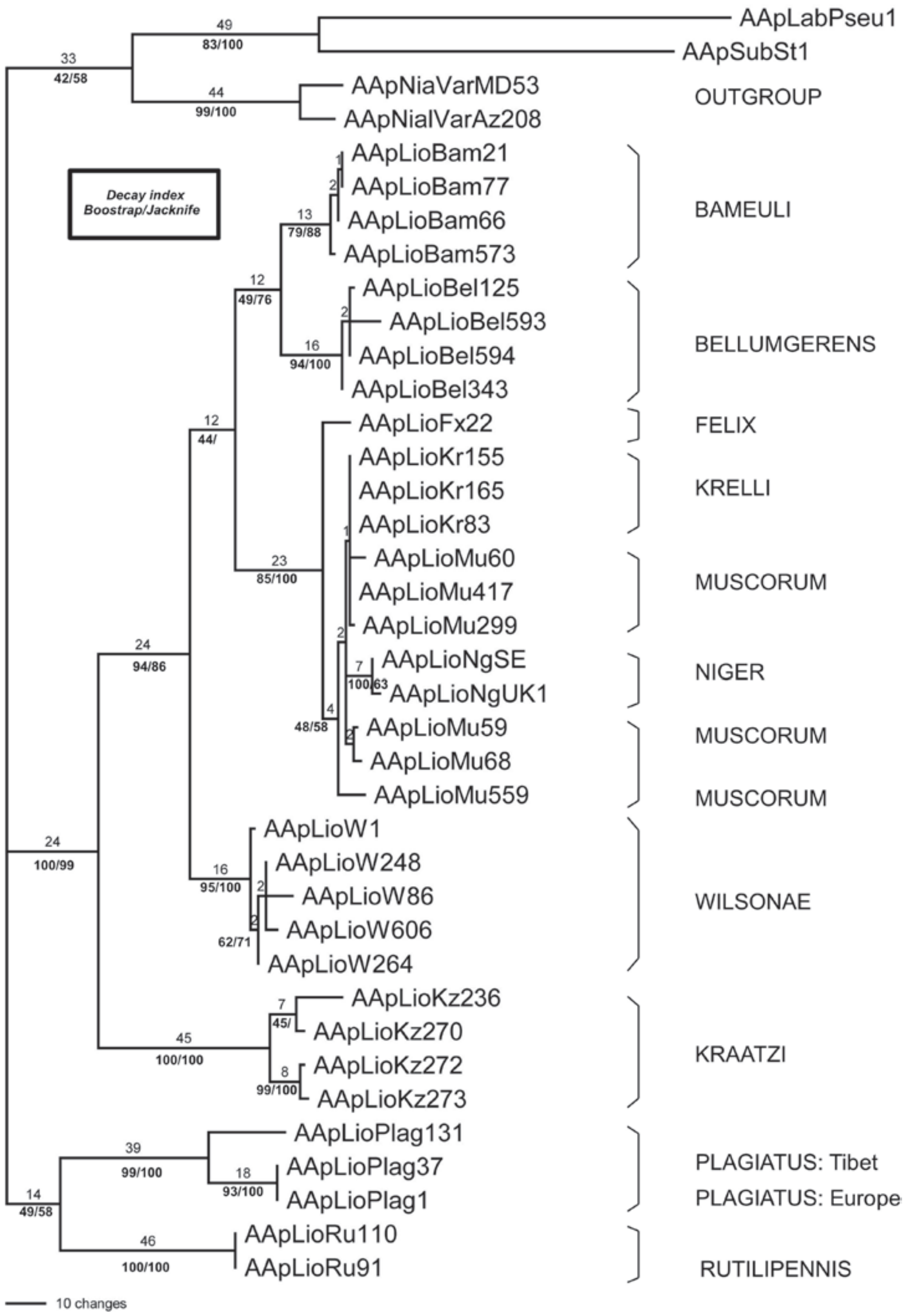

Figure 35. Molecular Majority consensus (80%) phylogeny of 28 equally most parsimonious trees derived from the exhaustive search on the combined dataset of mtDNA (cox1 and Cyt-B). Support values shown only for the supraspecific nodes decay indices above the nodes, bootstraps and jackknife values below them. Scale bar size equivalent to 10 base pair changes.

is a very deep split between the Qinghai material (subspecies *sinoplagiatus*) and the European material (p-distance 0.03203); and *A. felix* sp. nov. with the other *niger*-crown group species, from which is has a greater divergence than the average intragroup divergence (0.01364 vs 0.00525) and intermediate between the highest IS distances and lowest ES distances (East – West *A. kraatzi* [0.02696] or *A. bameuli* sp. nov. and *A. bellumgerens* sp. nov. [0.02731]).

The results are congruent with and supportive of the specific status of several undescribed species. Within the *niger* group, we find strong molecular support for the species status of *A. wilsonae* as concluded by Maté and Angus (2005).

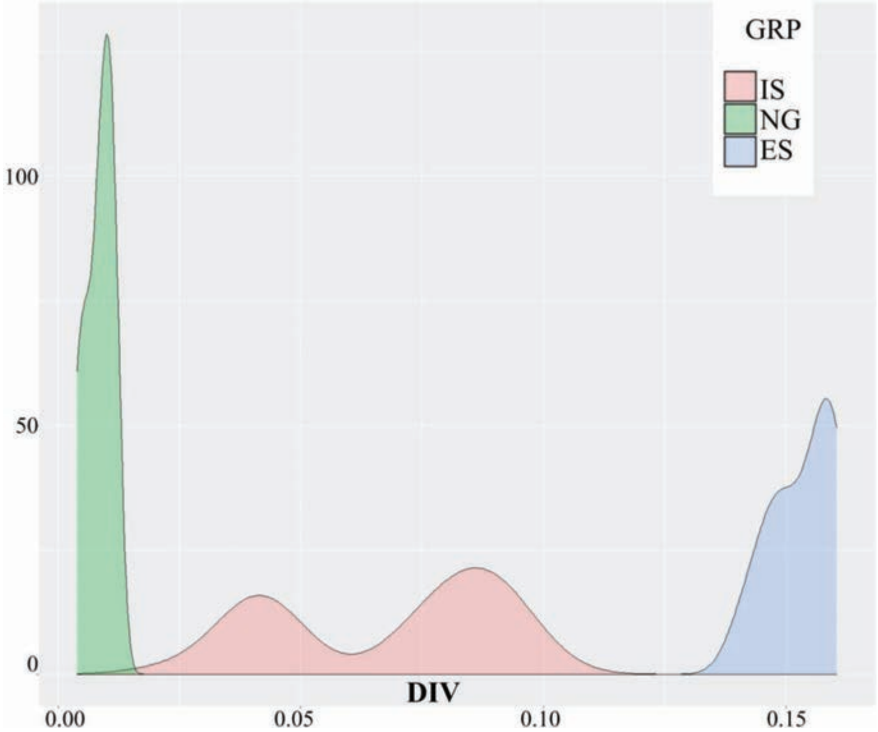

Figure 36. Intraspecific distance comparison of intraspecific (IS), interspecific (ES) and within niger-crown group (NG) distances. The distance distribution showed some overlap between the IS and NG distribution at the extreme but none with the ES distribution both the Wilcoxon's rank test (< 2e-16) and Kruskal-Wallis (< 0.000001) were highly significant for the latter.

At the time they noted that though the sampling was limited, the divergence between the three available species (*A. niger*, *A. plagiatus*, and *A. wilsonae*) was large enough to assume that all three were good species. In the present study we have a much larger the sample size in addition to a wider geographical area, which further supports the original hypotheses. Furthermore, the empirically derived divergence range (3.3–4.2%) is well above the commonly used cutoff 2–2.5% and far greater than the interspecific distances (< 1%) within *A. niger* or *A. wilsonae* (Table 5), and between *A. wilsonae* and any of the other *niger*-group species. This leads us to the conclusion that *A. wilsonae* is a *bona species* according to the molecular markers and reject Dellacasa and Dellacasa's (2005) synonymisation. Regarding the rest of the *niger*-group clade we also find strong molecular support for the specific status of *A. bameuli* sp. nov. and *A. bellumgerens* sp. nov., with distances > 4% between these taxa and others within the *niger* sensu lato group. The remaining species, conforming the *niger*-crown clade, have poor resolution and do not coalesce into monophyletic groups due to *A. muscorum* and *A. krelli* sp. nov. There are several reasons why this could be the case, such as incomplete lineage sorting or introgression, but considering the low divergences, it is likely that these lineages represent a very recent speciation event. Additional sampling and the sequencing of faster evolving nuclear genes will be necessary to elucidate their relationships.

The results for the sequenced *plagiatus* group species support their specific status but they do not form a monophyletic clade. Instead they are a paraphyletic group, with *A. rutilipennis*+*A. plagiatus* as the most basal sampled species and *A. kraatzi* as sister to the *niger* group. Furthermore, the deep divergence within *A. plagiatus* between the Chinese and European samples, is suggestive of a cryptic species complex. Though the sample size is insufficient to consider raising the Chinese populations to specific status, the molecular evidence, in conjunction with certain morphological traits such as the distinctly larger aedeagi and the spermathecae of the Chinese material, justifies recognition of a distinct subspecies inhabiting the Tibetan plateau.

Morphological analysis

Principal component analysis

The data were found to be suitable for PCA (MSA = 0.95, Bartlett's K-squared spherecity test = 174.32 ($p \leq 0.001$)) and the minimum number of factors to extract was determined to be two according, explaining over 80% of the variability.

Factor rotation under Varimax resulted in higher variance explained (cumulative loading 82%) but under Promax better separation was achieved (cumulative loading 67%). In either case factor loadings split along the same morphological features, with leg characters being positively loaded on factor 1 (PC1) and body measures (pronotal length and width, scutellar length and body height) on factor 2 (PC2). The other body measures (elytral length and width) were equally loaded on both components.

The resulting values clearly distinguished several groups. The generic groupings were highly divergent (Fig. 37) except for *A.* (*Labarrus*) which was not significantly different from *Liothorax*.

Because of this large morphological divergence between the genera, the dataset was reanalysed after excluding the outgroups *A.* (*Nialus*) and *A.* (*Subrinus*) to determine if the PCA values and loadings were overwhelmed by the subgeneric differences rather than the specific ones. The results of the analysis of the culled dataset were broadly similar to the complete dataset and cumulative variance explained remained almost unchanged (70% under Varimax and 66% under Promax, same loadings), indicating that the divergences and loadings were comparable, and henceforth all analyses were done on the full dataset.

Visual examination of the principal component bivariate plot (Fig. 38) and the boxplots (Fig. 39) demonstrated distinct groupings for several taxa. Within the *niger* group taxa (*A. niger*, *A. muscorum*, *A. krelli* sp. nov., *A. felix* sp. nov., *A. wilsonae*, *A. bameuli* sp. nov., and *A. bellumgerens* sp. nov.), the divergence of *A. wilsonae* from the other species is obvious (Fig. 36) and comparable to the position of the outgroup taxon *Labarrus*, occupying an intermediate place between the *niger*-group and *A. plagiatus*. The second major split concerned the species in the *niger*-crown group and the *bameuli-bellumgerens-alberti* group (3B group), with barely any overlap except for some *A. krelli* sp. nov. and *A. felix* sp. nov. specimens. Within this group, *L. bameuli* sp. nov. and *L. bellumgerens* sp. nov. broadly overlap, whereas *A. alberti* sp. nov. diverges from them along PC2 (shorter scutellum). Within the *niger* crown group (*A. niger*, *A. muscorum*, *A. krelli* sp. nov., and *A. felix* sp. nov.), *A. niger*, and *A. muscorum* form two groupings with partial overlap where the *A. niger* cf. specimens are placed (material from Czechia and western Russia which could not be karyotyped as *A. muscorum* or *A. niger*), whereas *A. krelli* sp. nov. and *A. felix* sp. nov. broadly overlap with each other.

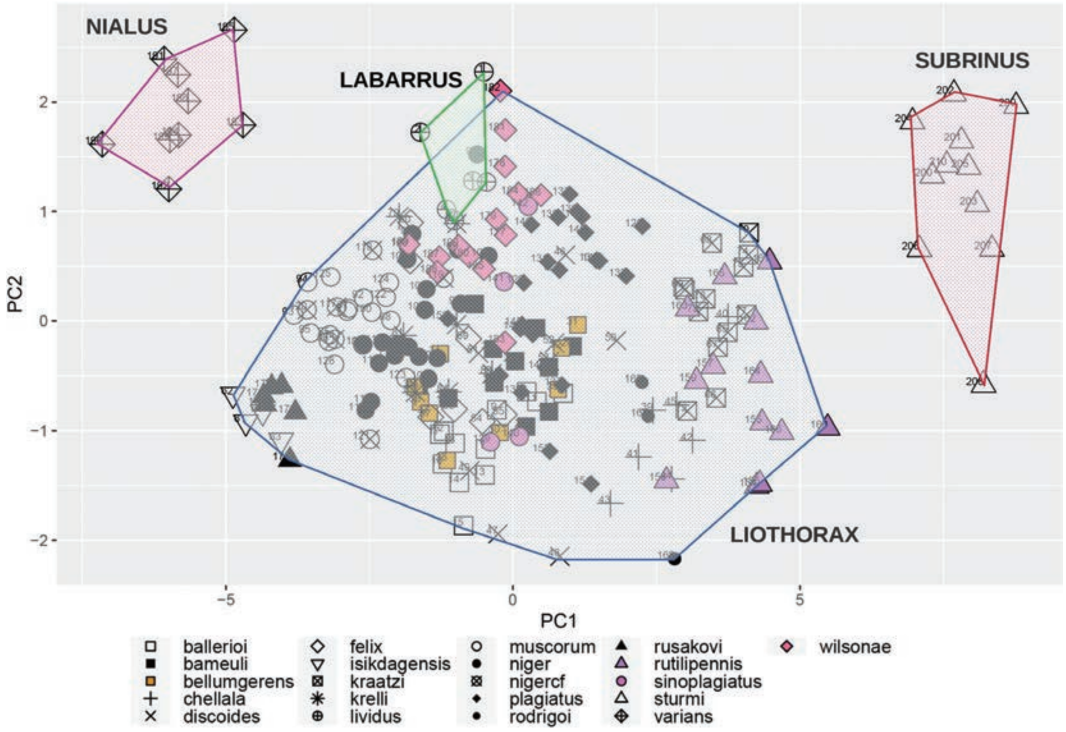

Figure 37. Bivariate plot of the principal components 1 and 2 derived from the linear morphological measurements. Subgeneric groupings indicated by the polygons enclosing the taxa, with vertices in the outermost specimens of each group.

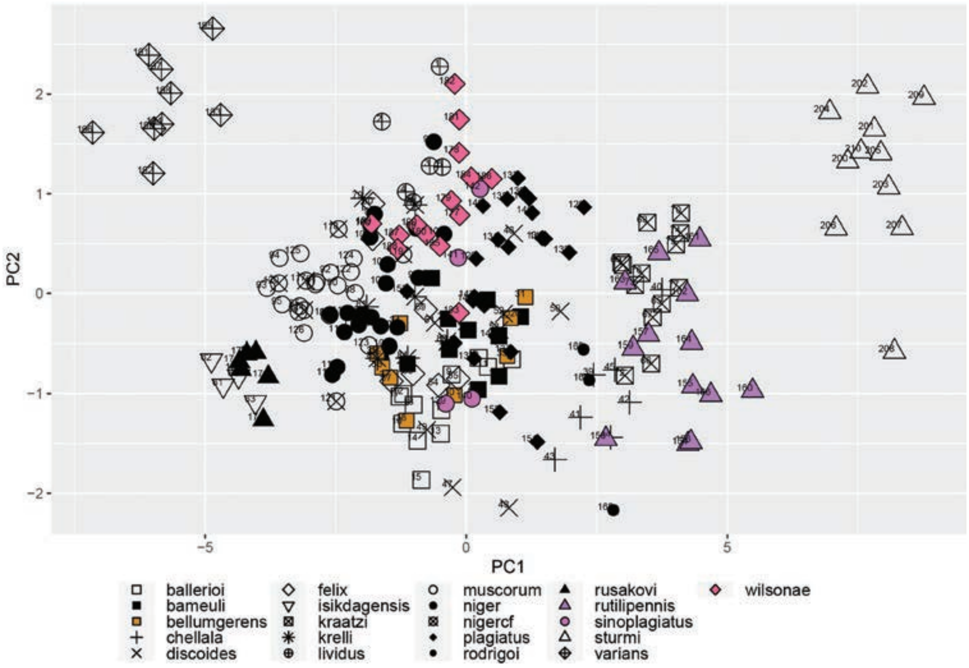

Figure 38. Bivariate plot of the principal components 1 and 2 showing the distribution of all the species in the morphospace as defined by the measurements taken in this study. For the translation of the symbols refer to the legend below the figure.

Within the *plagiatus* group, *A. plagiatus* sensu stricto was clearly separated from the rest of the species in the group, with no overlap at all with any species other than *A. discoides*. The other species of the group dispersed widely. There was a partial overlap between *A. rutilipennis*, *A. chellala* sp. nov. and *A. rodrigoi* sp. nov., but it was only due to three very divergent specimens (one from each species)

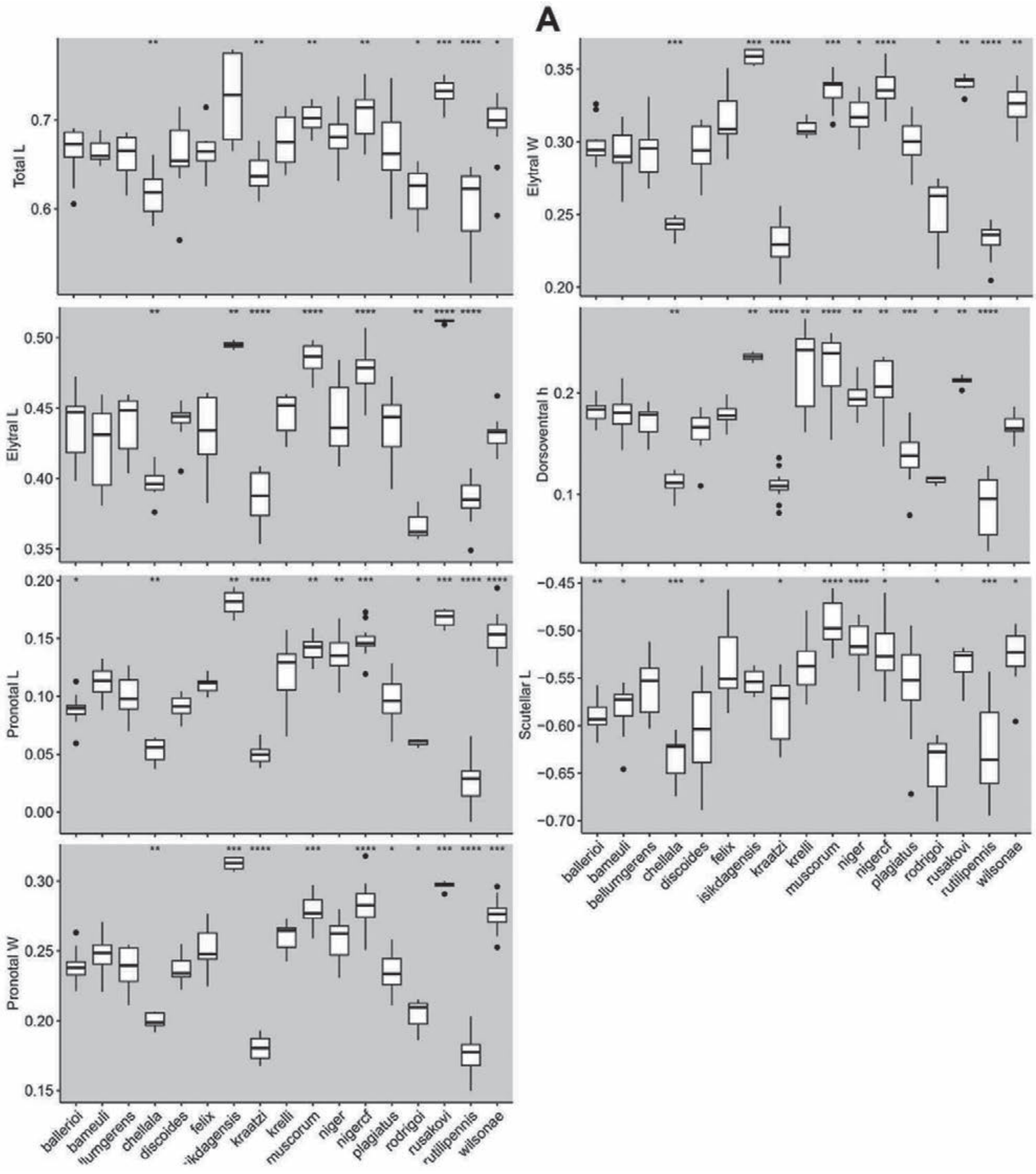

Figure 39. Boxplots of the allometrically corrected linear measurements for body measurements **A** and leg measurements **B** used in the PCA. Species names in the x axes and morphological features in the y axes.

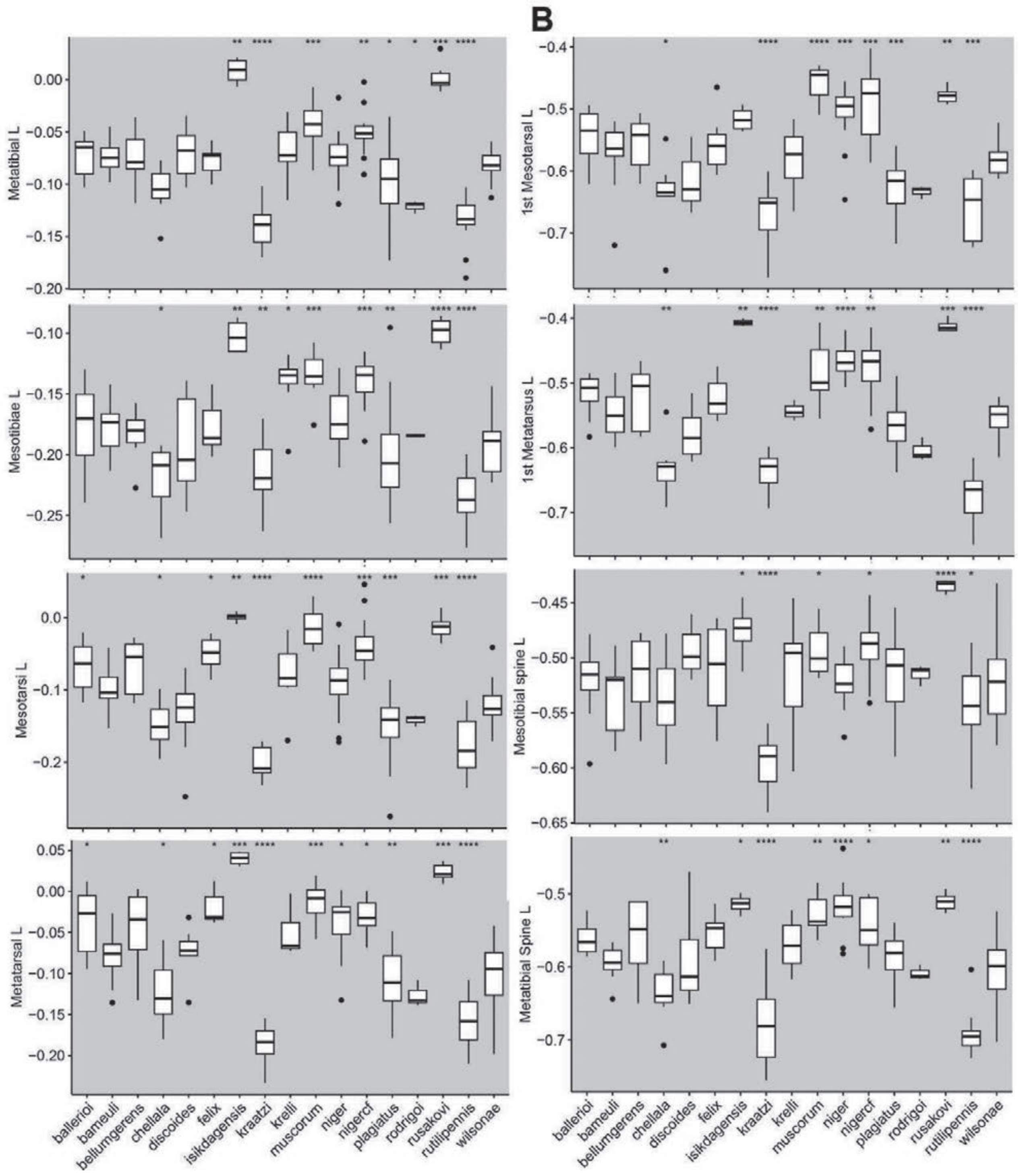

Figure 39. Continued.

which overlapped, while the majority clustered with conspecific specimens exclusively. Neither *A. discoides* nor *A. isikdagensis* overlapped at all with *A. rutilipennis* (as would have been expected according to the synonymy with *A. rutilipennis* sensu Dellacasa et al. (2007)). *Aphodius isikdagensis* formed a tight cluster next to *A. rusakovi* and well away from the other *Liothorax* but ultimately closer to the *A. niger* clade (as would be expected from the endophallus of *A. isikdagensis* but not *A. rusakovi*), whilst *discoides* was closest to the group of East Asian *A. plagiatus*. Morphologically it also showed a very spread-out distribution considering the relatively small sample size (8 specimens). Finally, *A. kraatzi* was recovered away from most of the other *plagiatus*-group species, overlapping *A. rutilipennis*.

Statistical analyses of individual characters

Morphological divergences between species pairs were highly significant on many characters, congruent with specific-level differentiation of the hypothesised species. All the characters demonstrated highly significant divergences in aggregate ($p < 0.001$, Wilcoxon's test and Tukey's test) and in most species-pair comparisons, with body proportions (width, length, and height) being the most significantly divergent, followed by the tibial and tarsal lengths. The results are summarised in a colour-coded table (Fig. 41), indicating the number of significant morphological differences in each species-pair comparison.

Within the *niger* clade, *A. wilsonae* was significantly divergent from all species in the *niger* group. *Aphodius wilsonae* differs from other *niger*-group species in having shorter meso- and metatarsi, 1st meso- and metatarsal segments, and a shorter mesotibial spine (Fig. 39B). These differences in the hind legs had previously been noted by Maté and Angus (2005). However, we can also report that *A. wilsonae* differs from the *niger* crown in being overall flatter and with shorter hind tibiae. From *plagiatus* it differed in having a significantly larger pronotum and being overall wider (Fig. 39A). The species in the *niger*-crown group (*A. niger*, *A. muscorum*, *A. krelli* sp. nov., and *A. felix* sp. nov.) were significantly to very significantly divergent in several morphological features compared to each other except for *A. krelli* sp. nov. *Aphodius felix* sp. nov. was significantly wider, with a wider and shorter pronotum (Fig. 39A), shorter legs and more flattened form than the other species, whereas *A. muscorum* had a longer and wider body (elytral length and width) and longer midlegs, particularly compared to *A. niger* sensu auctorum. *Aphodius krelli* sp. nov. occupied a middling position amongst the previous three species, differing the least from *A. felix* sp. nov. in its dorsoventral height and strongly from *A. niger* (shorter first metatarsal and first mesotarsal lengths and mesotibial length) and from *A. muscorum* (shorter first metatarsal and first mesotarsal lengths, narrower elytral width). The *niger*-crown group and the *bameuli-bellumgerens-alberti* group (3B group) differed significantly in several characters, namely the relative size of the pronotum (significantly smaller in the 3B group) and the shorter scutellum and more flattened shape (Fig. 39A) and the shorter middle legs. The closest species from the *niger* crown group to the 3B group was *A. felix* sp. nov., which was significantly wider. Within the 3B group there were no significant morphological differences. Both *A. rusakovi* and *A. isikdagensis* were significantly different from all other species morphometrically. They had significantly larger bodies (Fig. 39A) and longer legs (Fig. 39B), and were placed closest to *A. muscorum*, from which they differed in their longer hindlegs.

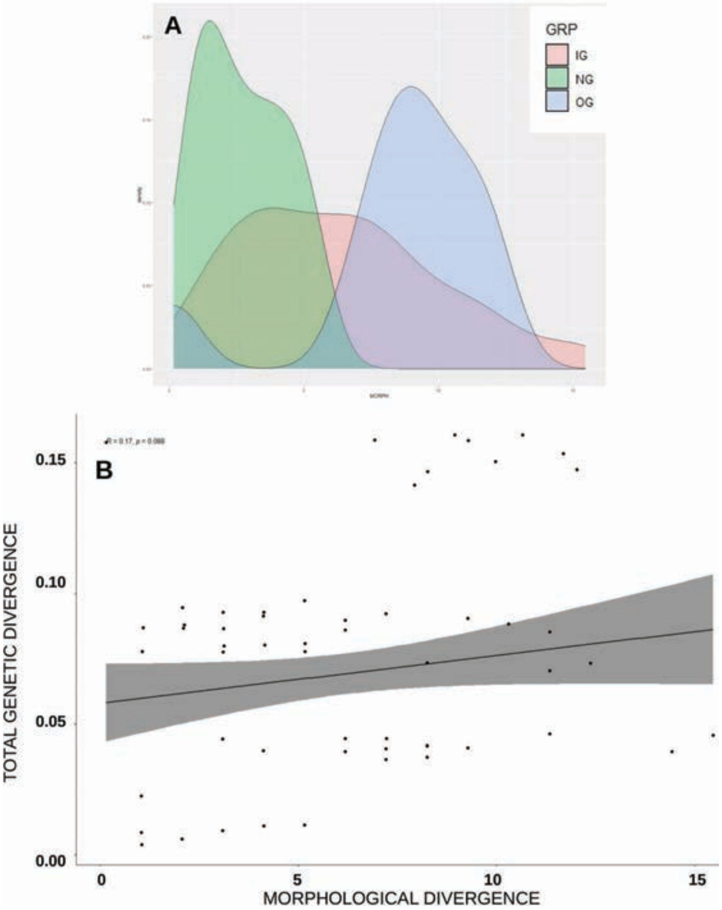

Figure 40. Comparison of the morphological distributions **A** at three phylogenetic levels: within the *niger*-crown group (NG), between species (IG) and between the genera/subgenera (OG)) **B** correlation between morphological and molecular divergence, demonstrating weak and non-significant positive correlation between both data sources.

In the *plagiatus* group, one of the major divergences was between *A. plagiatus* and most of the other species in the group (*A. rodrigoi* sp. nov., *A. chellala* sp. nov., and *A. rutilipennis*) in numerous characters. *Aphodius plagiatus* had a larger pronotum, was overall wider and more convex and had a longer scutellum (Fig. 39A). It was similar in gross morphology to *A. discoides*, from which it differed in being significantly more convex, and having a longer scutellum and shorter meso- and metatarsi. As for the other three species, *A. rodrigoi* sp. nov., *A. chellala* sp. nov., and *A. rutilipennis*, they were quite similar morphologically to each other and the differences amongst them were mostly not significant, the only exception being *A. chellala* sp. nov. which had a significantly bulkier prothorax. Finally, *A. kraatzi* had a highly divergent morphology compared to all other *Liothorax* and was closest to *A. rodrigoi* sp. nov. and *A. rutilipennis*, but still differing significantly in the relative length of the mesotibial spine and the remarkably shortened pronotal length.

Comparison of the morphological divergence at the three levels (Fig. 40A; within the *niger*-crown group, between species and between genera) shows a similar but non-significant result to the molecular divergences (Fig. 35). Hence, though the divergence values correlate with the phylogenetic distance, they overlap so broadly that they are non-significant. The lack of significance was driven mostly by the

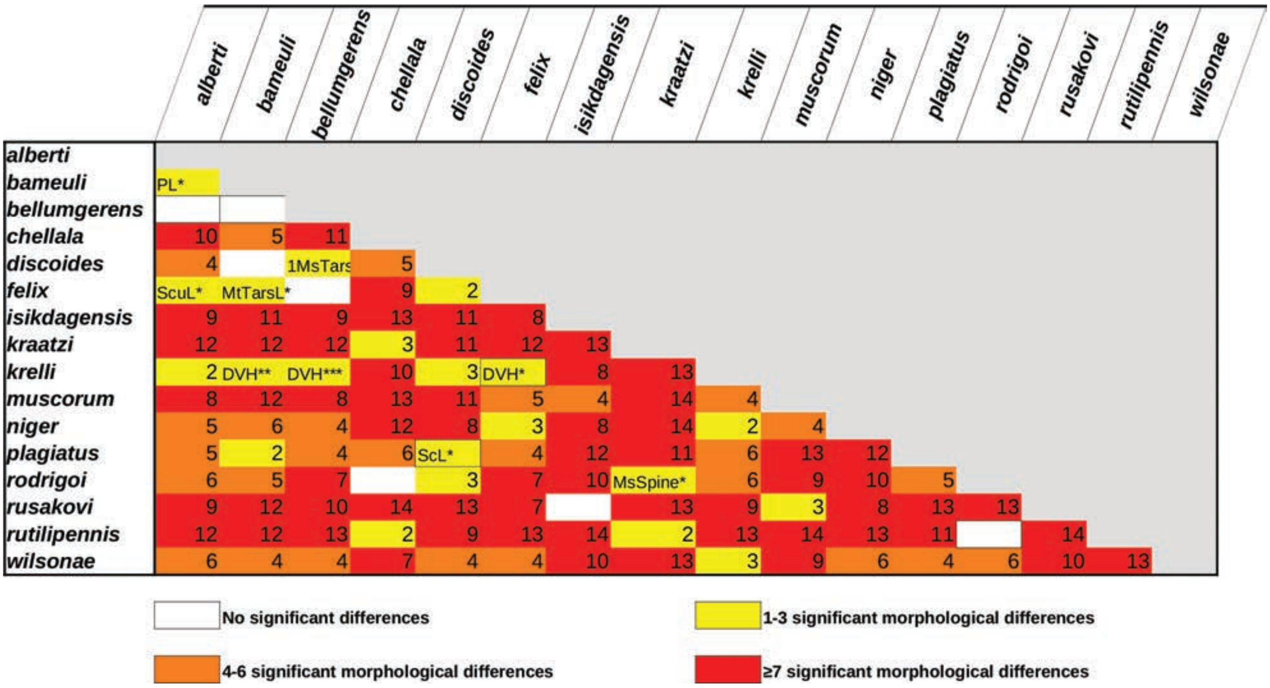

	alberti	bameuli	bellumgerens	chellala	discoides	felix	isikdagensis	kraatzi	krelli	muscorum	niger	plagiatus	rodrigoi	rusakovi	rutilipennis	wilsonae
alberti																
bameuli	PL*															
bellumgerens																
chellala	10	5	11													
discoides	4		1MsTars	5												
felix	ScuL*	MtTarsL*		9	2											
isikdagensis	9	11	9	13	11	8										
kraatzi	12	12	12	3	11	12	13									
krelli	2	DVH**	DVH***	10	3	DVH*	8	13								
muscorum	8	12	8	13	11	5	4	14	4							
niger	5	6	4	12	8	3	8	14	2	4						
plagiatus	5	2	4	6	ScL*	4	12	11	6	13	12					
rodrigoi	6	5	7		3	7	10	MsSpine*	6	9	10	5				
rusakovi	9	12	10	14	13	7		13	9	3	8	13	13			
rutilipennis	12	12	13	2	9	13	14	2	13	14	13	11		14		
wilsonae	6	4	4	7	4	4	10	13	3	9	6	4	6	10	13	

⬜ No significant differences

🟨 1-3 significant morphological differences

🟧 4-6 significant morphological differences

🟥 ≥7 significant morphological differences

Figure 41. Comparative matrix summarizing the number of significant differences in each species pair. Significance values were corrected to account for multiple comparisons (Bonferroni correction). When there is only one significant difference the level is shown (* <0.01 ** <0.001 ***<0.0001).

species in the 3B clade (which morphologically overlapped widely with each other as well as with some of the other *niger* group specimens) as well as the subgenus *Labarrus* (wide overlap with *A. wilsonae*). This is particularly obvious with the datapoints in the lower right quadrant in the bivariate plot (Fig. 40B) which corresponded to specimens in the 3B clade (*A. bameuli* sp. nov. and *A. bellumgerens* sp. nov.) which overlapped broadly both with the *niger*-crown group and *A. plagiatus*, as well as due to a single extreme specimen of *A. wilsonae* (specimen 183) which was morphologically divergent and placed just within the 3B group.

Discussion

Although *Liothorax* comprises a group of morphologically similar species, this study has found that it is possible to morphologically discriminate many of the species using continuous linear measurements of external, sex-independent morphological characters. Furthermore, these differences were statistically significant and congruent with other independent sources of evidence which support their species status.

The karyological and molecular results of this and previous papers have shown that within the western Palaearctic *Liothorax* there is an unrecognised diversity of species that have remained hidden due to their morphological similarity. However, this similarity is only an artefact of the character suites that have been used to date to identify species in the Aphodiini, as well as a failure to properly account for the significance of what Dellacasa and Dellacasa (2005) regard as "intraspecific variation", which the authors fail to define, as opposed to interspecific variation. In order to determine what this variation means, it is necessary to quantify it, not just intra- and interspecifically with as wide a geographical coverage as possible, but also within the context of the closest clades (genera/subgenera). This is also necessary on account of the need to accurately identify the cryptic diversity uncovered by the cytogenetic and molecular methods. Unfortunately the Aphodiinae are a morphologically conservative group, particularly compared to the better studied sister clade the Scarabaeinae, which has made their identification and classification difficult and heavily reliant on a small suite of characters, chiefly the aedeagus and epipharynx. Although there are some studies that have used morphometrics to study variation in epipharynx in Scarabaeidae (Pizzo et al. 2009; Tocco et al. 2011), this has been only amongst species pairs. Also, these studies have worked on the same limited data sets so there is a restrictive circularity in the classification of the group.

Within the *niger*-crown clade (*A. niger*, *A. muscorum*, *A. krelli* sp. nov., and *A. felix* sp. nov.), we have found support for the specific rank of these taxa. *Aphodius niger*, *A. wilsonae*, and *A. muscorum* have been found to be morphologically distinct from each other in this study, a result that is counter to the conclusions of Dellacasa and Dellacasa (2005) and Dellacasa et al. (2007). There is also strong and statistically significant support for the morphological distinctiveness of the *bameuli-bellumgerens-alberti* clade from the rest of the *niger*-clade taxa, although within the clade we could not find any morphological discriminant features. There was a broad overlap between *A. bameuli* sp. nov. and *A. bellumgerens* sp. nov., and although *A. alberti* sp. nov. diverged noticeably from the other two, this divergence was not significant. Similarly, within the *niger*-crown clade, it was difficult to distinguish *A. felix* sp. nov. and *A. krelli* sp. nov., probably due to noisy data (outlier specimen of *felix* along PC2 overlapped broadly with *krelli*) and insufficient sampling to overcome it. Future studies will address the lack of resolution by increasing the sampling size, which was rather low for these two otherwise easily distinguishable species. Similarly, larger samples of *niger* and *muscorum* should also improve the delimitation of these species and avoid the complications resulting from the indeterminate *niger* cf. material from peripheral areas. Fortunately, *A. bameuli* sp. nov., *A. bellumgerens* sp. nov., and *A. felix* sp. nov. show clear chromosomal differences.

The previously synonymised species *A. isikdagensis*, *A. discoides*, and *A. rutilipennis* have been found to be too morphologically divergent to be conspecific, contrary to previous studies on the group (Stebnicka 1990; Dellacasa et al. 2007). *Aphodius isikdagensis* (a member of the *A. niger* group, misidentified and wrongly synonymised with *A. rutilipennis*) nevertheless appeared closest to *A. rusakovi* and both were placed next to *A. muscorum*, supporting their inclusion in the *niger* group, as suggested by the aedeagal morphology of *A. isikdagensis*, but not *A. rusakovi*. This morphological affinity, as well as their close geographical distribution, could also be indicative of a close phylogenetic relationship. On the other hand, with the exception of some overlap with *A. discoides*, neither *A. rutilipennis*, *A. chellala* sp. nov., nor *rodrigoi* sp. nov. can be considered conspecific with *A. plagiatus* or *A. isikdagensis*, as their morphology is much too different from either, contradicting their synonymisation by previous authors (Stebnicka 1990; Dellacasa et al. 2001b). However their close morphometric similarity and the small sample size (for *A. rodrigoi* sp. nov. only three specimens were available for all measurements whilst for *A. chellala* sp. nov. only six) limited the statistical power such that they could not be discriminated from *A. rutilipennis*.

In addition, although morphological and molecular divergence were positively correlated, we did not find a significant statistical support for this association, even though the more genetically distant species were morphologically more divergent and vice versa. It is possible that the sample size was too small such that a few outliers overpowered the results. On the other hand, the discriminatory power of the PCA on the morphometric data between closely related taxa (for example between *plagiatus* and the other species in the *plagiatus* group, or between the major clades in the *niger* group), suggests that the gross morphology of the Aphodiini may be under strong selective pressure and not the drift like neutral evolution of mitochondrial molecular sequences. Possible reasons include ecomorphological selection, competitive displacement in sympatry, or a combination of both. A much larger sample of populations is required to answer this question, in particular since there were several species for which no molecular data were available (*A. chellala* sp. nov., *A. discoides*, *A. rodrigoi* sp. nov., *A. rusakovi*, and *A. isikdagensis*), and is beyond the scope of this paper. Similarly, although *A. niger* and *A. muscorum* are well characterised, the undetermined *A. niger* cf. specimens make it difficult to elucidate their exact distributions and to establish to what extent they overlap in Central Europe. Additional positively identified samples (via karyotyping) of these two species from Central and Eastern Europe is needed.

The present multifaceted study, drawing on evidence from morphology, karyology, and genetic analysis shows clearly that the known species of Palaearctic *Liothorax* comprise a monophyletic group of 16 distinct species. As implied by the title of this paper, this number is likely to be increased as more material and data from other populations and species from other areas becomes available. Also requiring clarification is the relationship of the Palaearctic *Liothorax* to those described from the Nearctic.

Acknowledgements

It is a pleasure to thank the many people who have helped us in the work described here. For help in arranging and carrying out collection in Hungary we thank Prof. Laszlo Bögre (Royal Holloway University of London) and his friend in Hungary Mihaly Bodnár who, with his sons Gergö and Daniel not only arranged permission for RBA to collect on the Hortobágyi National Park, but also took RBA to excellent collecting sites – making all the difference between success and failure. Mihaly also introduced RBA to Sandór Rozsa, Chief Ranger of the Aggteleki National Park. He not only gave permission to collect, but also showed interesting places, provided important information, and arranged accommodation for RBA and EMA. We thank Mattias Forshage (Stockholm) for putting the word around the Swedish dung-beetling community about our request for living *L. niger*, Hans-Erik Wanntorp for sending the material from Tullgarn, and Håkan Lundqvist for accommodating RBA and showing him collecting sites on Öland. In Czechia Aleš Bezděk accommodated DK and RBA and took us to the site on the airfield at Hosín near České Budějovice. We also thank the museum curators and private individuals who have lent specimens and provided valuable information: Ottó Merkl (MNSB), Jiří Hájek (NMP), Alberto Ballerio (Rome), Stefano Ziani (Imola), Alex Bellmann (Germany), Mercedes París (MNCN), and Carsten Zorn (Germany). We thank Andrey Frolov for the photograph of the *A. kraatzi* habitat, and for his assistance to RBA during his visit to ZIN in April 2014, and Yunus Yavuz for the use of his photograph of the type locality of *A. alberti*. RBA particularly thanks Max Barclay (NHMUK) and the Museum authorities for all the facilities associated with his position as a Scientific Associate in the Department of Life Sciences (Insects).

Additional information

Conflict of interest

The authors have declared that no competing interests exist.

Ethical statement

No ethical statement was reported.

Funding

No funding was reported.

Author contributions

RB Angus masterminded the paper, collected most of the livestock, did all the chromosome work and wrote most of the taxonomic section. JF Mate did all the DNA work and the statistical morphological analysis, and wrote some of the taxonomic section. EM Angus did nearly all the electron microscopy and helped RB Angus with livestock collection. David Kral advised throughout, helped with collection, and oversaw the manuscript.

Author ORCIDs

Robert B. Angus https://orcid.org/0000-0002-3860-5617
Jason F. Maté https://orcid.org/0000-0002-2505-7113
David Král https://orcid.org/0000-0002-7930-1927

Data availability

All of the data that support the findings of this study are available in the main text.

References

Paris Conference (1971) Standardization in human cytogenetics Birth Defects: Original Article series 8:7 1972 The National Foundation, New York. [Reprinted in] Cytogenetics 11(1972): 313–362. https://doi.org/10.1159/000130202

Ádám L (1994) A check-list of the Hungarian Scarabaeoidea with the description of ten new taxa. Folia Entomologica Hungarica 55: 5–17.

Angus RB (1982) Separation of two species standing as *Helophorus aquaticus* (L.) (Coleoptera, Hydrophilidae) by banded chromosome analysis. Systematic Entomology 7(3): 265–281. https://doi.org/10.1111/j.1365-3113.1982.tb00444.x

Angus RB (2010) Schwanengesang? Latissimus 27: 1–8.

Angus RB, Brown RE, Bryant LJ (2000) Chromosomes and identification of the sibling species *Pterostichus nigrita* (Paykull) and *P. rhaeticus* Heer (Coleoptera: Carabidae). Systematic Entomology 25(3): 325–337. https://doi.org/10.1046/j.1365-3113.2000.00108.x

Baraud J (1992) Coléoptères Scarabaeoidea d'Europe. Faune de France, France et Régions Limitrophes. Société Linnéenne de Lyon 78, 856 pp. [11 pls] https://doi.org/10.3406/linly.1992.11007

Baudi di Selve F (1870) Coleoptorum messis in insula Cypro et Asia minore ab Eugenio Truqui congregatae recensitio de Europaeis notis quibusdam additis. Pars tertia. Berliner Entomologische Zeitschrift 14: 49–90. https://doi.org/10.1002/mmnd.18710150113

Bedel J (1911) Faune des Coléoptères du basin de la Seine 1. Scarabaeidae 4. Société entomologique de France, Paris, 1–164. https://doi.org/10.5962/bhl.part.2981

Chan KO, Grissmer LL (2022) GroupStruct: An R package for allometric size correction. Zootaxa 5124(4): 471–482. https://doi.org/10.11646/zootaxa.5124.4.4

Costessèque R (2005) Les Aphodius de France Une clé de détermination. Magellanes, 79 pp.

Dellacasa G (1983) Sistematica e nomenclatura degli Aphodiini italiani. Monografie del Museo regionale di Scienzi naturali di Torino 1: 1–464.

Dellacasa M, Dellacasa G (2005) Comments on some systematic and nomenclatural questions in Aphodiinae with description of new genera and on Italian taxa. Memorie della Società Italiana de Entomologica 84: 47–101. https://doi.org/10.4081/memorieSEI.2005.45

Dellacasa G, Bordat P, Dellacasa M (2001a) A revisional essay of world-genus group taxa of Aphodiinae. Memorie della Società Italiana de Entomologica 79 (2000): 1–482.

Dellacasa G, Dellacasa M, Ziani S (2001b) Taxonomic position of *Aphodius turbatus* Baudi, 1870 and systematic redefinition of *Aphodius isikdagensis* Balthasar, 1952. Rivista del Museo civico de Scienze naturali “E. Caffi” 20 (2000): 3–11.

Dellacasa M, Gordon RD, Dellacasa G (2007) Systematic review to the genus *Liothorax* (Coleoptera: Scarabaeoidea: Scarabaeidae: Aphodiinae). Zootaxa 1407(1): 23–42. https://doi.org/10.11646/zootaxa.1407.1.4

Dellacasa G, Dellacasa M, Mann D (2010) The morphology of the labrum (epipharynx, ikrioma and aboral surface) of adult Aphodiini (Coleoptera: Scarabaeidae: Aphodiinae) and its implications for systematics. Insecta Mundi 0132: 1–21. https://digitalcommons.unl.edu/insectamundi/658

Dellacasa M, Dellacasa G, Král D, Bezděk A (2016) Tribe Aphodiini. In: Löbl I, Löbl D (Eds) Catalogue of Palaearctic Coleoptera. Volume 3. Scarabaeoidea – Scirtoidea – Dasciloidea – Buprestoidea – Byrrhoidea. Revised and Updated Edition. E. J. Brill, Leiden-Boston, 98–154.

Florín-Beltrán M (2001) La Mancha Húmeda: Valores ecológicos y problemática conservacionista. In: García E (Ed.) Ecología y Conservación de la Mancha Húmeda. Instituto Provincial de Investigaciones y Estudios Toledanos, Diputación Provincial de Toledo, Toledo, 65–92. https://doi.org/10.13140/2.1.4445.3764

Gusakov AA (2004) Novye vidy plastinchtousykh zhukov palearcticheskoj fauny. [New species of scarab beetles from the Palaearctic region]. Izdatel’skij dom Ejdos, Kaluga, 1–38.

Hata K, Edmonds WD (1983) Structure and function of the mandibles of adult dung beetles (Coleoptera: Scarabaeidae). International Journal of Insect Morphology & Embryology 12(1): 1–12. https://doi.org/10.1016/0020-7322(83)90031-4

Hebert PDN, Cywinska A, Ball SL, deWaard JR (2003) Biological identifications through DNA barcodes. Proceedings. Biological Sciences 270(1512): 313–321. https://doi.org/10.1098/rspb.2002.2218

International Commission for Zoological Nomenclature (1999) International Code of Zoological Nomenclature, 4th Ed. International Trust for Zoological Nomenclature, London, 306 pp.

International Commission for Zoological Nomenclature (2005) Opinion 2099 (Case 3254) *Aphodius niger* Illiger, 1798 (Insecta, Coleoptera): Specific name conserved. Bulletin of Zoological Nomenclature 62(1): 45.

Kimura M (1980) A simple method for estimating evolutionary rates of base substitutions through comparative studies of nucleotide sequences. Journal of Molecular Evolution 16(2): 111–120. https://doi.org/10.1007/BF01731581

Koichiro T, Stecher G, Kumar S (2021) MEGA11: Molecular Evolutionary Genetics Analysis Version 11. Molecular Biology and Evolution 38(7): 3022–3027. https://doi.org/10.1093/molbev/msab120

Krell F-T (1995) Type catalogue of some Scarabaeoidea species described by Linnaeus. The Linnean 11(4): 13–20.

Krell F-T, Mann DJ, Angus RB, Maté JF (2003) Case 3254 *Aphodius niger* Illiger, 1798 (Insecta, Coleoptera): Proposed conservation of the specific name. Bulletin of Zoological Nomenclature 60(2): 127–131.

Larsson A (2014) AliView: A fast and lightweight alignment viewer and editor for large datasets. Bioinformatics (Oxford, England) 30(22): 3276–3278. https://doi.org/10.1093/bioinformatics/btu531

Lawrence JF, Ślipiński A (2013) Australian Beetles Volume 1. Morphology, Classification and Keys. CSIRO Publishing, Collingwood, 561 pp. https://linnean-online.org/20869/#?s=0&cv=0 [*Scarabaeus plagiatus* [Ins Linn]]

Ljungberg H, Hall K (2009) Nyckel till svenska dyngbaggar. Lena Almqvist, Lässtyrelsen i Gotlands län, 33 pp.

Mann DJ, Garvey L (2014) *Aphodius* (*Liothorax*) *niger* (Illiger) (Scarabaeidae: Aphodiinae) inside and outside the New Forest. Coleopterist 23(3): 138–142.

Maté JF (2003) Radiation and diversification of *Aphodius* dung beetles. University of London PhD. Thesis, 300 pp.

Maté JF, Angus RB (2005) Description of a new species of *Aphodius* Illiger from the Iberian Peninsula and comments regarding the biogeography and ecology of the subgenus *Liothorax* Motschulsky. Koleopterologische Rundschau 75: 325–336.

Miller SA, Dykes DD, Polesky HF (1988) A simple salting out procedure for extracting DNA from human nucleated cells. Nucleic Acids Research 16(3): 1215. https://doi.org/10.1093/nar/16.3.1215

Motschulsky V (1860) Sur les collections Coléoptèrologiques de Linné et de Fabricius (continuation) 22. Lamellicornes. Etudes entomologiques 8 (1859): 163–168.

Müller K, Wickham H (2023) Tibble: Simple Data Frames. https://tibble.tidyverse.org/, https://github.com/tidyverse/tibble [Accessed 30/03/2023]

Nel A, De Villiers WM (1988) Mouthpart structure in adult scarab beetles (Coleoptera: Sacrabaeoidea). Entomologia Generalis 13(1–2): 95–114. https://doi.org/10.1127/entom.gen/13/1988/95

Nei M, Kumar S (2000) Molecular Evolution and Phylogenetics. Oxford University Press, New York, 325 pp. https://doi.org/10.1093/oso/9780195135848.001.0001

Phillips N (2017) Yarrr: A Companion to the e-Book “YaRrr!: The Pirate’s Guide to R”. Version 0.1.5. https://doi.org/10.32614/CRAN.package.yarrr

Pittino R (2010) Aphodiidae interessanti della regione sardo-corsa (Col. Scarabaeoidea). Bolletino della Societá entomologica italiana, Genova 112 (7–8): 127–134.

Pizzo A, Macagno ALM, Roggero A, Rolando A, Palestrini C (2009) Epipharynx shape as a tool to reveal differentiation patterns between insect sister species: insights from *Onthophagus taurus* and *O. illyricus* (Insecta: Coleoptera: Scarabaeidae). Organisms, Diversity & Evolution 9(3): 189–200. https://doi.org/10.1016/j.ode.2009.01.003

Rakovič M (1991) A treatise on some new and interesting *Aphodius* species with a list of species of the subgenus *Nialus* and related subgenera (Coleoptera, Scarabaeoidea, Aphodiidae). Annotationes Zoologicae et Botanicae 206: 1–16.

Reitter E (1892) Bestimmungs-Tabelle der Lucaniden und coprophagen Lamellicornen des palaearctisch Faunengebietes. Verhandlung des Naturforschenden Vereins in Brünn 30, 200 pp. [Published separately before the appearance of vol. 30]

Revelle W (2021) Psych: Procedures for Psychological, Psychometric, and Personality Research. Northwestern University, Evanston, Illinois. R package version 1.9.12.31. https://CRAN.R-project.org/package=psych

Rößner E (2012) Die Hirschkäfer und Blatthornkäfer Ostdeutschlands (Coleoptera:Scarabaeoidea). Herausgegeben und zu beziehen vom Verein der Freunde & Förderer des Naturkundemuseums Erfurt e. V. Große Arche14. 99084 Erfurt.

Rößner E, Frenzel E, Hillert O, Zeigler W (2016) Neue Nachweise von *Liothorax niger* (Illiger, 1798) (Coleoptera, Scarabaeidae, Aphodiinae) in Deutschland. Entomologische Nachrichten und Berichte 60: 191–196. https://www.academia.edu/49478986/%C3%9Fner_Frenzel_Hillert_Ziegler_2017?auto=download

RStudio Team (2020) RStudio: Integrated Development for R. RStudio, PBC, Boston, MA. http://www.rstudio.com/ [Accessed 29/03/2023]

Schmidt A (1916) Namenänderung und Beschreibung neuer Aphodiinen (Col.). Archiv für Naturgeschte (A) 82: 95–116.

Schneider CA, Rasband WS, Eliceiri KW (2012) NIH Image to ImageJ: 25 Years of Image Analysis. Nature Methods 9(7): 671–675. https://doi.org/10.1038/nmeth.2089

Shaarawi FA, Angus RB (1991) A chromosomal investigation of five European species of *Anacaena* Thomson (Coleoptera: Hydrophilidae). Insect Systematics & Evolution 21(4): 415–426. https://doi.org/10.1163/187631290X00319

Sidlauskas BL, Mol JH, Vari RP (2011) Dealing with allometry in linear and geometric morphometrics: a taxonomic case study in the *Leporinus cylindriformis* group (Characiformes: Anostomidae) with description of a new species from Suriname. Zoological Journal of the Linnean Society 162(1): 103–130. https://doi.org/10.1111/j.1096-3642.2010.00677.x

Simon C, Frati F, Beckenbach A, Crespi B, Liu H, Flook P (1994) Evolution, Weighting, and Phylogenetic Utility of Mitochondrial Gene Sequences and a Compilation of Conserved Polymerase Chain Reaction Primers. Annals of the Entomological Society of America 87(6): 651–701. https://doi.org/10.1093/aesa/87.6.651

Sorenson MD, Franzosa EA (2007) TreeRot, version 3. Boston University, Boston, MA. https://people.bu.edu/msoren/TreeRot.html [accessed 1/08/2022]

Stebnicka Z (1985) A new genus and species of Aulonocneminae from India with notes on comparative morphology (Coleoptera: Scarabaeidae). Revue Suisse de Zoologie 92(3): 649–658. https://doi.org/10.5962/bhl.part.81901

Stebnicka Z (1990) New synonymies and notes on some Aphodiinae (Coleoptera: Scarabaeidae). Revue Suisse de Zoologie 97(4): 895–899. https://doi.org/10.5962/bhl.part.79769

Sumner AT (2003) Chromosomes: organization and function. Blackwell, Oxford, 287 pp. https://doi.org/10.1002/9780470695975

Swofford DL (2003) PAUP*: Phylogenetic analysis using parsimony (and other methods). Version 4.0a169. Sinauer Associates.

Tocco C, Roggero A, Rolando A, Palestrini C (2011) Interspecific shape divergence in Aphodiini dung beetles: the case of *Amidorus obscurus* and *A. immaturus* (Coleoptera: Scarabaeoidea). Organisms, Diversity & Evolution 11(4): 263–273. https://doi.org/10.1007/s13127-011-0055-1

Wickham H, Averick M, Bryan J, Chang W, McGowan LD, François R, Grolemund G, Hayes A, Henry L, Hester J, Kuhn M, Pedersen TL, Miller E, Bache SM, Müller K, Ooms J, Robinson D, Seidel DP, Spinu V, Takahashi K, Vaughan D, Wilke C, Woo K, Yutani H (2019) Welcome to the tidyverse. Journal of Open Source Software 4(43): 1686. https://doi.org/10.21105/joss.01686

Wickham H, François R, Henry L, Müller K, Vaughan D (2021). dplyr: A Grammar of Data Manipulation. R package version 1.0.7. https://github.com/tidyverse/dplyr, https://dplyr.tidyverse.org [Accessed 30/03/2023]

ZooKeys 1207: 301–323 (2024)
DOI: 10.3897/zookeys.1207.124517

Research Article

Bivalves of superfamily Galeommatoidea (Mollusca, Bivalvia) from western South Africa, with observations on commensal relationships and habitats

Paul Valentich-Scott[1], Charles Griffiths[2], Jannes Landschoff[3,4], Ruiqi Li[5,6], Jingchun Li[5,6]

1 Santa Barbara Museum of Natural History, 2259 Puesta del Sol Road, Santa Barbara, CA 93105, USA
2 Department of Biological Sciences, University of Cape Town, Private Bag X3, Rondebosch 7701, South Africa
3 Sea Change Trust, Cape Town, Western Cape, South Africa
4 Department of Botany and Zoology, Stellenbosch University, Private Bag X1, Matieland, 7602, South Africa
5 Department of Ecology and Evolutionary Biology, University of Colorado Boulder, 1900 Pleasant Street, Boulder, CO 80309, USA
6 Museum of Natural History, University of Colorado Boulder, 265 UCB, Boulder, CO 80309, USA
Corresponding author: Paul Valentich-Scott (pvscott@sbnature2.org)

Abstract

The Galeommatoidea are a diverse but little-studied group of small bivalves, well known for the symbiotic relationships many species have with a range of invertebrate taxa. Four species collected from the Western Cape region of South Africa were examined and illustrated, providing new details on their habitat preferences, and depicting the mantle structure of live specimens for the first time. *Brachiomya ducentiunus* **sp. nov.**, is described herein, and an additional record of *Montacuta substriata* (Montagu, 1808) is reported from South Africa. *Brachiomya ducentiunus* and *Montacuta substriata* have obligate symbiotic relationships with different burrowing echinoids, while *Kellia becki* (WH Turton, 1932) and *Melliteryx mactroides* (Hanley, 1857) are free-living. DNA data and phylogenetic analyses are provided for three of the species.

Key words: Biodiversity, commensalism, heart urchin, South Atlantic Ocean, *Spatagobrissus mirabilis*, *Spatangus capensis*, symbiosis, taxonomy

Academic editor: Graham Oliver
Received: 1 April 2024
Accepted: 11 June 2024
Published: 22 July 2024

ZooBank: https://zoobank.org/682C6C4D-D59A-4D51-9D2B-9ABDEB841CD6

Citation: Valentich-Scott P, Griffiths C, Landschoff J, Li R, Li J (2024) Bivalves of superfamily Galeommatoidea (Mollusca, Bivalvia) from western South Africa, with observations on commensal relationships and habitats. ZooKeys 1207: 301–323. https://doi.org/10.3897/zookeys.1207.124517

Introduction

This study examines four galeommatoidean species collected near Cape Town, South Africa, mostly from the intertidal or inshore zones, but one from a depth of 122 m. We report on the characteristics and habits of each of these species, one of which is described as new to science.

The Galeommatoidea are perhaps the most poorly known, yet most diverse, of all groups of marine bivalve mollusks (Morton and Valentich-Scott 1989; Bouchet et al. 2002; Goto et al. 2012; Li et al. 2012; Huber 2015; Li et al. 2016), largely due to their small sizes, cryptic lifestyles, and frequent specialized symbiotic relationships with a wide diversity of marine invertebrate taxa.

The unusual lifestyles of Galeommatoidea have piqued the interest of scientists for more than two centuries. Turton (1822) noted that *Montacuta substriata* (Montagu, 1803) was found abundantly on an echinoid, attaching to its spines using “slender filaments issuing from the middle margin” (i.e., the byssal threads). Récluz (1844) further added to the knowledge of commensal relationships of various *“Erycina”* species (Galeommatoidea) and their invertebrate hosts. During the twentieth century a vast number of publications including pivotal papers by Yonge (1952), Morton (1962), Oldfield (1964), Gage (1966), and Morton and Valentich-Scott (1989) described the commensal relationships and functional morphology of various galeommatids.

The current century has seen a continuing high level of interest in galeommatoid biology, with many more details published about their host relationships and interactions (Lützen and Nielsen 2005); Passos and Domaneschi 2006; Rotvit et al. 2007). In the past 15 years considerable work has also been published on the phylogeny of the Galeommatoidea, along with a large expansion in our knowledge of the diversity of invertebrates with which they interact (Goto et al. 2012; Li et al. 2012). Huber (2015) also documented the Galeommatoidea globally, based on conchological characteristics. These studies revealed the morphological disparity and convergence of different galeommatoidean groups and presented new challenges to taxonomical classifications in this bivalve superfamily. These works also highlighted geographical gaps in our understanding of galeommatoidean diversity.

Zettler and Hoffman (2021) described and illustrated six galeommatoidean species from shallow to deep water off Namibia, Africa. Of the six species, four were new to science, indicating much is still unknown in the fauna of southwest Africa. Surprisingly, one of the recorded galeommatids, *Kurtiella bidentata* (Montagu, 1803), is also a fairly common, free living associate within ophiuroid-dominated communities in the North Atlantic (Oliver et al. 2016).

A number of authors have included descriptions or coverage of galeommatoidean bivalves in the course of broader treatments of the South African mollusk fauna. Sowerby’s ‘Marine Shells of South Africa’ (1892) included six species of galeommatids within the genera *Lasaea* Brown, 1827; *Kellia* Turton, 1822; and *Montacuta* Turton, 1822. Smith (1904) provided an extensive checklist of mollusks in the Port Alfred region, on the South African south coast, which included dozens of new species descriptions, including one species each of *Lepton* and *Tellimya*. In the most extensive account of South African galeommatids to date, Bartsch (1915) documented 25 species, of which 15 were new to science. This account was followed by Turton (1932), who documented an impressive 54 galeommatids, including 16 new species, mostly also from the Port Alfred region. Barnard (1964a) gave a detailed account of 14 galeommatids in his overview of South African mollusks and subsequently added two new genera and two new species from the region (Barnard 1964b). As their book on Southern African shells (which is otherwise the most comprehensive account available on the regional mollusk fauna) excludes many of the smaller bivalves, Kilburn and Rippey (1982) report on only five galeommatoideans, despite the fact that their publication covered the wider Southern African region (including Namibia and southern Mozambique).

Materials, methods, and abbreviations

Study locality

The area for the present study of galeommatoidean species has a mild Mediterranean subtropical climate, with warm, dry summers and cooler wet winters. The oceanographic regime of the wider region, the recognized biogeographic regions in the area, and the resulting patterns of marine biodiversity and endemicity are all described by Griffiths et al. (2010). A more detailed account of the physical oceanography of False Bay, one of few significant embayments along the almost linear South African coastline and the collection site of three of the four species covered in this report, is described in detail by Gründlingh and Largier (1991). A description of the coastal fauna of the broader Atlantic coastline of Southern Africa is provided by Branch and Griffiths (1989). The habitat of this region is vastly influenced by extensive kelp forests that grow along rocky reefs and intermixed sandy beaches and are altogether informally known as the "Great African Seaforest."

Abbreviations

The following abbreviations represent institutions at which we examined type specimens, reviewed images, or deposited voucher specimens of this study's subject species.

NHMUK	The Natural History Museum, London, UK
NMSA	KwaZulu-Natal Museum, Kwazulu-Natal, South Africa
SAM	Iziko South African Museum, Cape Town, South Africa
SBMNH	Santa Barbara Museum of Natural History, Santa Barbara, California, USA
UCM	Museum of Natural History, University of Colorado, Boulder, Colorado, USA
USNM	United States National Museum collection in the National Museum of Natural History, Smithsonian Institution, Washington, D.C., USA
ZC	Oxford Museum of Natural History, Oxford, UK

Examined taxa

The samples of *Brachiomya ducentiunus*, new species, were collected in 2016 and 2018 from Miller's Point, in False Bay on the Cape Peninsula (34.13°S, 18.28°E) by freediving and hand excavating specimens of its host, the burrowing echinoid *Spatagobrissus mirabilis* H. L. Clark, 1923, from coarse sand sediments in a water depth of approximately 3 m. Each echinoid was placed immediately after collection into a plastic bag and brought alive to an adjacent field laboratory, where symbiotic species were removed, counted, and preserved. The samples, including the type specimens, were collected by Jannes Landschoff, Craig Foster, and Charles Griffiths.

Samples of *Montacuta substriata* were found crawling on the oral surface spines of the heart urchin *Spatangus capensis* Döderlein, 1905, collected from a trawl sample on the RS *Africana* (cruise AFR289) during the 10 October 2016 austral spring demersal research survey (Trawl 094, Station No A32843, 122 m) at Agulhas Bank, approximately 110 km south off Mossel Bay (35.196°S, 22.056°E). The cruise was jointly organized by the former South African Departments of Agriculture, Forestry and Fisheries (DAFF) and the Department of Environmental Affairs (DEA), now merged into the Department of Forestry, Fisheries and the Environmental (DFFE). Samples were obtained from a single urchin by Jannes Landschoff using a German otter trawl design and a 75 mm mesh cod-end fitted with a 35 mm mesh liner (see Atkinson et al. 2011).

Kellia becki were collected by hand from beneath boulders in a mid-intertidal rock pool at Glencairn, on the east coast of the Cape Peninsula (34.162°S, 18.432°E), collected by Charles Griffiths in 2020.

Melliteryx mactroides were collected at Miller's Point in the small intertidal section north of the tidal pool (34.231°S, 18.476°E), collected by Jannes Landschoff in 2020.

Before being preserved in 96% ethyl alcohol, all samples were photographed alive, either in situ prior to collection or in the laboratory while still alive. We used either an Olympus Tough digital camera on microscope setting or a digital SLR camera and macro lens.

DNA amplification

Genomic DNA of the four species were extracted from mantle, foot or whole body of the specimens using the E.Z.N.A. Mollusc DNA Kit (Omega Bio-tek) following manufacturer's instructions. DNA concentrations were assessed using the Qubit Fluorometer (Invitrogen). Fragments of two nuclear genes (28S rRNA, Histone H3) and one mitochondrial gene (16S rRNA) were amplified for phylogenetic analyses. The 28S gene fragment was amplified using primers D23FLas (5'-CCGCATAGAGGCAAACGGGT-3') (Li et al. 2013) / D6R (5'-CGAAGTTTCCCTCAGGATAGCTGG-3') (Park and Ó Foighil 2000), following a standard PCR protocol with an annealing temperature at 52 °C. The 16S gene fragment was amplified using primers 16SLasF (5'-TAGATTAAGGGTTGGGCCTG-3')/16SLasR (5'-GCCTAAATGGTAAGACTGTTCG-3') (Valentich-Scott et al. 2013) following a touchdown protocol. The initial annealing temperature was 55 °C, and was decreased by 2 °C per cycle, until the final annealing temperature 48 °C was reached. The H3 gene was amplified using primers H3F (5'-ATGGCTCGTACsdCAAGCAGACVGC-3')/H3R (5'-ATATCCTTRGGCATRATRGTGAC-3') (Li et al. 2016) with an annealing temperature at 52 °C. PCR products were sequenced by Quintara Biosciences and DNA sequences were deposited in GenBank (See Table 1 for accession numbers).

Phylogenetic analyses

Due to specimen sizes and preservation condition, not all specimens amplified for all three genetic markers. Table 1 summarizes the PCR amplification results.

The same three genetic markers from other galeommatoidean species belonging to closely related genera were downloaded from GenBank (Suppl. material 1) that included many unidentified galeommatid taxa from the non-systematic paper by Li et al. (2016). Phylogenetic positions of *Kellia becki*, *Brachiomya ducentiunus*, and *Melliteryx mactroides* in relationship with other species were

Table 1. GenBank ID of successfully amplified DNA fragments from the four galeommatoidean species. Note that some species included multiple individuals from the same voucher lot. A dash indicates failed PCR amplification.

Voucher SBMNH	Species	28S	16S	H3
665157	*Montacuta substriata*	–	–	–
665157		–	–	–
666951	*Kellia becki*	–	PP431564	–
666970	*Brachiomya ducentiunus*	–	PP431565	PP454116
666970		–	PP431566	PP454117
666970		–	PP431567	PP454118
665156	*Melliteryx mactroides*	PP431562	PP431568	PP454119
665156		PP431563	PP431569	PP454120

assessed. For each genetic marker, sequences were aligned using MUSCLE 5.1 (edgar) implement in Geneious Prime 2023.2.1. Alignments of multiple genetic markers were concatenated when applicable. Maximum likelihood inferences were performed using RAxML 8.2.11 (Stamatakis et al. 2008) with the GTR CAT model and 100 bootstrap replicates. Bayesian phylogenies were constructed using MrBayes 3.2.6 (Huelsenbeck and Ronquist 2001) using the GTR model. For each dataset, two independent runs were performed for 100,000 generations with a 10,000 burn-in. Cumulative split frequencies were observed to be below 0.01 to ensure convergence.

Results

Systematic Account

Superfamily Galeommatoidea Gray, 1840
Family Lasaeidae Gray, 1842

***Brachiomya* Jespersen et al., 2004**

Brachiomya Jespersen, Lützen & C. Nielsen, 2004. Type species (original designation) *Solecardia stigmatica* (Pilsbry, 1921). Recent.

Description. Shell small (less than 5 mm); transversely ovate; anterior end narrower than posterior end; inequilateral; hinge plate narrow; both valves with a small triangular pseudocardinal tooth beneath umbos; ligament internal, in oblique resilifer; mantle folds wrapped over most of the shell and anteriorly extended into a large inhalant-pedal siphon, posteriorly into a smaller exhalent siphon; mantle with many slender, terminally spatulate tentacles; foot elongate; gills with inner demibranch only.

Discussion. Jespersen et al. (2004) distinguished *Brachiomya* from other galeommatoidean genera by the presence of extensive mid-mantle folds with many spatulate tentacles. Huber (2015) accepted *Brachiomya* as a monotypic genus. As Jespersen and Huber both postulated, we have found *Brachiomya* to group with members of the Lasaeidae. All species are likely to be obligate commensals with echinoid echinoderms.

Brachiomya ducentiunus **sp. nov.**

https://zoobank.org/25211096-71D8-41CA-A5CF-DADEDA4CD18B
Figs 1A–H, 2A–F, Suppl. material 2

Type locality. Miller's Point Lagoon, in False Bay, Western Cape Province, South Africa; 34.231°S, 18.477°E; 3 m; attached to spines, or crawling amongst spines of *Spatagobrissus mirabilis* (Clark, 1923), collected by Charles Griffiths, July 2018.

Type material. ***Holotype*** (Fig. 1A, B), SBMNH 713162, length 2.50 mm, height 1.75 mm, preserved in 70% EtOH. 13 ***Paratypes***, SAMC-A096817, same locality as holotype, largest specimen length 2.5 mm, height 1.7 mm, preserved in 70% EtOH, collected by Jannes Landschoff and Craig Foster, 9 June 2016. 7 ***Paratypes***, SBMNH 666970, same locality and collector as holotype (Fig. 1C–H), dried specimens mounted on SEM stub; length 2.17 mm, height 1.38 mm; length 2.40 mm, height 1.56 mm; length 1.87 mm, height 1.19 mm; length 2.42 mm, height 1.67 mm. 1 ***Paratype***, UCM 60476; length 1.5 mm, height 1.0 mm.

Description. Shell extremely thin, fragile, moderately inflated, translucent; inequilateral, slightly longer anteriorly; ovate-elongate; anterior end obliquely truncate in larger specimens; posterior end broadly rounded; ventral margin straight, slightly invaginated in some; dorsal margin gently sloping from umbos; shell margins weakly gaping; prodissoconch well defined, umbonate, smooth, subcircular; prodissoconch length ~ 350 μm; external sculpture of commarginal striae, with few widely spaced radial striae, especially anteriorly; umbos low, wide; hinge plate extremely narrow, with one minute pseudocardinal in each valve; ligament internal, very short. Length up to 2.7 mm.

***Mantle*.** Large, reflected, covering ~ 95% of outer shell surface when fully extended, but not fully covering umbos; mantle can be almost completely retracted into the shell; reflected portion with low papillae; mantle near shell margin with longer tentacles; anterior end with large cowl, serrate on end; cowl can be greatly extended (Fig. 2E, F; Suppl. material 2).

***Foot*.** Of moderate size, ~ the length of the shell when fully extended, vermiform, with slight heel. The species is an active crawler, and can also attach to the host by byssal threads. The foot has been observed to frequently wrap around the urchin spines as the bivalve crawls.

***Ctenidia*.** One demibranch on each side, comprised of ~ 30 narrowly spaced filaments in larger specimens.

***Brooding*.** Up to ten shelled juvenile specimens observed brooding in the dorsal portion of ctenidia in mature specimens.

Distribution. Only known from the type locality in False Bay, South Africa, and only found attached to the echinoid *Spatagobrissus mirabilis*; not observed free-living.

Commensal relationship and habitat. Found crawling on the oral surface of the heart urchin *Spatagobrissus mirabilis*. This host species was found to be living in a specialized microhabitat of coarse gravel and half-buried cobbles or boulders (at least at the type locality associated with kelp forests). At the type locality in 2018, of 10 sampled heart urchins, all had associated *Brachiomya* on their oral surface. Densities of *Brachiomya* ranged from 38 to 172 specimens on a single host. Two other commensal species were also recorded on these same urchins, a small but very common unidentified amphipod of family Lysianassidae, and a large, scale worm (family Polynoidae), of which only a

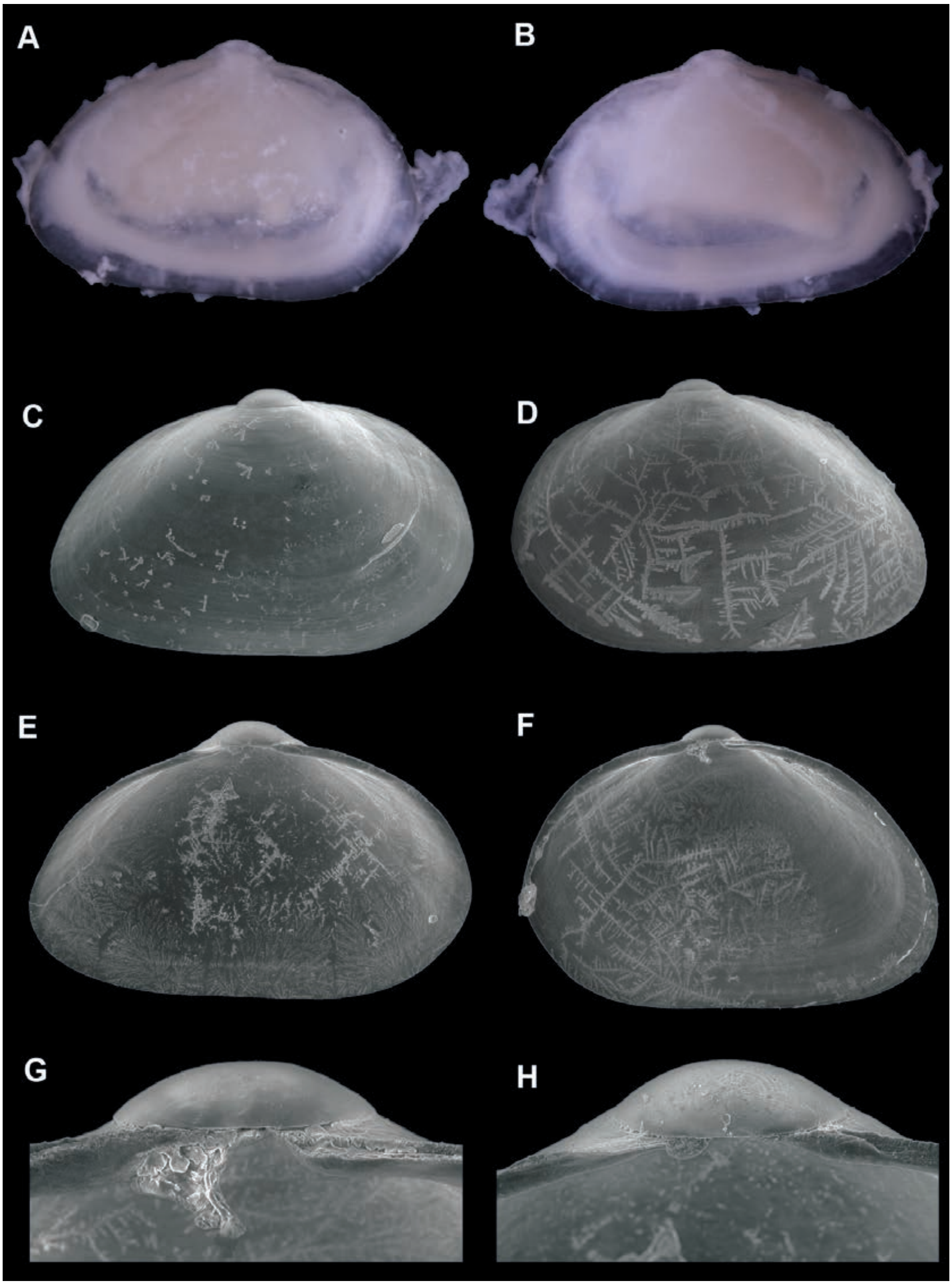

Figure 1. *Brachiomya ducentiunus* sp. nov. **A, B** holotype, SBMNH 713162, length 2.50 mm, height 1.75 mm **A** exterior of right valve **B** exterior of left valve **C–H** paratypes, SBMNH 666970, crystallization on exterior and interior of shell is from dried bleach, not a sculpture element **C** exterior of right valve, length 2.17 mm, height 1.38 mm **D** exterior of left valve, length 2.40 mm, height 1.56 mm **E** interior of left valve, length 1.87 mm, height 1.19 mm **F** interior of right valve, length 2.42 mm, height 1.67 mm **G** hinge of right valve **H** hinge of left valve.

few specimens were found. The amphipod and polychaete species also both appear to be new to science.

Discovery. Initially discovered via free-diving in 2016 at the type locality, collected by Jannes Landschoff and Craig Foster.

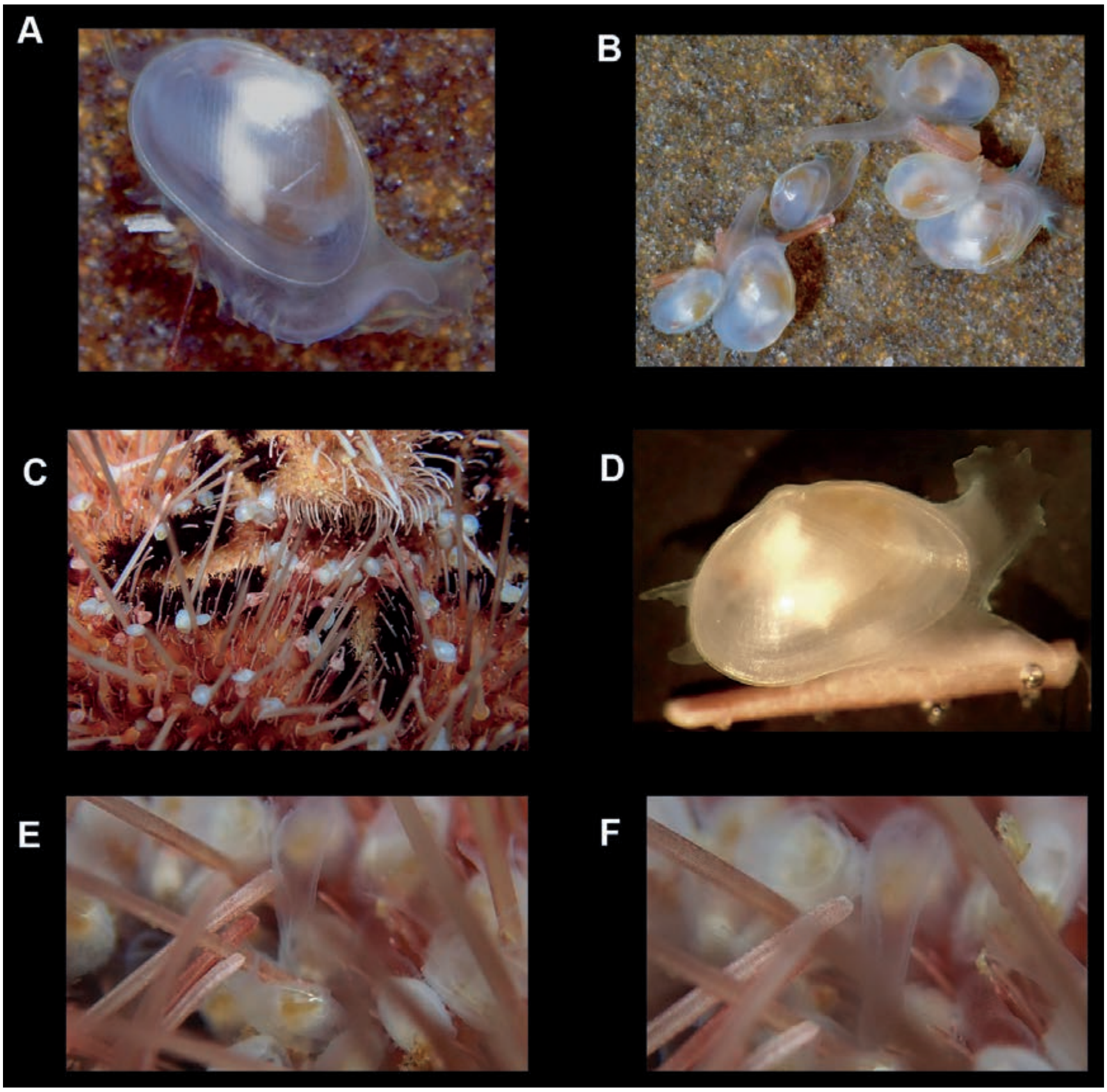

Figure 2. *Brachiomya ducentiunus* new species, living animals **A, B** crawling on hard substrate **C** overview of specimens crawling on the aboral surface of urchin *Spatagobrissus mirabilis* **D** crawling on urchin spine with mantle and foot extended **E, F** extended mantle between urchin spines.

Etymology. The name *ducentiunus* is from Latin, meaning “201.” The species was discovered while preparing and working on the ‘1001 Seaforest Species’ project, a research and storytelling program aimed at increasing awareness of regional kelp bed ecosystems colloquially referred to as ‘the Great African Seaforest’ (see www.seachangeproject.com). The number 201 was chosen as a unique identifier for the 1001 program, with the goal to link each hundredths species to a species described as new to science.

Comparisons. The Pacific and Asian *Brachiomya stigmatica*, which is the only other known species in the genus, is more evenly rounded anteriorly, has a strong rust-colored stripe medially, lacks radial striae, and has more developed teeth.

Montacuta Turton, 1822

Montacuta Turton, 1822. Type species (subsequent designation) *Ligula substriata* Montagu, 1808. Recent, North Atlantic Ocean.

Description. Shell small (length less than 5 mm), subovate to subelliptical, moderately thin, translucent to opaque, gaping ventrally in some; sculpture of commarginal striae and ribs, weak, widely spaced radial ribs in some; periostracum thin to thick, translucent to dark brown; hinge plate narrow, each valve with low anterior cardinal tooth; ligament internal, large, elongate; mantle sparsely papillate, reflected, covering some of outer shell surface; without mantle tentacles; foot elongate, thin, trigonal, heel absent; with one demibranch on each side.

Discussion. While this genus is widely distributed in the North Atlantic, Mediterranean, and eastern Australia, this is only the second record from southern Africa. Kamenev (2008) provides a comprehensive description of the genus along with SEM images of the type species, *Montacuta substriata*.

***Montacuta* cf. *substriata* (Montagu, 1808)**

Fig. 3A–F

Ligula substriata Montagu, 1808: 25.

Material examined. Four specimens from 122 m off Agulhas Bank, ~ 110 km south off Mossel Bay (35.196°S, 22.056°E).

Description. ***Shell*** thin, fragile, moderately inflated, opaque; inequilateral, much longer anteriorly; anterior and posterior ends broadly rounded (Fig. 3A, B); shell margins only weakly gaping, if at all; prodissoconch length ~ 300 μm; dissoconch sculpture of commarginal striae, irregular widely-spaced radial striae, plus 1–3 low, broad, irregular radial undulations in some; umbos narrow, pointed, slightly projecting; hinge plate narrow; both valves with short, stout anterior cardinal tooth, and long, thin posterior cardinal tooth (Fig. 3C, D); ligament in oblique resilifer between cardinal teeth. Length up to 3 mm.

Mantle not reflected.

***Foot*.** Large, equal to or slightly longer than the length of the shell when fully extended, trigonal, without heel; long ventral byssal groove extending to end of smooth foot tip. Can attach to the host by byssal threads.

***Ctenidia*.** With one demibranch on each side, comprised of ~ 20 widely-spaced filaments in larger specimens.

Type. Lost; Devon coast, United Kingdom.

Commensal relationship and habitat. Found crawling on the oral surface of the heart urchin *Spatangus capensis* Döderlein, 1905. Up to 20 specimens have been observed byssally attached to the host.

Locality information. Collected in 122 m off Agulhas Bank, ~ 110 km south off Mossel Bay (35.196°S, 22.056°E). Voucher specimens deposited as SBMNH 467288, SAMC-A096818, and UCM 60478.

Discussion. *Montacuta substriata* is a well-documented species in the North Atlantic (Oliver et al. 2016) and the Mediterranean (Gofas et al. 2011). Barnard (1964a) reported a single valve of this species in 100 fathoms (182 m). Cosel and Gofas (2019) did not report the species from tropical West Africa, nor have there been any other records from the African Atlantic or Indian Oceans. We acknowledge that there is likely limited gene flow between the populations of *Montacuta substriata* in the North Atlantic and Cape Town, especially in light of the apparent absence of the species in tropical West Africa. However, the

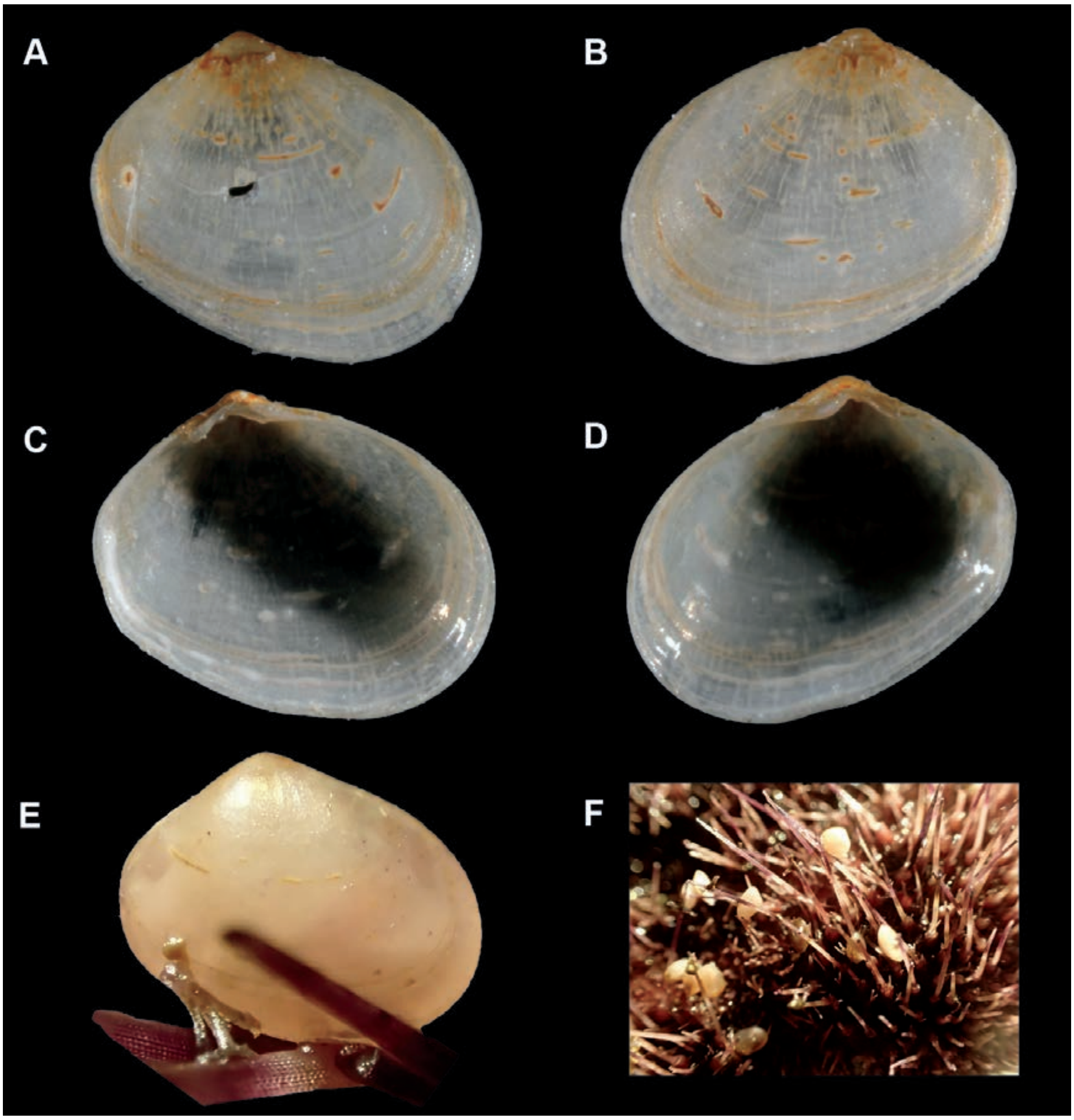

Figure 3. *Montacuta* cf. *substriata* **A–D** SBMNH 467288, length = 3.0 mm, height = 2.2 mm **A** exterior of right valve **B** exterior of left valve **C** Interior of left valve **D** Interior of right valve **E** specimen attached to urchin spine **F** living animals attached to urchin *Spatangus capensis*.

two populations match conchologically in all details although their hosts are different; *Spatangus capensis* in South Africa and *Spatangus purpureus* Müller, 1776 and *Enchinocardium flavescens* Müller, 1776, in the northeast Atlantic. Unfortunately, we have been unable to extract DNA from our specimens from the Agulhas Bank, so we are unable to completely confirm this identification. It is possible that the South African specimens represent a new species.

Kellia Turton, 1822

Kellia Turton, 1822. Type species (subsequent designation, Récluz 1844): *Mya suborbicularis* (Montagu, 1803). Recent, North Atlantic.

Chironia Deshayes, 1839. Type species (monotypy): *Chironia laperousii* Deshayes, 1839.

Diplodontina Stempell, 1899. Type species (monotypy): *Diplodontina tumbesiana* Stempel, 1899. Recent, Chile.

Description. Shell subovate to ovate-elongate, inflated, subequilateral, equivalve; umbos prosogyrate; sculpture of commarginal ribs, striae, or growth checks; periostracum thin, translucent, green to yellow, dehiscent to adherent; hinge plate narrow; two small cardinal teeth in left valve, one cardinal tooth in right valve; one elongate, posterior lateral tooth in both valves; ligament internal, robust, in elongate resilifer.

Discussion. There has been much taxonomic confusion with members of *Kellia*, especially in the southern hemisphere, and the genus needs a global revision. Kamenev (2004) documented many species of *Kellia* from the North Pacific and North Atlantic Oceans. The functional morphology of the genus has been documented by Oldfield (1961) and the sperm morphology by Jespersen and Lützen (2007)

Kellia becki **(W.H. Turton, 1932)**

Fig. 4A–H

Erycina becki W.H. Turton, 1932: 238.

Material examined. Two specimens from at Glencairn, South Africa (34.162°S, 18.432°E).

Description. ***Shell*** ovate, thin, fragile, highly inflated, semi-translucent; subequilateral; umbos broad, moderately inflated; anterior and posterior ends broadly rounded; shell margins not gaping; periostracum thin, adherent, yellow, iridescent; external sculpture of fine commarginal striae; hinge plate narrow; right valve with one small cardinal tooth and one thin posterior lateral tooth, with large gap between them; left valve with two very small cardinal teeth and one posterior lateral tooth; ligament oblique, broad, in shallow resilifer. Length up to 6 mm.

***Mantle*.** Translucent, reflected, extending well past shell margin dorsally, forming an extended facultative siphon posteriorly (Fig. 4H).

***Foot*.** Long, thin, translucent, without heel (Fig. 4H).

***Ctenidia*.** Specimens for internal examination not available.

Type. ZC-M003209, Port Alfred, South Africa.

Commensal relationship and habitat. Found on the undersides of rocks in intertidal pools. Although the errant polynoid polychaete, *Polynoe scolopendrina* Savigny, 1822, is also visible in some of the images provided herein, we do not suspect any commensal relationship between the *Kellia becki* and this polychaete and consider it to be a free-living, nestling species.

Comparisons. Huber (2015) considered *Kellia becki* to be the only member of this genus to be present in the Cape Town region. The Australian *Kellia rotunda* (Deshayes, 1856) had been recorded from South Africa by Bartsch (1915), W.H. Turton (1932), Barnard (1964a), and Kilburn and Rippey (1982), but these records were considered erroneous by Huber (2015), although he did mention the need to genetically compare these two species.

The specimens illustrated by Cosel and Gofas (2019: 486) in tropical West Africa as *Kellia suborbicularis* (Montagu, 1803) are very similar conchologically

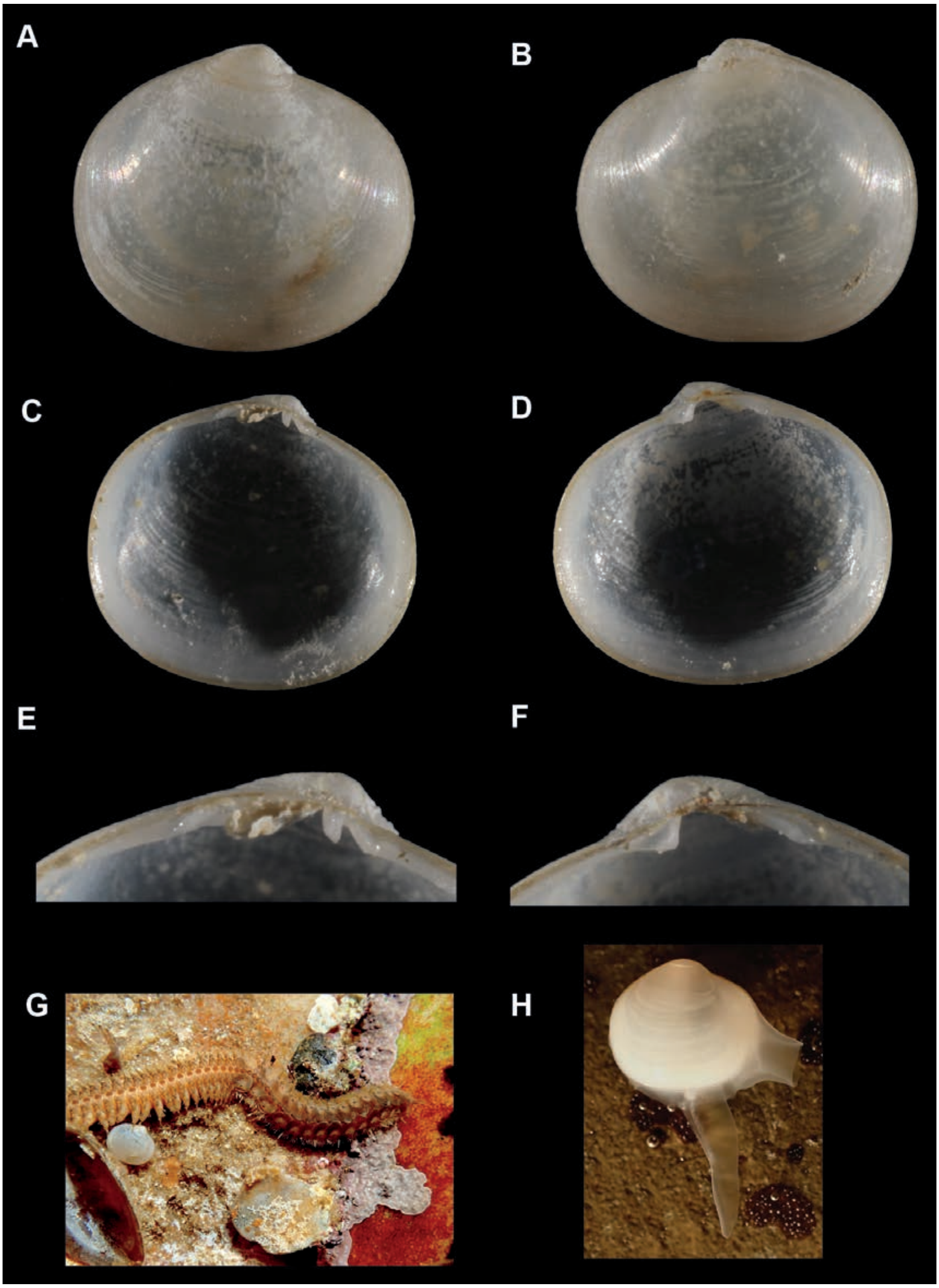

Figure 4. *Kellia becki* **A–F** SBMNH 669951, length = 5.6 mm, height = 4.9 mm **A** exterior of right valve **B** exterior of left valve **C** interior of left valve **D** interior of right valve **E** hinge of left valve **F** hinge of right valve **G** living animal on rock adjacent to polynoid polychaete, *Polynoe scolopendrina* **H** living animal with mantle and foot fully extended.

to our specimens from the Cape Peninsula. Genetic studies on these two populations, as well as other Atlantic species of *Kellia*, are needed.

Locality information. Collected intertidally from beneath boulders at Glencairn, on the east coast of the Cape Peninsula, South Africa (34.162°S, 18.432°E). Voucher specimens deposited as SBMNH 666951 and SAMC-A096819.

Melliteryx Iredale, 1924

Melliteryx Iredale, 1924. Type species (original designation): *Erycina acupuncta* Hedley, 1902. Recent, Australia.

Description. Shell subtrigonal, moderately inflated, subequilateral, equivalve; umbos narrow; sculpture of commarginal ribs, striae, or growth checks, with micro-pits in some; periostracum thick, tan, adherent, shiny to silky; hinge plate narrow; both valves with anterior and posterior lateral teeth; left valve with small central pseudocardinal directly below umbos, conjoined with anterior lateral tooth in some; right valve with small thickening near umbos; ligament internal, in elongate resilifer.

Discussion. The type species of the genus, *Erycina acupuncta* Hedley, 1902, was described from off New South Wales, Australia. Huber (2015) documents five additional species, including three from South Africa, one from the Indo-Pacific and one from New Zealand. See Discussion section below for additional comments on *Melliteryx*.

Melliteryx mactroides (Hanley, 1857)

Fig. 5A–H, Suppl. materials 3, 4

Pythina mactroides Hanley, 1857: 340.

Material examined. Three specimens from Miller's Point, False Bay, South Africa (34.231°S, 18.476°E).

Description. ***Shell*** trigonal, thick for size, moderately inflated, cream colored; subequilateral; umbos narrow, pointed; anterior and posterior ends broadly rounded; shell margins not gaping; periostracum thick, adherent, yellow to dark brown; exterior sculpture of fine commarginal striae, some with micro-pits; hinge plate broad; both valves with an anterior and posterior lateral tooth with a wide gap between them; left valve small central pseudocardinal tooth; anterior lateral tooth in right valve with small thickening near umbos; ligament oblique, narrow, in shallow resilifer. Length up to 6 mm.

Mantle. Translucent, only slightly reflected, forming a facultative siphon posteriorly (see Suppl. material 3).

Foot. Long, broad, translucent, with distinct heel. This species is an active crawler (see Suppl. material 3).

Ctenidia. With one demibranch on each side, comprised of ~ 75 narrowly spaced filaments in larger specimens.

Type. NHMUK 1967994, Cape of Good Hope, South Africa.

Commensal relationship and habitat. Found in small groups of 10–20 animals, clinging to the underside of rocks in the lower intertidal. We have found no directly associated hosts.

Comparisons. Huber (2015) documented two additional species of *Melliteryx* in South Africa, *Melliteryx jaeckeli* Huber, 2015, and *Melliteryx fortidentata* (Smith, 1904). *Melliteryx jaeckeli* has a much weaker hinge plate than *Melliteryx mactroides*, and we question whether this is the correct genus for the Smith species. *Melliteryx fortidentata* is inequilateral, with the umbos placed well off the center, compared to the subequilateral *Melliteryx mactroides*.

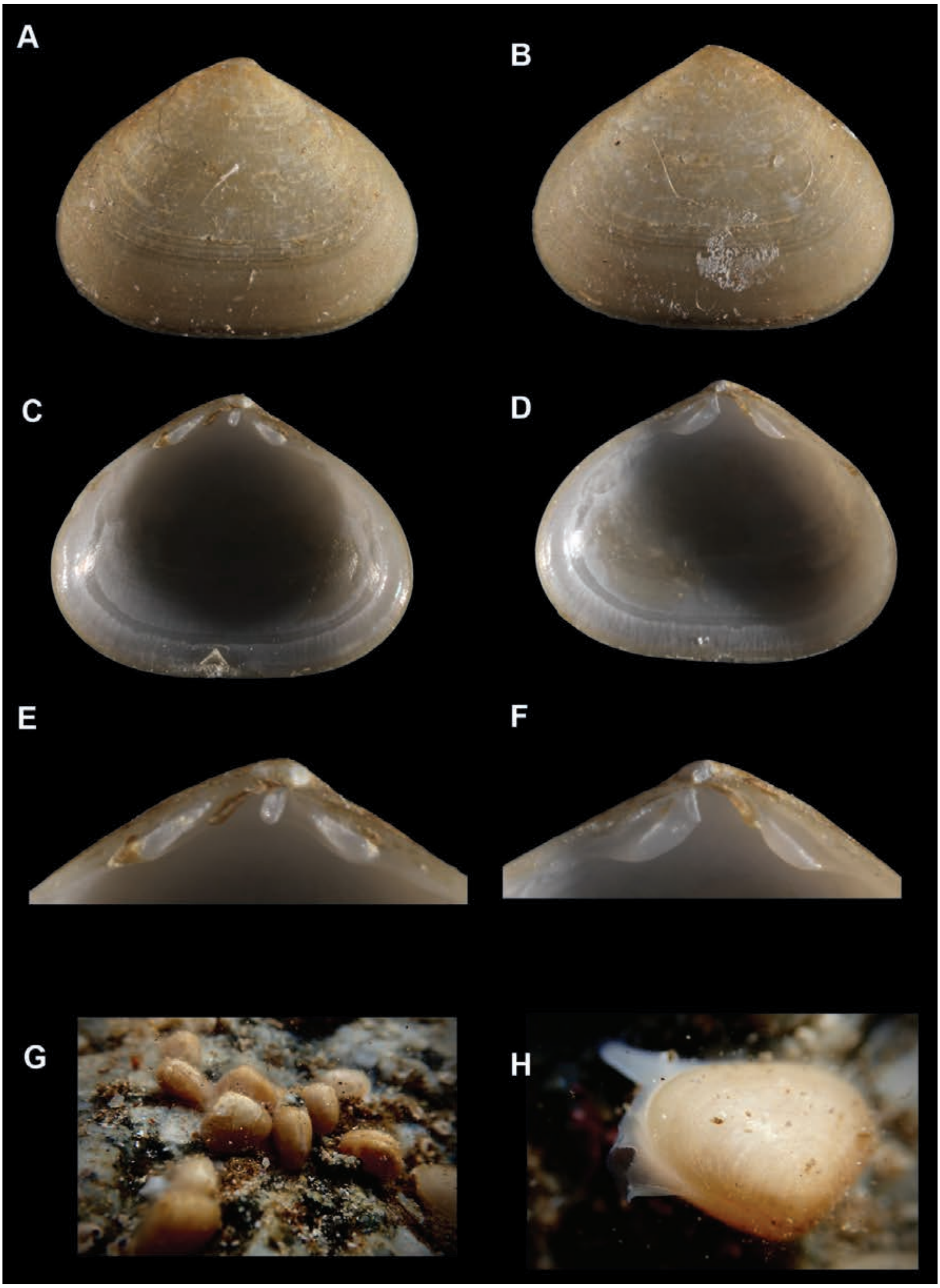

Figure 5. *Melliteryx mactroides* **A–F** SBMNH 665156, length = 6.0 mm, height = 5.0 mm **A** exterior of right valve **B** exterior of left valve **C** interior of left valve **D** interior of right valve **E** hinge of left valve **F** hinge of right valve **G** living animals crawling on a rock **H** living animal with foot and mantle extended (note biofilm present in **G** and **H**).

Locality information. Specimens were collected in the intertidal at Miller's Point (34.231°S, 18.476°E). Voucher specimens were deposited as SBMNH 665156, SAMC-A096820, and UCM 60477.

Discussion. We are following Huber (2015) and Cosel and Gofas (2019) with the placement of this species into the genus *Melliteryx*. As our molecular results indicate below there is little resolution of the genera due to lack of taxon sampling globally. With further genetic data it is possible that our South African species might fall into an undescribed genus.

Cosel and Gofas (2019) reported *Melliteryx mactroides* from tropical West Africa. The specimens they illustrate are more elongate than our specimens and have a weaker hinge plate. Additional study must be completed to determine if these are indeed the same species, or if the tropical West Africa specimens represent a new species.

On the shell exterior in living specimens of *Melliteryx mactroides* we observed a dense layer of filamentous biofilm (see Suppl. material 4). A similar biofilm was reported by (Gillan and De Ridder 1997) and (Gillan et al. 2000) in the North Atlantic galeommatid *Tellimya ferruginosa* (Montagu, 1808).

Molecular results

Phylogenetic positions of *Kellia becki*, *Brachiomya ducentiunus*, and *Melliteryx mactroides* are shown in Fig. 6. Topologies from the Maximum Likelihood and Bayesian analyses were consistent for all species. *Kellia becki* belong to a clade (Clade FS9 in Li et al. 2016) composed of other *Kellia* species, including *Kellia porculus* Pilsbry, 1904, *Kellia japonica* Pilsbry, 1895, and *Kellia suborbicularis*. It was recovered as a sister lineage to an unidentified *Kellia* species collected from Madagascar.

Brachiomya ducentiunus belongs to a clade of sea urchin commensals (Clade CS2 in Li et al. 2016), including species from the genera *Montacutella* and *Brachiomya*. *Brachiomya ducentiunus* and two other unidentified sea urchin commensal species from Madagascar form a well-supported clade.

The phylogenetic position of *Melliteryx mactroides* was less resolved compared to the other two species, likely due to a lack of taxon sampling in this group. *Melliteryx mactroides* was recovered with high confidence as part of the FS1 clade in Li et al. (2016), which includes the genera *Lasaea* Brown, 1827 and *Arthritica* Finlay, 1926. However, its position within this clade is uncertain. *Melliteryx mactroides* is currently grouped with an Australian species *Arthritica semen* (Menke, 1843) with low bootstrap or posterior support, and is quite divergent from *Arthritica semen* based on the branch length. *Melliteryx mactroides* also does not appear to be closely related to *Melliteryx acupuncta* from Australia or ?*Tellimya* sp. from Japan.

The phylogenetic position of our *Montacuta substriata* specimens could not be assessed due to unsuccessful PCR amplifications.

Discussion

We have documented and described four species of galeommatid bivalves, including one new to science. We did not discover any of the galeommatids from eastern South Africa listed by Smith (1904) or Bartsch (1915). We did, however, locate a single species, *Kellia becki*, which was described from Port Alfred by Turton (1932), and two species, *Melliteryx mactroides* and *Montacuta substriata*, reported by Barnard (1964a).

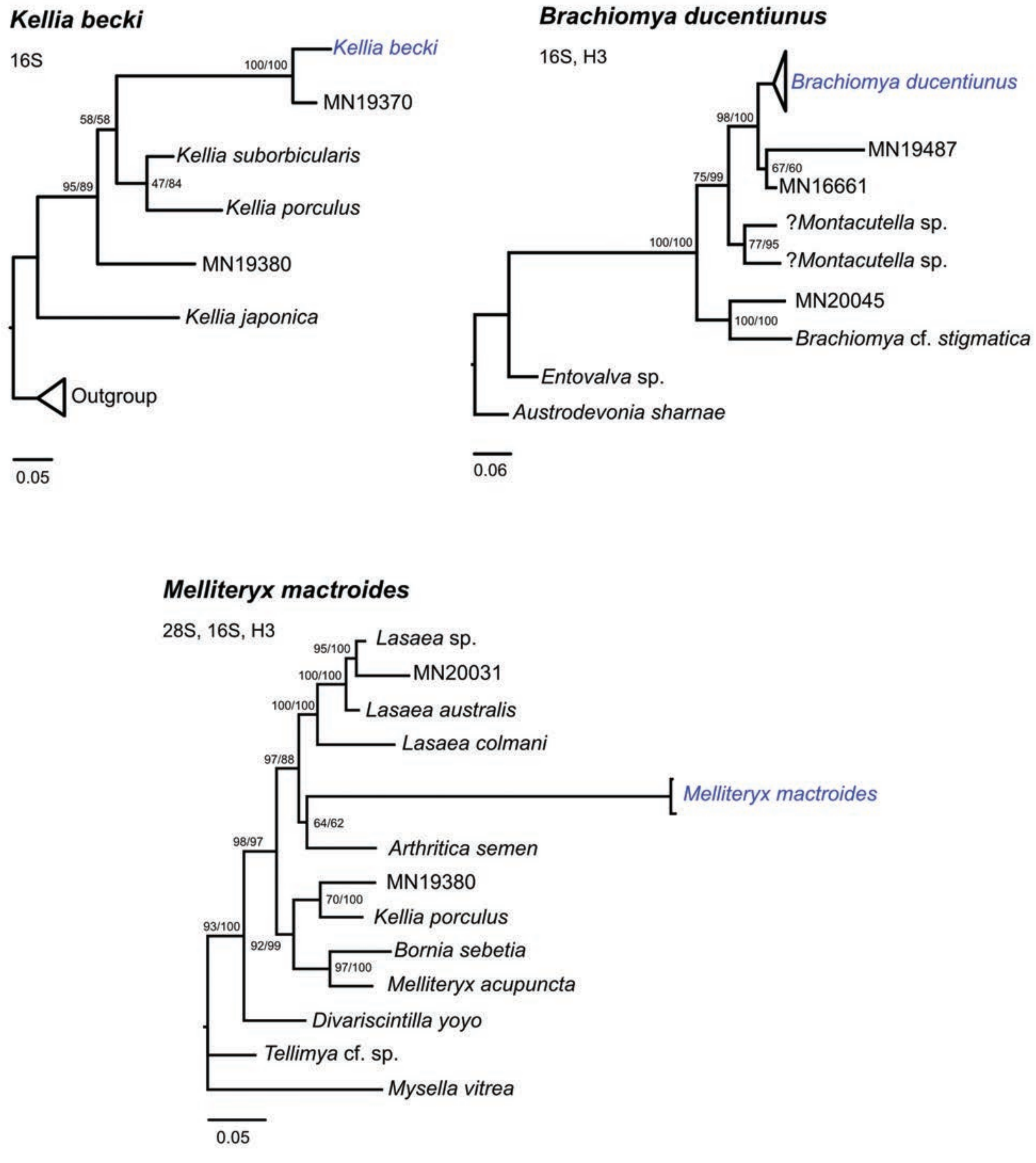

Figure 6. Phylogenetic positions of *Kellia becki*, *Brachiomya ducentiunus*, and *Melliteryx mactroides*.

The presence of the North Atlantic *Montacuta substriata* in Cape Town represents an unusual disjunct distribution, as Cosel and Gofas (2019) did not report this or indeed any other members of the genus, from tropical West Africa. Future studies may prove the South African specimens to be a new species. The possible presence of European, northeast Atlantic species in South Africa was raised by Sowerby (1892) who reported eleven bivalve species as being identical to their British counterparts. Gradually these were dismissed although a few remain to this day such as *Talochlamys multistriata* (Poli, 1795). A wider ranging molecular comparison of the north and south temperate faunas is warranted.

Our phylogenetic analyses provided us with intriguing, albeit sometimes confusing results (Fig. 6). *Kellia becki* formed a clade with other *Kellia* members, but was found to be distinct. This confirms its current taxonomical placement within the genus *Kellia*.

Brachiomya ducentinus belonged to a clade with *Brachiomya stigmatica* and also to an unidentified *Montacutella* Jespersen et al., 2004. It is also sister to an unidentified urchin-associated galeommatid from the biogeographically distant, Madagascar. Galeommatids are known for frequent evolutionary host switching and many groups do not exhibit high host fidelity (Goto et al. 2012; Li et al. 2016). The fact that echinoid-associated genera across a wide geographic range from a single clade indicates that this lineage exhibits exceptionally high host fidelity and perhaps host specialization. There is also a potential for bivalve-echinoid co-diversification to be detected in this group, which will require the host phylogeny to be constructed.

Our lack of sampling and understanding of the phylogeny of small commensal galeommatids is perhaps typified by the results with *Melliteryx mactroides* (Fig. 6). We compared two type species of galeommatids of the genera *Bornia* and *Melliteryx* to our South African samples. Interestingly, *Bornia sebetia* (da Costa, 1830), the type species of the genus, has a sister relationship to *Melliteryx acupuncta*, which is the type species of *Melliteryx*. However, they are both quite distant from our South African species. Our South African bivalve is more closely aligned with the intertidal Australian *Arthritica semen*. Ponder (2022) reviewed the Australian species of *Arthritica* and they have few similarities in shell morphology when compared to our species. Therefore, the taxonomical placement of our *Melliteryx* cannot be fully resolved until more taxon sampling is be done for this particular free-living clade. We are following Huber (2015) and Cosel and Gofas (2019) in the generic placement of this species until further genetic data is available.

Galeommatoidean bivalves and their hosts remain poorly known in South Africa and there are doubtless many more regional species that remain uncollected, especially those from deeper waters or commensal on other invertebrates.

Acknowledgements

We appreciate assistance with collections and type images by Tom White and Andreia Salvador (NHMUK), Ellen Strong (USNM), and Igor Muratov (NMSA). John Taylor (NHMUK) pointed us to literature on the biofilm hairs we observed on *Melliteryx mactroides* and also provided images of syntypes of *Melliteryx mactroides*. Peter Middelfart provided images of the type of *Erycina acupuncta*, the type species of *Melliteryx*.

Our thanks to the South African Departments of Environmental Affairs and of Forestry, Fisheries and the Environment, for the research collecting permit under which these specimens were collected and the Iziko South African Museum for information on their holdings and for housing type specimens collected during this study. We also acknowledge the entire team of the DFFE demersal offshore surveys in Cape Town, South Africa, especially Lara Atkinson and her extended team from the NRF-FBIP SeaMap, as well as the NRF/SAEON Egagasini Node, for playing a pivotal role in the demersal invertebrate monitoring program. As such Lara was instrumental for JL's participation in the research cruise that led to one of the discoveries in this paper. The Sea Change Trust and the team of the Sea Change Project are thanked for their ongoing research support in documenting species from the Great African Seaforest. Craig Foster, who is part of this team, is especially acknowledged for initially finding the host sea urchins and newly-described *Brachiomya* species in the kelp forest.

We are very grateful for excellent editorial and organizational assistance from Robert Dees. We appreciate the helpful and substantial comments by Michael L. Zettler and Graham Oliver, which greatly enhanced this manuscript.

Additional information

Conflict of interest

The authors have declared that no competing interests exist.

Ethical statement

No ethical statement was reported.

Funding

This study was in part performed with the support of Keystone Grant 542 '1001 Seaforest Species' from the Save Our Seas Foundation.

Author contributions

Conceptualization: PVS. Data curation: JL, RL. Formal analysis: JL, RL. Investigation: PVS, CG, JL. Methodology: JL, RL, CG, JL. Project administration: PVS. Writing – original draft: PVS. Writing – review and editing: JL, CG, PVS, JL.

Author ORCIDs

Paul Valentich-Scott https://orcid.org/0000-0003-0019-7643
Jannes Landschoff https://orcid.org/0000-0001-9836-1530
Ruiqi Li https://orcid.org/0000-0001-9428-6094

Data availability

All of the data that support the findings of this study are available in the main text or Supplementary Information.

References

Atkinson L, Leslie R, Field J, Jarre A (2011) Changes in demersal fish assemblages on the west coast of South Africa, 1986–2009. African Journal of Marine Science 33(1): 157–170. https://doi.org/10.2989/1814232X.2011.572378

Barnard KH (1964a) Contributions to the knowledge of South African marine Mollusca. Part V. Lamellibranchiata. South African Museum. Annals 47: 361–593.

Barnard KH (1964b) Two new genera of Erycinacea (Bivalvia) from South Africa. Proceedings of the Malacological Society of London 36: 33–37.

Bartsch P (1915) Report on the Turton Collection of South African marine mollusks, with additional notes on other South African shells contained in the United States National Museum. Govenment Printing Office, Washington, xii, 305 pp. https://doi.org/10.5479/si.03629236.91.i

Bouchet P, Lozouet P, Maestrati P, Heros V (2002) Assessing the magnitude of species richness in tropical marine environments: Exceptionally high numbers of molluscs at a New Caledonia site. Biological Journal of the Linnean Society. Linnean Society of London 75(4): 421–436. https://doi.org/10.1046/j.1095-8312.2002.00052.x

Branch GM, Griffiths CL (1989) The Benguela ecosystem part V. The coastal zone. Oceanography and Marine Biology – an Annual Review 28: 395–486.

Brown T (1827) Illustrations of the conchology of Great Britain and Ireland. Drawn from nature. WH Lizars & D Lizars, Edinburgh and S Highley, London, 144 pp.

Clark HL (1923) Echinoderm fauna of South Africa. Annals of the South African Museum 13: 221–435. [pls. 8–23]

Cosel R von, Gofas S (2019) Marine bivalves of tropical west Africa from Rio de Oro to southern Angola. Muséum National d'Histoire Naturelle, Paris, 1104 pp. https://doi.org/10.5852/fft48

da Costa O-G (1830) Catalogo sistematico e ragionato de testaces delle due Sicilie. 1st ed. Dalla Tipografia Della Minerva, Naples, 132 pp. [2 pls.] https://doi.org/10.5962/bhl.title.13093

Deshayes GP (1839) Nouvelles espèces de mollusques, provenant des côtes de la Californie, du Mexique, de Kamtschatka et de Nouvelle-Zélande.... Société Cuviérienne. Revue Zoologique 2: 356–361.

Deshayes GP (1856) Descriptions de nouvelles espèces du genre *Erycina*. Zoological Society of London, Proceedings for 1855[23]: 181–183.

Döderlein L (1905) Über Seeigel der deutschen Tiefsee-Expedition. Zoologischer Anzeiger 28: 621–624. https://doi.org/10.5962/bhl.title.46999

Finlay HJ (1926) A further commentary on New Zealand molluscan systematics. Transactions of the New Zealand Institute 57: 320–485.

Gage JD (1966) Observations on the bivalves *Montacuta substriata* and *M. ferruginosa*, "commensals" with spatangoids. Journal of the Marine Biological Association of the United Kingdom 46(1): 49–70. https://doi.org/10.1017/S0025315400017549

Gillan DC, De Ridder C (1997) Morphology of a ferric iron-encrusted biofilm forming on the shell of a burrowing bivalve (Mollusca). Aquatic Microbial Ecology 12: 1–10. https://doi.org/10.3354/ame012001

Gillan DC, Warnau M, De Vrind-De Jong E, Boulvain F, Preat A, De Ridder C, Gillan DC, Michel Warnau E (2000) Iron oxidation and deposition in the biofilm covering *Montacuta ferruginosa* (Mollusca, Bivalvia). Geomicrobiology Journal 17(2): 141–150. https://doi.org/10.1080/01490450050023818

Gofas S, Moreno D, Salas C (2011) Moluscos marinos de Andalucía. Málaga, Spain (Universidad de Málaga). I: i–xvi + 1–342, II: i–xii + 343–809.

Goto R, Kawakita A, Ishikawa H, Hamamura Y, Kato M (2012) Molecular phylogeny of the bivalve superfamily Galeommatoidea (Heterodonta, Veneroida) reveals dynamic evolution of symbiotic lifestyle and interphylum host switching. BMC Evolutionary Biology 12: 13 pp. https://doi.org/10.1186/1471-2148-12-172

Gray JE (1840) Mollusks. Synopsis of the contents of the British Museum, 42nd ed. G. Woodfall and Son, London, 105–152.

Gray JE (1842) Mollusks. Synopsis of the Contents of the British Museum, 48–92.

Griffiths CL, Robinson TB, Lange L, Mead A (2010) Marine biodiversity in South Africa: an evaluation of current states of knowledge. PLOS ONE 5: e12008. https://doi.org/10.1371/journal.pone.0012008

Gründlingh ML, Largier JL (1991) Physical Oceanography of False Bay: A review. Transactions of the Royal Society of South Africa 47: 387–400.

Hanley SCT (1857) Descriptions of four new species of Kelliadae in the collection of Hugh Cuming, Esq. Zoological Society of London, Proceedings for 1856 [24]: 340–341.

Hedley C (1902) Scientific results of the trawling expedition of H.M.C.S. "Thetis," off the coast of New South Wales, in February and March, 1898, Part 2: Mollusca. Part I. Brachiopoda and Pelecypoda. Australian Museum Memoir 4(5): 287–324. https://doi.org/10.3853/j.0067-1967.4.1902.1501

Huber M (2015) Compendium of bivalves 2. Hackenheim, Germany (ConchBooks), 907 pp.

Huelsenbeck JP, Ronquist F (2001) MRBAYES: Bayesian inference of phylogenetic trees. Bioinformatics (Oxford, England) 17(8): 754–755. https://doi.org/10.1093/bioinformatics/17.8.754

Iredale T (1924) Results from Roy Bell's molluscan collections. Proceedings of the Linnean Society of New South Wales 49: 179–278.

Jespersen Å, Lützen J (2007) Sperm ultrastructure in *Kellia suborbicularis* (Bivalvia: Galeommatoidea: Kellidae. Acta Zoologica (Stockholm, Sweden) 88(1): 59–63. https://doi.org/10.1111/j.1463-6395.2007.00251.x [sic]

Jespersen Å, Lützen J, Nielsen C (2004) On three species and two new genera (*Montacutella* and *Brachiomya*) of galeommatoid bivalves from the irregular sea urchin *Brissus latecarinatus* with emphasis on their reproduction. Zoologischer Anzeiger 243(1–2): 3–19. https://doi.org/10.1016/j.jcz.2004.04.001

Kamenev GM (2004) New species of the genus *Kellia* (Bivalvia: Kelliidae) from the Commander Islands, with notes on *Kellia comandorica* Scarlato, 1981. Malacologia 46: 57–71.

Kamenev GM (2008) Little-known arctic species *Montacuta spitzbergensis* (Bivalvia: Montacutidae) from the north-western Pacific with notes on *Montacuta substriata* and *Tellimya ferruginosa*. Journal of the Marine Biological Association of the United Kingdom 88(2): 347–356. https://doi.org/10.1017/S0025315408000568

Kilburn R, Rippey E (1982) Sea shells of Southern Africa. Macmillan South Africa, 249 pp.

Li J, Ó Foighil D, Middelfart PU (2012) The evolutionary ecology of biotic association in a megadiverse bivalve superfamily: sponsorship required for permanent residence in sediment. PLOS ONE 7: e42121. https://doi.org/10.1371/journal.pone.0042121

Li J, Ó Foighil D, Park J-K (2013) Triton's trident: Cryptic Neogene divergences in a marine clam (*Lasaea australis*) correspond to Australia's three temperate biogeographic provinces. Molecular Ecology 22(7): 1933–1946. https://doi.org/10.1111/mec.12220

Li J, Ó Foighil D, Strong EE (2016) Commensal associations and benthic habitats shape macroevolution of the bivalve clade Galeommatoidea. Proceedings of the Royal Society B, Biological Sciences 283: 20161006. https://doi.org/10.1098/rspb.2016.1006

Lützen J, Nielsen C (2005) Galeommatid bivalves from Phuket, Thailand. Linnean Society of London, Zoological Journal 144: 261–308. https://doi.org/10.1111/j.1096-3642.2005.00168.x

Menke KT (1843) Molluscorum Novae Hollandiae specimen. Libraria Aulica Hahniana, Hannover, 46 pp.

Montagu G (1803) Testacea Britannica, or natural history of British shells, marine, land, and fresh-water, including the most minute: systematically arranged and embellished with figures. Romsey (Hollis). 2 vols. 1: xxxvii + 292 pp; 2: 293–606. [16 pls.] https://doi.org/10.5962/bhl.title.33927

Montagu G (1808) Supplement to Testacea Britannica. With additional plates. White, London / Woolmer, Exeter, v + 183 + [5] pp, pls 17–30 (post-1 Oct.).

Morton JE (1962) Habitat and orientation in the small commensal bivalve mollusc, *Montacuta ferruginosa*. Animal Behaviour 10(1–2): 126–133. https://doi.org/10.1016/0003-3472(62)90140-9

Morton B, Valentich-Scott PH (1989) The Hong Kong Galeommatacea (Mollusca: Bivalvia) and their hosts, with descriptions of new species. Asian Marine Biology 6: 129–160.

Müller OF (1776) Zoologiae Danicae prodromus, seu animalium Daniae et Norvegiae indigenarum characteres, nomina, et synonyma imprimis popularium. Typis Hallagerii, Havni, Copenhagen, 282 pp. https://doi.org/10.5962/bhl.title.13268

Oldfield EW (1961) The functional morphology of *Kellia suborbicularis* (Montagu), *Montacuta ferruginosa* (Montagu) and *M. substriata* (Montagu) (Mollusca, Lamellibranchiata). Journal of Molluscan Studies 34(5): 255–295. https://doi.org/10.1093/oxfordjournals.mollus.a064872

Oldfield EW (1964) The reproduction and development of some members of the Erycinidae and Montacutidae (Mollusca, Eulamellibranchiata). Malacological Society of London. Proceedings 36: 79–120.

Oliver PG, Holmes AM, Killeen IJ, Turner JA (2016) Marine Bivalve Shells of the British Isles. Amgueddfa Cymru – National Museum Wales. http://naturalhistory.museumwales.ac.uk/britishbivalves [Accessed: 25 June 2024]

Park J-K, Ó Foighil D (2000) Genetic diversity of oceanic island *Lasaea* (Mollusca: Bivalvia) lineages exceeds that of continental populations in the northwestern Atlantic. The Biological Bulletin 198(3): 396–403. https://doi.org/10.2307/1542695

Passos FD, Domaneschi O (2006) A new species of *Mysella* Angas, 1877 (Bivalvia: Galeommatoidea) from Admiralty Bay, King George Island, South Shetlands, Antarctica, with data on its biology and functional anatomy. Polar Biology 29(5): 389–398. https://doi.org/10.1007/s00300-005-0068-3

Pilsbry HA (1895) Catalogue of the marine mollusks of Japan with descriptions of new species and notes on others collected by Frederick Stearns. Detroit (Stearns). viii + 196 pp. [11 pls.] https://doi.org/10.5962/bhl.title.10379

Pilsbry HA (1904) New Japanese Mollusca: Pelecypoda. Proceedings. Academy of Natural Sciences of Philadelphia 56: 550–561.

Pilsbry HA (1921) Marine Mollusks of Hawaii, VIII–XIII. Proceedings. Academy of Natural Sciences of Philadelphia 72: 296–328.

Poli JX (1795) 2: i–xlix, [1–2] Testacea utriusque Siciliae eorumque historia et anatome tabulis aeneis illustrata. Regio Typographeio, Parma, 75–264. [pls 19–39 pp]

Ponder WF (2022) The first galeommatoidean from inland waters: A new species of *Arthritica* (Bivalvia, Lasaeidae) from artesian springs in South Australia, with comments on other Australian members of the genus. Molluscan Research 43(1): 22–33. https://doi.org/10.1080/13235818.2022.2151070

Récluz CA (1844) Prodrome d'une monographie du genre erycine. Société Cuviérienne, Revue Zoologique 7: 291–299 (Aug.); (9): 325–336 (Sept.).

Rotvit L, Lützen J, Jespersen Å, Fox TH (2007) *Mysella gregaria* new species, a bivalve (Galeommatoidea: Montacutidae) commensal with an intertidal burrowing sea anemone from North Carolina, USA. The Nautilus 121: 191–200.

Savigny J-C (1822) Système des annélides, principalement de celles des côtes de l'Égypte et de la Syrie, offrant les caractères tant distinctifs que naturels des Ordres, Familles et Genres, avec la Description des Espèces. Description de l'Égypte ou Recueil des Observations et des Recherches qui ont été faites en Égypte pendant l'Expédition de l'Armée Française, publié par les Ordres de sa Majesté l'Empereur Napoléon le Grand. Histoire Naturelle, Paris 1: 1–128.

Smith EA (1904) On a collection of marine shells from Port Alfred, Cape Colony. Journal of Malacology 11: 21–44.

Sowerby GBI (1892) Marine shells of South Africa. A catalogue of all the known species with references to figures in various works, descriptions of new species, and figures of such as are new, little known, or hitherto unfigured. First. Sowerby, London, i–iv, 1–89. [pls. 1–5 pp] https://ia601603.us.archive.org/25/items/marineshellsofso00sowe/marineshellsofso00sowe.pdf

Stamatakis A, Hoover P, Rougemont J (2008) A Rapid Bootstrap Algorithm for the RAxML Web Servers. Systematic Biology 57: 758–771. https://doi.org/10.1080/10635150802429642

Stempell CLW (1899) Die Muscheln der Sammlung Plate (systematische Uebersicht). Zoologische Jahrbücher, Supplement 5 [Fauna Chilensis 2]: 217–250. [pl. 12]

Turton W (1822) Conchylia Insularum Britannicarum. The shells of the British Islands, systematically arranged. Collum, Exeter, xlvii + 279 pp. [20 pls.] https://doi.org/10.5962/bhl.title.10443

Turton WH (1932) The marine shells of Port Alfred, S. Africa. Humphrey Milford, London, xvi + 331 pp. [70 pls.]

Valentich-Scott PH, Ó Foighil D, Li J (2013) Where's *Waldo*? A new commensal species, *Waldo arthuri* (Mollusca, Bivalvia, Galeommatidae), from the northeastern Pacific Ocean. ZooKeys 316: 67–80. https://doi.org/10.3897/zookeys.316.4256

Yonge CM (1952) Studies on Pacific coast mollusks. VI. A note on *Kellia laperousii* (Deshayes). California. University of California Publications in Zoology 55: 451–454.

Zettler ML, Hoffman L (2021) New species in Galeommatoidea (Bivalvia) from Namibia. Iberus: Revista de la Sociedad Espanola de Malacologia 39: 195–208. https://doi.org/10.5281/ZENODO.5039263

Supplementary material 1

Three genetic markers from other galeommatoidean species belonging to closely related genera that were downloaded from GenBank and used for our analysis

Authors: Paul Valentich-Scott, Charles Griffiths, Jannes Landschoff, Ruiqi Li, Jingchun Li

Data type: xlsx

Link: https://doi.org/10.3897/zookeys.1207.124517.suppl1

Supplementary material 2

Brachiomya ducentiunus sp. nov., crawling between urchin spines highlighting elongated and serrated cowl

Authors: Paul Valentich-Scott, Charles Griffiths, Jannes Landschoff, Ruiqi Li, Jingchun Li

Data type: mp4

Link: https://doi.org/10.3897/zookeys.1207.124517.suppl2

Supplementary material 3

Melliteryx mactroides in situ on rocks highlighting active crawling and large foot

Authors: Paul Valentich-Scott, Charles Griffiths, Jannes Landschoff, Ruiqi Li, Jingchun Li

Data type: mp4

Link: https://doi.org/10.3897/zookeys.1207.124517.suppl3

Supplementary material 4

Melliteryx mactroides in situ on rocks highlighting biofilm on outside of shell

Authors: Paul Valentich-Scott, Charles Griffiths, Jannes Landschoff, Ruiqi Li, Jingchun Li

Data type: mp4

Link: https://doi.org/10.3897/zookeys.1207.124517.suppl4

ZooKeys 1207: 325–353 (2024)
DOI: 10.3897/zookeys.1207.121725

Research Article

A review of the genus *Zygota* (Hymenoptera, Diapriidae) in Germany with taxonomic notes on this genus and its distinction from *Pantoclis*

Jeremy Hübner[1], Vasilisa Chemyreva[2], Jan Macek[3], Victor Kolyada[4]

1 Bavarian State Collection of Zoology, Munich, Münchhausenstr. 21, 81247 Munich, Germany
2 Zoological Institute, Russian Academy of Sciences, 1 Universitetskaya Emb., St Petersburg 199034, Russia
3 National Museum, Department of Entomology, Praha, Czech Republic
4 Palaeontological Institute, Russian Academy of Sciences, Moscow 117997, Russia
Corresponding authors: Jeremy Hübner (huebner@snsb.de); Vasilisa Chemyreva (diapriidas.vas@gmail.com)

Abstract

This study provides a comprehensive overview of the genus *Zygota* Förster combining DNA barcoding and current morphology. Nineteen species of *Zygota* were found throughout Germany, including the newly described species *Zygota walli* **sp. nov.** First species records for Germany are: *Zygota balteata* Macek, 1997; *Z. comitans* Macek, 1997; *Z. spinosipes* (Kieffer, 1908); *Z. sordida* Macek, 1997; *Z. angularis* Macek, 1997 and *Z. vigil* Nixon, 1957. We also clarify diagnoses for the two related genera, *Pantoclis* Förster and *Zygota* to designate the boundaries of the *Zygota* genus and propose new synonymies: *Zygota caligula* Buhl, 1997 is a junior synonym of *Z. congener* (Zetterstedt, 1840); *Z. reticulata* Kozlov, 1978 is a junior synonym of *Z. ruficornis* (Curtis, 1831). Thirteen species of *Zygota* sensu Nixon (1957) are transferred to the genus *Pantoclis* with the following new combinations proposed: *Zygota brevinervis* (Kieffer, 1908) (= *Pantoclis brevinervis* (Kieffer, 1909), **comb. nov.**); *Z. brevipennis* (Kieffer, 1908) (= *P. brevipennis* (Kieffer, 1908), **comb. nov**.); *Z. caecutiens* (Kieffer, 1908) (= *P. caecutiens* (Kieffer, 1908), **comb. nov.**); *Z. cursor* (Kieffer, 1908) (= *P. cursor* (Kieffer, 1908), **comb. nov.**); *Z. fossulata* (Thomson, 1858) (=*P. fossulata* (Thomson, 1858), **comb. nov.**); *Z. fuscata* (Thomson, 1858) (= *P. fuscata* (Thomson, 1858), **comb. no**v.); *Z. hemiptera* (Thomson, 1858) (= *P. hemiptera* (Thomson, 1858), **comb. nov.**); *Z. microtoma* (Kieffer, 1909) (= *P. microtoma* (Kieffer, 1909), **comb. nov**.); *Z. soluta* (Kieffer, 1907) (= *P. soluta* (Kieffer, 1907), **comb. nov**.); *Z. striata* (Kieffer, 1909) (= *P. striata* (Kieffer, 1909), **comb. nov**.); *Z. subaptera* (Thomson, 1858) (= *P. subaptera* (Thomson, 1858), **comb. nov**.); *Z. sulciventris* (Kieffer, 1909) (= *P. sulciventris* (Kieffer, 1909), **comb. nov.**), and *Z. unicolor* (Kieffer, 1908) (= *P. unicolor* (Kieffer, 1908), **comb. nov.**).

Key words: Checklist, DNA-barcoding, integrative taxonomy, new records, new species, new synonymy, parasitoid wasps

Academic editor: Norman Johnson
Received: 29 February 2024
Accepted: 16 May 2024
Published: 24 July 2024

ZooBank: https://zoobank.org/78F95F50-E355-4D18-8236-20748CE3B113

Citation: Hübner J, Chemyreva V, Macek J, Kolyada V (2024) A review of the genus *Zygota* (Hymenoptera, Diapriidae) in Germany with taxonomic notes on this genus and its distinction from *Pantoclis*. ZooKeys 1207: 325–353. https://doi.org/10.3897/zookeys.1207.121725

Introduction

This article deals with the parasitoid wasps of the genus *Zygota* Förster (Diapriidae, Belytinae, Belytini), comprising mostly medium-sized (2.5–4.0 mm long) melanic and pubescent specimens with brightly colored appendages.

The genus has 75 described species worldwide, of which most are described from the Palearctic and Nearctic (Johnson 1992; Buhl 1995, 1997, 1998; Macek 1997). Although common, little is known about their biology and their hosts. In the past, morphology-based taxonomy of *Zygota* led to confusion and many reinterpretations of the genus. The generic diagnosis, key to the species of Central Europe, and diagnostic remarks based on available types were given by Macek (1997). According to the original description of the genus given by Förster (1856) *Zygota* can be easily distinguished from other Belytinae genera by the strengthened marginalis, open radial cell, and emarginated fore tibiae in males (Förster 1856). Förster's vague diagnosis was misinterpreted by the later authors Ashmead (1893, 1902) and Kieffer (1909), which Macek (1997, 2007) has pointed out in his revisionary works. He clarified the identity based on the designation of the neotype of *Zygota abdominalis* (Nees, 1834), and completed a revision of available types. However, the boundary between *Zygota* and its sister genus *Pantoclis* Förster is still unclear, as some species remained falsely placed inside *Zygota*. Nixon (1957) and later Kozlov (1978) placed all Belytini species with an open radial cell and unpunctured scutellum [except some few *Belyta* species (Macek 1995)] in the genus *Zygota*. The same genus concept was applied in Johnson's (1992) world catalog. Although the diagnosis of the genus *Zygota* was given by Macek (1997), the generic affiliation of many species was not discussed. For example, the taxonomy of the 14 species from 39 Palearctic species of *Zygota* listed by Johnson (1992) is still questionable. The genus *Pantoclis* has never been defined conclusively to exclude it from other Belytinae, because the diversity and lack of knowledge of *Pantoclis* species makes it extremely difficult to define. To understand the genus concept of *Zygota*, it must be distinguished from *Pantoclis*. We will, therefore, present a diagnosis for each.

Currently, there are 38 known species of *Zygota* in the Palearctic Region (Johnson 1992, Buhl 1995, 1997, Macek 1997). Full taxonomic treatments of the genera are given by Macek (1997) (only *Zygota*) and cataloged by Johnson (1992) (both, *Zygota* and *Pantoclis*). Macek (1997) has given a taxonomic interpretation only for 18 of these species. The present study thus aims to clarify the diagnosis of *Zygota* and the taxonomic position of the remaining 20 species, which are not discussed in Macek (1997). This revision is mostly based on material collected in Bavaria, Germany, in the framework of the German Barcode of Life (GBOL) III: Dark Taxa project (Hausmann et al. 2020). The most recent diversity evaluation that has been conducted for Germany was done over twenty years ago by Blank (2001). In his work, twenty *Zygota* taxa were recovered, of which two, *Z. excisipes* (Kieffer, 1916) and *Z. norvegica* (Kieffer, 1912), have been synonymized with *Z. excisor* (Zetterstedt, 1840) and *Z. ruficornis* (Curtis, 1831), respectively. For *Zygota subclausa* (Kieffer, 1907), Macek (1995, 1997) proposed the new combination *Belyta subclausa* (Kieffer, 1907). In total, 19 species of *Zygota* were reliably identified for the German fauna.

Material and methods

Most of the examined material was collected within the GBOL III project as well as from earlier collecting events in Bavaria and Baden-Wuerttemberg (Germany) led by the Bavarian State Collection of Zoology in Munich (SNSB-ZSM). Further material originates from the collection of the National Museum in Prague (NMPC) and the Russian collections in St. Petersburg (ZISP). In addition, type material from the Zoological Museum in Copenhagen (ZMUC) and the Natural History Museum (NHM) in London was examined. All specimens were morphologically identified as far as possible, including the closely related genus *Pantoclis*. Afterwards, individuals were Sanger sequenced under the usage of a voucher recovery approach. The genetic information was obtained at the Canadian Centre for DNA Barcoding (CCDB) in Guelph by the application of a voucher recovery protocol (https://ccdb.ca/). All mitochondrial CO1 sequences were aligned in MEGA11 (Tamura et al. 2021), and the alignment was then used to construct maximum likelihood trees with the online program IQ TREE version 2.0 (Trifinopoulos et al. 2016) using the default settings (1000 bootstrap alignments, substitution model: TIM+F+I+G4, 1000 iterations). Editing was done using FIGTREE version 1.4.4 (Rambaut 2010) and INKSCAPE version 1.1.1 (2021, available from: https://inkscape.org/de). Clustering and BIN-distance-analyses were conducted to infer species barriers among the CO1 barcodes using MEGA11 as well as ASAP (Puillandre et al. 2021). Suppl. material 3 gives an overview of the genetically examined material and the clustering results. All molecular data and collection metadata are publicly available on the Barcode of Life Data System (BOLD) platform (http://www.barcodinglife.org, Ratnasingham and Hebert 2007) in the dataset [DS-ZYGPAN dx.doi.org/10.5883/DS-ZYGPAN]. It is important to note that analysis was conducted on data that was downloaded from BOLD on 27 February 2024. Therefore, the results are based on the BIN-statuses of that time.

The morphological terminology and abbreviations follow those proposed by Yoder (2004) and as used in Hymenoptera Anatomy Ontology (Yoder et al. 2010); the measurements follow Yoder (2004) and Chemyreva (2015, 2018). Terms of relative position follow Goulet and Huber (1993). The terms of sculpture description follow Eady (1968). The accurate taxonomic treatments of the genera and species *Zygota* and *Pantoclis* are given in Macek (1997) and Johnson (1992). Taxa that have received an updated taxonomic treatment, such as new species or synonyms, are newly diagnosed here. Sufficiently detailed diagnoses for all other species were given by Macek (1997). The general distribution of species was obtained and updated from Blank (2001), Wall (1963), Buhl (1995, 1997), Macek (1997), and Chemyreva et al. (2023). New records are marked with an asterisk (*). The following abbreviations for locations in Germany are used: BW= Baden-Württemberg, BY= Bavaria. Museum acronyms: SNSB-ZSM – Bavarian State Collection of Zoology, Munich; ZISP – Zoological Institute of the Russian Academy of Sciences, St. Petersburg, Russia; ZMUC – Zoological Museum, University of Copenhagen. A series of images were taken using an Olympus OM-D camera mounted on a Leica M125 C binocular and stacked using HELICON FOCUS (Version 8).

Taxonomy

Genus *Pantoclis* Förster, 1856

Type species. *Pantoclis barycera* Förster, 1861 (Figs 1A, B, 5E).

Diagnosis. Body black to yellowish brown; males macropterous, females alate to brachypterous or wingless; occipital carina always with occipital pit

(Fig. 1B, red arrow); fore tibiae of males always unmodified with homogeneous pubescence (Fig. 3H); submetapleural carina usually present, complete (Fig. 2A, green arrow) [if submetapleural carina missing, then venation as described below]; radial cell open to closed, variable in shape (Fig. 14); radialis not parallel to parastigma [if parallel (Fig. 3G, J) then angle between stigmal and marginal veins as described below]; angle between stigmal and marginal veins 130 degrees (Fig. 3G, J) or more; S2 always smooth, without punctured area on it in anterior half (Fig. 4F); male genitalia usually slender, apex of aedeagus distinctly convex (Fig. 5I–L), lanceolate (Fig. 5F–L), rather truncate (Fig. 5E) [if genitalia short and stout with rounded aedeagus then fore wing with a closed radial cell], digitus usually diminished (Fig. 5E–L) [if not then fore wing with closed radial cell]; ovipositor usually long, at least as long as length of T2 [if ovipositor short then fore wing with closed radial cell].

Genus *Zygota* Förster, 1856

Zygota Förster, 1856: 128, 131, 133, 135. Type species: *Belyta abdominalis* Nees van Esenbeck, designated by Ashmead (1893).

Carinia Kieffer, 1905: 140. Type: *Carinia nitida* Kieffer, by monotypy and original designation. Synonymized with *Aclista* Förster by Kieffer (1910), with *Zygota* Förster by Muesebeck (1951).

Diagnosis. Body always black (only metasoma very rarely brown); males and females alate; occipital carina with or without occipital pit (Fig. 1C–F, red arrows); fore tibiae modified in some males or bear several stiff setae (Fig. 3B, E, F, I); submetapleural carina missing (Fig. 2B), or reduced; radial cell long, open at apex (except *Z. croton* Fig. 3C); radialis long and almost parallel to parastigma (Fig. 3D); angle between stigmal and marginal veins at most 120 degrees; some species with small depression (Fig. 4B) or micro-puncture sculpture on S2 in anterior half (Fig. 4A, C–E, green arrows); male genitalia short and stout, apex of aedeagus truncate or rounded, digitus large (Fig. 5A–D); complete ovipositor always short, at most as long as pygidium (8th + 9th tergite above, 7th sternite below).

Remarks. Based on the diagnoses and original descriptions of the species *Zygota caecutiens* (Kieffer, 1908), Z. *hemiptera* (Thomson, 1858), Z. *microtoma* (Kieffer, 1909), Z. *soluta* (Kieffer, 1907) and the generic diagnoses of *Zygota* and *Pantoclis*, these four species should be excluded from *Zygota* and considered as part of *Pantoclis*; *Pantoclis caecutiens* (Kieffer, 1908), comb. nov., *P. hemiptera* (Thomson, 1858), comb. nov., *P. microtoma* (Kieffer, 1909), comb. nov. and *P. soluta* (Kieffer, 1907), comb. nov. Moreover, based on the study of the type specimens the following species are transferred from *Zygota* to *Pantoclis*: *Pantoclis brevinervis* (Kieffer, 1909), comb. nov., *P. brevipennis* (Kieffer, 1908), comb. nov., *P. cursor* (Kieffer, 1908), comb. nov., *P. fossulata* (Thomson, 1858), comb. nov., *P. fuscata* (Thomson, 1858), comb. nov., *P. striata* (Kieffer, 1909), comb. nov., *P. subaptera* (Thomson, 1858), comb. nov., *P. sulciventris* (Kieffer, 1909), comb. nov. and *P. unicolor* (Kieffer, 1908), comb. nov. (see also Suppl. material 2 for an overview of type locations and the museums where the specimens are stored).

Zygota abdominalis **(Nees, 1834)**
Figs 1D, E, 4B, 5B–D

Belyta abdominalis Nees, 1834: 344, male.
Zygota abdominalis: Macek 1997: 37, male, female, neotype designation.

BOLD BIN. BOLD:AEJ6743.

Material examined. GERMANY: BY: NGS Schwarzes Moor, 09-Aug-2017, 1 ♂; Paehl, 21-Mar-2020, 24-Apr-2020, 4 ♂; Ammer mountains, 27-Aug-2016, 1 ♂; Kehlheim, 10-Apr-2017, 1 ♂; Balderschwang, 21-Sept–12-Oct-2017, 1 ♀, 4 ♂; Kehlheim, 23-Aug–08-Sept-2017, 1 ♂; NSG Romberg, 18-May–09-Jun-2018, 2 ♂; Paehl, 24-Apr–08-May-2020, 7 ♂; Rhoen mountains, 27-Jun–11-Jul-2018, 2 ♂; Ketterschwang, 01–16-Jul-2019, 1 ♂; Grafenreuth, 01–15-Jul-19, 4 ♂. BW: Malsch, 27-Jun–09-Jul-2011, 2 ♂; Gaggenau-Sulzbach, 02–21-Aug-2011, 1 ♀.

Distribution. Europe: Czech Republic, Germany, Poland, Russia (European part).

Zygota angularis **Macek, 1997**

Zygota angularis Macek, 1997: 54, male, female.

BOLD BIN. BOLD:ACQ5437.

Material examined. GERMANY: BY: Mittenwald, 30-Jul-2021, 1 ♂; Rhoen mountains, 11-Jul-2018, 3 ♂.

Distribution. Europe: Czech Republic, Germany*, Slovenia.

Zygota balteata **Macek, 1997**

Zygota balteata Macek, 1997: 40, male, female.

BOLD BIN. No BIN.

Material examined. GERMANY: BY: NSG Fellinger Mountain, 08-Jun-2013, 1 ♀, Grafenaschau, 2013, 1 ♀.

Distribution. Europe: Czech Republic, Germany*, Slovenia.

Zygota breviuscula **(Thomson, 1858)**
Figs 2B, 3E, 4A

Belyta breviuscula Thomson, 1858: 176, female.
Aclista sulcata Kieffer, 1909. Synonymized by Macek (1997).
Zygota larides Nixon, 1957. Synonymized by Macek (1997).

BOLD BIN. No BIN.

Material examined. GERMANY: BY: Ammer mountains, 05-Oct-2016, 1 ♀; Oberstdorf, 10–24-Jul-2016, 24-Jul-2016 and 28-Jun-2016, 15 ♂.

Distribution. Europe: Austria, Czech Republic, Germany, Hungary, Italy, Russia (European part), Slovenia, Sweden.

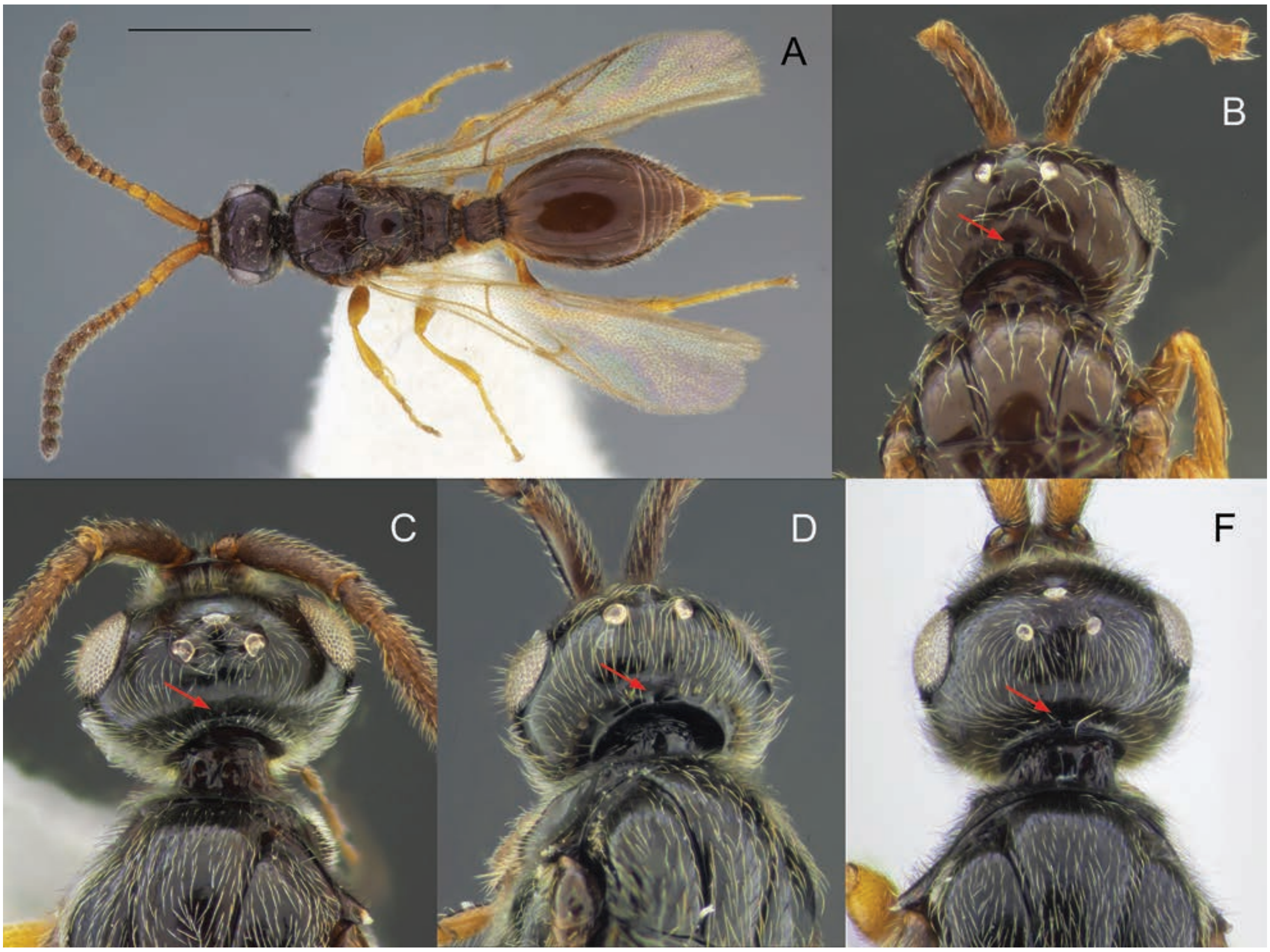

Figure 1. Morphological characters to identify the closely related genera *Zygota* and *Pantoclis* **A, E** female **B, C, D** males **A, B** *P. barycera* **C** *Z. walli* sp. nov. **D, E** *Z. abdominalis*. Scale bars: 1 mm (**A**); 0.5 mm (**B–F**).

Zygota claviscapa (Thomson, 1858)

Belyta claviscapa Thomson, 1858: 175, female, male.
Aclista brevicornis Kieffer, 1909. Synonymized by Macek (1997).

BOLD BIN. No BIN.

Material examined. Germany: BY: Garmisch-Partenkirchen, 2–13-Aug-2018, 3 ♂; Oberstdorf, 28-Jun-2016, 2 ♂; Grafenreuth, 1–15-Jul-19, 1 ♂.

Distribution. Europe: Austria, Czech Republic, England, Germany, Hungary, Ireland, Poland, Russia (European part), Scotland, Slovenia, Sweden.

Zygota comitans Macek, 1997

Zygota comitans Macek, 1997: 47, female, male.

BOLD BINs. BOLD:AEL3896, BOLD:AEJ0891.

Material examined. Germany: BY (BOLD:AEL3896): Moos, Isarmuendung, Hartholzauwald, 16-Jun-2021, 1 ♂; Chiemgauer Alpen, Ruhpolding, Fischbach, 02-Aug-2016, 1 ♂; Paehl, 24-Apr-2020, 1 ♂. BY (BOLD:AEJ0891): Berchtesgaden,

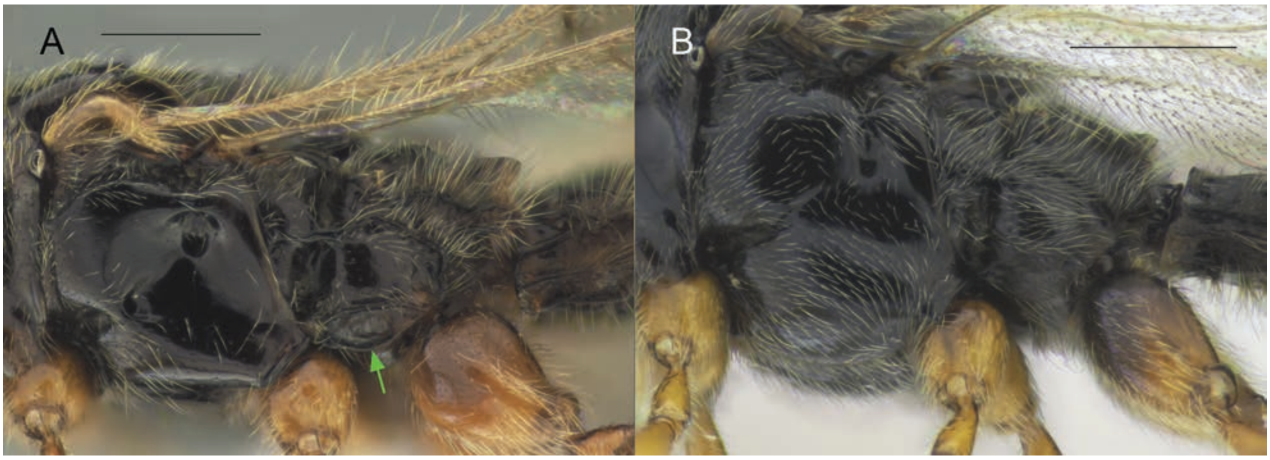

Figure 2. Morphological characters to identify the closely related genera *Pantoclis* (**A**) and *Zygota* (**B**) **A** *Pantoclis* spp., male **B** *Z. breviuscula*, male. Green arrow – submetapleural carina. Scale bars: 0.3 mm.

Bartholomae, NP Berchtesgarden, Wald, 13-Sep-2017, 1 ♀; Gaggenau, Michelbach, 21-Aug-2011, 1 ♀; Paehl, Niedermoor w Goasl, 19-Sep-2020, 1 ♀. BY (unsequenced material): Rhoen mountains, 27-Jun–11-Jul-2018, 3 ♂; Grafenaschau, 2013, 1 ♂; Oberstdorf, 28-Jun-2016, 1 ♂.

Distribution. Finland, Germany*, Poland, Slovenia, Sweden.

Zygota congener (Zetterstedt, 1840)

Figs 6A–F, 7A–F

Psilus (*Belyta*) *congener* Zetterstedt, 1840: 415, female, male.
Zygota caligula Buhl, 1997: 53, female. Syn. nov.

BOLD BIN. BOLD:AAI8609.

Material examined. ***Holotype*** of *Zygota caligula*: NORWAY: Mosvik, 14-Aug-1994, "MT. JT:19", "Smafa", P.N. Buhl det. 1996, Holotype, ZMUC 00021242, Zygota caligula, 1 ♀. GERMANY: BY: Garmisch-Partenkirchen, 02-Aug-2018, 13-Aug-2018, 09-Oct-2018, 4 ♂; Grafenaschau, 2013, 1 ♂ (Fig. 6E)

Diagnosis. Both sexes: postmarginal vein distinctly shorter than radial cell length (Fig. 7F); occipital pit present; mesopleuron with only small bare area medially or entirely pubescent (Fig. 6D); axillar depression with scattered setae and only 2 verriculate tubercles; propodeal spiracle distinctly enlarged (Fig. 6A); base of T2 with lateral corners (Fig. 6A); S2 without micro-puncture sculpture anteriorly. **Female:** female antenna with A6–A14 about 1.25 times as long as wide (Fig. 7B, C); T2 punctuated (Fig. 7B, C); T8 (apical) with median keel between cerci (Fig. 6E). **Male:** A3 strongly emarginate (Fig. 6B); fore tibia slightly modified, weakly humped interiorly, entirely pubescent and with a row of enlarged setae along its inner side (Fig. 6C); genitalia as in *Z. walli* sp. nov. and *Z. abdominalis* (Fig. 5A–D), digitus armed with 3 or 4 teeth.

Remarks. The female of *Zygota congener* is best recognized by the large propodeal spiracles (Fig. 6A) and the sharp median keel between the cerci on the apical tergite of the female (Fig. 6E). These two characters, together with other peculiarities of the morphology of *Z. congener*, correspond to the

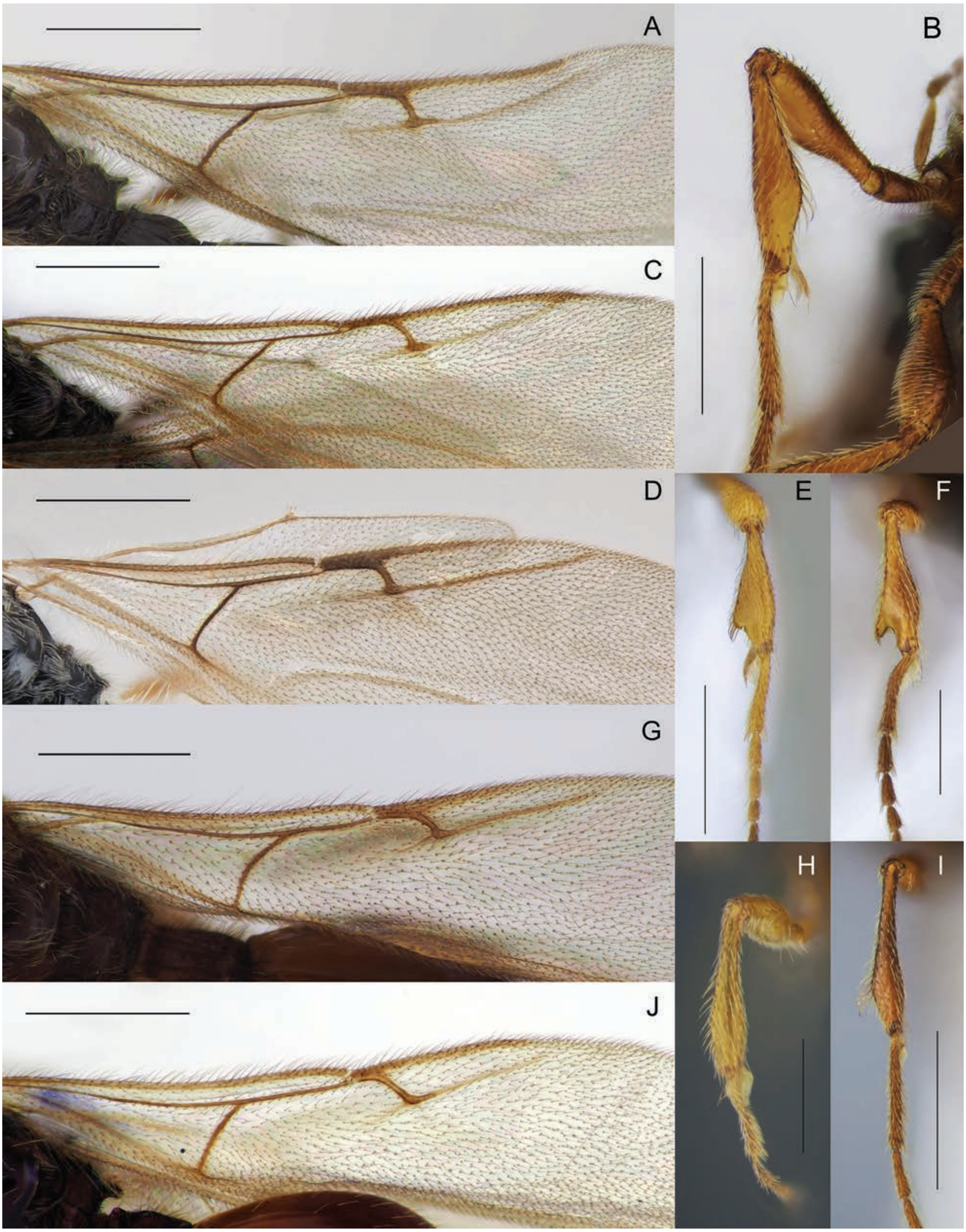

Figure 3. Venation (**A, C, D, G, J**) and fore tibia (**B, E, F, H, I**) morphology of males **A** *Zygota bensoni* **B** *Z. sordida* **C** *Z. croton* **D** *Z. walli* sp. nov. **E** *Z. breviuscula* **F** *Z. walli* sp. nov. **H** *Pantoclis* sp. **I** *Z. croton* **G, J** *Pantoclis* spp. Scale bars: 0.5 mm (**A–E, G, I, J**); 0.3 mm (**F, H**).

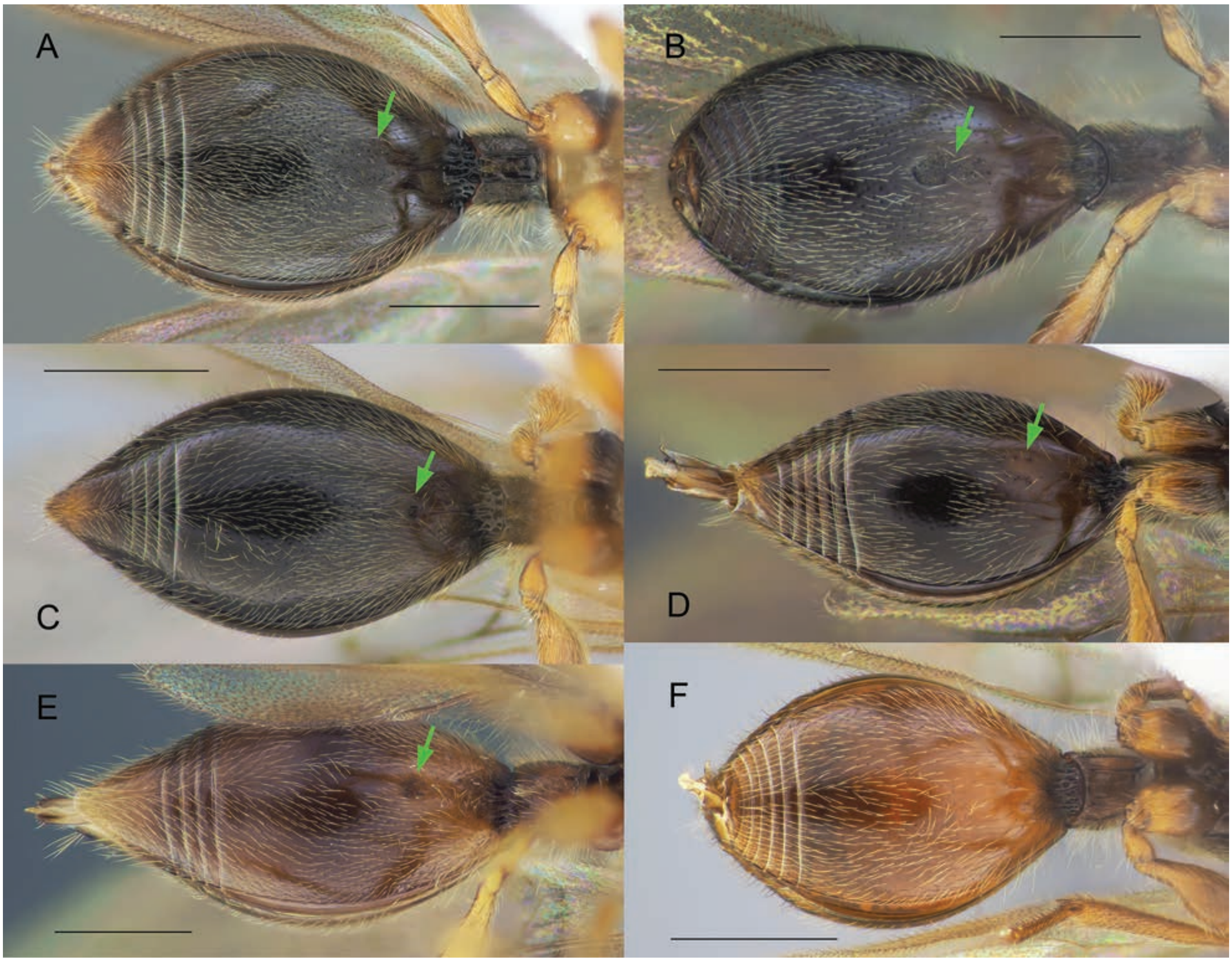

Figure 4. Ventral side of metasoma of females (**A, C, E**) and males (**B, D, F**) **A** *Zygota breviuscula* **B** *Z. abdominalis* **C, D** *Z. pubescence* **E** *Z. walli* sp. nov. **F** *Pantoclis* sp. Scale bar: 0.5 mm.

characters of the holotype of *Z. caligula* Buhl. For this reason, *Z. caligula* is considered here to be a junior synonym of *Z. congener*.

Distribution. Austria, Czech Republic, Denmark, Finland, Germany, Russia (European part), Slovenia, Sweden.

Zygota croton Nixon, 1957

Fig. 3C, I

Zygota croton Nixon, 1957: 29, 62, male, female.

BOLD BIN. BOLD:AEK1965.

Material examined. Germany: BY: Mittenwald, 30-Jul-2021, 1 ♂; Garmisch-Partenkirchen, 05-Jul-2018, 18-Jul-2018, 02-Aug-2018, 13-Aug-2018, 1 ♀, 16 ♂; Oberstdorf, 10-24-Jul-2016, 1 ♂.

Distribution. Europe: Austria, Czech Republic, France, Germany, Russia (European part), Scotland, Slovenia, Sweden.

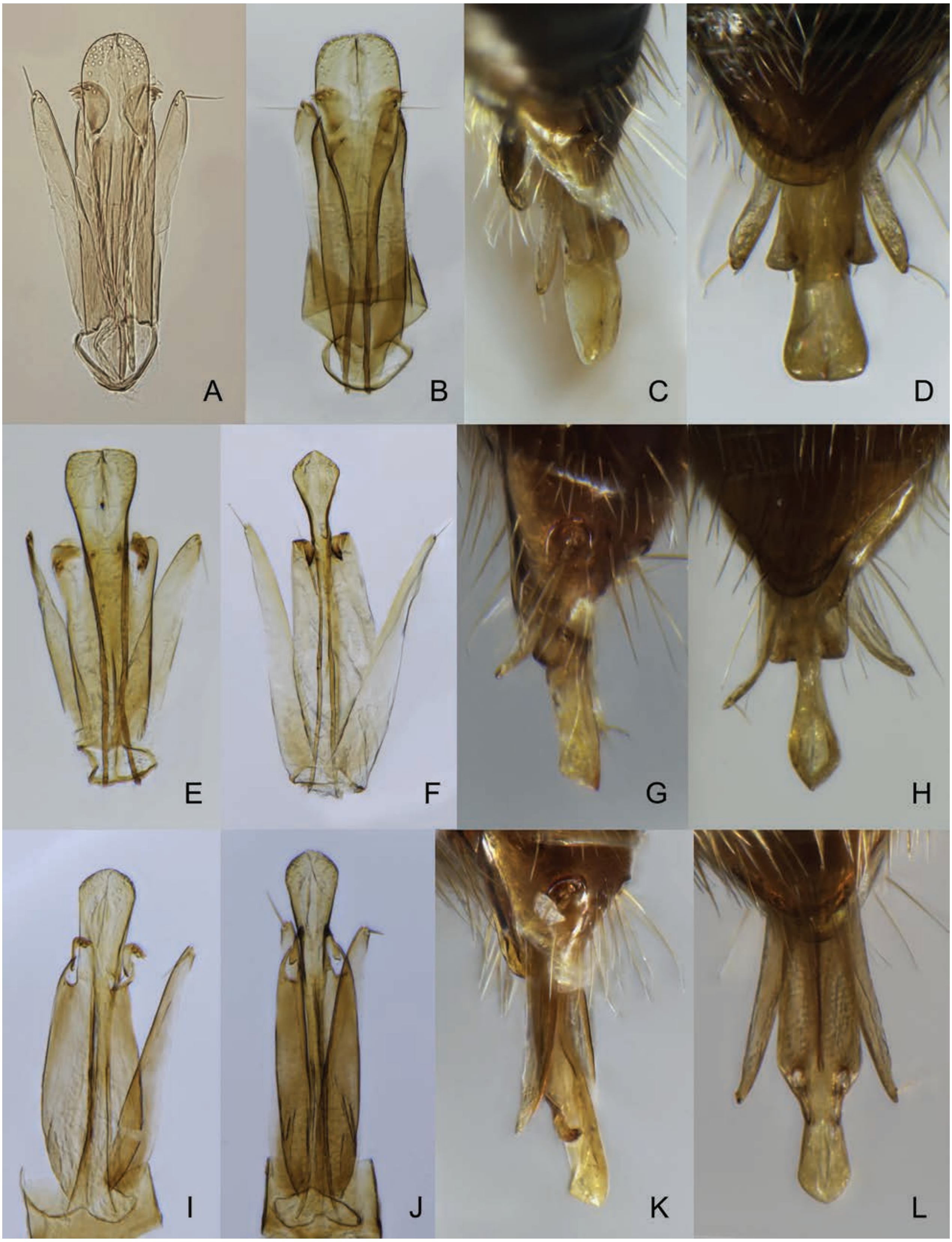

Figure 5. Male genitalia of *Zygota* and *Pantoclis* **A** *Z. walli* sp. nov. **B–D** *Z. abdominalis* **E** *P. barycera* **F–H** *Pantoclis* sp. 1 **I–L** *Pantoclis* sp. 2 **C, G, I, K** lateral view **A, B, D, E, F, H, J, L** ventral view.

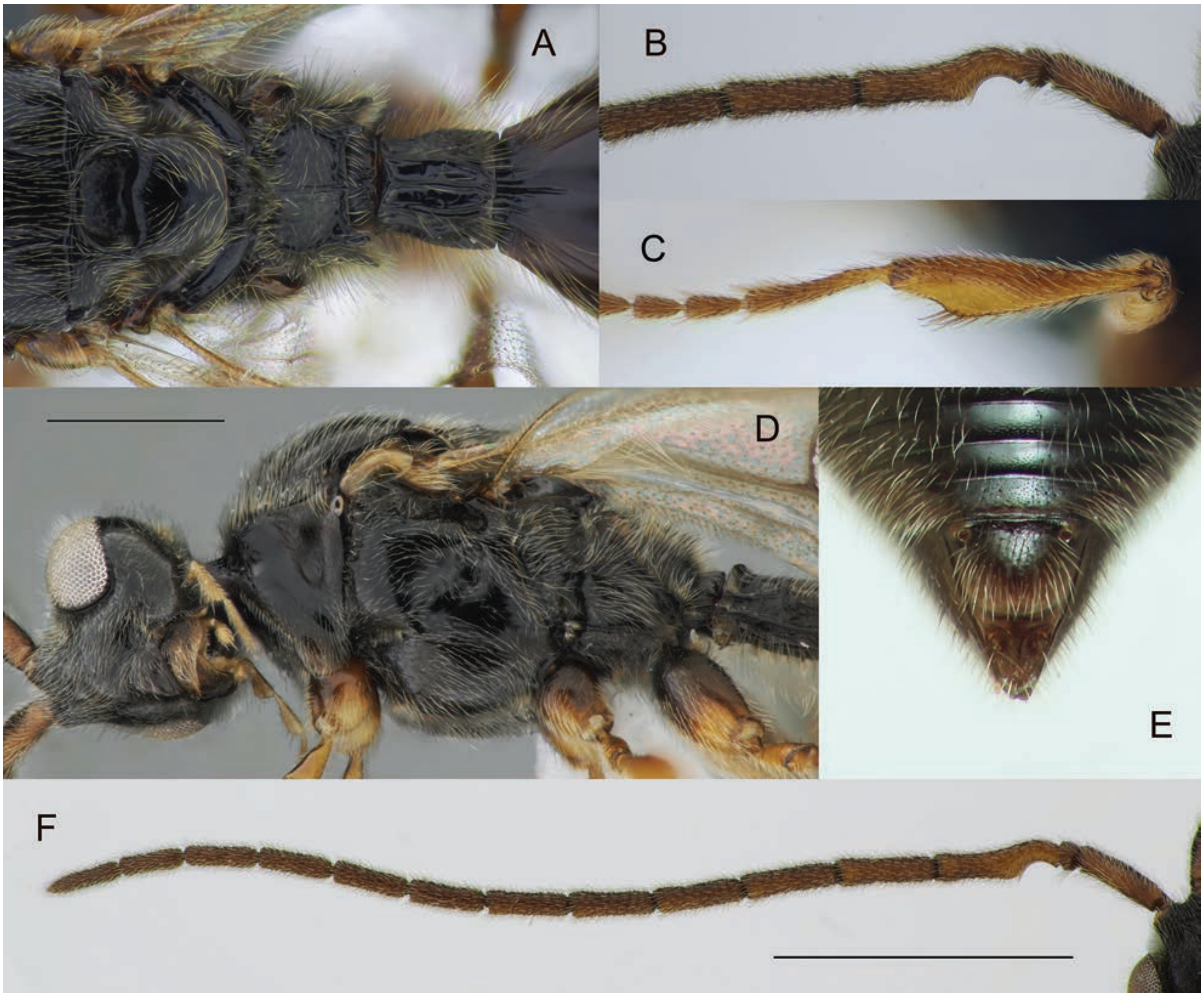

Figure 6. *Zygota congener*, male (**B–D, F**) and female (**A, E**) **A** mesosoma and petiole in dorsal view **B** A1–A5 in ventral view **C** fore tibia **D** head and mesosoma in lateral view **E** apex of metasoma in dorsal view (*Z. caligula* Buhl, holotype) **F** antennae in ventral view. Scale bars: 0.5 mm (**D**); 1 mm (**F**).

Zygota excisor (Zetterstedt, 1840)

Psilus (*Belyta*) *excisor* Zetterstedt, 1840: 415, male.
Aclista lanceolata Kieffer, 1909. Synonymized by Macek (1997).
Aclista lanceolata var. *fuscicornis* Kieffer, 1909. Synonymized by Macek (1997).
Aclista semirufa Kieffer, 1909. Synonymized by Macek (1997).
Aclista (*Zygota*) *excisipes* Kieffer, 1908. Synonymized by Macek (1997).

BOLD BIN. No BIN.

Material examined. Germany: BY: Lohr am Main, 06-Sep-2016, 1 ♂; Rhoen mountains, 11-Jul-2018, 1 ♂; Oberstdorf, 28-Jun-2016, 1 ♀; Ruhpolding, 19-Jul-2016, 1♂; Garmisch-Partenkirchen, 13-Aug-2018, 1 ♂.

Distribution. Europe: Austria, Czech Republic, Germany, Hungary, Italy, Poland, Russia (European part), Slovenia, Sweden.

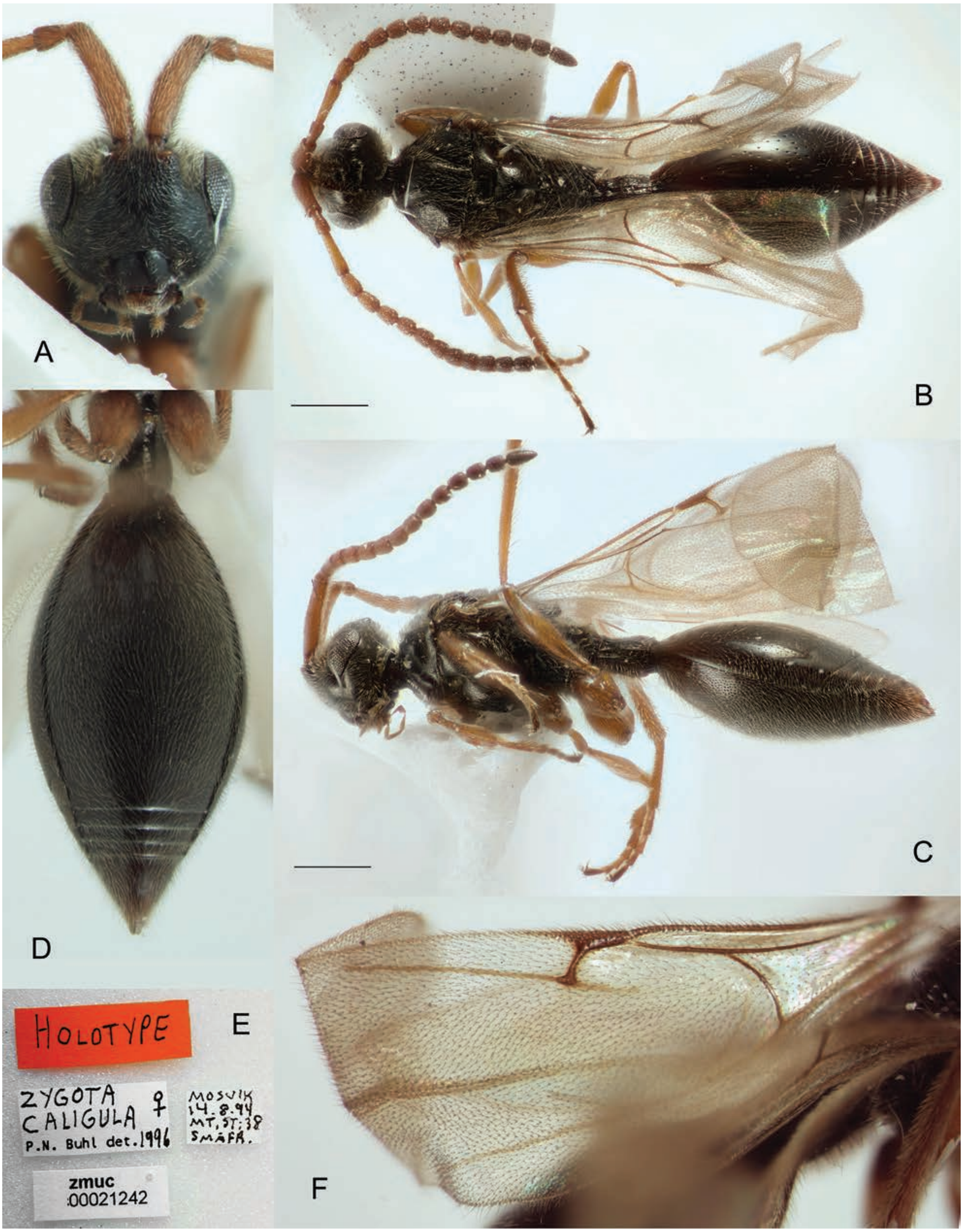

Figure 7. Holotype of the *Zygota caligula* Buhl **A** face **B** body in dorsal view **C** body in lateral view **D** metasoma, ventral view **E** type material labels **F** fore wing venation. Scale bar: 0.5 mm.

Zygota nigra **(Thomson, 1859)**

Belyta nigra Thomson, 1859: 175, female.
Aclista lanceolata Kieffer, 1909. Synonymized by Macek (1997).

BOLD BIN. BOLD:AEJ4945.

Material examined. Germany: BY: Mittenwald, 30-Jul-2021, 3 ♂, 1 ♂; Garmisch-Partenkirchen, 05-Jul-2018, 13-Aug-2018, 11-Sep-2018, 3 ♂.

Distribution. Europe: Algeria, Czech Republic, Germany, Russia (European part), Slovenia, Sweden.

Zygota parallela **(Thomson, 1859)**

Belyta parallela Thomson, 1859: 175, male.
Aclista macroneura Kieffer, 1909. Synonymized by Macek (1997).

BOLD BINs. BOLD:ACU1498, BOLD:AEJ0893.

Material examined. (BOLD:ACU1498) Germany: BY: Berchtesgaden, 11-Jun-2017, 3 ♂; Rhoen mountains, 27-Jun–11-Jul-2018, 2 ♀, 1 ♂; NSG Metzgergraben, 25-Jun-2016, 1 ♂; NSG Metzgergraben, 10–25-Jun-2016, 10 ♀, 37 ♂; Oberstdorf, 24-Jul-2016, 1 ♀, 17 ♂; Oberstdorf, 28-Jun-2016, 12 ♂; Siegenburg, 08–26-May-2017, 4 ♂; Grafenreuth, 01–15-Jul-2019, 1 ♀, 1 ♂; Paehl, 24-Apr-08-May-2020, 6 ♂; Rhoen mountains, 27-Jun-18-Jul-2018, 10 ♂; NSG “Schwarzes Moor”, 26-Jun–18-Jul-2017, 4 ♂. Material examined (BOLD:AEJ0893). Germany: BY: Sugenheim, 24-May-2021, 1? (ZSM-HYM-42355-A04); Garmisch-Partenkirchen, 13-Aug-2018, 1 ♀; Markt Nordheim, 02-May-2019, 1 ♂.

Distribution. Europe: Austria, Czech Republic, Germany, Hungary, Poland, Scotland, Slovenia, Sweden.

Zygota praetor **Nixon, 1957**

Zygota praetor Nixon, 1957: 58, 62, male, female.

BOLD BIN. No BIN.

Material examined. Germany: BY: Oberstdorf, 24-Jul-2016, 1 ♂.

Distribution. Europe: Czech Republic, Denmark, Germany, Ireland, Slovenia, Sweden.

Zygota pubescens **(Kieffer, 1909)**
Fig 4C, D

Aclista lanceolata var. *pubescens* Kieffer, 1909: 473. Female.
Pantoclis cameroni: Kieffer 1907. Synonymized by Macek (1997).

BOLD BIN. BOLD:ACC4346.

Material examined. Germany: BY: Mittenwald, 13-Jul-2021, 1 ♂; Paehl, 21-Mar-2020, 24-Apr–08-May-2020, 2 ♀, 1 ♂; Ketterschwang, 01–16-Jul-2019, 1 ♂; Balderschwang, 21-Sep–12-Oct-2017, 3 ♂; Rhoen mountains, 27-Jun–11-Jul-2018, 5 ♂; Garmisch- Partenkirchen, 02-Aug-2018, 1 ♀; NSG Allacher Lohe, 01-Sep-2021, 1 ♂; NSG Allacher Lohe, Munich, 08-Jun–23-Jun-2021, 3 ♂; NSG Metzgergraben, 10–25-Jun-2016, 2 ♂; Siegenburg 08–26-May-2017, 2 ♂; Oberstdorf, 10–24-Jul-2016, 2 ♂.

Distribution. Europe: Austria, Czech Republic, Germany, Italy, Russia (European part), Scotland, Slovenia, Sweden.

Zygota ruficornis **(Curtis, 1831)**

Fig. 8A–I

Cinetus ruficornis Curtis, 1831: 380, female.
Aclista dentatipes Kieffer, 1908: 447. Synonymized by Macek (1997).
Aclista norvegica Kieffer, 1912: 20. Synonymized by Macek (1997).
Zygota reticulata Kozlov, 1978: 575, female. Syn. nov.

BOLD BINs. BOLD:AEX2887, BOLD:AEK5610, BOLD:AEY0233.

Material examined. ***Holotype*** of *Zygota reticulata*: Russia: Kola Peninsula, Lake Vud'yavr basin, Khibiny Mountains, Kol'sk Mt., 18-Jun-1931, Fridolin leg., 1 ♀ (Fig. 8I). Germany: BY (BOLD:AEX2887): Mittenwald, 30-Jul-2021, 1 ♂. BY (BOLD:AEY0233): Paehl, 08-May-2020, 1 ♂; Mittenwald, 13-Jul-2021, 1 ♂. BY (BOLD:AEK5610): Mittenwald, 30-Jul-2021, 3 ♂; Garmisch-Partenkirchen, 18-Jul-2018, 02-Aug-2018, 4 ♂. BY (unsequenced material): Garmisch-Partenkirchen, 05-Jul-2018, 18-Jul-2018, 02-Aug-2018, 09-Oct-2018, 4 ♂; Garmisch-Partenkirchen, 13-Aug-2018, 1 ♀, 9 ♂; Bad Windsheim, 12-Jul-2020, 1 ♂; Aub, 21-May-2020, 1 ♂; Grettstadt, 20-May-2020, 1 ♀; Oberstdorf, 28-Jun-2016, 1 ♀, 6 ♂; Rhoen mountains, 27-Jun-11–Jul-2018, 21 ♂; Grafenreuth, 01–15-Jul-2019, 7 ♂; NSG Metzgergraben, 10–25-Jun-2016, 15 ♂; NSG Romberg, 18-May–09-Jun-2018, 3 ♂; Ketterschwang, 01–16-Jul-2019, 3 ♂; Siegenburg, 08–26-May-2017, 2 ♂; Garmisch-Partenkirchen, 02–13-Aug-2018, 2 ♂; NSG "Schwarzes Moor", 26-Jun–18-Jul-2017, 2 ♂; Paehl, 24-Apr–08-May-2020, 2 ♂; Kehlheim, 29-Jun–13-Jul-2017, 1 ♂; Lohr a. M., 03–14-Jun-2018, 1 ♂; NSG Allacher Lohe, Munich, 08–23-Jun-2021, 1 ♂. BW (unsequenced material): Malsch, 27-Jun–09-Jul-2011, 1 ♀, 4 ♂.

Diagnosis. Both sexes: postmarginal vein distinctly shorter than radial cell length (Fig. 8F); occipital pit present; mesopleuron with only small bare area on it medially or entirely pubescent (Fig. 8D); axillar depression with scattered setae and only 2 verriculate tubercles; base of T2 with small lateral corners (Fig. 8A). **Female:** T2 finely granulate (Fig. 8A); T8 without transverse or elongate carinae on it (Fig. 8B); S2 with a small pit in anteriorly half (as in Fig. 4C, green arrow). **Male:** A3 weakly emarginate (Fig. 8H); fore tibia broadened, with sharp projection and a row of strong setae on the top of it, bare at the apex on its anterior surface (Fig. 8G); S2 with a small area of micropuncture in anteriorly half (as in Fig. 4E, green arrow); digitus armed

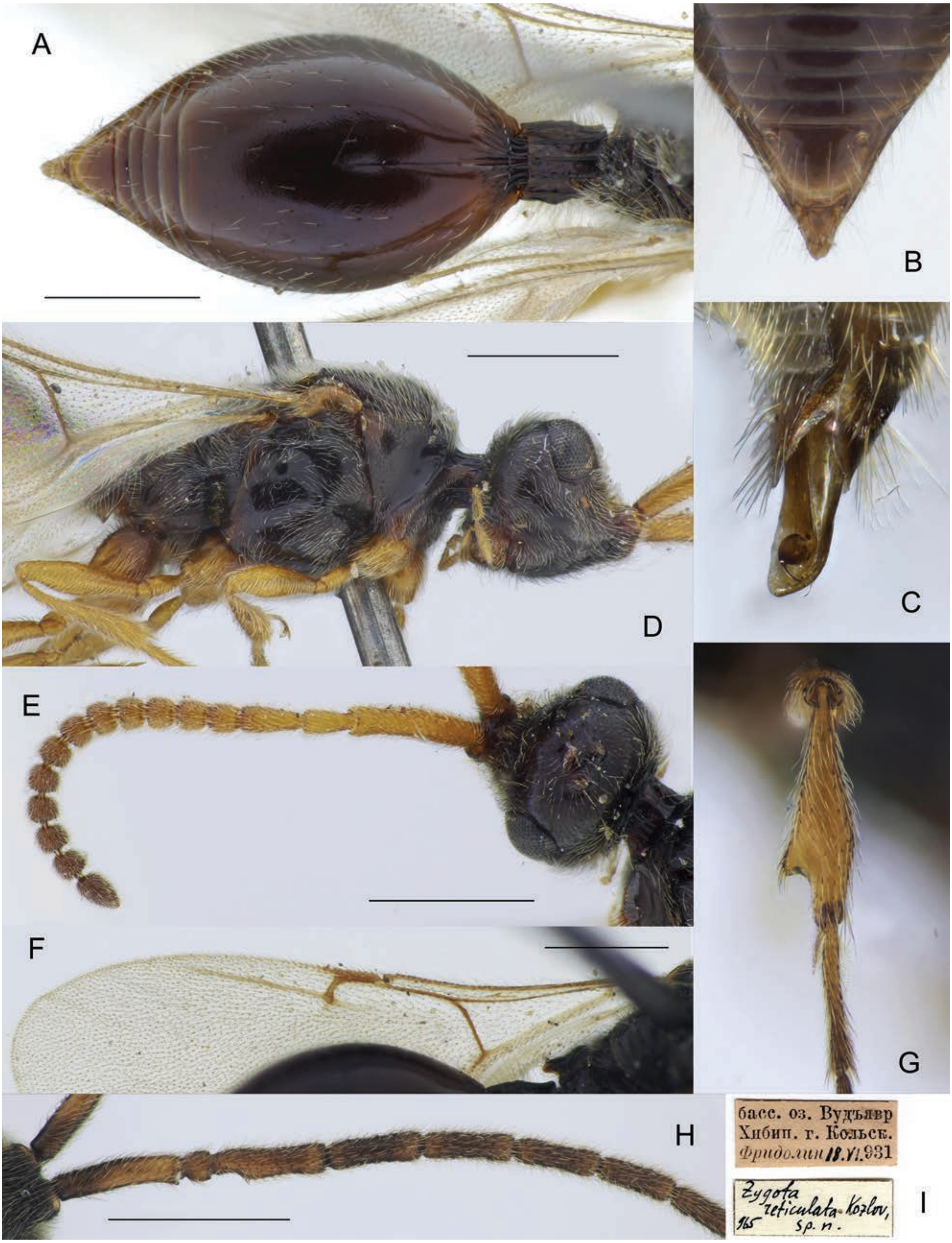

Figure 8. *Zygota ruficornis* male (**C, G, H**) and female (Z. *reticulata* Kozlov, holotype) (**A**, **B**, **D**, **E**, **F**) **A** metasoma, dorsal view **B** apex of metasoma, dorsal view **C** genitalia, lateral view **D** head and mesosoma, lateral view **E** antennae, dorsal view **F** fore wing **G** fore tibia **H** antenna, proximal part **I** label of the holotype. Scale bar: 0.5 mm.

with 1 long curved spine; spine extending from digitus at significant angle and not pushed towards it (Fig. 8C).

This species is very similar to *Z. pubescens* except as follows: female antenna stout, with A6–A14 distinctly transverse (A6–A14 subquadrate in Z. *pubescens*); male genitalia armed with a spine, which extends from digitus at significant angle (this spine pushed towards digitus in Z. *pubescence*). Both species are very common in Germany.

Distribution. Europe: Austria, Czech Republic, France, Germany, Hungary, Norway, Poland, Russia (European part), Scotland, Slovenia.

***Zygota sordida* Macek, 1997**

Fig. 3B

Zygota sordida Macek, 1997: 11, female, male.

BOLD BIN. No BIN.

Material examined. Germany: BY: Paehl, 24-Apr-2020, 1 ♂; Oberstdorf, 10–24-Jul-2016, 1 ♂.

Distribution. Europe: Austria, Czech Republic, Germany*, Slovenia.

***Zygota spinosa* (Kieffer, 1908)**

Aclista (*Zygota*) *spinosa* Kieffer, 1908: 448, male.
Zygota comes Nixon, 1957: 63, male. Synonymized by Macek (1997).
Zygota loris Nixon, 1957: 59, female. Synonymized by Macek (1997).

BOLD BINs. BOLD:AEL5584, BOLD:AER0775.

Material examined. Germany: BY (BOLD:AEL5584): Mittenwald, 13-Jul-2021, 30-Jul-2021, 2 ♂; Garmisch-Partenkirchen, 02-Aug-2018, 13-Aug-2018, 11-Sep-2018, 5 ♀, 6 ♂. BY (BOLD:AER0775): Garmisch-Partenkirchen, 02-Aug-2018, 1 ♂; Garmisch-Partenkirchen, 11-Sept-2018, 1 ♂.

Distribution. Austria, Czech Republic, Germany, Slovenia, Switzerland.

***Zygota spinosipes* (Kieffer, 1908)**

Aclista (*Zygota*) *spinosipes* Kieffer, 1908: 446, male.

BOLD BIN. BOLD:ACK3325, BOLD:AEY9457.

Material examined. Germany: BY (BOLD:ACK3325): Mittenwald, 30-Jul-2021, 1 ♀, 1 ♂; Garmisch-Partenkirchen, 11-Sep-2018, 2 ♀; NP Berchtesgaden, 09-Aug-2017, 1 ♀. BY (BOLD:AEY9457): Garmisch-Partenkirchen, 13-Aug-2018, 1 ♀; Mittenwald, 30-Jul-2021, 1 ♂, 1 ♀. BY (unsequenced material): Oberstdorf, 28-Jun-2016, 1 ♀.

Distribution. Europe: Czech Republic, Germany*, Italy, Russia (European part), Sweden.

Zygota vigil **Nixon, 1957**

Figs 9A–C, 10A–G

Zygota vigil Nixon, 1957: 65, male.

BOLD BIN. No BIN.

Material examined. Germany: BY: Garmisch-Partenkirchen, 18-Jul-2018, 1 ♂.

Diagnosis. Slender specimens with postmarginal vein clearly shorter than radial cell length (Fig. 9); marginal vein slightly longer than parastigma (Fig. 9C); occipital pit absent; mesopleuron with only small bare area medially (Fig. 10B); axillar depression with scattered setae and only 2 verriculate tubercles; petiole in dorsal view pubescent anteriorly; S2 without micro-puncture sculpture on its anterior half (Fig. 10C); emargination on A3 distinct but not deep, extending to 0.35 of the segment length; fore tibia not modified, entirely pubescent and with several enlarged setae along its inner side (Fig. 10D); petiole with inarticulated elongate carinae (Fig. 10E); base of T2 without lateral corners (Fig. 10E); digitus with two narrow and long spines (Fig. 9B).

Distribution. Europe: Austria, Germany*.

Remark. This species was described by Nixon based on a single male from Austria, but the type of the species was not found (J. Monks pers. com.). Unfortunately, it was not possible to create a BIN from the obtained sequence of the *Zygota vigil* male due to its length (461bp).

Zygota walli **sp. nov.**

https://zoobank.org/DC1B6471-36AC-4653-9044-4D277DFF9DF3

Figs 1C, 3D, F, 4E, 5A, 11A–F, 12A–E

BOLD BIN. BOLD:ACF9113, BOLD:AER4128.

Material examined. ***Holotype*** Germany. BY: Platt, Garmisch-Partenkirchen, 09-Oct-2028, lat. 47.406, long. 11.009, dv.zugsp6.6, ZSMHYM42437-A07, GBOL III leg., BOLD:ACF9113, SNSB-ZSM, 1 ♀.

Paratypes. BY (BOLD:ACF9113): Mittenwald, 13-Jul-2021, 30-Jul-2021, 1 ♀, 2 ♂; Garmisch-Partenkirchen, 05-Jul-2018, 09-Oct-2018, 2 ♀, 1 ♂.

Other material. Germany: BY (BOLD:AER4128): Garmisch-Partenkirchen, 2-Aug-2018 1 ♂; Mittenwald, 30-Jul-2021, 1 ♂; Garmisch-Partenkirchen, 09-Oct-2018, 1 ♂. BY (unsequenced material): Rhoen mountains, 11-Jul-2018, 1 ♂; Oberstdorf, 28-Jun-2016, 1 ♀; Garmisch-Partenkirchen, 13-Aug-2018, 1 ♂.

Diagnosis. Both sexes: postmarginal vein distinctly shorter than radial cell length (Figs 3D, 11B); occipital pit absent (Figs 1C, 11C); mesopleuron with only small bare area medially or entirely pubescent (Fig. 11D); axillar depression with scattered setae and only 2 verriculate tubercles; base of T2 with lateral corners (Fig. 12B); S2 with small sculptured area anteriorly (Fig. 4E, green arrow). **Female:** T2 mainly smooth with few scattered micropunctures (Fig. 12B); T8 with distinct transverse carinae (Fig. 11E, 12A). **Male:** A3 distinctly emarginated (Fig. 12C); fore tibia distinctly modified, broadened with sharp projection and a row of strong setae on the top of it, bare at the apex on its anterior sur-

Figure 9. *Zygota vigil* Nixon, male **A** whole insect in lateral view **B** male genitalia **C** fore wing venation. Scale bar: 1 mm.

face (Fig. 3F); digitus armed with 3 teeth (Fig. 5A). *Zygota walli* sp. nov. differs from all other species mentioned by Macek (1997) in the absence of the occipital pit (Fig. 1C, red arrow).

Description. Female (*holotype*). Body length 3.2 mm, antenna length 2 mm, wing length 2.6 mm. Body mainly black with metasoma dark brown; antennae, palpi, mandibles, tegula, legs and venation brown (Fig. 11B).

Figure 10. *Zygota vigil* Nixon, details of morphology, male **A, B** head and mesosoma in dorsal (**A**) and lateral (**B**) views **C, E** metasoma, in ventral (**C**) and dorsal (**E**) views **D** fore tibia **F, G** antennae in dorsal view. Scale bars: 0.5 mm (**B**); 1 mm (**F**).

Head in dorsal view as long (measured with antennal shelf) as wide. Toruli separated from each other by narrow and shallow furrow and from front posteriorly with deep pubescent depression. Ocelli small, OOL twice as long as POL. Eye densely pubescent. Eye diameter 1.2 as long as malar space. Pleurostomal distance as

Figure 11. *Zygota walli* sp. nov. female holotype (ZSMHYM42437-A07) **A** face **B** whole body in dorsal view **C** head, dorsal view **D** head and mesosoma in lateral view **E** apex of metasoma, dorso-lateral view **F** head and mesosoma in lateral view. Scale bar: 1 mm.

long as malar space. Occipital carina narrow, almost smooth, without occipital pit (Fig. 11C). Head in lateral view as high as long, in frontal view subtriangular, with face smooth and shining. Antennal shelf rugose below toruli in frontal view. Subantennal furrows very short (Fig. 11A). Epistomal sulcus distinct, clypeus convex and smooth. Tentorial pits situated in small hollows. Mandibles not prominent.

Antennae 15-segmented (Figs 11B, 12E). A1 cylindrical, as long as A2–A5 combined, slightly curved, with simple apical rim. A3–A14 as long as wide

Figure 12. Details of *Zygota walli* sp. nov. morphology, female (**A, B, D**) and male (**C, D**) **A** apex of metasoma **B** metasoma in dorsal view **C** A1–A4 in dorsal view **D** antenna in lateral view **E** antenna in dorsal view. Scale bar: 0.5 mm.

to slightly transverse: A7–A9 weakly wider than A13–A14. A15 1.7 times as long as wide.

Mesosoma convex, 1.2 times as wide as the head. Pronotal shoulders weakly convex, with transverse carina between them. Epomia with long lower branch and short lateral branch. Lateral part of pronotum strongly impressed, smooth and shining. Mesonotum convex, with percurrent notauli, converging posteriorly. Scutellum convex, smooth, with oval anterior scutellar pit. Axillar depressions smooth, densely pubescence, with a pair of vericulate tubercles. Mesopleuron smooth with deep mesopleural pit, with epicnemial and acetabular bridges (Fig. 11D). Metascutellum with strong median carina and lateral carinas. Metanotal trough smooth and bare. Propodeum slightly transverse, with round posterior rim. Median keel of propodeum simple. Both plicae parallel to each other, slightly projecting posteriorly. Lateral side of propodeum below plicae with lateral longitudinal carina, slightly projecting posteriorly. Fore tibia simple with homogeneous strengthened bristles on the inner side.

Wings. Marginal vein strongly developed, 3.9 times as long as wide (measured medially) and 1.45 times as long as distance from it to basal vein. Radial cell open, radialis long and nebulous (Fig. 11B). Postmarginal vein slightly shorter than stigmal vein; stigmal and postmarginal veins form 65° angle, stigmal vein 0.5 times as long as marginal vein.

Petiole cylindrical, entirely covered with semi-erect pubescence and elongate keels, ventrally with a row of verriculate tubercles. Base of T2 with slightly indicated lateral corners, short medial furrow and straight striation flanked at each side (Fig. 12B). S2 entirely pubescent, base of S2 with group of verriculate tubercles. Apical tergite (T8) with transverse sharp keel (Figs 11E, 12A), smooth and bare anteriorly and smooth and setose posteriorly from the transverse keel.

Male. Head distinctly transverse, as wide as mesosoma. Antennae 14-segmented with A4–A14 cylindrical, A3 with keel and emargination extending to 0.35–0.40 of the segment length (Fig. 12C, E). Fore tibia modified, acutely angled on the inner side and covered at the top with several minute bristles (Fig. 3F). Excavation on the fore tibia bare and shining in frontal view. Postmarginal vein 0.5–1.5 times as long as marginal vein (Fig. 3D). Marginal vein 1.3 times as long as distance from it to basal vein or slightly shorter. Petiole 1.5–2.1 times as long as its median width.

Etymology. This newly described species is named after the diapriid taxonomist Ingmar Wall who made himself a name in the Diapriidae research for years.

Distribution. Europe: Germany (Bavaria).

Discussion

As a result of our study, new combinations were proposed for 13 of 20 species which have a yet questionable taxonomic position, and two names (*Zygota caligula* Buhl and *Z. reticulata* Kozlov) were considered synonyms. One species of the genus *Zygota*, *Z. maura* (Kieffer, 1910) remains unstudied and inexplicable. Based on the emarginated fore tibia in males, mentioned in the original description, this species should be without doubt classified in the genus *Zygota* (Kieffer 1910). However, the type specimen of this species has not been found, and the description is not detailed enough to allow further conclusions at the species level or potential synonymies. The types of the two species *Z. strigata* Kozlov, 1978 and *Z. groenlandica* Buhl, 1995 were examined, and both are valid taxa of *Zygota*. *Zygota cilla* Nixon, 1957 and *Z. vigil* Nixon, 1957 were not included in Macek ́s (1997) revision because of the lack of relevant material. Nixon (1957) based both species on a single female (*Z. cilla*) and a single male specimen (*Z. vigil*), yet neither type has been found. The first discovery of a male *Z. vigil* since the description of the species is given here. A female of *Z. cilla*, which is unique in its morphology (Nixon 1957), was not found during this research. Thus, the taxonomic position of all Palearctic species (Johnson 1992, Buhl 1995, 1997, Macek 1997) listed in *Zygota* but not mentioned in Macek ́s (1997) revision, are discussed in this article.

Molecular-based analysis, which was conducted in the framework of this and previous works of GBOL III, has recovered rather poor results for the genus *Zygota* (and others of the Belytinae tribes Cinetini and Belytini; ~68% sequencing success rate) when compared to other diapriid taxa (~90%). Therefore, we recommend future studies invest their efforts into the development of a specific primer set to improve sequencing success. Nevertheless, we significantly improved the amount of genetic information that is available online. Prior to this study, BOLD listed a total of 391 public records that were assigned to 26 BINs globally. Our dataset DS-ZYGPAN presents 178 *Zygota* records and 19 BINs from Germany alone (see also Suppl. material 3).

In this study, some *Zygota* morphospecies were assigned to more than one BIN. This can happen for a variety of reasons: incomplete lineage sorting, heteroplasmy, NUMTs, hybridisation, recent speciation, cryptic species, phylogeographic effects, introgression or endosymbionts or their combinations can influence the outcome of genetically sorting of different OTUs (Raupach et al. 2016). Another factor that plays a key role in the construction of a BIN is the DNA barcoding gap difference between the highest intra- and smallest interspecific variation of a certain taxon. A typical threshold in the genetic distance between two species ranges from 10–15%, but this can vary immensely (Meier et al. 2006, Hebert et al. 2016, Raupach et al. 2016). In our case, 10–15% was indeed a fitting value to delimit species with CO1. A MEGA mean group distance analysis (Suppl. material 3) confirmed our morphological findings, namely, that specimens assigned to the same morphological species all displayed smaller genetic distances between one another than between other morpho-species: *Z. comitans* (mean group distance within all sequences of the BIN: 7%), *Z. spinosa* (5.4%), *Z. parallela* (5.8%), *Z. spinosipes* (6.3%), *Z. ruficornis* (three BINs; 5.3%, 3.5%, 4.3%) and *Z. walli* sp. nov. (2.6%). The corresponding specimens of each BIN cluster together in the taxonomic ML-tree (see Suppl. material 1). An ASAP analysis of the genetic material confirmed the BIN clusters for the genus *Zygota*. The highly variable genus *Pantoclis*, on the other hand, displayed less resemblance when comparing the BINs with ASAP clusters. All of those questionable records were only represented by one or two sequences in our dataset which might explain their uncertain placement.

A subset of the available CO1 sequence data of species of the tribe Belytini was used to construct a phylogenetic ML-tree (Fig. 13). Here, the genera *Zygota* and *Pantoclis* were displayed as well-supported sister groups within the Belytini. Fig. 14 shows a more detailed tree with records from all *Pantoclis* BINs we investigated. The data show that some species with an open radial cell are grouped and demonstrate close genetic relationships with species that clearly belong to *Pantoclis* and have a closed radial cell. These findings suggest that the character state of the radial cell reduction cannot be used as an appropriate feature for genus designation. Nixon (1957) also noticed these differences between *Zygota* species and the group of *Pantoclis* species with an open radial cell. He proposed to aggregate them into the *Z. fuscata* – species group "... because of the form of the radial cell and better development of the radialis, this group is transitional between *Pantoclis* and *Zygota* and has perhaps more relationships to the former genus [*Pantoclis*] than to *Zygota* s. str." (Nixon 1957). Nixon placed six species (*Z. fuscata*, *Z. microtoma*, *Z. striata*, *Z. brevinervis*, *Z. soluta*, *Z. fossulata*) in the *Z. fuscata* – species group which have been transferred to *Pantoclis* here.

In addition, the species transferred to the genus *Pantoclis* in this research are not similar to *Zygota* species in other key characteristics. Unlike *Zygota* species, males of *Pantoclis* never display a modified fore tibia and most of them have slender genitalia with lanceolate apex of aedeagus and a diminished digitus. On the contrary, some *Zygota* males have the digitus with a single strong curved spine, while similar structures are not known for the *Pantoclis* species. All females of *Zygota* show a very short ovipositor, while many *Pantoclis* females (with closed or

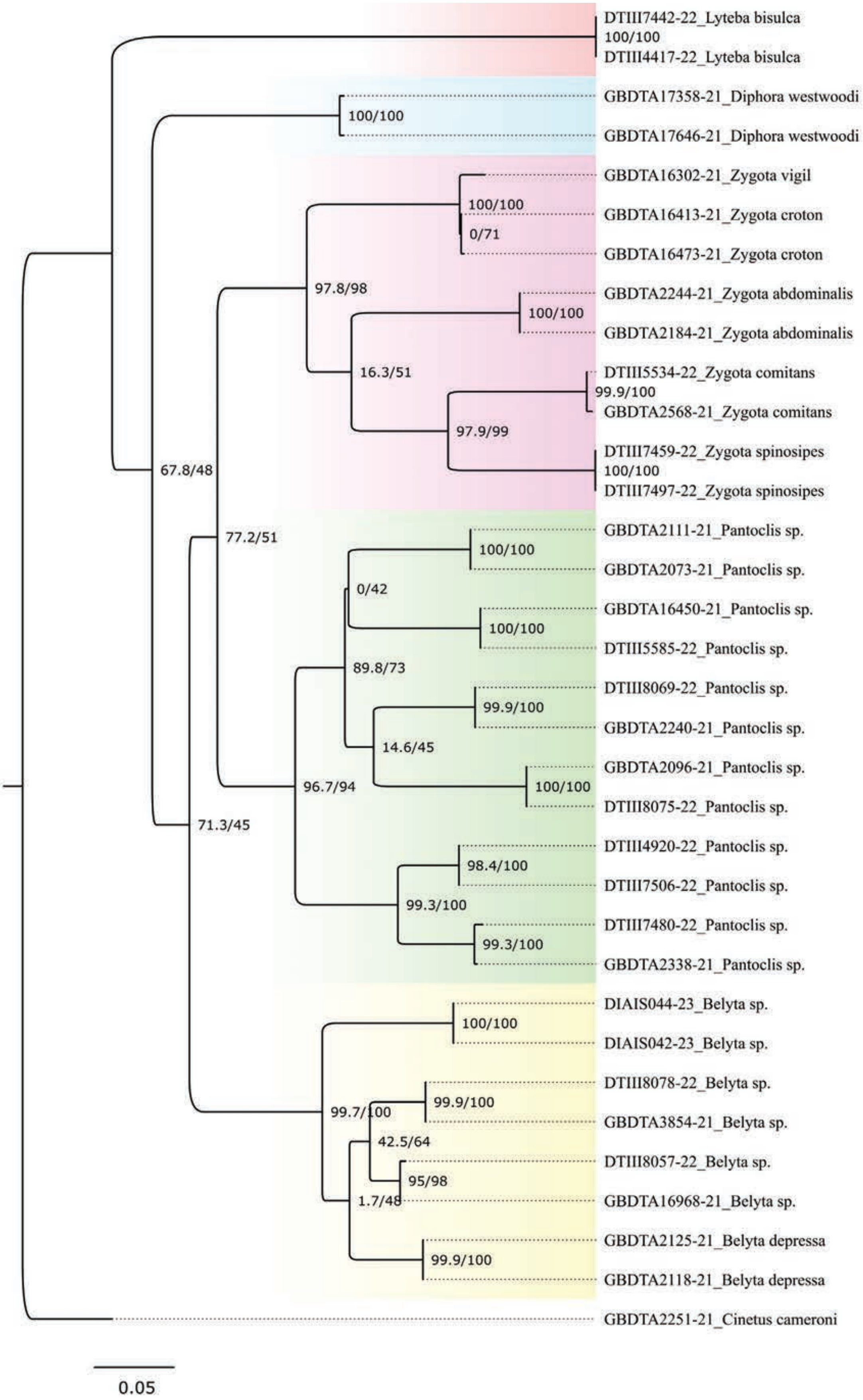

Figure 13. Phylogenetic ML consensus tree of barcoded Belytini specimens with bootstrap/jackknife values and *Cinetus cameroni* as an outgroup.

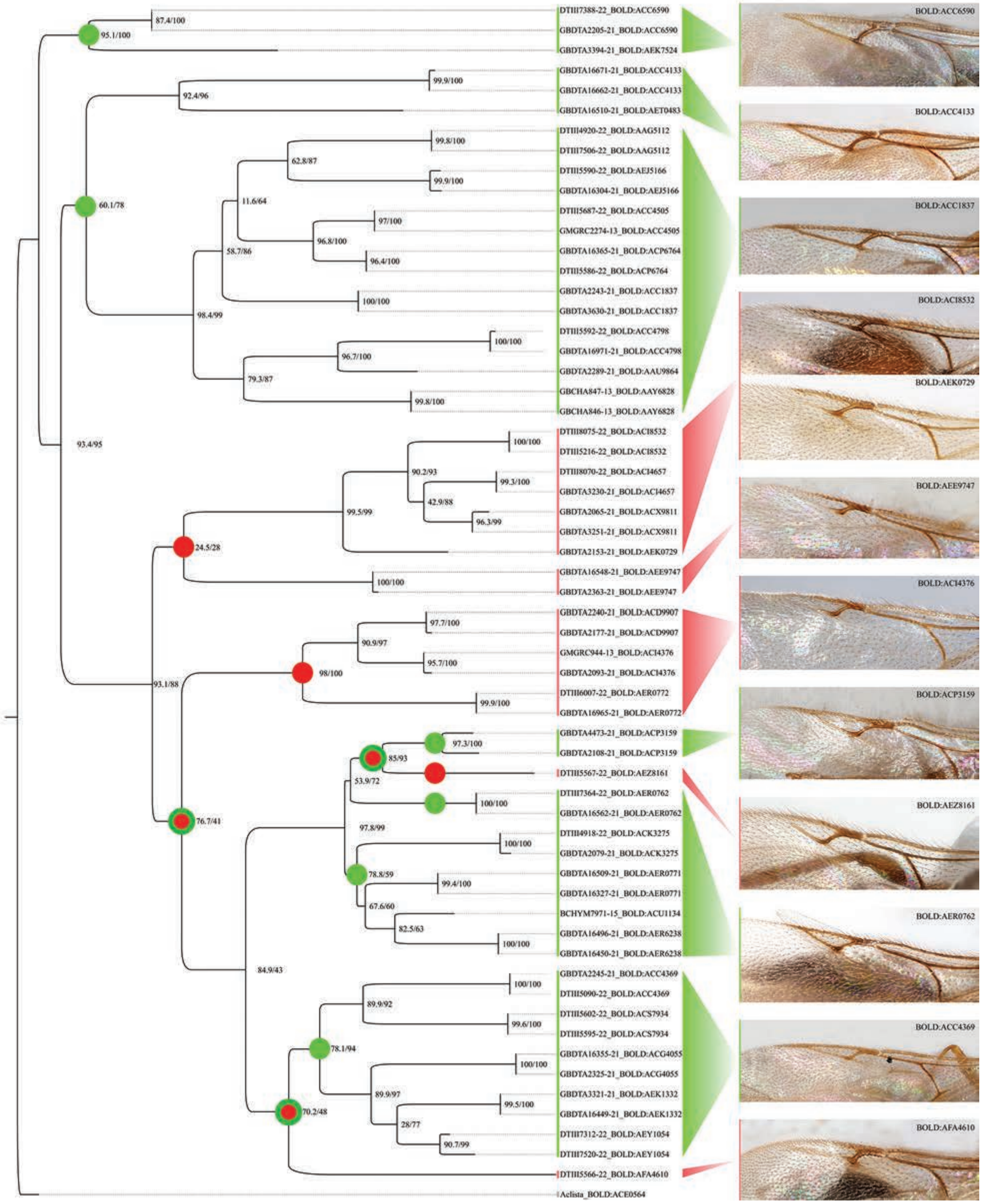

Figure 14. Phylogenetic ML tree of barcoded *Pantoclis* material and the polyphyletic appearance of their wing venation. Green represents the taxa with a closed radial cell while species with an open cell are color-coded red. Each node's support is displayed by the bootstrap and the jackknife values. *Aclista* was used as an outgroup.

open radial cell) show a long ovipositor (Fig. 1A). Thus, combining this morphological information with our understanding of the genus *Pantoclis* (see the diagnosis of the genus proposed above), and taking data on the venation variability based on the molecular data into consideration, we propose in this study, new combinations for 13 species previously listed in the genus *Zygota* (Suppl. material 2).

Because a detailed revision of *Pantoclis* is still lacking, it is important to note that the diagnosis presented here is preliminary. The high amount of variation in the morphology and the large species richness of the genus suggest that *Pantoclis* is paraphyletic. On the other hand, as a consequence of the taxonomic changes proposed here, the monophyly of the *Zygota* is now less controversial based on species morphology.

Acknowledgements

Thanks are due to Lars Vilhelmsen (ZMUC) and Joseph Monks (NHM) for providing crucial information and images of type material.

Additional information

Conflict of interest

The authors have declared that no competing interests exist.

Ethical statement

No ethical statement was reported.

Funding

This work was partly supported by Russian State Research (project 122031100272-3). Our work is part of the German Barcode of Life III: Dark Taxa project and was funded by the German Federal Ministry of Education and Research (FKZ 16LI1901B).

Author contributions

Conceptualization: VC. Data curation: JH, VC. Formal analysis: VK, JM, JH, VC. Funding acquisition: JH. Investigation: VK, JH, JM, VC. Project administration: VC. Resources: JH. Validation: VK, VC. Visualization: JH, VC. Writing – original draft: JH, JM, VC. Writing – review and editing: VK.

Author ORCIDs

Jeremy Hübner https://orcid.org/0009-0007-5624-8573
Vasilisa Chemyreva https://orcid.org/0000-0002-6547-6259
Jan Macek https://orcid.org/0000-0003-3104-325X
Viktor Kolyada https://orcid.org/0000-0001-8628-1365

Data availability

All of the data that support the findings of this study are available in the main text or Supplementary Information.

References

Ashmead WH (1893) 45 A Monograph of the North American Proctotrypidae. Government Printing Office, Washington, 472 pp. https://doi.org/10.5479/si.03629236.45.1

Ashmead WH (1902) Classification of the pointed-tailed wasps, or the superfamily Proctotrypidae. Journal of the New York Entomological Society 10: 240–247.

Blank SM (2001) Diapriidae. In: Dathe HH (Ed.) Verzeichnis der Hautflügler Deutschlands. Fauna Germanica. Entomofaunistische Gesellschaft e.V., Dresden, 34–43.

Buhl PN (1995) The proctotrupoid wasps of Greenland (Hymenoptera, Proctotrupoidea s.l.). Entomologiske Meddelelser 63: 7–10.

Buhl PN (1997) On some new or little known species of Belytinae from Norway (Hymenoptera: Diapriidae). Folia Entomologica Hungarica 58: 45–55. https://doi.org/10.1080/00305316.1998.10433766

Buhl PN (1998) New or little known Oriental and Australasian Belytinae (Hymenoptera: Diapriidae). Oriental Insects 32(1): 41–58. https://doi.org/10.1080/00305316.1998.10433766

Chemyreva VG (2015) Three new species of the parasitic wasps genus *Spilomicrus* Westwood (Hymenoptera: Diapriidae) from the East Palaearctic Region. Zootaxa 4059(1): 191. https://doi.org/10.11646/zootaxa.4059.1.11

Chemyreva VG (2018) The Eastern Palaearctic parasitic wasps of the genus *Spilomicrus* Westwood, 1832 (Hymenoptera: Diapriidae). Far Eastern Entomologist = Dal'nevostochnyi Entomolog 357: 1–20. https://doi.org/10.25221/fee.357.1

Chemyreva VG, Humala AE, Kolyada VA (2023) Faunistic notes on the Diapriidae family (Hymenoptera) of Karelia. Russian Entomological Journal 32: 187–193. https://doi.org/10.15298/rusentj.32.2.08

Eady RD (1968) Some illustrations of microsculpture in the Hymenoptera. Proceedings of the Royal Entomological Society of London. Series A, General Entomology 43(4–6): 66–72. https://doi.org/10.1111/j.1365-3032.1968.tb01029.x

Förster A (1856) Hymenopterologische Studien. 2. Heft. Chalcidiae und Proctotrupii. Ernst ter Meer, Aachen, 152 pp.

Goulet H, Huber JT (1993) Hymenoptera of the world: an identification guide to families. Centre for Land and Biological Resources Research, Ottawa, Ontario, 668 pp.

Hausmann A, Krogmann L, Peters RS, Rduch V, Schmidt S (2020) GBOL III: DARK TAXA. iBOL Barcode Bulletin 10. https://doi.org/10.21083/ibol.v10i1.6242

Hebert PDN, Ratnasingham S, Zakharov EV, Telfer AC, Levesque-Beaudin V, Milton MA, Pedersen S, Jannetta P, deWaard JR (2016) Counting animal species with DNA barcodes: Canadian insects. Philosophical Transactions of the Royal Society of London. Series B, Biological Sciences 371(1702): 20150333. https://doi.org/10.1098/rstb.2015.0333

Johnson N (1992) Catalog of world species of Proctotrupoidea, exclusive of Platygastridae (Hymenoptera). Memoirs of the American Entomological Institute 51: 1–825. https://doi.org/10.5281/zenodo.23657

Kieffer JJ (1909) Proctotrypidæ (suite). Species des Hyménoptères d'Europe et d'Algérie 10: 449–592.

Kieffer JJ (1910) Fam. Belytidae. Genera Insectorum 107: 1–47.

Kozlov MA (1978) Fam. Diapriidae. In: Medvedev GS (Ed.) Opredelitel' nasekomykh evropeyskoy chasti SSSR [Keys to the insects of the European part of USSR] 3(2): 548–608. [Leningrad: Nauka] [In Russian]

Macek J (1995) Revision of the European species of *Belyta* Jurine. Acta Musei Nationalis Pragae, Series B. Historia Naturalis 51: 1–22.

Macek J (1997) Revision of Central European species of *Zygota* (Hymenoptera: Diapriidae) with description of new species and taxonomic remarks on the genus. Folia Heyrovskyana 5(1): 31–57.

Macek J (2007) Revision of Central European species of the *Aclista scutellaris* complex (Hymenoptera: Diapriidae). Acta Entomologica Musei Nationalis Pragae 47: 211–228.

Meier R, Shiyang K, Vaidya G, Ng PKL (2006) DNA barcoding and taxonomy in Diptera: a tale of high intraspecific variability and low identification success. Hedin M (Ed.) Systematic Biology 55: 715–728. https://doi.org/10.1080/10635150600969864

Muesebeck CF (1951) Superfamily Proctotrupoidea. In: Walkley LM (Ed.) Hymenoptera of America north of Mexico: Synoptic Catalog. Agriculture monograph. U.S. Dept. of Agriculture, Washington, D.C, 655–718.

Nixon GEJ (1957) Hymenoptera: Proctotrupoidea, Diapriidae subfamily Belytinae. Handbooks for the Identification of British Insects 8: 1–107. https://doi.org/10.5281/zenodo.23920

Puillandre N, Brouillet S, Achaz G (2021) ASAP: Assemble species by automatic partitioning. Molecular Ecology Resources 21(2): 609–620. https://doi.org/10.1111/1755-0998.13281

Rambaut A (2010) FigTree. http://tree.bio.ed.ac.uk/software/figtree/

Ratnasingham S, Hebert PDN (2007) BARCODING: BOLD: The Barcode of Life Data System (http://www.barcodinglife.org): BARCODING. Molecular Ecology Notes 7: 355–364. https://doi.org/10.1111/j.1471-8286.2007.01678.x

Raupach MJ, Amann R, Wheeler QD, Roos C (2016) The application of "-omics" technologies for the classification and identification of animals. Organisms, Diversity & Evolution 16(1): 1–12. https://doi.org/10.1007/s13127-015-0234-6

Tamura K, Stecher G, Kumar S (2021) MEGA11: Molecular Evolutionary Genetics Analysis Version 11. Molecular Biology and Evolution 38(7): 3022–3027. https://doi.org/10.1093/molbev/msab120

Trifinopoulos J, Nguyen L-T, von Haeseler A, Minh BQ (2016) W-IQ-TREE: A fast online phylogenetic tool for maximum likelihood analysis. Nucleic Acids Research 44(W1): W232–W235. https://doi.org/10.1093/nar/gkw256

Wall I (1963) Erster Beitrag zur Kenntnis der Verbreitung der mitteleuropäischen Proctotrupoidea (mit besonderer Berücksichtigung von Südbaden) 1. Diapriidae: Belytinae. Beiträge zur Entomologie = Contributions to Entomology 13: 902–911. https://doi.org/10.21248/contrib.entomol.13.7-8.902-911

Yoder MJ (2004) Revision of the North American species of the genus *Entomacis* (Hymenoptera: Diapriidae). Canadian Entomologist 136(3): 323–405. https://doi.org/10.4039/n03-061

Yoder M, Mikó I, Seltmann K, Bertone M, Deans A (2010) A gross anatomy ontology for Hymenoptera. PLOS ONE 5(12): e15991. https://doi.org/10.1371/journal.pone.0015991

Supplementary material 1

ML-tree with a subset of all *Pantoclis* and *Zygota* BINs available from our data with one *Aclista* sequence as outgroup

Authors: Jeremy Hübner, Vasilisa Chemyreva, Jan Macek, Victor Kolyada

Data type: png

Link: https://doi.org/10.3897/zookeys.1207.121725.suppl1

Supplementary material 2

Type information for the taxonomically treated and transferred *Zygota* species

Authors: Jeremy Hübner, Vasilisa Chemyreva, Jan Macek, Victor Kolyada

Data type: xlsx

Link: https://doi.org/10.3897/zookeys.1207.121725.suppl2

Supplementary material 3

Cluster analyses of the genetic results

Authors: Jeremy Hübner, Vasilisa Chemyreva, Jan Macek, Victor Kolyada

Data type: xlsx

Link: https://doi.org/10.3897/zookeys.1207.121725.suppl3

ZooKeys 1207: 355–368 (2024)
DOI: 10.3897/zookeys.1207.127297

Research Article

First record of *Orthohalarachne attenuata* in *Arctocephalus australis* in mainland Argentina (Parasitiformes, Mesostigmata, Dermanyssoidea, Halarachnidae) with observations on its ambulacral morphology

Andrés Osvaldo Porta[1,2,3], Juan Pablo Loureiro[4], Marcela Karina Castelo[5]

1 *División de Aracnología, Museo Argentino de Ciencias Naturales Bernardino Rivadavia, Av. Ángel Gallardo 470 C1405DJR, Buenos Aires, Argentina*
2 *Universidad de Buenos Aires, Facultad de Ciencias Exactas y Naturales, Departamento de Ecología, Genética y Evolución, Instituto de Ecología, Genética y Evolución de Buenos Aires (IEGEBA, UBA-CONICET), Pabellón II, Ciudad Universitaria, Buenos Aires C1428EGA, Argentina*
3 *Departamento de Ciencias Exactas, Universidad Nacional del Oeste, Belgrano 369 C1718, San Antonio de Padua, Buenos Aires, Argentina*
4 *Fundación Mundo Marino, Av. X 157, San Clemente del Tuyú B7105, Provincia de Buenos Aires, Argentina*
5 *Laboratorio de Entomología Experimental – Grupo de Investigación en Ecología de los Mares (LEE-GIEM), Instituto de Ecología, Genética y Evolución de Buenos Aires (IEGEBA-CONICET/UBA), Departamento de Ecología, Genética y Evolución, Facultad de Ciencias Exactas y Naturales, Universidad de Buenos Aires, Pabellón II, Ciudad Universitaria, Buenos Aires C1428EGA, Argentina*
Corresponding author: Marcela Karina Castelo (marcela.castelo@conicet.gov.ar)

Abstract

Pinniped respiratory mites of the species *Orthohalarachne attenuata* have been recorded from various locations around the world but not from continental Argentina. In the present work, we document for the first time the presence of *O. attenuata* on *Arctocephalus australis* on the Argentine mainland. A total of 23 adult and 381 immature mites were collected from the nose and nasopharyngeal cavity during a necropsy. The mite ambulacrum is described in adults and larvae. This structure consists of a pretarsus, an extensible pulvillum, a pair of claws and paradactyli (pretarsus opercula). The ambulacral structures also have some peculiarities, such as the presence of longitudinal furrows in the claws, straight claws in legs II and III (as opposed to curved in legs I and IV), and the fin-shaped paradactyli. The morphology of the ambulacrum of this mite is interpreted as an adaptation for anchoring to different surfaces of the host, and the protective structures present in the larvae as an adaptation for the dispersal phase in the external environment.

Key words: Acari, attachment structures, marine mammals, mites, Otariidae, parasites

Academic editor: Farid Faraji
Received: 11 May 2024
Accepted: 17 June 2024
Published: 24 July 2024

ZooBank: https://zoobank.org/7840CD5F-CCD7-44CB-B38B-37FC6BB07800

Citation: Porta AO, Loureiro JP, Castelo MK (2024) First record of *Orthohalarachne attenuata* in *Arctocephalus australis* in mainland Argentina (Parasitiformes, Mesostigmata, Dermanyssoidea, Halarachnidae) with observations on its ambulacral morphology. ZooKeys 1207: 355–368. https://doi.org/10.3897/zookeys.1207.127297

Introduction

Mites of the family Halarachnidae Oudemans, 1906 (Acari, Mesostigmata) are obligate parasites of the respiratory tract of a variety of mammals (Lindquist et al. 2009) and are usually found in the mucosa of the nasal cavity, upper respiratory tract, and lungs. Species in the genus *Orthohalarachne* affect otariids (sea lions and fur seals) and odobenids (walruses). Two species of *Orthohalarachne* have been described that affect marine mammals: *O. diminuata* (Doetschman, 1944) and *O. attenuata* (Banks, 1910).

Orthohalarachne attenuata has been reported as a parasite of several species of pinnipeds in various parts of the world, but not from mainland Argentina (Table 1). Adults and larvae are found in the upper respiratory tract of their hosts (Kim et al. 1980). Newell (1947) reported that *Orthohalarachne* species are found in the North Atlantic, the Pacific coast of North America, and the Islas Malvinas (Falkland Islands).

In terms of mite development, the larva of *O. attenuata* is an active stage that attaches to nasal structures. It can survive for several days without feeding and, after dispersal among hosts, is followed by two short or suppressed nymphal stages that do not feed and are generally not observed (Furman and Smith 1973). The adult is an active feeding stage, with individuals typically attaching themselves to tissues via tarsal structures that pierce the respiratory epithelium with chelicerae and feed on lymph and other body fluids (Dowling 2006). Females of *O. attenuata* are up to 4 mm long due to their elongated opisthosoma (Banks 1910). Newell (1947) undertook a systematic revision of the halarachnid mites parasitising Pinnipedia by observing morphological characters with light microscopy and established the genus *Orthohalarachne*. With advances in microscopy techniques, it is now possible to analyse morphological characters that are difficult to observe by light microscopy alone. In this sense, the specific adaptations of the host-tissue anchoring structures have not been described in detail.

Table 1. Otarid and odobenid species documented as hosts of *Orthohalarachne attenuata* mites in different parts of the world.

Host species	Common name	Reference(s)	Geographic area(s)
Arctocephalus australis (Zimmermann, 1783)	South American sea lion	Katz et al. 2012; Gastal et al. 2016; Seguel et al. 2018; Duarte-Benvenuto et al. 2022	Cabo Polonio, Isla de Lobos (Uruguay); Rio Grande do Sul, San Pablo state (Brazil); Punta San Juan (Peru)
Arctocephalus philippii townsendi Merriam, 1897	Guadalupe fur seal	Pesapane et al. 2021	Central California coast (USA)
Arctocephalus pusillus doriferus Wood Jones, 1925	Australian fur seal	Domrow 1963, 1974; Seawright 1964; Tubb 1937	Port Lincoln, Lady Julia Percy Island, Portarlington, Dangerous Reef, Seal Rocks and Geelong (Australia); New South Wales coast (England)
Callorhinus ursinus Linnaeus, 1758	Northern fur seal	Dunlap et al. 1976; Kim et al. 1980; Kikuchi and Okuyama 1987; Kuzmina et al. 2021; Pesapane et al. 2021	Pribilof Islands, St. Paul Island, Alaska (USA). Hokkaido (Japan); Central California coast (USA)
Eumetopias jubatus (Schreber, 1776)	Steller sea lion	Fay and Furman 1982; Konishi and Shimazaki 1998	Alaska (USA); Hokkaido (Japan)
Neophoca cinerea Peron, 1816	Australian sea lion	Domrow 1974; Marlow 1975; Nicholson and Fanning 1981	Port Lincoln, Dangerous Reef, Seal Rocks and Geelong, Kangaroo Island (Australia)
Odobenus rosmarus divergens (Illiger, 1815)	Pacific walrus	Fravel and Procter 2016	Alaska (USA)
Otaria flavescens Shaw, 1800	Southern sea lion	Finnegan 1934; Gómez-Puerta and Gonzales-Viera 2015; Seguel et al. 2018; Rivera-Luna et al. 2023	Islas Malvinas (Argentina); Lima, Punta San Juan (Peru); Valdivia (Chile)
Zalophus californianus (Lesson, 1828)	California sea lion	Pesapane et al. 2021, 2022	Central California coast (USA)
Zalophus wollebaeki Sivertsen, 1953	Galapagos fur seal	Kuzmina et al. 2018; Pesapane et al. 2021	Central California coast (USA)

In this article, we report for the first time the presence of *O. attenuata* in continental Argentina parasitizing *A. australis*, describe in detail the morphology of the ambulacrum in adults and larvae using SEM techniques, and interpret these morphological features in terms of the mechanism of attachment of the mites to host tissues. Finally, we discuss the taxonomic status of *Orthohalarachne* mites in the context of previous descriptions.

Materials and methods

Methods of collection

Mites were collected from a South American fur seal, *Arctocephalus australis* (Zimmermann, 1783) (Carnivora, Otariidae) (Fig. 1A), rescued from the beaches of Las Toninas, Province of Buenos Aires, Argentina (36°29'00"S, 56°42'00"W) in August 2022. The animal was transferred to the Mundo Marino Foundation's Rescue and Rehabilitation Centre, where it was assisted in its recovery (ID M7422, young male). When the specimen did not recover and died, a necropsy was performed, and the entire respiratory system was removed. The sea lion's respiratory organs were then stored in the freezer, dissected, and washed for manual collection of mites. During the dissection of the respiratory organs, the nose,

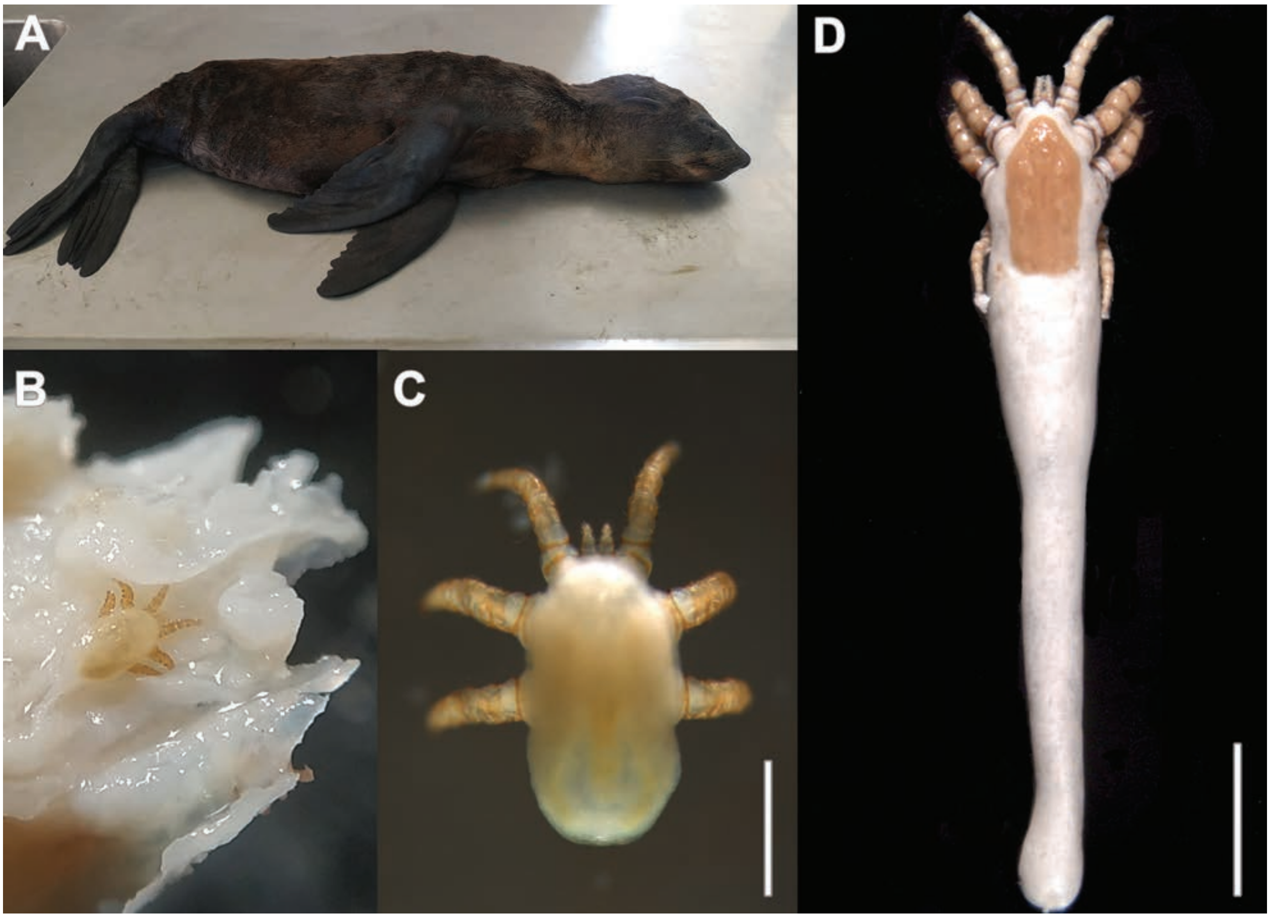

Figure 1. Marine mammal host and mites collected **A** young male of *Arctocephalus australis* (ID M7422), host of the collected mites **B** *Orthohalarachne attenuata*, larva (LEE-FCEN-UBA), in the turbinate tissue of the host **C** *O. attenuata*, larva (LEE-FCEN-UBA), dorsal habitus **D** *O. attenuata*, female (LEE-FCEN-UBA), dorsal habitus. Scale bars: 0.5 mm (**C**); 1 mm (**D**).

turbinates, nasopharynx, pharynx, trachea, and lungs were separated. All mites present in the respiratory tissues were then collected manually with forceps. The specimens collected in this way were counted and grouped by organ into larvae or adults and fixed in 96% alcohol in a freezer until used for taxonomic studies.

Specimen handling and imaging

Specimens for optical observation were mounted in Hoyer's medium following Walter and Krantz (2009). Measurements were made using an Olympus CH or Leica D2500 compound microscope. For scanning electron microscopy, specimens were dehydrated according to Pérez-Benavides et al. (2023). The specimens were processed in amyl acetate, mounted with copper adhesive tape, sputter-coated with gold-palladium (60:40) and examined with a ZEISS GeminiSEM 360.

Optical images of preserved specimens were taken using a Leica DFC 290 digital camera mounted on a Leica M165 C stereomicroscope in multiple focal planes, with focal planes aligned using Helicon Focus 4.62.2.

For the structural description of the mites, the morphological terminology follows Walter and Krantz (2009) and for the ambulacrum Alberti and Coons (1999). The studied material is housed in the Colección de Artrópodos of the Laboratorio de Entomología Experimental, Facultad de Ciencias Exactas y Naturales, Universidad de Buenos Aires (LEE-FCEN-UBA) and in the Arachnological National Collection, Museo Argentino de Ciencias Naturales Bernardino Rivadavia, in Buenos Aires, Argentina (MACN-Ar 46561 and 46562).

Results

We collected 381 larvae (Figs 1B, C, 5A, B) and 23 adults (Figs 1D, 2) from the nose and nasopharynx of *A. australis*. Based on leg and palpal chaetotaxy, idiosoma dimensions, body chaetotaxy, and dorsal sclerites, identity was assigned to *O. attenuata*.

The ambulacrum of adult females (Figs 3, 4) is composed of a pretarsus (*pt*, Figs 3A, 4G), a pair of large paradactyli or pretarsal opercula (*pd*), a pair of claws (*cl*), and a large and retractable pulvillus (*pv*) (Figs 3, 4). The paradactyli are large and fin-shaped (Fig. 3A, B, D–F) and do not have any denticles in the distal part. When the pulvillus is retracted, they completely cover the paradactyli (Figs 3D, E, 4A, B). The clearing for optical observation makes these structures difficult to observe. The claws are directed towards the ventral side of the leg and have different shapes and sizes depending on the leg. Legs II and III have relatively large and straight claws (Figs 3G, 4D) with deep longitudinal furrows on both sides of the structure. These furrows do not extend to the distal end (Figs 3H, 4E).

In contrast, the claws on legs I (Fig. 3B, C) and IV (Fig. 4F–I) are more curved and relatively smaller, with longitudinal furrows much shallower than in legs II and III. The pulvilli are smooth on all legs (Figs 3B, F, 4C, G, H) and, when expanded (*cfr*, Figs 3B, F, 4C, G), are rather large and directed anteriorly to the longitudinal axis of the tarsi. In larvae (Fig. 5) the ambulacrum is composed of the same structures as in adults, but the paradactyli are more elongated in the longitudinal axis (Fig. 5C, E, G), and cover most of the pretarsus and the claws when the pulvilli are expanded (Fig. 5D, F, H).

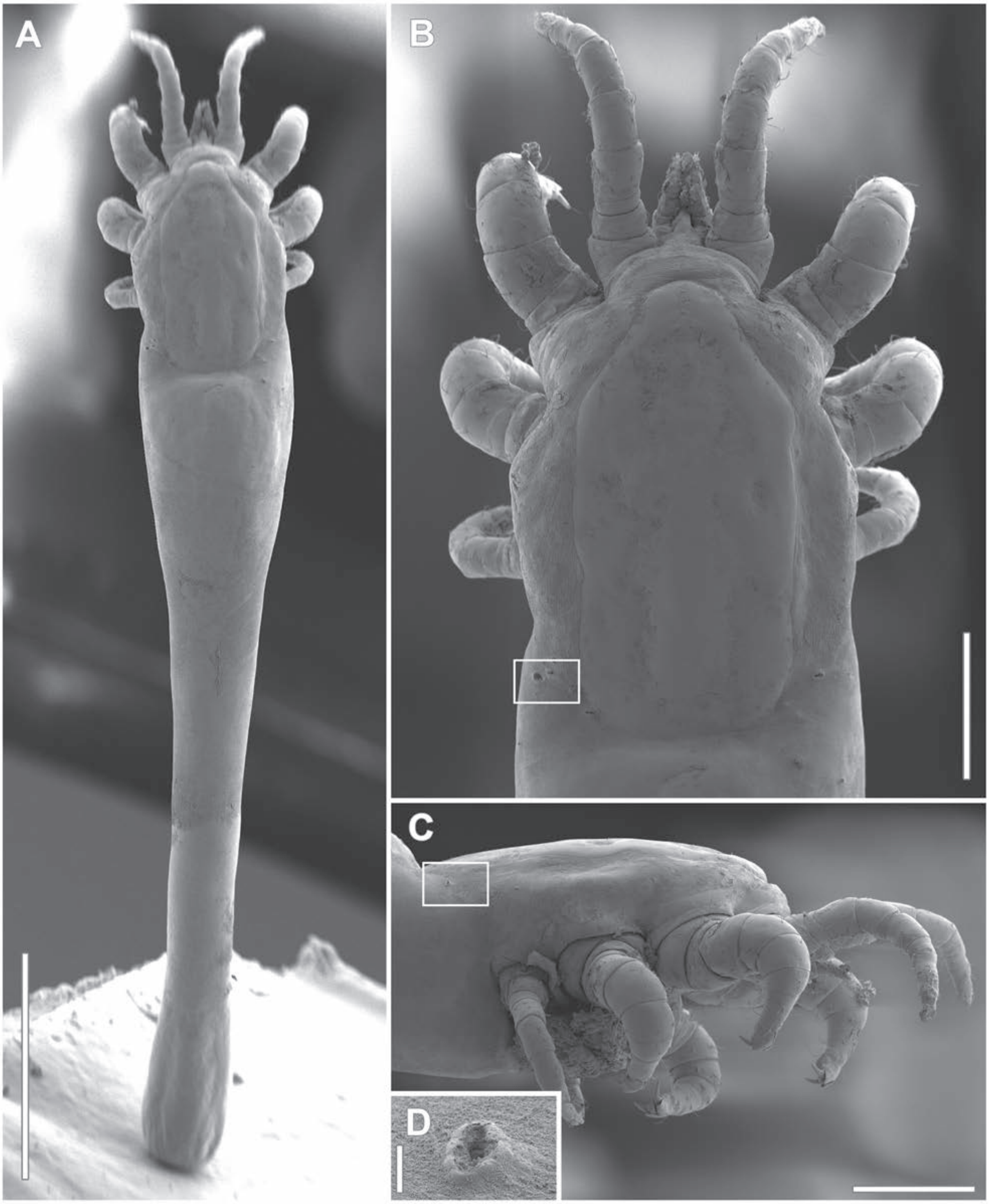

Figure 2. *Orthohalarachne attenuata*, females (MACN-Ar 46561) **A** dorsal habitus **B** same as in **A**, detail of anterior part, white box marks left stigma **C** lateral view of anterior part of body, white box marks left stigma **D** detail of the stigma. Scale bars: 1 mm (**A**); 300 µm (**B, C**); 10 µm (**D**).

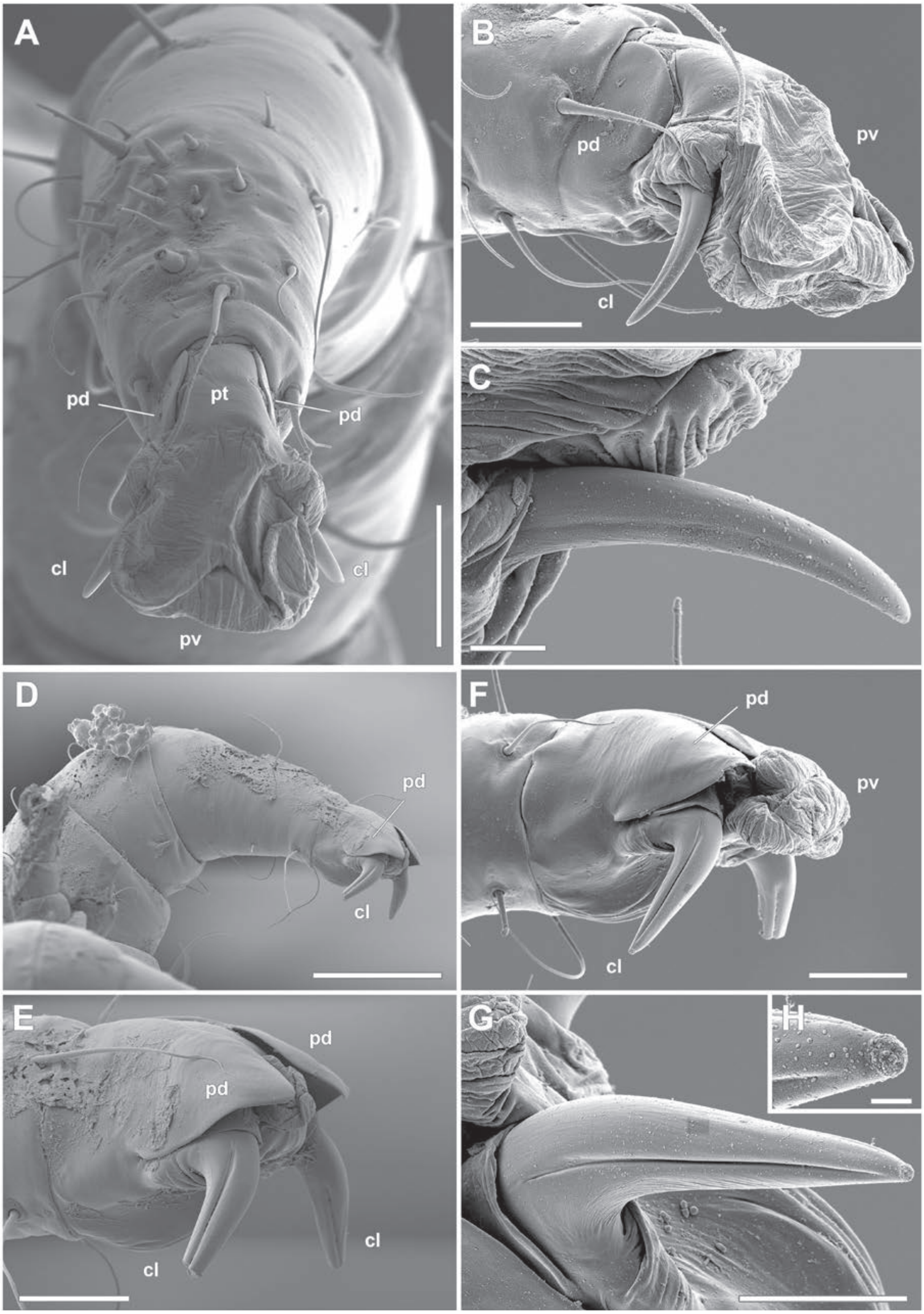

Figure 3. *Orthohalarachne attenuata*, females (MACN-Ar 46561) **A** tarsus and ambulacrum of right leg I, dorsodistal view **B** same as in **A**, detail of the ambulacrum, antiaxial view **C** same as in **B**, detail of the antiaxial claw; antiaxial view **D** tarsus and ambulacrum of left leg II, paraxial view **E** as in **D**, detail of the ambulacrum **F** ambulacrum of right leg II, antiaxial view **G** as in **F**, detail of the antiaxial claw; antiaxial view **H** as in **G**, detail of the distal part. Abbreviations: *cl*, claw; *pd*, paradactyl; *pt*, pretarsus; *pv*, pulvillus. Scale bars: 30 μm (**A**); 20 μm (**B, G**); 5 μm (**C**); 100 μm (**D**); 30 μm (**E, F**); 2 μm (**H**).

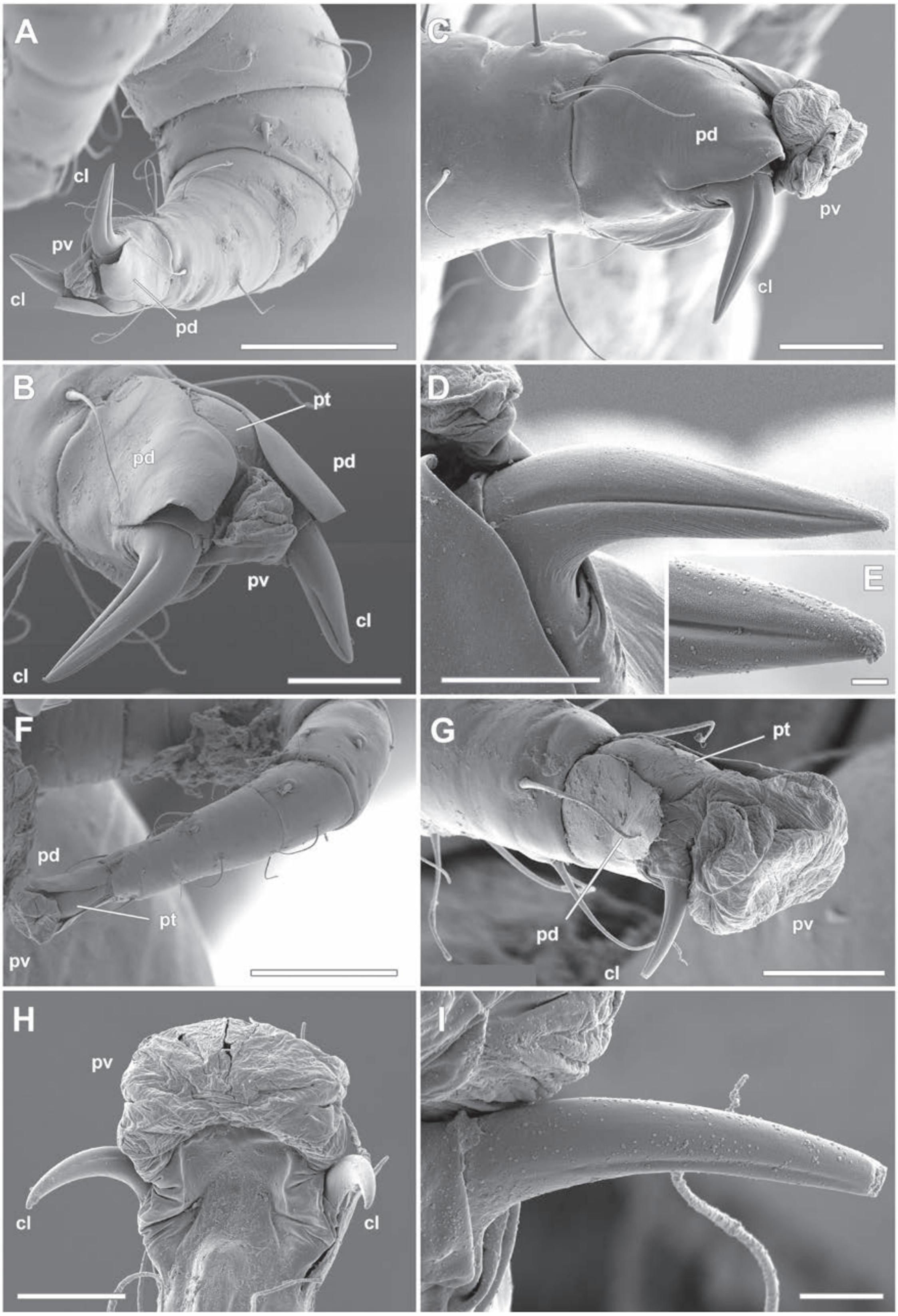

Figure 4. *Orthohalarachne attenuata*, females (MACN-Ar 46561) **A** right leg III, paraxial view **B** Same as in **A**, ambulacrum **C** ambulacrum of right leg III, antiaxial view **D** same as in **C**, detail of the antiaxial claw antiaxial view **E** as in **D**, detail of the distal part **F** tarsus and ambulacrum of left leg IV, dorsal view **G** ambulacrum of right leg IV, antiaxial view **H** ambulacrum of left leg IV, ventral view **I** same as in **G**, antiaxial claw. Scale bars: 100 µm (**A**); 30 µm (**B, C**); 20 µm (**D**); 2 µm (**E**); 100 µm (**F**); 30 µm (**G**); 20 µm (**H**); 5 µm (**I**).

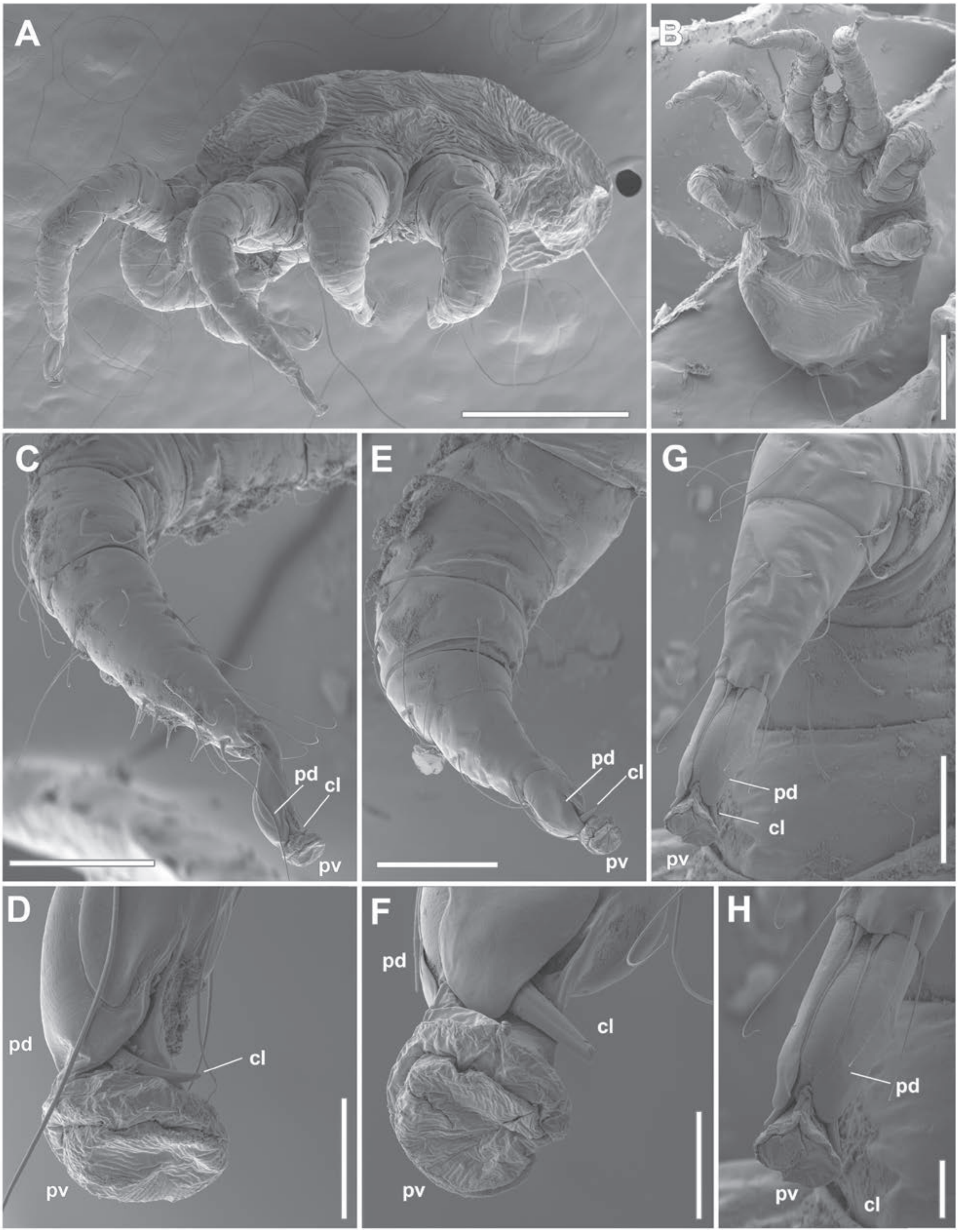

Figure 5. *Orthohalarachne attenuata*, larvae (MACN-Ar 46561) **A** habitus, lateral view **B** habitus ventral view **C** right leg I, paraxial view **D** as in **C**, ambulacrum **E** right leg II, paraxial view **F** as in **E**, ambulacrum **G** right leg III, dorsal view **H** as in **G**, ambulacrum. Scale bars: 300 µm (**A, B**); 100 µm (**C**); 20 µm (**D**); 100 µm (**E**); 20 µm (**F**); 60 µm (**G**); 20 µm (**H**).

Discussion

In this work, after an exhaustive taxonomic determination, we document for the first time the presence of *Orthohalarachne attenuata* parasitizing *A. australis* in continental Argentina, extending its known geographical distribution. Furthermore, we describe in detail the structure of the ambulacrum through SEM images of the adult and larvae, observing structural differences and details of its anchoring apparatus to the host that have never been described in such detail, reflecting the different function they have in locomotion at each stage of the life cycle.

Detailed studies describing the ambulacral morphology of dermanyssoid mites are scarce (Evans and Till 1965; Evans 1992; Alberti and Coons 1999; Montasser 2006; Krantz 2009; Di Palma and Mul 2019). In these mites (as free-living Gamasida), the ambulacrum consists of a pretarsus, a pair of claws, a pulvillus and the paradactyli (Alberti and Coons 1999). In general, the paradactyli (pretarsal opercula) may be variable or absent on the first pair of legs, with their distal end generally dentate (Evans and Till 1979: fig. 14G). In some taxa, however, paradactyli can have different shapes with modifications in orientation depending on the life history of the mite (e.g. Pugh et al. 1987). In *O. attenuata*, the shape of these structures differs in adults and larvae, probably fulfilling different functions depending on the life history of each stage. While larvae have elongated paradactyli that seem to cover the entire ambulacrum, even the claws (Fig. 5C–H), in adults they only protect the pulvillus when it is not expanded (*cfr*, Fig. 3D, E). The peculiar morphology of the paradactyli on the larval legs could be related to their high dispersal in the environment (Furman and Smith 1973). In this process, mite larvae are expelled from the infected host’s nose by sneezing, fall onto the substrate or onto the body of another host. The larvae must then crawl on their legs along hot, hard, or rough surfaces until they find the nostrils of a new host (Furman and Smith 1973). Therefore, we propose that paradactyli play an important protective role in locomotion during the host-finding process on the beach. In contrast, we observed that adult mites do not have tarsi with protective structures. During development, nymphs moult within the host’s respiratory tract and adults remain immobile, mainly in the most internal respiratory organs such as the nasopharynx, do not leave the host and remain attached to the internal mucosa for the rest of their lives. We propose that adults have tarsi with fewer protective structures as an adaptation to their reduced locomotor activity. Unfortunately, we did not collect nymphs of this species, but considering the differential development of tarsal claws in these stages (Furman 1977), it would be very interesting to study the development of these structures in nymphal stages using SEM techniques in a future work. However, it has been reported that it is very difficult to find halarachnid nymphs in otariids due to the extremely short duration of the protonymphal and deutonymphal stages, an adaptation in these mites to their highly specialised parasitic lifestyle (Furman and Smith 1973).

We interpret the presence of longitudinal furrows in the claws of these mites as an adaptation for attachment to the host’s respiratory mucosa, combined with the presence of straight claws on legs II and III, shaped like the head of a climbing axe, for attachment to a soft substrate. On the one hand, it is noteworthy that these claws appear to be firmly inserted into the turbinates and the mucosa of the nasal cavity. In fact, removal of the material results in breakage of the distal portion of the claw. On the other hand, the presence of a large, retractable, and smooth pulvillus is a common adaptation in dermanyssoid mites to adhere to a smooth surface, which would correspond to the anchoring of adults in the mucosa of the choanae and of larvae in the mucosa and hard tissue of the turbinates. Therefore, we propose that both structures, claw and pulvillus, may act alternatively as attachment devices depending on the substrate to which the mite is attached, as similar attachment structures have been recorded for other mites such as *Dermanyssus gallinae* (De Geer, 1778) (Di Palma and Mul 2019). When collecting mites from different host tissues, we observed that almost all adults were attached to the soft mucosa of the choanae, whereas larvae were mostly found in harder tissues such as the nose and turbinates. The differences in the structure of the ambulacrum of each stage would then correspond to the hardness characteristics of the host tissues in which the individuals of each stage were found. According to the life cycle of this mite, the characteristics of the tarsal structures found in larvae and adults in this work correspond to adaptations to parasitic life in organisms that have to alternate between being inside and outside the host depending on the stage of development.

With regard to the taxonomic status of *Orthohalarachne* mite species in the literature, a description of a mite species on another host with similar characteristics to *O. attenuata* is reported. The halarachnid mite *O. magellanica* (Finnegan, 1934) was described on *O. flavescens* Shaw, 1800 from the Islas Malvinas (Falkland Islands), but this description does not mention the leg chaetotaxy. In the revision of the family, Newell (1947) treated this species as valid and mentioned the relatively shorter dorsal shield (L/W = 1.75–1.8 vs 2.00–2.28 in *O. attenuata*) and the greatly enlarged male trochanter (Finnegan 1934: fig. 11) as diagnostic characters. Later, Domrow (1974: 20) subjectively synonymised this species with *O. attenuata* because “I see no real evidence in the original descriptions to justify the retention of the nominal taxa now combined under *H. attenuata*”. In papers dealing with South American records of *O. attenuata* (e.g. Gomez-Puerta and Gonzales-Viera 2015; Gastal et al. 2016; Ebmer et al. 2022; Rivera-Luna et al. 2023), *O. magellanica* is treated as a junior synonym of *O. attenuata*. In our specimens, the chaetotaxy, at least in number and arrangement, is similar to that reported by Furman (1977) for *O. attenuata*. The L/W ratio of the dorsal shield varies between 2.11 and 2.2 in non-compressed material, while in compressed (MACN-Ar 46562, Hoyer’s mounted) specimens this ratio varies between 1.73 and 2.00. This difference could be the reason for the different observations in the original description of *O. magellanica*. However, considering the stability of the leg chaetotaxy of halarachnid mites (Furman 1977) and the wide geographical distribution of the host species of *O. attenuata*, we believe that Domrow’s synonym remains to be tested using molecular data.

Acknowledgments

We thank the veterinarians and technicians of the Fundación Mundo Marino, especially Dolores Erviti and Candela Martelli, for their help and collaboration in collecting the samples, Nicolás López Carrion (La Plata Museum) for access to the bibliography, and Fabián Tricárico of MACN for help with the microscopy. We are grateful to David Verón for his contributions to the fieldwork, assistance with necropsies and access to stored material. Valuable edits that helped to improve this study were provided by Bruce Halliday and Owen Seeman. Thanks are also due to Farid Faraji, the subject editor, for his help with this manuscript.

Additional information

Conflict of interest

The authors have declared that no competing interests exist.

Ethical statement

No ethical statement was reported.

Funding

This work was partially supported by the Fundación Mundo Marino, Consejo Nacional de Investigaciones Científicas y Técnicas, Universidad de Buenos Aires (grant number UBACyT 2020 20020190100059BA) and the Agencia Nacional de Promoción de la Investigación, el Desarrollo Tecnológico y la Innovación – FONCyT (grant number PICT 2019-I-A- 00975).

Author contributions

Conceptualization: MKC. Data curation: AOP. Formal analysis: AOP. Funding acquisition: MKC, JPL. Investigation: MKC. Methodology: JPL, AOP, MKC. Project administration: JPL, MKC. Resources: AOP, MKC, JPL. Supervision: JPL, MKC. Visualization: AOP, MKC. Writing – original draft: MKC, AOP. Writing – review and editing: MKC.

Author ORCIDs

Andrés Osvaldo Porta https://orcid.org/0000-0002-9533-4139
Marcela Karina Castelo https://orcid.org/0000-0001-7107-6078

Data availability

All of the data that support the findings of this study are available in the main text.

References

Alberti G, Coons LB (1999) Acari – Mites. In: Harrison FW (Ed.) Microscopic Anatomy of Invertebrates. Volume 8: Chelicerate Arthropoda. Wiley-Liss, New York, 515–1265.

Banks N (1910) New American mites. Proceedings of the Entomological Society of Washington 12: 2–12. https://doi.org/10.1093/besa/2.2.12

Di Palma A, Mul MF (2019) How can *Dermanyssus gallinae* (De Geer 1778) (Acari: Anactinotrichida: Dermanyssidae) walk upwards on slippery surfaces? Avian Pathology 48(1): 10–16. https://doi.org/10.1080/03079457.2019.1608909

Doetschman WH (1944) A new species of endoparasitic mite of the family Halarachnidae (Acarina). Transactions of the American Microscopical Society 63(1): 68–72. https://doi.org/10.2307/3223339

Domrow R (1963) New records and species of Austromalayan laelapid mites. Proceedings of the Linnean Society of New South Wales 88: 199–220.

Domrow R (1974) Notes on halarachnine larval morphology and a new species of *Pneumonyssus* Banks (Acari: Dermanyssidae). Australian Journal of Entomology 13(1): 17–26. https://doi.org/10.1111/j.1440-6055.1974.tb02286.x

Dowling AP (2006) Mesostigmatid mites as parasites of small mammals: systematics, ecology, and the evolution of parasitic associations. In: Morand S, Krasnov BR, Poulin R (Eds) Micromammals and Macroparasites: from Evolutionary Ecology to Management. Springer Japan, Tokyo, 103–117. https://doi.org/10.1007/978-4-431-36025-4_7

Duarte-Benvenuto A, Sacristán C, Reisfeld L, Santos-Costa PC, Fernandes NCD, Ressio RA, Mello DMD, Favero C, Groch KR, Diaz-Delgado J, Catão-Dias JL (2022) Clinico-pathologic findings and pathogen screening in fur seals (*Arctocephalus australis* and *Arctocephalus tropicalis*) stranded in southeastern Brazil, 2018. Journal of Wildlife Diseases 58(1): 86–99. https://doi.org/10.7589/JWD-D-21-00060

Dunlap JS, Piperlij RC, Keyes MC (1976) Lesions associated with *Orthohalarachne attenuata* (Halarachnidae) in the northern fur seal (*Callorhinus ursinus*). Journal of Wildlife Diseases 12(1): 42–44. https://doi.org/10.7589/0090-3558-12.1.42

Ebmer D, Kniha E, Strauss V, Kübber-Heiss A, Komornik L, Balfanz F, Hering-Hagenbeck S, Walochnik J, Gärtner U, Prosl H, Taubert A, Voracek T, Hermosilla C (2022) First report of a severe nasopulmonary acariasis caused by *Orthohalarachne diminuata* Doetschman, 1944 (Acari: Halarachnidae) in a captive South American sea lion (*Otaria flavescens* Shaw, 1800). International Journal for Parasitology. Parasites and Wildlife 19: 248–256. https://doi.org/10.1016/j.ijppaw.2022.10.005

Evans GO (1992) Principles of Acarology. CAB international, Oxon, 563 pp. https://doi.org/10.1079/9780851988221.0000

Evans GO, Till WM (1965) Studies on the British Dermanyssidae (Acari: Mesostigmata). Part I. External Morphology. Bulletin of the British Museum, Natural History. Zoology 13: 247–294. https://doi.org/10.5962/bhl.part.16752 [Natural History]

Evans GO, Till WM (1979) Mesostigmatic mites of Britain and Ireland (Chelicerata: Acari-Parasitiformes), an introduction to their external morphology and classification. Transactions of the Zoological Society of London 35(2): 139–270. https://doi.org/10.1111/j.1096-3642.1979.tb00059.x

Fay FH, Furman DP (1982) Nasal mites (Acari: Halarachnidae) in the spotted seal, *Phoca largha* Pallas, and other pinnipeds of Alaskan waters. Journal of Wildlife Diseases 18(1): 63–68. https://doi.org/10.7589/0090-3558-18.1.63

Finnegan S (1934) On a new species of mite of the family Halarachnidae from the Southern sea lion. Discovery Reports 8: 319–328.

Fravel V, Procter D (2016) Successful diagnosis and treatment of *Orthohalarachne attenuata* nasal mites utilising voluntary rhinoscopy in three Pacific walrus (*Odobenus rosmarus divergens*). Veterinary Record Case Reports 4(1): e000258. https://doi.org/10.1136/vetreccr-2015-000258

Furman DP (1977) Observations on the ontogeny of halarachnid mites (Acarina: Halarachnidae). The Journal of Parasitology 63(4): 748–755. https://doi.org/10.2307/3279587

Furman DP, Smith AW (1973) In vitro development of two species of *Orthohalarachne* (Acarina: Halarachnidae) and adaptations of the life cycle for endoparasitism in mammals. Journal of Medical Entomology 10(4): 415–416. https://doi.org/10.1093/jmedent/10.4.415

Gastal B, Mascarenhas CS, Ruas JL (2016) Infection rates of *Orthohalarachne attenuata* and *Orthohalarachne diminuata* (Acari: Halarachnidae) in *Arctocephalus australis* (Zimmermann, 1783) (Pinipedia: Otariidae). Comparative Parasitology 83(2): 245–249. https://doi.org/10.1654/4797s.1

Gomez-Puerta LA, Gonzales-Viera O (2015) Ectoparásitos del lobo marino sudamericano (*Otaria flavescens*) de la costa peruana. Revista Peruana de Biología 22(2): 259–262. https://doi.org/10.15381/rpb.v22i2.11360

Katz H, Morgades D, Castro-Ramos M (2012) Pathological and Parasitological Findings in South American Fur Seal Pups (*Arctocephalus australis*) in Uruguay. ISRN Zoology 586079: 1–7. https://doi.org/10.5402/2012/586079

Kikuchi S, Okuyama Y (1987) A lung mite, *Orthohalarachnae attenuata* (Acarina: Halarachnidae) from the nasal cavity of a northern fur seal, *Callorhinus ursinus*. Japanese Journal of Sanitary Zoology 38(2): 85–91. https://doi.org/10.7601/mez.38.85

Kim KC, Haas VL, Keyes MC (1980) Populations, microhábitat preference and effects of infestations of two species of *Orthohalarachne* (Halarachnidae: Acarina) in the northern fur seal. Journal of Wildlife Diseases 16: 45–51. https://doi.org/10.7589/0090-3558-16.1.45

Konishi K, Shimazaki K (1998) Halarachnid mites infesting the respiratory tract of Steller sea lions. Biosphere Conservation 1(1): 45–48. https://doi.org/10.20798/biospherecons.1.1-45

Krantz GW (2009) Form and function. In: Krantz GW, Walter DE (Eds) A Manual of Acarology. Texas Tech University Press, Lubbock, 5–53.

Kuzmina TA, Spraker TR, Kudlai O, Lisitsyna OI, Zabludovskaja SO, Karbowiak G, Fonataine C, Kuchta R (2018) Metazoan parasites of California sea lions (*Zalophus californianus*): A new data and review. International Journal for Parasitology. Parasites and Wildlife 7(3): 326–334. https://doi.org/10.1016/j.ijppaw.2018.09.001

Kuzmina TA, Kuzmin Y, Dzeverin I, Lisitsyna OI, Spraker TR, Korol EM, Kuchta R (2021) Review of metazoan parasites of the northern fur seal (*Callorhinus ursinus*) and the analysis of the gastrointestinal helminth community of the population on St. Paul Island, Alaska. Parasitology Research 120(1): 117–132. https://doi.org/10.1007/s00436-020-06935-6

Lindquist EE, Krantz GW, Walter DE (2009) Order Mesostigmata. In: Krantz GW, Walter DE (Eds) A Manual of Acarology. Texas Tech University Press, Lubbock, 124–232.

Marlow BJ (1975) the comparative behaviour of the australasian sea lions *Neophoca cinerea* and *Phocarctos hookeri* (Pinnipedia: Otariidae). Mammalia 39(2): 159–230. https://doi.org/10.1515/mamm.1975.39.2.159

Montasser AA (2006) Scanning electron microscopy observations on male *Echinolaelaps echidninus* (Berlese, 1887) (Dermanyssoidea: Laelapidae) with emphasis on its gnathosoma, palpal organ and pulvilli. International Journal of Zoological Research 2(3): 204–212. https://doi.org/10.3923/ijzr.2006.204.212

Newell IM (1947) Studies on the morphology and systematics of the family Halarachnidae Oudemans 1906 (Acari, Parasitoidea). Bulletin of the Bingham Oceanographic Collection 10: 235–266.

Nicholson A, Fanning J (1981) Parasites and associated pathology of the respiratory tract of the Australian sea lion, *Neophoca cinerea*. Wildlife disease of the Pacific Basin and other countries. In: Fowler ME (Ed.) Proceedings of the Fourth International Conference of the Wildlife Disease Association, Sydney, 178–181. https://www.cabidigitallibrary.org/doi/full/10.5555/19820802483

Oudemans AC (1906) Über genitaltracheen bei chernetiden und Acari. Zoologischer Anzeiger 30: 135–140.

Pérez-Benavides AL, Ospina-Peñuela E, Gamboa J, Duran-Bautista EH (2023) Amyl acetate: An alternative technique to dry mount Chalcidoidea (Hymenoptera) from alcohol, faster and inexpensively. Journal of Insect Science 23(2): 4. https://doi.org/10.1093/jisesa/iead010

Pesapane R, Archibald W, Norris T, Fontaine C, Halaska B, Duignan P, Javeed N, Miller M, Foley J (2021) Nasopulmonary mites (Halarachnidae) of coastal Californian pinnipeds: Identity, prevalence, and molecular characterization. International Journal for Parasitology. Parasites and Wildlife 16: 113–119. https://doi.org/10.1016/j.ijppaw.2021.08.005

Pesapane R, Chaves A, Foley J, Javeed N, Barnum S, Greenwald K, Dodd E, Fontaine C, Duignan P, Murray M, Miller M (2022) Nasopulmonary mites (Acari: Halarachnidae) as potential vectors of bacterial pathogens, including *Streptococcus phocae*, in marine mammals. PLOS ONE 17(6): e0270009. https://doi.org/10.1371/journal.pone.0270009

Pugh PJA, King PE, Fordy MR (1987) Ambulacral structure in the terrestrial moiety of the intertidal Acari, and its relationship with the lifestyle of the Acari. Acarologia 28(1): 3–13.

Rivera-Luna H, Kniha E, Muñoz P, Painean J, Balfanz F, Hering-Hagenbeck S, Prosl H, Walochnik J, Taubert A, Hermosilla C, Ebmer D (2023) Non-invasive detection of *Orthohalarachne attenuata* (Banks, 1910) and *Orthohalarachne diminuata* (Doetschman, 1944) (Acari: Halarachnidae) in free-ranging synanthropic South American sea lions *Otaria flavescens* (Shaw, 1800). International Journal for Parasitology, Parasites and Wildlife 21: 192–200. https://doi.org/10.1016/j.ijppaw.2023.06.001

Seawright AA (1964) Pulmonary acariasis in a Tasmanian fur seal. The Journal of Comparative Pathology and Therapeutics 74: 97–IN20. https://doi.org/10.1016/S0368-1742(64)80013-8

Seguel M, Calderón K, Colegrove K, Adkesson M, Cárdenas-Alayza S, Paredes E (2018) Helminth and respiratory mite lesions in Pinnipeds from Punta San Juan, Perú. Acta Parasitologica 63(4): 839–844. https://doi.org/10.1515/ap-2018-0103

Tubb J (1937) Lady Julia Percy Island: Report of the expedition of the McCoy Society for Field Investigation and Research. No. 18. Crustacea. Proceedings of the Royal Society of Victoria 49: 408–411.

Walter DE, Krantz GW (2009) Collecting, rearing, and preparing specimens. In: Krantz GW, Krantz GW (Eds) A Manual of Acarology. Texas Tech University Press, Lubbock, 83–96.

ZooKeys 1207: 369–371 (2024)
DOI: 10.3897/zookeys.1207.128152

Corrigendum

Corrigendum: Liu W-B, Wang C-Y, Tang Y-N, Wang Y, Pei W-X, Yan C-C (2024) Six new species of *Cryptochironomus* Kieffer (Diptera, Chironomidae) from the Nearctic region. ZooKeys 1200: 275–302. doi:10.3897/zookeys.1200.119225

Wen-Bin Liu[1], Cheng-Yan Wang[1], Ya-Ning Tang[1], Ying Wang[1], Wen-Xuan Pei[1], Chun-Cai Yan[1]

1 *Tianjin Key Laboratory of Conservation and Utilization of Animal Diversity, Tianjin Normal University, Tianjin, 300387, China*
Corresponding author: Chun-Cai Yan (skyycc@tjnu.edu.cn)

Academic editor:
Fabio Laurindo da Silva
Received: 23 May 2024
Accepted: 29 June 2024
Published: 24 July 2024

ZooBank: https://zoobank.org/DA1BE2CC-CAAC-4CFE-BD29-37E5BA36BE32

Citation: Liu W-B, Wang C-Y, Tang Y-N, Wang Y, Pei W-X, Yan C-C (2024) Corrigendum: Liu W-B, Wang C-Y, Tang Y-N, Wang Y, Pei W-X, Yan C-C (2024) Six new species of *Cryptochironomus* Kieffer (Diptera, Chironomidae) from the Nearctic region. ZooKeys 1200: 275–302. doi:10.3897/zookeys.1200.119225. ZooKeys 1207: 369–371. https://doi.org/10.3897/zookeys.1207.128152

We recently published six new species of *Cryptochironomus* Kieffer (Diptera, Chironomidae) from the Nearctic region. However, the authors made some errors in couplet 4, in that the values given in the second alternative of the couplet do not agree with in the least the values that appear further down the key (couplet 7, etc.), and parentheses were missing in authorities of three species. In this corrigendum, we revise the key to Nearctic males of *Cryptochironomus*. We thank Dr. Martin Spies (Zoologische Staatssammlung München, München) for kindly pointing out the error in contradictions between couplets.

Key to Nearctic males of *Cryptochironomus* Kieffer

The key adapted from Sæther 2009.

1 Anal point broad and flat **2**
– Anal point narrow **3**
2 Mesal apical margin of gonostylus emarginate .... ***C. scimitarus* Townes, 1945**
– Mesal apical margin of gonostylus straight or nearly straight .... ***C. sorex* Townes, 1945**
3 Mesal apical margin of gonostylus emarginate .... ***C. argus* Roback, 1957**
– Mesal apical margin of gonostylus not emarginate **4**
4 Gonostylus ~ 4× as long as wide, AR about 3.7, Wing length 3.1–3.4 mm .... ***C. blarina* Townes, 1945**
– Gonostylus ~ 1.6–3.7× as long as wide; when AR higher than 3.6, Wing length higher than 3.4 mm or lower than 3.1 mm **5**
5 Gonostylus widened towards apex; frontal tubercles present; AR 1.99–5.1; LR$_1$ 1.12–1.73, 9–24 sensilla chaetica on P$_2$ **6**
– Gonostylus not distinctly widened towards apex; frontal tubercles mostly absent, when present AR 2.5–3.8, LR$_1$ 1.45–2.02 and mostly 1–6 sensilla chaetica on P$_2$; when AR higher than 3.5, LR$_1$ higher than 1.59 .... **10**
6 AR 1.99–2.76; LR$_1$ 1.60–1.7 .... **7**
– AR 3.54–5.12; LR$_1$ 1.12–1.39 .... **9**

7 Wing length 2.43–2.65; anal point widest at the base and slightly constricted at 1/3 distance from the base ...... ***C. beardi*** **Liu, sp. nov.**
– Wing length 2.05–2.37; anal point is parallel-sided with a rounded apex ... **8**
8 AR 1.99–2.37; thorax brown with dark brown spots ...... ***C. parallelus*** **Liu, sp. nov.**
– AR 2.48–2.76; thorax yellowish brown without spots ...... ***C. dentatus*** **Liu, sp. nov.**
9 AR 4.35–5.12, LR_1 1.12–1.21; gonostylus strongly widened towards apex ...... ***C. stylifera*** **Johannsen, 1908**
– AR 3.54–4.03, LR_1 1.23–1.39; gonostylus slightly widened towards apex ...... ***C. digitatus*** **(Malloch, 1915)**
10 LR_1 1.31–1.67, frontal tubercles absent **11**
– LR_1 1.45–2.02, when lower than 1.7 frontal tubercles present **13**
11 Wing length 4.99–5.78 mm; LR_1 1.48–1.67 ...... ***C. eminentia*** **Mason, 1986**
– Wing length 1.47–4.75 mm; LR_1 1.31–1.55 ...... **12**
12 Wing length 4.05 mm; gonostylus widest width near apex ...... ***C. ramus*** **Mason, 1986**
– Wing length 2.31–2.59 mm; gonostylus gradually tapered and pointed apically ...... ***C. taylorensis*** **Liu, sp. nov.**
13 Wing length 1.47–1.8 mm, gonostylus only ~ 2× as long as wide **14**
– Wing length 1.9–5.6 mm, gonostylus at least 2.5× as long as wide **5**
14 Wing length 1.8 mm, AR 2.75, frontal tubercles present ...... ***C. parafulvus*** **Beck & Beck, 1964**
– Wing length 1.47–1.69 mm, AR 2.29–2.49, frontal tubercles absent ...... ***C. ferringtoni*** **Liu, sp. nov.**
15 Gonostylus ~ 2.8–3.2× as long as wide, anal point slightly spatulate apically, frontal tubercles absent ...... ***C. ponderosus*** **(Sublette, 1964)**
– Gonostylus ~ 2.7× as long as wide, anal point tapering parallel-sided or slightly spatulate, frontal tubercles present or absent **16**
16 Frontal tubercles absent, wing length 2.0–5.6 mm **17**
– Frontal tubercles present, wing length 1.8–3.2 mm or 5.1–5.3 mm **18**
17 Gonostylus rounded apically, wing length 2.5–5.6 mm ...... ***C. curryi*** **Mason, 1986**
– Gonostylus tapering to the apex, wing length 2.02 mm ...... ***C. absum*** **Liu, sp. nov.**
18 Wing length 5.1–5.3 mm; AR 2.5–2.6 ...... ***C. conus*** **Mason, 1986**
– Wing length 1.8–3.2 mm; AR 2.5–3.4 ...... **19**
19 LR_1 1.56–1.73, mean 1.64; anal point slightly spatulate apically ...... ***C. imitans*** **Sæther, 2009**
– LR_1 1.60–2.02, mean 1.78, anal point parallel-sided ...... ***C. fulvus*** **(Johannsen, 1905)**

Additional information

Conflict of interest

The authors have declared that no competing interests exist.

Ethical statement

No ethical statement was reported.

Funding

No funding was reported.

Author contributions

All authors have contributed equally.

Author ORCIDs

Wen-Bin Liu https://orcid.org/0000-0001-6916-0692

Data availability

All of the data that support the findings of this study are available in the main text.

References

Liu W-B, Wang C-Y, Tang Y-N, Wang Y, Pei W-X, Yan C-C (2024) Six new species of *Cryptochironomus* Kieffer (Diptera, Chironomidae) from the Nearctic region. ZooKeys 1200: 275–302. https://doi.org/10.3897/zookeys.1200.119225